Publication No. FHWA-IF-02-034

PB2003-100459

April 2002

U.S. Department of Transportation
Federal Highway Administration

Office of Bridge Technology
400 Seventh Street, SW
Washington, DC 20590

Geotechnical Engineering Circular No. 5

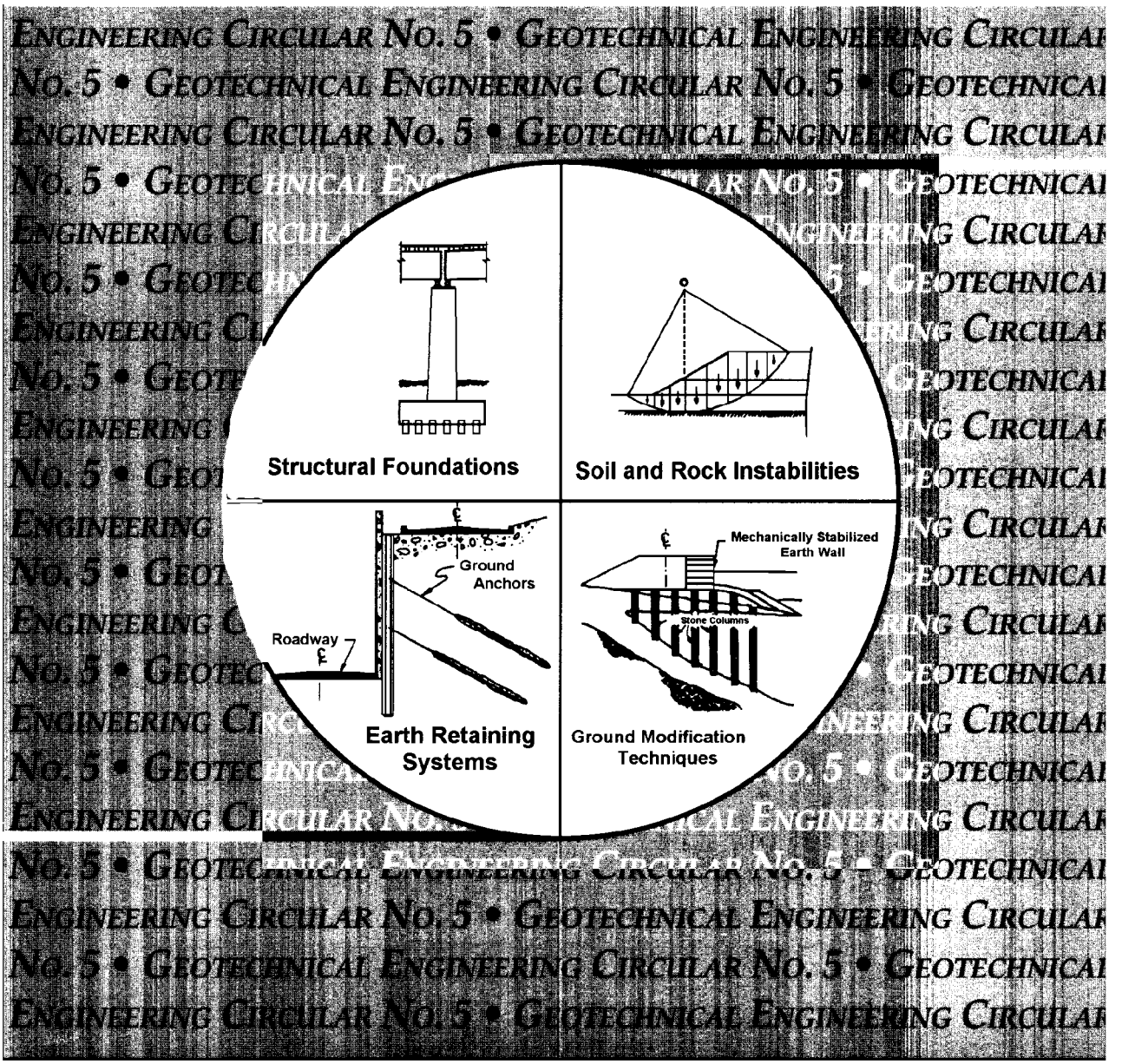

The FHWA geotechnical Engineering Circulars (GEC) are a series of comprehensive and practical manuals that provide state-of–the-practice methods and techniques to assist the highway engineer in the design and construction of highway facilities. No other agency or group has assembled such a complete set of manuals for geotechnical engineering. The manuals are modeled after the well-respected set of hydraulic engineering circulars and hydraulic design series, and they are expected to become a mainstay of geotechnical engineering practice worldwide.

The published circulars in this series are the following:

GEC No. 1 – Dynamic Compaction (FHWA-SA-95-037)
GEC No. 2 – Earth Retaining Systems (FHWA-SA-96-038)
GEC No .3 – Design Guidance: Geotechnical Earthquake
Engineering for Highways
Volume 1 – Design Principles (FHWA-SA-95-037)
Volume II – Design Examples (FHWA-SA-97-077)
GEC No. 4 – Ground Anchors and Anchored Systems (FHWA-IF-99-015)
GEC No. 5 – Evaluation of Soil and Rock Properties (FHWA-IF-02-034)

Geotechnical Engineering Circulars are currently being developed in the following areas:
Shallow Foundations
Soil Nail Walls

REPRODUCED BY: NTIS
U.S. Department of Commerce
National Technical Information Service
Springfield, Virginia 22161

PROTECTED UNDER INTERNATIONAL COPYRIGHT
ALL RIGHTS RESERVED
NATIONAL TECHNICAL INFORMATION SERVICE
U.S. DEPARTMENT OF COMMERCE

NOTICE

The contents of this report reflect the views of the authors, who are responsible for the facts and the accuracy of the data presented herein. The contents do not necessarily reflect the policy of the Department of Transportation. This report does not constitute a standard, specifications, or regulation. The United States Government does not endorse products or manufactures. Trade or manufacture's names appear herein only because they are considered essential to the objective of this document.

Technical Report Documentation Page

1. Report No.	2. Government Accession No.	3. Recipient's Catalog No.
FHWA-IF-02-034		

4. Title and Subtitle	4. Report Date
GEOTECHNICAL ENGINEERING CIRCULAR NO. 5 Evaluation of Soil and Rock Properties	April 2002
	6. Performing Organization Code:

7. Author(s)	8. Performing Organization Report No.
P.J. Sabatini, R.C. Bachus, P.W. Mayne, J.A. Schneider, T.E. Zettler	

9. Performing Organization Name and Address	10. Work Unit No.(TRAIS)
GeoSyntec Consultants 1100 Lake Hearn Drive, NE Atlanta, Georgia 30342-1523	11. Contract or Grant No. DTFH61-94-C-00099

12. Sponsoring Agency Name and Address	13 Type of Report and Period Covered
U.S. Department of Transportation Office of Bridge Technology Federal Highway Administration 400 Seventh Street, SW Washington, DC 20590	Technical Manual
	14. Sponsoring Agency Code

15. Supplementary Notes
FHWA COTR: Chien-Tan Chang
FHWA Technical Consultant: Jerry A. DiMaggio

16. Abstract This document presents state-of-the-practice information on the evaluation of soil and rock properties for geotechnical design applications. This document addresses the entire range of materials potentially encountered in highway engineering practice, from soft clay to intact rock and variations of materials that fall between these two extremes.

Information is presented on parameters measured, evaluation of data quality, and interpretation of properties for conventional soil and rock laboratory testing, as well as in situ devices such as field vane testing, cone penetration testing, dilatometer, pressuremeter, and borehole jack. This document provides the design engineer with information that can be used to develop a rationale for accepting or rejecting data and for resolving inconsistencies between data provided by different laboratories and field tests.

This document also includes information on: (1) the use of Geographical Information Systems (GIS) and Personal Data Assistance devices for the collection and interpretation of subsurface information; (2) quantitative measures for evaluating disturbance of laboratory soil samples; and (3) the use of measurements from geophysical testing techniques to obtain information on the modulus of soil. Also included are chapters on evaluating properties of special soil materials (e.g., loess, cemented sands, peats and organic soils, etc.) and the use of statistical information in evaluating anomalous data and obtaining design values for soil and rock properties. An appendix of three detailed soil and rock property selection examples is provided which illustrate the application of the methods described in the document.

17. Key Words	18. Distribution Statement
Soil properties, rock properties, laboratory testing, in-situ testing, subsurface investigation, data quality, data interpretation, shear strength, consolidation, hydraulic conductivity, modulus	No restrictions. This document is available to the public from the National Technical Information Service, Springfield, Virginia 22161.

19. Security Classif. (of this report)	20. Security Classif. (of this page)	21. No. of Pages	22. Price
Unclassified	Unclassified	385	

ACKNOWLEDGEMENTS

The authors would like to express their appreciation to Mr. Jerry A. DiMaggio, P.E. of the U.S. Department of Transportation Federal Highway Administration (FHWA) for providing significant technical assistance and review during preparation of the document. The authors would also like to thank Messer's Norman Norrish, P.Eng. and Duncan Wyllie, P.Eng. of Wyllie & Norrish Rock Engineers for providing technical assistance on rock property evaluation. The authors would also like to thank the following individuals who reviewed the document and served on the Technical Working Group for this project:

- Richard Cheney, P.E. – FHWA (retired);
- Nari Abar – Geostructural Engineering, Inc.
- David Shiells, P.E. – Virginia DOT;
- Lawrence Pierson – Oregon DOT;
- Sam Mansukhani – FHWA Midwestern Resource Center;
- Michelle Cribbs – FHWA

The authors would also like to acknowledge Geotesting Express Inc. for providing photographs.

Finally, the authors would like to thank Mrs. Ann Taylor and Mr. Michael Harris of GeoSyntec Consultants who drafted the figures and assisted in the layout of the document.

PREFACE

This document presents state-of-the-practice information on the evaluation of soil and rock properties for geotechnical design applications. This document was prepared to provide geotechnical engineers with tools to assist in the rational development of subsurface investigation programs, as well as in the execution of laboratory and field testing programs involving soil and rock, and interpretation of data from these programs. The document will be equally useful for structural engineers, engineering geologists, or geologists who may be responsible for field and laboratory testing programs. This document addresses the entire range of materials potentially encountered in highway engineering practice, from soft clay to intact rock and variations of materials that fall between these two extremes.

In reviewing texts and course materials that are currently available to the practicing engineer, it is recognized that two important areas have not been sufficiently addressed. These are: (1) the use and role of in-situ testing; and (2) the interpretation of conflicting, contradicting, and inconsistent data. Regarding the first point, it is recognized that over the past 20 years, several in situ testing techniques have moved from the arena of university research to routine engineering practice. In 2002, in situ testing plays a critical role in assessing soil properties and, to a lesser extent, rock properties, particularly by complementing laboratory-derived data. In this document detailed information on parameters measured, evaluation of data quality, and interpretation of properties are provided for conventional soil and rock laboratory testing, as well as in situ devices such as field vane testing, cone penetration testing, dilatometer, pressuremeter, and borehole jack. Regarding the second point, data resulting from the range of laboratory and in situ tests are often not completely consistent with other data obtained for the project and/or soil deposit. This document provides the design engineer with information that can be used to develop a rationale for accepting or rejecting data and for resolving inconsistencies between data provided by different laboratories and field tests.

This document relies on previous good practice in the evaluation of soil and rock properties. This good practice is extended by more recent developments in the areas of engineering property evaluation methods by including: (1) use of Geographical Information Systems (GIS) and Personal Data Assistance (i.e., handheld computer) devices for the collection and interpretation of subsurface information; (2) quantitative measures for evaluating disturbance of laboratory soil samples; and (3) use of measurements from seismic and geophysical testing techniques to obtain information on the modulus of soils for static deformation analyses. Other features of this document include a chapter on evaluating properties of special soil materials (e.g., loess, cemented sands, peats and organic soils), a chapter on the use of statistical information in evaluating anomalous data and obtaining design values for soil and rock properties, and an appendix of three detailed soil and rock property selection examples which illustrate the application of the methods described in the document for property evaluation.

TABLE OF CONTENTS

CHAPTER 1 1

1.1 INTRODUCTION 1

1.2 BACKGROUND 1

1.3 DOCUMENT ORGANIZATION 2

CHAPTER 2 4

2.1 INTRODUCTION 4

2.2 PROCESS OF SOIL AND ROCK PROPERTY SELECTION 4

2.3 USE OF CORRELATIONS TO ASSIST PROPERTY SELECTION 7

2.4 USE OF OBSERVATIONAL METHOD 9

CHAPTER 3 10

3.1 INTRODUCTION 10

3.2 PLANNING THE SUBSURFACE INVESTIGATION AND LABORATORY TESTING PROGRAM 10

3.2.1 General 10

3.2.2 Identify Data Needs 10

3.2.3 Gather and Analyze Existing Information 11

3.2.4 Conduct Site Visit 17

3.2.5 Develop Preliminary Site Model 18

3.2.6 Developing a Site Investigation Program 20

3.2.7 Developing a Laboratory Testing Program 22

CHAPTER 4 26

4.1 INTRODUCTION 26

4.2 BORING METHODS 27

4.3 SAMPLING METHODS 32

4.3.1 Disturbed Sampling of Soil 32

4.3.2 Undisturbed Sampling of Soil 34

TABLE OF CONTENTS (continued)

4.3.2.1 General 34

4.3.2.2 Overview of Thin-Walled Tube Sampling 39

4.3.3 Rock Coring 42

4.4 STANDARD PENETRATION TEST (SPT) 44

4.4.1 General 44

4.4.2 Procedures 45

4.4.3 Parameters Measured 45

4.5 CONE PENETRATION TESTS (CPT / CPTU / SCPTU) 48

4.5.1 General 48

4.5.2 Equipment 50

4.5.3 Procedures 52

4.5.4 Parameters Measured 54

4.6 FLAT DILATOMETER TEST (DMT) 56

4.6.1 General 56

4.6.2 Equipment 56

4.6.3 Procedures 56

4.6.4 Parameters Measured 58

4.7 PRESSUREMETER TEST (PMT) 58

4.7.1 General 58

4.7.2 Equipment 59

4.7.3 Procedures 59

4.7.4 Parameters Measured 60

4.8 VANE SHEAR TEST (VST) 62

4.8.1 General 62

4.8.2 Equipment 62

4.8.3 Procedures 63

4.8.4 Parameters Measured 64

4.9 USE OF DRILL RIGS TO PERFORM IN-SITU TESTS 65

4.10. IN-SITU TESTING IN ROCK 65

TABLE OF CONTENTS (continued)

4.10.1 General 65
4.10.2 Borehole Dilatometer 66
4.10.3 Borehole Jack 67
4.10.4 In-situ Direct Shear Testing 67
4.11 GEOPHYSICAL TESTING 68
4.12 LABORATORY SOIL TESTING 74
4.12.1 Introduction 74
4.12.2 Quality Assurance for Laboratory Testing 74
4.12.2.1 Sample Tracking 74
4.12.2.2 Sample Storage 78
4.12.2.3 Sample Handling 78
4.12.2.4 Specimen Selection 78
4.12.3 Effects of Sample Disturbance 79
4.12.4 Laboratory Index Tests for Soils 82
4.12.4.1 General 82
4.12.4.2 Moisture Content 82
4.12.4.3 Unit Weight 83
4.12.4.4 Atterberg Limits 83
4.12.4.5 Particle Size Distribution 86
4.12.4.6 Laboratory Classification 87
4.12.4.7 Specific Gravity 87
4.12.4.8 Organic Content 87
4.12.4.9 Electro Chemical Classification Tests 88
4.12.5 Laboratory Performance Tests for Soils 88
4.12.5.1 General 88
4.12.5.2 Consolidation 89
4.12.5.3 Soil Strength 92
4.12.5.4 Permeability 99
4.13 LABORATORY ROCK TESTS 102

4.13.1 Introduction 102
4.13.2 Laboratory Testing of Rock 104
4.13.2.1 Point-Load Strength Test 104
4.13.2.2 Unconfined Compressive Strength of Intact Rock Core 105
4.13.2.3 Elastic Moduli of Intact Rock Core 106
4.13.2.4 Laboratory Direct Shear Test 106

CHAPTER 5 108
5.1 INTRODUCTION 108
5.2 INTERPRETATION OF SUBSURFACE STRATIGRAPHY 108
5.2.1 General 108
5.2.2 Soil Classification by Soil Sampling and Drilling 108
5.2.3 Soil Classification by Cone Penetration Testing 112
5.2.4 Soil Classification using the Flat-Plate Dilatometer 117
5.2.5 Generating a Subsurface Profile 118
5.3 IN-SITU STRESS STATE 123
5.3.1 General 123
5.3.2 Overburden Stresses 123
5.3.3 Horizontal Stresses 124
5.4 CONSOLIDATION PROPERTIES OF SOIL 125
5.4.1 General 125
5.4.2 Laboratory Consolidation Tests 125
5.4.2.1 General 125
5.4.2.2 Soil Parameters from Laboratory Consolidation Tests 126
5.4.2.3 Selection of Samples for Laboratory Consolidation Testing 126
5.4.2.4 Evaluation of σ_p' from Laboratory Consolidation Tests 128
5.4.2.5 Evaluation of C_c and C_r 130
5.4.2.6 Laboratory Evaluation of c_v 131
5.4.2.7 Evaluation of $C_{\alpha\varepsilon}$ 134
5.4.3 Evaluation of σ_p' from In-situ Test Methods 136

5.4.4 Evaluation of c_h from CPTu Dissipation Data 140
5.4.5 Selection of Design Values for Consolidation Analyses 142
5.5 GENERAL STRESS-STRAIN AND STIFFNESS PROPERTIES 146
5.5.1 Background 146
5.5.2 Settlement Analysis for Soils 147
5.5.3 Method to Evaluate Equivalent Elastic Modulus 148
5.5.4 Evaluation of Shear Wave Velocity 151
5.5.4.1 General 151
5.5.4.2 Field Measurements of Shear Wave Velocity 151
5.5.5 Correlations for Small-Strain Shear Modulus 154
5.5.6 Evaluation of Modulus Degradation Value 155
5.5.7 Summary 156
5.6 SHEAR STRENGTH PROPERTIES OF SOIL 156
5.6.1 Introduction 156
5.6.2 Fundamental Concepts of Soil Shear Strength 159
5.6.2.1 Drained versus Undrained Loading 159
5.6.2.2 Drained Stress-Strain-Strength Behavior 160
5.6.2.3 Undrained Stress-Strain-Strength Behavior 162
5.6.2.4 Effective Stress Parameters 163
5.6.2.5 Total Stress Parameters 167
5.6.3 Relevance of Design Applications to Soil Shear Strength Evaluation 167
5.6.4 Laboratory Testing Methods for Evaluating Soil Shear Strength 168
5.6.4.1 Selection of Laboratory Testing Method 168
5.6.4.2 Triaxial Testing 169
5.6.4.3 Direct Shear Testing 175
5.6.4.4 Unconfined Compression Testing 178
5.6.4.5 Relevance of Laboratory Strength Tests to Field Conditions 179
5.6.5 Undrained Shear Strength from In-situ Tests 180
5.6.6 Drained Friction Angle of Granular Soils from In-situ Tests 184

5.6.7 Selection of Total Stress Parameters (s_u) for Undrained Strength Design Analyses 187
5.6.8 Selection of Effective Stress Parameters (ϕ', c') for Design Analyses 189
5.7 HYDRAULIC CONDUCTIVITY PROPERTIES OF SOIL 189
5.7.1 Introduction 189
5.7.2 Laboratory Output/Data Reduction 190
5.7.3 Correlation Methods 191
5.7.4 Interpretation Methods 193

CHAPTER 6 195
6.1 INTRODUCTION 195
6.2 ROCK MASS CLASSIFICATION 196
6.2.1 Description of Rock Masses 196
6.2.2 Core Recovery and Rock Quality Designation 200
6.2.3 CSIR Classification 202
6.3 ROCK UNIAXIAL COMPRESSIVE STRENGTH 204
6.4 ROCK DEFORMATION MODULUS VALUES 204
6.4.1 Intact Rock Modulus 204
6.4.2 Rock Mass Modulus 206
6.4.2.1 Method Based On Rock Mass Rating 206
6.4.2.2 Method Based on RQD 207
6.4.2.3 Use of In situ Tests to Evaluate Rock Mass Modulus 208
6.4.3 Selection of Rock Deformation Modulus for Design 211
6.5 ROCK SHEAR STRENGTH 211
6.5.1 Mohr-Coulomb Materials 211
6.5.2 Shear Strength Of Discontinuities 213
6.5.2.1 General 213
6.5.2.2 Friction Angle of Rock Surfaces 213
6.5.2.3 Surface Roughness 214
6.5.2.4 Measurement of Surface Roughness 216
6.5.2.5 Discontinuity Infilling 217

6.5.2.6. Effect of Water on Shear Strength 218
6.5.2.7 Laboratory Direct Shear Testing 222
6.5.3 Shear Strength Of Fractured Rock Masses 223
6.5.3.1 General 223
6.5.3.2 Strength Determination by Back Analysis of Failures 223
6.5.3.3 Hoek-Brown Strength Criteria for Fractured Rock Masses 224
6.5.4 Selection of Rock Shear Strength for Design 227

CHAPTER 7 229

7.1 INTRODUCTION 229

7.2 LOESS 231

7.2.1 Identification of Loess 231
7.2.2 Issues Related to Subsurface Exploration in Loess 231
7.2.3 Laboratory Strength Testing of Loess 232
7.2.4 Evaluation of Collapse Potential 232

7.3 EXPANSIVE SOILS 233

7.3.1 Identification of Expansive Soils 233
7.3.2 Evaluation of Expansion (Swell) Potential 235
7.3.3 Shear Strength Evaluation of Expansive Soils 236

7.4 ORGANIC SOILS AND PEAT 236

7.4.1 Introduction 236
7.4.2 Identification of Organic Soils and Peat 237
7.4.3 Issues Related to Subsurface Exploration and Sampling of Organic Soils and Peat 238
7.4.4 Shear Strength of Organic Soils and Peats 238
7.4.5 Compressibility of Organic Soils and Peats 239

7.5 COLLUVIUM AND TALUS 240

7.5.1 Identification of Colluvium and Talus 240
7.5.2 Issues Related to Subsurface Exploration and Testing in Colluvium 241
7.5.3 Issues Related to Subsurface Exploration and Testing in Talus 241
7.5.4 Compressibility of Colluvium and Talus 242

7.5.5 Shear Strength of Colluvium and Talus 242
7.6 SHALES AND DEGRADABLE MATERIALS 243
7.6.1 Identification of Degradable Materials 243
7.6.2 Slake Durability Test 244
7.6.3 Jar Slake Test 244
7.6.4 Point-Load Test 245
7.6.5 Use of Shale Material 245
7.7 CEMENTED SANDS 246
7.7.1 Identification of Cemented Sands 246
7.7.2 Issues Related to Subsurface Exploration and Testing in Cemented Sands 247
7.7.3 Interpretation of Laboratory and Field Testing Results in Cemented Sands 247
7.8 SENSITIVE CLAYS 248
7.8.1 Identification of Sensitive Clays 248
7.8.2 Issues Related to Subsurface Exploration and Testing in Sensitive Clays 249
7.8.3 Interpretation of Laboratory and Field Testing Results in Sensitive Soils 250
7.9 PARTIALLLY SATURATED SOILS 251
7.9.1 Identification of Partially Saturated Soils 251
7.9.2 Sampling and Testing Partially Saturated Soils 251
7.9.3 Interpretation of Laboratory and Field Testing Results of Partially Saturated Soils 252

CHAPTER 8 253
8.1 INTRODUCTION 253
8.2 RESOLVING INCONSISTENCIES BETWEEN TEST RESULTS 253
8.3 ESTIMATING VARIABILITY OF SELECTED PARAMETERS 254
8.4 FINAL SELECTION OF DESIGN PARAMETERS 255

REFERENCES 258

TABLE OF CONTENTS (continued)

APPENDIX A **SOIL AND ROCK PROPERTY SELECTION EXAMPLES**

Example 1 Soft to Medium Clay and Overconsolidated Clay Crust

Example 2 Piedmont Residual Soil, Weathered Rock, And Rock

Example 3 Heavily Overconsolidated Clays

APPENDIX B **CALCULATION OF THE COEFFICIENT OF CONSOLIDATION FROM LABORATORY DATA**

APPENDIX C **ALTERNATIVE APPROACH TO EVALUATE HORIZONTAL COEFFICIENT OF CONSOLIDATION VALUES FROM PIEZOCONE DISSIPATION TESTS**

LIST OF TABLES

Table		Page
1	Summary of information needs and testing considerations for a range of highway applications.	12
2	Sources of historical site data.	15
3	Guidelines for minimum number of investigation points and depth of investigation	24
4	Reference publications on in-situ testing	27
5(a)	Boring methods (modified after Day, 1999).	30
5(b)	Rock core drilling methods (modified after Day, 1999).	31
5(c)	Other exploratory techniques (modified after Day, 1999).	32
6(a)	Common samplers to collect disturbed soil samples (modified after NAVFAC, 1982).	33
6(b)	Specialty samplers to collect disturbed soil samples (modified after NAVFAC, 1982).	34
7	Nominally undisturbed soil samplers (modified after NAVFAC, 1982)	41
8	Factors affecting the SPT and SPT results (after Kulhawy and Mayne, 1990).	46
9	Corrections to the SPT (after Skempton, 1986)	47
10	In-situ testing methods used in soils.	49
11	In-situ testing methods used in rock.	66
12	Geophysical testing techniques.	70
13	Common soil laboratory tests.	75
14	Methods for index testing of soils.	76
15	Methods for performance testing of soils.	77
16	Sample quality designation system (Lacasse et al., 1985).	81
17	U.S. standard sieve sizes and corresponding opening dimension.	86
18	Time t_f to reach failure (after Head, 1986).	99
19	Recommended maximum hydraulic gradient for permeability testing	101
20	Common rock laboratory tests.	103
21	Summary information on rock laboratory test methods.	103
22	SPT N value soil property correlations for granular soils (after AASHTO, 1988).	110
23	SPT N value soil property correlations for cohesive soils (after AASHTO, 1988)	110
24	Casagrande method to evaluate σ_p'	128
25	Strain-energy method to evaluate σ_p'	129
26	Summary of correlations for C_c (modified after Holtz and Kovacs, 1986).	131
27	Modified time factors, T*, for analysis of CPTu dissipation data (after Teh and Houlsby, 1991)	141
28	Elastic constants of various soils based on soil type (modified after AASHTO, 1996).	148
29	Elastic constants of various soils based on SPT N value (modified after AASHTO, 1996).	148
30	Typical values of small-strain shear modulus.	154
31	Unconfined compressive strength of particles for rockfill grades in figure 73.	164
32	Summary of issues relevant to shear strength evaluation in support of the design of typical geotechnical features.	168
33	Conventional methods of interpretation for s_u from in-situ tests.	180

LIST OF TABLES (continued)

Table		Page
34	Relationship among relative density, SPT N value, and internal friction angle of cohesionless soils (after Meyerhof, 1956).	184
35	Comparison of hydraulic conductivity from empirical and field methods.	193
36	Description of geological mapping terms.	198
37	Rock material strengths	199
38	Weathering grades	199
39	Rock quality description based on RQD.	202
40	CSIR classification of jointed rock mass.	203
41	Typical elastic constants for intact rock (after Wyllie, 1999)	206
42	Estimation of E_M based on RQD (modified after Carter and Kulhawy, 1988)	207
43	Typical ranges of friction angles for a variety of rock types (after Barton, 1973; Jaeger and Cook, 1976)	214
44	Shear strength of filled discontinuities (modified after Hoek and Bray, 1977).	220
45	Approximate relationship between rock-mass quality and material constants used in defining nonlinear strength (Hoek and Brown, 1988).	225
46	Parameters used to develop strength envelopes in figure 105.	227
47	Summary of sampling difficulties and engineering characteristics of special materials.	229
48	Qualitative assessment of collapse potential (after ASTM D 5333)	233
49	Organic soils and peat classification properties (after Landva et al., 1983).	238
50	Evaluation of jar slake index, I_J.	245
51	Criteria for rockfill materials (after Strohm et al., 1978)	246
52	Values of coefficient of variation, V, for geotechnical properties and in situ tests (after Duncan, 2000).	256
A-1	Summary of soil property selection examples.	A-1
A-2	Summary of CPT subsurface profile interpretation.	A-7
A-3	Summary of CPTu subsurface profile interpretation.	A-9
A-4	Summary of laboratory testing on varved clay samples.	A-15
A-5	Parameters used for analysis of dissipation data	A-26
A-6	Evaluation of c_h from $CPTu_2$ dissipation data at 6.68 m.	A-26
A-7	Evaluation of c_h from $CPTu_2$ dissipation data at 17.65 m.	A-26
A-8	Summary of triaxial test data.	A-31
A-9	Vane shear data.	A-37
A-10	Index properties of Piedmont soils at the Alabama site	A-44
A-11	Summary of CPTu subsurface profile interpretation.	A-46
A-12	Summary of oedometer testing on Piedmont residual soils.	A-54
A-13	Test data and calculated elastic modulus from Menard PMT data at the Alabama site.	A-55
A-14	Test data and calculated unload-reload elastic modulus from full displacement PMT data (C-41) at the Alabama site.	A-56
A-15	Summary of elastic modulus values from various tests.	A-61
A-16	Stress-strain data for specimen B2-1-1 at 15 m.	A-63

LIST OF TABLES (continued)

Table		Page
A-17	Strength properties from CIUC triaxial tests on Piedmont soils from the Alabama site.	A-64
A-18	Soil stratigraphy from SPT and classification testing.	A-75
A-19	Summary of oedometer testing on heavily overconsolidated clays.	A-81

LIST OF FIGURES

Figure		Page
1	Soil and rock property selection flowchart.	5
2	Checklist items for site reconnaissance.	19
3	Large diameter auger boring.	29
4	Split barrel sampler.	33
5	Thin walled (Shelby) tube for sampling (with end caps)	35
6	Stationary piston sampler	36
7	Denison sampler	37
8	Pitcher sampler	38
9	Single and double tube rock core barrels (after FHWA-HI-97-021, 1997).	43
10	SPT performed at the back of a drill rig.	44
11	Stress normalization parameter, C_N, for sands	48
12	Cone and piezocone penetrometers.	52
13	Cone penetration testing from cone truck.	53
14	Measurement locations on cone penetrometers.	54
15	Illustration of unequal end areas of CPT (after Kulhawy and Mayne, 1990).	55
16	Flat plate dilatometer test equipment.	57
17	Pre-bored pressuremeter equipment.	61
18	Typical curves and characteristic pressures for pre-bored Menard pressuremeter.	61
19	(a) Rectangular vane; and (b) Parameters used to define vane dimensions.	63
20	Typical pressure-dilation graphs for a borehole dilatometer (after ISRM, 1987).	67
21	Typical setup for an in-situ direct shear test in an adit (after Saint Simon et al., 1979).	68
22	Disturbance during sampling and trimming (after Ladd and Lambe, 1963).	79
23	Lab and field consolidation curves.	80
24	Equipment used for Atterberg limits testing of soil.	84
25	Location of clay minerals on the Casagrande plasticity chart (Skempton, 1953).	85
26	Components of consolidation test.	89
27	Incremental load oedometer	90
28	Failure of a loose sand specimen in a triaxial cell; and (b) Load frame, pressure panel, and computerized data acquisition system.	93
29	Direct shear testing box.	94
30	Soil sample mounted in direct shear testing apparatus.	95
31	Rigid wall permeameter.	100
32	Flexible wall permeameter	101
33	Point load strength test equipment.	104
34	Laboratory direct shear testing equipment for rock.	107
35	Traditional drilling, sampling, and laboratory testing of collected samples.	109
36	Variability of SPT N values.	111
37	Comparison of SPT $(N_1)_{60}$ and CPT q_t values.	112
38	Soil classification based on q_t and FR (Robertson et al., 1986)	113
39	Soil classification based on q_t and Bq (Robertson et al., 1986).	113
40	Typical CPTu log.	115

LIST OF FIGURES (continued)

Figure		Page
41	CPTu log with subsurface stratigraphy interpretation	116
42	CPTu dissipation test in sand.	117
43	Soil classification based on DMT.	118
44	Summary plot of Atterberg limits data.	120
45	Boring location plan.	121
46	Interpreted subsurface profile.	121
47	Definition of C_c, C_r, C_s, σ_p'.	126
48	Profile of preconsolidation stress.	127
49	Illustration of Casagrande method to evaluate preconsolidation stress.	129
50	Illustration of strain-energy method to evaluate preconsolidation stress	130
51	Summary consolidation data showing c_v.	133
52	Evaluation of C_α	135
53	Correlation of σ_p' with CPT q_t data (after Kulhawy and Mayne, 1990).	137
54	Correlation of σ_p' with CPTu u_1 data (after Kulhawy and Mayne, 1990).	137
55	Correlation of σ_p' with CPTu u_2 data (after Kulhawy and Mayne, 1990).	138
56	Correlation of σ_p' with DMT p_o data (after Kulhawy and Mayne, 1990).	138
57	Correlation of σ_p' with self boring PMT p_L data (after Kulhawy and Mayne, 1990).	139
58	Correlation of σ_p' with VST $su_{,VST}$ data (after Kulhawy and Mayne, 1990).	139
59	$CPTu_2$ pore pressure dissipation curves	141
60	Rigidity index (after Keaveny and Mitchell, 1986).	142
61	Preconsolidation stress from oedometer and DMT.	144
62	Correlation of c_v to LL.	146
63	Strength measured by in-situ tests at peak of stress-strain curve	149
64	Stress-strain-strength curves for three geomaterials having the same strength yet different stiffness.	149
65	Variation of modulus with strain level	150
66	Field and laboratory methods to evaluate shear wave velocity.	152
67	Seismic dilatometer test.	154
68	Modulus degradation based on g=0.3.	155
69	Shear wave velocity profile from seismic cone sounding.	157
70	Various laboratory tests used to measure soil strength showing the imposed stresses and loading conditions.	158
71	Drained stress-strain behavior	160
72	Mohr-Coulomb failure criteria	161
73	Typical ranges of friction angle for rockfills, gravels, and sands (Terzaghi, Peck, and Mesri, 1996).	164
74	Relationship between ϕ' and PI (Terzaghi, Peck, and Mesri, 1996).	165
75	Relationship between c' and σ_p' (Mesri and Abdel-Ghaffar, 1993).	166
76	Residual friction angles for clayey soils (after Stark & Eid, 1994).	166
77	Stress-strain and Mohr circle representation for four UU tests performed on the same soil (after Day, 1999).	170

LIST OF FIGURES (continued)

Figure		Page
78	Interpretation of UU test data.	171
79	CIU triaxial compression test results.	173
80	Effective stress path in undrained shear.	174
81	Direct shear test results.	176
82	Area correction for direct shear test.	177
83	Typical stress-strain curve and Mohr circle representation of the state of stress for an unconfined compression test.	178
84	Shear modes for an embankment slip surface.	179
85	Plasticity based VST correction factors.	181
86	Example s_u profile (after Finno and Chung, 1992).	182
87	Correlation of ϕ' with SPT N_{60} data in clean sands.	185
88	Correlation of ϕ' with normalized CPT q_t data in clean sands.	186
89	Correlation of ϕ' with the DMT K_D parameter for clean sands.	186
90	Range of hydraulic conductivity values based on soil type.	192
91	Range of hydraulic conductivity based on grain size (after GeoSyntec, 1991).	194
92	Illustration of geological mapping terms (after Wyllie, 1999).	196
93	List of parameters and categories describing rock mass characteristics (after Wyllie, 1999).	197
94	Calculation of core recovery and RQD.	201
95	Axial and diametral stress-strain curves for intact rock tested in uniaxial compression.	205
96	Relationship between in situ modulus and rock mass rating (after Bieniawski, 1978; Serafim and Pereira, 1983).	207
97	Pressure-displacement plot for borehole jack.	210
98	Curve of E_{true} versus E_{calc} (after ASTM D 4971).	210
99	Relationships between shear stress and normal stress on rupture surface for five different geological conditions (TRB, 1996).	213
100	Effect of surface roughness and normal stress on the friction of a discontinuity surface.	214
101	Definition of joint roughness coefficient, JRC (Barton, 1973).	216
102	Simplified division of filled discontinuities into displaced and undisplaced, and NC and OC categories.	219
103	Results of direct shear test of filled discontinuity showing measurements of shear strength and roughness (after Wyllie, 1999).	222
104	Typical curved shear strength envelope defined by Hoek-Brown theory for rock mass strength (Hoek, 1983).	224
105	Illustration of use of nonlinear shear strength for three fractured rock mass types.	226
106	Classification chart for swelling potential (after Seed et al., 1962).	234
107	Guide to collapsibility, compressibility, and expansion based on in-situ dry density and liquid limit (after Mitchell and Gardner, 1975 and Gibbs, 1969).	235

LIST OF FIGURES (continued)

Figure		Page
108	Values of natural water content and compression index for peats, clays, and silts (after Mesri, Stark, Ajlouni, and Chen, 1997).	240
A-1	Boring log B1	A-4
A-2	Summary data for samples from Borings B1, B2, and B3	A-5
A-3	Subsurface soil layering based on CPT data and friction ratio.	A-6
A-4	Classification of soil type based on q_t and FR.	A-7
A-5	Subsurface soil layering based on CPTu data, friction ratio, and B_q parameter.	A-8
A-6	Classification of soil type based on q_t and B_q.	A-8
A-7	Subsurface soil layering based on DMT index values.	A-10
A-8	Classification and consistency of soil layers based on DMT data.	A-10
A-9	Index properties and "P_o" diagram for Boring B-1	A-12
A-10	Evaluation of σ_p' using the Casagrande method.	A-14
A-11	Evaluation of σ_p' using the strain energy method	A-16
A-12	Profile of σ_p' based on correlations with in-situ testing devices	A-17
A-13	Sample graphical evaluation for $C_{c\varepsilon}$ and $C_{r\varepsilon}$	A-19
A-14	Empirical correlations of C_c and $C_{c\varepsilon}$	A-20
A-15	Secondary compression results for Connecticut Valley varved clays investigation.	A-21
A-16	Laboratory-measured $C_{c\varepsilon}$ vs. depth.	A-22
A-17	c_v values from laboratory consolidation tests.	A-23
A-18	$CPTu_2$ pore pressure dissipation curves	A-25
A-19	Normalized $CPTu_2$ dissipation curves.	A-25
A-20	$C_{\alpha\varepsilon}$ values from laboratory consolidation tests.	A-28
A-21	Comparison of $C_{\alpha\varepsilon}$ and $C_{c\varepsilon}$ for laboratory consolidation tests.	A-28
A-22	K_o value calculated using in-situ testing devices	A-29
A-23	P_o diagram developed from 1-D consolidation data.	A-31
A-24	Stress - strain curve and stress path for a UU test on a Connecticut Valley varved clay specimen.	A-32
A-25	Stress - strain curve and stress path for a CIUC test on a Connecticut Valley varved clay specimen.	A-33
A-26	Effective stress properties from CIUC test data.	A-34
A-27	P_o diagram with OCR and s_u vs. depth.	A-35
A-28	Normalized strength property relationships for various shear modes.	A-35
A-29	Estimation of shear strength from in-situ tests: (a) VST; (b) empirical CPT, CPTu, & DMT based on correlations in table 33; and (c) based on Equation A-14 with $\phi'=18.2^o$	A-39
A-30	Residual soil classification and typical gneiss and schist weathering profile (after Sowers and Richardson, 1983)	A-40
A-31	Boring log for Alabama site	A-42
A-32	Summary index test data for samples from borings B-1, B-3, B-4, and B-6 at Alabama site	A-43
A-33	Subsurface layering based on CPTu data	A-45

LIST OF FIGURES (continued)

Figure		Page
A-34	Soil classification charts with CPTu data from Alabama site (signature 1).	A-47
A-35	Soil stratigraphy from DMT index values.	A-50
A-36	Classification and consistency of soil at Alabama site based on DMT data	A-50
A-37	Comparison of Alabama site data to published trend between CPT tip resistance and N-value as a function of mean grain size (Kulhawy & Mayne, 1990).	A-52
A-38	Comparison of Opelika, Alabama data to published trend between dilatometer modulus and N-value in Piedmont sandy silts (Mayne & Frost, 1989).	A-52
A-39	Comparison of Opelika, Alabama data to published trends between PMT modulus and N-Value in Piedmont soils (Martin, 1977).	A-53
A-40	Laboratory 1-D consolidation curves (a) Stress – Strain; (b) Stress – Strain Energy.	A-54
A-41	Menard pressuremeter data for the Alabama site.	A-56
A-42	Full displacement pressuremeter data for the Alabama site.	A-57
A-43	Dilatometer modulus E_D compared to pressuremeter modulus, E_P.	A-59
A-44	Calculation of elastic modulus from shear wave velocity data.	A-60
A-45	Stress-strain curve for CIUC tests on samples B2-1-1 at 15 m and B7-1 at 4 m.	A-62
A-46	Effective stress paths for CIUC tests shown in figure A-45.	A-65
A-47	Effective stress failure envelopes based on triaxial test data.	A-65
A-48	Estimate of effective stress friction angle at Alabama site using in-situ test data.	A-68
A-49	Rock core log.	A-71
A-50	Unconfined compression test results (sample depth 18 ft).	A-73
A-51	Unconfined compression test results (sample depth 40 ft).	A-73
A-52	Direct shear test results on rock joint (sample depth 74 ft).	A-73
A-53	Boring Log UHSPT1.	A-76
A-54	Summary test data from samples across site.	A-77
A-55	Atterberg limits results for soil samples.	A-77
A-56	Results of CPT measurements at site.	A-78
A-57	Classification of soils using CPT derived parameters.	A-79
A-58	Results of DMT measurements at site.	A-80
A-59	Classification of soils using DMT derived parameters.	A-81
A-60	Evaluation of $C_{c\varepsilon}$, $C_{r\varepsilon}$, and σ_p' using oedometer test results for sample at depth of 7 m.	A-82
A-61	σ_p' and OCR with depth from laboratory and in-situ tests.	A-83
A-62	Calculated K_o with depth from in-situ tests.	A-84
A-63	K_o correlated with K_D from DMT data (Kulhawy and Mayne, 1990).	A-85
A-64	K_o correlated with qt from CPT data (Kulhawy and Mayne, 1990).	A-85
A-65	Undrained shear strength, s_u, from laboratory and in-situ testing.	A-86
A-66	Guide to expansion and collapse potential (adapted from Holtz and Kovacs, 1986).	A-88

LIST OF FIGURES (continued)

Figure		Page
B-1	Casagrande logarithm of time method for c_v calculation	B-1
B-2	Taylor's square root of time method for c_v calculation.	B-3
C-1	Comparison of measured and predicted piezocone dissipation data.	C-2

LIST OF SYMBOLS

A	activity
a	cone radius
A_C	corrected area for cone penetrometer
A_c	percentage of ash from organic content test
a_n	net area ratio for cone penetrometer
A_s	surface area of cone sleeve
AR	area ratio
B	Skempton's pore pressure parameter
B_q	normalized pore pressure parameter for soil classification using CPTu
c'	effective stress cohesion intercept
c_T	total stress cohesion intercept
c'_i	instantaneous cohesion
C_B	borehole diameter correction factor
C_c	compression index
$C_{c\varepsilon}$	modified compression index or compression ratio
C_E	energy correction factor
CF	clay fraction
c_h	horizontal coefficient of consolidation
C_N	SPT stress normalization parameter
CP	collapse potential
C_R	rod length correction factor
C_r	recompression index
$C_{r\varepsilon}$	modified recompression index or recompression ratio
C_S	sampling method correction factor or swelling index
c_v	vertical coefficient of consolidation
C_α	coefficient of secondary compression
$C_{\alpha\varepsilon}$	modified coefficient of secondary compression
D	initial diameter of pressuremeter or vane diameter or distance between platens in a point-load strength test
d_{10}	effective grain size at 10% passing by weight
d_{15}	effective grain size at 15% passing by weight
d_s	equivalent particle diameter
D_e	diameter at sampler cutting tip
D_i	inside diameter of sampling tube
D_o	outside diameter of sampling tube
D_r	relative density
E	Young's modulus

LIST OF SYMBOLS (continued)

e	void ratio
E_D	dilatometer modulus
E_d	deformation modulus of rock from borehole dilatometer
E_M	rock mass modulus
E_{max}, E_o	small-strain Young's modulus
e_o	in-situ void ratio
E_P	pressuremeter elastic modulus
ER	energy ratio
E_R	intact rock deformation modulus
E_s	equivalent elastic modulus
E_{u-r}	pressuremeter elastic modulus evaluated using unload-reload cycle
FR	friction ratio
f_s	sleeve friction
G	shear modulus
G_d	interpreted shear modulus from borehole dilatometer test
G_{max},G_o	small-strain shear modulus
G_s	specific gravity
H	vane height
H_{DR}	drainage height
H_o	initial height
I	displacement influence factor
i	dilation angle
i_B	angle of vane taper at bottom
i_T	angle of vane taper at top
I_P, PI	plasticity index
ICR	inside clearance ratio
I_D	material index for dilatometer or slake durability
I_J	Jar Slake index
IL	incremental load
I_r	undrained rigidity index
I_s	point load strength
$I_{s(50)}$	size-corrected point load strength index
JCS	compressive strength of rock adjacent to the fracture surface
JRC	joint roughness coefficient
k	hydraulic conductivity
K_D	horizontal stress index
KE	kinetic energy

LIST OF SYMBOLS (continued)

k_h	horizontal hydraulic conductivity
k_m	calibration pressure-dilation curve (for borehole dilatometer)
K_o	at-rest lateral earth pressure coefficient
k_{PLT}	size correction factor for point load strength test
k_R	stiffness of rock (for borehole dilatometer)
k_s	stiffness of hydraulic system (for borehole dilatometer)
k_T	stiffness of overall system plus rock (for borehole dilatometer)
L	length of cell membrane in borehole dilatometer
LI	liquidity index
LL	liquid limit
M_s	mass of soil solids
m_v	volumetric compressibility coefficient
N	uncorrected Standard Penetration Test (SPT) blow count
N_{60}	standardized SPT blow count
$(N_1)_{60}$	normalized and standardized corrected blow count
N_{meas}	field recorded N-value
N_k	cone factor
OCR	overconsolidation ratio
P	point load breaking strength
p'	mean normal effective stress
p_1	expansion pressure
P_a	atmospheric pressure
PE	potential energy
p_f	yield pressure
P_i	applied pressure
p_L	limit pressure
PL	plastic limit
p_o	liftoff pressure or complete recompression pressure
p_r	yield point
p_u	minimum pressure during unloading in a pressuremeter unload/reload cycle
q	applied surface stress
q_c	uncorrected cone tip resistance
q_t	corrected cone tip resistance
q_u	unconfined compressive strength
R_P	uninflated radius of pressuremeter probe
R_T	temperature correction factor
S	normally consolidated undrained strength ratio

LIST OF SYMBOLS (continued)

$s_{collapse}$	settlement due to collapse
SL	shrinkage limit
s_r	remolded undrained shear strength
S_t	sensitivity
s_u	undrained shear strength
s_{uCIUC}	undrained shear strength from isotropically consolidated triaxial compression tests
s_{uDSS}	undrained shear strength from direct simple shear tests
s_{uVST}	undrained shear strength from vane shear test
s_{uUC}	undrained shear strength from unconfined compression tests
s_{uUU}	undrained shear strength from triaxial unconsolidated compression tests
t	time or vane edge thickness
T	torque and/or temperature
T*	modified time factor
t_{100}	time required to complete primary consolidation
t_{50}	time required to complete 50 percent primary consolidation
t_{90}	time required to complete 90 percent primary consolidation
t_f	minimum time required to fail a sample
T_{max}	maximum torque measured in vane shear test
T_{net}	maximum torque minus rod friction torque
t_p	time of primary consolidation
T_{rod}	rod friction torque
t_s	shear wave arrival times
U	degree of consolidation or normalized excess pore pressure
u_1	pore pressure at cone tip ($CPTu_1$)
u_2	pore pressure at cone shoulder ($CPTu_2$)
u_i	initial pore pressure at t=0
u_m	measured pore pressure during CPT
u_o	hydrostatic pore pressure or in-situ pore pressure condition
u_t	pore pressure at time t
V_m	mean volume of pressuremeter probe
V_o	initial volume of pressuremeter probe
V_s	shear wave velocity or volume of soil solids
w_i	initial moisture content
w_n	natural moisture content
z_m	gage offset zero reading in a flat plate dilatometer
z_w	depth of water table
%C	percent collapse

LIST OF SYMBOLS (continued)

1-U	normalized excess pore pressure
α	angle of taper
γ	unit weight
γ_b	buoyant unit weight
γ_d, γ_{dry}	dry unit weight
γ_s	shear strain
γ_{sat}	saturated unit weight
γ_t, γ_{tot}	moist (total) unit weight
ΔA	calibration factor for applied suction of membrane in air
ΔB	calibration factor for applied expansion of membrane in air
Δe	change in void ratio
ΔH_c	change in height of soil upon wetting
ΔR_m	increase in radius of pressuremeter probe
Δu	change in pore pressure
ΔW	change in work per unit volume
δ	deformation (of circular membrane)
$\dot{\delta}$	maximum rate of displacement
δ_f	displacement required to achieve peak strength of soil
δ_n	normal displacement
δ_s	shear displacement
ε	axial strain
ε_f	strain at end of increment
ε_i	strain at beginning of increment
ε_p	axial strain to reach peak strength
ε_V	vertical strain
μ	vane shear correction factor
ν	Poisson's ratio
ν_R	Poisson's ratio of rock
ρ	pump constant for borehole dilatometer
ρ_d, ρ_{dry}	dry mass density
ρ_t, ρ_{tot}	moist (total) mass density
σ'	effective stress
σ_1'	major principal effective stress
σ_3'	minor principal effective stress
σ_c	uniaxial compressive strength of rock or consolidation pressure
σ_f	stress at end of strain increment
σ_{ho}'	in-situ horizontal effective stress

LIST OF SYMBOLS (continued)

σ_i	stress at beginning of strain increment
σ_n	normal stress
σ_n'	effective normal stress
σ_p'	preconsolidation stress
σ_v'	vertical effective stress
σ_{vo}	total vertical stress
σ_{vo}'	in-situ vertical effective stress
τ	shear stress
τ_{max}	peak shear strength
τ_r	residual strength
ϕ	friction angle
ϕ'	effective stress friction angle
ϕ_i'	instantaneous friction angle
ϕ_r'	residual friction angle
ϕ_s'	secant friction angle
ϕ_T	total stress friction angle

CHAPTER 1

INTRODUCTION TO GEOTECHNICAL ENGINEERING CIRCULAR ON SOIL AND ROCK PROPERTIES

1.1 INTRODUCTION

The purpose of this document is to provide the practicing highway design professional with specific recommendations regarding the appropriate methods to obtain engineering properties of soil and rock materials that may be encountered during construction of a wide range of transportation facilities. The target audience for Geotechnical Engineering Circular (GEC) No. 5 includes primarily geotechnical engineers and civil engineers who are responsible for establishing subsurface exploration programs and directing/overseeing the field and/or laboratory testing programs. The document is equally intended for structural engineers, engineering geologists, or geologists who may be responsible for these programs. The document is written to provide both general and specific information regarding the assessment of soil and rock properties to a potentially diverse audience.

GEC No. 5 was developed in a very specific manner due in large part to the diverse background of potential readers. It is recognized that every civil engineer, and many geologists, have had classes related to this subject and there are several excellent textbooks and Federal Highway Administration (FHWA)-sponsored courses, demonstration projects, and guidance manuals dealing with the subject matter. Additionally, because site investigations and laboratory testing are critical steps in virtually all highway projects, every state Department of Transportation (DOT) has had to deal with the subject and resolve issues related to soil and rock properties on a day-to-day basis. Therefore, it is anticipated that almost every reader has an opinion, or at least an experience, regarding the subject of soil and rock properties. The purpose of this document is to provide each reader, regardless of their level of experience, with guidance related to appropriate techniques for evaluating soil and rock properties.

1.2 BACKGROUND

Textbooks and FHWA courses and documents are invaluable in terms of providing general recommendations concerning site investigation and laboratory testing. Basic information regarding how many holes to advance, how many samples to obtain, and how to conduct specific laboratory tests can be found in these sources. The one element missing from most of these documents/courses is a rationale for the "judgment" that must be applied to decide which specific tests are going to provide the specific information needed for a specific project and how to appropriately interpret these test results. Without judgment, the site exploration and field/laboratory testing phases can become prescriptive (e.g., advance ten boreholes to refusal, spaced at 60-m centers obtaining Standard Penetration Test (SPT) samples at 1.5-m vertical intervals). This approach may miss the fact that previous explorations in the area identified a weak 0.6-m thick clay layer at a depth of 5 m below ground surface that will control the stability of the proposed embankment constructed over the deposit. Therefore, there is a need to assist the design professional in making rationale decisions

when encountering real (as opposed to textbook) soil deposits. The designer must make decisions regarding: (1) the layout and organization of the subsurface exploration program; (2) the type of in situ or laboratory test to run on the encountered material; and (3) the proper techniques to employ in interpreting multiple test results and developing design parameters.

In reviewing the text and course materials that are currently available, it is recognized that two important areas are not addressed. First, over the past 15 to 20 years, several in situ testing techniques have moved from the arena of university research to routine engineering practice. Today, in situ testing plays a critical role in assessing soil properties and, to a lesser extent, rock properties, particularly by complementing laboratory-derived data. The designer needs to understand what in situ tests are applicable for specific soil deposits and specific soil properties. The second area that is not addressed in current literature is that the data resulting from the range of laboratory and in situ tests are often not completely consistent with other data obtained for the project and/or soil deposit. The designer needs to develop a rationale for accepting or rejecting data and for resolving potential inconsistencies between data provided by different laboratory and field tests.

This document was prepared to provide the design professional with tools to assist in the rational development of subsurface investigation as well as in the execution and interpretation of laboratory and field testing programs. This document attempts to provide this rationale for the entire range of materials potentially encountered by a state DOT. This includes soft clay to intact rock and all variations of material between these extremes.

1.3 DOCUMENT ORGANIZATION

To assist the reader, the rationale for evaluating soil and rock properties has been organized into eight specific chapters. After this initial Chapter 1 that provides a general introduction to the entire document, the remainder of the GEC No. 5 is organized as follows:

- Chapter 2 provides an overview of the remainder of the document by describing an FHWA-recommended "process" for obtaining soil and rock properties.
- Chapter 3 describes the rationale and procedures for developing a subsurface investigation program in soil and rock deposits.
- Chapter 4 provides a general introduction and description of field and laboratory tests, focusing on specific tests, the resulting data from the tests, and the limitations of the tests.
- Chapter 5 describes the procedures for selecting specific tests for soil and for interpreting the resulting data from these tests.
- Chapter 6 describes rock mass classification and the procedures for selecting specific tests for rock and rock masses and for interpreting the resulting data from these tests.
- Chapter 7 provides a discussion on special materials (e.g., expansive soils, loess, organic materials, colluvium, talus, and degradable materials) that could be encountered by a design professional.

- Chapter 8 provides a brief summary of techniques available to the engineer to resolve inconsistencies in test results from different tests and to appropriately select design values.

The final portion of the document presents three Property Selection Examples in which the concepts identified in Chapters 2 through 8 are put into practice. For each of the examples, a "real" soil profile is used and the example provides a step-by-step approach in conducting the subsurface investigation program, performing laboratory and field tests, and interpreting the test results to obtain recommended soil and rock properties that may be required for typical highway related designs.

A few final notes are warranted with regards to the document. It is expressly noted that the document presents a summary of the state of-the-practice as of the document date for a wide range of subsurface conditions. As such, many of the relatively "new" investigation and testing techniques that are currently available to DOTs, particularly in situ testing methods, have been included in the document. The document provides specific recommendations regarding the best tests to run for a given soil and the proper method to interpret these tests. By providing a rationale for obtaining realistic and appropriate soil and rock properties, it is anticipated that an "improved" or a "better" understanding and estimation of these properties will result relative to historical practices. The designer must assess how these properties affect the selected design, as many of the current design methods are semi-empirical and based largely on the historical (i.e., not the improved) techniques for evaluating soil and rock properties. Finally, it is intended that this document be read cover-to-cover, more as a "novel" than as a "cookbook." In the latter case, the reader may desire specific information regarding a specific test and therefore can read a few pages from the text to secure an answer. With this document, recommendations are made as explicit paragraphs and sometimes the rationale is explained as part of the overall philosophy. Therefore, it is intended that the reader initially read the document cover-to-cover. Later, reference to specific sections and to recommendations can be made, but this later reference is provided once the spirit of the entire document has been understood. Although the authors have attempted to address the widest range of potential conditions encountered by the designer, there will certainly be cases that are not addressed in this document. By applying the philosophy and extrapolating the recommendations to these new and potentially more complex scenarios, the authors believe the reader will be able to use this document for even the most complex highway design applications.

CHAPTER 2

THE PROCESS FOR SOIL AND ROCK PROPERTY SELECTION

2.1 INTRODUCTION

Most geotechnical engineering textbooks provide information related to the mechanics of conducting field and laboratory tests to obtain soil and rock properties. In addition, the American Society for Testing and Materials (ASTM) and American Association of State Highway and Transportation Officials (AASHTO) standards provide excellent guidance related to the specific procedures for performing the actual field and laboratory tests. There are, however, few resources that provide guidance to the design professional related to a rational process for selecting appropriate critical locations in the geologic deposit and then developing a specific laboratory and field testing program to obtain soil and rock properties appropriate for design. The goal of this chapter is to describe a "process" that has been used on a variety of large and small projects to integrate the various decision steps necessary to arrive at the final design parameters. In addition to describing this step-by-step formal process, guidance is provided on the: (1) appropriate use of correlations to aid in engineering property selection; and (2) use of the Observational Method to refine and improve selected soil and rock properties used in design.

2.2 PROCESS OF SOIL AND ROCK PROPERTY SELECTION

A rational approach for selecting soil and rock properties for engineering design can be summarized as a logical twelve-step procedure that encompasses the general activities of site investigation and field testing, laboratory testing and interpretation, and engineering design. This step-by-step process is presented on the flow chart in figure 1. A brief description of each step of this process is presented below. More extensive discussion and the methods used to implement these steps are provided throughout the remainder of this document.

Site Investigation and Field Testing

- *Review Available Information*: The best place to start the process of material property selection is to review any and all information that may be available. There are several sources for this information, many of the sources being in the public domain and readily available at modest expense.

- *Identify Required Material Properties*: No investigation should be initiated without specific goals being established that are related to design and construction issues that must be considered (i.e., performance requirements), engineering properties that are needed, and the type of structure that is to be constructed.

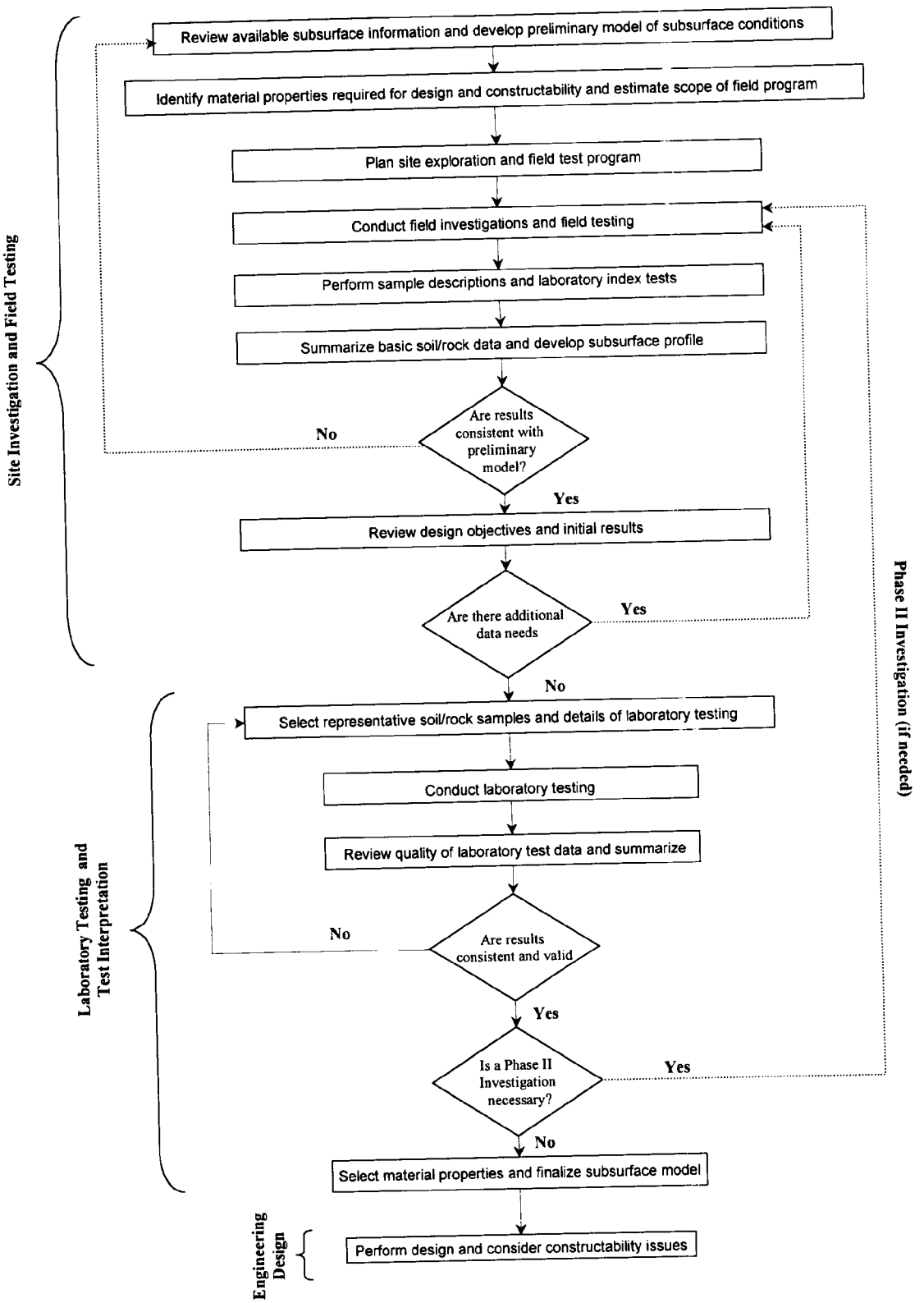

Figure 1. Soil and rock property selection flowchart.

- *Plan Site Investigation:* Historical information, which will provide anticipated subsurface conditions, coupled with knowledge of the specific design will allow an efficient site-specific investigation strategy to be developed. Contingency plans should be considered based on anticipated variabilities in subsurface conditions. Sampling intervals should be identified and an in situ testing program should be developed.

- *Conduct Site Investigation and Field Testing*: Once the investigation strategy is developed, it is ready to implement. Findings should be communicated to the geotechnical design engineer during the field work and modifications to the number and types of samples and testing should be determined, as required.

- *Describe Samples*: Results from the field investigation program and subsequent laboratory identification of samples should be compared to the anticipated conditions based on historical information. Selected laboratory samples can be reviewed by the design engineer to obtain first-hand observations. These samples should be used for performing simple laboratory index tests.

- *Develop Subsurface Profile*: Using results from the field investigation and the laboratory index tests, a detailed subsurface profile should be developed by the geotechnical design engineer. It is helpful at this step to review the initial site investigation objectives and expectations to be assured that the materials are consistent with expectations.

- *Review Design Objectives*: An on-going evaluation of field and available laboratory data relative to the design objectives should be performed during the implementation of the site investigation. If adjustments are needed or if additional data needs are identified, procedures should be initiated to obtain the necessary information.

Laboratory Testing and Test Interpretation

- *Select Samples for Performance Testing*: Prior to initiating the project-specific laboratory-testing program, the design engineer should review the recovered samples and confirm the testing that needs to be conducted (i.e., type, number, and required test parameters). If possible, selected samples should be extruded in the laboratory and reviewed by the design engineer.

- *Conduct Laboratory Testing*: Once the samples have been reviewed and the testing program is confirmed, it is time to continue the index tests and initiate the performance-testing program (with index test correlation for quality assurance). Preliminary results should be provided to the design engineer for review.

- *Review Quality of Laboratory Data*: If the data and interpreted laboratory test results are not consistent with expectations or if results indicate that the sample was disturbed, it is necessary to review progress and make adjustments. On some projects, results at this stage can be used to plan and initiate a more detailed and focused phase of investigation. A phased investigation approach is particularly helpful on large projects and in cases where there are many unknowns regarding the subsurface conditions or specific project requirements prior to conducting the proposed site investigation program.

- *Select Material Properties*: The laboratory and field test results should be interpreted and compared to project expectations and requirements. The role of the design engineer at this stage is critical as the full integration of field and laboratory test results must be coupled with the site-specific design. If test results are not completely consistent, the reason(s) should be evaluated, poor data should be eliminated, and similarities and trends in data should be identified. It may be necessary to return to the laboratory and conduct an additional review of sample extrusion, selection, and testing.

Engineering Design

- *Perform Design*: At this final stage, the design engineer has the necessary information related to the soil and rock properties to complete the design. Additionally, the design engineer also has first-hand knowledge related to the variability of the deposit and of the material properties. Design activities can proceed with knowledge of these properties and variabilities.

As referenced in chapter 1, this process is logical and is generally followed on many projects. In many cases, however, old "rules-of-thumb" and "status quo" approaches can result in an unconscious "by-passing" of critical steps. In particular, selection of the correct engineering property tests, their interpretation, and summarization are often poorly performed. Rigorous attention to this twelve-step procedure is required to assure efficient and thorough investigation and testing programs, especially since many projects are fragmented in which drilling, testing, and design are performed by different parties.

2.3 USE OF CORRELATIONS TO ASSIST PROPERTY SELECTION

If time and budget were not an issue, the design engineer could obtain as many samples as necessary and conduct as many laboratory or in situ tests as desired to obtain a complete assessment of subsurface soil and rock conditions. Engineering properties could be quantified and any inconsistent data could be set aside; additional testing could then be initiated. Unfortunately, time and budgets are major issues and the design engineer must make critical decisions at several steps throughout the design to obtain the most reliable and realistic soil and rock property information. As described previously, a critical step in obtaining these properties lies in the selection of a specific test and the interpretation of the test results. For any number of reasons (e.g., cost, sampling difficulties, etc.), it may be difficult to obtain the specific parameter(s) of interest. Fortunately, the design engineer can often use well-developed and/or site-specific correlations to obtain the desired parameter. Also, correlations serve as a quality assurance check on determined test results.

Correlations to engineering properties come in many forms, but all have a common theme; specifically, the desired correlation utilizes a large database of results based on past experience. In the best case, the correlation and experience have been developed or "calibrated" using the specific local soil; in other cases the correlation may be based on reportedly similar soils. The reliance or use of correlations to obtain soil and rock properties is justified and recommended in the following cases: (1) specific data are simply not available and are only possible by indirectly comparing to other properties; (2) a limited amount of data for the specific property of interest are available and the correlation can provide a complement to these limited data; or (3) the validity of certain data is in question and a comparison to previous test results allows the accuracy of the selected test to be

assessed. **Correlations in general should never be used as a substitute for an adequate subsurface investigation program, but rather to complement and verify specific project-related information.** Examples of each of the three cases follows:

- *Specific Data are Unavailable*: Several examples of this type exist. Most notable is the strength of uncemented clean sands. Undisturbed sampling is prohibitively expensive and correlations to Standard Penetration Testing (SPT), Cone Penetration Testing (CPT), and other in situ tests results have been shown to be quite reliable. As another example, suppose that the strength of a soil in triaxial extension is desired and only triaxial compression data are available. By reviewing previous published comparisons of compression and extension test results for similar soils, it is possible to approximate the triaxial test extension test results.

- *Limited Data are Available*: For a given application, suppose that only a few, high-quality consolidation tests were performed. Compression properties were found to correlate well with Atterberg limits testing results. It is therefore concluded that additional consolidation test results are not required and that numerous Atterberg limits tests can be used to confidently assess compression properties.

- *Assessing Data Validity*: Consider that results from tests on two similar soils are inconsistent. By comparing the results to those for similar soils it may be possible to identify whether the data are simply inconsistent of if some of the data are incorrect.

There are several sources of correlation data for a range of geotechnical materials and properties. Many geotechnical textbooks and reference manuals include correlations as part of the text (e.g. Holtz and Kovacs, 1981; NAVFAC, 1982). The Electric Power Research Institute (EPRI) (Kulhawy and Mayne, 1990) commissioned the preparation of a very useful document that includes several correlations for laboratory and in situ tests.

Regardless of the specific correlation, the following critical components need to be explicitly recognized:

- The selected correlation is only as good as the data used to develop the correlation. Many correlations for sands were developed for clean, uncemented, uniform sands primarily for assessing liquefaction potential. Be careful in using this correlation to assess properties in a well-graded silty sand deposit. Select the appropriate correlation carefully.

- A correlation provides an "approximate" answer and will undoubtedly exhibit scatter among the data points. Assess the data and the scatter by using upper and lower bound (i.e., best case/worst case) scenarios in the design calculations.

- The selected correlation will be most accurate if "calibrated" to local soil conditions. Many state DOTs have developed useful correlations based on specific project experience in their state.

2.4 USE OF OBSERVATIONAL METHOD

Once an appropriate value for the design has been selected, it is possible to complete the design and proceed to construction. There is one final step that can be performed to validate the data and possibly improve the accuracy of the selected value. This three step process involves: (1) using the design value and the actual estimated loading to predict a field response; (2) systematically monitor the field performance; and (3) "back calculate" the actual property of interest. This process of prediction, monitoring, and reassessment is known as the Observational Method (Terzaghi and Peck, 1967). Two examples of this technique follow:

- In soil, the use of piezometers to monitor the rate of pore pressure dissipation and measured settlements of a large area fill can result in a more accurate estimate of the compressibility and time rate of consolidation characteristics of soft soils as well as provide information to maximize the rate of fill placement.

- In rock, the use of instrumented rock bolts and displacement monitoring instrumentation can provide valuable information regarding the kinematics of block stability and the strength of the jointed rock mass.

The Observational Method is an invaluable aid and ideally should be a part of every geotechnical project. Sadly, this approach is often overlooked due to budget concerns, and in many cases is not even considered by the design engineer. Where appropriately used, the Observational Method can have significant benefits not only to the project at hand, but also for other projects in the area because a full-scale assessment of the engineering properties can be made. It is strongly recommended that the Observational Method be included as a basic tenet of all projects.

CHAPTER 3

PLANNING A SUBSURFACE INVESTIGATION AND LABORATORY TESTING PROGRAM

3.1 INTRODUCTION

To evaluate soil and rock properties required for geotechnical design related to transportation projects, subsurface investigation and laboratory testing programs are developed and executed. The data collection efforts associated with these activities should occur early in the project; failure to conduct an appropriately scoped investigation and laboratory-testing program will result in potential data gaps and/or the need to re-mobilize to the site for supplementary testing. Data gaps can cause significant delays in the project and can potentially lead to either an overconservative and costly design or an unconservative and unsafe design. It is, therefore, imperative that the subsurface and laboratory testing programs be carefully planned to ensure that the information collected in the field and the laboratory will be sufficient to develop soil and rock properties for design and construction.

This chapter will present general guidelines related to the development of subsurface investigation and laboratory testing programs for the evaluation of soil and rock properties. Since the selection of sampling and testing methods will be driven by the scope of the project and geologic conditions, critical project related issues must be understood prior to field and laboratory planning activities. For heterogeneous deposits and special materials (i.e., colluvium, organic soils, etc.) greater effort will be required during the planning stage of the investigation to assess the applicability of specific tools and sampling devices.

3.2 PLANNING THE SUBSURFACE INVESTIGATION AND LABORATORY TESTING PROGRAM

3.2.1 General

Planning subsurface investigation and laboratory testing programs requires the engineer to be aware of parameters and properties needed for design and construction, as well as to understand the geologic conditions and site access restrictions. Specific steps include: (1) identify data needs; (2) gather and analyze existing information; (3) develop a preliminary site model; (4) develop and conduct a site investigation; and (5) develop and conduct a laboratory-testing program. Specific planning steps are addressed in the following sections.

3.2.2 Identify Data Needs

The first step of an investigation and testing program requires that the engineer understand the project requirements and the site conditions and/or restrictions. The ultimate goal of this phase is to

identify geotechnical data needs for the project and potential methods available to assess these needs. During this phase it is necessary to:

- identify design and constructability requirements (e.g., provide a grade separation, transfer loads from bridge superstructure, provide for a dry excavation);
- identify performance criteria (e.g., limiting settlements, right of way restrictions, proximity of adjacent structures) and schedule constraints;
- identify areas of concern on site and potential variability of local geology;
- develop likely sequence and phases of construction;
- identify engineering analyses to be performed (e.g., bearing capacity, settlement);
- identify engineering properties and parameters required for these analyses;
- evaluate methods to obtain parameters and assess the validity of such methods for the material type and construction methods; and
- evaluate number of tests/samples needed and appropriate locations for them.

As an aid to assist in the planning of site investigation and laboratory testing, table 1 provides a summary of the information needs and testing considerations for various geotechnical applications. A discussion of specific field and laboratory test methods is provided in chapter 4.

3.2.3 Gather and Analyze Existing Information

Before any equipment is mobilized to the site, existing data for the site, both regionally and locally, should be evaluated as a logical first step in the investigation. This is an important and inexpensive step that is often overlooked. There are many readily available data sources that can be used to identify major geologic processes that have affected the site, site history. geologic constraints, man-made features, and access issues. The planning step can be extremely cost effective and productive. Existing data will provide information which can reduce the scope of the subsurface investigation, help guide the location of testing and sampling points, and reduce the amount of time in the field due to unexpected problems. For example, historical aerial photographs can be used to identify an area where fill had been placed, where a landslide scarp exists, or major geologic structures such as faults, bedding planes, and continuous joint sets. A list of potential information sources along with the type of information available is presented in table 2.

Table 1. Summary of information needs and testing considerations for a range of highway applications.

Geotechnical Issues	Engineering Evaluations	Required Information for Analyses	Field Testing[1]	Laboratory Testing[1]
Shallow Foundations	• bearing capacity • settlement (magnitude & rate) • shrink/swell of foundation soils (natural soils or embankment fill) • chemical compatibility of soil and concrete • frost heave • scour (for water crossings) • extreme loading	• subsurface profile (soil, groundwater, rock) • shear strength parameters • compressibility parameters (including consolidation, shrink/swell potential, and elastic modulus) • frost depth • stress history (present and past vertical effective stresses) • chemical composition of soil • depth of seasonal moisture change • unit weights • geologic mapping including orientation and characteristics of rock discontinuities	• vane shear test • SPT (granular soils) • CPT • dilatometer • rock coring (RQD) • nuclear density • plate load testing • geophysical testing	• 1-D Oedometer tests • direct shear tests • triaxial tests • grain size distribution • Atterberg Limits • pH, resistivity tests • moisture content • unit weight • organic content • collapse/swell potential tests • rock uniaxial compression test and intact rock modulus • point load strength test
Driven Pile Foundations	• pile end-bearing • pile skin friction • settlement • down-drag on pile • lateral earth pressures • chemical compatibility of soil and pile • driveability • presence of boulders/ very hard layers • scour (for water crossings) • vibration/heave damage to nearby structures • extreme loading	• subsurface profile (soil, ground water, rock) • shear strength parameters • horizontal earth pressure coefficients • interface friction parameters (soil and pile) • compressibility parameters • chemical composition of soil/rock • unit weights • presence of shrink/swell soils (limits skin friction) • geologic mapping including orientation and characteristics of rock discontinuities	• SPT (granular soils) • pile load test • CPT • vane shear test • dilatometer • piezometers • rock coring (RQD) • geophysical testing	• triaxial tests • interface friction tests • grain size distribution • 1-D Oedometer tests • pH, resistivity tests • Atterberg Limits • organic content • moisture content • unit weight • collapse/swell potential tests • slake durability • rock uniaxial compression test and intact rock modulus • point load strength test

[1] Corresponding AASHTO and ASTM Standard references are provided in chapter 4 for field and laboratory tests.

Table 1. Summary of information needs and testing considerations for a range of highway applications (continued).

Geotechnical Issues	Engineering Evaluations	Required Information for Analyses	Field Testing[1]	Laboratory Testing[1]
Drilled Shaft Foundations	• shaft end bearing • shaft skin friction • constructability • down-drag on shaft • quality of rock socket • lateral earth pressures • settlement (magnitude & rate) • groundwater seepage/ dewatering • presence of boulders/ very hard layers • scour (for water crossings) • extreme loading	• subsurface profile (soil, ground water, rock) • shear strength parameters • interface shear strength friction parameters (soil and shaft) • compressibility parameters • horizontal earth pressure coefficients • chemical composition of soil/rock • unit weights • permeability of water-bearing soils • presence of artesian conditions • presence of shrink/swell soils (limits skin friction) • geologic mapping including orientation and characteristics of rock discontinuities • degradation of soft rock in presence of water and/or air (e.g., rock sockets in shales)	• technique shaft • shaft load test • vane shear test • CPT • SPT (granular soils) • dilatometer • piezometers • rock coring (RQD) • geophysical testing	• 1-D Oedometer • triaxial tests • grain size distribution • interface friction tests • pH, resistivity tests • permeability tests • Atterberg Limits • moisture content • unit weight • organic content • collapse/swell potential tests • rock uniaxial compression test and intact rock modulus • point load strength test • slake durability
Embankments and Embankment Foundations	• settlement (magnitude & rate) • bearing capacity • slope stability • lateral pressure • internal stability • borrow source evaluation (available quantity and quality of borrow soil) • required reinforcement	• subsurface profile (soil, ground water, rock) • compressibility parameters • shear strength parameters • unit weights • time-rate consolidation parameters • horizontal earth pressure coefficients • interface friction parameters • pullout resistance • geologic mapping including orientation and characteristics of rock discontinuities • shrink/swell/degradation of soil and rock fill	• nuclear density • plate load test • test fill • CPT • SPT (granular soils) • dilatometer • vane shear • rock coring (RQD) • geophysical testing	• 1-D Oedometer • triaxial tests • direct shear tests • grain size distribution • Atterberg Limits • organic content • moisture-density relationship • hydraulic conductivity • geosynthetic/soil testing • shrink/swell • slake durability • unit weight
Excavations and Cut Slopes	• slope stability • bottom heave • liquefaction • dewatering • lateral pressure • soil softening/progressive failure • pore pressures	• subsurface profile (soil, ground water, rock) • shrink/swell properties • unit weights • hydraulic conductivity • time-rate consolidation parameters • shear strength of soil and rock (including discontinuities) • geologic mapping including orientation and characteristics of rock discontinuities	• test cut to evaluate stand-up time • piezometers • CPT • SPT (granular soils) • vane shear • dilatometer • rock coring (RQD) • in situ rock direct shear test • geophysical testing	• hydraulic conductivity • grain size distribution • Atterberg Limits • triaxial tests • direct shear tests • moisture content • slake durability • rock uniaxial compression test and intact rock modulus • point load strength test

[1] Corresponding AASHTO and ASTM Standard references are provided in chapter 4 for field and laboratory tests.

Table 1. Summary of information needs and testing considerations for a range of highway applications (continued).

Geotechnical Issues	Engineering Evaluations	Required Information for Analyses	Field Testing[1]	Laboratory Testing[1]
Fill Walls/ Reinforced Soil Slopes	• internal stability • external stability • settlement • horizontal deformation • lateral earth pressures • bearing capacity • chemical compatibility with soil and wall materials • pore pressures behind wall • borrow source evaluation (available quantity and quality of borrow soil)	• subsurface profile (soil, ground water, rock) • horizontal earth pressure coefficients • interface shear strengths • foundation soil/wall fill shear strengths • compressibility parameters (including consolidation, shrink/swell potential, and elastic modulus) • chemical composition of fill/ foundation soils • hydraulic conductivity of soils directly behind wall • time-rate consolidation parameters • geologic mapping including orientation and characteristics of rock discontinuities	• SPT (granular soils) • CPT • dilatometer • vane shear • piezometers • test fill • nuclear density • pullout test (MSEW/RSS) • rock coring (RQD) • geophysical testing	• 1-D Oedometer • triaxial tests • direct shear tests • grain size distribution • Atterberg Limits • pH, resistivity tests • moisture content • organic content • moisture-density relationships • hydraulic conductivity
Cut Walls	• internal stability • external stability • excavation stability • dewatering • chemical compatibility of wall/soil • lateral earth pressure • down-drag on wall • pore pressures behind wall • obstructions in retained soil	• subsurface profile (soil, ground water, rock) • shear strength of soil • horizontal earth pressure coefficients • interface shear strength (soil and reinforcement) • hydraulic conductivity of soil • geologic mapping including orientation and characteristics of rock discontinuities	• test cut to evaluate stand-up time • well pumping tests • piezometers • SPT (granular soils) • CPT • vane shear • dilatometer • pullout tests (anchors, nails) • geophysical testing	• triaxial tests • direct shear • grain size distribution • Atterberg Limits • pH, resistivity tests • organic content • hydraulic conductivity • moisture content • unit weight

(1) Corresponding AASHTO and ASTM Standard references are provided in chapter 4 for field and laboratory tests.

Table 2. Sources of historical site data.

Source	Functional Use	Location	Examples
Utility Maps	• Identifies buried utility locations • Identifies access restrictions • Prevents damage to utilities	Local agencies/utility companies	Power line identification prior to an intrusive investigation prevents extensive power outage, expensive repairs, and bodily harm
Aerial Photographs	• Identifies manmade structures • Identifies potential borrow source areas • Provides geologic and hydrological information which can be used as a basis for site reconnaissance • Track site changes over time	Local Soil Conservation Office, United States Geological Survey (USGS), Local Library, Local & National aerial survey companies	Evaluating a series of aerial photographs may show an area on site which was filled during the time period reviewed
Topographic Maps	• Provides good index map of site area • Allows for estimation of site topography • Identifies physical features in the site area • Can be used to assess access restrictions	USGS, State Geological Survey	Engineer identifies access areas/restrictions, identifies areas of potential slope instability; and can estimate cut/fill capacity before visiting the site
Existing Subsurface Investigation Report	• May provide information on nearby soil/rock type; strength parameters; hydrogeological issues; foundation types previously used; environmental concerns	USGS, United States Environmental Protection Agency (USEPA), State DOTs	A five year old report for a nearby roadway widening project provides geologic, hydrogeologic, and geotechnical information for the area, reducing the scope of the investigation
Geologic Reports and Maps	• Provides information on nearby soil/rock type and characteristics; hydrogeological issues, environmental concerns	USGS and State Geological Survey	A twenty year old report on regional geology identifies rock types, fracture and orientation and groundwater flow patterns

Table 2. Sources of historical site data (continued).

Source	Functional Use	Location	Examples
Water/Brine Well Logs	• Provide stratigraphy of the site and/or regional area • Varied quality from state to state • Groundwater levels	State Geological Survey/Natural Resources	A boring log of a water supply well two miles from the site area shows site stratigraphy facilitating evaluations of required depth of exploration
Flood Insurance Maps	• Identifies 100 and 500 yr. floodplains near water bodies • May prevent construction in a floodplain • Provide information for evaluation of scour potential	Federal Emergency Management Agency (FEMA), USGS, State/Local Agencies	Prior to investigation, the flood map shows that the site is in a 100 yr floodplain and the proposed structure is moved to a new location
Soil Survey	• Identifies site soil types • Permeability of site soils • Climatic and geologic information	Local Soil Conservation Service	The local soil survey provides information on near-surface soils to facilitate preliminary borrow source evaluation
Sanborn Fire Insurance Maps	• Useful in urban areas • Maps for many cities are continuous for over 100 yrs. • Identifies building locations and type • Identifies business type at a location (e.g., chemical plant) • May highlight potential environmental problems at an urban site	State Library/Sanborn Company (www.sanborncompany.com)	A 1929 Sanborn map of St. Louis shows that a lead smelter was on site for 10 years. This information prevents an investigation in a contaminated area.

Of the information sources listed in table 2, utility maps, existing subsurface investigation reports in the area, geologic reports/maps, and soil surveys often provide extremely valuable information. Although historic reports may provide useful data, the information they contain should be used with caution. The data should be scrutinized as to its reliability by evaluating the consistency of the information and the overall quality of the report. Review of construction or performance monitoring records will provide helpful information regarding subsurface conditions and variability. On some projects, it may be worthwhile to develop a geologic summary report that provides information on regional and local geology, hydrogeology, and unstable areas (e.g., karstic areas, fault zones, etc.).

3.2.4 Conduct Site Visit

After review of the available data and prior to mobilizing investigation equipment to the project site, a site visit should be performed. During the site visit, the engineer should carefully observe all relevant physical features of the area and record detailed notes. These observations should include:

- utility locations (overhead and underground);
- access issues (e.g., location, width, and condition of all potential access roads; trees; power lines; buildings; right-of-way);
- conditions of nearby structures (record location, type, and depth of existing structures and foundations);
- geologic constraints (e.g., rivers, streams, bluffs, outcrops);
- topographic conditions (e.g., ditches, hills, valleys);
- soil/rock type (e.g., clay, sand, rock outcrops, conditions when wet);
- surface conditions (e.g., desiccated surface, lack of vegetation, debris, ponded water, deposits of colluvium or talus, evidence of rock/soil slope failures);
- geomorphic controls (e.g., landslides, floodplains, karst, erosional/depositional conditions);
- flood levels/drainage issues;
- zonation of rock mass with information on location, orientation, and type of boundary between zones of relatively uniform geology;
- adjacent property use; and
- potential borrow source areas (if applicable).

If possible, the engineer should meet with local landowners to obtain information on springs, historic landslides, old mine workings, etc. and to obtain permission for gaining access to private property.

Potential drilling locations should be noted for subsequent subsurface investigation. A topographic map of the project site should be prepared prior to the site visit and the map should be used by the engineer during the site visit. The previously referenced observations should be noted on the topographic map and a preliminary layout of the subsurface investigations borings/soundings should be marked. Temporary field stakes can often be established for these locations during the site visit. Additional information can be gained by driving along roads in the general site area and observing roadcuts and rock outcrops. In hilly areas, roadcuts provide some of the most accessible and useful means of obtaining subsurface information prior to the use of intrusive investigation methods. Seeps along the face of a roadcut may provide an idea of the relative proximity of the water table to the ground surface and the structure of the subsurface geologic units.

Information gathered during a site reconnaissance visit will aid in the selection of a drill rig, sampler type, boring/sampling locations, personnel safety needs, and potential problems which may preclude construction of certain geotechnical design elements. The site visit also allows the engineer to make an initial estimate of subsurface conditions, as well as an estimation of the time needed to complete the field investigation and testing program. Conducting the site visit after collecting and interpreting existing data allows for an efficient data collection effort. Figure 2 provides a checklist of information items that should be collected during the site reconnaissance stage of a project. Checklists and/or field reconnaissance forms are useful while conducting site visits to ensure that pertinent data are not forgotten or overlooked. A copy of the field reconnaissance report should be provided to the drill crew prior to drilling.

3.2.5 Develop Preliminary Site Model

A preliminary site model should be developed using the information obtained from existing data and the site visit. The preliminary model should consist of the soil and rock stratigraphy, potential site restrictions, and anticipated groundwater levels. The model should be divided into zones of interest (i.e., geotechnical units) based on the necessary design parameters and objectives. This model will obviously change as results of the detailed investigation are collected.

While developing the preliminary site model, particular attention should be given to the possibility of encountering heterogeneities. In many geologic settings, these include boulders and significant variations in bedrock surface elevation, which may affect the design and investigation. If boulders are suspected at a site, unexpected "top of rock" elevations should be questioned and it may be necessary to drill several feet into "rock" in order to resolve this issue. In addition, soils containing large amounts of gravel or boulders may cause damage to intrusive in situ testing equipment or limit the feasibility of these test methods.

Based on the information gathered thus far in the planning phase, it may be possible to eliminate or favor specific designs. For example, the preliminary site model may indicate that extensive boulder and gravel deposits are present at the site, which could eliminate the possibility of a driven pile design. Alternatively, the preliminary site model might show subsurface conditions to be particularly favorable to a proposed design.

- ☐ Date_____
- ☐ Prepared by: _____
- ☐ Organization_____

☐ **ACCESSIBILITY**
- ☐ Easy
- ☐ By Vehicle only
- ☐ Difficult by car - Walk only
- ☐ Requires 4-wheeled drive
- ☐ Dozer and Grading Required
- ☐ Inaccessible
- ☐ Details _____

☐ **VISIT TO SITE**
- ☐ Date/Time of Day
- ☐ Visitors
- ☐ Weather Conditions
  - ☐ Sunny
  - ☐ Cloudy
  - ☐ Rain
  - ☐ Snow
  - ☐ Icy
  - ☐ Freezing

☐ **GROUND COVER**
- ☐ Asphalt
- ☐ Grass
- ☐ Flowers
- ☐ Bushes
- ☐ Trees
- ☐ Forest
- ☐ Soil
- ☐ Gravel
- ☐ Concrete
- ☐ Rock Outcroppings
- ☐ Evidence of fill/debris
- ☐ Prior Construction
- ☐ Existing Buildings
- ☐ Roadways
- ☐ Other

☐ **EXISTING TERRAIN**
- ☐ Level Ground
- ☐ Sloping Conditions
- ☐ Gentle Dip
- ☐ Steep
- ☐ Hummocky
- ☐ Rolling Hills
- ☐ Mountainous

☐ Other remarks_____

☐ **SITE HYDROLOGY**
- ☐ Dry - Barren
- ☐ Desert
- ☐ Surface Water Conditions
  - ☐ None
  - ☐ Swampy
  - ☐ Pond
  - ☐ Lake
  - ☐ Ocean
  - ☐ Stream
  - ☐ River
- ☐ Subsurface Water
  - ☐ None
  - ☐ Not Obvious
  - ☐ Major Aquifer
  - ☐ Water Wells
  - ☐ Pumping from deep wells
  - ☐ Other Details_____

☐ **SITE DRAINAGE**
- ☐ Runoff Features
  - ☐ Erosion
  - ☐ Ponding
  - ☐ Waterfalls
  - ☐ Piping
  - ☐ Swale
  - ☐ Other
- ☐ Natural
  - ☐ Excellent
  - ☐ Good
  - ☐ Fair
  - ☐ Poor
- ☐ Artificial Drains
  - ☐ Stormwater System
  - ☐ Retention Pond
  - ☐ Vertical wick drains
  - ☐ Pumping Stations
  - ☐ Other

☐ **SOIL AND ROCK CONDITIONS**
- ☐ Surface Soils
  - ☐ Topsoil
  - ☐ Presence of Fills
  - ☐ Evidence of Debris
  - ☐ Pollutants/Contaminants
  - ☐ Agrarian types/farming
  - ☐ Evidence of slope instability
    - ☐ Landslides/slips
  - ☐ Creep
  - ☐ Cracking
  - ☐ Scour
  - ☐ Heave
  - ☐ Subsidence
- ☐ Cut/Quarry Operations
- ☐ Fill/Borrow
- ☐ Other_____

☐ Subsurface Soils
- ☐ USCS soil types:
  - ☐ GM, GC, GP, GW
  - ☐ SM, SC, SP, SW
  - ☐ CL, CH, ML, MH
  - ☐ Pt, OL, OH
  - ☐ Other_____

☐ Surface Rocks
- ☐ Loose cobbles
- ☐ Boulders
- ☐ Rock outcroppings

☐ Type of rocks
- ☐ Igneous
- ☐ Sedimentary
- ☐ Metamorphic
- ☐ Details

☐ Rock Features
- ☐ Jointing Patterns
- ☐ Faults
- ☐ Discontinuities
- ☐ Weathering
- ☐ Planes of weakness
- ☐ Evidence of talus
- ☐ Karst/sinkholes
- ☐ Caves
- ☐ Other

☐ **INVESTIGATIVE OPERATIONS**
- ☐ Existing test pits
- ☐ Existing boreholes
- ☐ Cased holes
- ☐ Blasting operations
  - ☐ Dynamite
  - ☐ ANFO
  - ☐ Rippers
  - ☐ Percussive Drills
- ☐ Erratics/ boulders
  - ☐ Coreholes
  - ☐ Diamond drilling
  - ☐ Wireline drilling
- ☐ Exploratory Adits
  - ☐ Vertical shafts
  - ☐ Tunnels
  - ☐ Pilot Holes

Other info:_____

☐ **PRIOR INFORMATION**
- ☐ Tax map records
  - ☐ Federal Documents
  - ☐ State records
  - ☐ County tax maps
  - ☐ City records files
  - ☐ Personal files
  - ☐ Interviews with neighbors and nearby businesses:_____

☐ **TOPOGRAPHIC DATA**
- ☐ USGS Quadrangle Maps
- ☐ State Survey
- ☐ County Surveys
- ☐ Site Survey
  - ☐ Transit/Level
  - ☐ Aerial Photos
  - ☐ GPS data
- ☐ Details_____

☐ **GEOLOGIC INFORMATION**
- ☐ USGS Geologic Maps
- ☐ State Geologic Surveys
- ☐ Field Mapping by geologists
- ☐ Specimens for lab analysis
- ☐ Details on geologic setting

☐ **UTILITIES**
- ☐ Existing overhead lines
- ☐ Marked gas lines
- ☐ Easements
- ☐ Manholes
- ☐ Sewer outfalls
- ☐ Power substations
- ☐ Electromagnetic readings
  - ☐ Ground penetrating radar, VEM surveys
  - ☐ Magnatometer
  - ☐ Resistivity measurements
- ☐ Other_____

☐ NOTES & REMARKS_____

Figure 2. Checklist items for site reconnaissance

3.2.6 Developing a Site Investigation Program

For many projects and for many site conditions, the most difficult and crucial part of the planning phase involves the decisions regarding sampling/investigation method, boring locations, number of samples, number and types of laboratory tests, and the number of confirmatory samples. At this stage, the types of potential sampling/investigation methods should have been identified and assessed. During the site visit, it is often possible to eliminate certain techniques. Specific tools for sampling and testing are discussed in chapter 4 and include:

- Undisturbed sampling: Thin walled tubes, block samples, rock core
- Disturbed sampling: SPT, augering, non-core rock drilling
- Non-intrusive: Geophysical and remote sensing methods
- In-situ soil and rock testing: CPT, flat-plate dilatometer test (DMT), vane shear test (VST), pressuremeter, borehole dilatometer, in situ direct shear test, etc.

Many engineers underestimate the importance in selecting an appropriate investigation technique(s) and sampling method(s), since in-house SPT capabilities are a presumptive "one size fits all" investigation/sampling approach (e.g., SPT sampling at 1.5-m intervals in borings on 60-m spacing). Experience has shown the short-falls of this approach and the benefit of a focused site-specific strategy. For example, in cases where extensive laboratory tests are not needed but it is necessary to gather large amounts of data concerning stratigraphy and subsurface material variability, intrusive non-sampling methods such as the CPT and DMT could be considered. The CPT method is quick and allows for stratigraphic mapping over a site area much more quickly and economically than the use of other intrusive methods. Additionally, data from the CPT can be input into stress history and strength correlations to obtain specific design parameters. When the penetrometer is fit with a pore pressure transducer (CPTu), detailed stress history and strength correlations for clays can be evaluated, estimates of groundwater elevation can be predicted, and flow characteristics can be assessed. The DMT can provide stratigraphic information similar to that from the CPT, but the DMT data are better suited for assessment of modulus values for settlement calculations.

The number of borings and their locations in a site area will depend on the proposed structure, design parameters, access issues, geologic constraints, and expected stratigraphy and heterogeneity. Some minimum guidelines for boring spacing are provided in table 3. This table was developed based on a number of FHWA documents including *Drilled Shafts: Construction Procedures and Design Methods* (FHWA-IF-99-025), *Design and Construction of Driven Pile Foundations* (FHWA-HI-97-013), and *Advanced Technologies for Soil Slope Stability* (FHWA-SA-94-005). This table should be used only as a first step in estimating the minimum number of borings for a particular design, as actual boring spacings will be dependent upon the project type and geologic environment. In areas underlain by heterogeneous soil deposits and/or rock formations, it will probably be necessary to exceed the minimum guidelines from table 3 to capture variations in soil and/or rock type and to assess consistency across the site area. For situations where large-diameter rock-

socketed shafts will be used or where drilled shafts are being installed in karstic formations, it may be necessary to advance a boring at the location of each shaft. In a laterally homogeneous area, drilling or advancing a large number of borings may be redundant, since each sample tested would exhibit similar strength and compressibility properties. In all cases, it is necessary to understand how the design and construction of the geotechnical feature will affect the soil and/or rock mass in order to optimize the investigation.

The engineer or geologist should plot the proposed boring locations on a site topographic map prior to initiation of drilling. They should review the notes taken during the site visit considering access restrictions and not arbitrarily or randomly select boring locations. Alternate boring locations should be considered and a contingency plan (e.g., move a maximum of 15 m from a boring location if unable to drill at a particular location) should be discussed in case a boring needs to be relocated due to access restrictions or unexpected geologic conditions. Field personnel unfamiliar with the objectives and rational behind the planning of the site investigation should maintain contact with the office during field activities and discuss issues such as the relocation of a boring. Arbitrary or random boring selection will increase the chances of boring relocation, confusion, and wasted time in the field. Final boring locations should be surveyed and recorded as part of the permanent project record.

The guidelines for depth interval selection should also be developed in recognition of specific site/project conditions and design property/parameter requirements. For preliminary screening, disturbed samples might be taken continuously in the upper 3 m, at 1.5 m intervals up to 30 m, and possibly every 3 m at depths greater than 30 m. For characterization and assessment of design properties in fine-grained soils, a minimum of one undisturbed sample should be taken for each stratum, with additional samples taken at 3 to 6 m intervals with depth. Undisturbed samples may not need to be taken in each boring if the deposit is relatively homogeneous with closely spaced borings. These are general minimum guidelines and intervals may need to be increased depending upon the project requirements and site geologic conditions. The sampling interval may need to be increased when soil/rock conditions change frequently with depth; however, these changes need to be considered in the context of the design. Therefore, ongoing communication with the office/design engineer is absolutely essential. Once the site stratigraphy has been established, it may not be necessary to sample every time there is a change in stratigraphy if the changes have no impact on design. For example, it may not be necessary to sample alternating layers of coarse grained deposits where settlement is of concern, and for designs concerned with bearing capacity, although samples below the anticipated extent of the area influenced by the load may be reduced, samples should be obtained in case the type of foundation changes between preliminary and final design.

The sampling interval will vary between individual projects and regional geologies. If soils are anticipated to be difficult to sample or trim in the lab due to defects, etc., the frequency of sample collection should be higher than average to offset the number of samples that may be unusable in the lab for performance property evaluation (e.g., shear strength). When borings are widely spaced, it may be appropriate to collect undisturbed samples in each boring. For closely spaced borings or in deposits of lateral uniformity, undisturbed samples may only be needed in select borings. If a thin clay seam is encountered during drilling and not sampled, the boring may need to be offset and re-drilled to obtain a sample.

It is often quite helpful to combine in situ soundings using CPT, CPTu, DMT, or pressuremeter with conventional disturbed/undisturbed sampling. For example, by performing CPT or CPTu soundings prior to conventional drilling and sampling, it may be possible to target representative and/or critical areas where samples can be later obtained. This combination may reduce some of the potential drilling redundancy in heterogeneous environments. The use of geophysical methods can be used to provide useful information on ground in-between boring locations.

For investigations for rock slopes and foundations, it is important to consider structural geology, in addition to information obtained as part of a rock-coring program. For example, the orientation and characteristics of a clay-filled discontinuity is critical information that will be used to judge whether a rock slope will be stable or unstable or whether a structural foundation will undergo minor or significant settlement. However, a detailed structural geologic assessment may provide enough information to significantly limit the scope of a rock-coring program. For example, drilling and coring may not be required where applied loads are significantly less than the bearing capacity of the rock, where there is no possibility of sliding instability in a rock slope, or where there are extensive rock outcrops from which information can be obtained to confidently establish the subsurface conditions for design and constructability assessments (Wyllie, 1999).

As the reader can see from this discussion, it is difficult and really unnecessary to establish a prescriptive drilling, sampling, and testing protocol that is applicable to all sites. The engineer is most effective when: (1) applying these conventional guidelines with site and/or project-specific requirements/constraints; and (2) recognizing the advantages and limitations of sampling equipment and in-situ testing methods.

3.2.7 Developing a Laboratory Testing Program

The final planning step includes the development of a laboratory-testing program. Prior to planning the laboratory-testing program, it is again necessary to review the design needs of the project. Specifying unnecessary laboratory tests will add time and cost to the project and consume samples. Table 1 lists laboratory tests that may be applicable to specific designs. One can see from this table that moisture content, Atterberg limits, grain size distribution, and unit weight tests are recommended for most design applications in soils. As will be discussed in chapter 5, index tests are not specifically used in the design but are invaluable in establishing general conditions and assessing inherent material variabilities. Although this table provides useful guidelines, additional tests may be required or tests may be eliminated depending on individual site conditions.

Once a list of necessary tests has been developed and the field program has been executed, the engineer should review field notes, borings, and design plans to identify "critical areas". Critical areas correspond to borings/locations where the results of the laboratory tests could result in a significant change in the proposed design. Samples from these critical areas should be identified for performance testing. As will be discussed in chapter 5, performance tests provide design-specific parameters. For example, if unexpected clay deposits were discovered in the area of a proposed footing, 1-D consolidation testing would be required to assess potential settlements. If the test results show that settlements may be excessive under the proposed design, the footing may have to be moved, redesigned, or deep foundation support considered. Similarly, if the same footing was

proposed for use on a rock slope, the presence of an unfavorably oriented clay-filled discontinuity would likely make it necessary to obtain an undisturbed rock core sample for direct shear testing of the clay-filled discontinuity. The engineer should also consider the site area in context of the required design parameters and the samples available for laboratory analysis. It is necessary to select samples for laboratory analysis that will accurately characterize the site. In heterogenous areas, many samples may be required to obtain comprehensive parameters; in homogeneous areas, few samples may be required.

A laboratory-testing program should be performed on representative and critical specimens from geologic layers across the site. To assess the locations where tests should be performed, it is useful to evaluate sample location maps and geologic cross sections. By evaluating a sample location map, it will be easy to quickly identify the locations of disturbed and undisturbed samples that may be used in the laboratory testing program. The generation of detailed subsurface cross sections (see section 5.2), including stratigraphy, in-situ testing results, and laboratory index test results, if available, will be useful when identifying representative samples for laboratory performance testing.

Table 3. Guidelines for minimum number of investigation points and depth of investigation.

Application	Minimum Number of Investigation Points and Location of Investigation Points	Minimum Depth of Investigation
Retaining walls	A minimum of one investigation point for each retaining wall. For retaining walls more than 30 m in length, investigation points spaced every 30 to 60 m with locations alternating from in front of the wall to behind the wall. For anchored walls, additional investigation points in the anchorage zone spaced at 30 to 60 m. For soil-nailed walls, additional investigation points at a distance of 1.0 to 1.5 times the height of the wall behind the wall spaced at 30 to 60 m.	Investigate to a depth below bottom of wall between 1 and 2 times the wall height or a minimum of 3 m into bedrock. Investigation depth should be great enough to fully penetrate soft highly compressible soils (e.g. peat, organic silt, soft fine grained soils) into competent material of suitable bearing capacity (e.g., stiff to hard cohesive soil, compact dense cohesionless soil, or bedrock).
Embankment Foundations	A minimum of one investigation point every 60 m (erratic conditions) to 120 m (uniform conditions) of embankment length along the centerline of the embankment. At critical locations, (e.g., maximum embankment heights, maximum depths of soft strata) a minimum of three investigation points in the transverse direction to define the existing subsurface conditions for stability analyses. For bridge approach embankments, at least one investigation point at abutment locations.	Investigation depth should be, at a minimum, equal to twice the embankment height unless a hard stratum is encountered above this depth. If soft strata is encountered extending to a depth greater than twice the embankment height, investigation depth should be great enough to fully penetrate the soft strata into competent material (e.g., stiff to hard cohesive soil, compact to dense cohesionless soil, or bedrock).
Cut Slopes	A minimum of one investigation point every 60 m (erratic conditions) to 120 m (uniform conditions) of slope length. At critical locations (e.g., maximum cut depths, maximum depths of soft strata) a minimum of three investigation points in the transverse direction to define the existing subsurface conditions for stability analyses. For cut slopes in rock, perform geologic mapping along the length of the cut slope.	Investigation depth should be, at a minimum, 5 m below the minimum elevation of the cut unless a hard stratum is encountered below the minimum elevation of the cut. Investigation depth should be great enough to fully penetrate through soft strata into competent material (e.g., stiff to hard cohesive soil, compact to dense cohesionless soil, or bedrock). In locations where the base of cut is below ground-water level, increase depth of investigation as needed to determine the depth of underlying pervious strata.

Table 3. Guidelines for minimum number of investigation points and depth of investigation (continued).

Application	Minimum Number of Investigation Points and Location of Investigation Points	Minimum Depth of Investigation
Shallow Foundations	For substructure (e.g., piers or abutments) widths less than or equal to 30 m, a minimum of one investigation point per substructure. For substructure widths greater than 30 m, a minimum of two investigation points per substructure. Additional investigation points should be provided if erratic subsurface conditions are encountered.	Depth of investigation should be: (1) great enough to fully penetrate unsuitable foundation soils (e.g., peat, organic silt, soft fine grained soils) into competent material of suitable bearing capacity (e.g. stiff to hard cohesive soil, compact to dense cohesionless soil or bedrock) and; (2) at least to a depth where stress increase due to estimated footing load is less than 10% of the existing effective overburden stress and; (3) if bedrock is encountered before the depth required by item (2) above is achieved, investigation depth should be great enough to penetrate a minimum of 3 m into the bedrock, but rock investigation should be sufficient to characterize compressibility of infill material of near-horizontal to horizontal discontinuities.
Deep Foundations	For substructure (e.g., bridge piers or abutments) widths less than or equal to 30 m, a minimum of one investigation point per substructure. For substructure widths greater than 30 m, a minimum of two investigation points per substructure. Additional investigation points should be provided if erratic subsurface conditions are encountered. Due to large expense associated with construction of rock-socketed shafts, conditions should be confirmed at each shaft location.	In soil, depth of investigation should extend below the anticipated pile or shaft tip elevation a minimum of 6 m, or a minimum of two times the maximum pile group dimension, whichever is deeper. All borings should extend through unsuitable strata such as unconsolidated fill, peat, highly organic materials, soft fine-grained soils, and loose coarse-grained soils to reach hard or dense materials. For piles bearing on rock, a minimum of 3 m of rock core shall be obtained at each investigation point location to verify that the boring has not terminated on a boulder. For shafts supported on or extending into rock, a minimum of 3 m of rock core, or a length of rock core equal to at least three times the shaft diameter for isolated shafts or two times the maximum shaft group dimension, whichever is greater, shall be extended below the anticipated shaft tip elevation to determine the physical characteristics of rock within the zone of foundation influence.

CHAPTER 4

TOOLS AND TECHNIQUES FOR MEASURING SOIL AND ROCK PARAMETERS

4.1 INTRODUCTION

The purpose of this section is to provide information on various in-situ and laboratory testing methods that are currently used to establish site-specific soil and rock properties for design and construction. The execution of a conventional subsurface exploration and testing program usually includes rotary drilling, Standard Penetration Testing (SPT), disturbed and undisturbed sample recovery, and laboratory testing. Although procedures for these commonly performed activities are codified in AASHTO and ASTM standards and are well known to most geo-professionals, important testing details are sometimes overlooked that can result in marginal data quality. This section was prepared to help identify the importance of selecting and conducting the appropriate field and laboratory testing method.

In-situ testing methods are becoming increasingly used on transportation projects, however testing procedures and testing limitations are not as well understood as more conventional methods of subsurface exploration and testing. In this section, procedures for various in-situ and laboratory testing methods are presented as they relate to obtaining high-quality data for evaluation of engineering properties. Information on equipment calibration, measured test parameters, quality control, and the appropriate range of ground conditions that are appropriate for each test is also presented.

In-situ tests discussed in this section include: (1) SPT; (2) CPT; (3) piezocone penetration testing (CPTu); (4) seismic piezocone testing (SCPTu); (5) DMT; (6) pressuremeter testing (PMT); and (7) vane shear testing (VST). Many state DOTs perform these tests directly using agency-owned equipment. In many cases however, the agency may directly contract to an outside contractor for these services or they may be contracted for as part of an overall project development package. Several technical reports and manuals are available that describe these methods. A brief list of these references is provided in table 4. Those agencies that perform or contract for these testing services are encouraged to obtain the references identified in table 4.

Table 4. Reference publications on in-situ testing.

Test Method	AASHTO/ ASTM Designation	Reference
SPT	AASHTO T206 ASTM D 1586	U.S. Department of Transportation, Federal Highway Administration, (1997) *Subsurface Investigations*, Training Course in Geotechnical and Foundation Engineering, FHWA HI-97-021
CPT, CPTu, SCPTu	ASTM D 3341, D5778	U.S. Department of Transportation, Federal Highway Administration, (1988) *Guidelines for Using the CPT, CPTu, and Marchetti DMT for Geotechnical Design*, FHWA-SA-87-023-024. Lunne, T., Robertson, P.K., and Powell, J.J.M. (1997) *Cone Penetration Testing in Geotechnical Practice*, E & F Spon, 312 pp.
DMT	Suggested ASTM Method Schmertmann, 1986	U.S. Department of Transportation, Federal Highway Administration (1992) *The Flat Dilatometer Test*, FHWA-SA-91-044. Marchetti, S., and Crapps, D.K. (1981) Flat Dilatometer Manual, Internal Report of GPE, Inc. (Gainesville, FL), available at http://www.gpe.org.
PMT	ASTM D 4719	U.S. Department of Transportation, Federal Highway Administration, (1989) *The Pressuremeter Test for Highway Applications*, FHWA-IP-89-008. Clarke, B.G. (1995) *Pressuremeters in Geotechnical Design*, Blackie Academic & Professional, 364 pp.
VST	ASTM D 2573	American Society of Testing and Materials, (1988) *Vane Shear Strength Testing in Soils: Field and Laboratory Studies*, ASTM STP 1014, 378 pp.

The remainder of this section is devoted to describing the specific tools and techniques used to drill, sample and test soil and rock materials. In addition, summary information on the use of geophysical methods as a supplement to drilling, sampling, in-situ testing, and laboratory testing of soil and rock is presented.

4.2 BORING METHODS

Geotechnical borings are a critical component of any subsurface exploration program. They are performed to satisfy several objectives including those listed below.

- identification of the subsurface distribution of materials with distinctive properties, including the presence and geometry of distinct layers;
- determination of data on the characteristics of each layer by retrieving samples for use in evaluating engineering properties;

- acquisition of groundwater data; and
- provide access for introduction of in-situ testing tools.

There are many types of equipment used in current practice for advancing a soil or rock boring. Typical types of soil borings are listed in table 5(a), rock coring methods in table 5(b), and other exploratory techniques in table 5(c). Detailed information on soil and rock boring procedures are beyond the scope of this document, but can be found in AASHTO (1988), FHWA HI-97-021 (1997), and ASTM D 4700. A brief description of typical soil boring methods is provided below (Day, 1999).

- *Discontinuous Auger boring:* An auger is an apparatus with a helical shaft that can be manually or mechanically advanced to bore a hole into soil. Auger drilling is shown in figure 3. The practice of advancing a borehole with a mechanical auger consists of rotating the auger while at the same time applying a downward pressure on the auger to penetrate soil and possibly weak or weathered rock. The augers may be continuous, where the length of the helix is along the entire length of the shaft, or discontinuous when the auger is at the bottom of the drill stem. There are basically two types of discontinuous augers: discontinuous flight augers and bucket augers. Commonly-available discontinuous flight augers have diameters ranging from 0.05 to 1.2 m and bucket augers have diameters ranging from 0.3 to 2.4 m. For discontinuous flight auger borings, the auger is periodically removed from the hole and the soil lodged in the grooves of the flight auger is removed. When using a bucket auger, the soil in the bucket is periodically removed. A casing is generally not used for discontinuous flight and bucket auger borings. Therefore, these methods are not recommended for boreholes deeper than 10 m where the hole may cave-in during the excavation of loose or soft soils, or when the boring is below the groundwater table. In firm stiff clays, discontinuous auger borings can be performed to depths in excess of 10 m.

- *Continuous flight auger.* As the name implies, continuous flight augers have the auger flights continuous along the entire length of the auger. There are two types of continuous flight augers: solid stem and hollow stem. For both of these type augers the drill cuttings are returned to the ground surface via the auger flights. The solid stem auger must be removed from the borehole to allow access to the hole for sampling or testing. Because the auger must be periodically removed from the borehole, a solid stem auger is not appropriate in sands and soft soils, or in soil deposits exhibiting high groundwater. A hollow-stem flight auger has a circular hollow core that allows for sampling through the center of the auger. The hollow-stem auger acts like a casing and allows for sampling in loose or soft soils or when the excavation is below the groundwater table. A plug is necessary when advancing hollow stem augers to prevent cuttings from migrating through the hollow stem. The plug is removed to permit SPT sampling. In loose sands and soft clays extending below the water table, drilling fluids are often used (and maintained) in order to minimize and mitigate disturbance effects.

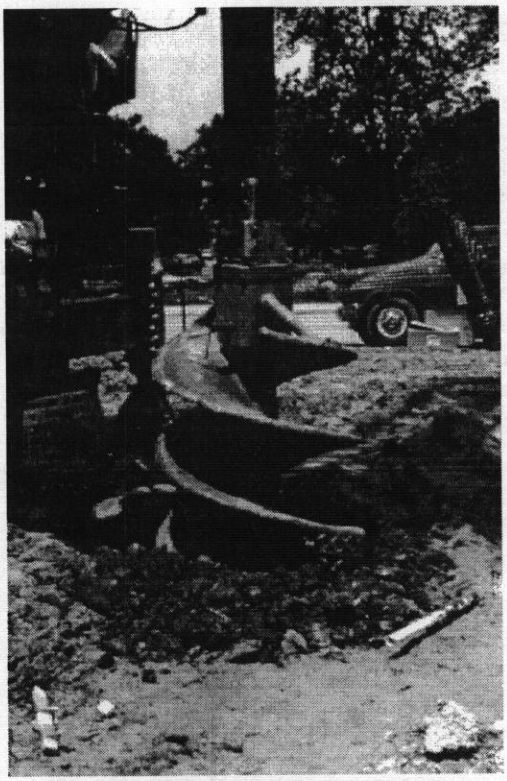

Figure 3. Large diameter auger boring.

- *Wash-type borings*. Wash-type borings use circulating drilling fluid (e.g., water or mud), to remove cuttings from the borehole. Cuttings are created by the chopping, twisting, and jetting action of the drill bit that breaks the soil or rock into small fragments. If bentonite or polymeric drilling muds cannot be used to maintain an open borehole, casings are often used to prevent cave-in of the borehole. The use of casing will require a significant amount of additional time and effort but will result in a protected borehole. When drilling mud is used during subsurface boring, it will be difficult to classify the soil using auger cuttings. Also, the outside of samples may become contaminated with drilling mud.

The previously described methods are typically used for soil exploration, while the following methods are primarily used in rock exploration.

- *Rotary coring*. This type of boring equipment is most commonly used for rock exploration when an intact core of the rock is desired. This technique uses power rotation of the drilling bit as circulating fluid removes cuttings from the hole. The drilling bits are specifically designed to core rock, and inner/outer tubes or casings are used to capture the intact core. Table 5(b) lists various types of rotary coring techniques for rock, although many of these techniques are applicable in stiff soil.

- *Percussion drilling*. This type of drilling equipment is often used to penetrate hard rock for subsurface exploration or for the purpose of drilling wells. The drill bit works much like a

jackhammer, rising and falling to break up and crush the rock material. Air is commonly used to clean the cuttings to the ground surface. Table 5(c) includes a description on use of the percussion drilling techniques.

Table 5(a). Boring methods (modified after Day, 1999).

Method	Procedure	Applications	Limitations / Remarks
Auger boring (ASTM D 1452)	Dry hole drilled with hand or power auger; samples recovered from auger flights	In soil and soft rock; to identify geologic units and water content above water table	Soil and rock stratification destroyed; sample mixed with water below the water table
Hollow-stem auger boring	Hole advanced by hollow-stem auger; soil sampled below auger as in auger boring above	Typically used in soils that would require casing to maintain an open hole for sampling	Sample limited by larger gravel; maintaining hydrostatic balance in hole below water table is difficult
Wash-type boring	Light chopping and strong jetting of soil; cuttings removed by circulating fluid and discharged into settling tub	Soft to stiff cohesive materials and fine to coarse granular soils	Coarse material tends to settle to bottom of hole; Should not be used in boreholes above water table where undisturbed samples are desired.
Becker Hammer Penetration Test (BPT)	Hole advanced using double acting diesel hammer to drive a 168 mm double-walled casing into the ground.	Typically used in soils with gravel and cobbles; Casing is driven open-ended if sampling of materials is desired	Skin friction of casing difficult to account for; unsure as to the repeatability of test
Bucket Auger boring	A 600 to 1200-mm diameter drilling bucket with cutting teeth is rotated and advanced. At the completion of each advancement, the bucket is retrieved from the boring and soil is emptied on the ground.	Most soils above water table; can dig harder soils than above types and can penetrate soils with cobbles and boulders if equipped with a rock bucket	Not applicable in running sands; used for obtaining large volumes of disturbed samples and where it is necessary to enter a boring to make observations

Table 5(b). Rock core drilling methods (modified after Day, 1999)[1].

Method	Procedure	Type of sample	Applications	Limitations / Remarks
Rotary coring of rock (ASTM D 2113; AASHTO T 225)	Outer tube with diamond (or tungsten carbide) bit on lower end rotated to cut annular hole in rock; core protected by stationary inner tube; cuttings flushed upward by drill fluid	Rock cylinder 22 to 100 mm wide and as long as 3 m, depending on rock soundness. Standard coring size is 54 mm diameter.	To obtain continuous core in sound rock (percent of core recovered depends on fractures, rock variability, equipment, and driller skill)	Core lost in fracture or variable rock; blockage prevents drilling in badly fractured rock; dip of bedding and joint evident but not strike
Rotary coring of rock, wire line	Same as ASTM D 2113, but core and stationary inner tube retrieved from outer core barrel by lifting device or "overshot" suspended on thin cable (wire line) through special large-diameter drill rods and outer core barrel	Rock cylinder 28 to 85 mm wide and 1.5 to 3 m long	To recover core better in fractured rock which has less tendency for caving during core removal; to obtain much faster cycle of core recovery and resumption of drilling in deep holes	Core lost in fracture or variable rock; blockage prevents drilling in badly fractured rock; dip of bedding and joint evident but not strike
Rotary coring of swelling clay, soft rock	Similar to rotary coring of rock; swelling core retained by third inner plastic liner	Soil cylinder 28.5 to 53.2 mm wide and 600 to 1500 mm long encased in plastic tube	In soils and soft rocks that swell or disintegrate rapidly in air (protected by plastic tube)	Sample smaller; equipment more complex than other soil sampling techniques

Note: (1) See section 4.3.3 for additional discussion on types of core barrels (i.e., single-, double-, or triple-tube).

Table 5(c). Other exploratory techniques (modified after Day, 1999).

Method	Procedure	Type of sample	Applications	Limitations / Remarks
Borehole camera	Inside of core hole viewed by circular photograph or scan	No sample, but a visual representation of the material	To examine stratification, fractures, and cavities in hole walls	Best above water table or when hole can be stabilized by clear water
Pits and Trenches	Pit or trench excavated to expose soils and rocks	Chunks cut from walls of trench; size not limited	To determine structure of complex formations; to obtain samples of thin critical seams such as failure surface	Moving excavation equipment to site, stabilizing excavation walls, and controlling groundwater may be difficult; useful in obtaining depth to shallow rock and for obtaining undisturbed samples on pit/trench sidewalls; pits need to be backfilled
Rotary or cable tool well drill	Toothed cutter rotated or chisel bit pounded and churned	Pulverized	To penetrate boulders, coarse gravel; to identify hardness from drilling rates	Identification of soils or rocks difficult
Percussive Method (jack hammer or air track)	Impact drill used; cuttings removed by compressed air	Rock dust	To locate rock, soft seams, or cavities in sound rock	Drill becomes plugged by wet soil

4.3 SAMPLING METHODS

4.3.1 Disturbed Sampling of Soil

Disturbed sampling provides a means to evaluate stratigraphy by visual examination and to obtain soil specimens for laboratory index testing. Disturbed samples are usually collected using split-barrel samplers (figure 4; AASHTO T206, ASTM D 1586), although several other techniques are available for disturbed sample collection in boreholes (see table 6(a) and 6(b)). Shallow disturbed samples can also be obtained using hand augers and test pits. Direct push methods, such as GeoProbe sampling, can be used to obtain continuous disturbed samples but have similar limitations in sampling depth as solid stem and bucket augers (i.e., less than 10 m unless in firm to stiff clays). Discrete direct push samples can be obtained at depth using free-floating or retractable piston samplers. Samples obtained via disturbed sampling methods can often be used for index property testing in the laboratory but explicitly should not be used to prepare specimens for consolidation and strength (i.e. performance) tests.

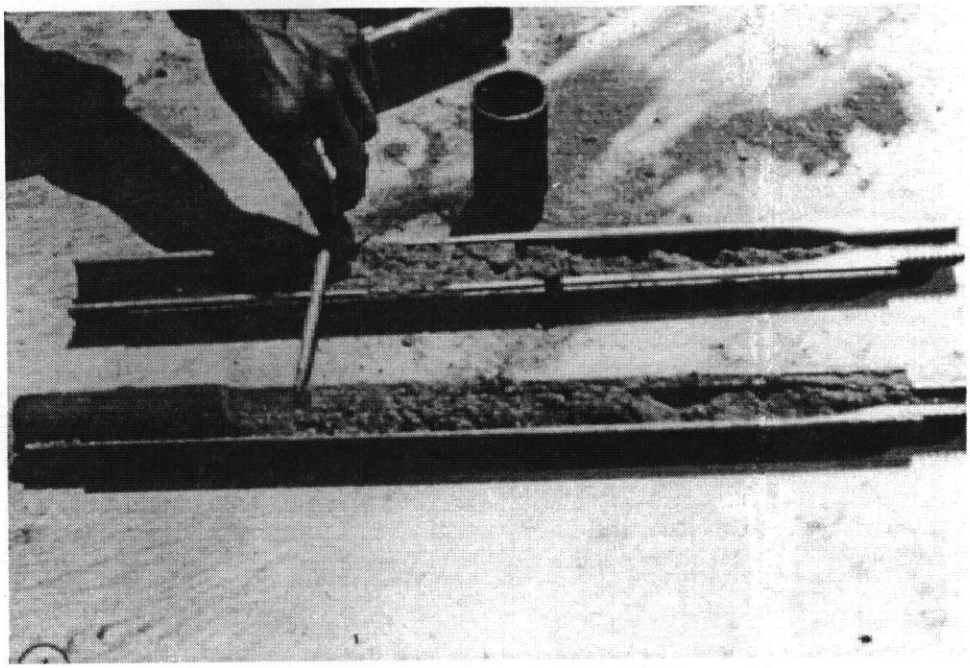

Figure 4. Split barrel sampler.

Table 6(a). Common samplers to collect disturbed soil samples (modified after NAVFAC, 1982).

Sampler	Typical Dimensions	Soils that Give Best Results	Method of Penetration	Cause of Low Recovery	Remarks
Split Barrel	Standard is 50 mm outside diameter (OD) and 35 mm inside diameter (ID);	All soils finer than gravel size particles that allow sampler to be driven; gravels invalidate drive data; A soil retainer may be required in granular soils.	64 kg (140 lb) hammer driven	Gravel may block sampler	A SPT is performed using a standard penetrometer and hammer (see text); samples are extremely disturbed
Continuous helical-flight auger	Diameters range 76 to 406 mm; penetrations to depths exceeding 15 m	Most soils above water table; will not penetrate hard soils or those containing cobbles or boulders	Rotation	Hard soils, cobbles, boulders	Method of determining soil profile, bag samples can be obtained; log and sample depths must account for lag time between penetration of bit and arrival of sample at surface, to minimize errors in estimated sample depths

Table 6(b). Specialty samplers to collect disturbed soil samples (modified after NAVFAC, 1982).

Sampler	Typical Dimensions	Soils that Give Best Results	Method of Penetration	Cause of Low Recovery	Remarks
Disc auger	Up to 1070 mm diameter; usually has maximum penetration depth of 8 m	Most soils above water table; will not penetrate hard soils or those containing cobbles or boulders	Rotation	Hard soils, cobbles, boulders	Method of determining soil profile, bag samples can be obtained; log and sample depths must account for lag time between penetration of bit and arrival of sample at surface, to minimize errors in estimated sample depths
Bucket auger	Up to 1220 mm diameter common; larger sizes available; with extensions, depth over 24 m are possible	Most soils above water table; can penetrate harder soils than above types and can penetrate soils with cobbles and boulders if equipped with a rock bucket	Rotation	Soil too hard to penetrate	Several bucket types available, including those with ripper teeth and chopping tools; progress is slow when extensions are used
Test boring of large samples, Large Penetration Test (LPT)	50- to 75-mm ID and 63- to 89- mm OD samplers (examples, Converse sampler, California Sampler)	In sandy to gravelly soils	Up to 160 kg (350 lb) hammer driven	Large gravel, cobbles, and boulders may block sampler	Sample is intact but very disturbed; A resistance can be recorded during penetration, but is not equivalent to the SPT N-value and is more variable due to no standard equipment and methods

4.3.2 Undisturbed Sampling of Soil

4.3.2.1 General

Undisturbed soil samples are required for performing laboratory strength and consolidation testing on generally cohesive soils ranging from soft to stiff consistency. High-quality samples for such testing are particularly important for approach embankments and for structural foundations and wall systems that may stress compressible strata. In reality, it is impossible to collect truly undisturbed samples since changes in the state of stress in the sample will occur upon sampling. The goal of high-quality undisturbed sampling is to minimize the potential for: (1) alteration of the soil structure; (2) changes in moisture content or void ratio; and (3) changes in chemical composition of the soil. Due to cost and ease of use, the thin-walled Shelby tube (figure 5) is the most common equipment for obtaining relatively undisturbed samples of soils. Depending upon cohesive soil type (e.g., stiffness and whether significant granular material is in the soil matrix), alternative sampling equipment may be used to obtain nominally undisturbed soil samples including: (1) stationary piston (figure 6); (2) hydraulic piston; (3) Denison (figure 7); and (4) pitcher samplers (figure 8). Summary information on these samplers is provided in table 7 and detailed procedures for these sampling techniques are provided in FHWA HI-97-021. Although not common for typical transportation-

related projects, a variety of special samplers are available to obtain samples of soil and soft rocks such as the retractable plug, Sherbrooke, and Laval samplers.

When dealing with relatively shallow soils that are very stiff, brittle, partially cemented, or contain coarse gravel or stones, the best method to obtain large relatively undisturbed samples is by block sampling. Block sampling involves isolating a soil column, encasing it in paraffin wax, and covering it with an open-ended box or tube (usually about 30-cm square). The bottom is cut, sealed and covered, and the sample is transported to the laboratory. This technique is difficult to implement for deep deposits of materials.

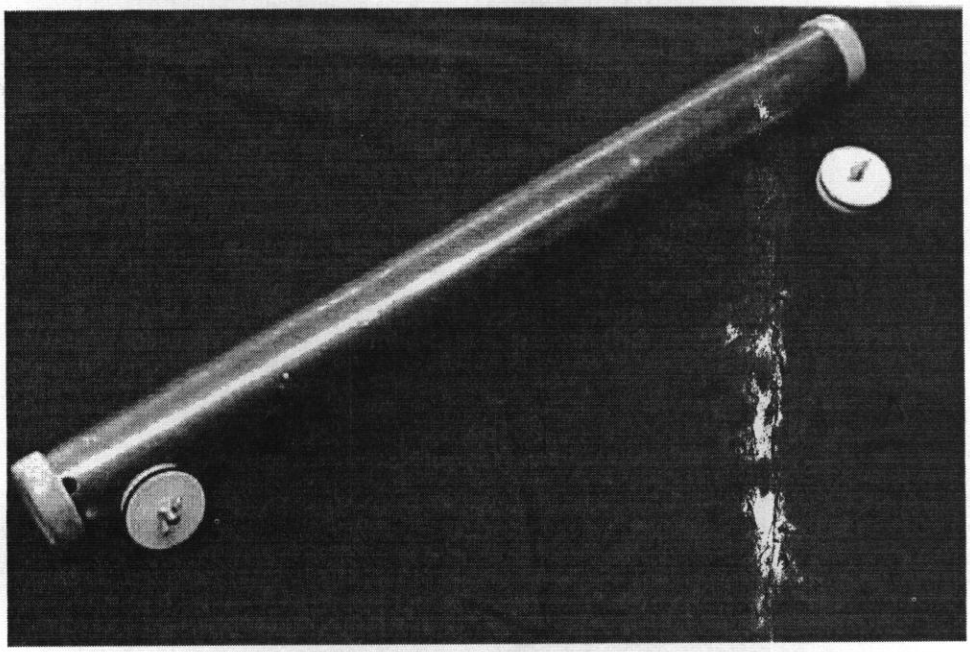

Figure 5. Thin walled (Shelby) tube for sampling (with end caps).

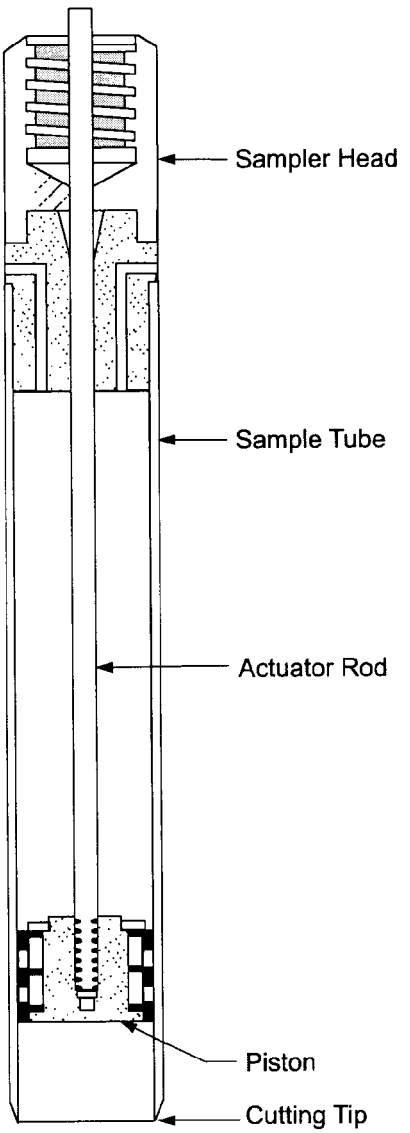

Figure 6. Stationary piston sampler.

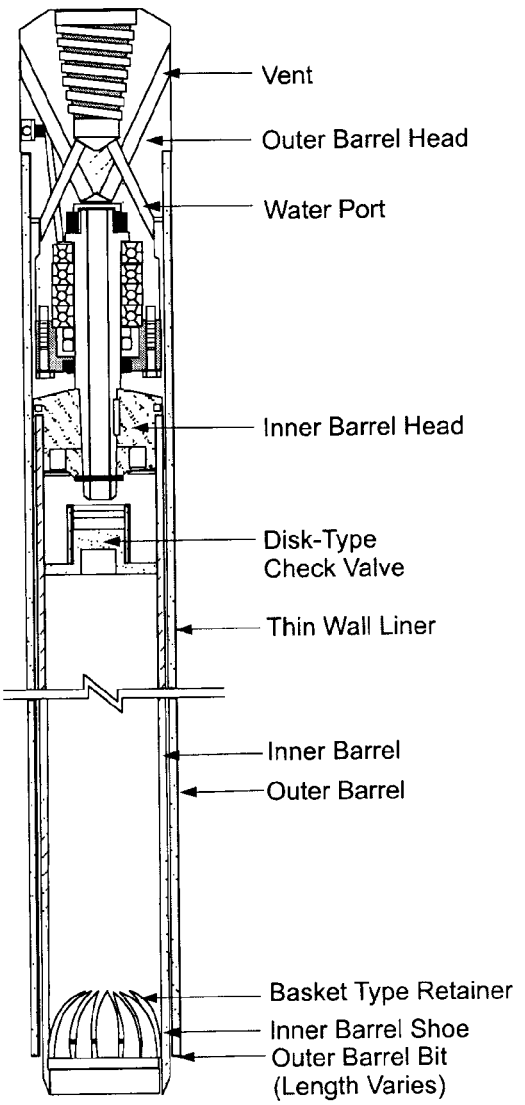

Figure 7. Denison Sampler.

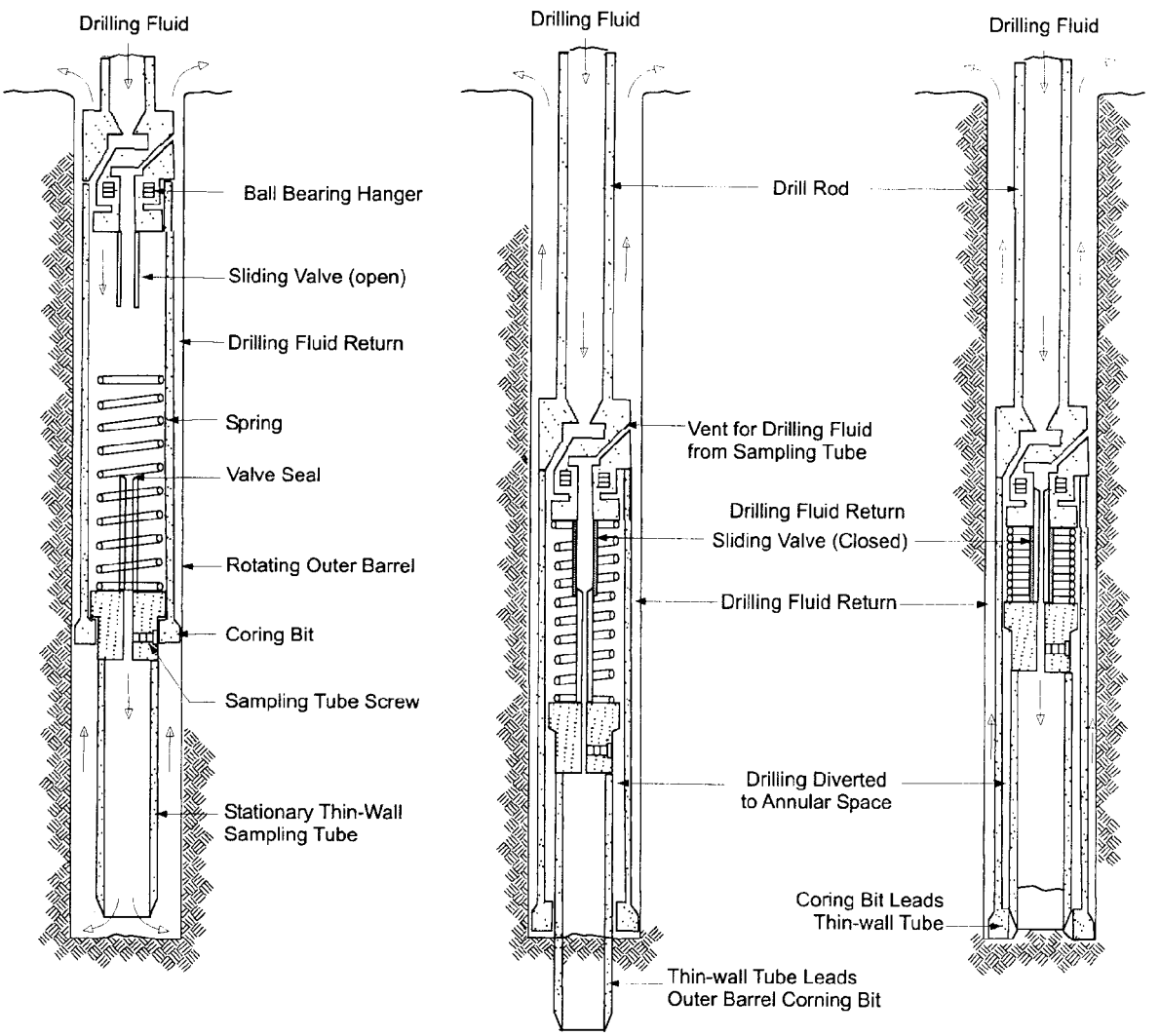

Figure 8. Pitcher sampler.

4.3.2.2 Overview of Thin-Walled Tube Sampling

The importance of appropriate sampling practice cannot be overemphasized. Poor sampling practices, exposure to extreme temperatures, and careless handling of samples will result in misleading test results that may result in uneconomical or unsafe designs. Issues related to good practice for undisturbed sampling are provided in this section.

- Geometry of a Thin-Walled Tube: The inside clearance ratio (ICR) and the area ratio (AR) are parameters that are used to evaluate the disturbance potential for different types of soil samplers. These parameters are defined as follows:

$$AR = \frac{D_o^2 - D_i^2}{D_i^2} \qquad \text{(Equation 1)}$$

$$ICR = \frac{D_i - D_e}{D_e} \qquad \text{(Equation 2)}$$

where D_e = diameter at the sampler cutting tip, D_i = inside diameter of the sampling tube, and D_o = outside diameter of the sampling tube. For a sample to be considered undisturbed, the ICR should be approximately 1 percent and the AR should be 10 percent or less. Using a tube with this ICR value minimizes the friction buildup between the soil sample and the sampler during the advancement of the sampler. Using a tube with an AR value less than 10 percent enables the sampler to cut into the soil with minimal displacement of the soil. Thin-walled tubes (e.g., Shelby tubes) are typically manufactured to meet these specifications, but a thicker walled tube with an ICR of zero is commonly used in the Gulf states (i.e., Texas, Louisiana) to sample very stiff overconsolidated clays. The use of the thicker walled tube minimizes buckling of the sampler in the stiff deposits, and the ICR of zero minimizes sample expansion within the tube. Additional information on suitable geometry for thin-walled tubes is provided in ASTM D 1587.

- Sample Tube Inspection and Storage: Tubes received from the manufacturer should be inspected to assure that no damage has occurred to the ends of the tubes. Plastic end caps, which will later be used to facilitate securing of the sample, should be placed on the ends of the tube at this time.

- Cleaning Borehole Prior to Sampling: Depending upon the methods used, drilling and sampling procedures will cause some disturbance in the vicinity of the advancing face of a borehole. This is especially the case if a sample is overdriven, if casing is advanced ahead of the borehole, or during continuous sampling operations. It is recommended that a borehole be advanced and cleaned to two to three diameters below the bottom of the previous sample to minimize disturbance. Additionally, after advancement of the borehole, caving may occur at the bottom of the hole. Thus, the bottom of the borehole should be cleaned out thoroughly before advancing the sampling device. Improper cleaning will lead to severe disturbance of the upper material (accumulated settled material), and possibly

disturbance of the entire sample. Cleaning is usually performed by washing materials out of the hole. It should be ensured that the jet holes are not directed downward, for this will erode soft or granular materials to an unknown depth. All settled material should be removed to the edge of the casing. In deep or wide borings, special cleaning augers may be used to decrease time for cleaning and produce a cleaner hole.

- Tube Advancement and Retrieval: Tubes should be advanced without rotation in a smooth and relatively rapid manner. The length of the sampler advancement should be limited to 610 mm for a 762-mm long tube to minimize friction along the wall of the sampler and allow for loose material in the hole. The amount of recovery should be compared to the advanced length of the sampler to assess whether material has been lost, the sample has swelled, or some caved material has been collected at the top of the tube. The possible presence of caved material should be noted at the top of the tube so that no laboratory moisture content or performance tests are performed on that material. After advancing to the target depth, the drill rod should be rotated one full turn to shear off the bottom of the sample. A waiting period of 5 to 15 minutes is recommended for tubes in soft soils to permit the sample to reach equilibrium inside the tube and prevent the sample from falling out the bottom of the tube during retrieval. This waiting period may be reduced for stiffer soils.

- Preparation for Shipment: Upon removal of the sample from the borehole, the ends should be capped using the plastic end caps and the tube should be labeled. The label should be written directly on the tube with a permanent marking pen, and include: (1) tube identification number; (2) sample depth; (3) top and bottom of sample; (4) length of recovery; (5) sampling date; (6) job name and/or number; and (7) sample description. Tube samples that are intended for laboratory performance testing (i.e., strength, consolidation, hydraulic conductivity) should never be extruded from the tube in the field and stored in alternative containers. Samples should only be extruded in the laboratory under controlled conditions. After the sample is collected, seal the upper end of the tube with nonshrinking wax. After the upper wax has dried, remove at least 25 mm of material from the lower end of the tube and seal the bottom of the tube with nonshrinking wax. The use of relatively low temperature wax will minimize shrinkage and potential moisture migration within the sample. The space between the wax seal and the top of the tube should be filled with sawdust or moist sand. The tube should be kept vertical, with the top of the sample in the upright position. If the sample needs to be inverted for purposes such as sealing, care should be taken to ensure the sample does not slide within the tube.

- Shipment: Sample tubes need to be packed in accordance with guidelines provided in ASTM D 4220, or in an equivalent sample box. Tubes should be isolated from other sample tubes, and fit snugly in the case to protect against vibration or shock. The cushioning material between the samples should be at least 25 mm thick, and the cushioning on the container floor should be at least 50 mm thick. The samples should not be exposed to extreme heat or cold. If possible, the engineer should deliver the samples to the lab or use an overland freight service to ship samples. Typical handling practices of air freight services will lead to additional disturbance of the sample. The use of a chain of custody form for sample traceability records is encouraged.

Table 7. Nominally undisturbed soil samplers (modified after NAVFAC, 1982).

Sampler	Typical Dimensions	Soils that Give Best Results	Method of Penetration	Cause of Disturbance or Low Recovery	Remarks
Shelby tube (ASTM D 1587; AASHTO T 207)	76 mm OD and 73 mm ID most common; available from 50 to 127 mm OD; 760-mm sampler length standard	Cohesive fine-grained or soft soils; gravelly and very stiff soils will crimp tube	Pressing with relatively rapid, smooth stroke; can be carefully hammer driven but this will induce additional disturbance	Erratic pressure applied during sampling, hammering, gravel particles, crimping of tube edge, improper soil types for sampler, pressing tube greater than 80% of tube length	Simplest device for undisturbed samples; boring should be clean before sampler is lowered; little waste area in sampler; not suitable for hard, dense or gravelly soils
Stationary piston	76 mm OD most common; available from 50 to 127 mm OD; 760-mm sampler length standard	Soft to medium clays and fine silts; not for sandy soils	Pressing with continuous, steady stroke	Erratic pressure during sampling, allowing piston rod to move during press, improper soil types for sampler	Piston at end of sampler prevents entry of fluid and contaminating material requires heavy drill rig with hydraulic drill head; samples generally less disturbed compared with Shelby tube; not suitable for hard, dense, or gravelly soil
Hydraulic piston (Osterberg)	76 mm OD is most common; available from 50 to 101 mm OD; 910-mm sampler length standard	Silts and clays, some sandy soils	Hydraulic or compressed air pressure	Inadequate clamping of drill rods, erratic pressure	Needs only standard drill rods; requires adequate hydraulic or air capacity to activate sampler; samples generally less disturbed compared with Shelby tube; not suitable for hard, dense, or gravelly soil
Denison	89 to 177 mm OD, producing samples 60 to 160 mm; 610-mm sampler length standard	Stiff to hard clay, silt, and sands with some cementation, soft rock	Rotation and hydraulic pressure	Improper operation of sampler; poor drilling procedures	Inner tube face projects beyond outer tube, which rotates; amount of projection can be adjusted; generally takes good samples; not suitable for loose sands and soft clays
Pitcher sampler	105 mm OD; uses 76-mm diameter Shelby tubes; sample length 610 mm	Same as Denison	Same as Denison	Same as Denison	Differs from Denison in that inner tube projection is spring controlled; often ineffective in cohesionless soils
Foil Sampler	Continuous samples 50 mm wide and as long as 20 m	Fine grained soils including soft sensitive clays, silts, and varved clays	Pushed into the ground with steady stroke; Pauses occur to add segments to sample barrel	Samplers should not be used in soils containing fragments or shells	Samples surrounded by thin strips of stainless steel, stored above cutter, to prevent contact of soil with tube as it is forced into soil

4.3.3 Rock Coring

When considering equipment for rock coring, the dimensions, type of core barrel, type of coring bit, and drilling fluid are important variables. The minimum depth of rock coring should be determined based on the local geology of the site and type of structure to be constructed. Coring should also be performed to a depth that assures that refusal was not encountered on a boulder.

Four different types of core barrels are described in ASTM D 2113 including: (1) Single Tube (figure 9(a)); (2) Rigid Double Tube (figure 9(b)); (3) Swivel Double Tube (figure 9(c)); and (4) Triple Tube. A brief description of issues related to rock coring is provided subsequently. Additional information on drilling rigs, methods of circulating drill cuttings (i.e., fluid or air), hole diameters, and casings are provided in ASTM D 2113.

Since the double core barrel isolates the rock from the drilling fluid stream to yield better recovery, it is the minimum standard of core barrel that should be used in practice when an intact core is required. The inner tube of a swivel-type core barrel does not rotate during drilling, resulting in less disturbance and better recovery in weak and fractured rock. Rigid type double tube core barrels should not be used where core recovery is a concern. Triple tube swivel-type core barrels will produce better recovery and less core breakage than a double tube barrel.

Conventional drilling and wireline techniques are applicable for rock coring. Wireline techniques are generally preferred by drillers for deep cores since the production rates are higher and the method facilitates deeper sampling. Wireline drilling can be used for any project, but is typically used for coring at depths greater than 25 m.

The standard size rock core is NX 54 mm (2 1/8 in.) diameter. Generally larger core sizes will lead to less mechanical breakage and yield greater recovery, but the associated cost for drilling will be much higher. Since the size of the core will affect the percent recovery, this should be clearly recorded on the log. Additionally, the core length can increase recovery in fractured and weathered rock zones. In these zones a core length of 1.5 meters is recommended, and core lengths should not be greater than 3 m under any conditions because of the potential to damage the long cores.

The coring bit is manufactured in accordance with one of the following designs: (1) diamond; (2) carbide insert; or (3) sawtooth. Bit selection will be based on the anticipated rock formation as well as the expected drilling fluid. Diamond bits are applicable in all rock types, and permit higher rates of coring when compared to other bits. Carbide insert bits are cheaper than diamond bits and can be used in soft to medium-hard rock. While sawtooth bits are the cheapest of the three, they have no salvage value, lead to slower coring, and are typically only used in soft rock.

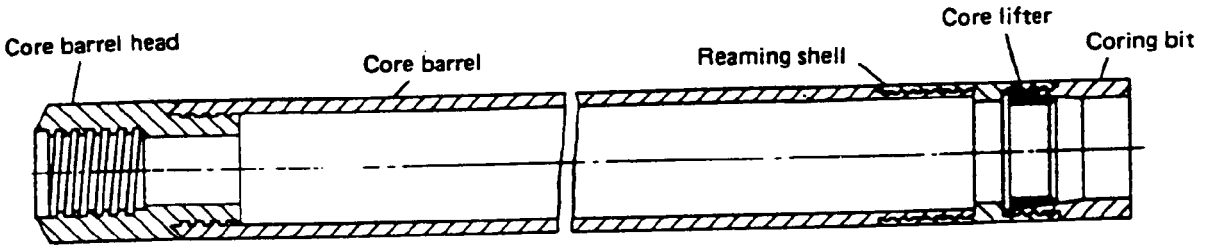

(a)

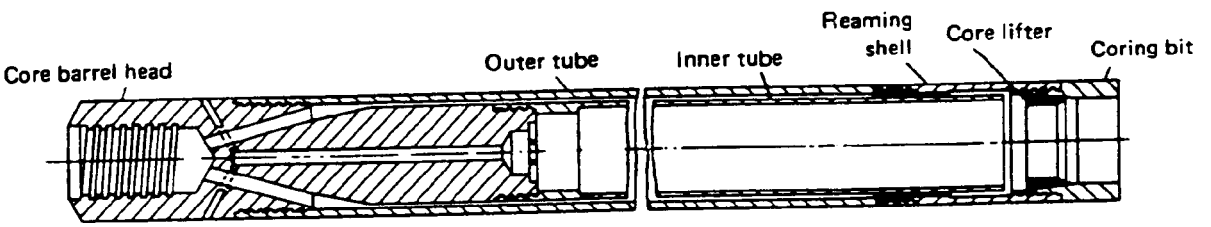

(b)

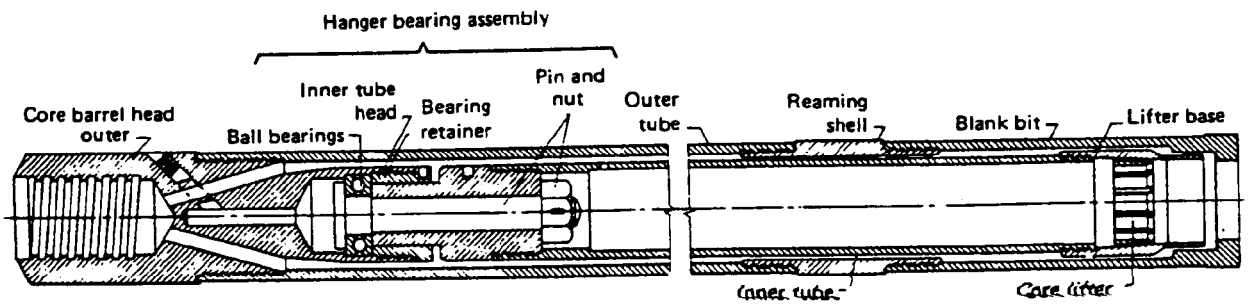

(c)

Figure 9. Single and double tube rock core barrels (after FHWA-HI-97-021, 1997).

Observations of drilling conditions and measurements of core properties taken in the field should be recorded on the boring log. These include: (1) size, type, and design of the core barrel; (2) length of each core run, core recovery, and rock quality designation (RQD); (3) engineer or geologists

description of the formation; (4) structural descriptions including dip of strata, dip of jointing, presence of fissures, presence of fractures, and any other pertinent information; (5) depth, thickness, and apparent nature of joint filling; and (6) notations concerning drilling time and character. Cores in a split core barrel should be photographed immediately upon removal from the borehole. Core recovery and RQD are parameters often used in shear strength evaluations for rock masses. These parameters are defined in section 6.2.2.

4.4 STANDARD PENETRATION TEST (SPT)

4.4.1 General

The most commonly used in-situ test in the world is the Standard Penetration test (SPT) (AASHTO T206, ASTM D 1586). The SPT is a simple and rugged test suitable for most soil types except gravel and is usually performed using a conventional geotechnical drill rig (see figure 10). SPTs are recommended for essentially all subsurface investigations since a disturbed sample can be obtained for baseline soil property interpretation. Many engineers have experience using SPT resistance for design purposes, even though the standard accepted correlations are often based on limited laboratory reference tests. Additionally, variability associated with hammer types used (i.e., donut, safety, automatic) and specific testing errors result in relatively poor correlations for evaluating performance properties for design, especially for cohesive soils. The test does provide a rough index of the relative strength and compressibility of the soil in the vicinity of the test.

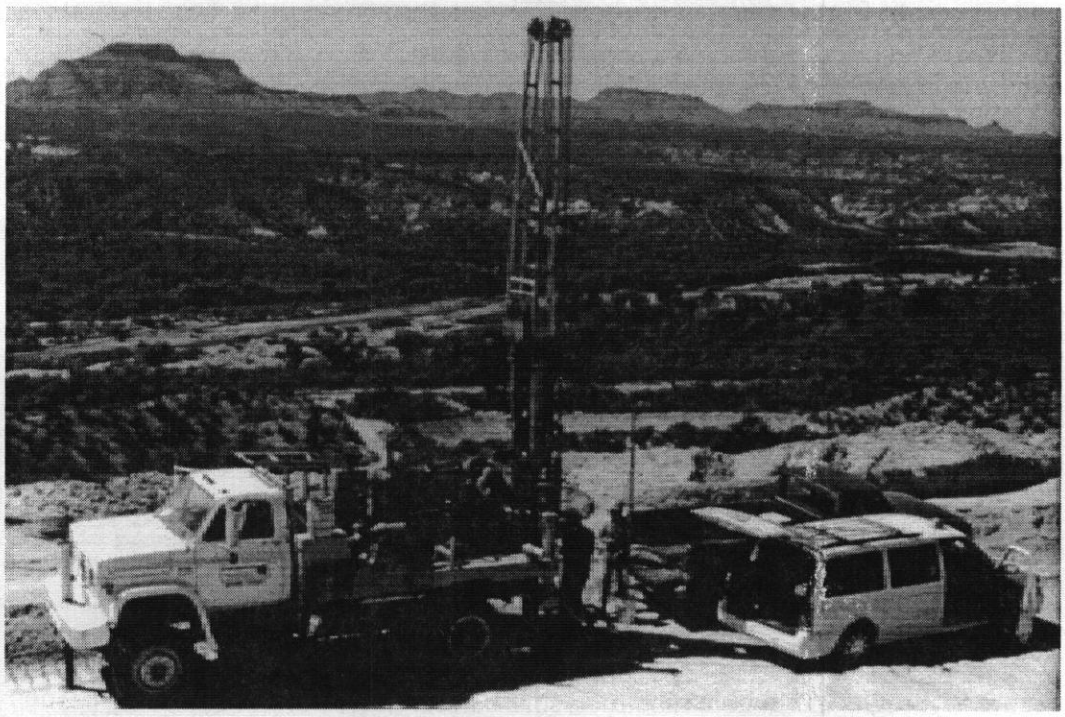

Figure 10. SPT performed at the back of a drill rig.

4.4.2 Procedures

Standard Penetration Test procedures consist of repeatedly dropping a 63.5-kg hammer from a height of 760 mm to drive a split-spoon (i.e., split-barrel) sampler three successive 150-mm long increments. The number of blows required to drive the sampler is recorded for each 150-mm increment. The initial 150-mm increment is considered a seating drive. The blows required for the second and third 150-mm increments are totaled to provide blows/300 mm. This total is referred to as the as the SPT resistance or "N-value". Blow counts taken for each 150-mm interval should be recorded, even for the seating increment. Additionally, the total recovery of soil during the 450-mm drive should be recorded. Depending upon sampler geometry, resistance for a fourth 150-mm increment is sometimes recorded. Due to sampler side friction, the values for the fourth 150-mm increment should not be used in the calculation of N-values, but may provide additional insight into soil stratigraphy.

Since the SPT is highly dependent upon the equipment and operator performing the test, it is often difficult to obtain repeatable results. The main factors affecting the SPT results are summarized in table 8. The SPT should not be relied on in soils containing coarse gravel, cobbles, or boulders, because the sampler can become obstructed, resulting in high and unconservative N values. The test should not be relied on for cohesionless silts because dynamic effects at the sampler tip can lead to erroneous strength and compressibility evaluations. The test also has little meaning in soft and sensitive clays (Kulhawy and Mayne, 1990).

When performing an SPT and recording information on the field log, the following items are of note: (1) N is always recorded as an integer; (2) a test is ended and noted as "refusal" if 50 blows over a 25-mm increment has been recorded. At this point, the blows per 25 mm (or in.) is recorded (i.e., 100/50 mm or 50/ 25 mm); and (3) if the N-value is less than one, then the engineer or geologist should record that the penetration occurred due to the weight of the hammer (WOH) or the weight of rods (WOR).

4.4.3 Parameters Measured

The measured N-value is the number of blows required to drive the split spoon sampler a distance of 300 mm. The efficiency of the system can be obtained by comparing the kinetic energy, KE, (i.e., $KE=\frac{1}{2}mv^2$), with the potential energy, PE, of the system, (i.e., PE=mgh). The energy ratio (ER) is defined as KE/PE. For routine engineering practice in the United States, correlations for engineering properties are based on SPT N values measured based on a system which is 60 percent efficient, i.e., ER=60 percent. The N values corresponding to 60 percent efficiency are termed N_{60}. Numerous correction factors to the measured N-value are necessary because of energy inefficiencies and procedural variation in practice. When all factors are applied to the field recorded N-value (N_{meas}), the corrected value is calculated as:

$$N_{60} = N_{meas} C_E C_B C_S C_R \qquad \text{(Equation 3)}$$

where correction factors are presented in table 9 and include the effects of energy (C_E), borehole diameter (C_B), sampling method (C_S), and rod length (C_R). As can be noted from table 9, values of

the correction term for energy, i.e., C_E, vary over a relatively wide range. For this reason, accurate estimates of C_E are more important than estimates of the other correction factors. More accurate estimates of C_E should be evaluated by directly measuring the energy ratio (ER) of a particular SPT setup according to procedures in ASTM D 4633. Commercially available equipment can be used to perform this calibration. Hammer systems used for standard penetration testing should be periodically calibrated using the procedures outlined in ASTM D 4633.

Table 8. Factors affecting the SPT and SPT results (after Kulhawy and Mayne, 1990).

Cause	Effects	Influence on SPT N Value
Inadequate cleaning of hole	SPT is not made in original in-situ soil, and therefore soil may become trapped in sampler and may be compressed as sampler is driven, reducing recovery	Increases
Failure to maintain adequate head of water in borehole	Bottom of borehole may become quick	Decreases
Careless measure of drop	Hammer energy varies (generally variations cluster on low side)	Increases
Hammer weight inaccurate	Hammer energy varies (driller supplies weight; variations of 5 – 7 percent common)	Increases or decreases
Hammer strikes drill rod collar eccentrically	Hammer energy reduced	Increases
Lack of hammer free fall because of ungreased sheaves, new stiff rope on weight, more than two turns on cathead, incomplete release of rope each drop	Hammer energy reduced	Increases
Sampler driven above bottom of casing	Sampler driven in disturbed, artificially densified soil	Increases greatly
Careless blow count	Inaccurate results	Increases or decreases
Use of non-standard sampler	Correlations with standard sampler invalid	Increases or decreases
Coarse gravel or cobbles in soil	Sampler becomes clogged or impeded	Increases
Use of bent drill rods	Inhibited transfer of energy of sampler	Increases

Table 9. Corrections to the SPT (after Skempton, 1986).

Factor	Equipment Variable	Term	Correction
Energy Ratio	Donut Hammer Safety Hammer Automatic Hammer	$C_E = ER/60$	0.5 to 1.0[1] 0.7 to 1.2[1] 0.8 to 1.5[1]
Borehole Diameter	65 to 115 mm 150 mm 200 mm	C_B	1.0 1.05 1.15
Sampling method	Standard sampler Non-standard sampler	C_S	1.0 1.1 to 1.3
Rod Length	3 to 4 m 4 to 6 m 6 to 10 m 10 to >30 m	C_R	0.75 0.85 0.95 1.0

[1] Values presented are for guidance only. Actual ER values should be measured per ASTM D 4633

Since N-values of similar materials increase with increasing effective overburden stress, the corrected blowcount (N_{60}) is often normalized to 1-atmosphere (or about 100 kPa) effective overburden stress using overburden normalization schemes. The normalized corrected blowcount is referred to as $(N_1)_{60}$, and is equal to:

$$(N_1)_{60}=C_N N_{60} \quad \text{(Equation 4)}$$

where C_N is the stress normalization parameter calculated as:

$$C_N = (P_a/\sigma_{vo}')^n \quad \text{(Equation 5)}$$

where P_a is atmospheric pressure in the same units as σ_{vo}', and n is a stress exponent typically equal to 1 in clays (e.g., Olsen, 1997; Mayne & Kemper, 1988) and 0.5 to 0.6 in sands (e.g., Seed et al., 1983; Liao & Whitman, 1986; Olsen, 1997). Figure 11 illustrates a correlation for C_N that is used for sands. There exist several soil specific correlations for C_N, as reported in the literature. C_N may vary slightly from the general values identified previously, depending upon the specific correlation.

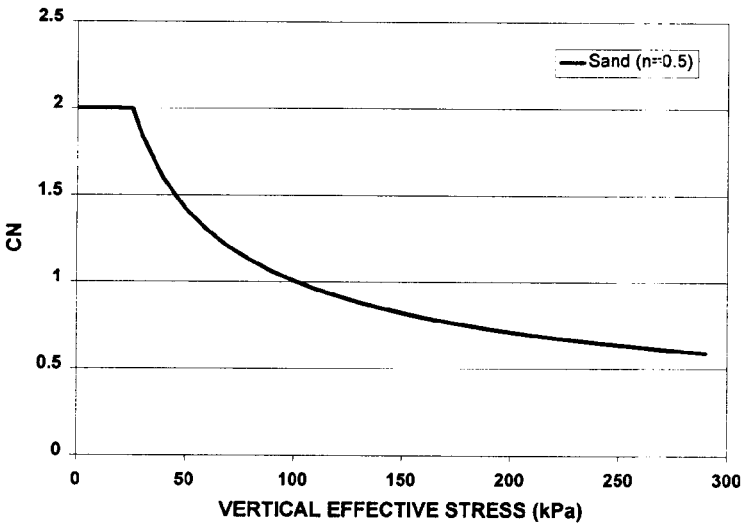

Figure 11. Stress normalization parameter, C_N, for sands.

4.5 CONE PENETRATION TESTS (CPT / CPTU / SCPTU)

4.5.1 General

The cone penetration test (CPT) involves the hydraulic push of an instrumented steel probe at constant rate to obtain continuous vertical profiles of stress, pressures, and/or other measurements. No borehole, cuttings, or spoil are produced by this test. Testing is conducted in accordance with ASTM D 5778. The cone penetration test can be conducted without the use of a pore pressure measurement (i.e., CPT) or can be conducted using a device to measure penetration pore pressure using a piezocone (i.e., CPTu). Some equipment includes the ability to measure the propagation of shear waves using a seismic piezocone; this test designated as SCPTu. Details concerning cone penetration tests are summarized in table 10. Additionally, other in-situ tests that will be discussed subsequently are presented in this table.

Table 10. In-situ testing methods used in soil.

Method	Procedure	Applicable Soil Types	Applicable Soil Properties	Limitations / Remarks
Electric Cone Penetrometer (CPT)	A cylindrical probe is hydraulically pushed vertically through the soil measuring the resistance at the conical tip of the probe and along the steel shaft; measurements typically recorded at 2 to 5 cm intervals	Silts, sands, clays, and peat	Estimation of soil type and detailed stratigraphy Sand: ϕ', D_r, σ_{ho}' Clay: s_u, σ_p'	No soil sample is obtained; The probe may become damaged if testing in gravelly soils is attempted; Test results not particularly good for estimating deformation characteristics
Piezocone Penetrometer (CPTu)	Same as CPT; additionally, penetration porewater pressures are measured using a transducer and porous filter element	Silts, sands, clays, and peat	Same as CPT, with additionally: Sand: u_o / water table elevation Clay: σ_p', c_h, k_h OCR	If the filter element and ports are not completely saturated, the pore pressure response may be misleading; Compression and wear of a mid-face (u_1) element will effect readings; Test results not particularly good for estimating deformation characteristics
Seismic CPTu (SCPTu)	Same as CPTu; additionally, shear waves generated at the surface are recorded by a geophone at 1-m intervals throughout the profile for calculation of shear wave velocity	Silts, sands, clays, and peat	Same as CPTu, with additionally: V_s, G_{max}, E_{max}, ρ_{tot}, e_o	First arrival times should be used for calculation of shear wave velocity; If first crossover times are used, the error in shear wave velocity will increase with depth
Flat Plate Dilatometer (DMT)	A flat plate is hydraulically pushed or driven through the soil to a desired depth; at approximately 20 to 30 cm intervals, the pressure required to expand a thin membrane is recorded; Two to three measurements are typically recorded at each depth.	Silts, sands, clays, and peat	Estimation of soil type and stratigraphy Total unit weight Sand: ϕ', E, D_r, m_v Clays: σ_p', K_o, s_u, m_v, E, c_h, k_h	Membranes may become deformed if overinflated; Deformed membranes will not provide accurate readings; Leaks in tubing or connections will lead to high readings; Good test for estimating deformation characteristics at small strains
Pre-bored Pressuremeter (PMT)	A borehole is drilled and the bottom is carefully prepared for insertion of the equipment; The pressure required to expand the cylindrical membrane to a certain volume or radial strain is recorded	Clays, silts, and peat; marginal response in some sands and gravels	E, G, m_v, s_u	Preparation of the borehole most important step to obtain good results; Good test for calculation of lateral deformation characteristics
Full Displacement Pressuremeter (PMT)	A cylindrical probe with a pressuremeter attached behind a conical tip is hydraulically pushed through the soil and paused at select intervals for testing; The pressure required to expand the cylindrical membrane to a certain volume or radial strain is recorded	Clays, silts, and peat in sands	E, G, m_v, s_u	Disturbance during advancement of the probe will lead to stiffer initial modulus and mask liftoff pressure (p_o); Good test for calculation of lateral deformation characteristics

Table 10. In-situ testing methods (continued).

Method	Procedure	Applicable Soil Types	Applicable Soil Properties	Limitations / Remarks
Vane Shear Test (VST)	A 4 blade vane is slowly rotated while the torque required to rotate the vane is recorded for calculation of peak undrained shear strength; The vane is rapidly rotated for 10 turns, and the torque required to fail the soil is recorded for calculation of remolded undrained shear strength	Clays, Some silts and peats if undrained conditions can be assumed; not for use in granular soils	s_u, S_t, σ_p'	Disturbance may occur in soft sensitive clays, reducing measured shear strength; Partial drainage may occur in fissured clays and silty materials, leading to errors in calculated strength; Rod friction needs to be accounted for in calculation of strength; Vane diameter and torque wrench capacity need to be properly sized for adequate measurements in various clay deposits

Symbols used in table 10.

ϕ': effective stress friction angle
D_r: relative density
σ_{ho}': in-situ horizontal effective stress
s_u: undrained shear strength
σ_p': preconsolidation stress
c_h: horizontal coefficient of consolidation
k_h: horizontal hydraulic conductivity
OCR: overconsolidation ratio
V_s: shear wave velocity
G_{max}: small-strain shear modulus
G: shear modulus
E_{max}: small-strain Young's modulus
E: Young's modulus
ρ_{tot}: total density
e_o: in-situ void ratio
m_v: volumetric compressibility coefficient
K_o: coefficient of at-rest earth pressure
S_t: sensitivity

4.5.2 Equipment

Equipment necessary for performing a cone penetration test includes a penetrometer, cone rod or drill rod, electrical cable, a data acquisition system, and hydraulic actuator attached to equipment exhibiting sufficient reaction mass to advance the penetrometer. This can be a conventional drilling rig or, more commonly, a dedicated CPT truck commonly weighing 20 to 25 tons.

A standard cone penetrometer is a 35.7-mm diameter cylindrical probe with a 60° apex at the tip, 10-cm^2 projected tip area, and a 150-cm^2 sleeve surface area. More robust penetrometers are available with a 44-mm diameter body, a 15-cm^2 projected tip area, and 200- to 225-cm^2 sleeve surface area. A 15-cm^2 penetrometer will generally provide the same response as a 10-cm^2 probe. The size of a cone is identified by the projected tip area, e.g. a 10-cm^2 cone or a 15-cm^2 cone. Figure 12 shows a number of different cone penetrometers and piezocones. Standard cone rod is typically 1 m in length with a 35.7 mm outer diameter and a 22 mm inner diameter. Alternatively, the penetrometer can be pushed with standard AW or EW drill rod.

A cone cable will run through the hollow cone/drill rods and attach to a data acquisition system at the ground surface. The data acquisition system will generally consist of an analog signal conditioner, an analog to digital (A-D) converter, and computer processor. Current data acquisition

systems are attached to one or two computer monitors so the operator and engineer can observe data recorded during the sounding in real time. Real time monitoring allows for decisions to be made in the field with respect to the sounding. This is helpful if auxiliary tests, such as a pore pressure dissipation tests, are to be performed in certain soil layers, or if the test is to be terminated once a certain layer is encountered. Printers can be attached to the computer processor to obtain a real-time printout of the data during the test. Printed data are a good backup in case an unforeseen incident causes the computer to crash and lose the data. Data are typically recorded every 2 to 5 cm of vertical penetration.

For a piezocone penetration test (CPTu), the penetration porewater pressures are monitored using a transducer and porous filter element. The filter element position can be located at the mid-face on the cone (u_1) or behind the cone tip at the shoulder (u_2), with the latter required for the correction of tip resistance. Filter elements consist of high-density polypropylene, ceramic, or sintered metal. The high-density polypropylene filters wear easily in sands and may clog in clays. Since polypropylene filters are inexpensive and disposable, they should generally be replaced after each test. Ceramic and sintered metal can be re-used many times, but should be switched frequently and cleaned to prevent clogging. Filter compression and wear may influence u_1 results, and the position of the u_1 filter may vary between cone manufacturers. The u_2 position is more standardized and is required for tip correction. It is not as affected by filter compression as the u_1 location. In most cases it is recommended to specify the u_2, but on critical projects where detailed stratigraphy and or stress history are desired it may be advantageous to have the subcontractor bring additional tips with u_1 filter locations. This allows for flexibility in testing, if it is necessary to switch filter location in the middle of the program due to encountered soil conditions. A u_1 element is recommended for profiling in stiff fissured geomaterials where $u_2 \approx 0$.

For the seismic piezocone test, a geophone is located approximately 500 mm uphole from the cone tip. The geophone detects shear waves generated at the ground surface at intervals of approximately 1-meter, corresponding to successive rod additions.

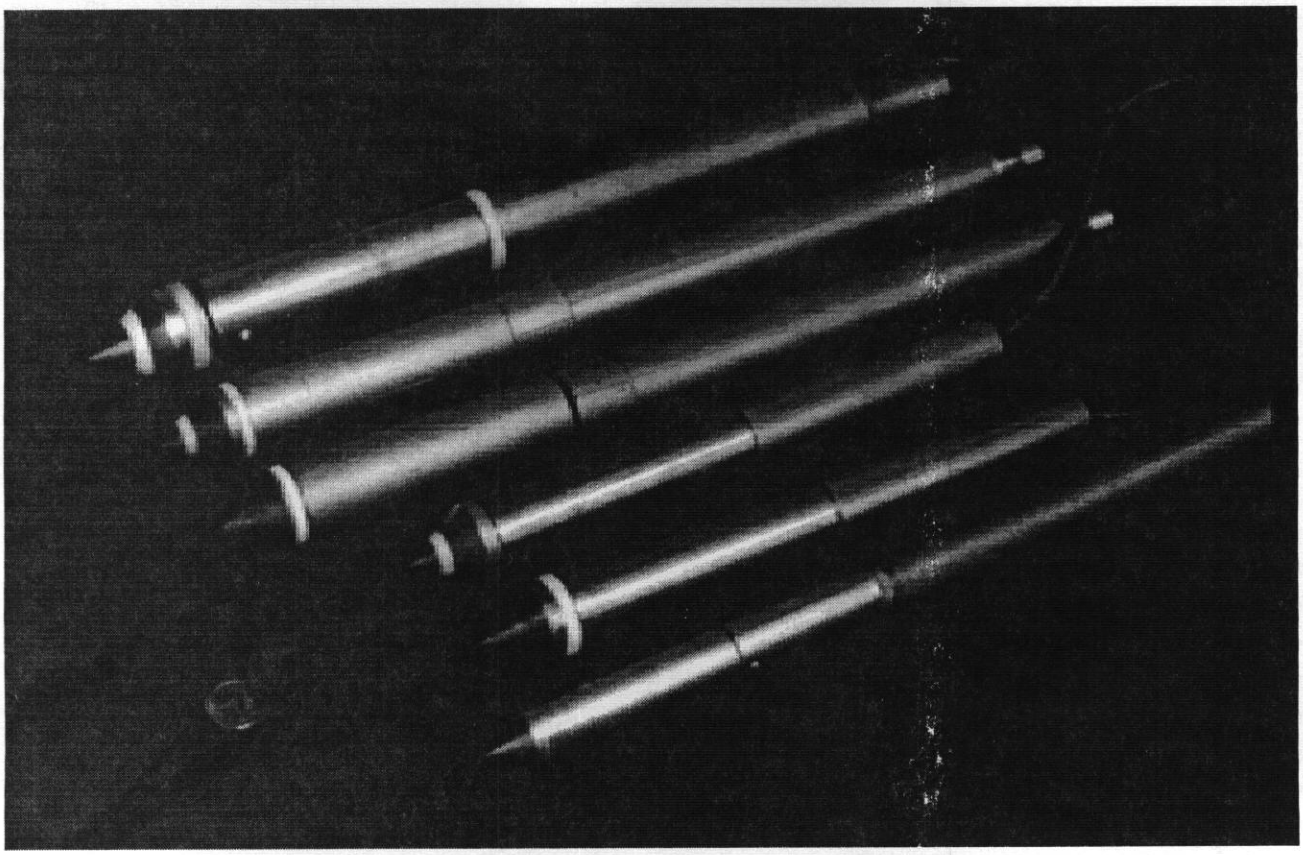

Figure 12. Cone and piezocone penetrometers (note the quarter for scale).

4.5.3 Procedures

Test procedures for the CPT consist of hydraulically pushing the cone at a rate of 2 cm/s in accordance with ASTM D 5778 using either a standard drill rig or specialized cone truck (see figure 13). The advance of the probe requires the successive addition of rods at approximately 1 m or 1.5 m intervals. Readings of tip resistance (q_c), sleeve friction (f_s), inclination (i), and pore pressure (u_m) are taken at least at every 5-cm (i.e., 2.5-sec interval). For the seismic cone test, shear wave arrival times (t_s) are typically recorded at rod breaks corresponding to 1-m or 1.5-m intervals in the strata.

Careful saturation of the porous filter and transducer ports is paramount for piezocone testing. Poor saturation will lead to a compressible measurement system, and thus the full magnitude of the penetration pore pressure response will not be recorded. If water or water mixtures are used as the saturation fluid, a fluid filled membrane should be wrapped around the element to maintain saturation until the probe enters the ground. Glycerin and silicon oil are typically viscous enough to prevent desaturation of the element before penetration into the ground.

Typically a pause in penetration will occur to add new rods. This is referenced as the rod break. The depth at each rod break should be recorded and compared to the expected depth. Inconsistent depths typically result from: (1) multiple readings at a pause in penetration due to decompression of the rod string; or (2) double recording of an interval due to the depth sensor being activated during retraction of the pushing head. The extra readings typically will show significantly reduced tip resistance and sleeve friction values due to decoupling of the cone from the soil matrix. These readings should be deleted from the CPT record and the depth of the sounding should be corrected.

For the seismic piezocone (SCPTu), downhole shear wave velocity tests are performed at each 1-m rod break. A special instrumented hammer is used to trigger a surface source rich in shear waves (e.g., typically a horizontal steel beam). The steel beam is coupled to the ground under a hydraulic outrigger of a cone truck or drill rig, or under the tire of a support vehicle. The horizontal distance between the source beam and cone rod should be minimized (typically < 1.5 m) to ensure a relatively vertically-propagating shear wave. A horizontal geophone located within the penetrometer serves as a receiver for the signal, which is displayed on the screen of an oscilloscope. First arrival times for shear waves are recorded with respect to depth, to provide interpretations of shear wave velocity of the overlying soil material.

Figure 13. Cone penetration testing from cone truck.

4.5.4 Parameters Measured

Electric and electronic penetrometers have standard readings of tip resistance (q_c) and sleeve friction (f_s), as shown in figure 14(a). Piezocone penetrometers measure penetration porewater pressures using filters located at the shoulder (u_2; figure 14(b)) or the midface (u_1; figure 14(c)). A horizontal geophone in the seismic piezocone (figure 14(d)) can be used to record mechanically induced shear waves from the surface, leading to determination of shear wave arrival time (t_s) and shear wave velocity (V_s).

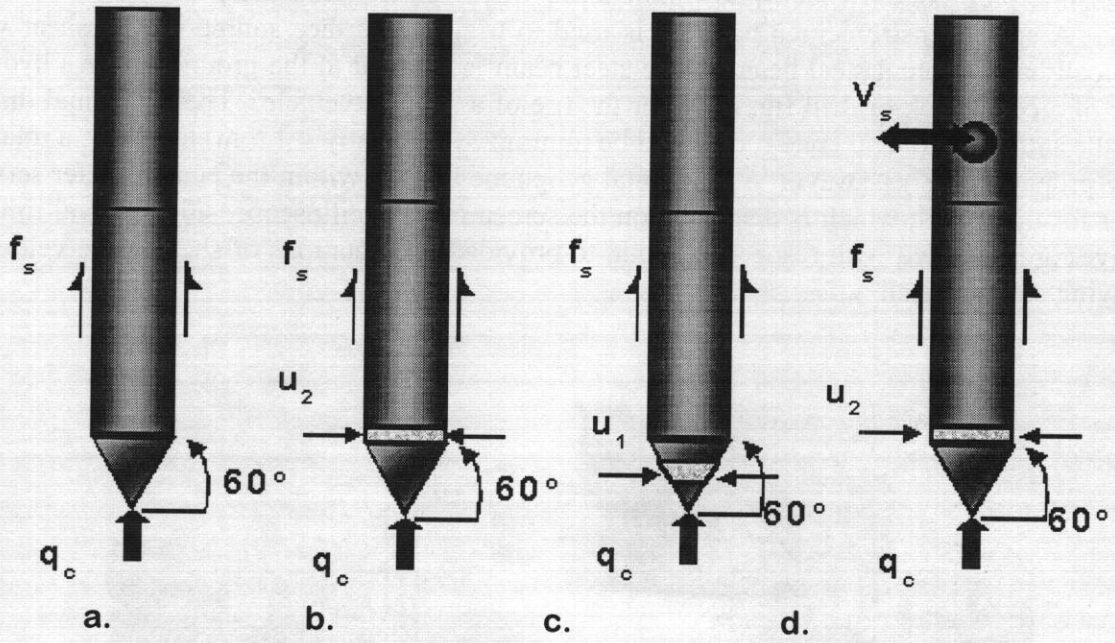

Figure 14. Measurement locations on cone penetrometers:
a. Electric Cone Penetrometer, CPT; b. Piezocone Penetrometer (filter behind tip), $CPTu_2$;
c. Piezocone Penetrometer (mid-face filter) $CPTu_1$; d. Seismic Piezocone, $SCPTu_2$.

The cone tip resistance (q_c) is the measured axial force over the projected tip area. It is a point stress related to the bearing capacity of the soil. In sands, the tip resistance is primarily controlled by the effective stress friction angle (ϕ'), relative density (D_r), and effective horizontal stress-state (σ_{ho}'). For intact clays, the tip resistance is primarily controlled by the undrained shear strength (s_u) and preconsolidation stress (σ_p'). Particularly in clays and silts, the measured q_c must be corrected for porewater pressures acting on the cone tip geometry, thus obtaining the corrected tip stress, q_t (Lunne, et al., 1997):

$$q_t = q_c + (1\text{-}a_n)u_2 \qquad \text{(Equation 6)}$$

where a_n is the net area ratio determined from laboratory calibration and u_2 is the shoulder penetration porewater pressure. The net area ratio is approximated as the ratio of the unequal end areas of the cone (see figure 15). The net area ratio (a_n) is penetrometer-specific and is obtained by isotropic pressurization of the cone in a triaxial cell. It is best to use penetrometers with an $a_n \geq 0.80$

to minimize the necessary correction, although many 15 cm^2 cones have $a_n \approx 0.75$. Contract specifications should always request the a_n calibration curves and clear indication that q_c readings have been adjusted to provide the proper q_t values. A general rule of thumb is that $q_t > 5$ MPa in sands, while $q_t < 2$ MPa in soft to medium clays and silts. It should be noted that the tip resistance in overconsolidated clays can occasionally be larger than 5 MPa.

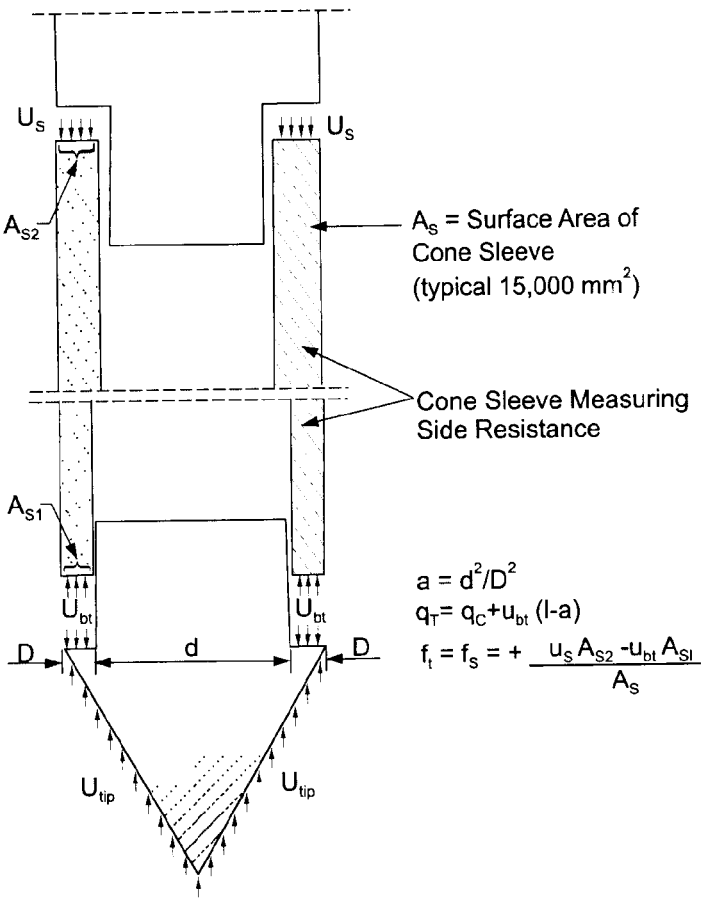

Figure 15. Illustration of unequal end areas of CPT (after Kulhawy and Mayne, 1990).

The sleeve friction (f_s) is a shear stress determined as load acting over the cylindrical surface area of a smooth sleeve. This value is often expressed as the Friction Ratio (FR) given as $f_s / q_t \times 100$, which is indicative of soil type (Lunne et al., 1997). Often, FR is less than one percent in clean sands and greater than four percent in clays and silts of low to medium sensitivity. In highly sensitive clays, FR may be approximately one percent or less.

The penetration porewater pressures are monitored using a transducer and porous filter element. These readings represent the fluid pressures between the soil particles during penetration. At the shoulder position, the pressures are near hydrostatic in sands ($u_2 \approx u_o$) whilst considerably higher than hydrostatic ($u_2 > u_o$) in soft to firm to stiff intact clays. Using values for total stress, σ_{vo}, and

hydrostatic pore pressure, u_o, the pore pressure parameter, $B_q = (u_2 - u_o) / (q_t - \sigma_{vo})$, is used as a means to normalize CPTu data for the purpose of soil classification and undrained shear strength estimation (see chapter 5 for discussion on the use of B_q for soil classification). At the mid-face location (u_1), penetration porewater pressures are always positive, while at the u_2 location measurements range from positive in intact (i.e., non fissured) materials to as low as negative one atmosphere (-100 kPa) in fissured clays and dense silts. The parameter resulting from a CPT, CPTu, and SCPTu are combined to provide several useful index and performance parameters. Details of these parameters are provided in chapter 5.

4.6 FLAT DILATOMETER TEST (DMT)

4.6.1 General

The flat plate dilatometer (DMT) involves pushing an instrumented steel blade into the subsurface soils and periodically stopping the penetration to obtain specific pressure measurements at the selected depth. No borehole cuttings or spoil are generally produced by this test, although it is possible to advance a conventional soil boring and then perform the DMT downhole within the borehole.

4.6.2 Equipment

The flat plate dilatometer system consists of a high strength steel blade, tubing, pressure gauge readout unit, and a nitrogen gas tank. The tapered steel blade is approximately 240-mm long, 95-mm wide, 15-mm thick, with an 18° wedge tip. A 60-mm diameter inflatable steel membrane exists on the face of the blade. The DMT tubing contains a wire, which is connected to an audible alarm within the control panel. The alarm notifies the operator to take specific pressure readings (i.e., the A, B, and C pressures, discussed subsequently). Figure 16 shows a flat plate dilatometer blade and the associated equipment.

4.6.3 Procedures

While there is no ASTM standard for the flat plate dilatometer (DMT), a suggested method has been outlined in Schmertmann (1986). Since the DMT operates using a pressure-based system, all connections should be sufficiently tightened with a wrench to eliminate leaks.

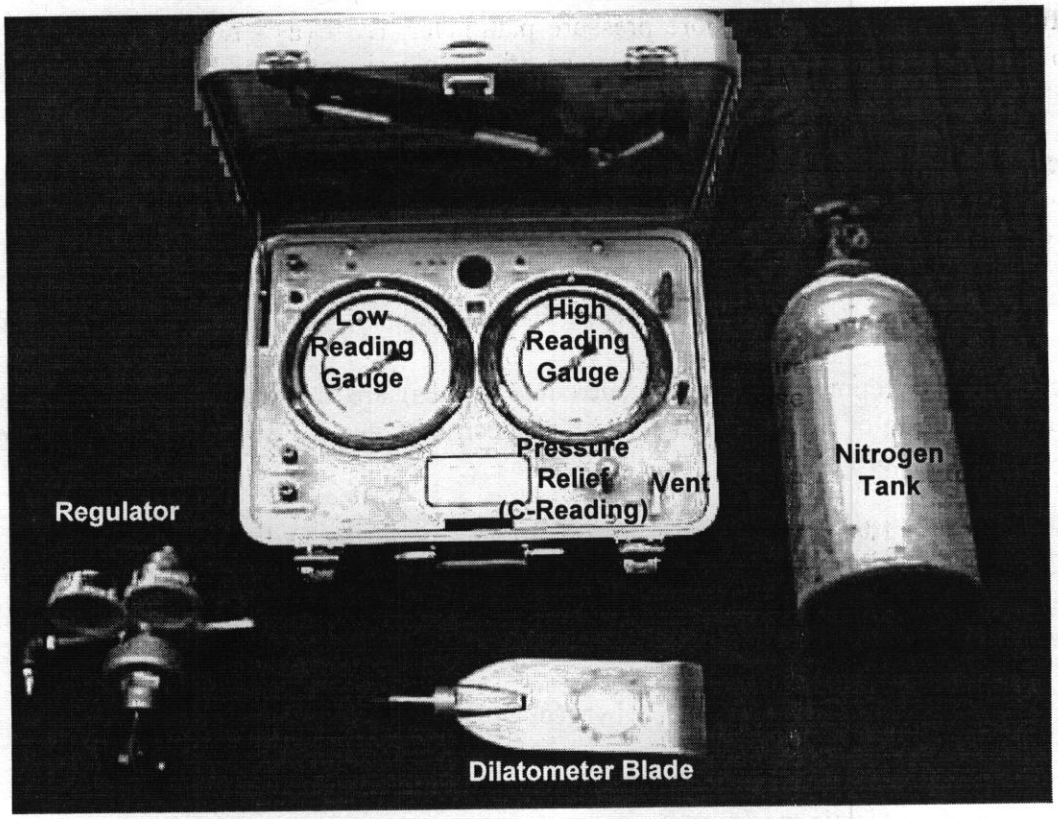

Figure 16. Flat plate dilatometer test equipment.

The blade is pushed into the ground at 20 mm/sec utilizing a similar truck and hydraulic system as described for the cone penetration test. Discrete tests are performed typically at 200-mm intervals. For each test, a 60-mm diameter flexible circular membrane on the face of the blade is inflated with nitrogen pressure to provide the A- and B-readings corresponding to the deformation, δ, of the circular membrane. Specifically the A-reading: (A) is the lift-off pressure where $\delta=0$; and the B-reading (B) is the expansion pressure where $\delta=1.1$ mm. A third reading may be recorded during deflation of the membrane and is noted as the closing pressure, or the C-reading.

The test should start within 15 seconds of reaching the desired depth, the A-reading should be taken within 15-30 seconds after beginning the test, and the B-reading should be taken within the next 15-30 seconds. After the B-reading is attained, the system is vented to prevent overexpansion of the membrane. The C-reading is recorded when the membrane is flush with the face of the blade during slow venting of the gas pressure. After deflation of the membrane, the blade is pushed to the next test depth and the inflation cycle is repeated.

4.6.4 Parameters Measured

The A- and B- readings need to be corrected for membrane stiffness effects to obtain the liftoff pressure, p_o, and expansion pressure, p_1. Correction of the readings has been presented by Schmertmann (1986):

$$p_o = 1.05(A + \Delta A - z_m) - 0.05(B - \Delta B - z_m) \quad \text{(Equation 7)}$$

$$p_1 = B - \Delta B - z_m \quad \text{(Equation 8)}$$

where ΔA and ΔB (reported as positive absolute values) are the calibration factors for applied suction and expansion of the membrane in air, respectively, and z_m is the gage offset zero reading. For a new gage, z_m is often zero.

The two dilatometer pressures, p_o and p_1, are combined with the hydrostatic water pressure, u_o, to provide three index parameters developed by Marchetti (1980). Hydrostatic water pressure should be evaluated based on available pore pressure information. The material index, I_D, is related to the soil classification and is presented as:

$$I_D = (p_1 - p_o) / (p_o - u_o) \quad \text{(Equation 9)}$$

The dilatometer modulus, E_D, is related to the compressibility of the soil. The equation for this parameter is based on elastic theory and is presented as:

$$E_D = 34.7 (p_1 - p_o) \quad \text{(Equation 10)}$$

The horizontal stress index, K_D, is related to the in-situ horizontal stress-state of the soil. The index K_D will always be greater than K_o due to disturbance caused during insertion of the blade. This parameter is presented as:

$$K_D = (p_o - u_o) / \sigma_{vo}' \quad \text{(Equation 11)}$$

A soil classification and consistency scheme has been developed utilizing the material index, I_D, and Dilatometer Modulus, E_D, and is presented in Schmertmann (1986). Other useful correlations to engineering properties are presented in chapter 5.

4.7 PRESSUREMETER TEST (PMT)

4.7.1 General

The pressuremeter test (PMT) involves inflating a cylindrical probe against the sidewalls of a boring. In general, the instrument is placed in a pre-bored hole prior to expansion, although it is possible to self-bore the instrument to the test location. The pressuremeter can be used to obtain specific strength and deformation properties of the subsurface soils.

4.7.2 Equipment

Pressuremeter equipment consists of an expandable cylindrical probe, inner rubber membrane, pressure lines, and an outer slotted tube or Chinese lantern. The pressuremeter probe may consist of either one cell or three cells that are hydraulically or pneumatically expanded to obtain a pressure versus volume curve or pressure versus radial strain curve. The inner rubber membrane is expanded at a specific test depth, and the outer slotted tube or Chinese screen expands with the membrane. The slotted tube or screen protects the membrane from punctures induced by gravel or other sharp objects.

Developments in pressuremeter testing include the self-boring pressuremeter, full displacement pressuremeter; and the cone pressuremeter. These devices do not require the independent preparation of a borehole. The latter two are thus a potentially higher production test. The self-boring pressuremeter is primarily used for research. Unfortunately, the probe penetration during a full displacement test leads to a highly disturbed zone of soil, which complicates interpretation of the field data. These instruments have not yet been extensively used on DOT projects.

Pressuremeter dimensions have not been standardized, which may lead to error when attempting to compare test data from different probes. Commonly, a 76-mm diameter probe is used and a thin walled Shelby tube can be conveniently pushed and extracted prior to the PMT. Typical probe diameters for Menard type (i.e., pre-bored) pressuremeters are presented in ASTM D 4719, and it is recommended that the length to diameter (L:D) ratio be at least 6.5L:1D to minimize end effects (see figure 17). For the full displacement and cone pressuremeters, the diameter is typically that of a 15 cm^2 cone (43.7 cm) and the suggested length to diameter ratio is 10L:1D

4.7.3 Procedures

The most important aspect of the pressuremeter test (ASTM D 4719) is the preparation of the borehole. The sidewalls of the borehole should be smooth, consistent, and of the appropriate uniform diameter. The borehole should not be less than 1.03D, or greater than 1.2D, where D is the initial diameter of the pressuremeter.

The PMT proceeds by incrementally increasing the inflation pressure while monitoring the radial deformation or volume. A loading increment should be selected to yield accurate results without producing an excessively long test. Seven to ten load increments of 25 to 200 kPa are typically used, depending upon the anticipated soil conditions. Loading increments are generally applied at typically one to three minute intervals. Operator judgment and experience are typically used in deciding when it is appropriate to increase or decrease the load. In general, the load versus deformation response is monitored and when the response stabilizes under a given load, the next load increment is applied.

It is good practice to perform the PMT using a phase of monotonic loading, a phase including a drained creep test, and at least one unload-reload cycle. The purpose of the creep test is to assess the time-dependent deformation behavior of the material. In a creep test, a constant pressure is maintained in the pressuremeter and the corresponding time-dependent deformation is recorded.

Depending on the soil type and the magnitude of the staged load, the creep testing stage may take several minutes to as long as an hour. In general, this test should be conducted for approximately 5 to 10 minutes for a clayey soil, for 3 to 5 minutes for silty soils, and for 2 to 3 minutes for sandy soils. Within these time periods, the displacement of the membrane is anticipated to have generally stabilized. Soft soils at a high load ratio will require the longest time to complete.

The purpose of unload-reload cycle is primarily to assess the elastic behavior of the material. Since the initial loading includes disturbance effects as well as both recoverable and irrecoverable deformations, an evaluation of the "elastic" modulus based on the initial pressuremeter response will likely underestimate the actual small-strain deformations of the material during loading under the field-applied stress. In general, it is recommended to include approximately two unload steps and three to four reload steps for each unload-reload cycle. To avoid inducing plastic deformations during the unloading cycle, it is recommended that no more than 80 percent of the applied pressure be removed before the reload cycle is initiated. In addition, care must be taken to release the pressure slowly during the unload cycle to allow the pressure in the pressuremeter membrane to equilibrate with the gage pressure when the pressure and deformation readings are recorded. If not conducted carefully, the membrane will appear to move outward when the pressure is decreased, because the pressure in the membrane will actually be higher than the gage pressure. If time permits (i.e., an unload–reload cycle may take nearly as long to complete as a monotonic-loading only pressuremeter test), it is recommended to run more than one unload-reload test. Finally, it is desirable to conduct one of the unload-reload cycles prior to achieving the yield pressure, p_f.

A typical pressuremeter curve for pre-bored Menard type pressuremeter is shown on figure 18. This shows a monotonic loading stage, followed by an unload-reload cycle, a creep stage, a second unload-reload cycle and a final monotonic load increase.

4.7.4 Parameters Measured

The following characteristic pressures on the pressuremeter curve are shown on figure 18:

- p_o – the pressure at which recompression of the disturbed soil is complete and expansion into undisturbed soil is started.
- p_f – an inflection point known as the creep or yield pressure where the soil changes from pseudo elastic to plastic where shear is initiated.
- Creep test – prior to performing an unload reload test, a creep test should be performed. This allows deformation to continue at a constant pressure until strain rates of 0.1%/min are recorded.
- p_u – the minimum pressure during unloading, in the unload – reload cycle.
- p_r – the yield point during the reloading portion of an unload – reload cycle where recompression ends and the soil reinitiates plastic shearing.

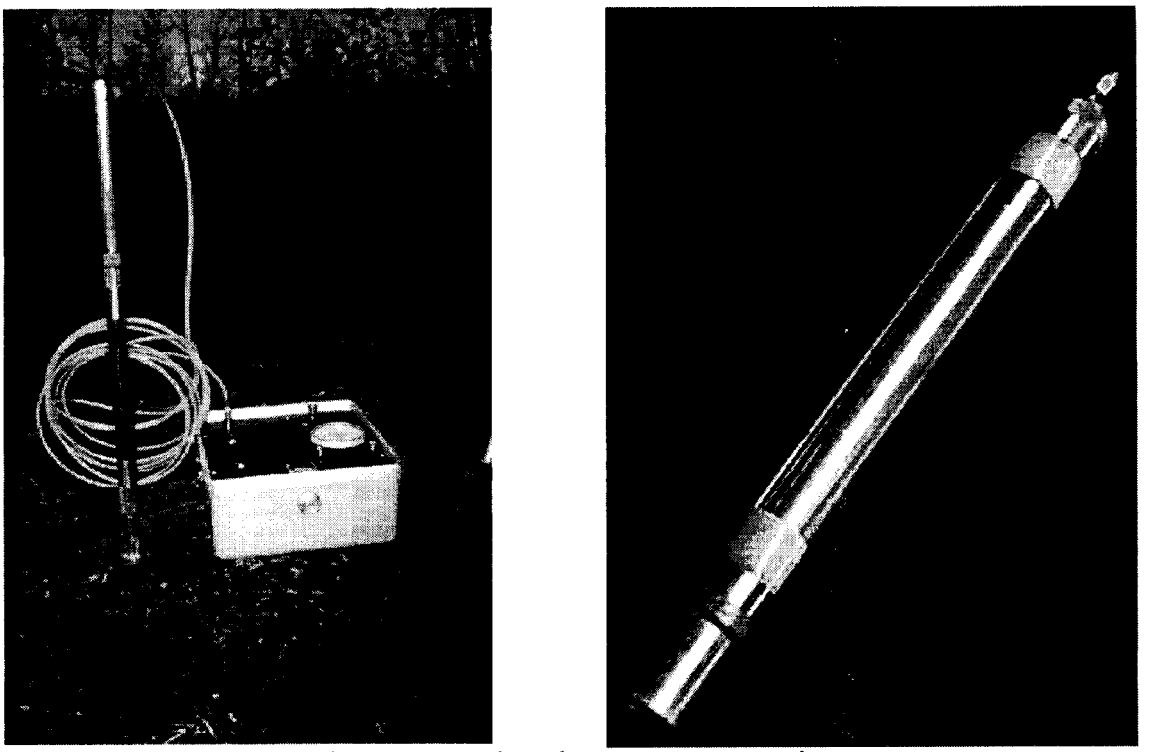

Figure 17. Pre-bored pressuremeter equipment.

- p_L – the limit pressure where the curve becomes asymptotic on a pressure versus volume curve. The value of p_L is taken as the extrapolated pressure when the volume is equal to $2 \cdot V_o$, where V_o is the initial volume of the pressuremeter.

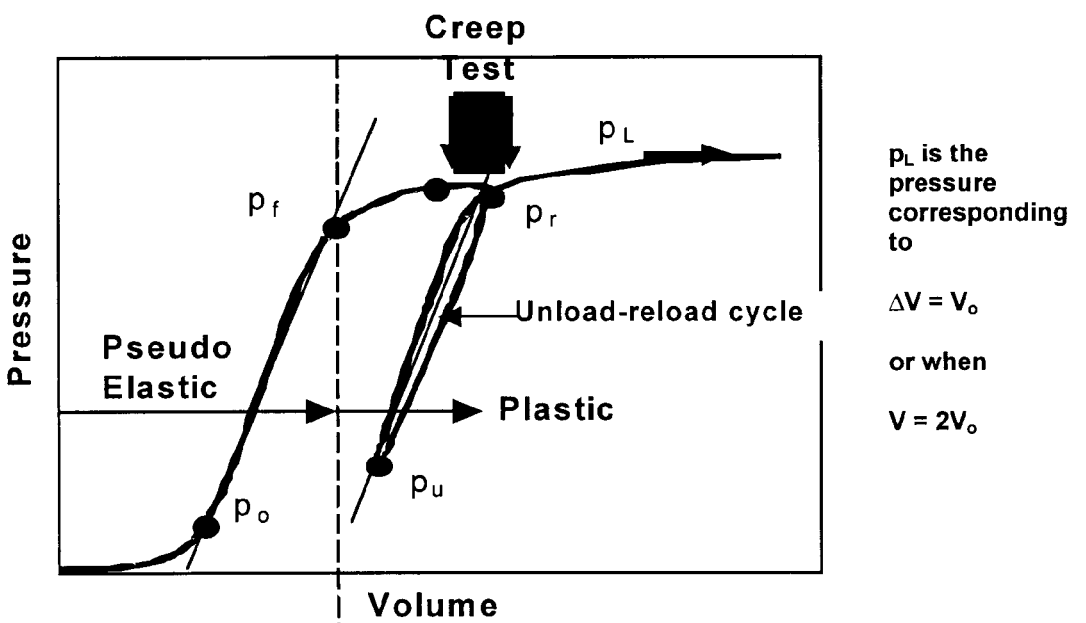

Figure 18. Typical curves and characteristic pressures for pre-bored Menard pressuremeter.

The pseudo-elastic modulus from pressuremeter tests is calculated by one of two methods, depending upon whether the data are plotted on an applied stress versus probe volume curve or an applied stress versus probe radius curve. The equation to calculate the pressuremeter elastic modulus from an applied stress versus probe volume curve is (ASTM D 4719):

$$E_P = 2(1+\nu)(V_0 + V_m)\frac{\Delta P}{\Delta V} \qquad \text{(Equation 12)}$$

where ν is the Poisson ratio (usually taken as 0.33), V_0 is the initial volume of the probe, V_m is the average volume of the probe over the stress range of consideration (i.e., $(V_{final} - V_{initial})/2$ for a given stress increment), and $\Delta P / \Delta V$ is the slope of the linear portion of the stress versus probe volume curve (between p_o and p_f or between p_u and p_r). If the slope is taken as the unload-reload portion of the curve, this should be noted as $E_{u\text{-}r}$.

The equation to calculate the pressuremeter elastic modulus from an applied stress versus probe radius curve is (ASTM D 4719):

$$E_P = (1+\nu)(R_P + \Delta R_m)\frac{\Delta P}{d\Delta R} \qquad \text{(Equation 13)}$$

where ν is the Poisson ratio (usually taken as 0.33), R_P is the uninflated radius of the probe, ΔR_m is the increase in radius of the probe to where E_p is measured, and $\Delta P / d\Delta R$ is the slope of the linear portion of the applied stress versus radius curve between p_o and p_f or p_u and p_r.

4.8 VANE SHEAR TEST (VST)

4.8.1 General

The vane shear test (VST) involves the use of a simple rotated blade to evaluate the undrained shear strength in soft to stiff clays and silts. The use of the VST should be limited to soils in which slow (6^o / min) rotation of the blade will lead to undrained shearing.

4.8.2 Equipment

Equipment necessary for a VST includes a four-sided vane with a height to diameter (H/D) ratio of 2, rods, and a torque-measuring device. Additional equipment may include a rod sheath, protection shoe, or slip coupling to account for rod friction, and a gear drive to provide a constant rate of rotation.

The standard vane has a diameter (D) of 65 mm, a height (H) of 130 mm, and a vane edge thickness (t) of 2 mm. However, vane sizes range from a diameter of 38 to 92 mm, a height of 76 to 184 mm, a blade thickness between 1.6 and 3.2 mm, and are attached to a 12.7-mm diameter rod. The rod diameter may need to be increased in stiff materials to prevent yielding of the rod during rotation. The vane may be rectangular, double-tapered, or single-tapered (i.e., tapered at the bottom of the

vane). Using a tapered vane will facilitate placement of the vane in stiffer materials. A typical vane and a summary of the geometric parameters used to identify a vane are provided in figure 19.

Vane size selection is a function of the anticipated strength of the soil and accuracy of the torque wrench. Larger vanes are typically used in soft soils and smaller vanes used in stiffer soils. While a large vane will provide better resolution than a smaller vane, it may cause more disturbance during insertion, be more difficult to rotate and thus lead to additional disturbance, or result in loads that overstress the capacity of the torque wrench. A number of different sized vanes, as well as torque wrenches with varying capacity, should be brought to the field to accommodate potentially variable conditions.

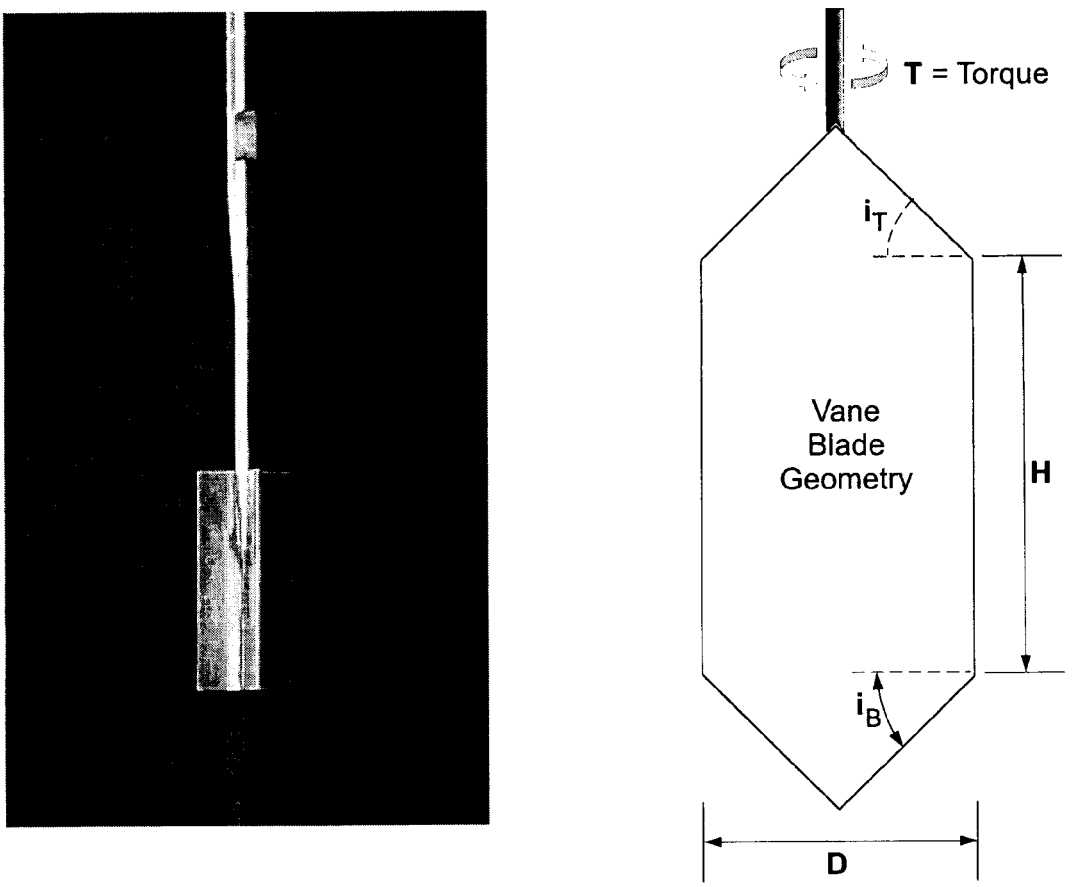

Figure 19. (a) Rectangular vane; and (b) Parameters used to define vane dimensions.

4.8.3 Procedures

Procedures for the vane shear test are outlined in ASTM D 2573. Depending upon what type of vane shear device is used, there is the potential for friction to develop along the rod. The torque-

measuring equipment can record this friction. This rod friction needs to be minimized and accounted for in the calculation of shear strength. Typical methods to account for rod friction include: (1) rods protected within a sheath; or (2) measurement of rod friction with a slip coupling. If the vane test is performed below the bottom of a borehole, the depth to the top of the vane from the bottom of the borehole should be equal to about 4 borehole diameters to minimize disturbance effects.

The VST should be started within 5 minutes of insertion, and the vane should be rotated at 6° per minute. This usually results in a time to failure between 2 and 5 minutes and is usually fast enough to assure undrained conditions, but time to failure may be up to 10 to 15 minutes in very soft clays. Readings of torque at 30 second to 1-minute intervals are recommended to provide an assessment of the soil response. Additionally, systems are currently available which record the applied torque with time or angle of rotation. Systems that use a gear drive to rotate the vane can eliminate some of the potential operator error, but limit the flexibility necessary to test extremely soft soils.

4.8.4 Parameters Measured

Three parameters can be obtained from the vane shear test: (1) undrained shear strength ($s_{u,VST}$); (2) remolded undrained shear strength ($s_{r,VST}$); and (3) sensitivity ($S_{t,VST}$). It should be noted that the subscript VST is added to each parameter to note that the parameter was obtained using vane shear test data. The undrained shear strength, remolded shear strength, and sensitivity will differ depending upon the mode of shear, as well as the strain level and degree of remolding.

During rotation, the torque (T) is measured and the maximum torque (T_{max}) is used to calculate the undrained shear strength based on the vane geometry. Prior to calculation of undrained shear strength ($s_{u,VST}$), the torque associated with rod friction (T_{rod}) must be subtracted from the measured torque ($T_{net} = T_{max} - T_{rod}$). Best practice involves using a sheath (or a slip coupling) to eliminate rod friction, and thus T_{net} would equal T_{max}. The undrained shear strength for a standard rectangular vane (H/D = 2) is expressed as:

$$s_{u,VST} = \frac{6T_{net}}{7\pi D^3} \qquad \text{(Equation 14)}$$

where D is the diameter of the vane (see figure 19). For the general case of rectangular or tapered vanes, the following equation is used to calculate undrained shear strength:

$$s_{u,VST} = \frac{12T_{net}}{\pi D^2\left(D/\cos i_T + D/\cos i_B + 6H\right)} \qquad \text{(Equation 15)}$$

where D is the diameter of the vane, H is the height of the vane, i_B is the angle of taper at the bottom, and i_T is the angle of taper at the top. These parameters are graphically displayed in figure 19(b).

The remolded strength is achieved in the same manner as the peak strength, except the torque reading is taken during rotation of the vane following 10 rapid turns. The torque associated with rod

friction should be recorded prior to the remolded test, and then subtracted from the maximum torque recorded for calculations of $s_{r,VST}$. The sensitivity of the soil from vane shear tests is expressed as:

$$S_{t,VST} = \frac{s_{u,VST}}{s_{r,VST}} \qquad \text{(Equation 16)}$$

4.9 USE OF DRILL RIGS TO PERFORM IN-SITU TESTS

When using a drill rig to perform in-situ tests such as the CPT, DMT, and PMT, it will be necessary to carefully pass wires, cables, and tubing through the drill rod and couplings. The inside diameter of the coupling will typically be the limiting diameter. The ends of cables will typically be the largest diameter of the cable or tubing system and should therefore be smaller than the diameter of the drill rod couplings. Typically, AW drill rod is used when CPTs are performed from drill rigs. Wires, cables, and tubing will need to exit through a coupling at the ground surface. The top coupling should have a slot in the side to enable cables and tubing to pass through without being pinched or cut.

It is important to ensure that the adapter for the in-situ testing device be appropriately attached to the drill rod. Threads for the CPT and DMT are usually proprietary and manufacturers of CPT and DMT equipment do not typically have drill rod adapters readily available. For this reason, it is best practice to have a drilling equipment supplier weld the CPT or DMT adapter to the appropriate drill rod coupling.

Casing may be needed to support the borehole above the zone of testing for the VST and PMT tests. Typical casing sizes are provided in FHWA HI-97-021 (1997). Appropriate casing sizes and diameters will be a function of the probe diameter and are outlined in ASTM D 2573 for the VST and ASTM D 4719 for the PMT.

If non-standard equipment is used to advance the probe, such as a drill rig or GeoProbe truck, the time for advancement of each rod should be recorded for CPT and DMT tests. A CPT contractor may be able to use the data acquisition system to record time of penetration along with depth, tip resistance, sleeve friction, and penetration pore pressure. It should be specified that the subcontractor provide time information along with depth information, if their system is capable of recording time. The penetration should be maintained relatively constant, at a rate of 20 $\pm$ 5 mm/sec for the CPT and DMT. Any pauses in penetration should be noted on a log.

4.10. IN-SITU TESTING IN ROCK

4.10.1 General

In-situ testing to evaluate rock mass deformation modulus and shear strength is sometimes required for the design of foundations for major structures such as dams and bridges, however, such testing is not performed for structural foundations or slopes associated with typical highway applications. Circumstances where in-situ rock testing may be carried out for highway projects include

foundations comprising closely fractured and weak rock that could compress, resulting in settlement of the structure, or continuous, low strength discontinuities on which sliding could take place. The need for in-situ testing would arise when it is not possible to obtain undisturbed samples, or sufficiently large samples, for laboratory testing. This section provides an overview of specific in-situ testing methods that may be used for rock (see table 11) and is based largely on information presented in Wyllie (1999).

Three methods of in-situ deformation modulus and shear strength testing are described in this section. These include: (1) borehole dilatometer; (2) borehole jack; and (3) in-situ direct shear test.

Table 11. In-situ testing methods used in rock.

Method	Procedure	Rock Properties	Limitations / Remarks
Borehole Dilatometer	The dilatometer is lowered to the test elevation and the flexible rubber membrane is expanded exerting a uniform pressure on the sidewalls of the borehole.	Modulus of fractured rock mass	Poisson's ratio of rock must be assumed; test only affects a small area of the rock mass but several tests over the depth of influence can be performed
Borehole Jack	Jacks exert a unidirectional pressure to the walls of a borehole by means of two opposed curved steel platens	Modulus of fractured rock mass	Measured modulus value must be corrected to account for stiffness of steel platens; test method can be used to provide an estimate of anisotropy
Plate Load Test	Load is applied to a steel plate or concrete foundation using a system of hydraulic jacks and a reaction frame anchored to the foundation rock	Modulus of fractured rock mass	Loaded area is limited so may not be effectively testing rock mass if joints are widely spaced; modulus values corrected for plate geometry, effect of rock breakage, rock anisotropy, and steel plate modulus
In-situ Direct Shear Test	Testing is typically performed in an adit where reaction for the shear load is provided by an adit wall. Normal load applied via a jack system that uses the adit roof for reaction	Peak and residual shear strength of discontinuity or discontinuity infilling	Need to isolate a block of rock above the discontinuity surface without disturbing the infilling

4.10.2 Borehole Dilatometer

The borehole dilatometer is similar to the pressuremeter used in soil. At each testing depth, a uniform radial pressure is exerted on the walls of the drill hole by means of a flexible rubber sleeve. As with the pressuremeter, the volumetric expansion of the borehole can be measured by the inflation medium (generally oil or water) as the pressure is raised, or by electronic transducers that measure radial displacement of the inside of the sleeve. For the latter type, the measurement devices are generally arranged at right angles that further enables the anisotropy of the rock to be evaluated. The expansion volume of the borehole can be measured with a calibrated hand-operated screw pump. Alternatively, the volumetric expansion can be measured directly in the probe.

Because of the generally stiff character of most rock (even fractured rock), the hydraulic system should be relatively stiff and the system should be calibrated prior to and after testing. Figure 20 shows typical pressure-dilation graphs for a calibration test carried out in a material of known modulus; this figure also shows the result of a test carried out in rock. A complete test usually consists of three loading and unloading cycles, with dilation and pressure readings being taken on both the loading and unloading cycles.

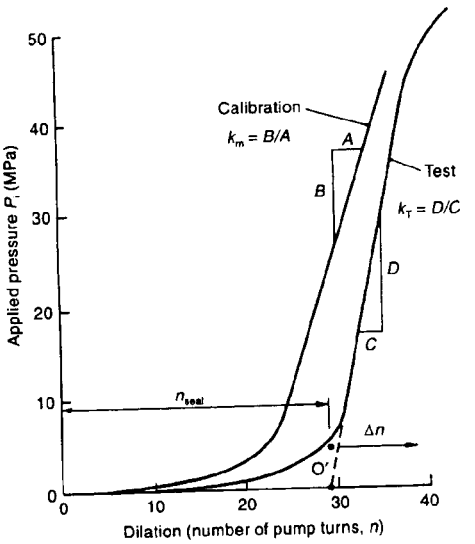

Figure 20. Typical pressure-dilation graphs for a borehole dilatometer (after ISRM, 1987).

4.10.3 Borehole Jack

As an alternative to the flexible dilatometer and in rock that may be too stiff for the dilatometer, the borehole jack (ASTM D4971) can be used to measure rock mass deformability in a drill hole. The jack exerts a directional pressure by means of semi-cylindrical steel loading platens, with the deformation being measured with linear variable differential transformers (LVDTs) built into the jack. Calculation of the modulus is carried out in a similar manner to that of the dilatometer, except that allowance must be made for the more complicated boundary conditions (i.e., pressure is not exerted uniformly in the borehole) and the relative stiffness of the steel platens compared to the in-situ rock mass.

4.10.4 In-situ Direct Shear Testing

In-situ direct shear testing is typically not performed due to the expense associated with the test setup. This test may be appropriate, however, for critical cases in which the shear strength of an undisturbed, potentially sensitive, infilling is required for design analyses. In cases where the infilling is displaced, it is likely that laboratory direct shear tests carried to residual conditions on recompacted infilling material would be sufficient. Figure 21 shows a schematic illustration of an

in-situ direct shear test performed in an adit. Testing can be conducted on a rock surface using cables anchored into the rock adjacent to the test site to supply the reaction for loading in the direction normal to the shear load.

Legend:

1. Rock anchor
2. Hand-placed concrete
3. Wide flange steel beam
4. Hardwood
5. Steel plates
6. 30 ton jack
7. Dial gauge
8. Steel rollers
9. Reinforced concrete pad
10. Bearing plate
11. Styrofoam
12. 50 ton jack
13. Steel ball

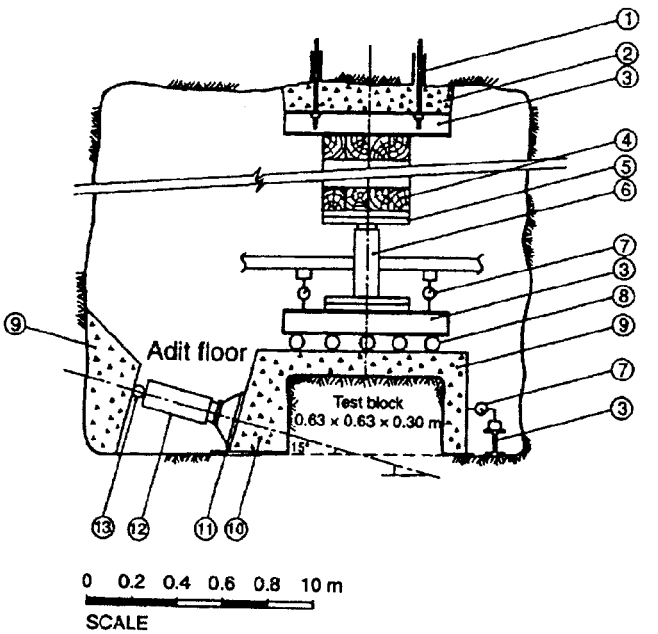

Figure 21. Typical setup for an in-situ direct shear test in an adit (after Saint Simon et al., 1979).

4.11 GEOPHYSICAL TESTING

Geophysical testing is often used as part of the initial site exploration phase of a project and/or to provide supplementary information collected by widely-spaced observations (i.e., borings, test pits, outcrops etc.). Geophysical testing can be used for establishing stratification of subsurface materials, the profile of the top of bedrock, depth to groundwater, limits of types of soil deposits, rippability of hard soil and rock, and the presence of voids, buried pipes, and depths of existing foundations. Data from geophysical testing should always be correlated with information from direct methods of exploration.

Geophysical testing offers some notable advantages and some disadvantages that should be considered before the technique is recommended for a specific application. The advantages are summarized as follows:

- Many geophysical tests are non-invasive and thus offer significant benefits in cases where conventional drilling, testing, and sampling are difficult (e.g., deposits of gravel, talus deposits) or where potentially contaminated soils may occur in the subsurface.

- In general, geophysical testing covers a relatively large area, thus providing the opportunity to characterize large areas with few tests. It is particularly well-suited to projects that have large longitudinal extent compared to lateral extent (such as for new highway construction).

- Geophysical measurement assesses the characteristics of soil and rock at very small strains, typically on the order of 0.001 percent thus providing information on truly elastic properties.

- For the purpose of obtaining information on the subsurface, geophysical methods are relatively inexpensive when considering cost relative to the relatively large areas over which information can be obtained.

Some of the general disadvantages of geophysical methods include:

- Most methods work best for situations in which there is a large difference in stiffness between adjacent subsurface units.

- It is difficult to develop good stratigraphic profiling if the general stratigraphy consists of hard material over soft material

- Results are generally interpreted qualitatively and therefore useful results can only be obtained by an experienced engineer or geologist familiar with the particular testing method.

- Specialized equipment is required (compared to more conventional subsurface exploration tools).

There are a number of different geophysical in-situ tests that can be used for stratigraphic information and in the determination of engineering properties. Table 12 provides a summary of the various geophysical methods that are currently available in U.S. practice. Additional information on the procedures used for these methods is provided in AASHTO (1988), FHWA-HI-97-021 (1997), and Campanella (1994). Additional general discussion regarding the major headings in table 12 is presented, with particular emphasis on the potential application to highway engineering.

- Seismic Methods: These methods are becoming increasingly popular for highway and general geotechnical engineering practice, as they have the potential to provide quantitative data regarding the shear wave velocity of the subsurface materials. The shear wave velocity is directly related to small-strain material stiffness, which in turn, is often correlated to strength and soil/rock type. As such, these techniques are often used for assessing the vertical stiffness profile in a soil deposit and for assessing the interface between soil and rock.

- Electrical Methods: These methods are usually used when attempting to locate voids or locally distinct materials. With regards to highway applications, these procedures may be applicable for assessing the potential for karst activity along a potential transmission corridor, or for locating specific underground drums and/or voids. The techniques provide qualitative information only and are usually part of a two- or three-phased investigation program.

Table 12. Geophysical testing techniques.

Method	Basic Field Procedures	Applications	Limitations
SEISMIC METHODS			
Seismic Refraction	Impact load is applied to the ground surface. Seismic energy refracts off soil/rock layer interfaces and is recorded on the ground surface using several dozen geophones positioned along a line or performing repeated events using a single geophone.	• depth to bedrock • depth to water table • thickness and relative stiffness soil/rock layers	• does not work if stiffness decreases with depth or if soft layer underlies stiff layer • works best when sharp stiffness discontinuity is present
Spectral-Analysis-of-Surface-Waves (SASW) (additional information provided in section 5.5.4.2)	Impact load is applied to the ground surface. Surface waves propagate along ground surface and are recorded on the ground surface with two geophones positioned along a line.	• depth to bedrock • measurement of shear wave velocity • thickness and stiffness of surface pavement layer • qualitative indicator of cracking in pavement	• resolution decreases significantly with increasing depth • accurate interpretation may require a significant amount of expertise • interpretation is difficult if a stiff layer overlies a soft layer and soft layer properties are desired
ELECTRICAL METHODS			
DC Resistivity	DC current is applied to the ground using electrodes. Voltages are measured at different points on the ground surface with other electrodes positioned along a line.	• depth to water table • inorganic groundwater contamination • groundwater salinity • soil layer thickness • delineation of certain vertical features (e.g., sinkholes, contamination plumes, waste trenches)	• slow; must install electrodes directly in the ground • resolution decreases significantly with increasing depth • resolution is difficult in highly heterogeneous deposits
Electromagnetics	Electrical coils are held over the ground. Current passing through the coils induces a magnetic field in the ground, which is measured with receiver coils.	• groundwater salinity • inorganic groundwater contamination • detection of buried metal objects • delineation of certain vertical features (e.g., sinkholes, contamination plumes, waste trenches)	• extra effort is required to characterize depth of target • resolution decreases significantly with increasing depth
Ground Penetrating Radar (GPR)	Electromagnetic energy is pulsed into the ground. This energy reflects off boundaries between different soil layers and is measured at the ground surface.	• depth to water table • identification of buried objects • thickness of pavement layers • void detection	• not effective below the water table or in clay • depth of penetration is limited to about 10 meters

Table 12. Geophysical testing techniques (continued).

Method	Basic Field Procedures	Applications	Limitations
GRAVITY AND MAGNETIC METHODS			
Gravity	The Earth's gravitational field is measured at the ground surface.	• identification of subsurface voids • identification of large objects possessing unusually high or low densities	• results are non-unique (i.e. more than one subsurface condition can give the same results) • primarily, large-scale reconnaissance tool; applications in engineering are limited
Magnetics	The Earth's magnetic field is measured at the ground surface.	• identification of ferrous materials • identification of soil/rock containing large amounts of magnetic minerals	• results are non-unique (i.e. more than one subsurface condition can give the same results) • primarily a large-scale reconnaissance tool; applications in engineering are limited
NEAR-SURFACE NUCLEAR METHODS			
Neutron Moisture Content	Instrument is placed on the ground surface and neutrons are emitted into the ground. Energy of returning neutrons is related to the moisture content in the ground (hydrogen atoms decrease the energy of the neutrons detected at the sensor).	• estimate of water content in compacted soil • estimate of asphalt content in asphalt concrete • can be quantitative if properly calibrated to site conditions	• limited investigation depth (a few inches) • possible health and safety hazard if operators not properly trained • will detect hydrogen ion (i.e. gas, clay) in non-water bearing stratum
Gamma Density	Instrument is placed on the ground surface and gamma radiation is emitted into the ground. Returning gamma energy is a function of material density (denser materials absorb more gamma energy so less is detected at the sensor)	• estimate of density of soil or asphalt concrete	• limited investigation depth (less than one foot); • investigation depth further limited to a few inches if ground cannot be penetrated • possible health and safety hazard if operators not properly trained

Table 12. Geophysical testing techniques (continued).

Method	Basic Field Procedures	Applications	Limitations
BOREHOLE METHODS			
Crosshole/ Downhole (additional information provided in section 5.5.4.2)	Energy sources and geophones are placed in boreholes and/or on ground surface; interval travel times are converted into seismic wave velocity as a function of depth in the borehole	• measurement of wave velocities for seismic site response analysis • depth to water table • correlation of lithologic units with surface seismic • identification of thin layers at depth	• requires one or more boreholes and significant support field equipment
Suspension Logger	Field instrument is placed in a fluid-filled borehole and used to measure P- and S-wave velocities in surrounding soil or rock.	• measurement of wave velocities for seismic site response analysis • correlation of lithologic units with surface seismic • identification of thin layers at depth	• requires borehole and significant support field equipment, which is expensive • borehole must be fluid-filled
Electrical Logging	Field instrument is placed in a borehole. Electrical fields are directly applied or electromagnetically induced into surrounding soil or rock and electrical resistivity is measured.	• estimate of soil/rock permeability or porosity • identification of inorganic contaminant plumes or saltwater intrusion • identification of thin layers at depth	• requires borehole and significant support field equipment, which is expensive • generally cannot operate in a cased borehole • may require fluid-filled borehole • results may be dependent upon drilling mud salinity
Nuclear Logging	Field instrument is placed in a borehole. Surrounding soil or rock is irradiated with neutrons particles and/or gamma energy. Energy and neutrons returning to the instrument are measured and related to rock density, porosity and pore fluid type.	• estimate of soil/rock type, density, porosity, and pore fluid density • identification of thin layers at depth	• requires borehole and significant support field equipment, which is expensive • possible health and safety hazard if operators are not properly trained
Lithology Logging	Field instrument is placed in a borehole; naturally occurring electrical fields and radiation levels are related to soil or rock type	• classification of soil or rock type • identification of thin layers at depth	• requires borehole and significant support field equipment, which is expensive • may require fluid-filled borehole • results are dependent upon site-specific conditions and/or borehole fluid salinity

- Gravity and Magnetic Methods: These methods are similar to the previously described electrical methods, except that they rely on the correlations between the influence of voids and subsurface anomalies and differences in the earth's micro-gravitational field and/or the magnetic fields, rather than the changes in the electrical fields.

Near-surface Nuclear Methods: These techniques have been used for several years in the field of soil construction. Through careful calibration, it is possible to reliably assess the moisture content and density of compacted soils. These techniques have gained widespread adoption as reliable quantitative techniques

Borehole Methods: Downhole geophysical techniques have been recognized as providing reliable indications of a wide range of soil properties. The downhole/crosshole techniques have proven to provide reliable measure of shear wave velocity. As reported previously, this parameter is directly related to small-strain stiffness and is correlated to strength and soil type. The downhole logging techniques have seen little use in highway construction, but they have been the mainstay for deep geologic characterization in oil exploration and deep geologic characterization. The principal advantage is the ability to obtain several different geophysical tests/ indicators by "stringing" these tools together in a deep boring.

With specific regards to highway construction, the authors have identified a few typical examples where geophysical testing could be used to compliment conventional exploration.

Highly Variable Subsurface Conditions: In several geologic settings, the subsurface conditions along a transportation corridor may be expected to be variable. This variability could be from underlying karst development above limestone, alluvial deposits, including buried terrace gravels, across a wide floodplain, buried boulders in a talus slope. For these cases, conventional exploration techniques may be very difficult and if "refusal" is encountered at one depth, there is a strong likelihood that different materials underlie the region. In these cases, a preliminary subsurface characterization profile using geophysical testing could prove advantageous in designing future focused investigations.

Regional Studies: Along a transmission corridor it may be necessary to assess the depth to (and through) rippable rock. Alternative alignments may or may not be possible, but the cost implications may be significant. Therefore, it is important to obtain a profile related to rock/soil stiffness. Geophysical testing is a logical consideration for this application, as a precursor to invasive investigation.

Settlement Sensitive Structures: The prior two examples related to cases where the geophysical testing served as the front–end of a multi-phase project. In the case where a settlement-sensitive structure is to be founded on deposits of sands, the in situ modulus of the sand deposit is critical. After assessing the characteristics of the site, it may be helpful to quantify the deformation modulus via geophysical testing at the specific foundation site.

These examples demonstrate that geophysical testing has a potentially important role in the subsurface characterization of soils and rocks. Like the other "tools" described in this document, the particular selection of the appropriate technology is very much a function of the site conditions and

the goals of the characterization program. In this document, focus is placed on geophysical testing techniques that can be used to measure soil shear wave velocity, V_s, such as seismic refraction, SASW, and seismic cone penetrometer. The relevance and evaluation of this parameter for static deformation analysis of various geotechnical structures is provided in chapter 5.

4.12 LABORATORY SOIL TESTING

4.12.1 Introduction

Laboratory testing of soil samples recovered during subsurface explorations is the most common technique to obtain engineering properties necessary for design. A laboratory-testing program consists of index tests to obtain general information on material consistency and performance tests to measure specific properties (e.g., shear strength, compressibility, hydraulic conductivity) for design and constructability assessments. This section provides information on common laboratory test methods for soil including testing equipment, general procedures related to each test, and parameters measured by the tests. A discussion of the interpretation of these tests to obtain properties is provided in chapter 5.

Laboratory soil testing will be required for most projects and it is therefore necessary to appropriately select the types and quantities of laboratory tests to be performed. A careful review of all data obtained during the field investigation is essential to developing an appropriately scoped laboratory-testing program. In some cases, owners may wish to hire external testing laboratories to perform select tests. It is necessary that testing requests be clear and sufficiently detailed. Unless specialized testing is required, the owner should require that all testing be performed in accordance with appropriate specification for laboratory testing such as those codified in AASHTO and ASTM. Table 13 provides a listing of commonly-performed laboratory tests. Tables 14 and 15 provide a summary of typical soil index and performance tests, respectively. Additional information on these tests is provided in subsequent sections.

4.12.2 Quality Assurance for Laboratory Testing

4.12.2.1 Sample Tracking

Whether the laboratory testing is performed in-house or is subcontracted, samples will likely be assigned a laboratory identification number that differs from the identification number assigned in the field. A list should be prepared which matches the laboratory identification number with the field identification number. This list can also be used to provide tracking information to ensure that each sample arrived at the lab. When requesting laboratory testing, both the field identification number and the laboratory identification number should be used on the request form. A spreadsheet or database program is useful to manage sample identification data.

Table 13. Common soil laboratory tests.

Test Category	Name of Test	Test Designation	
		AASHTO	ASTM
Visual Identification	Practice for Description and Identification of Soils (Visual-Manual Procedure)	-	D 2488
	Practice for Description of Frozen Soils (Visual-Manual Procedure)	-	D 4083
Index Properties	Test Method for Determination of Water (Moisture) Content of Soil by Direct Heating Method	T 265	D 2216
	Test Method for Specific Gravity of Soils	T 100	D 854; D 5550
	Method for Particle-Size Analysis of Soils	T 88	D 422
	Test Method for Classification of Soils for Engineering Purposes	M 145	D 2487; D 3282
	Test Method for Amount of Material in Soils Finer than the No. 200 (75-μm) Sieve		D 1140
	Test Method for Liquid Limit, Plastic Limit, and Plasticity Index of Soils	T 89; T 90	D 4318
Compaction	Test Method for Laboratory Compaction Characteristics of Soil Using Standard Effort (600 kN. m/m^3)	T 99	D 698
	Test Method for Laboratory Compaction Characteristics of Soil Using Modified Effort (2,700 kN.m/m^3)	T 180	D 1557
Strength Properties	Test Method for Unconfined Compressive Strength of Cohesive Soil	T 208	D 2166
	Test Method for Unconsolidated, Undrained Compressive Strength of Cohesive Soils in Triaxial Compression	T 296	D 2850
	Test Method for Consolidated, Undrained Compressive Strength of Cohesive Soils in Triaxial Compression	T 297	D 4767
	Method for Direct Shear Test of Soils under Consolidated Drained Conditions	T 236	D 3080
	Test Methods for Modulus and Damping of Soils by the Resonant-Column Method	-	D 4015
	Test Method for Laboratory Miniature Vane Shear Test for Saturated Fine-Grained Clayey Soil	-	D 4648
	Test Method for CBR (California Bearing Ratio) of Laboratory-Compacted Soils	-	D 1883
	Test Method for Resilient Modulus of Soils	T 294	-
	Test Method for Resistance R-Value and Expansion Pressure of Compacted Soils	T 190	D 2844
Consolidation and Swelling Properties	Test Method for One-Dimensional Consolidation Properties of Soils	T 216	D 2435
	Test Method for One-Dimensional Consolidation Properties of Soils Using Controlled-Strain Loading	-	D 4186
	Test Methods for One-Dimensional Swell or Settlement Potential of Cohesive Soils	T 258	D 4546
	Test Method for Measurement of Collapse Potential of Soils	-	D 5333
Permeability	Test Method for Permeability of Granular Soils (Constant Head)	T 215	D 2434
	Test Method for Measurement of Hydraulic Conductivity of Saturated Porous Materials Using a Flexible Wall Permeameter	-	D 5084
Corrosivity	Test Method for pH for Peat Materials	-	D 2976
	Test Method for pH of Soils	-	D 4972
	Test Method for pH of Soil for Use in Corrosion Testing	T 289	G 51
	Test Method for Sulfate Content	T 290	D 4230
	Test Method for Resistivity	T 288	D 1125; G57
	Test Method for Chloride Content	T 291	D 512
Organic Content	Test Methods for Moisture, Ash, and Organic Matter of Peat and Other Organic Soils	T 194	D 2974

Table 14. Methods for index testing of soils.

Test	Procedure	Applicable Soil Types	Applicable Soil Properties	Limitations / Remarks
Moisture Content, w_n	Dry soil in oven at 100 ± 5 °C	Gravel, sand, silt, clay, peat	e_o, γ	Simple index test for all materials
Unit Weight and Density	Extract a tube sample; measure dimensions and weight;	Soils where undisturbed samples can be taken, i.e., silt, clay, peat	γ_{tot}, γ_{dry}, ρ_{tot}, ρ_{dry}, σ_{vo}	Not appropriate for clean granular materials where undisturbed sampling is not possible. Very useful index test.
Atterberg Limits, LL, PL, PI, SL, LI	LL – Moisture content associated with failure at 25 blows of specimen in Casagrande cup PL – Moisture content associated with crumbling of rolled soil at 3.2 mm	Clays, silts, peat; silty and clayey sands to determine whether SM or SC	Soil classification	Not appropriate in non-plastic granular soil. Recommended for all plastic materials.
Mechanical Sieve	Place air dry material on a series of successively smaller screens of known opening size and vibrate to separate particles of a specific equivalent diameter	Gravel, sand, silt	Soil classification	Not appropriate for clay soils. Useful, particularly in clean and dirty granular materials
Wash Sieve	Flush fine particles through a U.S. No. 200 sieve with water;	Sand, silt, clay	Soil classification	Needed to assess fines content in dirty granular materials
Hydrometer	Allow particles to settle, and measure specific gravity of the solution with time.	Fine sand, silt, clay	Soil classification	Helpful to assess relative quantity of silt and clay
Specific Gravity	The volume of a known mass of soil is compared to the known volume of water in a calibrated pyncnometer	Sand, silt, clay, peat	Used in calculation of e_o	Particularly helpful in cases where unusual solid minerals are encountered
Organic Content	After performing a moisture content test at 110 °C, the sample is ignited in a muffle furnace at 440 °C to measure the ash content.	All soil types where organic matter is suspected to be a concern	Not related to any specific performance parameters, but samples high in organic content will likely have high compressibility	Recommended on all soils suspected to contain organic materials

Symbols used in table 14.

e_o: in-situ void ratio
γ: unit weight
γ_{tot}: total unit weight
γ_{dry}: dry unit weight
ρ_{tot}: total density
ρ_{dry}: dry density
σ_{vo}: total vertical stress

Table 15. Methods for performance testing of soils.

Test	Procedure	Applicable Soil Types	Soil Properties	Limitations / Remarks
1-D Oedometer	Incremental loads are applied to a soil specimen confined by a rigid ring; deformation values are recorded with time; loads are typically doubled for each increment and applied for 24 hours each.	Primarily clays and silts; Granular soils can be tested, but typically are not.	σ_p', OCR, C_c, $C_{c\varepsilon}$, C_r, $C_{r\varepsilon}$, C_{α},, $C_{\alpha\varepsilon}$, c_v, k	Recommended for fine grained soils. Results can be useful index to other critical parameters
Constant rate of Strain Oedometer	Loads are applied such that Δu is between 3 and 30 percent of the applied vertical stress during testing	Clays and silts; Not applicable to free draining granular soils.	σ_p', C_c, $C_{c\varepsilon}$, C_r, $C_{r\varepsilon}$, c_v, k	Requires special testing equipment, but can reduce testing time significantly
Unconfined Compression (UC)	A specimen is placed in a loading apparatus and sheared under axial compression with no confinement.	Clays and silts; cannot be performed on granular soils or fissured and varved materials	$s_{u,UC}$	Provides rapid means to approximate undrained shear strength, but disturbance effects, test rate, and moisture migration will effect results
Unconsolidated Undrained (UU) Triaxial Shear	The specimen is not allowed to consolidate under the confining stress, and the specimen is loaded at a quick enough rate to prevent drainage	Clays and silts	$s_{u,UU}$	Sample must be nearly saturated. Sample disturbance and rate effects will affect measured strength.
Isotropic consolidated drained compression (CIDC)	The specimen is allowed to consolidate under the confining stress, and then is sheared at a rate slow enough to prevent build-up of porewater pressures	Sands, silts, clays	ϕ', c', E	Can be run on clay specimen, but time consuming. Best triaxial test to obtain deformation properties
Isotropic consolidated undrained compression (CIUC)	The specimen is allowed to consolidate under the confining stress with drainage allowed, and then is sheared with no drainage allowed, but porewater pressures measured	Sands, silts, clays, peats	ϕ', c', $s_{u,CIUC}$, E	Recommended to measure pore pressures during test. Useful test to assess effective stress strength parameters. Not for measuring deformation properties
Direct Shear	The specimen is sheared on a forced failure plane at a constant rate, which is a function of the hydraulic conductivity of the specimen	Compacted fill materials; sands, silts, and clays	ϕ', ϕ'_r	Requires assumption of drainage conditions. Relatively easy strength test.
Flexible Wall Permeameter	The specimen is encased in a membrane, consolidated, backpressure saturated, and measurements of flow with time are recorded for a specific gradient	Relatively low permeability materials (k $\leq 1x10^{-5}$ cm/s); clays & silts	k	Recommended for fine grained materials. Backpressure saturation required. Confining stress needs to be provided. System permeability must be at least an order of magnitude greater than that of the specimen. Time needed to allow inflow and outflow to stabilize.
Rigid Wall Permeameter	The specimen is placed in a rigid wall cell, vertical confinement is applied, and flow measurements are recorded with time under constant head or falling head conditions	Relatively high permeability materials; sands, gravels, and silts	k	Need to control gradient. Not for use in fine grained soils. Monitor for sidewall leakage.

Symbols used in table 15.

ϕ':	peak effective stress friction angle	OCR:	overconsolidation ratio	$C_{c\varepsilon}$:	modified compression index
ϕ'_r	residual effective stress friction angle	c_v:	vertical coefficient of consolidation	C_r:	recompression index
c':	effective stress cohesion intercept	E:	Young's modulus	$C_{r\varepsilon}$:	modified recompression index
s_u:	undrained shear strength	k:	hydraulic conductivity	C_α:	secondary compression index
σ_p':	preconsolidation stress	C_c:	compression index	$C_{\alpha\varepsilon}$:	modified secondary compression index

4.12.2.2 Sample Storage

Undisturbed soil samples should be transported and stored so that that the moisture content is maintained as close as possible to the natural conditions (AASHTO T 207, ASTM D 4220 and 5079). Samples should not be placed, even temporarily, in direct sunlight. Undisturbed soil samples should be stored in an upright position with the top side of the sample up.

As storage time increases, moisture will migrate within a tube. Potential for disturbance and moisture migration within the sample will increase with time, and samples tested after 30 days should be noted on the laboratory data sheet. Excessive storage time can lead to additional sample disturbance that will affect strength and compressibility properties. Additionally, stress relaxation, temperature changes, and storage in a room with humidity below 90 percent will have detrimental effects to the samples. Long-term storage of soil samples should be in temperature and humidity controlled environments. The temperature control requirements may vary from sub freezing to ambient and above, depending on the environment of the parent formation. The relative humidity for soil storage normally should be maintained at 90 percent or higher.

Long-term storage of soil samples in sampling tubes is not recommended. During long term storage the sample tubes may corrode. This accompanied by the adhesion of the soil to the tube may develop such resistance to extrusion that some soils may experience internal failures during extrusion. Often these failures cannot be seen by the naked eye; x-ray radiography (ASTM D 4452) will likely be necessary to confirm the presence of such conditions. If these samples are tested as "undisturbed" specimens, the results may be misleading.

4.12.2.3 Sample Handling

Careless handling of undisturbed soil samples may cause major disturbances that could lead to serious design and construction consequences. Samples should always be handled by experienced personnel in a manner that ensures that the sample maintains structural integrity and natural moisture condition. Saws and knives used to prepare soil specimens should be clean and sharp. Preparation time should be kept to a minimum, especially where the maintenance of the moisture content is critical. Specimens should not be exposed to direct sun, freezing, or precipitation.

4.12.2.4 Specimen Selection

The selection of representative specimens for testing is one of the most important aspects of sampling and testing procedures. Selected specimens must be representative of the formation or deposit being investigated. The senior laboratory technician, the geologist and/or the geotechnical engineer should study the drilling logs, understand the geology of the site, and visually examine the samples before selecting the test specimens. Samples should be selected on the basis of their color, physical appearance, and structural features. Specimens should be selected to represent all types of materials present at the site, not just the worst or the best. Samples with discontinuities and intrusions may prematurely fail in the laboratory. If these features are small and randomly located, however, they would not necessarily cause such failures in the field. Such local failures should be noted but not selected as representative of the deposit.

4.12.3 Effects of Sample Disturbance

As a result of drilling, sampling, sample extrusion, and trimming to form a specimen for testing, nominally undisturbed specimens from samples obtained using methods presented in table 7 will become disturbed. These processes change the effective stress condition in the soil sample; that is, the effective stress in the soil at the time after a sample is trimmed and prepared for testing is different than that of the same soil in the ground. Figure 22 provides an illustration of the stress changes that a soil undergoes as it is transferred from the ground (given by point A at an at-rest (K_o) condition) to a laboratory specimen. At point F in figure 22, significant stress relief has occurred, and the specimen is at a higher void ratio than the in-situ condition. Since the laboratory sample is at a higher void ratio (i.e., less dense) than it was in-situ, a laboratory strength test performed on the specimen would likely exhibit a lower strength and a higher compressibility relative to the same soil at the in-situ void ratio.

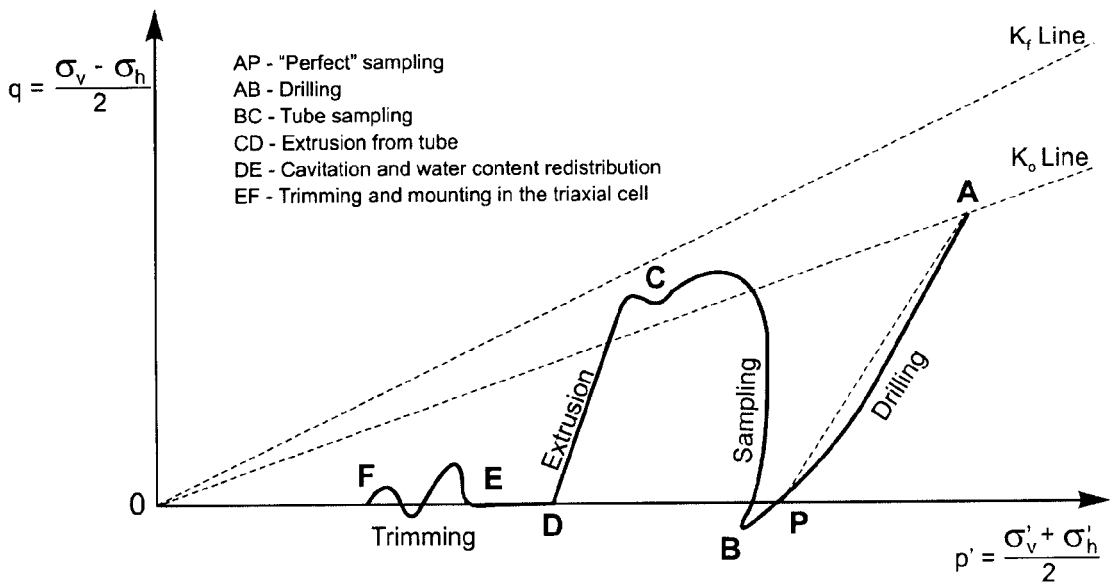

Figure 22. Disturbance during sampling and trimming (after Ladd and Lambe, 1963).

The effects of disturbance listed above provide a basis for evaluating laboratory shear strengths from unconsolidated-undrained (UU) tests and consolidated-undrained (CIU) strength tests. It should be noted that with CIU tests there is some recompression and restoration of void ratio, while results of a UU test will be much more affected by disturbance induced changes in void ratio and structure of the specimen. Figure 23 illustrates the "field" or undisturbed consolidation curve for a normally consolidated sample as well as the disturbed curve developed from laboratory data. The void ratio in the ground is given by point A. A UU test on a disturbed specimen will be performed at a void ratio shown by point B since the sample will be unloaded prior to testing, whereas for a CIU test on a disturbed sample, in which the sample is reconsolidated to the in-situ effective stress, the void ratio will be at point C. Since soil strength is a function of void ratio, among other properties, it can be seen that the UU strength may be less than that for the in-situ sample and the CIU strength may be greater. In summary, for both a UU and a CIU test, if the sample is disturbed it will not be possible to reestablish in the

laboratory the unique void ratio and effective stress combination that existed in the ground, although clearly the CIU test can provide a much better representation of the in situ soil conditions as compared to a UU test. Efforts must therefore concentrate on obtaining high quality, undisturbed samples for laboratory strength testing.

Additional test-related issues such as direction of shearing, sample disturbance, and rate effects, will play a role in differences between laboratory and field values of strength. For example, shear rates used in a UU test are much faster than that which would be expected for most field situations. In general, the faster a clay sample is sheared under undrained conditions, the greater will be the measured undrained strength. Based on this discussion, it would seem as though disturbance and shear rate produce "compensating errors" in the UU test. Also, many engineers assume that the disturbance effect is greater than the shear rate effect leading to the conclusion that UU strengths must be less than the actual undrained strength of the soil so that characterization of undrained strengths from UU tests is therefore conservative. Such a generalization should not be relied upon when selecting undrained strengths for design. Undrained strengths based on UU testing must be supplemented with additional CIU testing and/or in situ testing. Additional discussion on the selection of shear strength values based on UU and CIU testing is provided in chapter 5.

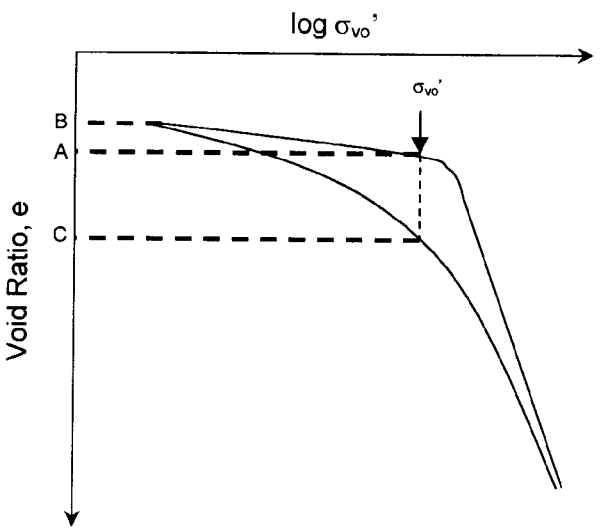

Figure 23. Lab and field consolidation curves.

Based on the previous discussion, it is clear that minimization of disturbance during sampling and testing is required. Also, since some disturbance is inevitable, procedures and "rules-of-thumb" are available to assess sample disturbance and the potential effects of this disturbance on soil properties. Quantification of sample disturbance in cohesive soils can be assessed using: (1) laboratory odometer curves; and (2) radiographic testing.

Sample disturbance will generally affect laboratory oedometer curves in three ways (see figure 23):

- The strain to reach the in-situ effective stress will be greater for the disturbed sample when compared to the strain (or change in sample height) of an undisturbed specimen (compare point C to point A in figure 23).

- The preconsolidation stress is difficult to determine due to rounding of the consolidation curve. This generally leads to an under estimation of the preconsolidation stress.

- The recompression curve for the disturbed sample will have a steeper slope than that of an undisturbed specimen, while the apparent virgin compression curve will likely be flatter than that of the undisturbed specimen.

Depending upon the stress history of the deposit and the stress ranges of the design, sample disturbance can effect the selection of soil properties to different degrees. As shown in table 16, the quality of a specimen can be assessed based on results of oedometer tests. Additionally, the quality of a specimen prepared for strength testing can be assessed if the strain to reach σ_{vo}' during the consolidation phase is monitored and an estimate of OCR for the specimen is known. Table 16 attempts to correlate disturbance to the initial elastic stiffness of a sample. That is, for a given OCR, the loading of the sample up to the preconsolidation stress is "elastic" and the response should be relatively stiff. As the amount of strain required to reach the initial effective stress in the ground increases, so does the likelihood that the sample is disturbed.

Table 16. Sample quality designation system (Lacasse et al., 1985).

Range of OCR	Depth Interval (m)	Very good test if $\varepsilon_v <$ (%)	Acceptable test if $< \varepsilon_v <$ (%)	Likely to be very disturbed if $\varepsilon_v >$ (%)
1 – 1.2	0 – 10	3	3 – 5	5
	10 – 50	2	2 – 4	4
1.2 – 1.5	0 – 10	2	2 – 4	4
	10 – 50	1	1 – 3	3
1.5 – 2	0 – 10	1.5	1.5 – 3.5	3.5
	10 – 50	1.0	1 – 2.5	2.5
2 – 3	0 – 10	1.0	1 – 3	3
	10 – 50	0.75	0.75 – 2	2
3 – 8	0 – 10	0.5	0.5 – 1	1
	10 – 50	0.5	0.5 – 2	2

ε_v = strain required to reach σ_{vo}'

X-ray photographs of soil specimens can be used to assess sample quality. Radiography (ASTM D 4452) utilizes X-ray photographs to assess density variation or consistency of a sample, and thus identify potential areas of defects and disturbance. X-ray photographs may be taken on samples within tubes or liners, or on extruded samples. Radiography can be used to identify:

- variation in soil types;
- macrofabric features such as bedding planes, varves, fissures, and shear planes;
- presence of intrusions such as gravel, shells, calcareous soils, peat, and drilling mud;

- presence of voids and cracks; and
- variation in the degree of disturbance that may range from curvature of soil layers near the tube edges to extreme disturbance noted by large voids and cracks (typically at the end of the tubes).

Since these features are often within the sample and not apparent from visual identification, radiography provides a non-destructive means for selecting representative samples for laboratory performance testing. Radiography is particularly useful where a limited number of samples are available for testing or complexities in sampling are likely to induce disturbance. Radiographic testing requires special testing equipment (usually from an outside laboratory) but the testing is not expensive. The radiographic images provide information to ensure that high quality samples are used for laboratory performance tests.

4.12.4 Laboratory Index Tests for Soils

4.12.4.1 General

Data generated from laboratory index tests provide an inexpensive way to assess soil consistency and variability among samples collected from a site. Information obtained from index tests is used to select samples for engineering property testing as well as to provide an indicator of general engineering behavior (e.g., high plasticity clay based on plasticity index (PI) may indicate high compressibility, low hydraulic conductivity, and high swell potential). Common index tests discussed in this section include moisture content, unit weight (wet density), Atterberg limits, particle size distribution, visual classification, specific gravity, and organic content. Index testing should be conducted on soil materials from every project. Information from these tests should be assessed prior to a final decision regarding the specimens selected for subsequent performance testing.

4.12.4.2 Moisture Content

The moisture (or water) content test is one of the simplest and least expensive laboratory tests to perform. Moisture content is defined as the ratio of the mass of the water in a soil specimen to the dry mass of the specimen. Natural moisture contents (w_n) of sands are typically $0 \leq w_n \leq 20$ %, whereas for inorganic and insensitive silts and clays, general ranges are: $10 \leq w_n \leq 40$ %. However, depending upon the mineralogy, formation environment, and structure of clay, it is possible to have more water than solids (i.e., $w > 100\%$). Therefore soft and highly compressible clays, as well as sensitive, quick, or organically rich clays, can exhibit water contents $40 \leq w_n \leq 300$ % or more.

Moisture content can be tested in a number of different ways including: (1) a drying oven (ASTM D 2216); (2) a microwave oven (ASTM D 4643); or (3) a field stove or blowtorch (ASTM D 4959). While the microwave or field stove (or blowtorch) methods provide a rapid evaluation of moisture content, potential errors inherent with these methods require confirmation of results using ASTM D 2216. The radiation heating induced by the microwave oven and the excessive temperature induced by the field stove may release water entrapped in the soil structure that would normally not be released at 110° C, yielding higher moisture content values than would occur from ASTM D 2216.

Field measurements of moisture content often rely on a field stove or microwave, due to the speed of testing. When dealing with compacted material, it is common to use a nuclear gauge (ASTM D 3017) in the field to rapidly assess moisture contents. It is noted that nuclear gage readings may indicate widely varying moisture contents for micaceous soils. Results from these techniques should be "calibrated" or confirmed using the drying oven (ASTM D 2216).

Sampling, handling, and storage may alter the in-situ moisture content tests. Because the top end of the sample tube may contain water or collapse material from the borehole, moisture content tests should not be performed on material near the top of the tube. Also, as storage time increases, moisture will migrate within a specimen and lead to altered moisture content values. If the sample is not properly sealed, drying of the sample and moisture loss will likely occur.

4.12.4.3 Unit Weight

In the laboratory, soil unit weight and mass density are easily measured on tube samples of natural soils. The moist (total) mass density is $\rho_t = M_t/V_t$, whereas the dry mass density is given by $\rho_d = M_s/V_t$. The moist (total) unit weight is $\gamma_t = W_t/V_t$, whereas the dry unit weight is defined as $\gamma_d = W_s/V_t$. The interrelationship between the total and dry mass density and unit weight is given by:

$$\rho_d = \rho_t/(1+w_n) \qquad \text{(Equation 17)}$$

and the relationship between total and dry unit weight is given by:

$$\gamma_d = \gamma_t/(1+w_n) \qquad \text{(Equation 18)}$$

The terms density and unit weight are often incorrectly used interchangeably. The correct usage is that density implies mass measurements while unit weight implies weight measurements. For this document they will be referenced as "density (unit weight)", if the usage is independent of the specific definition.

Field measurements of soil mass density (unit weight) are generally restricted to shallow surface samples, usually when placing compacted fills, and can be accomplished using drive tubes (ASTM D 2937), sand cone method (ASTM D 1556), or nuclear gauge (ASTM D 2922). To obtain unit weights or mass densities with depth, either high-quality thin-walled tube samples must be obtained (ASTM D 1587), or relatively expensive geophysical logging by gamma ray techniques (ASTM D 5195) can be employed.

4.12.4.4 Atterberg Limits

The Atterberg limits of a fine grained (i.e., clayey or silty) soil represent the moisture content at which the behavior of the soil changes. The tests for the Atterberg limits are referred to as index tests because they serve as an indication of several physical properties of the soil, including strength, permeability, compressibility, and shrink/swell potential. These limits also provide a relative indication of the plasticity of the soil, where plasticity refers to the ability of a silt or clay to retain water without changing state from a semi-solid to a viscous liquid. In geotechnical engineering practice, the Atterberg

limits generally refers to the liquid limit (LL), plastic limit (PL), and shrinkage limit (SL). These limits are defined below.

- Liquid Limit (LL) - This upper limit represents the moisture content at which any increase in moisture content will cause a plastic soil to behave as a liquid. The LL is defined as the moisture content at which a standard groove cut in a remolded sample will close over a distance of ½ inch at 25 blows of the liquid limit device (figure 24).

- Plastic Limit (PL) - This limit represents the moisture content at which the transition between the plastic and semisolid state of a soil. The PL is defined as the moisture content at which a thread of soil just crumbles when it is carefully rolled out to a diameter of 3.2 mm.

- Shrinkage Limit (SL) – The moisture content corresponding to the behavior change between the semisolid to solid state of the soil. The SL is also defined as the moisture content at which any further reduction in moisture content will not result in a decrease in the volume of the soil.

  A measure of a soils plasticity is the plasticity index (PI) which as calculated as PI = LL – PL. The PI is a useful index since numerous engineering correlations have been developed relating PI to clay soil properties, including undrained and drained strength and compression index. Results are typically presented on Casagrande's Plasticity chart (see figure 25). On this chart, the equation for the A-line and U-line are, respectively:

$$A - line : PI = 0.73\,(LL - 20) \qquad \text{(Equation 19)}$$

$$U - line : PI = 0.9\,(LL - 8) \qquad \text{(Equation 20)}$$

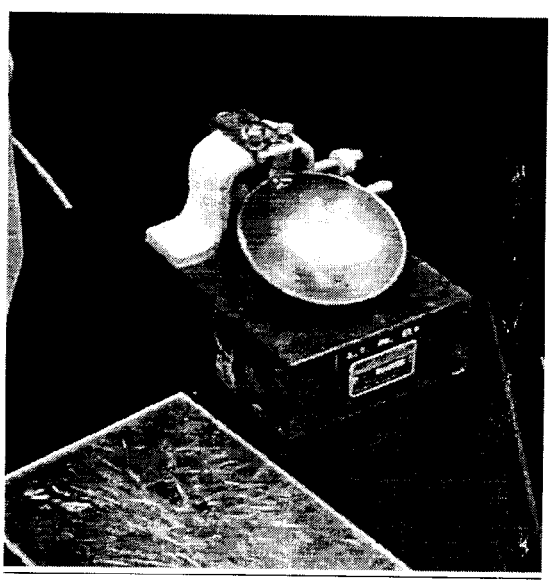

Figure 24. Equipment used for Atterberg limits testing of soil.

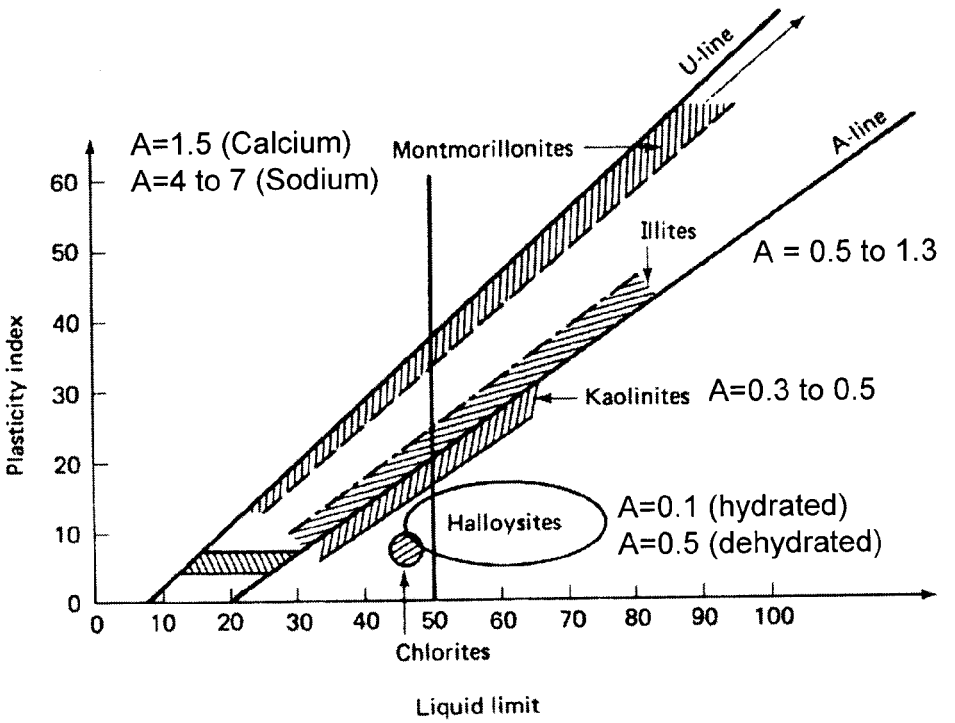

Figure 25. Location of clay minerals on the Casagrande plasticity chart (Skempton, 1953).

Other indices based on the Atterberg Limits include the liquidity index (LI) and the activity (A) of a soil. These are defined as:

$$LI = (w_n - PL) / PI \qquad \text{(Equation 21)}$$

$$A = PI / CF \qquad \text{(Equation 22)}$$

where w_n is the moisture content of the soil and CF is the clay fraction that corresponds to the percentage of particles exhibiting an equivalent diameter (d_s) < 0.002 mm. The use of the liquidity index and activity can provide very useful information concerning the likely behavior of a soil, even though Atterberg limits are performed on completely remolded materials. For example, a LI less than or equal to zero is generally indicative of a heavily overconsolidated soil that may be desiccated or highly expansive. A soil with a LI equal to unity implies that the soil is at its liquid limit and is likely to be relatively weak and compressible. A LI greater than unity indicates that the soil is sensitive. Soils with a LI greater than approximately 0.7 will likely undergo significant consolidation settlements when loaded.

Values for activity can be correlated to the type of clay mineral that, in turn, provides important information relative to the expected behavior of a clay soil. A clay soil that predominantly comprises montmorillonite behaves very differently from a clay soil comprising kaolinite. Figure 25 also shows the activities of various clay minerals and location on the Casagrande's plasticity chart.

4.12.4.5 Particle Size Distribution

Particle size distribution by mechanical sieve and hydrometer are useful for soil classification purposes. Procedures for grain size analyses are contained in ASTM D 422 and AASHTO T88. Testing is accomplished by placing air-dried material on a series of screens of known opening size. Each successive screen has a smaller opening to capture progressively smaller particles. Testing of the finer grained particles is accomplished by suspending the chemically dispersed particles in water column and measuring the specific gravity of the liquid as the particles fall from suspension.

Particle size testing is relatively straightforward, but results can be misleading if procedures are not performed correctly and equipment is not maintained in good condition. If the sieve screen is distorted, large particles may be able to pass through sieve openings that typically would retain the particles. Material lodged within the sieve from previous tests could become dislodged during shaking, increasing the weight of material retained on the following sieve, thus sieves should be cleaned after each test. A wire brush may distort finer sieve meshes during cleaning, so a plastic brush should be used to clean the U.S. No. 40 sieve and finer. Table 17 shows U.S. standard sieve sizes and associated opening sizes.

Table 17. U.S. standard sieve sizes and corresponding opening dimension.

U.S. Standard Sieve No.	Sieve Opening (mm)	Sieve Opening (in.)
3	6.35	0.25
4	4.75	0.187
6	3.35	0.132
8	2.38	0.0937
10	2.00	0.0787
12	1.68	0.0661
16	1.20	0.0469
20	0.85	0.0331
30	0.60	0.0232
40	0.425	0.0165
50	0.30	0.0117
60	0.25	0.0098
70	0.21	0.0083
100	0.15	0.0059
140	0.106	0.0041
200	0.075	0.0029
270	0.053	0.0021
400	0.0375	0.0015

Representative samples with fines (particles with diameter less than 0.075 mm or the U.S. No. 200 sieve) should not be oven dried prior to testing because some particles may cement together leading to a calculated lower fines content from mechanical sieve analyses than is actually present. When fine-grained particles are a concern, a wash sieve (ASTM D 1140) should be performed to assess the fines content. Additionally, if the clay content is an important parameter, hydrometer analyses need to be performed. It should be noted that the hydrometer test provides approximate analysis results due to oversimplified assumptions, but the obtained results can be used as a general index of silt and clay content. Depending upon the chemical makeup of the fine grained particles, the traditional sodium hexametaphosphate solution used to disperse the clay particles may not provide adequate dispersion. If the clay particles are not dispersed, the hydrometer data would lead to the interpretation of a low clay content. In some cases the concentration of dispersing agent may need to be increased or a different dispersing agent may need to be used.

4.12.4.6 Laboratory Classification

In addition to field identification (ASTM D 2488), soils should be classified in the laboratory using the Unified Soil Classification System (USCS) in accordance with ASTM D 2487 or the AASHTO soil classification system (AASHTO T 145). The differences in these two systems are beyond the scope of this document, and the reader is referred to Holtz and Kovacs (1981) and AASHTO (1988) for a comparison of these two classification systems. The USCS will be used throughout the remainder of this document. Classification in the laboratory occurs in a controlled environment and more time can be spent on this classification than the identification exercise performed in the field. Laboratory and/or field identification is important so that defects and features of the soil can be recorded that would not typically be noticed from index testing or standard classification. Some of the features include mica content, joints, and fractures.

4.12.4.7 Specific Gravity

The specific gravity of solids (G_s) is a measure of solid particle density and is referenced to an equivalent volume of water. Specific gravity of solids is defined as $G_s = M_s/(V_s \times \gamma_w)$ where M_s is the mass of the soil solids and V_s is the volume of the soil solids. Since many sands are comprised of quartz and/or feldspar minerals and many clays consist of the kaolinite and/or illite clay minerals in composition, and since the specific gravity of these minerals are confined to a relatively narrow range, the typical values of specific gravity of most soils also lie within the narrow range of $G_s = 2.7 \pm 0.1$. Exceptions include soils with appreciable organics (i.e., peat), ores (mine tailings), or calcareous (high calcium carbonate content) constituents. It is common to assume a reasonable G_s value, although laboratory testing by AASHTO T100 or ASTM D 854 or D 5550 can be used to verify and confirm its magnitude, particularly on projects where little previous experience exists and unusually low or high unit weights are measured.

4.12.4.8 Organic Content

A visual assessment of organic materials may be very misleading in terms of engineering analysis. Laboratory test method AASHTO T194 or ASTM D 2974 should be used to evaluate the percentage of

organic material in a specimen where the presence of organic material is suspected based on field information or from previous experience at a site. The test involves heating a sample to temperatures of 440°C and holding this temperature until no further change in mass occurs. At this temperature, the sample turns to ash. Therefore, the percentage of organic matter is (100% - % ash) where the % ash is the ratio of the weight of the ash to the weight of the original dried sample. The sample used for the test is a previously dried sample from a moisture content evaluation. Usually organic soils can be distinguished from inorganic soils by their characteristic odor and their dark gray to black color. In doubtful cases, the liquid limit should be determined for an oven-dried sample (i.e., dry preparation method) and for a sample that is not pre-dried before testing (i.e., wet preparation method). If drying decreases the value of the liquid limit by about 30 percent or more, the soil may usually be classified as organic (Terzaghi, Peck, and Mesri, 1996).

Soils with relatively high organic content have the ability to retain water, resulting in high moisture content, high primary and secondary compressibility, and potentially high corrosion potential. Organic soils may or may not be relatively weak depending on the nature of the organic material. Highly organic fibrous peats can exhibit high strengths despite having a very high compressibility.

4.12.4.9 Electro Chemical Classification Tests

Electro chemical classification tests provide the engineer or geologist with quantitative information related to the aggressiveness of the soil conditions and the potential for deterioration of a foundation material. Electro chemical tests include (1) pH; (2) resistivity; (3) sulfate ion content; and (4) chloride ion content. If the pH of the soil is below 4.5 or the resistivity is less than 1000 ohms/cm, the soil should be treated as an aggressive environment. If the soil resistivity is between 3000 ohms/cm and 5000 ohms/cm, chloride ion content and sulfate ion content tests should be performed. If results from these tests indicate chloride ion content greater than 100 ppm or sulfate ion content greater than 200 ppm, then the soil should be considered as aggressive. Tests to characterize the aggressiveness of a soil environment are important for design applications that include metallic elements, especially for ground anchors comprised of high strength steel and for metallic reinforcements in mechanically stabilized earth walls.

4.12.5 Laboratory Performance Tests for Soils

4.12.5.1 General

Design soil properties for deformation, shear strength, and permeability characteristics are evaluated using laboratory-testing methods. To contrast most index tests, performance tests are usually more costly and time consuming. The results, however, provide specific data regarding engineering performance. This section provides information on equipment and testing procedures for consolidation, shear strength, and permeability testing.

4.12.5.2 Consolidation

Equipment

The oedometer (or one-dimensional consolidometer) is the primary laboratory equipment used to evaluate consolidation and settlement potential of cohesive soils. Results from oedometer tests can be used to assess the rate of consolidation (t_{100}), creep characteristics (C_α), stress history (σ_p'), and swell potential. A consolidation test is typically performed on undisturbed samples obtained from the deposit to evaluate settlement potential of in-situ foundation soils, however recompacted materials can also be tested to assess the settlement performance of compacted fills. The equipment for a consolidation test includes: (1) a loading device that applies a vertical load to the soil specimen; (2) a metal ring (fixed or free) that laterally confines the soil specimen and restricts deformation to the vertical direction only; (3) porous plates placed on the top and bottom of the sample; (4) a dial indicator or linear variable differential transducer (LVDT); (5) a timer; and (6) a surrounding container to permit the specimen to remain submerged during the test. Figure 26 shows the components of a consolidation test.

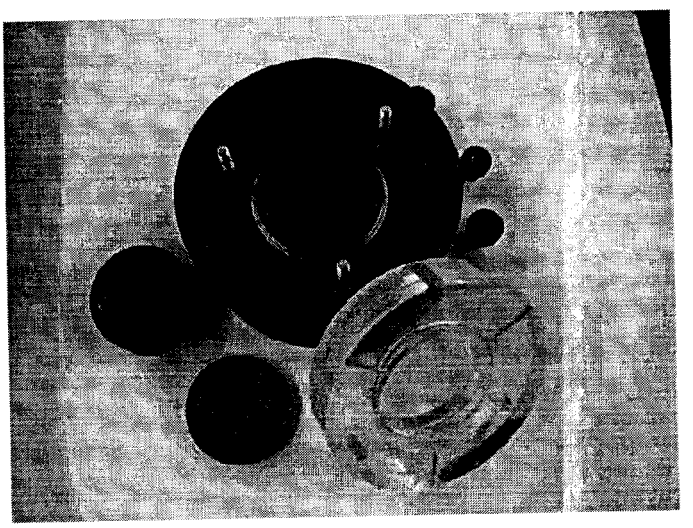

Figure 26. Components of consolidation test (photograph courtesy of GeoTesting Express).

The consolidation-loading device may be a weighted lever arm (figure 27), a pneumatic device, or an automated loading frame (figure 28(b)). Automated loading frames are recommended for use in production testing because they provide the most flexibility in testing options. The pneumatic device provides flexibility in loads and load increment ratios that can be applied during testing. A weighted lever arm provides a robust, relatively simple system for consolidation testing, however, because data are generally recorded manually, it is difficult to expedite testing or vary the loading schedule since data reduction cannot typically be performed in real time.

Consolidation cells may be either fixed ring or floating ring. Friction and drag are created in the ring as the specimen compresses in relation to the ring. In a fixed ring test the sample compresses from the top only, potentially resulting in high incremental side shear forces. In a floating ring test the sample compresses from the top and bottom thus providing the advantage of minimizing drag forces. However, the floating ring method has the disadvantages of being more difficult to set up, allowing for potential sidewall leakage that would result in an inaccurate assessment of the coefficient of consolidation, and

soil may squeeze out near the junction of the sidewall and the bottom porous plate. For these reasons, the fixed ring method is most commonly used.

Measurement of deflection can be done with either dial indicators or electronic LVDT. Properly calibrated, each device should provide the same accuracy, but the electronic output of a LVDT can be incorporated into automated recording systems for quicker, more efficient, and higher resolution readings. A timer will be required to assess duration of loading increments. Monitoring of time for manual systems can be accommodated using a wall clock with a second hand. The internal clock of a computer is used for automated systems.

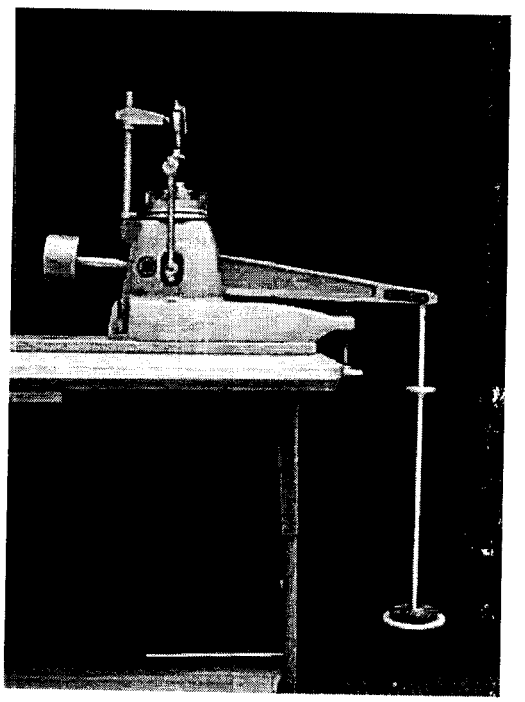

Figure 27. Incremental load oedometer.

Procedures

Consolidation properties of clay soils are evaluated in the laboratory using the one-dimensional consolidation test. The most common laboratory method is the incremental load (IL) oedometer (ASTM D 2435) shown in figure 27. High-quality undisturbed samples using thin-walled tubes (ASTM D 1587), piston samplers, or other special samplers are required for laboratory consolidation tests.

The consolidation test is relatively expensive and time consuming as compared to simpler index type tests, but results are necessary to assess the compressibility properties of the soil. As will be shown in subsequent sections of this document, this test is one of the most valuable tests for fine grained soil as it provides valuable data regarding stress history, as well as compressibility. It is important to carefully consider all laboratory testing variables and their potential effects on computed properties. Information that will need to be provided to a laboratory for a consolidation test will include the loading schedule (i.e., loads and duration of loads). It is important to carefully evaluate the loading schedule to be used.

The loading sequence selected for a consolidation test will depend on the type of soil being tested and the particular application (e.g., embankment, shallow foundation) being considered for the project. The selection of a loading schedule should never be left to the discretion of the laboratory. As an example, if the clay soil is heavily overconsolidated, it is possible that a laboratory-determined maximum load for the consolidation test will not be sufficient to exceed σ_p'.

The range of applied loads for the test should well exceed the effective stresses that are required for settlement analyses. This range should cover the smallest and largest effective stresses anticipated in the field and will depend on depth, foundation loads, and excavations. The anticipated preconsolidation stress should be exceeded by at least a factor of four during the laboratory test. If the preconsolidation stress is not significantly exceeded during the loading schedule, σ_p', and C_c (or $C_{c\varepsilon}$) may be underestimated due to specimen disturbance effects. A load-increment-ratio (LIR) of 1 defined as $\Delta\sigma_V/\sigma_V' = 1$, is commonly used for most tests corresponding to a doubling of the vertical stress applied to the specimen during each successive increment. As the stress approaches the value of σ_p', smaller LIR increments are recommended to facilitate an accurate estimate of σ_p'. Typically, laboratories provide a unit cost for a consolidation test that may be based on 6 to 8 load increments with a separate cost for each additional increment.

It is recommended that an unload-reload cycle be performed, especially for cases where accurate settlement predictions are required, specifically to obtain a value for C_r. Since most samples will inevitably be somewhat disturbed, a C_r value based on the initial loading of a consolidation test sample will be higher than that for an undisturbed sample, resulting in an overestimation of settlements in the overconsolidated region. A C_r value based on an unload-reload cycle is likely to be more representative of the actual modulus in the overconsolidated region. It is recommended that the unload-reload cycle be performed at a stress slightly less than σ_p'.

The duration of each load increment should be selected to ensure that the sample is approximately 100 percent consolidated prior to application of the next load. For relatively low to moderate plasticity silts and clays, durations of 3 to 12 hours will be appropriate for loads in the normally consolidated range. For fibrous organic materials, primary consolidation may be completed in 15 minutes. For high plasticity materials, the duration for each load may need to be 24 hours or more to ensure complete primary consolidation and to evaluate secondary compression behavior. Conversely, primary consolidation may occur in less than 3 hours for loads less than σ_p'. If the time period is too short for a given load increment (i.e., the sample is not allowed to achieve approximately 100 percent consolidation before the next load increment is applied), then values of C_c (or $C_{c\varepsilon}$) may be underestimated and values of c_v may be overestimated. The duration of time required, however, can be optimized using pneumatic, hydraulic, or electro-mechanical loading systems that include automated loading and data acquisition systems. Continuous deformation versus time measurements and the square root of time method (described in chapter 5) can be used to estimate the beginning and end of primary consolidation during the test. Once the end of primary consolidation is detected, the system can automatically apply the next load increment. Alternatively, some laboratories can provide real-time deformation versus time plots to enable the engineer to evaluate whether 100 percent primary consolidation has been achieved.

The constant rate of strain (CRS) version of the consolidation test (ASTM D 4186) applies the loading continuously and measures stress and pore pressures by transducers in real time, thereby reducing testing times from approximately 1 week by IL oedometer to about 1 day by a CRS consolidometer.

While expediting the testing time duration, the CRS consolidation test requires special instrumentation and equipment that is not normally available in state DOT laboratories. A discussion of the CRS and other consolidation methods are described in Head (1986) and Lowe et al. (1969).

Secondary compression should be assessed on the basis of the deformation versus a log-time response (see section 5.4.2.7). The consolidation test for each load increment should be run long enough to establish a log-linear trend between time and deformation.

4.12.5.3 Soil Strength

General

Soil shear strength is influenced by many factors including the effective stress state, mineralogy, packing arrangement of the soil particles, soil hydraulic conductivity, rate of loading, stress history, sensitivity, and other variables. **As a result, shear strength of soil is not a unique property.** Laboratory measured shear strength values will also vary because of boundary conditions, loading rates, and direction of loads. In this section, typical laboratory strength tests including unconfined compression (AASHTO T208; ASTM D 2166), triaxial (AASHTO T234; ASTM D 4767), and direct shear (AASHTO T236; ASTM D 3080) are introduced and in chapter 5, the evaluation of soil strength from these laboratory tests is provided. A detailed discussion on testing equipment and procedures is beyond the scope of this document. The interested reader should review the AASHTO and ASTM standards for detailed information on these tests. This section also describes information that must be conveyed to a laboratory-testing firm to ensure that the strength testing performed is consistent with the requirements imposed by the design (e.g., selection of confining pressures consistent with the imposed loads).

Unconfined Compression (UC) Tests

The unconfined compression test is a quick, relatively inexpensive means to obtain an approximate estimation of undrained shear strength of cohesive specimens. This test unfortunately is commonly used in practice because of its simplicity and low cost. In most cases, undrained strength results from an unconfined compression test are conservative. The maximum stress, q_u, measured at failure is equal to two times the undrained strength (s_u). In this test a cylindrical specimen of the soil is loaded axially, without any lateral confinement to the specimen, at a sufficiently high rate to prevent drainage. Since there is no confinement, residual negative pore pressures that may exist in the sample following sample preparation control the state of effective stress. This test cannot be performed on granular soils, dry or crumbly soils, silts, peat, or fissured or varved materials. Because there is no control on the effective stress state of the specimen, this test is not recommended for evaluating strength properties for compressible clay soils subjected to embankment or structural foundation loads. The reliability of this test decreases with respect to increasing sampling depth because the sample tends to swell after sampling resulting in greater particle separation and reduced shear strength. Testing the full diameter extruded specimen as soon as possible after removal from the tube can minimize swelling. This reduces disturbance and preserves natural moisture content.

Triaxial Tests

Equipment – Triaxial systems today use electronic instrumentation to provide continuous monitoring of test data (see figure 28). Force is measured using a force transducer or load cell that is typically mounted outside the triaxial cell, but more advanced systems have incorporated the transducer within the testing cell to reduce rod-friction effects. LVDTs are used to monitor deformations. Additionally, volume measurements can be taken with a device that makes use of an LVDT to measure the rise or fall of a bellofram cylinder. This change in movement is calibrated to the volume of water the sample will take in or push out. Pressure transducers are mounted on the base of the test cell to monitor the confining pressure and the pore pressure within the sample.

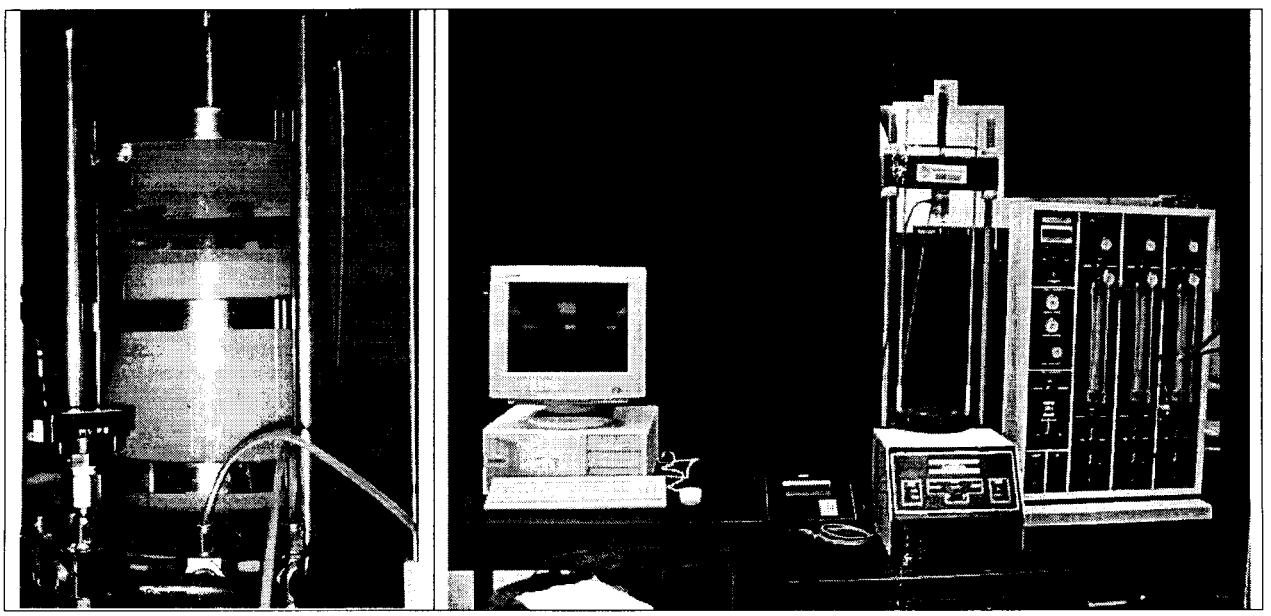

Figure 28. (a) Failure of a loose sand specimen in a triaxial cell; and
(b) Load frame, pressure panel, and computerized data acquisition system

Unconsolidated-Undrained (UU) Test – In this test, no drainage or consolidation is allowed during either the application of the confining stress or the shear stress. This test models the response of a soil that has been subject to a rapid application of confining pressure and shearing load. It is difficult to obtain repeatable results for UU testing due to sample disturbance effects. Like the UC tests, the accuracy of the UU test is also dependent on the soil sample retaining its original structure until testing occurs. The undrained strength of the soil, s_u, is measured in this test.

Consolidated-Drained (CD) Test – In this test, the specimen is allowed to completely consolidate under the confining pressure prior to performing the shearing portion of the test. During shearing, load is applied at a rate slow enough to allow drainage of pore water and no buildup of pore water pressures. The time required to conduct this test in low permeability soil may be as long as several months; therefore it is not common to conduct this test on low permeability soils. This test models the long-term (drained) condition in soil. Effective stress strength parameters (i.e., ϕ' and c') are evaluated in this test.

Consolidated-Undrained (CU) Test – The initial part of this test is similar to the CD test in that the specimen is allowed to consolidate under the confining pressure. Shearing occurs, however, with the drainage lines closed, thus during shearing there is continual pore water pressure development. The rate of shearing for this test is more rapid than that for a CD test. Pore pressures should be measured during shearing so that both total stress and effective stress strength parameters can be obtained. It is noted that the effective stress parameters evaluated for most soils based on CU testing with pore pressure measurements is similar to that obtained for CD testing, thus making CD tests not necessary for typical applications.

Direct Shear Tests

Equipment – The apparatus and procedures for direct shear testing are discussed in ASTM D 3080. A specimen is prepared in a split square or circular box (see figure 29), and is sheared as one box is displaced horizontally with respect to the other using upper and lower loading frames (see figure 30). Load cells are used to monitor the shear force and LVDTs are used to monitor both horizontal and vertical deformation. Using this instrumentation, as well as a loading frame that provides a constant rate of horizontal deformation, it is possible to automate the direct shear test.

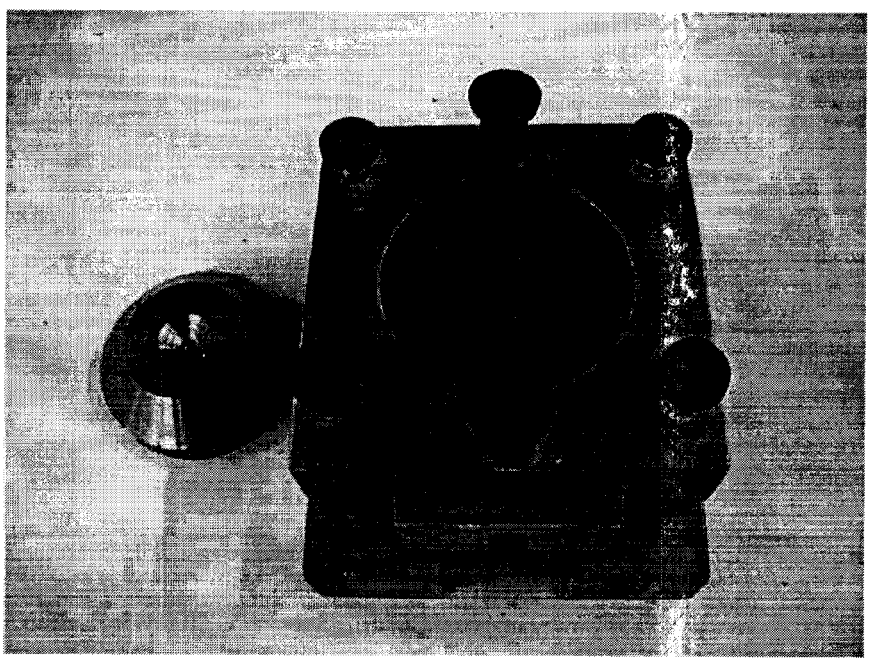

Figure 29. Direct shear testing box (photograph courtesy of GeoTesting Express).

Test Procedures – In the direct shear test, the soil is first consolidated under an applied normal stress. The soil is then sheared at a constant rate after consolidation is completed (which will be instantaneous in cohesionless soils), which should be selected as a function of the hydraulic conductivity of the specimen. Direct shear testing is commonly performed on compacted materials used for embankment fills and retaining structures. This testing can also be performed on natural materials; however, the lack of control on soil specimen drainage makes the evaluation of undrained strength unreliable. This test can be used to evaluate the drained strength of natural materials by shearing the sample at a slow enough

rate to reasonably ensure that no porewater pressures develop. In addition to peak effective stress friction angle (ϕ'), the direct shear test can be used for the evaluation of effective stress residual strengths ($c'_r \approx 0$; ϕ'_r). These parameters are necessary for stability and landslide analyses. Residual strengths are associated with very large deformations and shear strains along a predefined or preferential slip surface. A reversing direct shear test can be used to evaluate residual shear strengths. In this test, the direction of shearing in the test is reversed several times thereby causing the accumulation of displacements at the slip surface.

For designs involving geosynthetics, the strength of the interface between the soil and geosynthetic or geosynthetic and geosynthetic are often necessary parameters. Direct shear machines have been modified to test the shear strength of various interfaces, as described in ASTM D 5321.

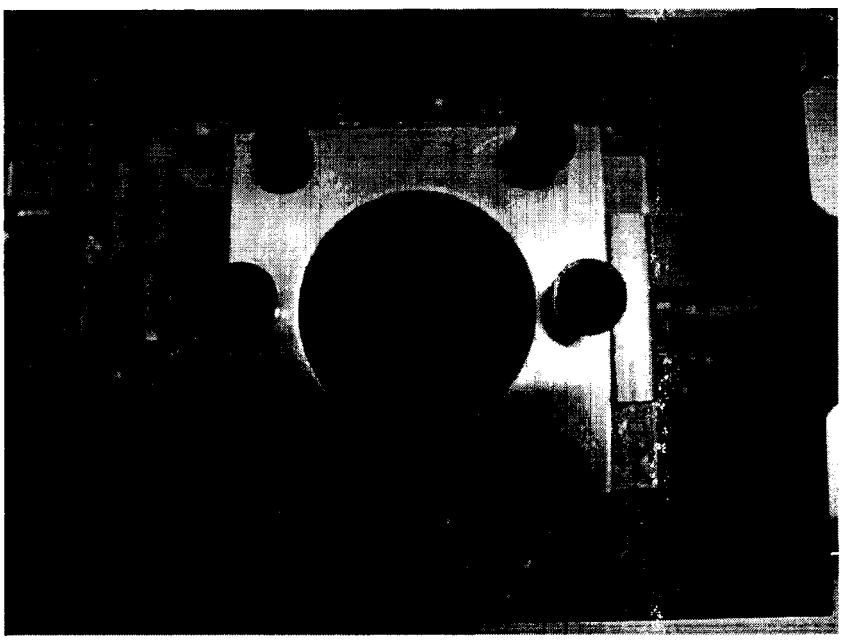

Figure 30. Soil sample mounted in direct shear testing apparatus (photograph courtesy of GeoTesting Express).

Factors Affecting Strength Testing Results

In chapter 2, a flowchart describing the process of evaluating design soil and rock properties was presented. That flowchart included a step wherein information collected from subsurface investigations and baseline laboratory test data (i.e., index test results) are summarized to facilitate development of a subsurface profile and as a tool to assist in developing a program for required laboratory performance tests such as strength and consolidation testing on specimens from tube samples. This section provides a discussion of specific factors relevant to laboratory unconfined compression, triaxial, and direct shear testing and how these factors affect measured shear strength values. In chapter 5, specific recommendations are developed with respect to selecting a particular test for a particular application where multiple tests may be appropriate.

Sample Disturbance

The degree of disturbance affecting samples will vary according to the type of soil, sampling method, and skill of the driller. All samples will experience some degree of disturbance due to the removal of in-situ stresses during sampling and laboratory preparation for testing. Due to disturbance-induced alteration of the in-situ soil structure, internal migration of pore water, and reduction in the effective stress state of the sample, shear strength values obtained from UC and UU tests will be unrepeatable and may be higher or lower than corresponding field strengths. Recompression of a sample during the consolidation phase of a CIU test will reduce the void ratio of the specimen that may lead to higher laboratory strengths relative to the in-situ condition, but destruction of natural bonding during sampling will typically more than offset this strength increase. Table 16 should be used to judge the degree of disturbance of the samples and strength results from samples designated as very good or acceptable can be considered to be appropriate. Shear strengths from samples designated as likely to be very disturbed should be used with caution for design calculations.

Mode of Shearing

Experience has shown the undrained soil shear strength also depends on the direction of shearing. That is, a soil loaded in compression will likely have a shear strength that is different than if the soil is loaded in extension. The effects are not as recognized for drained (effective stress) strength in compression and extension, or partially drained conditions. Most triaxial tests will be performed with isotropic consolidation and vertical compression, as most commercial laboratories are not equipped to perform various modes of shearing. The engineer must consider how the actual strength mobilized under field conditions differs from that measured using laboratory (or in-situ) methods. For example, when considering design of a temporary anchored wall in soft to medium clay, the undrained strength used to evaluate the earth pressures acting on the wall may be determined from a triaxial compression test. The lateral capacity of the wall toe, however, is more appropriately evaluated using the undrained strength from a triaxial extension test. The extension loading path more accurately approximates the unloading caused by a soil excavation as compared to a compression loading path and, more importantly, experience has shown that the shear strength of the soil located inside the excavation can be less than that of the soil located in the retained ground for certain clay soils.

It is recognized that for most typical projects the use of alternative loading paths is not practical. However, information and existing correlations relating undrained strength from isotropically consolidated (CU) triaxial tests to other loading paths can be used to adjust the CU strength to a value more appropriate for the loading condition imposed by the structure to be built. This is discussed further in chapter 5.

Confining Pressures

Soil shear strength is governed by the effective stresses in the soil. Therefore, it is important to carefully consider the range of effective stresses that a soil will be subjected to during the design life of a structure. These stresses will be affected by changes in the level of the ground water table, effects of capillary rise, design loads of potential structures, as well as many other possibilities. For laboratory testing considerations, this means that for each sample tested, the in-situ (or current) effective stress condition and that which will exist after the design feature (e.g., shallow foundation, embankment, retaining wall, cut slope) has been constructed needs to be calculated.

For laboratory strength testing, three different confining stresses are generally used for each sample at a unique depth, thus requiring three specimens from the same undisturbed sample. For each specimen, the shear strength is measured and a shear strength envelope is developed. Details regarding the evaluation of shear strength are provided in chapter 5. In some cases, it may be difficult to prepare three specimens from one tube due to defects, fissures, poor recovery, etc. Testing can be done using only one or two specimens if the number of specimens is limited, but the engineer should investigate the reasons for the inability to prepare three specimens and should exercise judgment in interpreting the test results.

Loading ranges typically include the effective overburden stress at the sample depth, one half the effective overburden stress at the sample depth, and a third stress condition superceding the anticipated design load or two to four times the effective overburden stress at the depth sampled, whichever is greater. To calculate the range of effective stresses, the final effective stress at the elevation of the sample should be plotted as a function of depth. For surface loadings such as that due to embankments and shallow foundations, stress distributions with depth should be calculated using appropriate methods.

For UU tests, the soil specimen is not re-consolidated to the effective stress in the ground. In selecting confining pressures, the total stress at the elevation of the soil sample in the ground is reapplied to the specimen with the test apparatus drain lines closed. If it is assumed that the water content of the specimen just prior to testing is the same as that in the ground and if the sample is saturated, the reapplication of total stresses equal in magnitude to those which were in the ground, should theoretically restore the sample to its in-situ effective stress condition. Because of inevitable sample disturbance, more pressure is transferred to the porewater resulting in a lower effective stress as compared to that in the ground. The lower preshear effective stress results in lower than actual shear strength. UU test results are considered unreliable at depths greater than 6 m for normally consolidated samples and over 12 m for overconsolidated soils because of this reduction in effective stress.

Specimen Size

The specimen size for testing must be provided to the laboratory. Triaxial testing specimens are cylindrical with a minimum diameter of 33 mm, and a length to diameter (L:D) ratio between 2 and 2.5. Undisturbed samples from tubes, which are typically 76 mm in diameter, need to be trimmed to fit the caps and bases of the triaxial device. A specimen trimmed with care to 35.6 mm diameter is generally the best practice for triaxial test specimen preparation for CU or CD testing to minimize the disturbance related to the side walls of the samples. If UU tests are performed, specimens should be extruded directly from the sampling tube and tested untrimmed at full diameter to minimize disturbance effects.

Laboratory testing for undrained strength of heavily overconsolidated, fissured soils is difficult since typical sample diameters may not be sufficient to capture the affects of fissures and cracks on strength. In many cases, the actual strength of the soil can be up to 50 percent less than that measured in the laboratory. Additional discussion on the strength testing of stiff, fissured soil materials are provided in chapter 5.

Saturation

Backpressure saturation procedures are typically used to saturate soil samples for triaxial testing. A backpressure of at least 1 atm (100 kPa) should be applied, but 2 to 3 atm (200 to 300 kPa) of backpressure are recommended. Samples need to be saturated for drained tests to permit volume change

measurements to be made and, for undrained tests, to permit pore pressures during shearing to be measured. Saturation by backpressure methods involves raising the pressure inside the specimen to dissolve gas into the pore fluid. Since the cell pressure is raised an equal value along with the internal specimen pressure, the effective stress of the sample remains constant. The pore pressure parameter, $B=\Delta u/\Delta\sigma_3$, should be equal to at least 0.95 for the specimen to be considered saturated. If the B-value remains constant as the back pressure is increased, the specimen can be considered essentially saturated.

Displacement at Failure

The engineer should estimate the amount of deformation or strain necessary to achieve the ultimate strength of the material in a laboratory strength test. The purpose of this is to ensure that the full stress-strain curve of the sample is recorded during the test. For example, large-displacement (or residual) shear strength values may be required to perform stability analyses for a preexisting slip plane, such as the case for a landslide. The engineer should provide the laboratory with a minimum strain (or displacement) value to ensure that the laboratory does not prematurely stop a test. In most cases, UC and triaxial tests run to 15 percent axial strain will be sufficient. For truly normally consolidated samples tested in compression, strains on the order of 20 to 25 percent may be required to reach the peak soil strength.

Rate of Shearing

The rate of shearing needs to be carefully considered before beginning either a triaxial or direct shear test, especially for fine grained soils. The selection of shearing rates for undrained shearing tests on clays needs to be slow enough to ensure equalization of pore pressures within the sample. For drained tests on clays, the shearing rate must be slow enough to allow for excess pore pressures to dissipate through the pervious boundaries. For both CU and CD tests, the time to failure, t_f, is estimated using table 18. This table also shows the affect of using side drains. Typical triaxial tests incorporate porous stones on the top and bottom of the specimen. The use of filter strips along the side of the specimen (i.e., side drains) serves to reduce the time required to dissipate excess pore pressures in the specimen by allowing drainage in the radial direction. The t_{100} value in table 18 is the time to complete primary consolidation, which can be evaluated using time rate versus deformation data from the consolidation portion of the strength test. Since most laboratories do not record time rate consolidation data during the consolidation phase of a CIU test, this data will need to be requested from the testing laboratory prior to testing. Next, the axial strain to reach peak strength, ε_p, is estimated Strains required to reach peak conditions depend on the type of clay, OCR of the clay, and the imposed loading during shear (i.e., compression, extension, etc.). Typical values for compression loading of an isotropically consolidated specimen are 20 to 25 percent at OCR = 1 and decreasing to a few percent at high OCR (>20). A maximum rate of displacement, $\dot{\delta}$, can then be calculated so that ε_p is reached after t_f for a specimen with an initial height H_o as:

$$\dot{\delta}=\varepsilon_p H_o/(12.7\, t_{100}) \qquad \text{(Equation 23)}$$

Table 18. Time t_f to reach failure (after Head, 1986).

Type of test	No side drains	With side drains
CU	0.51 t_{100}	1.8 t_{100}
CD	8.5 t_{100}	14 t_{100}

Although not commonly performed on fine-grained soils, in the case of consolidated drained (CD) direct shear tests, the shearing rate can be selected based on ASTM 3080 wherein the minimum time required to fail a sample, t_f, is calculated as:

$$t_f = 50 \cdot t_{50} = 11.7 \cdot t_{90} \qquad \text{(Equation 24)}$$

where t_{50} and t_{90} are the times required to complete 50 percent and 90 percent primary compression, respectively. The times t_{50} and t_{90} may be evaluated using the square root of time or logarithm of time method (see chapter 5) to assess the vertical displacements measured with time under the constant normal load prior to shearing. Once t_f is calculated, the displacement required to achieve the peak strength of the soil (using a conventional size direct shear box), δ_f, can be estimated as 1 to 2 mm for hard clays, 2 to 5 mm for stiff clays, and 8 to 10 mm for plastic clay (Bardet, 1997). The maximum shear rate for the CD test is then selected so that the test takes at least as long as t_f to reach the displacement δ_f.

4.12.5.4 Permeability

Equipment

Laboratory permeability testing is performed to determine the hydraulic conductivity of a soil specimen. For natural soils, tests are conducted on specimens from tube samples and for fill and borrow soils, tests are made on recompacted materials. Two types of tests are commonly performed, the rigid wall test (AASHTO T215; ASTM D 2434) and the flexible wall test (ASTM D 5084). Rigid wall permeameters are not recommended for low permeability (i.e., $k \leq 10^{-6}$ cm/s) soils due to the potential for sidewall leakage. The equipment for the rigid wall test includes a rigid wall permeameter, water tank, vacuum pump, and manometer tubes (see figure 31). The permeameter must be large enough to minimize sidewall leakage, and thus the diameter of the rigid wall device should be at least 8 to 12 times that of the largest soil particle. Porous stones and filter paper must not restrict flow through the soil, but must also retain the fine particles. A vacuum pump is used to remove air from the samples and to saturate the specimens prior to testing. Manometer outlets should be available on the sides of the cell to measure head loss over the specimen.

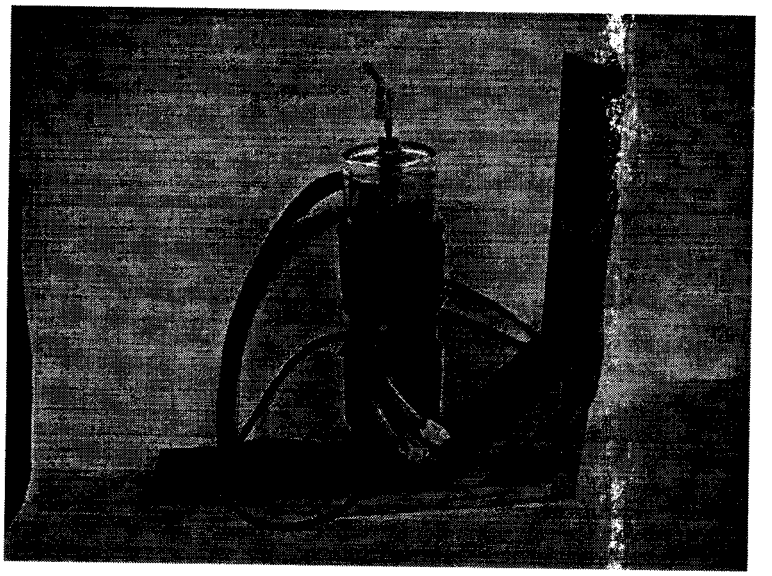

Figure 31. Rigid wall permeameter (photograph courtesy of GeoTesting Express).

Constant head and falling head tests can be performed using a flexible wall permeameter cell, cell reservoir, headwater reservoir, tailwater reservoir, top and base caps, flexible membrane, porous stones, and filter paper. With this equipment, the specimen can be tested at a range of confining stresses under backpressure saturation. The separate headwater and tailwater reservoirs can be monitored, and falling head or constant head tests can be performed. Since the flexible membrane encases the specimen, side leakage is prevented. Flexible wall permeameter cells (see figure 32) consist of influent and effluent lines as well as pore stones and filter paper. The hydraulic conductivity of the system may be found to be lower than that of the material due to small diameter flow lines and low permeability porous stones. This is not acceptable. The hydraulic conductivity of the system should be tested to ensure it is at least one order of magnitude greater than that anticipated for the material.

Procedures

Laboratory determinations of hydraulic conductivity (k) for materials with a hydraulic conductivity less than or equal to $1x10^{-3}$ cm/s are usually performed in flexible wall permeameters (ASTM D 5084). Rigid wall permeameters are typically used for sandy and gradually soils (ASTM D 2434) with a hydraulic conductivity greater than $1x10^{-3}$ cm/s. The flexible membrane used to encase the specimen prevents sidewall leakage for fine-grained soils that would occur in a rigid wall system. Rigid wall systems are used for granular materials because the permeability of the flexible wall system (valves, pore stones, tubing, etc.) may be less than that of the specimen, and thus the test would reflect a permeability lower than that of the specimen.

The confining stress of the hydraulic conductivity test will need to be specified to the laboratory. As confining stress increases, the hydraulic conductivity of fine grained soils will typically decrease due to consolidation of the specimen and reduction of void ratio. The confining stress should be equal to the anticipated effective stress-state in the soil.

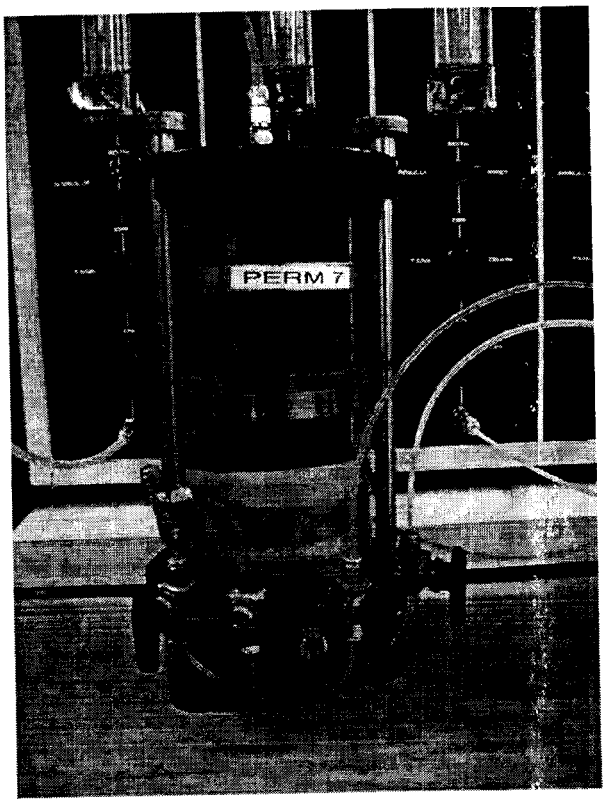

Figure 32. Flexible wall permeameter (photograph courtesy of GeoTesting Express).

The hydraulic gradient, defined as the difference in hydraulic head across the specimen divided by the length of the specimen, should also be specified to the laboratory. Typical hydraulic gradients in field situations are less than 5, however the use of such a small gradient will result in extremely long testing times for materials having hydraulic conductivities less than $1x10^{-6}$ cm/s. If the hydraulic gradient across the specimen is too high, turbulent flow will occur and result in hydraulic conductivity values that are too low. Suggested hydraulic gradient values are a function of the anticipated hydraulic conductivity, as presented in table 19.

Table 19. Recommended maximum hydraulic gradient for permeability testing.

Hydraulic Conductivity, cm/sec	Recommended Maximum Hydraulic Gradient
1×10^{-3} to 1×10^{-4}	2
1×10^{-4} to 1×10^{-5}	5
1×10^{-5} to 1×10^{-6}	10
1×10^{-6} to 1×10^{-7}	20
less than 1×10^{-7}	30

Saturation of the specimen is necessary to achieve accurate results. Backpressure saturation procedures should be used to achieve B-values greater than 0.95, or constant B-values over a range of increasing back pressure values. In a rigid wall test, air is evacuated from the sample using a pump and then saturation from the bottom of the specimen upward is performed (see ASTM D 2434).

A hydraulic conductivity test should be ended when steady flow is occurring. The hydraulic conductivity is considered to be steady when four or more consecutive hydraulic conductivity measurements fall within ±25 percent of the average k value if k is greater than 1×10^{-10} m/s, or if four or more measurements fall within ±50 percent of the average if k is less than 1×10^{-10} m/s.

Since the hydraulic conductivity is defined at a temperature, T (in degrees Celsius), of 20 °C, a temperature correction factor, R_T, may need to be incorporated into the calculations. To apply this temperature correction factor, the temperature of the permeant will need to be provided by the laboratory. The corrected hydraulic conductivity value, i.e., k_{20} is given as $k_{measured} \times R_T$. Temperature correction factors are presented in ASTM D 5084 and can also be calculated according to equation 25.

$$R_T = (-0.02452\ T + 1.495) \qquad \text{(Equation 25)}$$

4.13 LABORATORY ROCK TESTS

4.13.1 Introduction

This section provides information on common laboratory test methods for rock including testing equipment, general procedures related to each test, and parameters measured by the tests. A discussion of the interpretation of these tests to obtain properties is provided in chapter 6. Table 20 provides a list of commonly performed laboratory tests for rock associated with typical projects for highway applications. Although other laboratory test methods for rock are available including triaxial strength testing, rock tensile strength testing, and durability testing related to rock soundness, most design procedures for structural foundations and slopes on or in rock are developed based on empirical rules related to RQD, degree of fracturing, and to the unconfined compressive strength of the rock. The use of more sophisticated rock laboratory testing is usually limited to the most critical projects. Details on other laboratory rock testing procedures are provided in FHWA- HI-97-021 (1997). Table 21 provides summary information on typical rock index and performance tests.

Table 20. Common rock laboratory tests.

Test Category	Name of Test	ASTM Test Designation
Point Load Strength	Suggested method for evaluating point load strength	D 5731
Compressive Strength	Compressive strength of intact rock core specimen (in unconfined compression)	D 2938
Direct Shear Strength	Laboratory direct shear strength tests for rock specimens under constant normal stress	D 5607
Durability	Slake durability of shales and similar weak rocks	D 4644
Strength-Deformation	Elastic moduli of intact rock core specimens in uniaxial compression	D 3148

Table 21. Summary information on rock laboratory test methods.

Test	Procedure	Applicable Rock Types	Applicable Rock Properties	Limitations / Remarks
Point-Load Strength Test	Rock specimens in the form of core, cut blocks, or irregular lumps are broken by application of concentrated load through a pair of spherically truncated, conical platens.	Generally not appropriate for rock with uniaxial compressive strength less than 25 MPa	Provides an index of uniaxial compressive strength	Can be performed in the field with portable equipment or in the laboratory; in soft or weak rock, test results need to be adjusted to account for platen indentation
Unconfined Compressive Strength of Intact Rock Core	A cylindrical rock specimen is placed in a loading apparatus and sheared under axial compression with no confinement until peak load and failure are obtained.	Intact rock core	Uniaxial compressive strength	Simplest and fastest test to evaluate rock strength; fissures or other anomalies will often cause premature failure
Laboratory Direct Shear Test	A rock specimen is placed in the lower half of the shear box and encapsulated in either synthetic resin or mortar. The specimen must be positioned so that the line of shear force lies in the plane of the discontinuity to be investigated. The specimen is then mounted in the upper shear box and the normal load and shear force are applied.	Used to assess peak and residual shear strength of discontinuity	Peak and residual shear strength	May need to perform in-situ direct shear test if design is controlled by potential slip along a discontinuity filled with very weak material
Elastic Moduli of Intact Rock Core	Procedure is similar to that for unconfined compressive strength of intact rock. Lateral strains are also measured	Intact rock core	Modulus and Poisson's ratio	Modulus values (and Poisson's ratio) vary due to nonlinearity of stress-strain curve.
Slake Durability[1]	Dried fragments of rock are placed in a drum made of wire mesh that is partially submerged in distilled water. The drum is rotated, the sample dried, and the sample is weighed. After two cycles of rotating and drying, the weight loss and the shape of size of the remaining rock fragments are recorded.	Shale or other soft or weak rocks	Index of degradation potential of rock	

Note: (1) This test is described further in chapter 7.

4.13.2 Laboratory Testing of Rock

4.13.2.1 Point-Load Strength Test

The point load strength test is an appropriate method used to estimate the unconfined compressive strength of rock in which both core samples and fractured rock samples can be tested. The test is conducted by compressing a piece of the rock between two points on cone-shaped platens (see figure 33) until the rock specimen breaks in tension between these two points. Each of the cone points has a 5-mm radius of curvature and the cone bodies themselves include a 60° apex angle. The equipment is portable, and tests can be carried out quickly and inexpensively in the field. Because the point load test provides an index value for the strength, usual practice is to calibrate the results with a limited number of uniaxial compressive tests on prepared core samples. The point load test is also used with other index values to assess degradation potential of shales (see chapter 6).

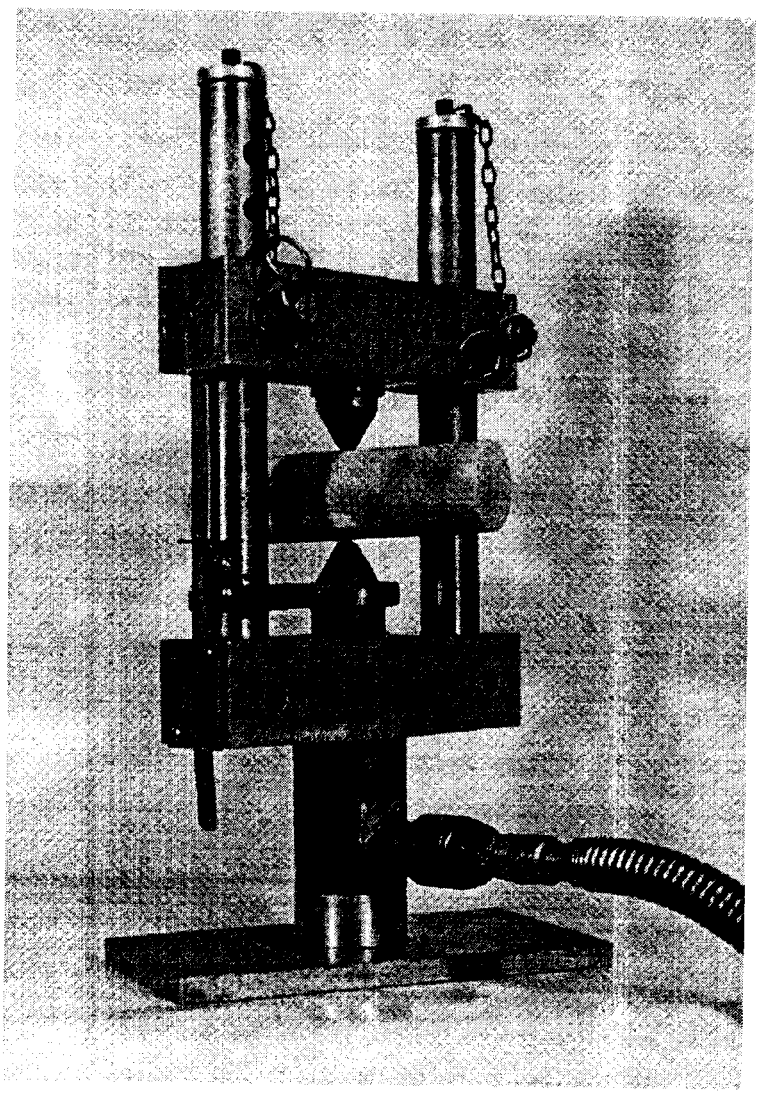

Figure 33. Point load strength test equipment.

If the distance between the platens is D and the breaking load is P, then the point load strength, I_s is calculated as:

$$I_s = \frac{P}{D_e^2} \qquad \text{(Equation 26)}$$

where D_e is the equivalent core diameter which is given by: (1) $D_e = D^2$ for diametral tests; or (2) $D_e = 4 \times A$ for axial, block, or lump tests where $A = W \times D$. The area A is the minimum cross-sectional area of a lump sample for a plane through the platen contact points where W is the specimen width.

The size-corrected point load strength index, $I_{s(50)}$ of a rock specimen is defined as the value of I_s that would have been measured by a diametral test with D = 50 mm. For tests performed on specimens other than 50 mm in diameter, the results can be standardized to the size-corrected point load strength index according to:

$$I_{s(50)} = k_{PLT} I_s \qquad \text{(Equation 27)}$$

The value of the size correction factor, k_{PLT}, is given by:

$$k_{PLT} = (D/50)^{0.45} \ (D \text{ in } mm) \qquad \text{(Equation 28)}$$

It has been found, on average, that the uniaxial compressive strength, σ_c, is about 20 to 25 times the point load strength index, with a value of 24 commonly used, i.e.,

$$\sigma_c = 24 I_{s(50)} \qquad \text{(Equation 29)}$$

However, tests on many different types of rock show that the ratio can vary between 15 and 50, especially for anisotropic rocks. Consequently, the most reliable results are obtained if a series of uniaxial calibration tests are carried out. Point load test results are not acceptable if the failure plane lies partially along a pre-existing fracture in the rock, or is not coincident with the line between the platens. For tests in weak rock where the platens indent the rock, the test results should be adjusted by measuring the amount of indentation and correcting the distance D (Wyllie, 1999).

4.13.2.2 Unconfined Compressive Strength of Intact Rock Core

The unconfined compressive strength of intact rock core can be evaluated reasonably accurately using ASTM D 2938. In this test, rock specimens or regular geometry, generally rock cores, are used. The rock core specimen is cut to length so that the length to diameter ratio is 2.5 to 3.0 and the ends of the specimen are machined flat. The ASTM test standard provides tolerance requirements related to the flatness of the ends of the specimen, the perpendicularity of the ends of the specimens, and the smoothness of the length of the specimen. The specimen is placed in a loading frame. Axial load is then continuously applied to the specimen until peak load and failure are obtained. The unconfined (or uniaxial) compressive strength of the specimen is calculated by dividing the maximum load carried by the specimen during the test by the initial cross-sectional area of the specimen.

This test is more expensive than the point load strength test, but is also more accurate. Careful consideration of the design requirements should be made in deciding whether to perform this test or the simpler point load strength test.

4.13.2.3 Elastic Moduli of Intact Rock Core

This test is performed similarly to the unconfined compressive test discussed above, except that deformation is monitored as a function of load. This test is performed when it is necessary to estimate both elastic modulus and Poisson's ratio of intact rock core. Because of this, it is common to measure both axial (or vertical) and lateral (or diametral) strain during compression. It is preferable to use strain gauges glued directly to the rock surface as compared to LVDT mounted on the platens since slight imperfections at the contact between the platens and the rock may lead to movements that are not related to strain in the rock (Wyllie, 1999).

4.13.2.4 Laboratory Direct Shear Test

The apparatus and procedures for direct shear testing are discussed in ASTM D 5607. This test is typically used to evaluate the shear strength of a rock discontinuity. Overall, the equipment for the direct shear test on rock is similar to that for soil including a direct shear testing machine, a device for applying normal pressure, and displacement monitoring devices. A schematic for the test set up is shown in figure 34. For testing of rock specimens, an encapsulating material such as a high strength gypsum cement is poured around the specimen in the upper and lower holding ring. The specimen is sheared as one holding ring is displaced horizontally with respect to the other such that the discontinuity surface is exactly parallel to the direction of the shear load. Load cells are used to monitor the shear force and LVDTs or dial gauges are used to monitor both horizontal and vertical deformation. Multiple LVDTs should be used to monitor vertical deformation and potential overturning of the specimen.

In this test, plots of shear stress versus shear displacement and normal displacement and shear displacement are prepared. Normal stresses should be adjusted to account for potential decreases in the shear contact area. After the sample is sheared, the sample is then reset to its original position, the normal load is increased, and another test is performed. Each test will produce a pair of shear stress and normal stress values for both peak and residual conditions. From this, the friction angle of the discontinuity surface can be evaluated. Evaluation of the friction angle is described in chapter 6.

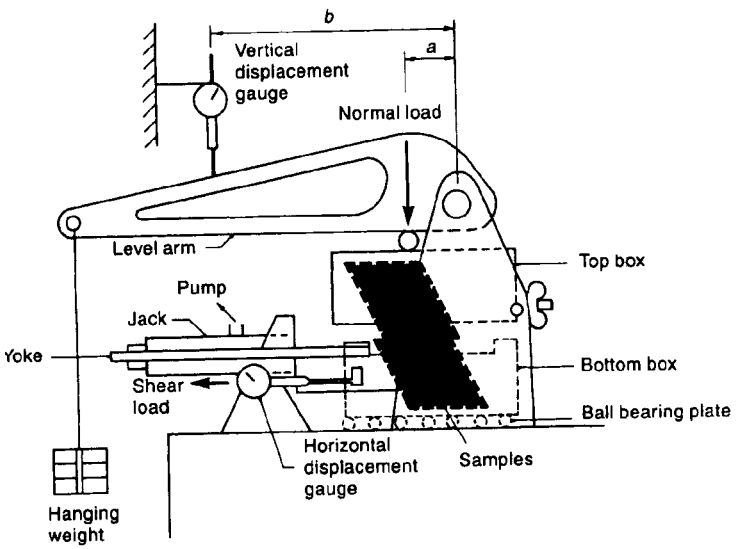

Figure 34. Laboratory direct shear testing equipment for rock (after Wyllie, 1999, Foundations on Rock, Figure 3.19, p. 74, E&FN Spon).

CHAPTER 5

INTERPRETATION OF SOIL PROPERTIES

5.1 INTRODUCTION

The interpretation of soil properties based on measured data and/or derived parameters from laboratory and in-situ tests is presented in this chapter. Numerous textbooks on soil mechanics and foundation engineering describe the basic methods used to interpret soil properties from laboratory tests such as one-dimensional consolidation and triaxial shear tests (e.g., Lambe and Whitman, 1969; Bardet, 1997). In this chapter, guidance on soil property interpretation is presented with a specific focus on practical issues, including the assessment of data quality and the selection of properties for design where multiple methods are available to obtain a property. The soil properties presented in this section include: (1) subsurface stratigraphy; (2) in-situ stress state; (3) deformation (i.e., consolidation, elastic deformation properties, and secondary compression); (4) shear strength; and (5) hydraulic conductivity.

In this section, the selection of properties for design calculations concerning, for example, settlements, time rate of settlement, and shear strength is presented. In selecting design soil properties, it is typical to use terminology such as "average", "conservative", "lower-bound", or "worst-case" in the context of describing a single design property or set of design properties. The selection of properties must consider the design application, potential construction issues related to the implementation of the design, the design life of the structure, and the criticality of the structure.

5.2 INTERPRETATION OF SUBSURFACE STRATIGRAPHY

5.2.1 General

Methods used to provide information on subsurface stratigraphy and soil type include the SPT with recovery of disturbed samples, electric cone penetration test (CPT), piezocone penetration test (CPTu), and flat plate dilatometer test (DMT). In this section, the evaluation of soil stratigraphy based on data collected from each of these tests is described. This section also provides information on developing a subsurface profile for use in geotechnical design analyses.

5.2.2 Soil Classification by Soil Sampling and Drilling

Routine sampling practice involves the recovery of auger cuttings, drive samples, and thin-walled tubes pushed into the ground. First, a vertical boring is advanced using rotary drilling methods that may involve solid flight augers (limited to depths < 10 m), hollow-stem augers (limited to depths < 30 m), and wash-boring techniques. At select depths, a hollow thick-walled tube is lowered to the bottom of the borehole and driven into the ground to recover a disturbed soil sample. The driving record (i.e., number of blows to drive the spoon 300 mm) is also the basis for the SPT resistance, or N value. The 450-mm long drive samples are usually collected at discrete 1.5-m intervals, although

smaller and larger testing intervals have been used. Figure 35 depicts the general process of traditional drilling, sampling, and laboratory testing of collected samples.

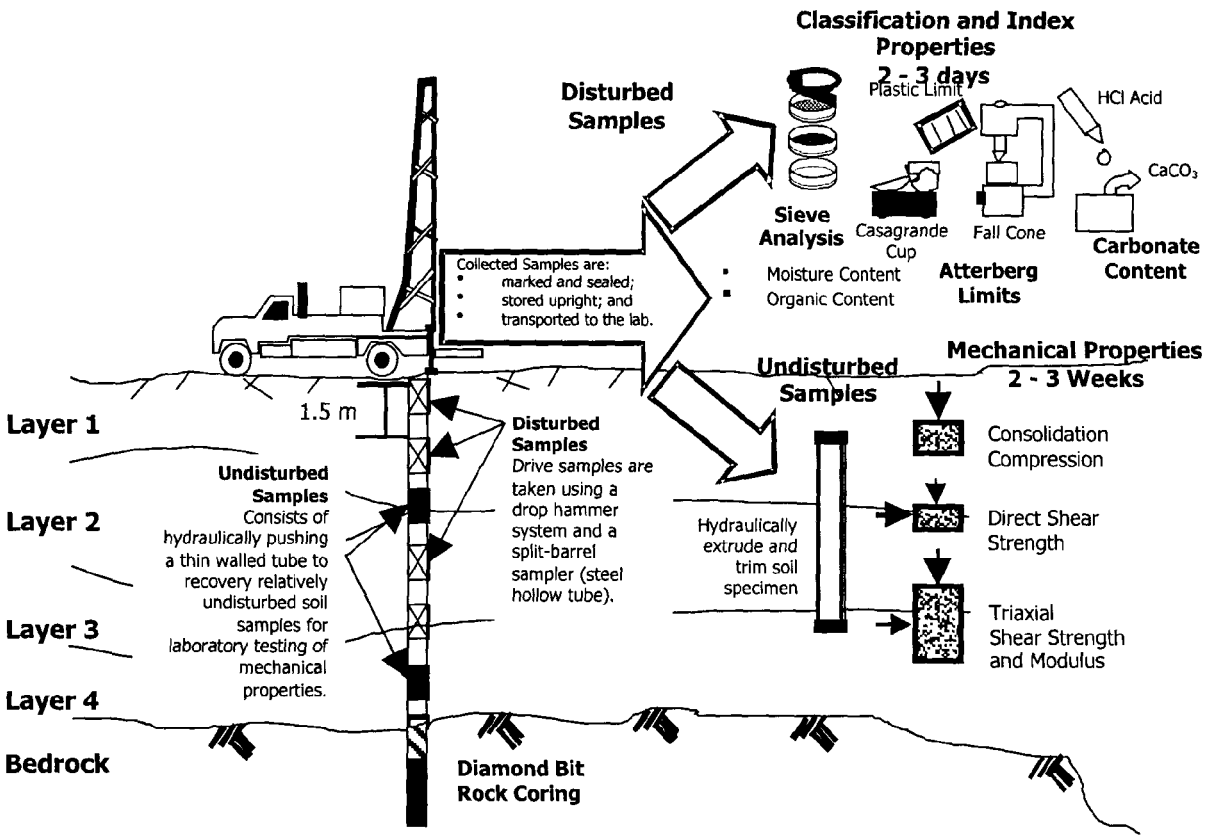

Figure 35. Traditional drilling, sampling, and laboratory testing of collected samples.

More recently, sampling by a combination of direct-push and percussive forces has become available (e.g., Geoprobe sampling), whereby 25-mm diameter continuously-lined plastic tubes of soil are recovered. Although disturbed samples of soil are recovered, the full stratigraphic profile can be examined for soil type, layers, seams, lenses, and color changes.

Standard penetration testing coupled with disturbed sample description, identification, and classification is the most commonly used method to obtain stratigraphic profiling information for most traditional projects. Although SPT samples are disturbed, the samples are usually of sufficient quality to permit visual identification and laboratory classification. These classifications are used with recorded SPT N values to develop a subsurface profile and to facilitate "first-order" estimates of engineering properties of the soil. Tables 22 and 23 provide baseline correlations between N values and relative density (granular soils) and consistency (cohesive soils). When establishing a stratigraphic profile using a SPT boring, significant changes in N values should be used to identify changes in material types.

Table 22. SPT N value soil property correlations for granular soils (after AASHTO, 1988).

N value	Relative Density
0-4	Very loose
5-10	Loose
11-24	Medium Dense
25-50	Dense
> 50	Very Dense

Table 23. SPT N value soil property correlations for cohesive soils (after AASHTO, 1988).

N value	Consistency
0-1	Very soft
2-4	Soft
5-8	Medium Stiff
9-15	Stiff
16-30	Very Stiff
31-60	Hard
>60	Very Hard

As discussed in chapter 4, N values are highly dependent on the energy efficiency of the SPT method. Inconsistency in the N values across a site may be due to variations in energy efficiency between different drill rigs and crews; therefore, N values should be corrected to $(N)_{60}$, as described in section 4.4.3. Failure to correct these N values could result in confusion when attempting to correlate subsurface units between borings. Figure 36 shows an example of actual variability of SPT N value measurements due to varying energy efficiencies for three different drill rigs and crews. For the data included in this figure, each crew used hollow stem auger techniques and a safety hammer with a cathead and rope system. The borings were performed in Piedmont residual soil consisting of silty fine sands. From this figure it is noted that variability in N-values by 50 percent or more in similar soils is not uncommon. Similar variations have been reported with different hammers.

During drilling operations, the field engineer or geologist should work closely with the driller. An experienced driller can distinguish changes in material type and can often identify the material based on resistance. The driller should be instructed at the beginning of the job and on a daily basis to alert the engineer or geologist of important observations such as, for example, loss of drilling fluid, odors, or auger refusal. Such observations should be noted on the field log since this information will be useful in developing the site stratigraphy for design analyses. For example, the loss of drilling fluid may occur in fractured rock, highly permeable units, or large void spaces; organic odors from the borehole may indicate an organic unit such as peat; chemical odors may indicate the presence of contaminated soil; and refusal may indicate the depth to bedrock or the presence of an obstruction such as a buried object or boulder.

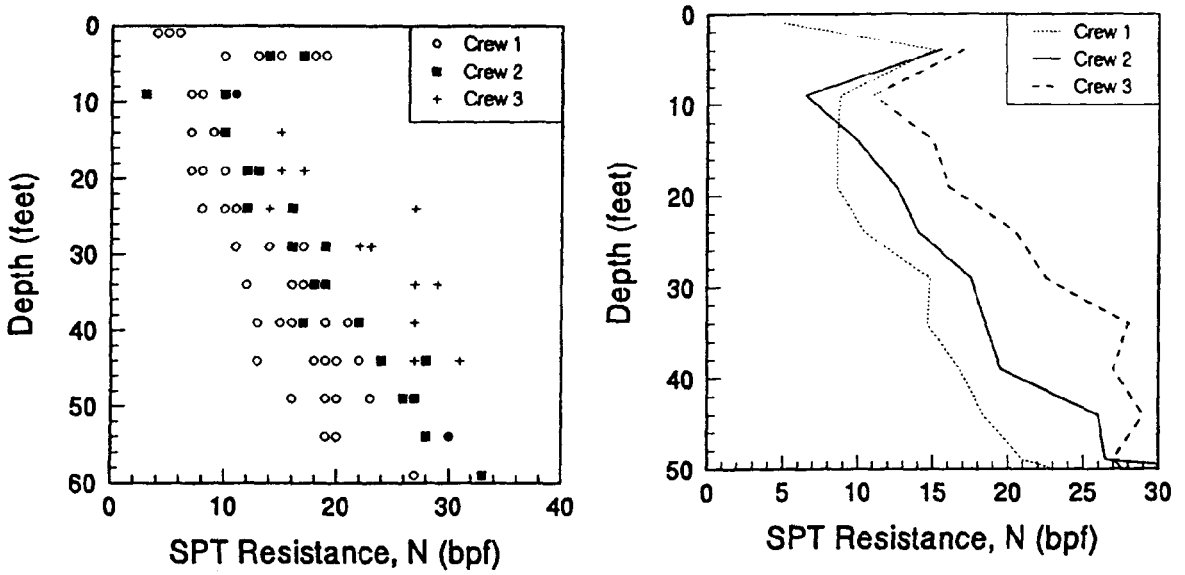

Figure 36. Variability of SPT N values.

The engineer or geologist should record for each boring the initial depth to water, the groundwater elevation at the end of drilling, and the groundwater elevation 24 hours after drilling at each location. If possible, at the end of the investigation, the groundwater levels should also be recorded in each boring. Groundwater level information is most valuable if the levels in all of the borings can be measured in one day, in the shortest amount of time possible since groundwater levels may fluctuate daily. Cave-in depths should also be recorded as these may indicate groundwater activity, even though no water may have been observed. For more reliable groundwater levels, all borings should be protected from surface water infiltration at the end of drilling.

Sampling intervals for SPTs are typically performed at 1.5 m intervals, although continuous sampling may be used for the upper reaches (up to 6 m) of a soil deposit. Where very detailed stratigraphy is required, it is more cost-effective to supplement SPTs with other in-situ devices such as the CPT or CPTu. These devices can be used to evaluate very thin soil layers. The ability to accurately characterize the thickness of potentially problematic soil layers cannot be overemphasized as costs associated with improving such layers are directly related to the thickness of the layer. Additionally, the materials in these layers may be shown to effectively control the entire design. As an example, figure 37 shows a summary of SPT $(N_1)_{60}$ values for two borings advanced at site near Charleston, South Carolina. Based on SPT $(N_1)_{60}$ values alone, it may be concluded that the thickness of a potentially liquefiable layer (i.e., as evidenced by SPT N values less than say 10 for this site) may be on the order of 5 to 13 ft (1.5 to 4 m). Two cone penetration tests were performed near the two borings and the presence of a potentially liquefiable layer was confirmed (based on low q_t values and classification as silty sand to sand; see discussion of classification using CPT in section 5.2.3). Additional cone testing was performed across the site to delineate the extent of the liquefiable zone.

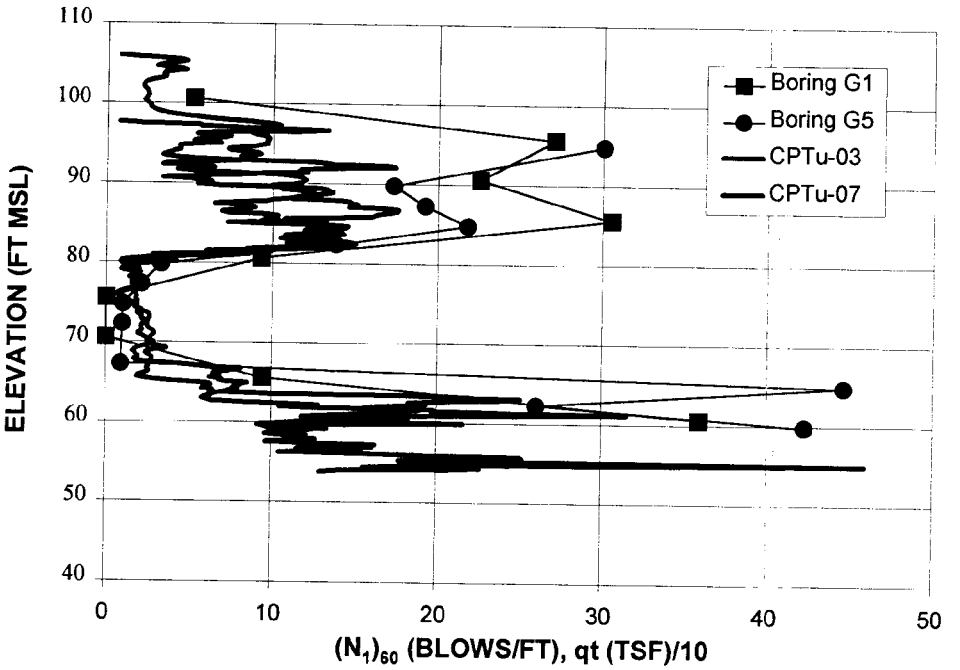

Figure 37. Comparison of SPT $(N_1)_{60}$ and CPT q_t values.

5.2.3 Soil Classification by Cone Penetration Testing

Cone penetration testing (CPT) may be used to obtain detailed site stratigraphy information. The CPT is rapid, relatively inexpensive, and facilitates the collection of continuous subsurface stratigraphy data. Soil classification using the CPT is based on measured values for cone tip resistance (q_t), and sleeve friction (f_s) presented as friction ratio (FR) defined as the ratio of sleeve friction to cone tip resistance (i.e., $FR = R_f = f_s/q_t \cdot 100$). The piezocone (CPTu) can also be used for soil classification based on measured pore pressure (u_2) during advancement of the penetrometer.

In general, the tip resistance (q_t) in sands is greater than 5 MPa whereas the tip resistance for clayey and silty materials is typically less than 2 MPa. Penetration porewater pressures in sands are often near hydrostatic values since the permeability of sands is relatively high such that negligible excess penetration porewater pressures are induced by penetration of the piezocone. In soft to firm, normally to lightly overconsolidated clays, measured u_2 values are often 3 to 10 times the value of hydrostatic porewater pressure. When using a penetrometer with the pore pressure transducer located at the shoulder position (i.e., the u_2 position), measured porewater pressures in heavily overconsolidated and fissured clays and dense silts are often negative due to the demonstrated behavior for these materials to dilate during undrained shearing. It is noted that porewater pressures measured using a penetrometer with the pore pressure transducer located at the tip position (i.e., the u_1 position) are always positive, regardless of the soil. Penetration porewater pressures that are lower than expected may indicate poor saturation of the filter element.

In addition to the previously referred general characteristic, friction ratio, tip resistance, and pore pressure data have been used with empirical soil behavioral classification charts for detailed soil

classification. Examples of these charts are shown in figures 38 and 39 and the use of these charts is illustrated in Soil Property Selection Example No. 1 and No. 2.

When using pore pressure data from CPTu, the normalized pore pressure parameter B_q should be used:

$$\textit{Normalized Pore Pressure Parameter}, B_q = \frac{u_2 - u_o}{q_t - \sigma_{vo}} \qquad \text{(Equation 30)}$$

It is noted that the term "classification" used here does not refer to a standard classification system such as USCS. Since more traditional laboratory classification is based on a mechanical analysis of "disassembled" particles and remolded fines material, it is impossible for a CPT to provide the same "classification" information since the CPT readings provide information on the in-situ soil. Therefore, the CPT and CPTu should be considered to provide an assessment of soil behavior type and an indirect assessment of soil "classification".

The CPT and CPTu typically record data (q_c, f_s, u_2) at 1-sec duration time intervals, therefore permitting nearly continuous subsurface profiling. Typically, these data are not plotted manually on the classification charts (i.e., figures 38 and 39) since most CPT contractors have software available that automatically classifies each set of data using these charts.

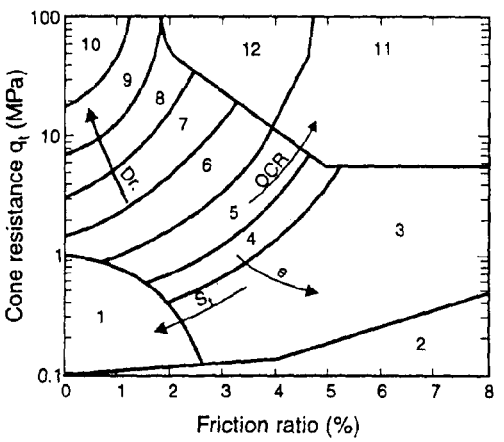

Figure 38. Soil classification based on q_t and FR (Robertson et al., 1986).

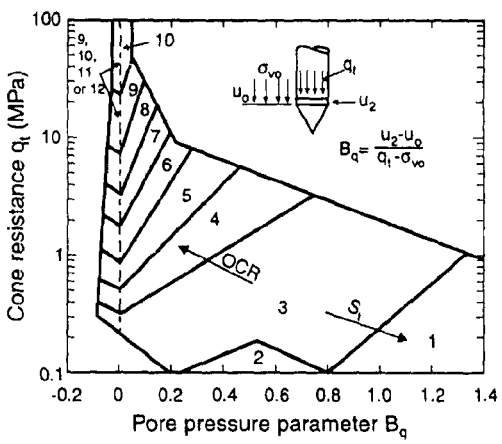

Figure 39. Soil classification based on q_t and B_q (Robertson et al., 1986).

Soil Behavior Type (Robertson et al.,1986; Robertson & Campanella, 1988)

1 – Sensitive fine grained	5 – Clayey silt to silty clay	9 – sand
2 – Organic material	6 – Sandy silt to silty sand	10 – Gravelly sand to sand
3 – Clay	7 – Silty sand to sandy silt	11 – Very stiff fine grained*
4 – Silty clay to clay	8 – Sand to silty sand	12 – Sand to clayey sand*
	** Overconsolidated or cemented*	

To develop a subsurface profile for design analyses based on CPT or CPTu data, the logs should first be reviewed to establish soil units based on distinct breaks in the q_t, f_s, FR, and u_2 signatures. Figure 40 shows a CPT log for an embankment constructed over dredged material, natural clays, and sands. The soil classification column shows numerous classifications based on the nearly continuous data. To develop a profile for design, distinct breaks in the actual cone data (e.g., q_t signatures) should be reviewed. A review of figure 41 indicates that a significant change in material type occurs at approximately a depth of 18 ft (5.5 m) as defined by a distinct drop in q_t and f_s along with a sharp increase in u_2. These trends indicate that at this depth the CPT has penetrated into a clay unit characterized by low q_t, high FR, and increased pore pressures due to the lower hydraulic conductivity of the clay. Another distinct break occurs at 32 ft (9.8 m) as evidenced by increased q_t, decreased FR, and decreased u_2 to essentially hydrostatic pressure. These trends in the data indicate that a sandy material has been encountered. Also shown on this profile are SPT blowcount data from an adjacent boring. Thus, the CPT characterization presented here is consistent with the SPT boring. It is worth noting that although the SPT N value is similar for the lower portion of the dike sands and the dredged material (with SPT N = 11), the CPT signature does indicate that there is a distinction between these two materials as evidenced by the rapid decrease in tip resistance. The distinction between these two layers was also confirmed by reviewing disturbed SPT samples for the project.

Once the main units have been identified, the soil classification columns of the logs should be reviewed. For the example shown in figure 41, the upper sand unit has been classified into three soil types (i.e., sand, silty sand, and sandy silt). Figure 38 and 39 shows the close proximity of each of these categories to each other and how scatter in the data from one unit could be plotted in several different zones. Such variations within a unit should generally be considered negligible, meaning that such distinctions will not typically need to be considered in developing a subsurface profile for design analyses. When dividing the subsurface into units, more attention should be given to overall groupings rather than to individual classifications. Experience has shown that minor variations in grain size throughout a unit across a site explain this subtle classification difference, although these changes generally have little to no significant change in engineering properties.

Groundwater elevations can also be evaluated using the CPTu provided that relatively clean sands exist within the subsurface. Under hydrostatic conditions, the groundwater elevation can be obtained by extrapolating the water pressure readings in a relatively clean sand unit back to zero (see figure 40). Pore pressure readings in clay or silt should not be used for this purpose. Alternatively, a pore pressure dissipation test can be performed in a sand layer to ensure that all penetration pore pressures have dissipated. Figure 42 shows the results of a dissipation test in a sand layer in which dissipation occurs instantaneously. For the example shown in figure 42, the dissipation test was performed at a depth of 35.6 ft. The pore pressure head measured was approximately 24 ft indicating that the ground water table was located at approximately a depth of 12 ft. The in-situ pore pressure condition, u_o, can also be evaluated by performing full dissipation tests in more fine-grained materials such as clays and silts, however, the tests will take much longer due to the lower hydraulic conductivity of these materials. Estimation of u_o from CPTu pore pressure dissipation tests in low hydraulic conductivity materials is usually not practical. On the other hand, in a Piedmont silty soil, full dissipation occurs within 1 to 2 minutes and thus u_2 data at rod breaks can be used to estimate u_o. The use of dissipation tests to obtain time rate of settlement information is discussed in section 5.4.4.

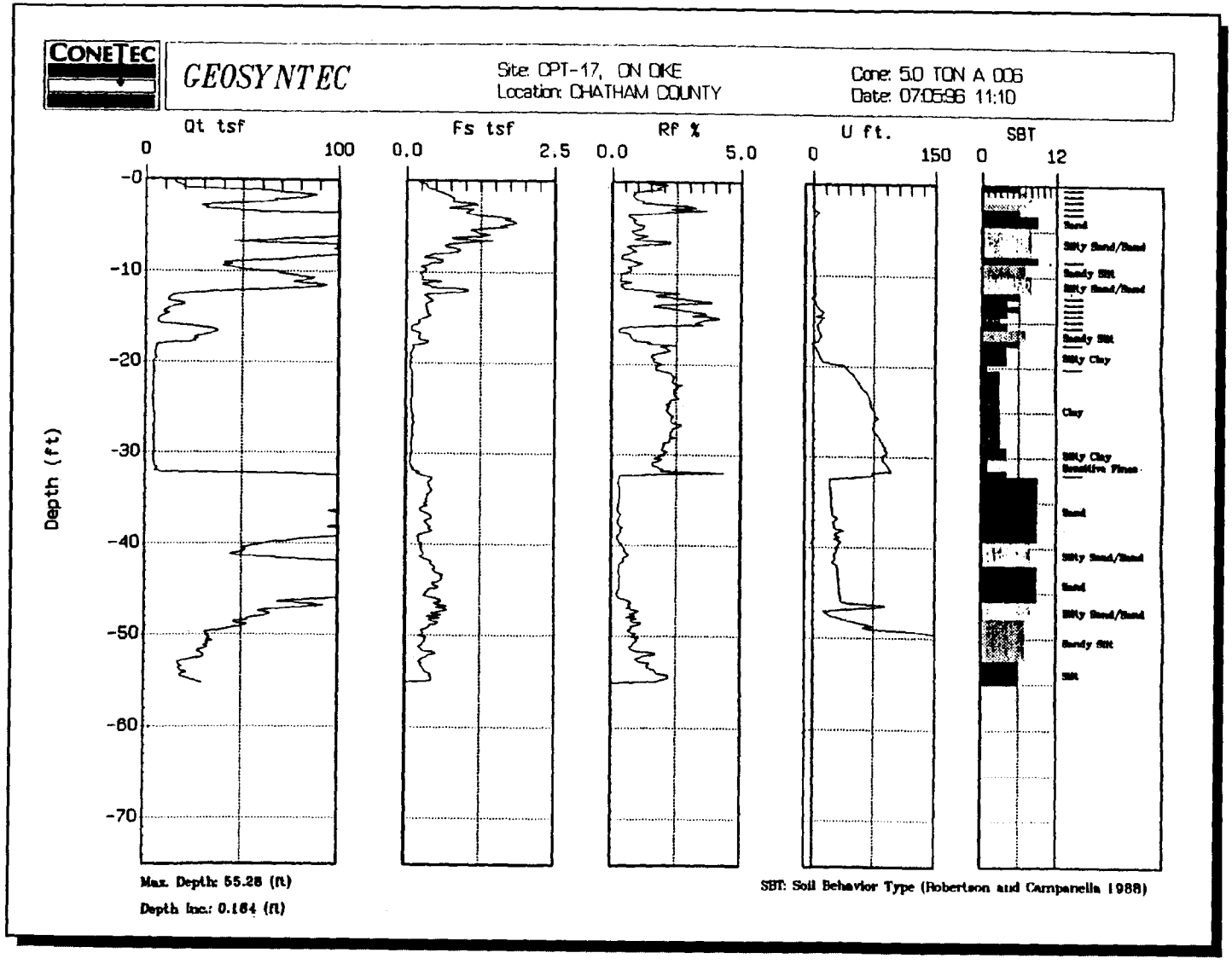

Figure 40. Typical CPTu log.

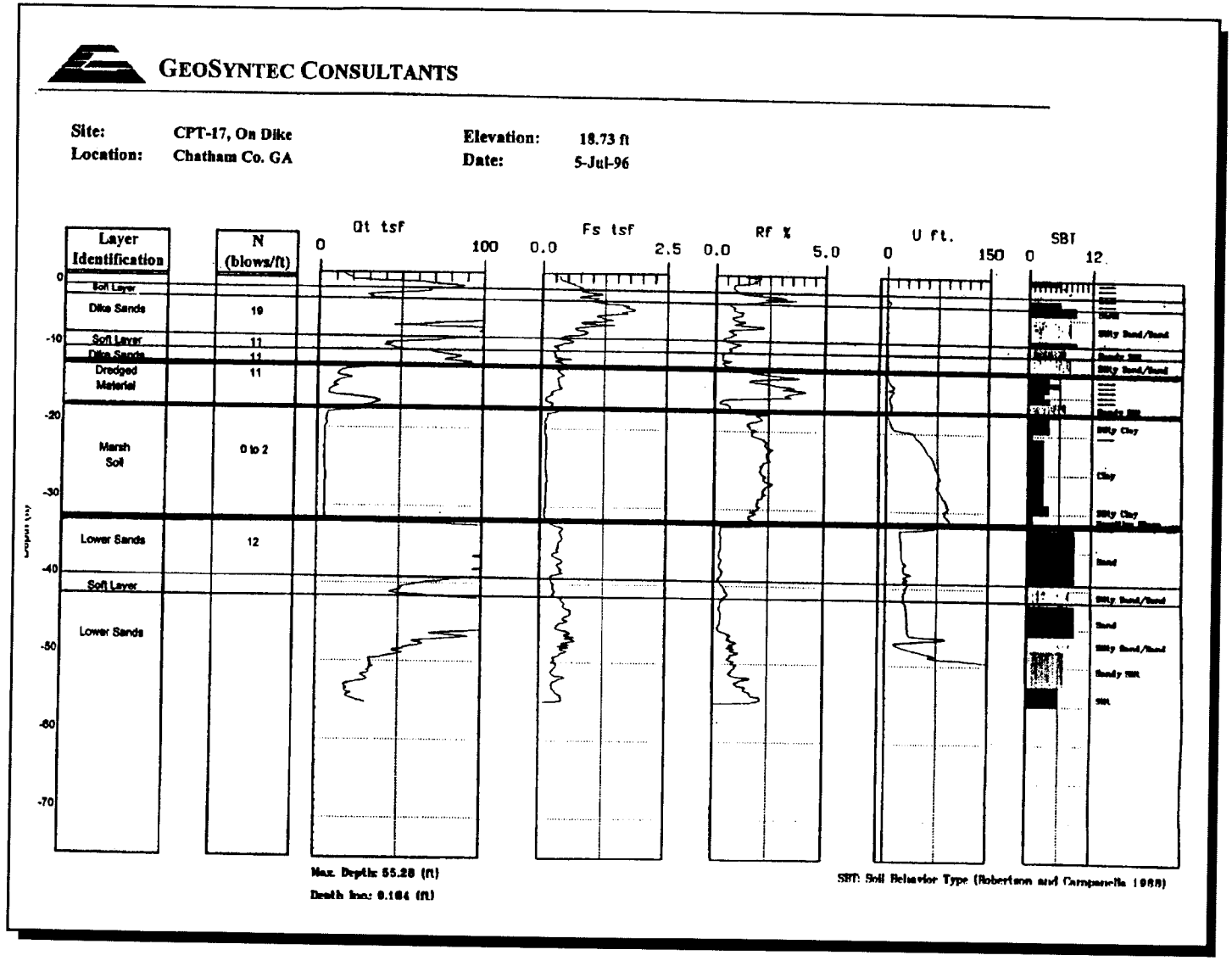

Figure 41. CPTu log with subsurface stratigraphy interpretation.

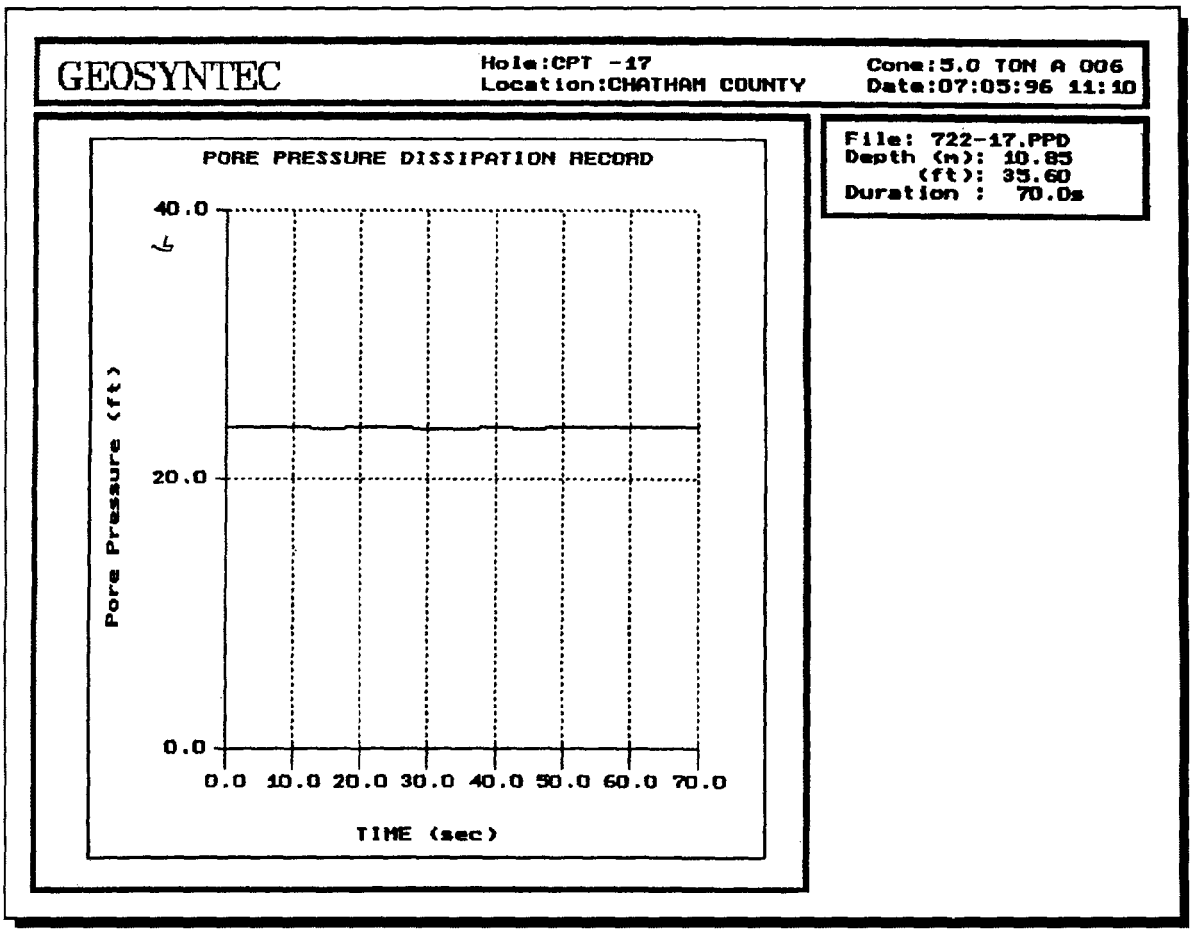

Figure 42. CPTu dissipation test in sand.

The CPT is most useful when results are correlated to known subsurface stratigraphy conditions. If the CPT is used in conjunction with other intrusive investigation methods (e.g., SPT), at least one CPT boring should be placed adjacent to a boring. If possible, the CPT results should be correlated with the physical samples recovered from an adjacent boring. With this correlation, similar CPT results across the site, possibly far from a sampling location, can be related to a particular soil type.

5.2.4 Soil Classification using the Flat-Plate Dilatometer

The DMT uses empirical charts for indirect soil classification. The chart shown in figure 43 utilizes the relationship between dilatometer modulus (E_D) and material index (I_D) to evaluate: (1) soil type (i.e., clay, silt, sand); and (2) consistency (soft vs. hard, loose vs. dense). Soil type is categorized by the following ranges:

- Clay: $I_D < 0.6$
- Silt: $0.6 < I_D < 1.8$
- Sand: $I_D > 1.8$

In the absence of other data, this DMT classification can be used in preliminary design, but should be confirmed by comparing classification results with other site-specific testing of either soil type and/or behavior such as that from laboratory classification, SPT, and CPT data (if available).

When using a DMT for soil classification and stratigraphy, the previously referenced comments regarding the CPT are applicable. Specifically, the DMT should be correlated on a site-specific basis with SPT and/or tube samples wherever possible. Additionally, it is recognized that since the DMT (like the CPT) provides quantified data on regular intervals, subtle differences in the data can result in a different "classification" while not representing a difference in engineering parameters.

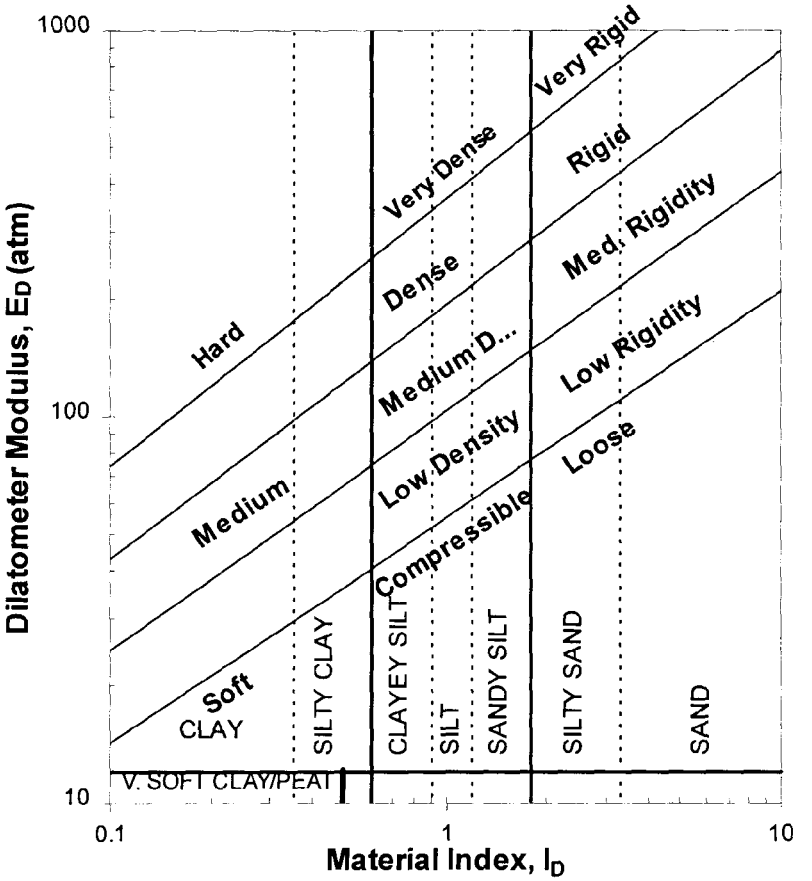

Figure 43. Soil classification based on DMT.

5.2.5 Generating a Subsurface Profile

A primary objective of any subsurface investigation is to obtain sufficient data to enable a two-dimensional drawing depicting the site geostratigraphy. This drawing is called a subsurface profile. A sufficient quantity of data must be collected to characterize soil variability with respect to aerial and vertical distribution across the site. The purpose of stratigraphic profiling is to develop a simple

working model that depicts the major subsurface layers exhibiting distinct engineering characteristics.

Once the stratigraphic information is compiled from the previously discussed methods (i.e., borings, CPT soundings, DMT soundings), final logs should be generated. The final logs are created using field notes and boring logs. Results of each boring, CPT, and DMT should be used to develop a preliminary model of soil units at each boring/sounding location, including elevation and depth intervals. This model should be added to and modified as each log is analyzed. Once an initial screening has been conducted on all of the logs, each of the completed logs should be placed on a large flat surface that is scaled to present the data in close proximity to each other, yet spaced horizontally and vertically on the surface to reflect their relative location in the field. The distinct units in each log should be compared with those in the adjacent logs. Attention to depth, soil type, distinct features (e.g., shell fragments, root matting, etc.), and engineering properties (e.g., Atterberg limits, strength, settlement parameters, etc.) will help in the correlation. The engineer or geologist should try to match these units across the site area, keeping in mind that conditions may change laterally depending on the geologic conditions. For example, alluvial units in floodplain deposits may "pinch out" laterally (i.e., localized lenses of material may exist over relatively short lateral distances). Thus, the importance of local and regional geology cannot be over emphasized.

Index properties such as Atterberg Limits, moisture content, and density provide information required to establish the stratigraphy in relation to the design parameters. Plotting these values with depth (see figure 44) can provide baseline information on the engineering properties of fine-grained soils. For example, natural moisture contents near or greater than the liquid limit indicate that a soil is normally consolidated and likely to be sensitive (i.e., loss of soil structure and strength upon disturbance). Overconsolidated clays or desiccated crusts may be identified by natural moisture contents near the plastic limit. Significant changes in index properties with depth should be used in conjunction with other data (e.g., CPT) to identify subsurface units.

After completing this exercise and grouping subsurface units based on their engineering properties, the engineer or geologist should create cross-sections of the site subsurface conditions. This entails plotting the borings at their respective elevations and relative positions horizontal to one another. Often, the vertical scale is exaggerated compared to the horizontal scale. The different strata are grouped based on color, texture, consistency, and soil type of the recovered samples or profiles from the soundings. If possible, at least two cross-sections, roughly perpendicular to each other should be constructed, as these will provide for an understanding of lateral trends in stratigraphy. Groundwater elevations should be plotted on the cross-section based on site-wide measurements taken on one day. It is likely that the conceptual model based on these cross sections will be modified as additional data are collected and evaluated. An example boring location plan and subsurface profile are shown in figures 45 and 46. If sufficient information is available, an additional graphical figure with three-dimensional perspective (i.e., a fence diagram) can be developed.

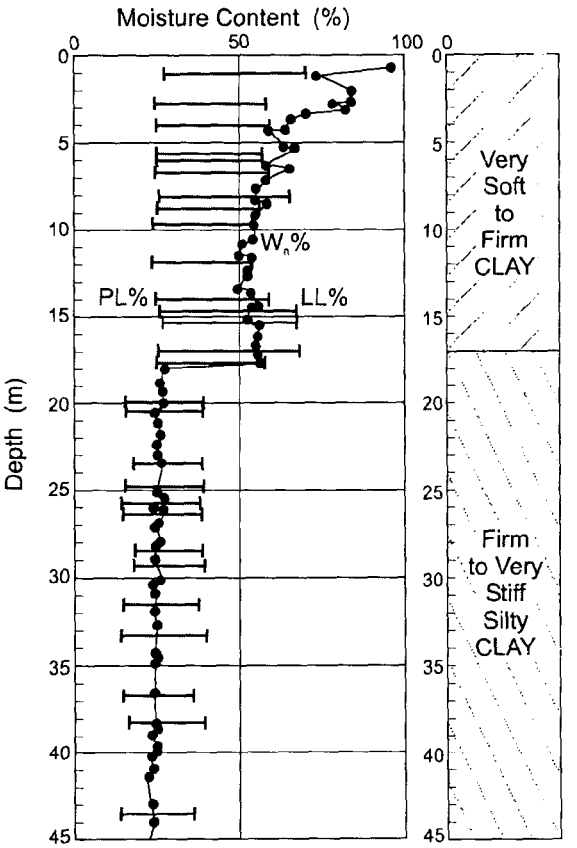

Figure 44. Summary plot of Atterberg limits data.

Historical boring logs from the area can be used to supplement current boring logs in developing a subsurface profile, however, such historical logs need to be carefully reviewed well in advance of drilling activities to ensure that the data are accurate. In some cases, boring log locations are referenced to the center alignment of a roadway or highway without actually surveying the location of the borehole. It is imperative to ensure that a consistent coordinate system has been used to establish the correct relative location of all borings. Since borings would have likely been performed over an extended period of time or for different contracts along a roadway alignment (i.e., project centerlines are commonly changed during project development), it is possible that coordinate systems will not be consistent. Simply stated, if a historical boring cannot be confidently located on a site plan due to these issues, then the boring has limited usefulness for establishing stratigraphy. Also, it is likely that different drill rigs with different operators and different energy efficiencies were used in the collection of SPT data on historical boring logs. This must be recognized when attempting to correlate engineering properties to SPT blow count values. The engineer, however, should consider that while these issues represent potential limitation in the usage of historical borings, it is necessary to review these borings relative to the design under consideration. As an example, a historical boring may indicate a thick layer of very soft clay as evidenced by weight of rod/weight of hammer. While shear strength and consolidation properties cannot be reliably estimated based on SPT blow count values, the historical boring may provide useful information concerning the depth to a firm stratum.

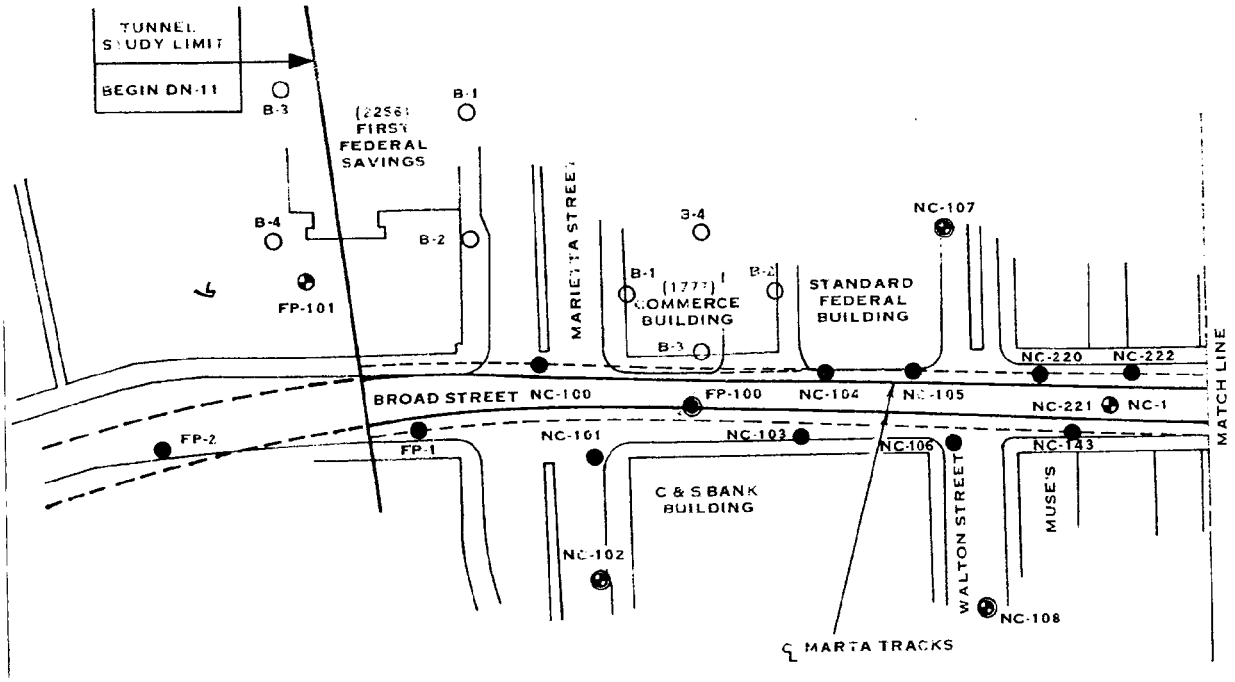

Figure 45. Boring location plan

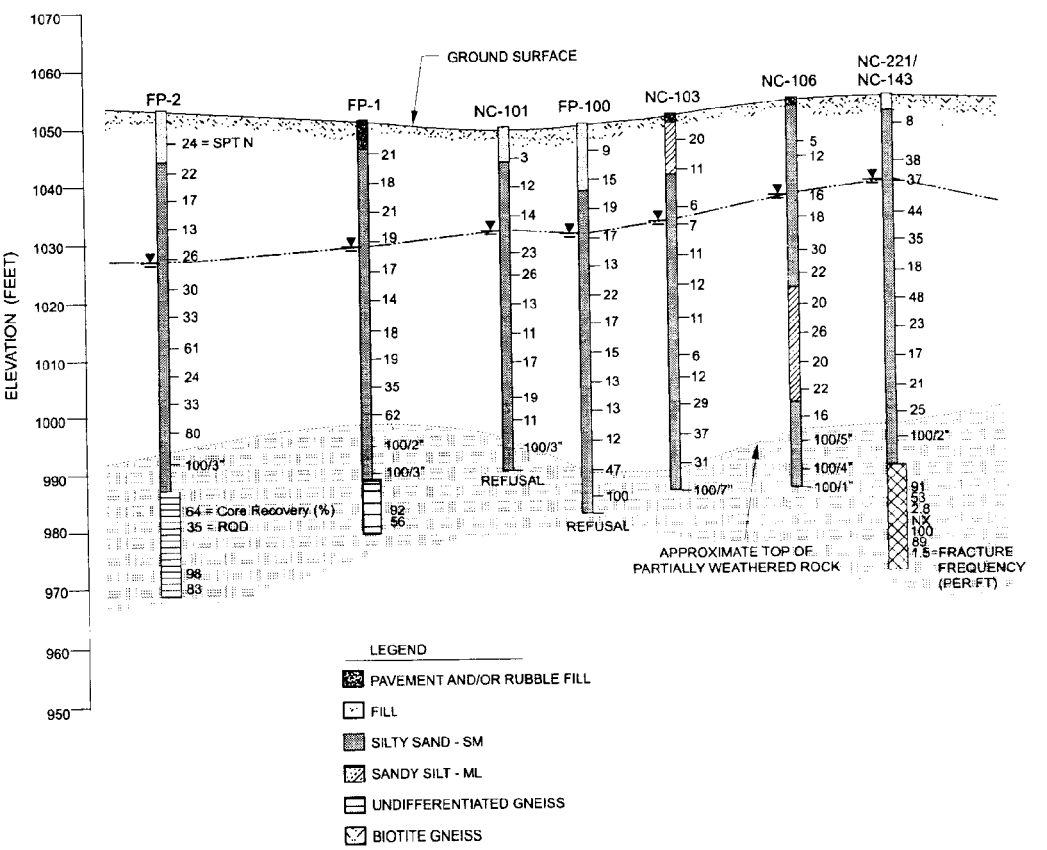

Figure 46. Interpreted subsurface profile.

Most DOTs have collected large amounts of subsurface data from previous investigations within their states. Unfortunately, much of these data are archived with related project data once the project has been completed, and thus may not be readily available or accessible for use during future projects. Additionally, the subsurface data may not be fully utilized if the locations of the borings are not identified or if the plan drawing of the project site is not maintained with the boring logs. To overcome this problem, many DOTs currently use longitude and latitude to identify the boring locations, in lieu of (or in companion with) the conventional positioning format that uses station and offset. To fully appreciate and use these historical data, the profession now realizes the benefits of using electronic boring logs and/or establishing an electronic database of the subsurface information. Unfortunately, the vast majority of the historical subsurface boring information is provided via paper copies, as it was not common (and still is relatively uncommon) to record electronic boring records.

Several DOTs have recently commenced using electronic boring records for their projects. Not only does this provide a redundant record to compliment the paper copy, but it also preserves data in a way that has the potential for automated electronic data management. One of the most useful techniques applied and recommended by the authors, and increasingly used by DOTs, involves the use of a centralized database and Geographic Information System (GIS) techniques that are maintained by the DOT. In its most simplistic form, the electronically stored data are managed and assessed visually using GIS software, where each boring location is identified on a plan map. The authors have found that an appropriately developed database and GIS can be used to great advantage by the DOT. Specifically, in addition to the previously mentioned advantages related to electronic data records, to compliment the paper logs, it is possible to: (1) catalog the borings that previously have been conducted; (2) inventory data regarding specific problematic formations across the state; and (3) develop cross sections that depict subsurface conditions across a site or within a region. This type of application tool can facilitate the development of subsequent subsurface investigations that are appropriately focused and that optimize the utility of existing data.

Recently, the authors have been involved in projects that augment and extend the concepts of database management and GIS technologies described above. Specifically, the authors note that a forms-based or map-based system can be used to develop electronic data records related to subsurface characterization. Using this technique, a handheld computational device (e.g., handheld computer, Palm, Jornada, etc.) can be used in such a manner that the inspector is directed to complete an electronic checklist on the handheld computer. The checklist includes information regarding the top and bottom of the encountered stratigraphic units, characteristics of the strata (e.g., primary and secondary descriptors, color, consistency) in accordance with recommendations presented in ASTM D 2487. In addition, the inspector is prompted to provide information regarding any obtained samples, including the sampling interval, type of sample, etc. In short, using the handheld computer and a properly organized electronic form, it is possible to systematically collect all subsurface information that would normally appear on a conventional boring log. The primary difference is that now the information is available as electronic data, and not just a paper record.

After the subsurface data are recorded, the handheld computer is synchronized with a host computer. At this point, the collected field data are transferred to a geotechnical database that is maintained on the host computer. Information in the database can be interpreted/viewed using GIS technologies. Importantly, this database can be queried to provide specific information for input into a dedicated boring log program, where a paper copy record of the boring log can be printed. Using this system of data management, three advantages are realized: (1) the field data do not have to manually entered

into a database or directly typed on a boring log; (2) the prompts that are programmed on the handheld computer assure a degree of consistency and uniformity in the recorded data that has heretofore not been possible; and (3) the recorded data become part of a database where they can be treated as data, not merely electronic information. Edits to the information in the database that are noted after synchronization and printing can simply be made in the database itself, and do not involve the handheld computer.

5.3 IN-SITU STRESS STATE

5.3.1 General

The current state of stress in the ground is required for the design of most geotechnical features. This state of stress is defined by the total and effective vertical and horizontal stresses, as well as the preconsolidation stress. The overburden stresses depend on gravity and buoyancy forces whereas horizontal stresses and the preconsolidation stress are more complex and depend upon the stress history of the soil.

5.3.2 Overburden Stresses

This section provides a summary of the methods used to calculate effective overburden stresses. The total vertical (overburden) stress is calculated as the cumulative sum of the total unit weights (γ_T) with depth, $\sigma_{vo} = \Sigma(\gamma_T)dz$, summed from the ground surface ($z = 0$) to the depth of interest. If the depth to the water table is designated z_w and the depth of interest is z, then $u_o = \gamma_w(z-z_w)$. The effective vertical stress is then calculated as:

$$\sigma'_{vo} = \sigma_{vo} - u_o \qquad \text{(Equation 31)}$$

The unit weight or density of the soil can be assessed using techniques described previously in chapter 4 for recovered samples. Alternatively, for soils located at depths below the groundwater table, soils can be assumed to be completely saturated and the saturated unit weight of soil is taken as:

$$\gamma_{sat} = \frac{\gamma_w(G_s + e_o)}{(1+e_o)} \qquad \text{(Equation 32)}$$

where G_s = specific gravity of solids ($\approx 2.7 \pm 0.1$ for many soils) and e_o = in-situ void ratio.

Above the water table, the soil may be dry, partially dry, partially saturated, or completely saturated due to capillarity effects. In the case of clean sands, it is often assumed that the soil is dry, and therefore, the unit weight of soil is given by:

$$\gamma_d = \frac{\gamma_w G_s}{(1+e_o)} = \frac{\gamma_{sat}}{(1+w_n)} \qquad \text{(Equation 33)}$$

Moreover, for a completely dry soil, the pore pressure is zero. Therefore, the total and effective overburden stresses are equal. In clays, however, capillarity effects can result in complete saturation for heights of 10 meters or more above the water table and therefore γ_{sat} may be appropriate. A corresponding negative hydrostatic porewater pressure occurs above the phreatic surface (free water table) which is calculated by the relation: $u_o = \gamma_w (z - z_w)$. In this case of negative pore pressure, the effective vertical stress is larger than is the case of dry soil at the same depth.

5.3.3 Horizontal Stresses

The horizontal state of stress in natural soils is a difficult parameter to assess accurately, however, for most design applications involving transportation projects, the horizontal stress can be estimated with sufficient accuracy using the correlations described in this section.

The effective horizontal stress in the ground (σ_{ho}') is related to the vertical effective stress by the at-rest lateral earth pressure coefficient, K_o:

$$K_o = \sigma'_{ho} / \sigma'_{vo} \qquad \text{(Equation 34)}$$

In the absence of direct measurements, laboratory testing on a variety of soils using oedometer and triaxial specimens have shown that the magnitude of K_o depends strongly on the stress history and frictional characteristics of the deposit. For normally consolidated soils, the value of K_o can be estimated using the following relationship:

$$K_o = 1 - \sin\phi' \qquad \text{(Equation 35)}$$

The magnitude of K_o increases during unloading (such as that caused by removal of soil overburden) and becomes greater than unity for OCR values exceeding about 4. For overconsolidated soils (clays, silts, sands, and gravels), K_o can be calculated according to the following equation:

$$K_o = (1 - \sin\phi')OCR^{\sin\phi'} \qquad \text{(Equation 36)}$$

Studies involving field tests in these materials have shown generally good agreement with these correlations, however additional factors such as cementation, aging, structuring, and desiccation may alter the magnitude of in-situ K_o. Where a more accurate assessment of K_o is required for design, it is recommended that either laboratory triaxial tests on undisturbed samples subjected to K_o consolidation or in-situ pressuremeter, total stress cells, Iowa stepped blade, or hydraulic fracture testing be performed. Information on the latter three in situ tests can be found in Tavenas et al. (1975), Handy et al. (1982), and Jamiolkowski et al. (1985). For K_o consolidation in a triaxial test, cell pressures are automatically controlled to maintain a condition of zero lateral strain (i.e., the K_o condition).

5.4 CONSOLIDATION PROPERTIES OF SOIL

5.4.1 General

In this section, the interpretation of laboratory-measured consolidation properties for cohesive soils is presented. These properties relate to primary settlement, (C_c and C_r), secondary settlement (C_α), time rate of settlement (c_v), and stress history (σ_p'). As will be demonstrated later, the consolidation characteristics of a soil provide invaluable information regarding the strength characteristics of the same soils. Interpretation of σ_p' from various in-situ test methods and evaluation of c_h from CPTu dissipation data is also provided.

Consolidation properties are required to perform time-dependent settlement analyses of soils for embankments, structural foundations, and retaining structures. Consolidation refers to the time dependent decrease in volume of a soil due to the dissipation of pore pressures within the soil mass. Shortly after a soil is first loaded (i.e., after immediate or undrained distortional settlements have occurred) the stresses are transmitted to the pore fluid in the soil mass resulting in excess pore pressures. As these pore pressures dissipate with time, the load is gradually transferred to effective stress within the soil skeleton. The resulting increase in effective stress results in a decrease in volume that causes settlements. The general consolidation characteristics of various major soil types can be used to evaluate whether a settlement problem should be anticipated for a particular geotechnical feature according to the following:

- Gravels, sands, and non-plastic silts: These soils consolidate rapidly under load and do not typically present settlement problems unless close tolerances are required for the project.
- Plastic silt-clay mixtures: Soft silts and clays are more compressible than stiff silts and clays. Settlement may continue long after construction is complete.
- Organic soils: These soils are very compressible as well as biodegradable and can result in large settlements that occur for many years.

5.4.2 Laboratory Consolidation Tests

5.4.2.1 General

Consolidation properties of cohesive soils are typically evaluated in the laboratory using the one-dimensional consolidation test. The most common laboratory method is the incremental load (IL) oedometer (ASTM D-2435). The constant rate of strain (CRS) version (ASTM D-4186) applies the loading continuously while measuring stress and pore pressures by transducers, thereby reducing testing times from 1 to 2 weeks by IL oedometer to say 1 day by the CRS consolidometer. High-quality undisturbed samples using thin-walled tubes, piston samplers, or other special samplers are required for laboratory consolidation tests. Tests performed on disturbed samples will result in computed consolidation properties that may result in conservative or unconservative design evaluations. Important issues relative to consolidation testing such as sample disturbance effects have been described in chapter 4.

5.4.2.2 Soil Parameters from Laboratory Consolidation Tests

Consolidation test results are traditionally shown in a graph of void ratio (e) versus logarithm of applied vertical effective stress (σ_v') in the oedometer, as illustrated in figure 47. Each of the compression indices are defined by the change in void ratio per log cycle stress (= $\Delta e/\Delta \log \sigma_v'$) for the respective ranges of recompression (C_r), virgin compression (C_c), and swelling or rebound (C_s). An alternate version of presenting consolidation test results is using a plot of vertical strain as the ordinate axis, whereby $\varepsilon_v = \Delta e/(1+e_o)$. In this case, the compression indices are reported as the recompression ratio, $C_{r\varepsilon} = C_r/(1+e_o)$, and compression ratio, $C_{c\varepsilon} = C_c/(1+e_o)$.

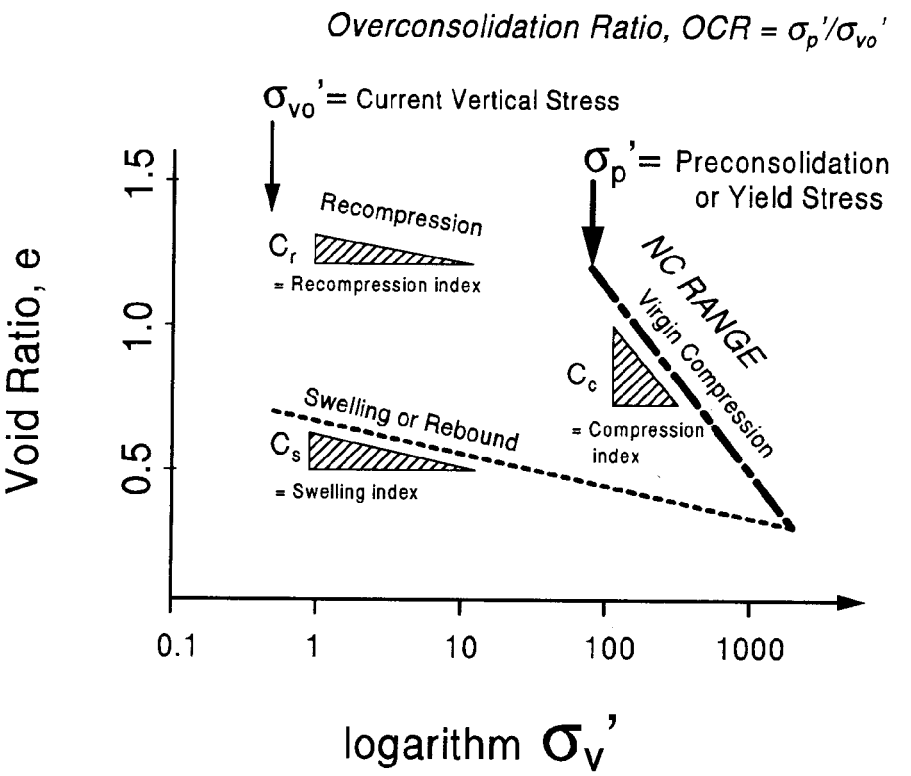

Figure 47. Definition of C_c, C_r, C_s, and σ_p'.

The maximum preconsolidation stress delineates the region of semi-elastic behavior (corresponding to overconsolidated states) from the region of primarily plastic behavior (associated with normal consolidation). The degree of preconsolidation is expressed using the overconsolidation ratio, where OCR = σ_p'/σ_{vo}'. Other important parameters obtained from the consolidation test include the constrained modulus ($D = \Delta\sigma_v/\Delta\varepsilon_v = 1/m_v$), and time-dependent parameters: coefficient of vertical consolidation (c_v) and coefficient of secondary compression (C_α).

5.4.2.3 Selection of Samples for Laboratory Consolidation Testing

Information on subsurface stratigraphy and basic index properties should be used to select the number and depths of undisturbed samples for laboratory consolidation testing. The number of

samples should be selected to facilitate the development of a profile of preconsolidation stress with depth. The selection of samples for consolidation testing (and shear strength testing) should be performed in a rational manner since such laboratory tests are time consuming, expensive, and provide important performance properties.

The procedure used to select samples includes developing a plot of the vertical effective stress, σ_{vo}', with depth (see Soil Property Selection Example No. 1 in appendix A). The location of each undisturbed sample should be plotted for its specific boring and the vertical effective stress evaluated. For consolidation tests, it is imperative that the test be carried out to stress levels much greater than the estimated preconsolidation stress to facilitate an accurate evaluation of the actual preconsolidation stress. It is useful to develop an estimated profile of preconsolidation stress with depth so that critical points can be noted. The engineer should recognize that the preconsolidation stress (σ_p') (or alternatively the OCR) of fine-grained materials is an important property because it significantly affects settlement calculations and the evaluation of undrained shear strength. An example plot showing preconsolidation stress with depth is shown in figure 48.

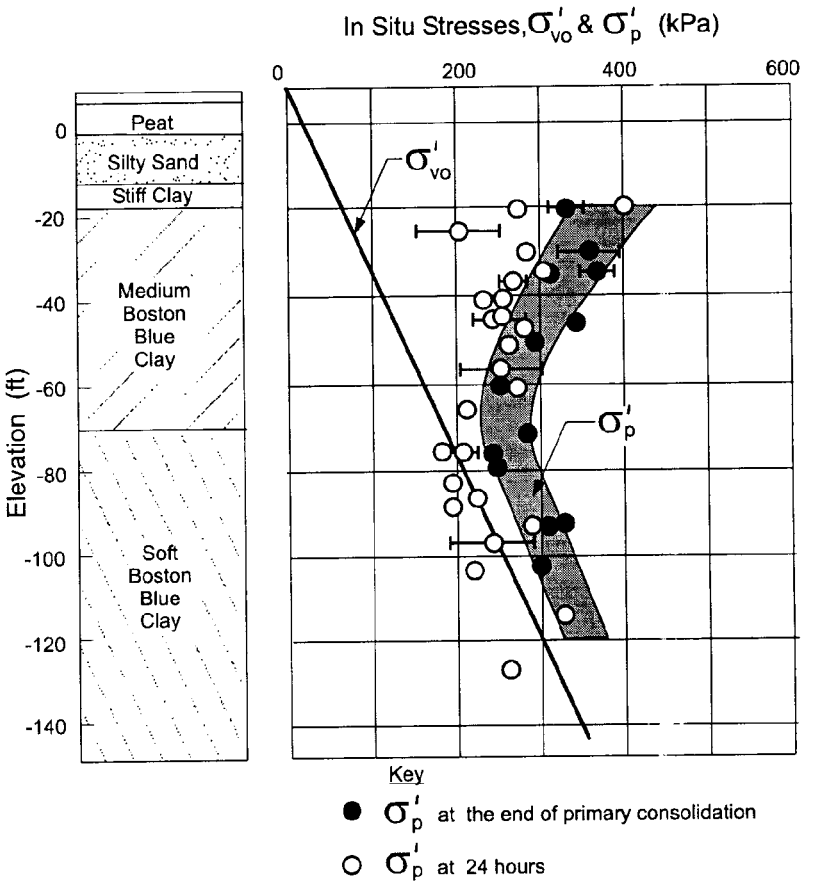

Figure 48. Profile of preconsolidation stress.

5.4.2.4 Evaluation of σ_p' from Laboratory Consolidation Tests

Standard oedometer tests are conducted on small specimens taken from the field and the characteristic e-logσ_v' graphs show a change in slope at the preconsolidation stress. Sampling disturbance effects typically "lower" the overall e-logσ_v' curve relative to field conditions (see figure 23). Consequently, the value of σ_p' is often underestimated in routine testing and interpretation. Sample disturbance can be quantified using the measured strain level that corresponds to σ_{vo}' (see table 16).

The preconsolidation stress from oedometer tests is normally interpreted from the e-logσ_v' relationship using the Casagrande graphical technique. In many clays and silts, this approach may be adequate in evaluating a reasonable value of σ_p' for engineering purposes. The steps involved in the Casagrande method are provided in table 24.

In very soft, sensitive, or structured materials, particularly those affected by sample disturbance, swelling, and the release of stress associated with removal from the ground, alternative graphical techniques can be utilized to better delineate the magnitude of σ_p'. Herein, the strain-energy method (Becker et al., 1987) is recommended for interpreting σ_p'. The strain-energy method, however, is valid for evaluating σ_p' for any laboratory consolidation test, not just for samples that are considered to be disturbed. The strain-energy method involves plotting the cumulative strain energy (i.e., the product of stress times strain) for each load increment in a laboratory consolidation test. The point where the strain energy plot exhibits a large incremental increase represents the preconsolidation stress for the soil. The strain-energy method is outlined in table 25.

Example calculations of σ_p' using both the Casagrande and strain-energy methods are provided in Soil Property Selection Example No. 1 and No. 2 in appendix A.

Table 24. Casagrande method to evaluate σ_p'.

1. Construct a line tangent to the steepest portion of the consolidation curve (within the normally consolidated range).
2. Locate the point of maximum curvature in the area of the laboratory curve where the slope transitions from shallow to steep. Construct a horizontal line from this point of maximum curvature.
3. Construct a tangent line to the curve from the point of maximum curvature.
4. Construct a line that bisects the angle between the horizontal line constructed in Step 2 and the tangent line constructed in Step 3.
The point of intersection between the bisector line (Step 4) and the first tangent line (Step 1) is the location of the preconsolidation pressure. A diagram of the Casagrande method is provided in figure 49.

Table 25. Strain-energy method to evaluate σ_p'.

1.Compute the change in work per unit volume for each strain increment according to:

$$\Delta W = \frac{(\sigma_i' + \sigma_f')}{2} * (\varepsilon_f - \varepsilon_i) \qquad \text{(Equation 37)}$$

where: ΔW = change in work (kPa/m^3) per unit volume

σ_i = stress at beginning of strain increment (kPa)

σ_f = stress at end of strain increment (kPa)

ε_i = strain at beginning of increment (dimensionless)

ε_f = strain at end of increment (dimensionless)

2. Plot stress versus summation of work for each respective stress increment. For plotting purposes, it is assumed that the stress value corresponding to the summation of work is the stress at the end of the strain increment.

3. A noticeable change in slope should be evident when data are plotted. A curve connecting the data should have a sharp transition from a flatter slope in the recompression range (slope 1) to a steeper slope (slope 2) in the virgin compression range. Construct a trend line through the data that represent a line with slope 1. Construct a second line through the data that represent a line with slope 2.

4. The stress where these two trend lines intersect is the preconsolidation stress. The strain-energy method is illustrated in figure 50.

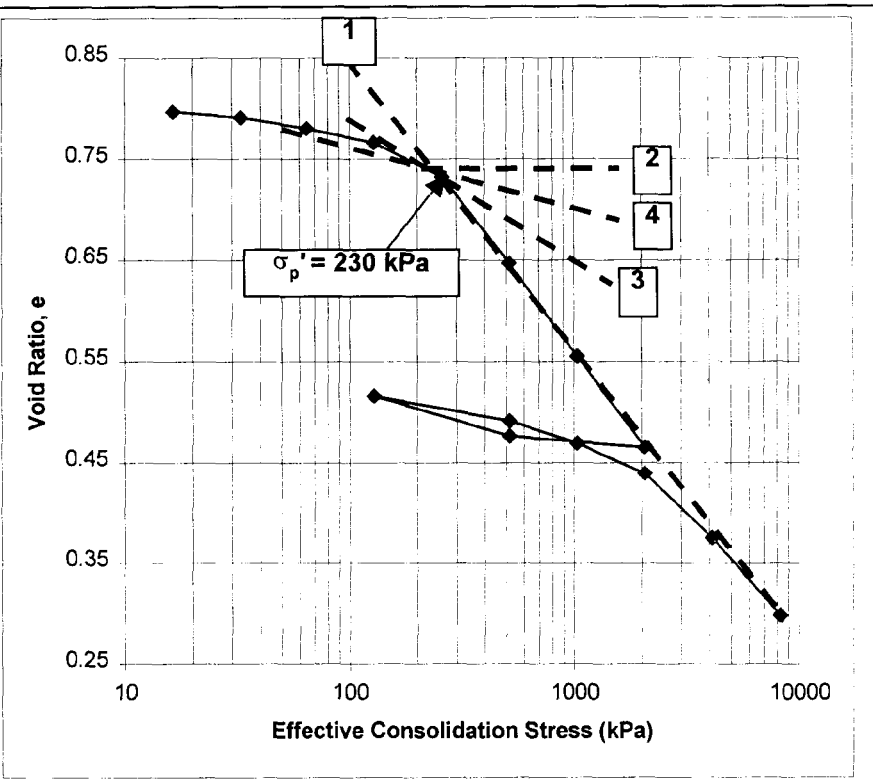

Figure 49. Illustration of Casagrande method to evaluate preconsolidation stress.

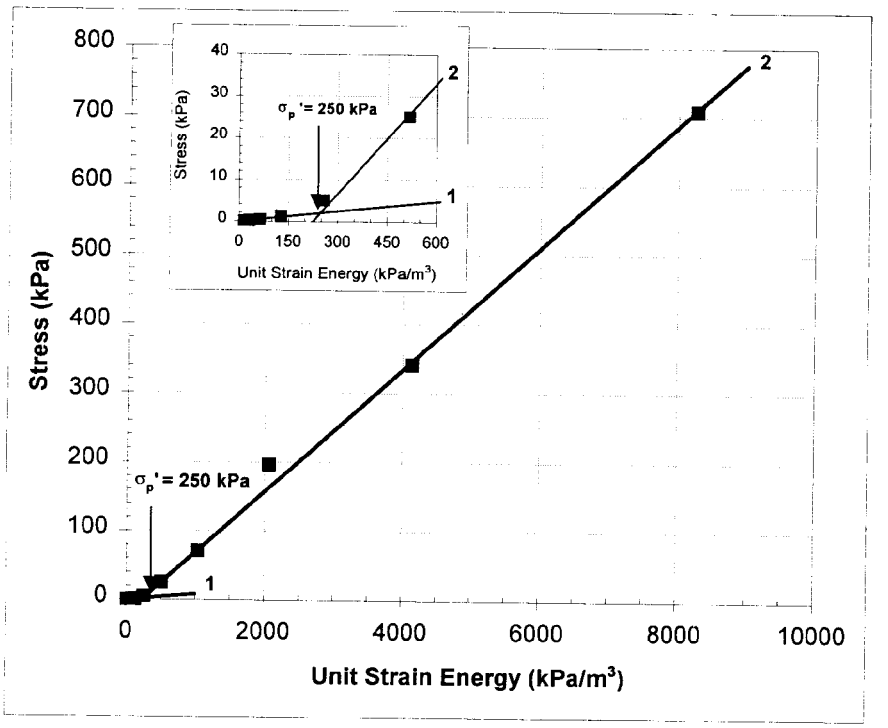

Figure 50. Illustration of strain energy method to evaluate preconsolidation stress.

5.4.2.5 Evaluation of C_c and C_r

Compression parameters can be estimated by correlation or by direct laboratory-measurement. The compression index, C_c, and recompression index, C_r, are index values required for primary consolidation settlement predictions. These parameters have been defined in figure 47. The value of C_c is evaluated by drawing a best-fit tangent line to data on an e-log σ_{vc}' representation of consolidation data along the virgin (i.e., part of curve where stresses are greater than σ_p') portion of the curve. The modified compression index, $C_{c\varepsilon}$, is evaluated similarly on a plot of ε_v-log σ_{vc}'. The line drawn to evaluate C_c (or $C_{c\varepsilon}$) should include the stress range defined by the calculated σ_p' and the final effective stresses in the ground. Typically, values of C_r (or $C_{r\varepsilon}$) are 10 to 20 percent of the value of C_c (or $C_{c\varepsilon}$).

Numerous correlations relating simple soil classification properties (e.g., LL, w_n) to C_c and $C_{c\varepsilon}$ are available in the literature for silts and clays. These correlations can be used to make first-order predictions of settlements, but should not be relied upon for final design, unless the correlation has been developed using site-specific laboratory consolidation test data. These correlations may be of limited value, however, for highly structured soils that are sensitive. Several correlations that are based on relatively large databases are provided in table 26. Other correlations are presented as part of Soil Property Selection Example No. 1 in appendix A.

Table 26. Summary of correlations for C_c (modified from Holtz and Kovacs, 1986).

Equation	Applicable Soils
$C_c = 0.009\ (LL - 10)$	Undisturbed clays of low to medium sensitivity
$C_c = 0.007\ (LL - 7)$	Remolded clays
$C_c = 0.01\ w_n$	Chicago clays

Interpreting a compression and recompression index value for design should be based on a rational assessment of the data. The objective is to assign a value to each behaviorally different subsurface layer or to assign some representative value for the entire subsurface. Assessments to be made in evaluating compression data include: (1) depth ranges where the material is more silty or sandy as compared to other depth ranges; (2) depth of transition from a crust layer to an underlying softer clay layer; and (3) assessment of sampling disturbance.

The sampling disturbance indices previously discussed offer a useful means to evaluate calculated C_c or $C_{c\varepsilon}$ values. As previously discussed measured C_c (or $C_{c\varepsilon}$) values from disturbed samples will be lower than those measured from undisturbed samples. Available data in the literature indicates that modified compression index values for disturbed samples may be, on average, about 15 to 25 percent lower than values from "field-measured" (i.e., undisturbed) curves. It is noted, however, that the effects of sample disturbance on the evaluation of C_c (or $C_{c\varepsilon}$) can be minimized by carrying the consolidation test out to a stress level of approximately 8 times the estimated preconsolidation stress. A reasonably accurate assessment of C_c (or $C_{c\varepsilon}$) can then be made by drawing a tangent line to the straight line portion of the consolidation curve at these high stress levels. It is recognized that such high stress levels may not be able to be achieved for standard laboratory equipment, especially if the estimated preconsolidation stress is itself quite large. However, since soils with high preconsolidation stresses pose little concern for typical geotechnical features (since loading will not likely cause the soil to experience stresses greater than its preconsolidation stress), then a sufficiently accurate estimate of C_c (or $C_{c\varepsilon}$) can be made for these soils at more moderate loading levels.

5.4.2.6 Laboratory Evaluation of c_v

The time rate of settlement is typically represented in geotechnical practice via the coefficient of vertical consolidation, c_v and the coefficient of horizontal consolidation, c_h. The parameter c_v is used for evaluating time rate of settlement for shallow foundations and large aerial fills whereas the parameter c_h is used for estimating pore pressure dissipation around driven piles and for designing wick drains. Graphical procedures used to evaluate c_v from laboratory consolidation data include Casagrande's logarithm of time method and Taylor's square root of time fitting method. Casagrande's method uses the time to complete 50 percent primary consolidation and evaluates c_v according to:

$$c_v = \frac{0.197 H_{DR}^2}{t_{50}} \qquad \text{(Equation 38)}$$

where H_{DR} is the drainage height (equal to one-half the average thickness of the oedometer test specimen for each load increment for a double drained specimen) and t_{50} is the time required to achieve 50 percent primary consolidation. For the square root of time method, the time for 90 percent primary consolidation, t_{90}, is used and c_v is calculated according to:

$$c_v = \frac{0.848 H_{DR}^2}{t_{90}} \qquad \text{(Equation 39)}$$

Procedures for these methods are provided in appendix B. Each of these methods is approximate and will result in different calculated values for c_v even though the same deformation-time data are used for both methods. The use of the logarithm of time method requires that a substantial part of the consolidation curve be defined after 90 percent consolidation is complete to facilitate a good approximation of t_{90}. For the square root of time method, the test does not need to be carried out beyond t_{90}. It is noted, however, that if secondary compression is to be evaluated, the test will need to be carried out beyond the time to reach 100 percent of primary consolidation. For some soils, such as soils which undergo significant secondary compression, these graphical methods may be difficult to implement to obtain the time to the end of primary consolidation since their deformation versus time response may not "look" like those used to develop the graphical methods. Recalling that the definitions of the time of primary consolidation, t_p, is the time at which all excess pore pressure has dissipated for a given load (i.e., $\Delta u=0$), it may be beneficial to perform CRS oedometer tests for these soils since pore pressures are measured during the test.

Significant scatter of calculated c_v values in the overconsolidated range may result from the following: (1) consolidation occurs quite rapidly at these load levels making the determination of the time for the end of primary consolidation difficult; and (2) in very stiff clays, fissures may exist at low stress levels which will affect drainage rates. Some of the inherent variability associated with evaluation of this parameter can be minimized by concentrating the interpretation on values corresponding to a reload cycle and to values associated with virgin compression. Values from initial loading should not be used due to inevitable sample disturbance effects.

A value for c_v should be calculated for each load increment for each consolidation test. For each test, values of c_v should be plotted as a function of log σ_{vc}' (i.e., c_v vs. log σ_{vc}' plot). High quality data will typically exhibit a sharp reduction in calculated c_v values near the preconsolidation stress. Figure 51 shows a summary plot for a consolidation test. Index properties should also be reported with the consolidation test plots.

Engineers typically use a constant value of c_v to perform time rate of settlement analyses, however, it should be noted that c_v is not a constant value for a test on a particular soil (see figure 51). Values for c_v depend on many factors including whether the preconsolidation stress has been exceeded. For load increments less than the preconsolidation stress, consolidation occurs relatively rapidly and c_v values can be relatively high. The typical trend for most clayey soils is that c_v values are higher in the overconsolidated range and exhibit a relatively rapid decrease as the preconsolidation stress is approached. Values for c_v will be lowest for effective stresses that exceed σ_p'.

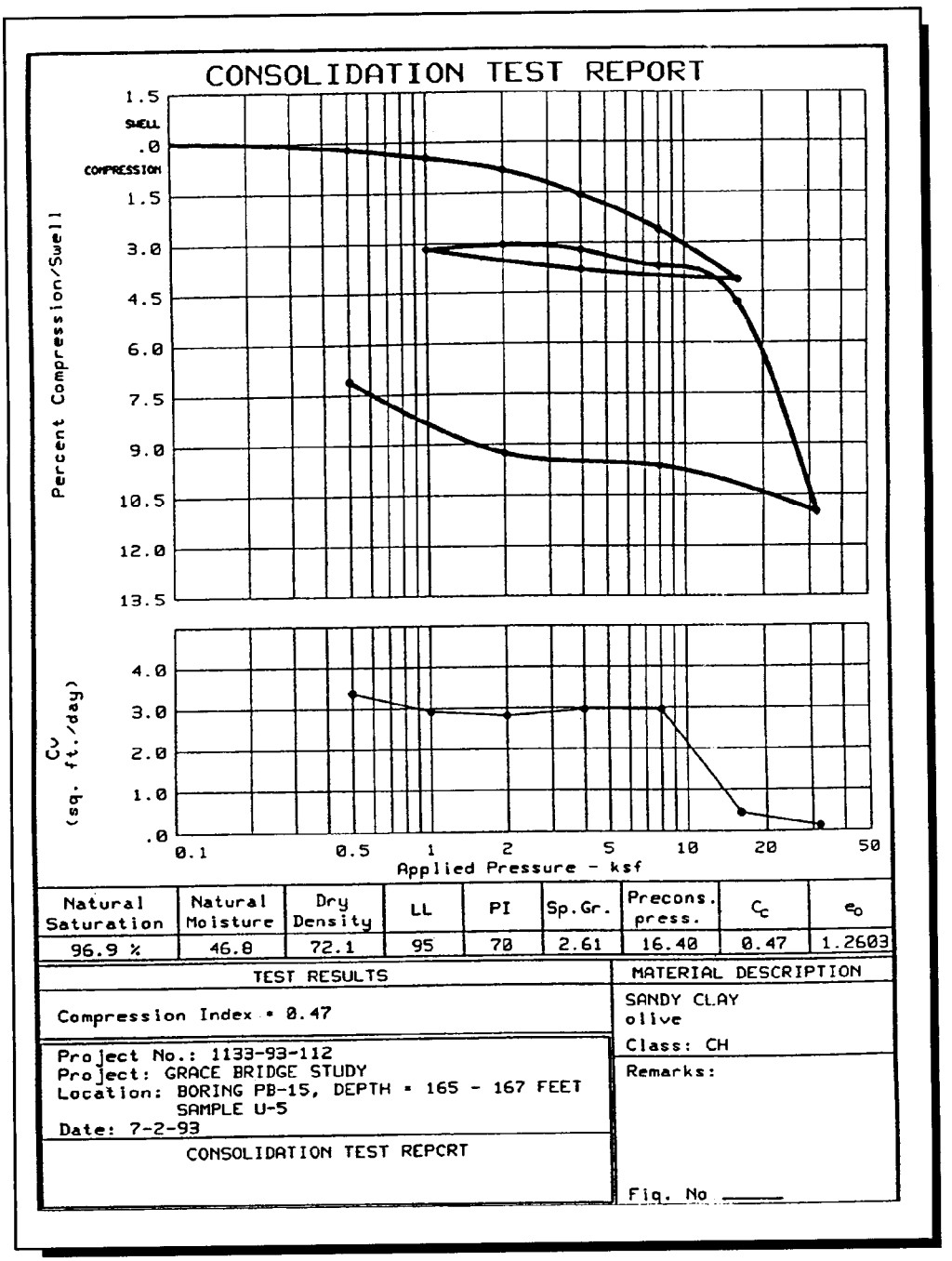

Figure 51. Summary consolidation data showing c_v.

A rational approach to selecting a c_v value for design would include first assessing whether the design loads are sufficiently high to consolidate the compressible layer to stress levels beyond the preconsolidation stress. If stress levels after consolidation are below approximately $0.8\sigma_p'$, an average c_v value associated with stress levels below $0.8\sigma_p'$ should be used for design. If the compressible layer will consolidate to stress levels in excess of σ'_p (or greater than $0.8\sigma_p'$ as described herein), then the average c_v value for the range of stresses from σ_p' to the final vertical

effective stress in the ground should be used. This value, however, should not exceed the average value obtained for the overconsolidated stress range (i.e., less than $0.8\sigma_p'$).

A value for c_v based on laboratory consolidation results may vary significantly from actual values in the field. As previously discussed, time rate of settlement analyses based on consolidation test results on disturbed samples will likely result in an overprediction of the time actually required for primary consolidation to be completed in the field. In addition, laboratory tests only simulate vertical drainage whereas most natural soil deposits have interbedded seams or layers of more permeable material within the low permeability layer. These smaller layers will permit lateral drainage as well, which will tend to decrease the time required to complete primary consolidation. All of these factors tend to make predictions of the time rate of settlement to be conservatively overestimated. The coefficient of consolidation can be obtained most accurately in the field using measured pore pressures from piezometers installed at several depths within a clay layer. Alternatively, monitoring the actual time rate of settlement in the early stages of loading can be used to assess the appropriate value of c_v and this value can be used to refine the predicted time to complete primary consolidation.

The parameter c_v is also important for developing a fill placement plan for an embankment that is to be constructed over clays. Failures of embankments constructed over clays are often caused by placing the fill too rapidly, i.e., not providing sufficient time to enable construction-induced pore pressures in the clay foundation to stabilize. If time permits, staged construction represents the most cost-effective solution and it is therefore worth the effort to perform high quality laboratory tests to evaluate the c_v parameter. Oftentimes, staged construction over an extended period of time is deemed inappropriate because of the need to put the structure into service as soon as possible. With this, ground improvement techniques may be necessary.

5.4.2.7 Evaluation of $C_{\alpha\varepsilon}$

In geotechnical design analyses, it is assumed that secondary settlement occurs after primary consolidation is completed. As noted earlier, secondary compression settlements may be relatively large for organic soils. For normally consolidated soils, the ratio of the coefficient of secondary compression to the compression index ($C_\alpha/C_c = C_{\alpha\varepsilon}/C_{c\varepsilon}$) is relatively constant for a given soil. On average, the value of C_α/C_c is 0.04 ± 0.01 for inorganic clays and silts. For organic clays and silts, the value averages 0.05 ± 0.01. For peats, the value averages 0.06 ± 0.01. These values may be used to assess actual values from laboratory tests or for preliminary analyses. If the final effective stress in the ground is less than the preconsolidation stress, then C_r should be used instead of C_c to estimate the secondary compression index.

The coefficient of secondary compression is calculated using the portion of the deformation versus time plot for a consolidation test that corresponds to a time after primary consolidation is completed. For soils that are expected to demonstrate significant secondary settlements, it is important that load durations extend to times after primary consolidation is completed. Figure 52 shows a plot of deformation (for a particular load increment) versus logarithm of time for a soil sample. The coefficient of secondary compression, C_α, is evaluated according to the following equation:

$$C_\alpha = \frac{\Delta e}{\log t_2/t_1} \qquad \text{(Equation 40)}$$

where Δe is the change in void ratio over an elapsed time equal to t_2-t_1. The times t_1 and t_2 occur after the time to the end of primary consolidation, t_p. Alternatively, the modified coefficient of secondary compression, $C_{\alpha\varepsilon}$, can be evaluated similarly using a plot of volumetric strain versus logarithm of time.

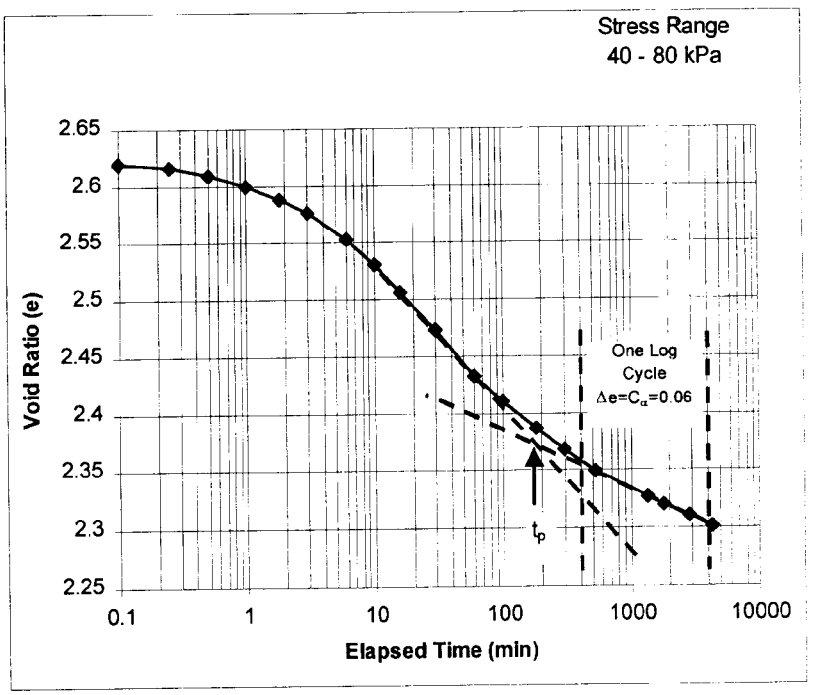

Figure 52. Evaluation of C_α.

Values of $C_{\alpha\varepsilon}$ (or C_α) are affected by stress history in that maximum values for $C_{\alpha\varepsilon}$ are evaluated for stress levels greater than the preconsolidation stress (i.e., at stresses corresponding to virgin compression). Therefore, to assess a value of $C_{\alpha\varepsilon}$ (or C_α) to be used for design analyses, the final effective stress in the ground after primary consolidation is completed should be evaluated. If the final effective stress is less than approximately $0.8\sigma_p'$, then an average value of $C_{\alpha\varepsilon}$ (or C_α) evaluated in the overconsolidated range may be used for design. If final effective stresses in the ground exceed σ_p', then it is conservative to select $C_{\alpha\varepsilon}$ (or C_α) value corresponding to stresses in the range of 1 to 2 times σ_p'. It is noted that for samples that are disturbed, laboratory-measured values of C_α (or $C_{\alpha\varepsilon}$) may be underestimated in the normally consolidated range as compared to results from high-quality undisturbed samples. Therefore, the effects of disturbance on measured secondary compression values need to be carefully assessed, especially for soils that may undergo significant secondary compression such as organic clays and peats.

5.4.3 Evaluation of σ_p' from In-situ Test Methods

The use of in-situ tests for profiling σ_p' in clayey soils is attractive since it may be possible to discern a rather complicated and varied stress history that includes multiple effects (e.g., erosion, reloading, aging, plus cementation). Also, in-situ tests are conducted quickly and inexpensively, thus allowing an immediate assessment of the state of overconsolidation and its variation across a site. However, in-situ data provide only indirect measures of preconsolidation and therefore should be used to supplement values obtained from laboratory consolidation tests. Calibration of in-situ test correlations is prudent and accomplished by benchmarking the data against values provided from consolidation, triaxial, and index tests run on undisturbed samples, as well as the stress history based on an understanding of the local geologic setting. Site-specific correlations between in-situ tests and laboratory tests, however, may be cost-prohibitive on small projects.

Analytical derivations are available to evaluate the OCR of cohesive soils using the cone penetrometer, piezocone, flat dilatometer, and pressuremeter. These methods, via a correlation, relate OCR to a specific measured parameter in the in-situ test. These correlations are presented elsewhere (see Kulhawy & Mayne, 1990). Herein, simple empirical and statistical expressions for estimating σ_p' from in-situ test results are presented. These correlations can be used to provide first-order estimates of σ_p' and to complement preconsolidation stress values evaluated from laboratory oedometer tests. Preliminary estimates of σ_p' for intact (i.e., not fissured) natural clays may be made using the approximate generalized trends as follows for each of the in-situ tests:

Cone Penetration Test (figure 53):	$\sigma_p' = 0.33\ (q_T - \sigma_{vo})$	(Equation 41)
Type 1 Piezocone (face element) (figure 54):	$\sigma_p' = 0.47\ (u_1 - u_0)$	(Equation 42)
Type 2 Piezocone (shoulder element) (figure 55):	$\sigma_p' = 0.54\ (u_2 - u_0)$	(Equation 43)
Flat (Plate) Dilatometer Test (figure 56):	$\sigma_p' = 0.51\ (p_0 - u_o)$	(Equation 44)
Self Boring Pressuremeter Test (figure 57):	$\sigma_p' = 0.45\ p_L$	(Equation 45)
Field Vane Test (figure 58):	$\sigma_p' = 3.54\ (s_{u,\,VST})$	(Equation 46)

Note that stress measures in these figures are normalized to atmospheric pressure, P_a.

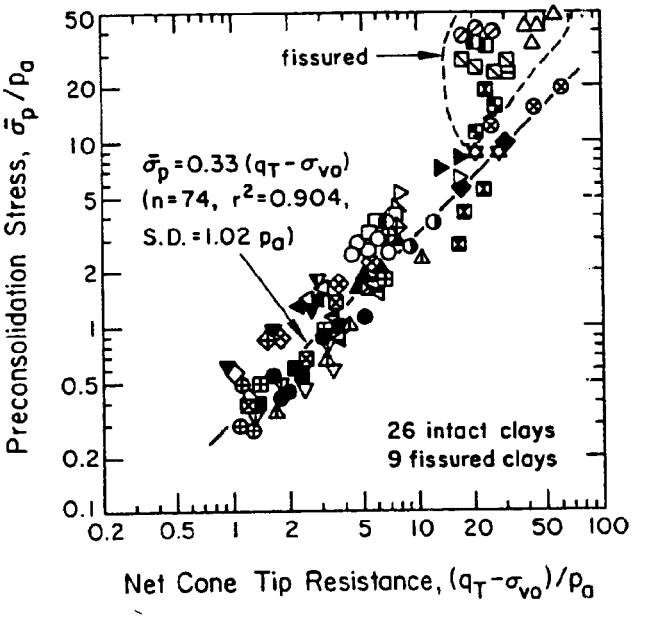

Figure 53. Correlation of σ_p' with CPT q_t data (after Kulhawy and Mayne, 1990).

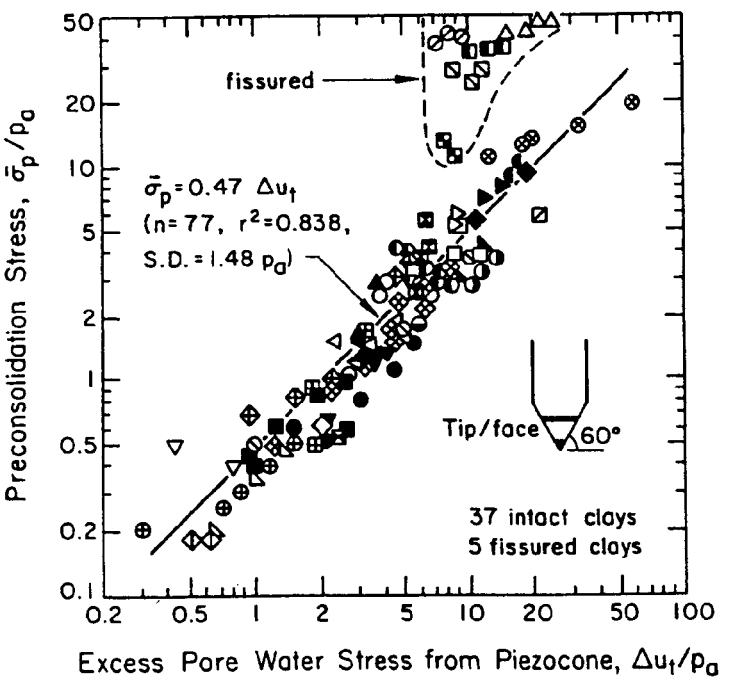

Figure 54. Correlation of σ_p' with CPTu u_1 data (after Kulhawy and Mayne, 1990).

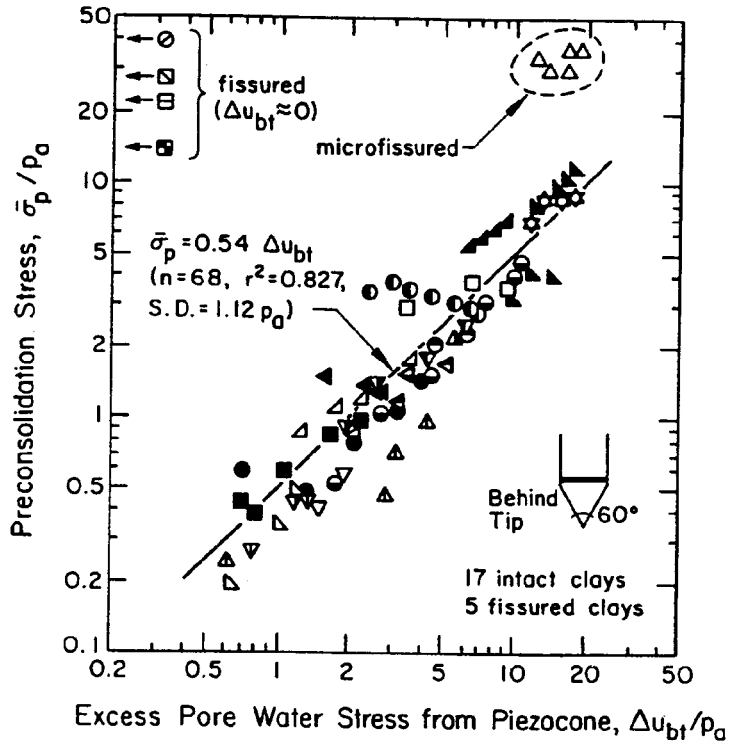

Figure 55. Correlation of σ_p' with CPTu u_2 data (after Kulhawy and Mayne, 1990).

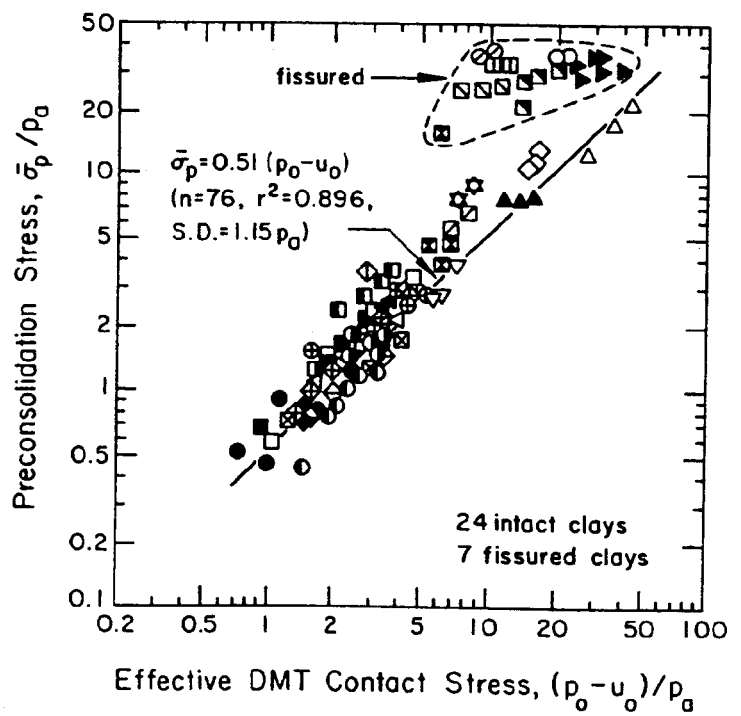

Figure 56. Correlation of σ_p' with DMT p_0 data (after Kulhawy and Mayne, 1990).

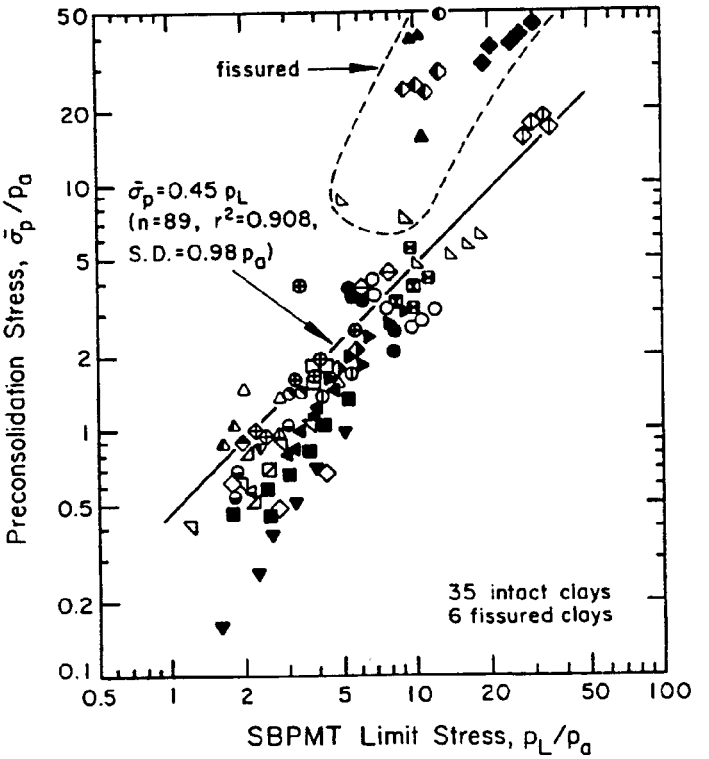

Figure 57. Correlation of σ_p' with self-boring PMT p_L data (after Kulhawy and Mayne, 1990).

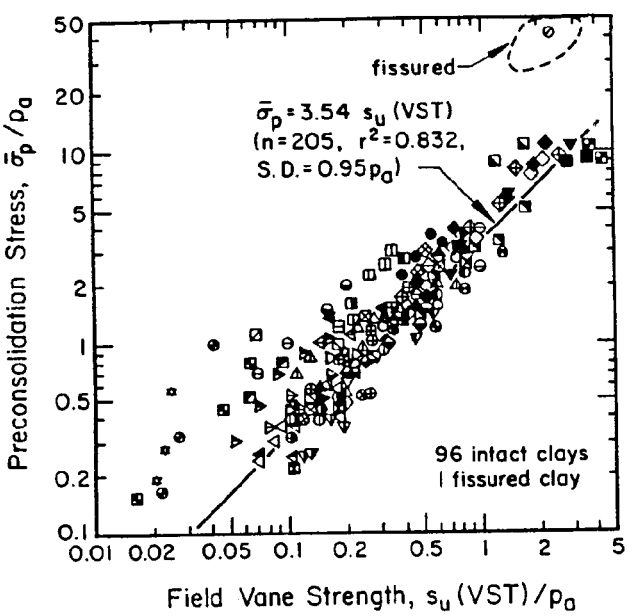

Figure 58. Correlation of σ_p' with VST s_u, VST data (after Kulhawy and Mayne, 1990).

Based on data shown in figures 53 through 58, it can be concluded that values of σ_p' from these empirical correlations compare favorably to values obtained from laboratory testing, except as noted below.

- The piezocone with a shoulder element (i.e., $CPTu_2$) will measure negative penetration pore water pressures in fissured clays and dense silts indicating that the above correlation for σ_p' is not valid for such soils.

- Each correlation tends to underpredict values of σ_p' for stiff fissured clays. The use of these correlations for stiff fissured clays is therefore conservative.

Although not shown, correlations have been developed for correlating SPT N values to σ_p'. This correlation is poor and therefore SPT results should not be used, even as a first-order estimator, to evaluate σ_p' for soft to medium clays.

5.4.4 Evaluation of c_h from CPTu Dissipation Data

In this section, procedures are presented to evaluate the coefficient of lateral consolidation, c_h, from piezocone dissipation test results. To calculate c_h using a piezocone, the modified time factor, T* must be evaluated. The parameter T* is related to the degree of consolidation. Values of T* are shown in table 27 for various stages of dissipation. The degree of consolidation, U, is defined with relation to the dissipation of excess penetration porewater pressure as:

$$U = 1 - \frac{u_t - u_o}{u_i - u_o} \qquad \text{(Equation 47)}$$

where: u_t = pore pressure at time t;
u_i = initial pore pressure at t=0; and
u_o = hydrostatic pore pressure at equilibrium (i.e., static conditions based on elevation of ground water table).

Based on this equation, when $u_t = u_i$, the degree of consolidation is zero whereas if $u_t = u_o$, the degree of consolidation is 100 percent.

Normalized excess pore pressures (defined as 1-U) are based on the dissipation from the initial excess pore pressure not the maximum excess pore pressure measured during a dissipation test. This is specifically noted since, in some cases, the maximum excess pore pressure does not correspond to the initial excess pore pressure. Figure 59 shows pore pressure dissipation test results at two depths within a clay deposit.

Table 27. Modified time factors, T*, for analysis of CPTu dissipation data (after Teh and Houlsby, 1991).

Degree of Consolidation, U (%)	Normalized Excess Pore Pressure, (1 – U)	T* for Piezocone with Element Located Mid-Face, u_1	T* for Piezocone with Element Located Behind the Tip, u_2
20	0.8	0.014	0.038
30	0.7	0.032	0.078
40	0.6	0.063	0.142
50	0.5	0.118	0.245
60	0.4	0.226	0.439
70	0.3	0.463	0.804
80	0.2	1.04	1.60

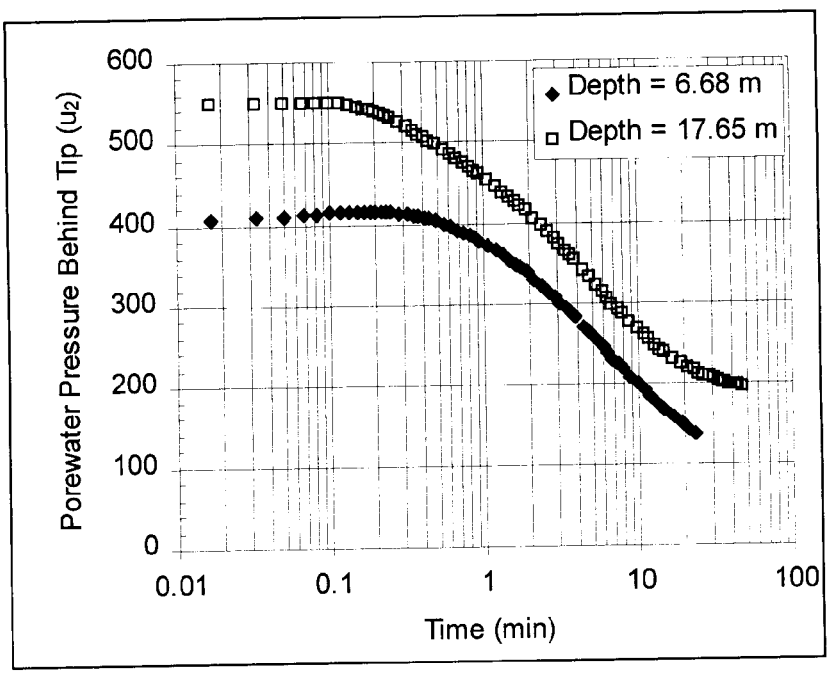

Figure 59. CPTu_2 pore pressure dissipation curves.

Values for c_h can be estimated for various degrees of consolidation; however evaluations for design analyses should be based on a degree of consolidation of 50 percent or greater. The parameter c_h is calculated according to the following:

$$c_h = \frac{T^* a^2 \sqrt{I_r}}{t} \qquad \text{(Equation 48)}$$

where a is the radius of the cone (equal to ½ D, see figure 15), I_r is the undrained rigidity index (=G/s_u where G is the soil shear modulus and s_u is the undrained strength), and t is the time at which the pore pressure measurement is taken. The parameter I_r can be evaluated directly for use in equation 48 from figure 60. Calculations are provided in Soil Property Selection Example No. 1 in appendix A that demonstrates the application of equation 48. An alternate method to evaluate c_h based on piezocone dissipation test results is provided in appendix C.

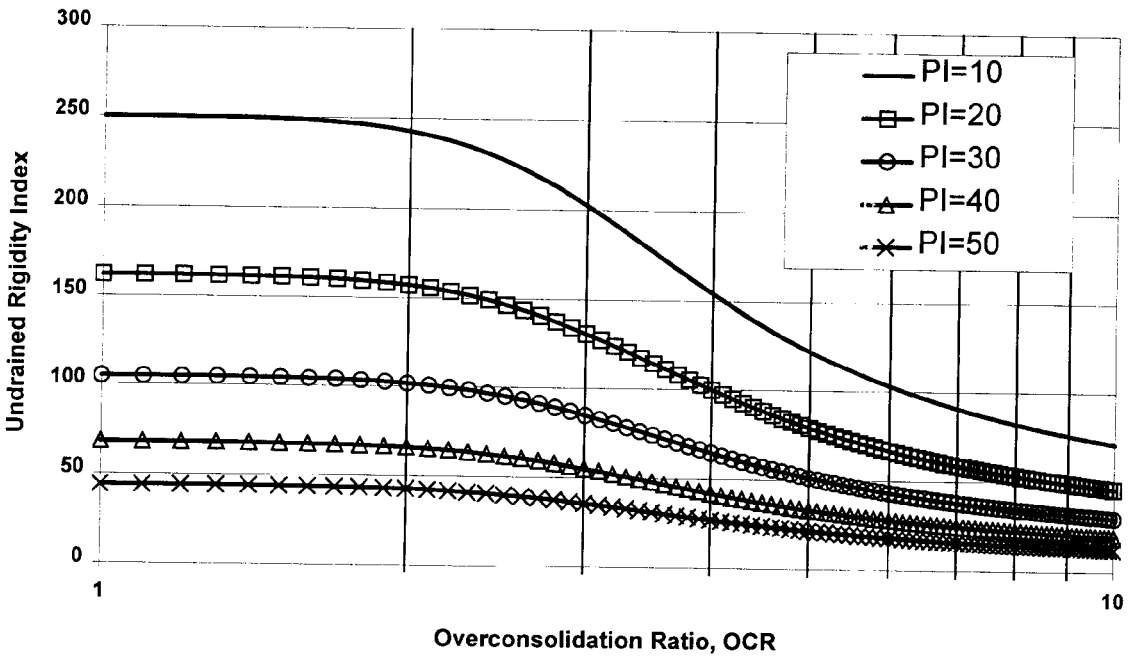

Figure 60. Rigidity index (after Keaveny and Mitchell, 1986).

5.4.5 Selection of Design Values for Consolidation Analyses

General

With respect to consolidation parameters and properties, the design engineer must consider whether the magnitude of settlement must be controlled to strict tolerances to ensure good performance of the structure or whether settlements must only be controlled to a more nominal tolerance. For example, settlements of embankments are typically not very critical due to the flexibility of the embankment; however, the settlement of an approach embankment needs to be very accurately assessed in an attempt to "match" the settlement of the bridge abutment. For mechanically stabilized earth (MSE) structures, allowable differential settlement along the wall alignment can vary between allowing significant differential settlement for geotextile-reinforced slopes to more stringent requirements for walls with full-height precast concrete facings. Such relative tolerances will ultimately guide the selection of settlement parameters. Where tolerances are very strict, conservative parameters will be

selected and site-specific variations will be assessed; where tolerances are more relaxed, average parameters will likely be selected for design. Ultimately the design engineer must ask the question, "what is the implication on the performance of the structure (for both limit states and serviceability states) if the selected design properties are significantly different than actual properties?"

Compression Parameters

Compressibility properties including C_c (or $C_{c\varepsilon}$), C_r (or $C_{r\varepsilon}$), and C_α (or $C_{\alpha\varepsilon}$) should be evaluated from one-dimensional consolidation tests. As discussed, computed values will depend on degree of sample disturbance, stress level at which the parameter is computed relative to the preconsolidation stress, and inherent variability. For settlement calculations, the range of calculated values and average values for these parameters for each compressible soil unit should be evaluated and plotted versus depth. Settlement analyses can be carried out extremely rapidly using spreadsheets or settlement analysis programs (e.g., EMBANK (FHWA, 1993)) so that the effect of parameter values at the upper and lower end of the range can be evaluated.

Preconsolidation Stress

Both laboratory and in-situ tests can be used to evaluate preconsolidation stress, recognizing that laboratory test data are required to correlate values derived from in-situ tests. As an example, figure 61 shows a comparison of calculated values of σ_p' from laboratory oedometer curves and from the correlation described previously for the DMT (i.e., equation 44). Results compare favorably and demonstrate the utility of in-situ testing for profiling preconsolidation stress. For the particular project example illustrated in figure 61, oedometer tests were performed at approximately 1.5 to 3-m intervals. For more typical transportation-related projects, oedometer tests will likely be performed at greater intervals based on project schedule and cost. For this project example, if the number of oedometer tests were reduced to be more consistent with that for a typical project, then the interpreted DMT data would accurately fill in data gaps between oedometer test results. Once again, however, high-quality oedometer tests must be performed to establish values of preconsolidation stress for which in-situ test results can be compared.

A profile of σ_p' (or OCR = σ_p'/σ_{vo}') with depth should be developed for the site. This parameter represents the most important value relative to settlement and shear strength evaluations for designs involving cohesive deposits. As with compressibility properties, an upper and lower bound profile should be developed based on laboratory tests and plotted with a profile based on particular in-situ test(s) (if used). There are no specific rules to judge the appropriateness of any particular value, however sample disturbance will typically be the most important factor affecting results. The sample disturbance indices will be useful in assessing why, for example, a particular test provides a value of preconsolidation stress that seems too low.

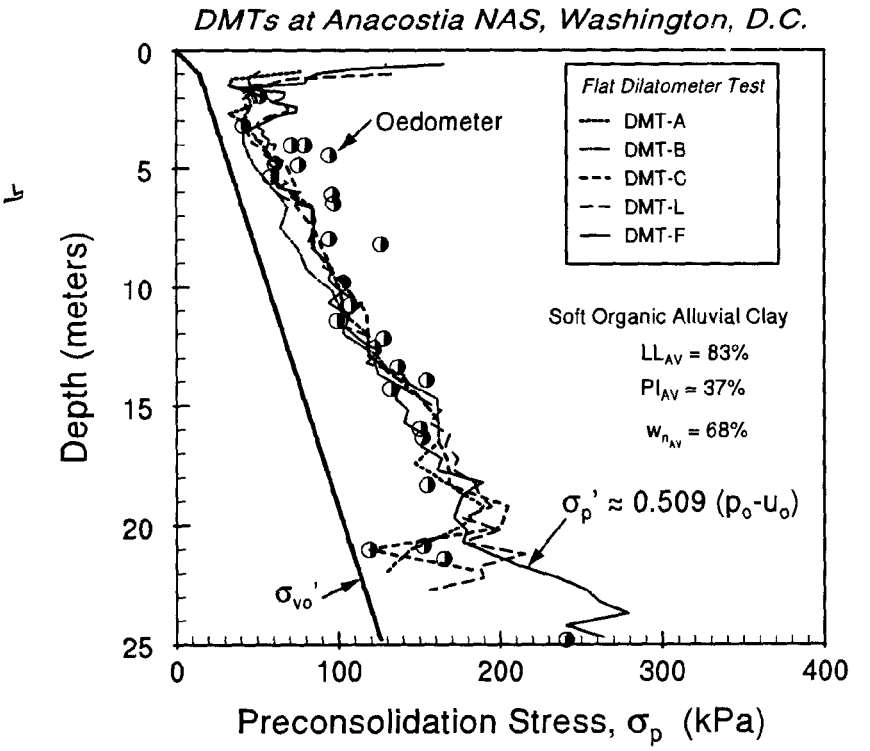

Figure 61. Preconsolidation stress from oedometer and DMT.

Specific data quality issues that should be considered in evaluating preconsolidation stress are described below:

- Assess whether a consolidation curve that does not exhibit a sharp break is the result of sample disturbance or that the soil sample may contain relatively significant amounts of non-cohesive material (i.e., sand, non-plastic silt), which will result in a consolidation curve without a distinct break.

- Make sure that the consolidation curve used to compute the preconsolidation stress corresponds to end of primary consolidation conditions. Most laboratories do not perform analyses to evaluate the end of primary condition, but simply provide consolidation curves that represent the end of the test (see figure 48 for comparison of σ_p' for laboratory tests after 24 hours and for tests carried out to the end of primary consolidation).

- The preconsolidation stress can only be reasonably estimated from laboratory oedometer tests if the test has been carried out to sufficiently high pressures. As a general rule of thumb, tests should be carried out to loads equal to approximately 4 to 8 times the estimated σ_p'. Previous testing and/or geologic information should be used to estimate σ_p'.

It is particularly important to accurately compute preconsolidation stress values for relatively shallow depths where in-situ effective stresses are low. An underestimate of the preconsolidation

stress at shallow depths will result in overly conservative estimates of settlement for shallow soil layers.

Coefficient of Consolidation

Laboratory consolidation test data are used to estimate the vertical coefficient of consolidation, c_v whereas a piezocone can be used with pore pressure dissipation test data to estimate the horizontal coefficient of consolidation, c_h. The general trend associated with coefficient of consolidation is that the c_v values are stress dependent and that higher values are to be expected for effective stresses less than the preconsolidation stress. Due to the numerous simplifying assumptions associated with conventional consolidation theory, for which the coefficient of consolidation is based, it is unlikely that even the best estimates of c_v or c_h from high-quality laboratory tests will result in predictions of time rate of settlement in the field that are significantly better than a prediction within one order of magnitude. In general, the in-situ value of c_v is larger than the value measured in the laboratory test. Therefore, a rational approach is to select average, upper, and lower bound values for the appropriate stress range of concern for the design application. These values should be compared to values obtained from previous work performed in the same soil deposit. Under the best-case conditions, these values should be compared to values computed from measurements of excess pore pressures during construction of other structures. Figure 62 provides a general correlation for c_v that can be used to judge the reasonableness of computed c_v values obtained from oedometer test data.

Calculations performed concerning time rate of settlement for the actual field conditions should be performed using the average, upper, and lower bound values discussed above. The results of these calculations should be compared relative to specific project constraints. For example, a range of c_v values may result in calculated times to the end of primary consolidation for field conditions of 6 to 60 days. This would indicate that even under worst-case conditions, it is likely that consolidation will be completed during construction. Where calculated c_v or c_h values result in a range of time rates of settlement which encompass "go, no-go" decisions, then the installation of piezometers should be considered.

Values for c_v obtained from laboratory oedometer tests should be compared to values for c_h obtained from piezocone tests. Although the time rate of consolidation in the lateral direction should be greater than that in the vertical direction, for most relatively isotropic soils the ratio of lateral to vertical consolidation may only be as high as two. Soils that are highly stratified such as varved clays may have a ratio on the order of ten or more.

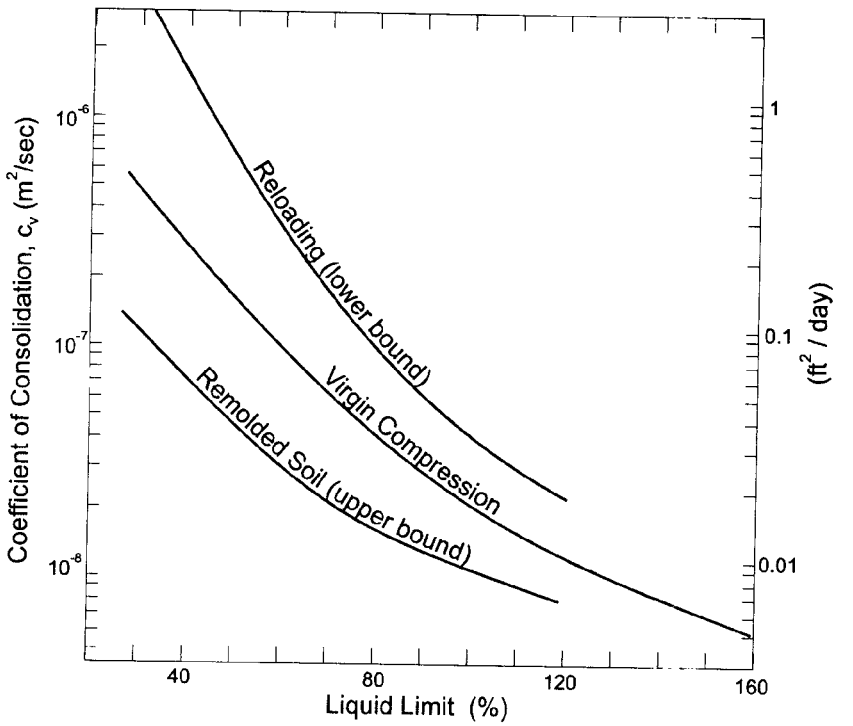

Figure 62. Correlation of c_v to LL.

Coefficient of Secondary Compression

The analysis of secondary compression settlements includes evaluating time-dependent (creep) settlements for a given period of time. In engineering analyses, it is commonly assumed that the coefficient of secondary compression can be represented as a constant value over the period of interest implying that the rate of secondary compression is independent of the thickness of the compressible layer. The accurate interpretation of C_α and $C_{\alpha\varepsilon}$ is directly linked to the ability to accurately evaluate the time to the end of primary consolidation in a laboratory consolidation test. As discussed, the coefficient of secondary compression is expected to vary with final effective stress level and an average value can be developed based on the recommendations provided in section 5.4.2.7. Computed values from consolidation tests should be compared to computed values for C_c and C_r and the ratios C_α/C_c and C_α/C_r should be compared to the expected values listed in section 5.4.2.7 (e.g., $C_\alpha/C_c = 0.05 \pm 0.01$ for organic silts and clays). Additional discussion on the evaluation of secondary compression properties for organic clays, organic silts, and peats is provided in chapter 7.

5.5 GENERAL STRESS-STRAIN AND STIFFNESS PROPERTIES

5.5.1 Background

There are numerous semi-empirical methods available for calculating settlements in soils. Some of these methods apply elasticity theory to calculate settlements based on a selected elastic modulus value. The difficulties associated with selecting a single modulus value to characterize the soil have

resulted in very conservative assessments of settlements in soils resulting from foundation loadings. This section describes a method that uses the shear wave velocity of the soil as a means to evaluate an appropriate modulus value for use in evaluating settlements in soils subject to vertical (or axial) loadings. Although not presented here, the method can be extended to evaluate primary consolidation settlements in cohesive soils.

For completeness, several historical correlations for elastic modulus based on soil type and SPT N values are presented first. These values can be used in preliminary calculations for foundation settlements. However, it is strongly recommended that where "go, no-go" decisions regarding the use of shallow foundations as compared to deep foundations need to be made, that the method presented herein for evaluating elastic modulus values based on soil shear wave velocity be considered.

5.5.2 Settlement Analysis for Soils

Settlements are often calculated based on results from in-situ tests and used either in empirical relationships or using equations from elasticity theory. The empirical expressions are particularly dependent on site-specific geologies, local practices, and specific test method (e.g., SPT, CPT, PMT, DMT). A review of the traditional methods used to evaluate settlements in sands is provided in FHWA/RD-86/185 (1987). Several methods use an elastic modulus value and a general elasticity equation to calculate settlements in granular soils and immediate settlements in clayey soils.

The general equation for displacement at the center of an applied surface loading is of the form:

$$s = \frac{qBI}{E_s} \cdot (1 - \nu^2) \qquad \text{(Equation 49)}$$

where q = applied surface stress ($\Delta\sigma_v$ at z = 0), B = width of the loaded area, I = displacement influence factor, E_s = equivalent elastic modulus, and ν = Poisson's ratio of the soil. The influence factors (I) depend on surface area geometry, layer thickness, degree of homogeneity, and relative rigidity of the loaded area. Values of I are given in table and chart forms for foundations (e.g., Harr, 1966; Poulos & Davis, 1974) and embankments (e.g., Giroud, 1968), or else can be generated on a simple spreadsheet using stress distributions (e.g., Mayne & Poulos, 1999). Equations are also available for evaluating settlement of a deep foundation element (i.e., a driven pile or drilled shaft) subject to axial compression loading.

Table 28 and 29 provide correlations for E_s based on soil type and from uncorrected SPT N values.

Table 28. Elastic constants of various soils based on soil type (modified after AASHTO, 1996).

Soil Type	Range of Equivalent Elastic Modulus (kPa)
Clay • Soft sensitive • Medium stiff • Very stiff	 • 2,500 to 15,000 • 15,000 to 50,000 • 50,000 to 100,000
Loess	• 15,000 to 60,000
Silt	• 2,000 to 20,000
Fine sand • Loose • Medium dense • Dense	 • 8,000 to 12,000 • 12,000 to 20,000 • 20,000 to 30,000
Sand • Loose • Medium dense • Dense	 • 10,000 to 30,000 • 30,000 to 50,000 • 50,000 to 80,000
Gravel • Loose • Medium dense • Dense	 • 30,000 to 80,000 • 80,000 to 100,000 • 100,000 to 200,000

Table 29. Elastic constants of various soils based on SPT N value (modified after AASHTO, 1996).

Soil Type	Equivalent Elastic Modulus (kPa)
Silts, sandy silts, slightly cohesive mixtures	400 $(N_1)_{60}$
Clean fine to medium sands and slightly silty sands	700 $(N_1)_{60}$
Coarse sands and sands with little gravel	1,000 $(N_1)_{60}$
Sandy gravels	1,200 $(N_1)_{60}$

5.5.3 Method to Evaluate Equivalent Elastic Modulus

For deformation analyses, correlations such as that presented above for the SPT have been developed to obtain a modulus value from penetration test data (e.g, Schmertmann, 1970; Mitchell & Gardner, 1975). As shown in figure 63, however, a relevant soil modulus for a deformation analysis is situated close to the initial stress state of the material, while the penetration readings correspond to the peak (i.e., fully mobilized strength) of the stress-strain-strength curve.

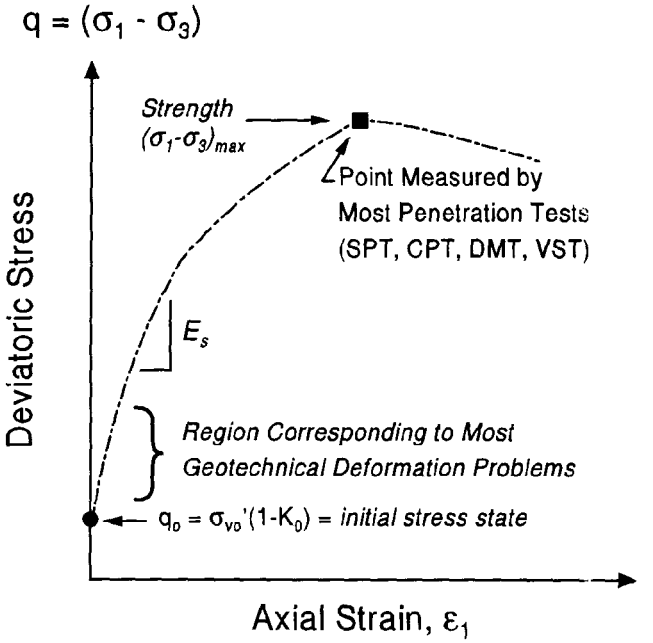

Figure 63. Strength measured by in-situ tests at peak of stress-strain curve.

Although the strength of a soil is in many cases proportional to its stiffness characteristics, different materials can have similar shear strength but have significant differences in stiffnesses (see figure 64).

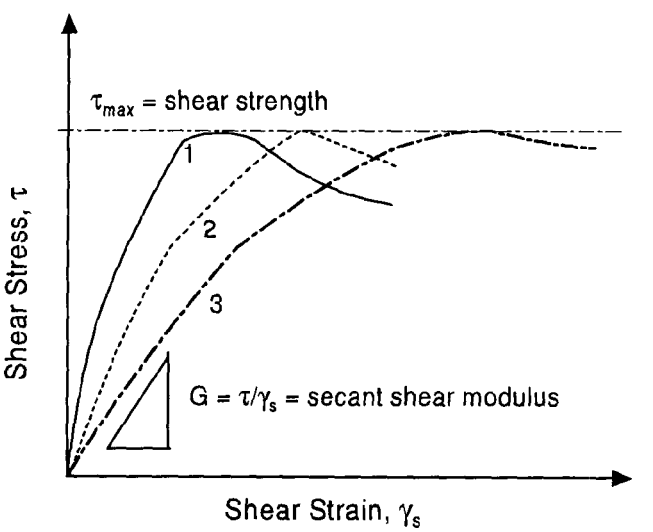

Figure 64. Stress-strain-strength curves for three geomaterials having the same strength yet different stiffnesses.

In certain geologic materials, it has been possible to develop calibrated correlations between specific tests (e.g., PMT, DMT) with performance-monitored data obtained from full-scale structures, including foundations and embankments, or with reference values from laboratory tests. Generally, these tests provide a modulus somewhere along the stress-strain curve, yet the specific position along the stress-strain curve is not well-defined, as indicated by figure 65.

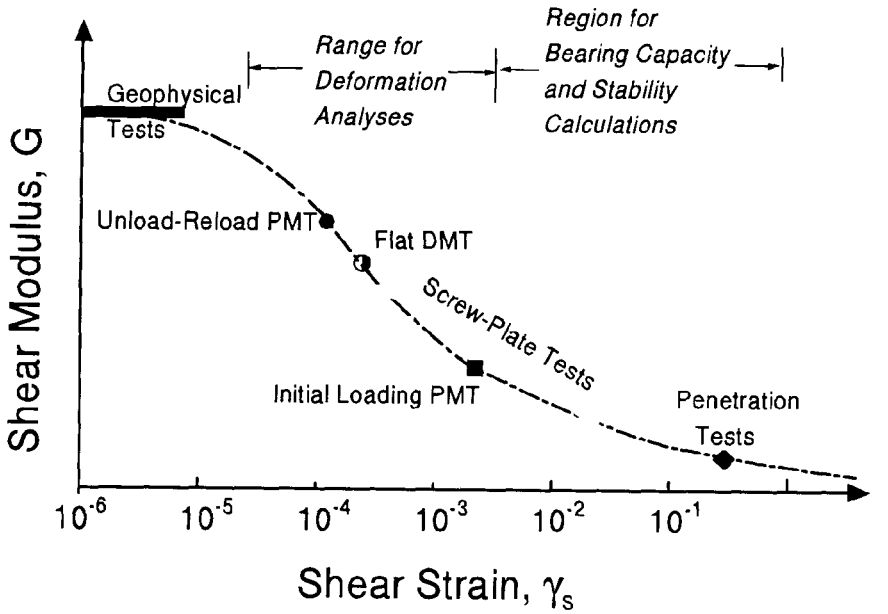

Figure 65. Variation of modulus with strain level.

Of particular note, the small-strain modulus from geophysical tests provides an excellent reference value, as this is the maximum stiffness that the soil can exhibit at a given void ratio and confining stress. Herein, a generalized approach based on the small strain stiffness from shear wave measurements will be discussed, whereby the initial modulus (E_0) is reduced to a value consistent with an appropriate working stress level for the desired factor of safety (FOS) for the structure. This reduction factor is also referred to as the modulus degradation value, E/E_o.

The equivalent elastic modulus value, E_s, can be calculated as:

$$E_s = \left(\frac{E}{E_o}\right) E_o \qquad \text{(Equation 50)}$$

where E_0 is the small-strain elastic Young's modulus. This modulus is related to the small-strain shear modulus, G_o, according to:

$$E_o = 2G_o\,(1+\nu) \qquad \text{(Equation 51)}$$

Recent research has confirmed that Poisson's ratios for many soils are lower than once thought. For drained loading, appropriate values are $0.1 < \nu < 0.2$ for stages of loading up to typical working load levels (e.g. Jamiolkowski, et al. 1994).

The small strain (initial) shear modulus of soil, G_o, is related to the shear wave velocity, V_s, and the mass density of the soil, ρ, by the equation:

$$G_o = \rho V_s^2 \qquad \text{(Equation 52)}$$

Mass density of the soil is related to total unit weight of the soil, γ_t, by the acceleration of gravity, g:

$$\rho = \frac{\gamma_t}{g} \qquad \text{(Equation 53)}$$

The mass density of soils can be reasonably estimated from soil classification and location relative to the water table. Combining equations 50 to 52 results in the following expression for the equivalent elastic modulus:

$$E_s = \left(\frac{E}{E_o}\right) 2\rho V_s^2 (1+\nu) \qquad \text{(Equation 54)}$$

The required parameters necessary to evaluate the equivalent elastic modulus (E_s), therefore include: (1) Poisson's ratio; (2) shear wave velocity, V_s; and (3) modulus degradation value, E/E_o. A value of 0.1 for Poisson's ratio may be assumed for drained loadings in granular materials at working load levels. In subsequent sections, field procedures are described for evaluating shear wave velocity. Correlations are also provided which relate small strain shear modulus, G_o, to measured parameters from in-situ tests. These correlations may be used if shear wave velocity information is not available for a particular project. Finally, a chart solution is provided for evaluating the modulus degradation value.

5.5.4 Evaluation of Shear Wave Velocity

5.5.4.1 General

Measurements of shear wave velocity, V_s, can provide a reliable means for evaluating the small strain shear modulus (G_o). The parameter G_o is applicable to static monotonic loading and dynamic loading and for drained and undrained behavior. Thus, the value of G_o can be established as a benchmark of stiffness for deformation analysis of all geotechnical problems. In addition, the small strain characteristics may be most appropriate for seismic design considerations.

5.5.4.2 Field Measurements of Shear Wave Velocity

The measurement of V_s (and G_o, see Equation 52) in soils can be accomplished by a variety of laboratory and field methods, as depicted in figure 66. Provided that high-quality undisturbed samples can be obtained during field drilling explorations, laboratory tests can be conducted on specimens of natural soils. Current practice, however, relies more often on field measurement of V_s and G_o.

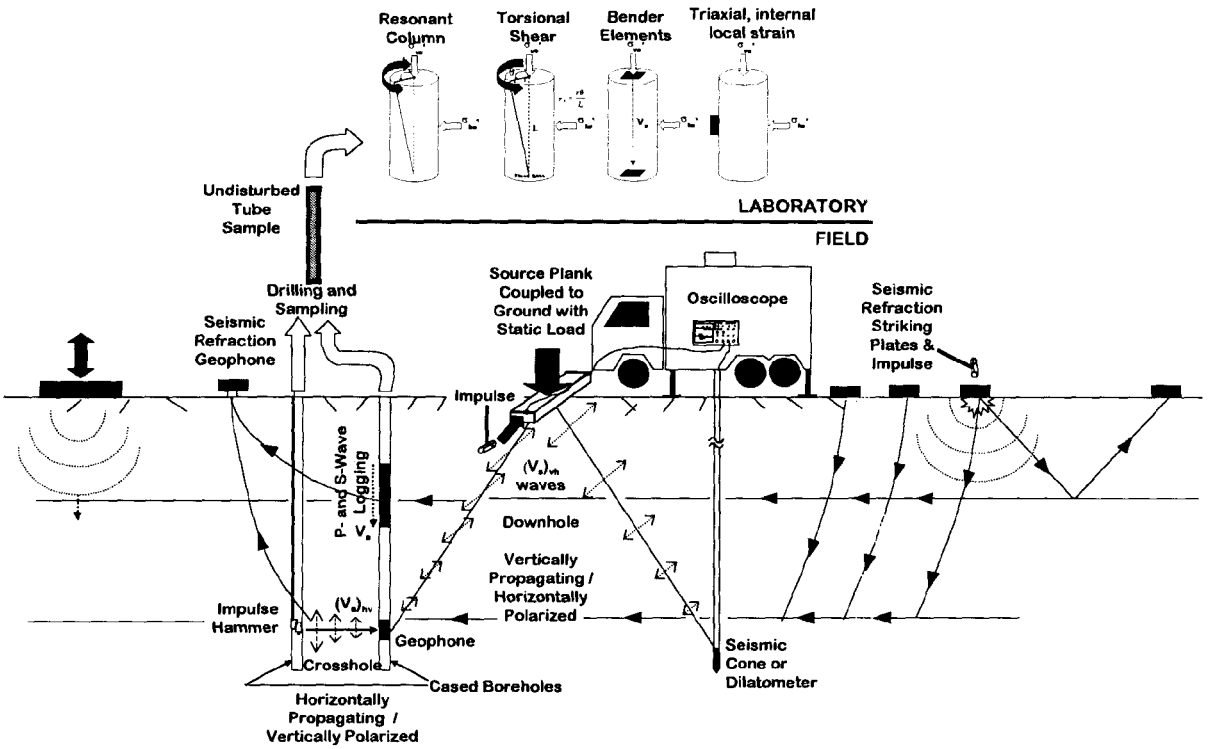

Figure 66. Field and laboratory methods to evaluate shear wave velocity.

Geophysical techniques for subsurface exploration are described in detail by Woods (1994). Geophysical techniques commonly used in geotechnical practice are briefly summarized in the following paragraphs. Two general types of techniques are available to measure shear wave velocity in the field:

- intrusive techniques whereby measurements are made using probes and sensors that are lowered in boreholes or pushed into the ground; and
- non-intrusive techniques whereby the measurements are made using sources and receivers at the ground surface.

Borehole Seismic Surveys

In a borehole seismic survey, one or more boreholes are drilled into the soil to the desired depth of exploration. Wave sources and/or receivers are then lowered into the boreholes to perform the desired tests. There are three approaches to borehole seismic surveys:

- *Cross Hole Survey*: In a cross hole survey, the energy source is located in one boring and the detector (or detectors) is placed at the same depth as the energy source in one or more surrounding boreholes at a known spacing. Travel time between source and receiver is measured to determine the wave velocity.

- *Down Hole Surveys*: In a down hole survey, the energy source is located on the surface and the detector, or geophone, is placed in the borehole. The travel time is measured with the geophone placed at progressively increasing depth to evaluate the wave velocity profile.

- *Up Hole Surveys*: Geophones are laid out on the surface in an array around the borehole. The energy source is set off within the borehole at successively decreasing depths starting at the bottom of the hole. The travel times from the source to the surface are analyzed to evaluate wave velocity versus depth. The energy source is usually either explosives or a mechanical pulse instrument composed of a stationary part and a hammer held against the side of the borehole by a pneumatic or hydraulic bladder.

The cross hole technique is generally the preferred technique for a borehole survey as it offers the highest resolution and greatest accuracy. However, cross hole measurements require a very precise evaluation of the distance between the energy source and the detector, as well as multiple vertical holes. An inclinometer reading is generally performed in the boreholes used in a cross hole survey to correct the results for deviation of the boreholes from verticality. Cross hole geophysical testing is codified in ASTM D 4428.

It has become convenient and economical to incorporate geophones within penetrometers and probes used for in-situ soil tests, and thus permit downhole testing in conjunction with routine in-situ testing soundings. The commercially-available seismic cone (Robertson, et al. 1986; Campanella, 1994) and seismic dilatometer (Martin and Mayne, 1998) are hybrid tests that combine penetration testing with downhole geophysics, thus allowing the determination of both small-strain and high-strain properties within a single sounding. Figure 67 shows a schematic illustration of a seismic dilatometer test.

Seismic Refraction and Seismic Reflection Methods

Seismic refraction and reflection exploration surveys are conducted from the surface and do not require boreholes. The resolution of the methods is relatively poor and decreases with depth. These methods are most suitable as a means of identifying the depth to competent rock and the location of prominent soil horizons that have a large contrast in density and stiffness compared to the overlying soil. Additional discussion is not warranted because these technologies generally cannot provide sufficiently accurate deformation parameters.

Spectral Analysis of Surface Waves (SASW)

Spectral Analysis of Surface Waves (SASW) is a non-intrusive geophysical technique used primarily for evaluating subsurface shear wave velocity profiles. SASW testing evaluates shear wave velocity indirectly by direct measurement of Rayleigh, or surface wave, velocity. Rayleigh wave velocity is closely related in magnitude to the shear wave velocity. SASW results are representative of the average properties of an assumed relatively large mass of material. SASW can be a very cost-effective method of investigation. Ease and speed of field measurements and automated algorithms for data processing and inversion allow for evaluation of subsurface conditions at a relatively large number of points at a fraction of the cost of conventional intrusive exploration techniques.

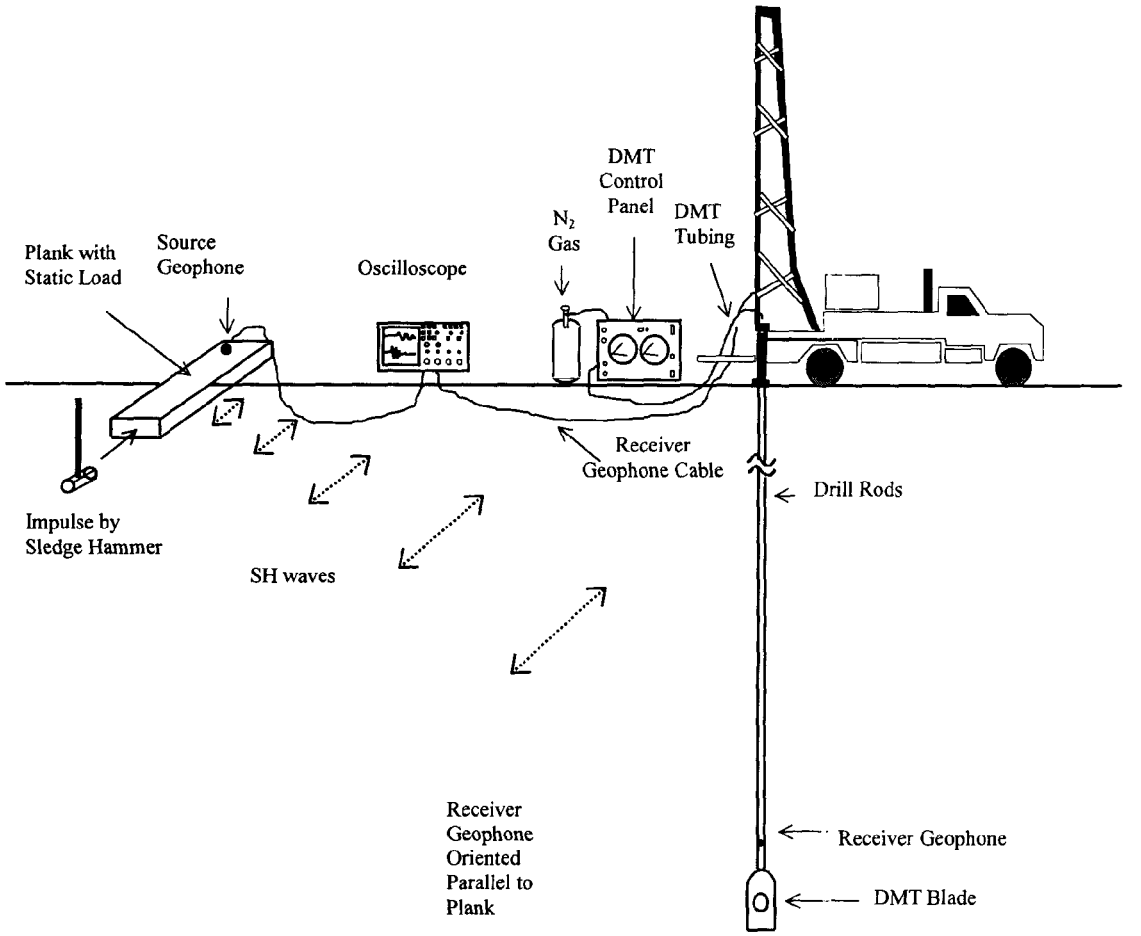

Figure 67. Seismic dilatometer test.

5.5.5 Correlations for Small-Strain Shear Modulus

In addition to using shear wave velocity information, the small-strain shear modulus, G_o, can be estimated using empirical correlations. Table 30 presents the typical range for G_o for several generic soil types.

Table 30. Typical values of small-strain shear modulus.

Soil Type	Small-strain shear modulus, G_o (kPa)
Soft clays	2,750 to 13,750
Firm clays	6,900 to 34,500
Silty sands	27,600 138,000
Dense sands and gravels	69,000 to 345,000

The small-strain shear modulus can be correlated to the SPT N_{60} value and to the CPT q_c value according to the following:

$$G_o = 15{,}560 (N_{60})^{0.68} \quad \text{(Equation 55)}$$

$$G_o = 1{,}634 (q_c)^{0.25} (\sigma'_{vo})^{0.375} \quad \text{(Equation 56)}$$

Units of kPa are used in equations 55 and 56. Additional correlations for small-strain shear modulus are provided in FHWA-SA-97-076 (1997).

5.5.6 Evaluation of Modulus Degradation Value

The small-strain shear modulus (and hence the small-strain Young's modulus) should be reduced for use in foundation deformation calculations since strains associated with foundation loadings are a few orders of magnitude greater than those corresponding to the small-strain values for G_o and E_o. A graphical procedure can be used as a simple means to reduce the small-strain stiffness (E_0) to those at working stress levels. To use this graphical procedure, the stress ratio, as defined as q/q_{ult}, at the desired working stress (q) is required. By definition q/q_{ult} = 1/FOS. Figure 68 illustrates the suggested trends for intact (i.e., non-fissured) clays and uncemented sands. For monotonic loading of these soils, a value of the dimensionless parameter g = 0.3 can be used. The parameter g is simply a curve-fitting parameter for the hyperbolic relationship shown in figure 68. The value of 0.3 has been confirmed as reasonable for first-order approximations based on results from laboratory shear tests as well as backcalculations from full-scale foundation load tests (Burns and Mayne, 1996; Kates, 1996). It is noted that the use of g=0.3 for highly structured soils and cemented materials is conservative (i.e., the calculated modulus value using g=0.3 for these soils is likely to result in a conservative estimate of settlements).

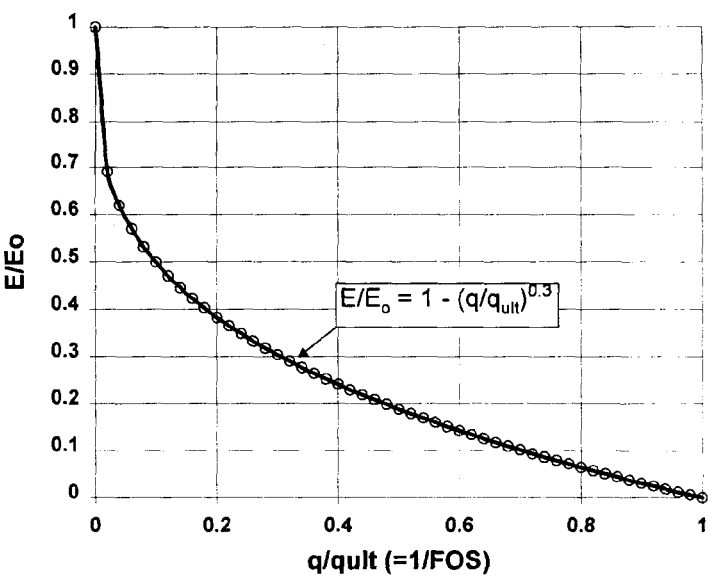

Figure 68. Modulus degradation based on g= 0.3.

5.5.7 Summary

A method for evaluating an equivalent elastic modulus has been presented. The modulus value can be used in settlement calculations of structures in soils for which the settlement analysis method used requires an elastic modulus. The method uses the soil shear wave velocity and small-strain modulus value (i.e., E_o or G_o) in the evaluation of the modulus. The evaluation of the equivalent elastic modulus is summarized below and is illustrated in Soil Property Selection Example No. 2 in appendix A.

- Develop a profile of shear wave velocity versus depth at the location of the structure. Shear wave velocity should be evaluated using geophysical or in-situ testing techniques. Figure 69 shows a shear velocity profile obtained using a commercially available seismic piezocone.

- Develop a profile of small strain shear modulus, G_o, using the shear wave velocity profile and unit weight measurements or from correlations.

- Divide the profile into distinct zones based on the shear modulus profile or develop a single average value over each distinct zone within the depth of interest.

- Based on the design FOS for the structure, evaluate E/E_o using figure 68 and the modified hyperbola with a "g" exponent equal to 0.3.

- Calculate the equivalent elastic modulus, E_s, using equation 54 and use this value in settlement analyses such as that of the form given in equation 49.

5.6 SHEAR STRENGTH PROPERTIES OF SOIL

5.6.1 Introduction

As part of the design analyses for most geotechnical projects, the load-carrying capacity of the supporting soil is evaluated. These capacity evaluations include, for example, bearing capacity of a shallow foundation, side and tip resistance of drilled shafts and driven piles, stability analyses of slopes and embankments and passive soil capacity for the toe of a retaining structure. These analyses are concerned with comparing actual loads imposed on the system to the limit (or failure) state of the supporting soil. This limit state of stress corresponds to the shear strength of the soil.

For a given soil, shear strength is anything but a unique property. This concept is often overlooked, even by experienced geotechnical engineers. The soil strength to be used in design analyses must be qualified in relation to whether the appropriate strength is: *drained* or *undrained, peak, fully softened* or *residual, intact* or *remolded, static* or *cyclic, compression* or *extension;* and other facets, such as direction of loading, rate of loading, and boundary conditions. As a consequence, soil strength is not a fundamental property, but instead, a specific behavioral response to a certain set of loading conditions.

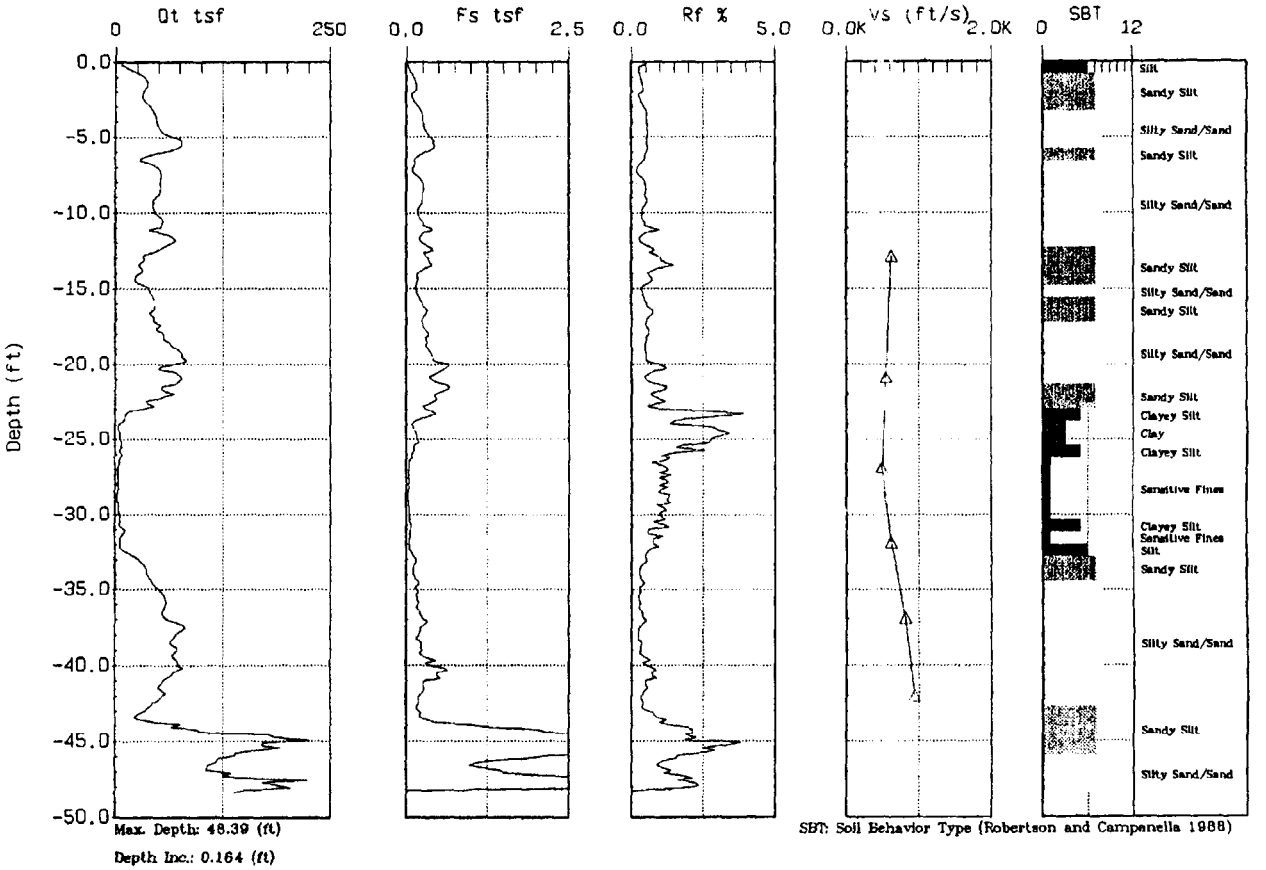

Figure 69. Shear wave velocity profile from seismic cone sounding.

Figure 70 provides an overview of the various laboratory tests used to measure soil strength showing the imposed stresses and loading conditions. Laboratory testing for most highway projects may include unconfined compression, triaxial shear, and direct shear. Other tests including direct simple shear, plane strain, torsional shear, hollow cylinder, cubical triaxial, and ring shear are also available, but are most often used on large projects (e.g., use of direct simple shear testing on the Central Artery Project in Boston) or in universities.

A variety of in-situ testing devices are also available for evaluating drained soil strength in granular soils and undrained strength in cohesive soils through the use of engineering correlations and theoretical equations. Currently, however, no in-situ test provides a reliable evaluation of effective stress strength (c′ and ϕ') of clays, however ongoing research with piezocones appears promising. Field penetration tests (SPT, CPT, DMT) can be readily used to evaluate the strength of sands (ϕ').

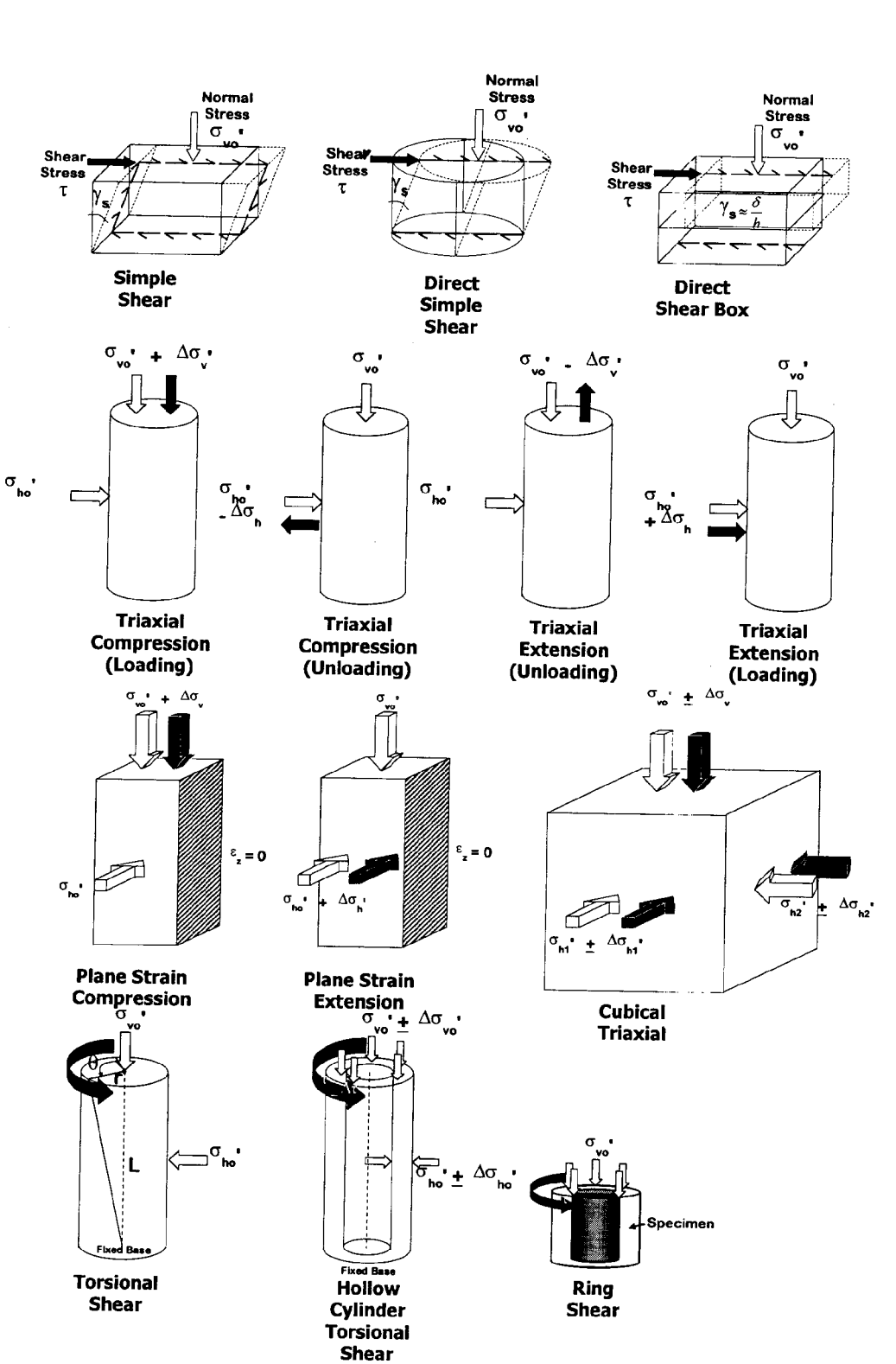

Figure 70. Various laboratory tests used to measure soil strength showing the imposed stresses and loading conditions.

This section provides state-of-the practice information on the evaluation of soil shear strength (i.e., ϕ', c', and s_u) for design analyses. Information on laboratory, in-situ, and correlative techniques to evaluate shear strength are presented. Also, fundamental information relating to shear strength evaluation including concepts of drained and undrained behavior and total and effective stress analyses are presented as they relate to shear strength evaluation. The numerous factors that affect the selection of shear strength values for design analyses are presented in terms of their relevance to specific design requirements for typical highway and transportation design and construction applications. A description of the process used to evaluate shear strength data from several test methods is provided at the end of this section for effective stress and total stress strength parameters for soils.

5.6.2 Fundamental Concepts of Soil Shear Strength

5.6.2.1 Drained versus Undrained Loading

In geotechnical practice, it is most important to distinguish between "**drained**" and "**undrained**" strengths. These terms refer to the ability of the porewater in the soil to move between soil particles resulting in volume change, and the accompanying generation (or lack) of excess porewater pressures, Δu. Soils can also exhibit any number of partially drained strengths, however, design analyses are typically performed using drained and undrained strengths, as these represent limits to the expected range of behavior.

For a saturated soil subjected to *undrained loading*, no drainage of porewater from the void spaces can occur, and thus the soil undergoes no change in volume. During undrained loading, changes in total stress ($\Delta\sigma$) cause the development of either positive porewater pressures ($\Delta u > 0$) that will tend to decrease the effective stress in the soil or negative porewater pressures ($\Delta u < 0$) that will tend to increase the effective stress in the soil.

The *drained loading* of a saturated soil means that the water in the void spaces is free to move so that no excess pore water pressures develop ($\Delta u = 0$). There is usually a change (i.e., increase or decrease) in void ratio and a corresponding change in volume. Again, water may be present, but is free to move either out of the soil mass (termed *contractive* soil behavior) or into the soil mass (termed dilatant soil behavior). Contractive behavior results in a decrease in volume (e.g., settlement) and dilative behavior causes an increase in volume (e.g., swelling). Clean sands have such a high permeability (e.g., $k > 10^{-3}$ cm/s) that, under static loading, they are almost always drained. Sands, however, will behave in an undrained mode when subjected to rapid loading, such as that imposed by an earthquake whereby the entire deposit is engaged and water cannot drain.

All clays exhibit drained behavior when the rate of loading is very slow, so slow that it does not interfere with the rate of water migration that is controlled by its low permeability (e.g., $k < 10^{-6}$ cm/s). Drained behavior in clays should be considered in evaluating the long-term stability (and ground movements) of cut slopes. The same clay that behaves in a drained manner in these applications, however, may initially behave in an undrained mode in the short-term if the rate of loading is too fast to permit water inflow. The short-term stability of excavations and slopes constructed in soft to medium clays is represented by undrained loading conditions.

5.6.2.2 Drained Stress-Strain-Strength Behavior

In this section, the stress-strain-strength behavior of soils is introduced for the simple case of drained loading. To illustrate this, a graph of measured shear stress (τ) versus shear strain (γ_s) from a direct simple shear test is used (figure 71). It is recognized that the direct simple shear test is not commonly performed, but it is most useful in introducing drained stress-strain strength behavior of soils. The more common direct shear (box) test is very similar to the direct simple shear and thus the same basic principles apply. The slope of the τ-γ_s curve is the shear modulus (G), as designated by point ① in figure 71. The term modulus can have several definitions, including *initial* (corresponding to small-strains), *secant* (always through the origin of the measured response or $G = \tau/\gamma_s$), and *tangent* (local incremental slope or $G = \Delta\tau/\Delta\gamma_s$). An unload-reload cycle can also be introduced and this is defined by the tangent value.

The maximum stress on the τ-γ_s curve is commonly interpreted as the ***peak shear strength*** (τ_{max}), corresponding to point ② in figure 71. Figure 71 shows two stress-strain curves, each one corresponding to different effective consolidation stresses (i.e., σ_{v1}' and σ_{v2}'). For each specimen, the measured peak strength (τ_{max}) is plotted versus effective consolidation stresses as shown in figure 71. A linear fit is generally forced (minimum of two data sets) to provide the simplified straight line Mohr-Coulomb failure criterion:

$$\tau_{max} = c' + \sigma' \tan \phi' \qquad \text{(Equation 57)}$$

where ϕ' = effective stress friction angle and c' = effective cohesion intercept.

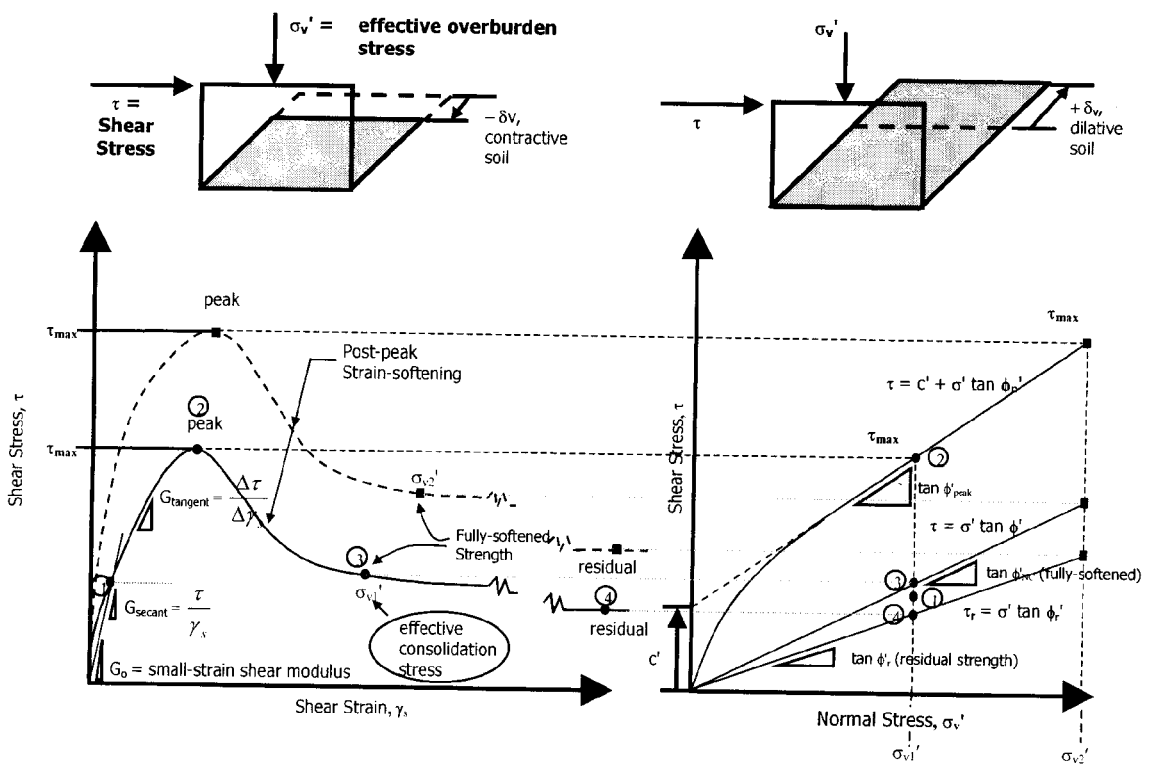

Figure 71. Drained stress-strain behavior.

During drained shearing, the soil specimen will likely undergo a change in total volume. If the soil decreases in volume during shear, the response is termed ***contractive*** behavior. This response is indicative of loose sands and soft clays. If the soil increases in volume during shearing, a ***dilative*** (or *dilatant*) behavior is observed. This response is common in hard clays and dense sands. If no change in volume occurs during drained shear loading ($\Delta V/V_0 = 0$), the corresponding stress state is called the ***critical state***. The complete description of soil behavior by this arrangement is termed *critical-state soil mechanics*, which encompasses normally- and overconsolidated soils for undrained, semi-drained, and drained loading, for both contractive and dilatant behavior (Schofield and Wroth, 1968; Wood, 1990). However, in current U.S. practice, the concept of critical state soil mechanics is not consistently recognized, although this concept is an excellent representation of soil behavior. In current U.S design practice., drained and undrained are not specifically viewed as they relate to volume change conditions. Rather, the adoption of the simplified Mohr-Coulomb strength criterion is widespread and it is normally taken that "drained conditions" are analyzed using effective stress parameters (i.e., ϕ', c') and "undrained conditions" are analyzed by total stress methods (i.e., $c=c_u=s_u$). For cohesive soils, the drained analysis corresponds to long-term conditions and undrained analyses to short-term conditions. For cohesionless soils (i.e., those with relatively high hydraulic conductivity values), drained analyses alone are performed. The Mohr-Coulomb strength parameters, ϕ' and c', are defined in figure 72.

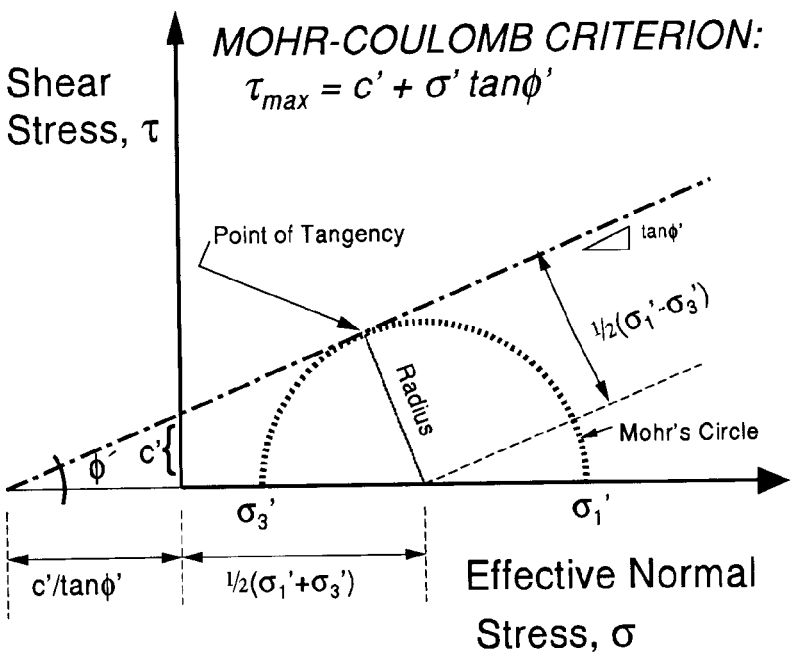

Figure 72. Mohr-Coulomb failure criteria.

Referring to drained strength characteristics in figure 71, after the peak shear strength (τ_{max}) is reached during drained loading, the shear stress reduces to a stable value termed the *fully-softened strength*, depicted as point ③ in figure 71. The fully softened strength is intermediate between the peak strength and the residual strength and there are no specific procedures to identify the fully

softened strength. Conceptually, the fully softened strength is close in value to the peak strength of the same soil in a normally-consolidated condition. This can be expressed as:

$$\tau = \sigma' \tan \phi_{NC}' \qquad \text{(Equation 58)}$$

where ϕ_{NC}' is the peak strength (or critical-state strength) of the normally-consolidated soil. Note that for long-term analyses, the effective cohesion intercept is a small value for the normally consolidated case and is therefore assumed to be zero ($c' = 0$).

For clays, if drained loading continues for very large shearing strains, the shear stress value drops even further to the *residual strength*, denoted τ_r and indicated by point ④. The residual strength is related to the mineralogical frictional characteristics of the soil in which the plate-like clay particles align themselves in a direction parallel to the shear plane that is developed at these very large strains. The residual strength can be represented by:

$$\tau_r = \sigma' \tan \phi_r' \qquad \text{(Equation 59)}$$

In commercial practice, ϕ_r' is obtained using 8 to 10 repeated cycles of shearing on the same specimen in a direct shear box using the same direction of shear and the same normal load. The more elaborate ring shear device is purposely suited for obtaining true residual values of ϕ_r'. The ring shear testing device is illustrated in figure 70 and additional information on the ring shear-testing device can be found in Terzaghi, Peck, and Mesri (1996).

For design of geotechnical features constructed on or in clay soils that exhibit peak, fully softened, and residual shear strength, the design engineer must consider the level of deformations that may be expected within the soil mass to appropriately select the strength to be used for design calculations. As an example, consider the evaluation of soil pressures acting on an anchored wall constructed in overconsolidated clay. Since the portion of shear strength at peak resulting from the cohesion intercept (c' in figure 71) tends to reduce relatively rapidly with increasing deformations beyond peak, soil deformations associated with flexible anchored walls may be sufficient to appreciably reduce this cohesion. Therefore, unless local experience indicates that a particular value of cohesion intercept can be reliably accounted for, zero cohesion should be used in the analyses of flexible anchored walls for long-term (drained) conditions. Since the anticipated deformations are relatively small, conservative drained shear strength for analysis of anchored walls is therefore the fully softened strength.

Residual strengths should be used for geotechnical projects that are designed for a location in which there is evidence of an existing failure surface within the clay (e.g., a structural system used to stabilize an active landslide) or in cases where large deformations are anticipated. For these conditions, it can be assumed that sufficiently large deformations have occurred to reduce the strength to a residual value and therefore, the residual strength can be used for design analyses.

5.6.2.3 Undrained Stress-Strain-Strength Behavior

The undrained shear stress-shear strain curve is similar to that observed for drained loading, except that excess porewater pressures are also generated ($\Delta u \neq 0$). During undrained shearing, a

contractive soil will exhibit positive pore pressures, while a dilative soil will show negative pore pressures. From the undrained τ-γ_s curve, the peak value of τ_{max} is designated as the *undrained shear strength* (s_u or c_u).

Instability under undrained conditions develops mainly for a contractive soil where the soil attempts to mobilize frictional shearing resistance and which also causes the soil to contract under the prevailing confining stresses. This tendency to contract during shear is typical for normally to lightly overconsolidated soft to medium clay soils. Since this tendency cannot be realized, due to the clay soil permeability in relation to the rate of shearing, positive porewater pressures are generated in the soil which reduce the effective stress and hence the mobilized frictional shearing resistance. In such cases the short term undrained shearing resistance of the soil is less than would have been the case if drainage (contraction of the soil volume) could have occurred. The short-term condition is critical for temporary walls constructed in, and for embankments constructed on, normally to lightly overconsolidated clay soils.

In clay soils subjected to unloading conditions that result from excavation to form a highway cut slope, the soil attempts to expand as it mobilizes frictional shearing resistance. This is resisted causing negative porewater pressure to be developed that increases the effective stress in the soil and hence increases the mobilized frictional shearing resistance. Thus, in overconsolidated clay subject to excavation, the short-term (undrained) strength and stability potentially exceeds that which would apply once drainage has occurred. For the examples cited, the engineer needs to be careful to assess both short-term and long-term strengths in their analyses. For dilative soils, the tendency to dissipate pore pressure will reduce the effective stress and thus the strength.

5.6.2.4 Effective Stress Parameters

Granular soils such as gravels, sand, and non-plastic silts have effective stress failure envelopes that pass through the origin indicating that $c' = 0$ for these materials. In fact, only cemented sands and some overconsolidated clay appear to have a true c' value (i.e., $c' \neq 0$). The value of ϕ' for sands depends on mineralogy and packing arrangement that is related to relative density and effective confining stress level (Bolton, 1986). Ranges of ϕ' for clean quartzitic (silica) sands are typically $30° \leq \phi' \leq 50°$, whereas calcareous (corraline) sands may exhibit somewhat higher values. The value of ϕ' generally is recorded at low confining stresses. Figure 73 shows typical ranges of friction angle for rockfills, gravels, and sands over a wide range of confining stresses and with initial porosities ranging from 0.17 to 0.48. The rockfill grades shown on figure 73 are summarized in table 31. To use this figure, the engineer must select the range of confining stresses that the granular soil will be subject to in the field. If this range is relatively large, the friction angle of the soil will vary over the range of confining stresses. A conservative single value can be selected based on the largest confining stresses, or a strength envelope can be developed (in particular for slope stability analyses) in which values of ϕ' are selected to be representative of smaller confining stress increments. Alternatively, values of ϕ' used for design analyses for cohesionless soils are typically based on correlation to a measured parameter value from a penetration test (i.e., N_{60} from SPT, q_t from CPTu, or K_D from DMT) as discussed in section 5.6.6.

Table 31. Unconfined compressive strength of particles for rockfill grades in figure 73.

Rockfill Grade	Particle unconfined compressive strength (MPa)
A	≥220
B	165 to 220
C	125 to 165
D	85 to 125
E	≤85

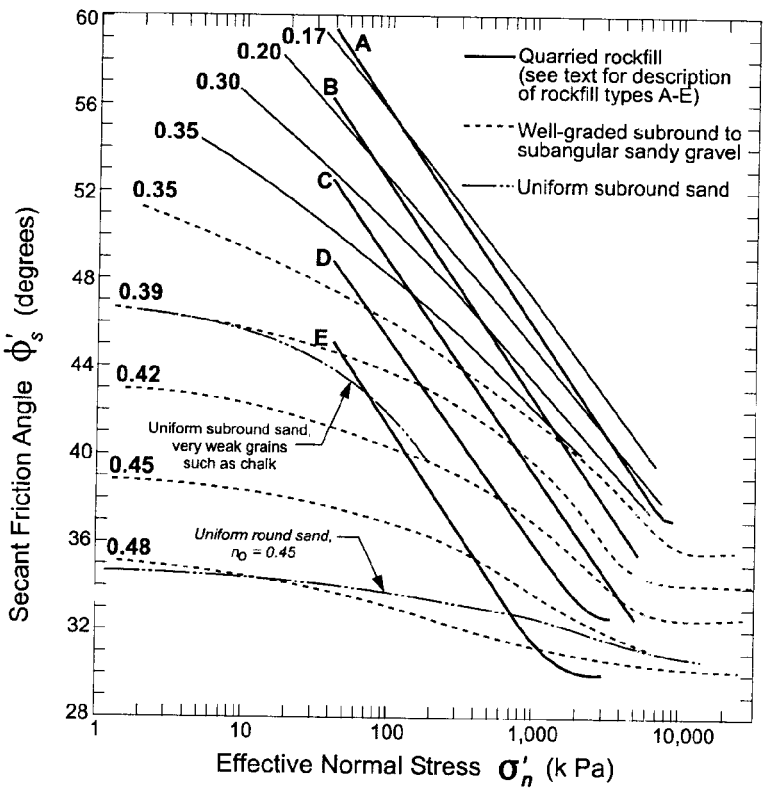

Figure 73. Typical ranges of friction angle for rockfills, gravels, and sands (Terzaghi, Peck, and Mesri, 1996).

For clays, empirical correlations have been developed to relate ϕ' to the plasticity characteristics of the soil. Figure 74 shows a slight trend of ϕ' decreasing with increasing PI (Mesri and Abdel-Ghaffar, 1993), yet values can be ± 8° in variance. Considering the overall importance of ϕ' in stability calculations, foundations, and landslide analyses, it is essential to directly assess ϕ' by means of consolidated drained direct shear tests, consolidated drained triaxial tests, or consolidated undrained triaxial tests with porewater pressure measurements. The consequences of estimating ϕ' can be economically unwise. As an example, for relatively long, shallow slip surfaces that may be associated with a landslide, the required forces that would need to be resisted by some form of

stabilization system (e.g., retaining wall, micropiles) would vary significantly depending on the drained friction angle of the soil. It is highly recommended that state DOTs develop historical data summaries of ϕ' versus PI to check validity of future test results.

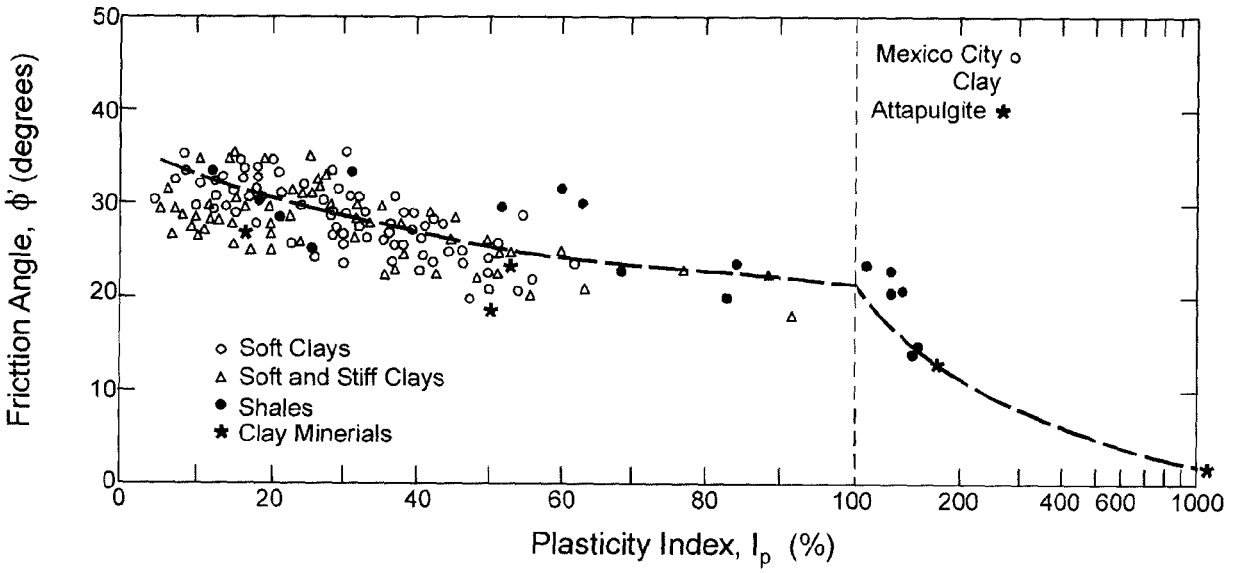

Figure 74. Relationship between ϕ' and PI (Terzaghi, Peck, and Mesri, 1996).

The short-term value of effective cohesion intercept is related to the preconsolidation stress and current effective stress state, as shown by figure 75. However, for long-term analyses involving most insensitive clays, silts, and uncemented sands, it is best to adopt $c' = 0$, unless extensive laboratory testing is conducted or sufficient experience exists to prove bonding or cementation. Conservative recommended values of effective cohesion intercept are as follows:

Short Term: $c' = 0.024\ \sigma_p'$

Long Term: $c' = 0$

The correlation shown in figure 76 (Stark and Eid, 1994) can be used to estimate residual friction angles for preliminary analyses that involve clayey soils that have been subject to large displacements.

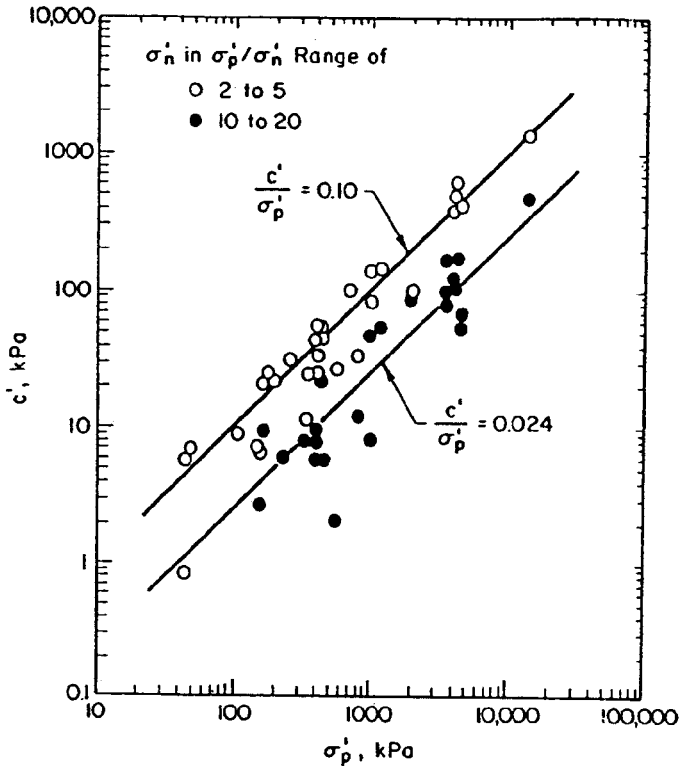

Figure 75. Relationship between c′ and σ_p' (Mesri and Abdel-Ghaffar, 1993).

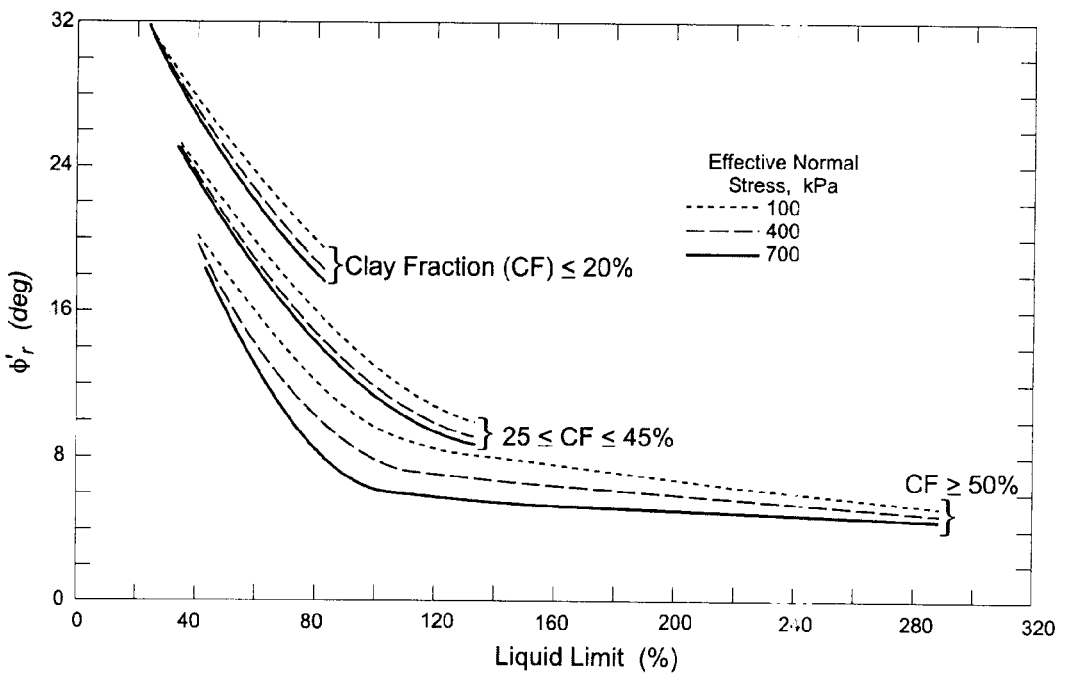

Figure 76. Residual friction angles for clayey soils (after Stark and Eid, 1994).

5.6.2.5 Total Stress Parameters

Total stress analyses for soils that do not drain during the loading period involve the principle that if an element of soil in the laboratory is subjected to the same changes in stress under undrained conditions as an element of the same soil in the field, the same excess pore pressures will develop. Thus, if the total stresses in the laboratory and the field are the same, the effective stresses will also be the same. Because soil strength is governed by effective stresses, the strength measured in laboratory tests should be the same as the strength in the field when the pore pressures and total stresses are the same. Thus, under undrained conditions, strengths can be related to total stresses, making it unnecessary to specify undrained excess pore pressures for design analyses.

Although the total stress principle is simple, experience has shown that many factors influence the pore pressures that develop under undrained loading. As a result, determining undrained strengths by means of laboratory and in-situ testing requires considerable attention to detail if reliable results are to be achieved. Shear strengths for use in undrained total stress analyses must be measured using test specimens and loading conditions that closely duplicate the conditions in the field. Alternatively, they can be reliably measured using the appropriate in-situ test.

Total stress type analyses using the "$\phi = 0$" approach are perhaps the most widely used form of analyses performed by highway engineers for design capacity analyses involving clays. For this condition, the Mohr-Coulomb relationship reduces to the form $\sigma_1' = \sigma_3' + 2c$ or $c=c_u=s_u= ½ (\sigma_1'-\sigma_3')$ = undrained shear strength. Since s_u is stress dependent, its value is commonly normalized by the vertical effective overburden stress (σ_{vo}') at the depth where s_u is measured. The interpretation of s_u from laboratory and in-situ tests is discussed subsequently in this chapter.

5.6.3 Relevance of Design Applications to Soil Shear Strength Evaluation

The selection of an appropriate value for soil shear strength to be used in the analysis of a particular geotechnical structure should consider, at a minimum, the following: (1) how fast will construction occur relative to the hydraulic conductivity of the soil (i.e., drained or undrained strengths); (2) how does the direction of applied load affect measured shear strengths and the appropriate strength to be used for an analysis; (3) how do the expected levels of deformation for the geotechnical structure affect the selection of shear strength; and (4) how does the manner in which the feature is constructed affect the shear strength to be used in analysis. Table 32 provides a summary of specific issues related to the design and construction of typical highway design elements that should be considered in developing and implementing a laboratory and in-situ testing program for evaluating soil shear strength. Issues related to the evaluation of shear strength for rock are described in chapter 6.

Table 32. Summary of issues relevant to shear strength evaluation in support of the design of typical geotechnical features.

Design Element	Issues Relevant To Shear Strength Evaluation
Shallow Foundation	• Soil shear strength information required for depths up to 2 times the width of the footing, unless weak zones are found below this depth. The depth of bottom of footing will be based, in part, on requirements with respect to frost penetration depths and scour depths.
Drilled Shaft	• The excavation of a hole to construct a drilled shaft results in stress relief and disturbance in the soil that ultimately results in a reduction in shear strength from that corresponding to in-situ (i.e., before construction) conditions. The magnitude of the stress relief and disturbance will depend upon the method of construction, soil type, saturation condition, and type of strength (e.g., side shear or end bearing).
Driven Pile	• The shear strength of the soil may vary significantly between the time when the pile (or pile group) is first driven and tested to the time when the superstructure loads are applied to the pile (or pile group). The time-dependent phenomena of strength increase is referred to as "pile set-up" and is often observed for driven piles in saturated NC to moderately OC clay and fine-grained material. A decrease in strength with time is referred to as "relaxation" and is often observed for heavily OC clays, dense silts, dense fine sands, and weak laminated rock. Shear strengths should therefore be evaluated for both long and short term conditions. • Changes in site conditions that affect the in-situ the effective stress state may increase or decrease shear strength and pile capacity. These may include site dewatering or additional surface loading from an embankment. • An increase in granular soil strength may occur due to densification during driving. This increased strength will need to be considered such that an appropriate pile driving system can be selected for construction.
Retaining Walls	• The analysis of non-gravity cantilevered and anchored walls require an evaluation of earth pressures on the active side and passive side of the excavation. For undrained loadings in some clayey soils, particularly low to medium plasticity materials, there can be a large difference in undrained strength between the strength used for the active side and the passive side of the excavation. • For soils that may exhibit peak, fully softened, and residual conditions, an estimate of the tolerable deflection of the wall system needs to be made and this deflection used to select the appropriate strength condition for analysis.
Slopes	• The shear strength of discontinuities (e.g., fissures) in soil (and rock) needs to be evaluated since it may represent the critical (i.e., lowest) shear strength for design. • Weathering and other physiochemical reactions may occur at a quick enough rate to weaken soil bonds and reduce shear strength. • Strength loss may occur in cut slopes due to soil softening (in presence of water) and continuing deformations. Large deformation residual strengths should be used for long-term analyses.

5.6.4 Laboratory Testing Methods for Evaluating Soil Shear Strength

5.6.4.1 Selection of Laboratory Testing Method

The laboratory shear strength testing method and testing parameters used should model the actual field problem being considered and provide a reliable assessment of shear strength. As previously noted, laboratory strength testing of natural granular soils is not typically performed due to sampling difficulties, however, the shear strength of compacted granular materials such as that used for

backfill in retaining structures and embankment fill is typically evaluated using the direct shear device.

The well known unconfined compression (UC) and unconsolidated undrained (UU) tests are often used to evaluate s_u in cohesive materials. Although simple to perform, the UC and UU tests are particularly misleading because of difficulties caused by sampling disturbance, high strain rate, and uncertain drainage effects, and therefore they are not recommended as the sole method to evaluate undrained shear strength for design analyses, but can be used to complement other strength data. Hand torvane and pocket penetrometer tests should not be considered at all for the evaluation of undrained strength for design analyses. These tests provide an index of soil consistency as an aid in selecting the type of testing device for measuring undrained strength and should not be relied upon for engineering analyses.

Ideally, laboratory specimens for shear strength testing should be reconsolidated in the laboratory such that at least the original effective stress states (σ_{vo}' and σ_{ho}') in the ground are applied to the specimen to simulate in-situ conditions. In research laboratories, it is possible to consolidate the specimens under K_0 conditions using automated triaxial devices. In most commercial laboratory triaxial systems, an isotropic stress state ($\sigma_c' = \sigma_{vo}'$) is imposed because of simplicity in procedure. These isotropic triaxial tests are suitable in providing an appropriate effective stress friction angle (ϕ') for most soil types, however, the undrained shear strengths from isotropically consolidated triaxial tests will likely be higher than those that should be used for design analyses of embankments, foundations, and retaining walls (e.g., Mayne, 1988). Procedures are available, however, to adjust the measured undrained strength in a triaxial compression test to values specifically applicable to particular field loading conditions. These procedures are discussed in this chapter.

In this section, the interpretation of soil shear strength using triaxial, direct shear, and unconfined compression direct simple shear testing methods are presented.

5.6.4.2 Triaxial Testing

On transportation-related projects, triaxial shear strength testing is performed on undisturbed samples of cohesive soils. Triaxial testing can be generally classified as: (1) unconsolidated-undrained (UU); (2) consolidated-undrained (CU); and (3) consolidated-drained (CD).

Unconsolidated Undrained Triaxial Test

In the UU test, the total stress undrained shear strength of the soil is calculated based on the measured compressive strength of the soil. Shear strengths calculated from UU tests correspond to the depth at which the sample was taken from in the ground. Figure 77 shows the stress-strain and Mohr circle representation for four UU tests performed on the same soil. Theoretically, if each sample is 100 percent saturated and at the same moisture content, the shear strength (which is the radius of the Mohr circle) will be the same. This is because shear strength is directly related to the void ratio of the sample. If the void ratio of each sample is the same, then since volume change is not allowed during shearing, the measured shear strength from each UU test will be the same. In most cases, however, due to sampling difficulties and inevitable differences in moisture content, samples taken from approximately the same depth will not exhibit this response.

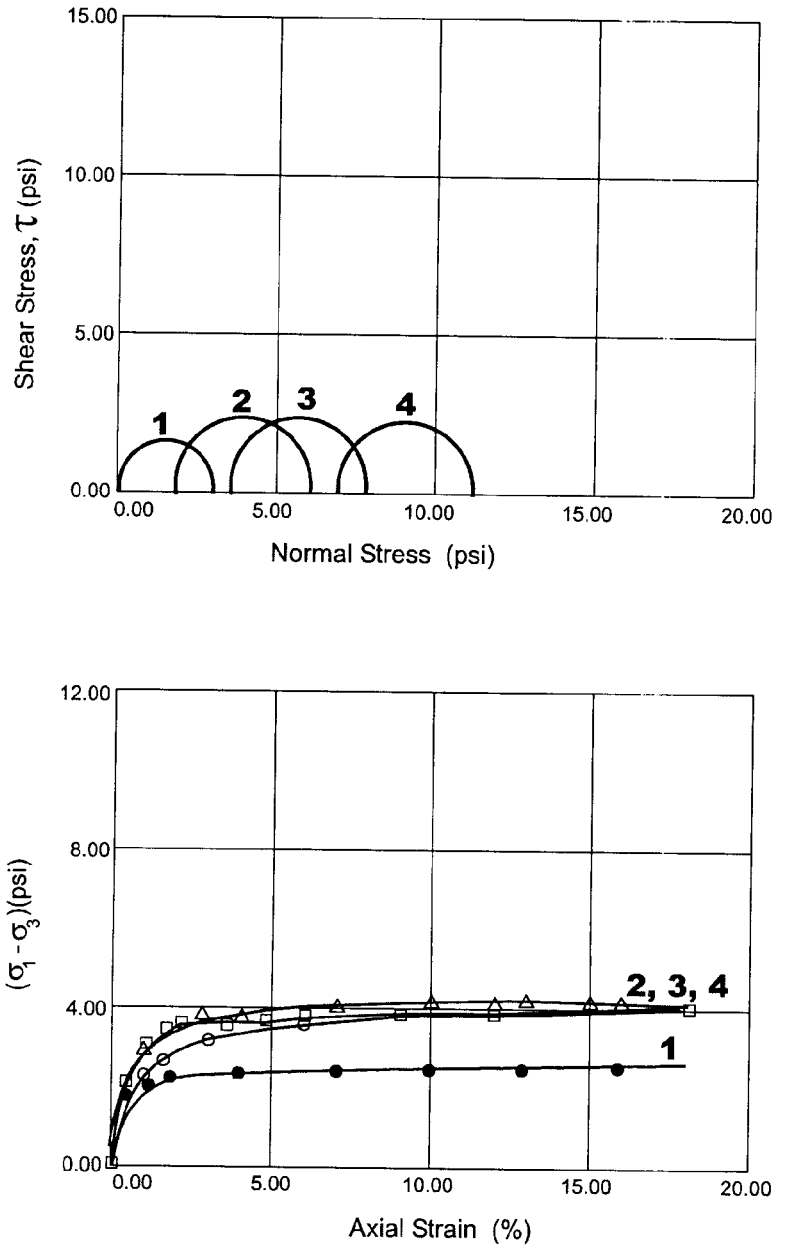

Figure 77. Stress-strain and Mohr circle representation for four UU tests performed on the same soil (after Day, 1999).

UU test results should be interpreted using the ϕ=0 concept. As an example, consider figure 78 in which the measured shear strength was not the same for each specimen. This may be due to sample disturbance or other factors. However, some commercial laboratories will report a best-fit envelope through triaxial data, including UU data, such as that shown in figure 78. **Such an interpretation is incorrect**; for *each* test, the undrained strength (i.e., radius of each individual Mohr circle) should be evaluated.

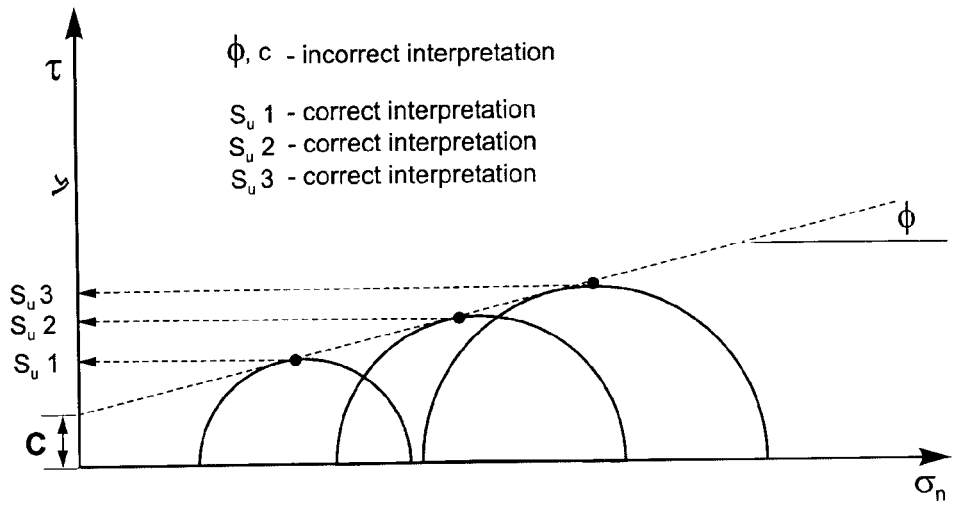

Figure 78. Interpretation of UU test data.

For soils that are partially saturated, such as compacted clays or naturally occurring clays above the water table, undrained strengths should be measured from UU tests performed on specimens with the same void ratio and degree of saturation as the soil in the field. Such soils will not exhibit a constant value for s_u. It is therefore important that tests be performed over a range of confining pressures that represent the range of stresses to be expected in the field. For each test, plot the confining pressure and corresponding undrained shear strength. This exercise will likely result in a nonlinear envelope of shear strength. Many slope stability programs enable the user to input an envelope of shear strength as a series of points (i.e., normal stress and shear stress).

There are significant problems associated with interpreting undrained shear strengths via UU tests for soils that are saturated. First, inevitable sample disturbance will result in measured shear strengths less than the actual strengths. Second, since the shearing portion of the test occurs so rapidly, it is likely that the measured strengths will be higher than a strength corresponding to typical rates of shear. Third, when the sample is removed from the tube, the total stress on the sample is zero, implying that residual negative pore pressures are in the sample. These pore pressures will obviously affect the effective stress condition in the sample and will therefore influence the measured strength. Although these factors may result in "compensating errors", it is not advisable to rely on undrained shear strengths obtained from UU data alone as the sole source of undrained strength information for design analyses. Data from UU tests should be used to complement data from consolidated undrained triaxial tests and from interpreted undrained strengths from in-situ testing, as discussed subsequently.

Consolidated Undrained Triaxial Test

The CU triaxial test provides data that can be used to interpret total stress strength parameters. Consolidated undrained triaxial testing with pore pressure measurements provides data for both total and effective stress strength interpretation. Unlike the UU test, the sample in a CU test is reconsolidated in the laboratory to a predetermined consolidation pressure.

Results of triaxial tests can be plotted either as Mohr circles or as stress path plots. Stress path plots, also referred to as p'-q or p-q plots, depict a series of points that represent the maximum shear stress on the Mohr Circles (i.e., τ corresponding to the top of the Mohr circle at a normal stress of $\sigma_n = \frac{1}{2}(\sigma_1 + \sigma_3)$. The coordinates for each point are $p = \frac{1}{2}(\sigma_1 + \sigma_3)$ and $q = \frac{1}{2}(\sigma_1 - \sigma_3)$. A line drawn through these points represents the total stress path for the triaxial test. If effective stresses are used, then $p' = \frac{1}{2}(\sigma_1' + \sigma_3') = p - \Delta u$. The parameter q is the same since $(\sigma_1' - \sigma_3') = (\sigma_1 - \Delta u - (\sigma_3 - \Delta u)) = \sigma_1 - \sigma_3$. A graphical example of the effective stress path for three specimens consolidated to different consolidation stresses and sheared in undrained triaxial compression (see figure 79 for stress-strain and pore pressure-strain curves for the three specimens) is shown in figure 80. As with a Mohr circle evaluation of the strength parameters, a best-fit line may be drawn through the data and the test result parameters α' and a' can be calculated. To evaluate the Mohr-Coulomb effective stress strength parameters from an effective stress path plot the following equations are used:

$$\sin\phi' = \tan\alpha'$$
$$c' = \mathbf{a}'/\cos\phi' \qquad \text{(Equation 60)}$$

As noted above, both total stress and effective stress parameters can be obtained from CU tests with pore pressure measurements. Effective stress parameters may be used for the evaluation of long-term conditions for cohesive soils since ϕ' and c' can be directly calculated. It is noted, however, that an effective stress analysis also requires knowledge of the in-situ pore pressures. For many design applications, it is very difficult to estimate these pore pressures with reasonable certainty. Analyses for short-term conditions in cohesive soils are performed using total stress parameters. The recommended approach for evaluating undrained shear strengths from CU tests for saturated soils for use in short-term total stress analyses includes developing a relationship between undrained shear strength s_u (which assumes $\phi = 0$) and vertical effective stress.

As discussed in chapter 4 and as illustrated on figure 23, for soils that are normally to lightly overconsolidated (i.e., OCR < 1.5), a CU test performed on a disturbed laboratory specimen that is reconsolidated back to the in-situ effective stress will likely overestimate the undrained strength since the specimen will be more dense (i.e., be at a lower void ratio) at a particular effective stress in the laboratory as compared to that at the same effective stress in the ground at the depth of the sample. Because of this, CU tests should be performed at consolidation pressures greater than the effective stress in the ground to compensate for the effects of disturbance. Because consolidation to higher pressures will result in higher undrained strengths, the undrained strength measured using a CU test at consolidation pressures greater than those corresponding to the depth at which the sample was taken is not a correct measure of the undrained strength for the depth in the ground where the sample for the CU test was taken. Using this information, however, a relationship between undrained strength and consolidation pressure can be developed. Typically, the undrained strength ratio, defined as s_u/σ_{vo}', is calculated and used for this relationship. For a slope stability analysis, for example, the program will calculate the effective vertical stress for each slice and then based on the relationship between undrained strength and effective vertical stress, the appropriate undrained strength will be assigned. Alternatively, a constant value of s_u can be assigned to each soil layer in the stability analysis.

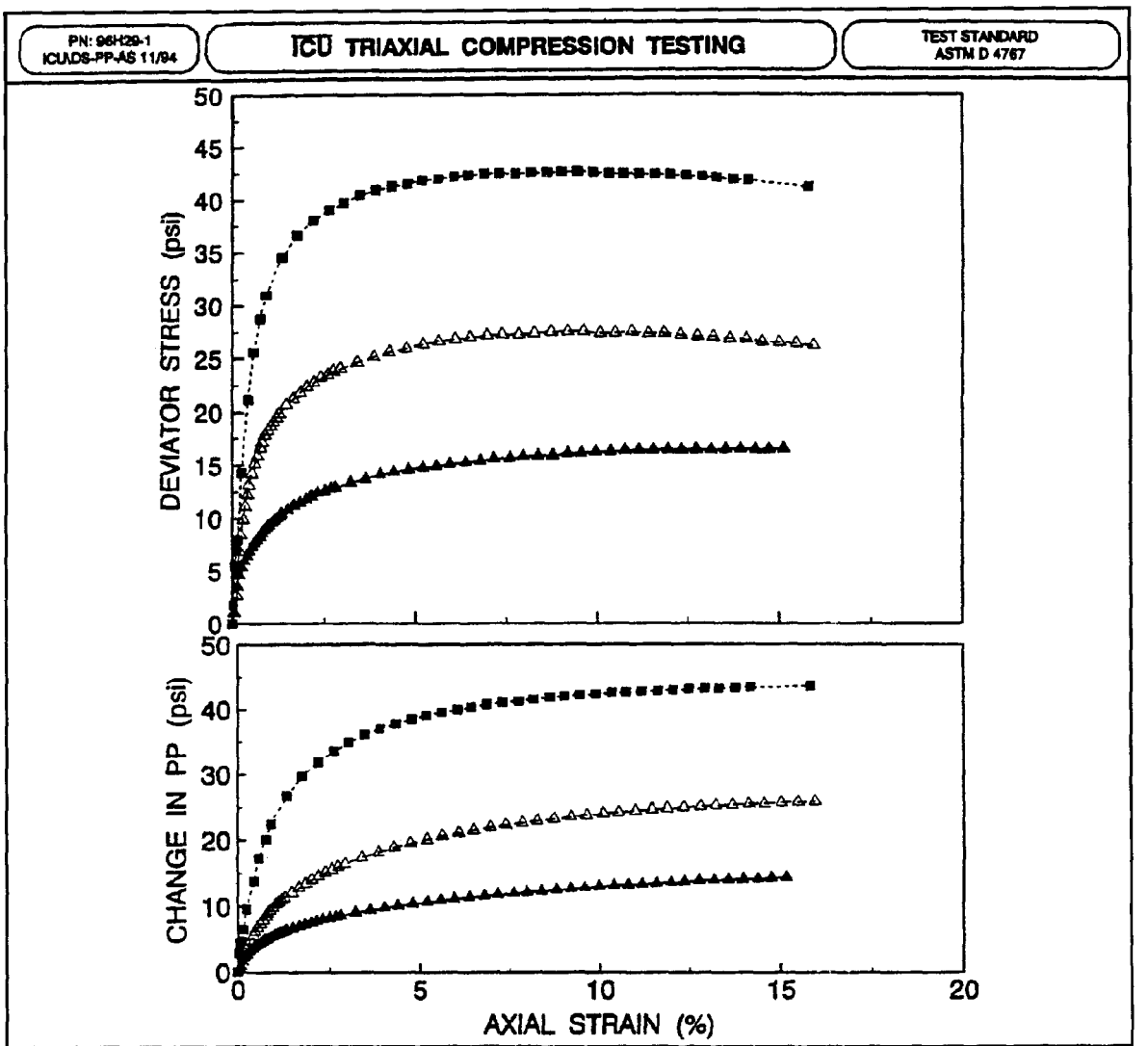

SYMBOLS	SITE SAMPLE ID	LAB SAMPLE NO.	W_i (%)	γ_i (pcf)	σ'_c (psi)	REMARKS
▲ ——	TB-15 (18.0' TO 20.0')	96G129.2	113.0	38.9	18.5	
△ - - - -		96G129.3	119.8	36.2	36.3	
■ -------		96G129.4	71.1	57.2	56.5	
□ ——						
● ——						
○						

NOTES: W_i - Initial Moisture Content, %
γ_i - Initial Dry Unit Weight, pcf
σ'_c - Consolidation Pressure, psi
PP - Pore Water Pressure, psi

Figure 79. CIU triaxial compression test results.

PN: 96H129-2
ICU\O-P 11/94

ICU TRIAXIAL COMPRESSION TESTING

TEST STANDARD
ASTM D 4767

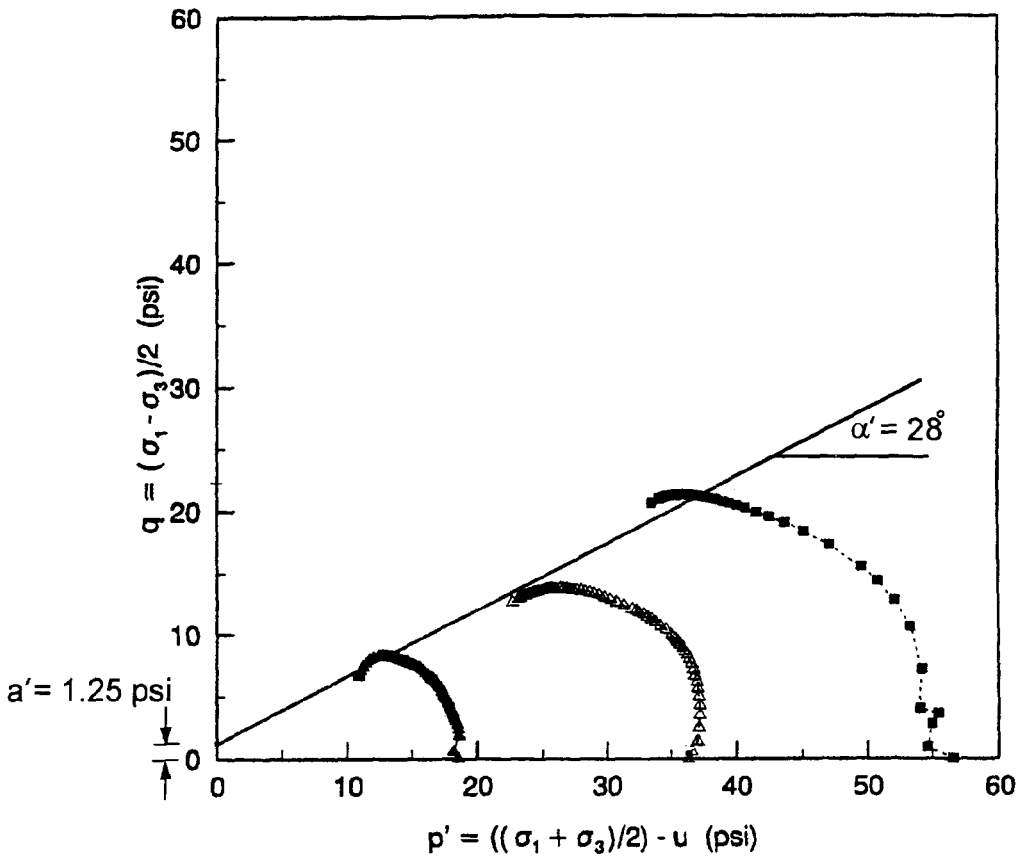

SYMBOLS	SITE SAMPLE ID	LAB SAMPLE NO.	W_i (%)	γ_i (pcf)	σ'_c (psi)	REMARKS
▲ ———	TB-15 (18.0' TO 20.0')	96G129.2	113.0	36.9	18.5	
△ – – – –		96G129.3	119.8	36.2	36.3	
■ ·····		96G129.4	71.1	57.2	56.5	
□ ———						
● ———						
○ ·····						

NOTES: W_i - Initial Moisture Content, %
γ_i - Initial Dry Unit Weight, pcf
σ'_c - Consolidation Pressure, psi

Figure 80. Effective stress path in undrained shear.

An important issue relative to the interpretation of CU tests for total stress undrained analyses, is that a total stress friction angle and cohesion intercept, i.e., ϕ_T and c_T that may be calculated from a Mohr circle representation of the total stresses at failure from CU tests, should not be used for analyses that assume undrained conditions. Undrained analyses are based on no consolidation of cohesive deposits under the application of, for example, an embankment loading. As an example, the incorrect effect of using ϕ_T and c_T evaluated based on CU test results as input data for a staged-loading stability analysis would be that as soon as fill is placed, the foundation soils would "experience" an increase in shear strength corresponding to the equation:

$$\tau = \sigma_n \tan\phi_T + c_T \qquad \text{(Equation 61)}$$

Since the normal stress, σ_n, will increase due to the placement of fill, the shear strength of the soil will increase instantaneously according to equation 61. This is incorrect. To correctly model the effect of placing fill, but not realizing an immediate increase in shear strength, requires that the shear strength be written according to the ϕ=0 concept, such that:

$$\tau = \sigma_n \tan(0) + s_u = s_u \qquad \text{(Equation 62)}$$

In this case, the undrained strength of the foundation soils will not increase as a result of the placement of the fill but will instead be correctly based on the undrained strength corresponding to the state of stress in the soil before the load was placed. For a staged construction analysis, this would include the increased effective stresses in the ground resulting from the previously placed fill which has been allowed time to consolidate and gain strength.

5.6.4.3 Direct Shear Testing

Direct shear testing is commonly performed on compacted materials used for embankment fills and retaining structures. This testing can also be performed on natural materials; however, the lack of control on soil specimen drainage makes the evaluation of undrained strength unreliable. This test can be used to evaluate the drained strength of natural materials by shearing the sample at a slow enough rate to reasonably ensure that no porewater pressures develop.

During the direct shear test, the normal stress and shear stress are measured on a horizontal failure surface. In interpreting the shear strength of a soil from a direct shear test, it is assumed that the normal stress on the failure plane is equal to the confining pressure placed on the sample at the beginning of the test (corrected for changes in specimen area as the specimen is sheared) and that the shear stress on the failure plane is calculated as the applied shear force divided by the corrected area. For a given soil, usually three tests are performed, each at a different confining pressure, σ_n. The results are plotted as shown in figure 81.

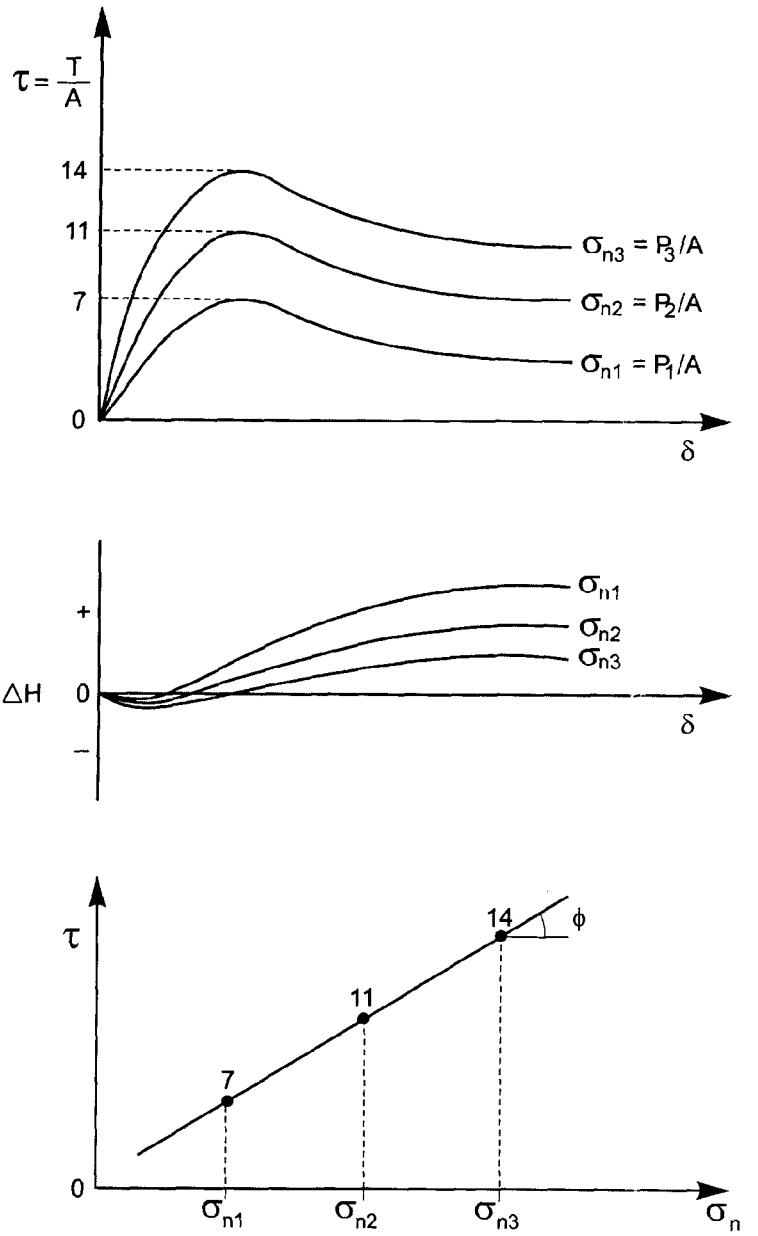

Figure 81. Direct shear test results.

As shown in figure 82, the contact area between the two specimen halves varies with the relative displacement, δ, between the upper and lower shear box. The corrected area A_c of the sheared specimen for a square box length, a is:

$$A_c = a(a-\delta) \qquad \text{(Equation 63)}$$

and for the cylindrical box of internal diameter D:

$$A_c = \frac{D^2}{2}\left(\theta - \frac{\delta}{D}\sin\theta\right) \qquad \text{(Equation 64)}$$

where $\theta = \cos^{-1}(\delta/D)$ (in radians). The area correction needs to be applied to both the normal stress and the shear stress. For a typical sample diameter of 6.3 cm, the error on shear and normal stresses may be 20% when δ =1 cm (Bardet, 1997), so it is important to make the appropriate correction, particularly if specific values of τ are used in analyses (e.g., when using the test results to obtain undrained shear strengths).

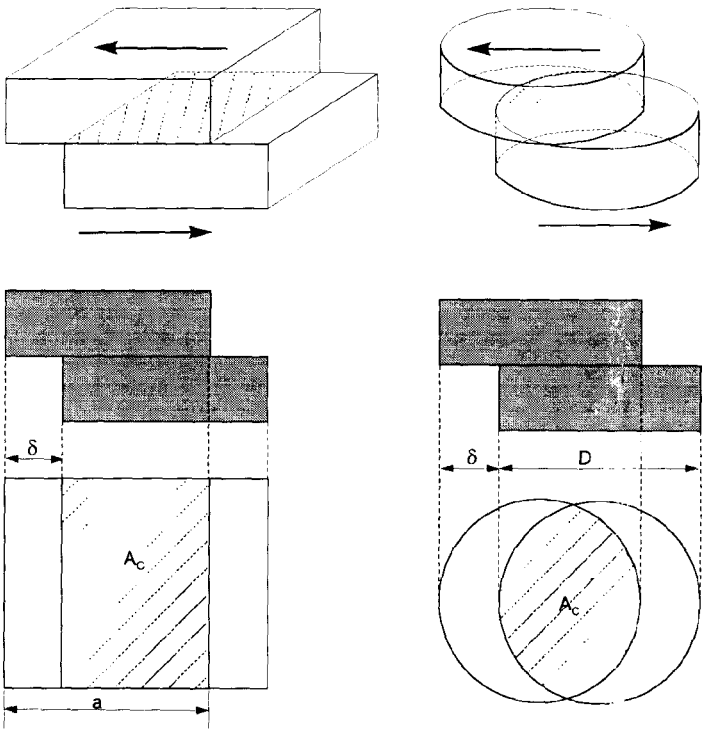

Figure 82. Area correction for direct shear test.

Direct shear testing performed on recompacted soils should be performed for a normal stress range consistent with the anticipated range of stresses for the field application. Tests should be performed at varying compaction and density conditions to be representative of the anticipated compaction conditions that can be achieved in the field. Consideration should be given to the potential for the soils to become saturated after construction and, if saturation is possible, tests should be performed on saturated (or submerged) samples. Tests should always be carried out until a stable large-displacement shear stress is measured.

The direct shear test is applicable to evaluating the shear strength of stiff, fissured materials or other materials that may contain pre-existing shear surfaces. In those cases, the specimen may be trimmed in such a manner so that the existing shear surface is oriented horizontally.

5.6.4.4 Unconfined Compression Testing

This test is typically performed on cohesive soils and provides a rapid means to obtain an approximate value of the undrained shear strength of cohesive soils. In this test, a cylindrical soil specimen is loaded axially in compression. This test cannot be performed on granular soils, or fissured or varved materials. This test represents a special case of the UU test wherein the total confining pressure is equal to zero. Since residual negative pore pressures reside within the specimen, however, the actual state of stress prior to shear is unknown.

Figure 83 shows a representative stress-strain curve and Mohr circle representation of the state of stress for a soil tested in unconfined compression. In a UC test, a peak in the stress-strain curve usually evidences failure, although a limiting strain value (e.g., say 15%) may be used to define failure for soils that do not exhibit a discernable peak value. When the failure envelope is assumed to be purely cohesive (i.e., ϕ=0) as shown on figure 83, the Mohr circle is tangent to the horizontal line $\tau=s_u$.

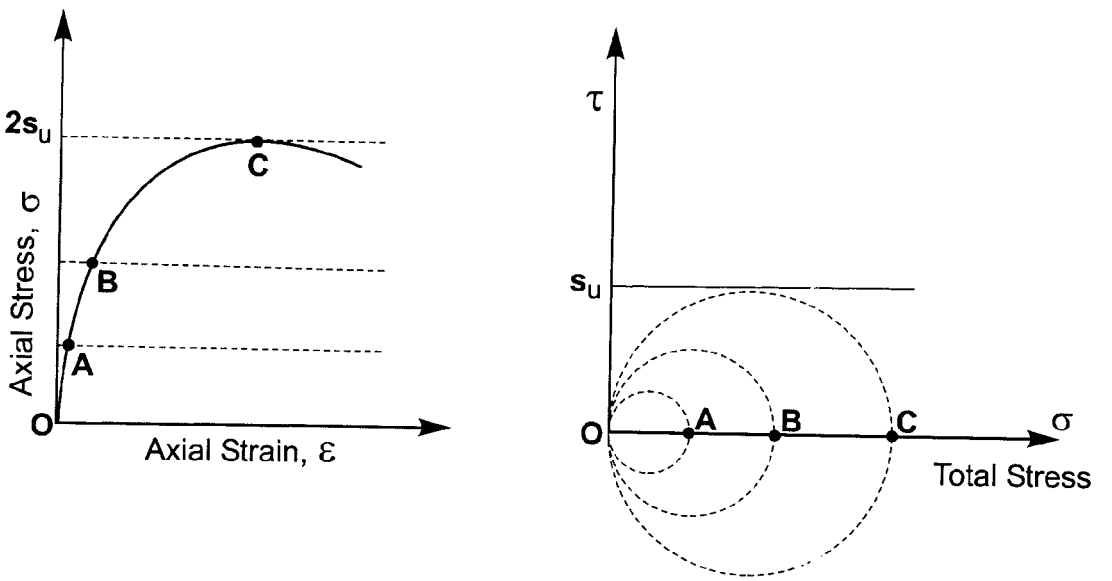

Figure 83. Typical stress-strain curve and Mohr circle representation of the state of stress for an unconfined compression test.

In most cases, the undrained strength measured in an unconfined compression test is less than that which would be measured in the field or for a triaxial compression test, even a laboratory UU triaxial test result. The unconfined compression test does not include a reconsolidation phase wherein the stresses in the ground are applied to the specimen. Also, sample disturbance can result in significant underestimation of actual strength. Because the undrained strength of a soil is affected by moisture content where, for example, a small change in moisture content may result in a significant change in undrained strength, it is necessary to take great care in preserving the in-situ (or field) moisture content of the soil specimen, particularly during sample preparation. If possible, all sample preparation work should be performed in a humidity controlled room.

5.6.4.5 Relevance of Laboratory Strength Tests to Field Conditions

As noted, the undrained strength to be used for design analyses depends on the direction of loading. For example, figure 84 shows an embankment with an assumed slip surface. This figure indicates that three different modes of soil shearing would be involved in evaluating the average shear strength along the failure surface. Therefore, accurate evaluation of undrained strength to be used in the stability analysis of an embankment constructed over soft to medium clays must somehow recognize the differences in measured undrained strengths for each of these shearing modes. Also, many field situations involve plane strain conditions such as that for a continuous footing, retaining wall, or long embankment; therefore the use of triaxial testing conditions may not be accurate. It is recognized, however, that to perform all laboratory tests that may be pertinent to a particular field loading condition may be impractical, especially for relatively small projects. Therefore, CU triaxial tests with pore pressure measurements are recommended as a standard reference test. Using the results of the CU test, the results of all other tests can be compared conveniently, even those tests following different stress paths to failure than the CU test. This is demonstrated in subsequent sections.

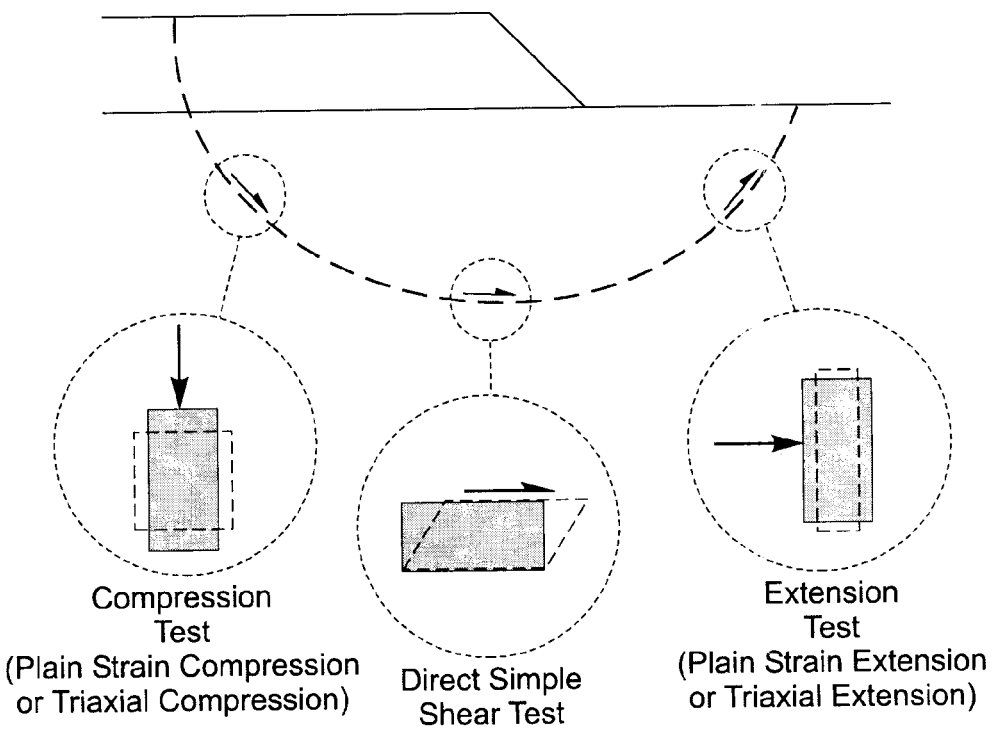

Figure 84. Shear modes for an embankment slip surface.

5.6.5 Undrained Shear Strength from In-situ Tests

The interpretation of undrained strength from in-situ tests involves a direct relationship to convert the in-situ test measurement (e.g., K_D from DMT, q_t from CPT) to s_u, based on empirical, analytical, or numerical methods. The common approaches for the vane, cone, piezocone, pressuremeter, dilatometer, plate, and SPT are summarized in table 33. The correlations presented in this table can be used to provide preliminary estimates of s_u. The use of the correlations in table 33 is illustrated in Soil Property Selection Example No. 1 in appendix A.

Table 33. Conventional methods of interpretation for s_u from in-situ tests.

IN-SITU TEST	COMMENTS	REFERENCES
VST: $s_{uv} = 6T/(7\pi D^3)$ for H/D = 2	Static equilibrium analysis Empirical: $\mu \approx 2.5(PI)^{-0.3} \leq 1.1$	Chandler (1988, ASTM 1014)
PMT: $s_{upmt} = dp/d(\ln \varepsilon_v)$ $s_{upmt} = (p_L - p_o)/N_c$	Cavity expansion theory Empirical bearing factor $N_c = 5.5$	Windle & Wroth (1977, ICSMFE). Baguelin et al. (1972, JSFMD).
SPT: $s_{u(N60)} = f_1 N_{60} p_a/100$	Empirical: $f_1 = 4.5$ for PI = 50 Empirical: $f_1 = 5.5$ for PI = 15	Stroud (1974, ESOPT-1) Stroud (1989, PTUK)
CPT: $s_{ucpt} = (q_c - \sigma_{vo})/N_c$	Limit plasticity theory Cavity expansion theory	Meyerhof (1951, Geotechnique) Vesic (1977, NCHRP)
$s_{ucpt} = (q_t - \sigma_{vo})/N_{kt}$	Corrected cone tip resistance, q_t N_{kT} = 10 (TC) = 15 (DSS) = 20 (TE)	Aas, et al. (1986, ASCE GSP 6)
$CPTu_2$: $s_{ucptu2} = \Delta u/N_u$	$N_{u2} = 7.9$ (uncorrected vane) Charts: $N_u = f(I_r, A_f, u_1$ or $u_2)$ Cavity expansion + critical state	Tavenas, et al. (1982, ESOPT). Robertson and Campanella (1983) Mayne & Bachus (1989, ISOPT)
DMT: $s_{uDMT} = 0.22\,\sigma_{vo}'(\frac{1}{2}K_D)^{1.25}$ $s_{uDMT} = (p_o - u_o)/10$ $s_{uDMT} = d_s\sigma_{vo}'\,(0.5K_D)^{1.25}$	Based on mix of UU, UC, VST Cavity expansion theory Empirical and test-dependent: TC: $d_s = 0.20$ VST: $d_s = 0.19$ DSS: $d_s = 0.14$	Marchetti (1980, JGE). Schmertmann (1991) Lacasse & Lunne (1988, ISOPT)
PLT: $s_{uplt} = q_{ult}/6.18$	Limit plasticity theory	Meyerhof (1951, Geotechnique)

Symbols used in table 33

VST = vane shear test
PMT = pressuremeter test
SPT = standard penetration test
CPT = cone penetration test
$CPTu_2$ = piezocone test
DMT = flat dilatometer test
PLT = plate load test

The correlations shown in table 33 that convert a measured in-situ test parameter to an undrained strength are widely used in practice. The "conversion factors" used in these correlations (e.g., N_{KT} for CPT) must be calibrated to the results from high-quality laboratory tests for the specific soil deposit and to a particular mode of shearing. For example, some practicing engineers have adopted a value of 15 for N_{KT} for CPT, although the appropriate value for a particular deposit may be significantly higher or lower than 15. Also, many engineers use the vane shear test to evaluate s_u for soft clays that cannot be easily sampled for laboratory tests. Engineers use the vane shear correction factor μ to account for shear rate and strength anisotropy effects. This μ factor is a function of PI and can be written as:

$$\mu \approx 2.5\,(PI)^{-0.3} \leq 1.1 \qquad \text{(Equation 65)}$$

Although the vane shear test is widely accepted and used, the scatter of the data originally used to develop the μ factors (see figure 85) is significant. Additional limitations associated with the use of these correlations are provided below.

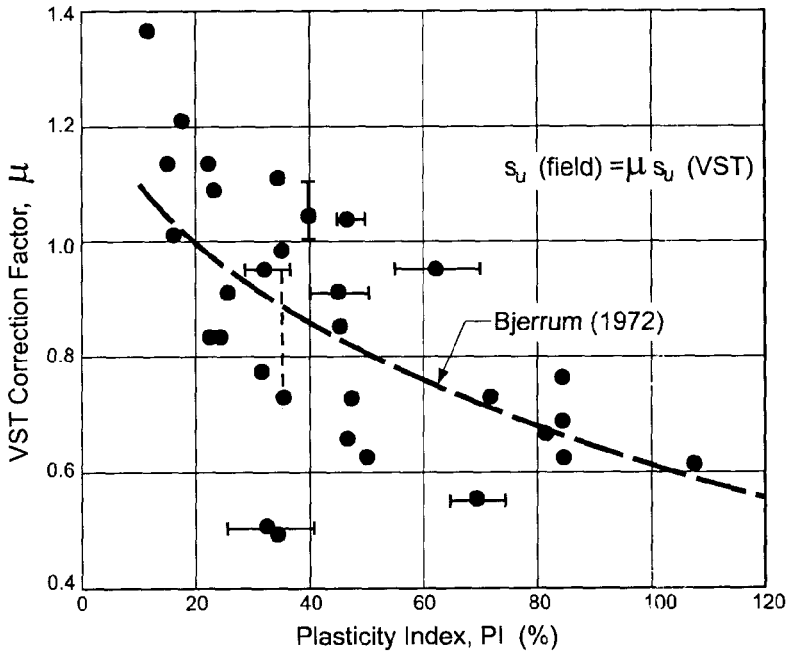

Figure 85. Plasticity based VST correction factors.

Several difficulties exist in using the approaches summarized in table 33 to convert in-situ tests directly to undrained strength. First, each in-situ testing device loads the soil in a different direction at a different rate, and therefore, the effects of boundary conditions, strength anisotropy, and strain rate influence the results. Second, each field test utilizes different models as the basis for interpretation (e.g., limit plasticity, limit equilibrium, cavity expansion, numerical method, or empirical correlation) such that large inconsistencies exist when the results are compared. Thirdly, each field test has been calibrated to its own particular laboratory reference test (e.g., vane shear test and consolidated anisotropically undrained compression (CAUC) triaxial test as is reported, Chandler, 1988), and consequently, a wide number of interrelationships would be required to convert results from one test to another test. Given this, it is clear that measured undrained strengths from different in-situ tests and laboratory tests are expected to be quite different, resulting in difficulties in selecting appropriate undrained strengths for design applications. See the example profile of s_u with depth for a soft clay/silt site in figure 86 as an illustration.

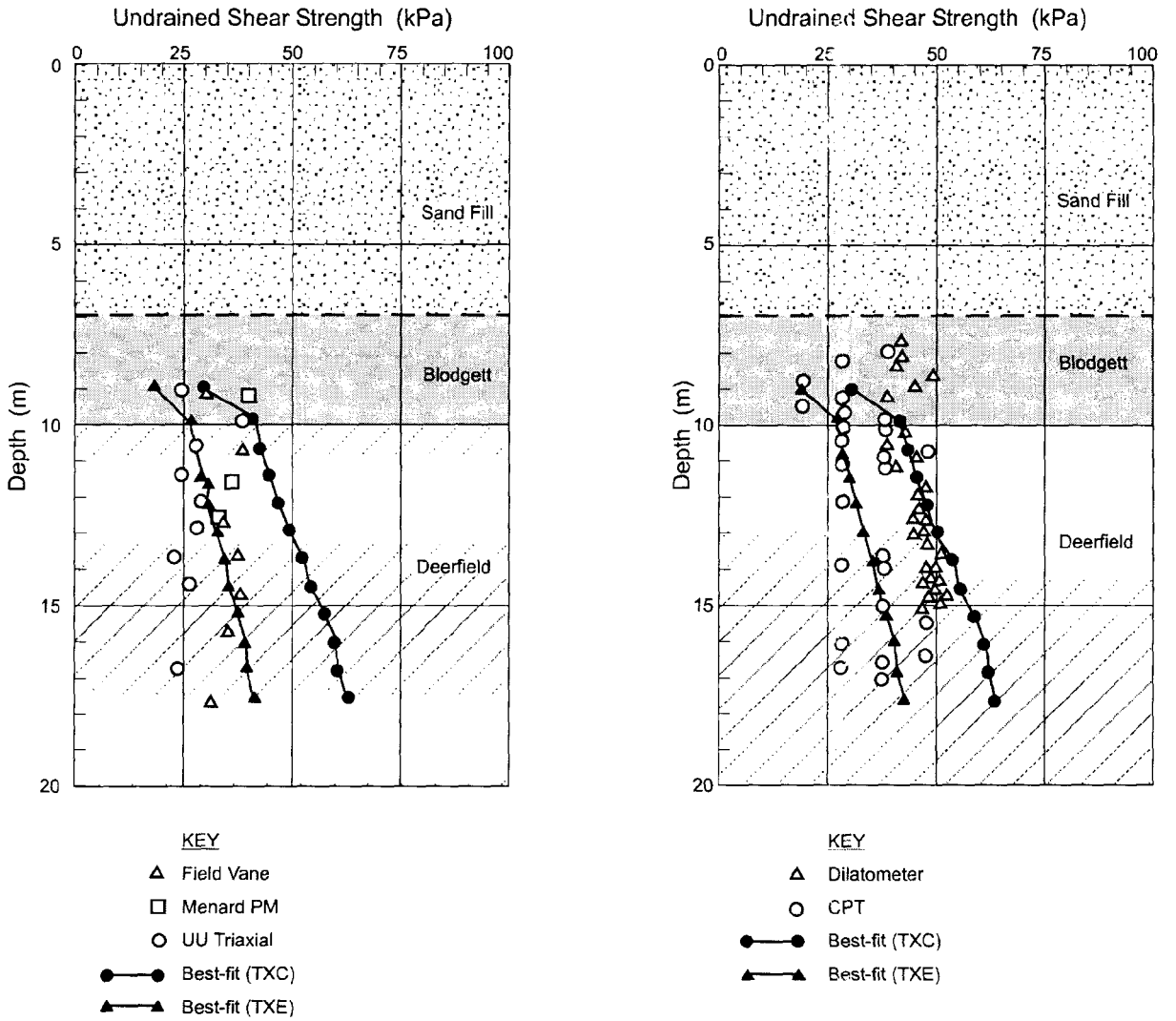

Figure 86. Example s_u profile (after Finno and Chung, 1992) (Note: for clarity, the comparison of testing results has been shown on two separate figures).

To use in-situ tests to evaluate s_u, it is recommended that the in-situ results be referenced to the preconsolidation stress (σ_p'). This is advantageous since each of the laboratory test modes (e.g., isotropically consolidated undrained compression (CIUC), plane strain compression (PSC), and other modes corresponding to isotropic and anisotropic consolidation, compression, extension, or simple shear loading, and triaxial or plane strain conditions) all provide a different measured s_u value for a given soil, whereas the preconsolidation stress (σ_p') is uniquely defined from one-dimensional consolidation. In using in-situ tests, the equations developed in section 5.4.3 that relate σ_p' to measured in-situ test parameters can be used with the results of one-dimensional laboratory consolidation tests to develop a profile of σ_p' with depth. The recommended relationship between s_u and σ_p' is described below.

Undrained shear strength can be expressed in a form that relates to the stress history (i.e., OCR) of the deposit:

$$s_u/\sigma_{vo}' = S\ OCR^m \qquad \text{(Equation 66)}$$

where S = normally-consolidated undrained strength ratio (also given in symbol form as $[(s_u/\sigma_{vo}')_{NC}]$ and m = exponent. Experimental studies have shown the parameters S and m to vary with test mode (Jamiolkowski, et al. 1985; Koutsoftas and Ladd, 1985; Kulhawy and Mayne, 1990). Values for S typically range from 0.15 to 0.30 and m is typically 0.8. Theoretical relationships based on critical-state soil mechanics (Wroth, 1984) have shown that S depends on test mode and increases with ϕ' of the clay, while the exponent parameter relates to the compression indices by:

$$m \approx 1 - C_s/C_c. \qquad \text{(Equation 67)}$$

As previously discussed, the laboratory-shearing mode that best approximates the range of conditions encountered for typical design analyses is the direct simple shear mode. The undrained shear strength from this test, i.e., s_{uDSS}, represents an overall "average" strength that is intermediate between triaxial compression and triaxial extension, as well as between plane strain compression and extension. The s_{uDSS} has been shown suitable for direct use in analyses of slopes, foundation bearing capacity, and embankment stability (e.g. Larsson, 1980; Ladd, 1991). In this regard, for overconsolidated intact clays, the recommended relationship is:

$$(s_u/\sigma_{vo}')_{DSS} = 0.23\ OCR^{0.80} \qquad \text{(Equation 68)}$$

The value of 0.23 for $(s_u/\sigma_{vo}')_{NC}$ was developed from a large database of DSS testing results. For soils with preferential shear planes that are near horizontal (e.g., varved clays), the value for $(s_u/\sigma_{vo}')_{NC}$ may be as low as 0.16. Work performed by Mayne (1988), however suggests that the value of $(s_u/\sigma_{vo}')_{NC}$ is influenced by the drained friction angle of the soil and can be written in general as:

$$\left(s_u/\sigma_{vo}'\right)_{NC} = \frac{\sin\phi'}{2} \qquad \text{(Equation 69)}$$

Therefore, equation 68 can be written as:

$$\left(s_u/\sigma_{vo}'\right)_{DSS} = \frac{\sin\phi'}{2} OCR^{0.80} \qquad \text{(Equation 70)}$$

For very soft clays where the degree of overconsolidation is small (OCR < 2), the expression can be approximated by:

$$s_{uDSS} \approx 0.21\ \sigma_p' \qquad \text{(Equation 71)}$$

The use of these equations coupled with the interpreted profile of preconsolidation stress, σ_p', can be easily implemented into a spreadsheet and used to generate profiles of undrained shear strength with depth for cohesive soil deposits based on in-situ and laboratory oedometer results. Profiles of undrained strength developed from these equations can also be used to judge potential outlier data from laboratory and in-situ tests. The information presented in this section can be used to develop

undrained strength profiles for use in design analyses. Section 5.6.7 provides a detailed discussion on the development of undrained strength profiles.

5.6.6 Drained Friction Angle of Granular Soils from In-situ Tests

It is common practice to evaluate the effective stress or drained friction angle of granular materials from in-situ penetration tests via a correlation to a measured test parameter. In this section, correlations are presented for the SPT, CPT, and DMT. These correlations can be easily implemented into a spreadsheet to evaluate friction angle as a function of depth within granular deposits.

Friction Angle Based on SPT

Table 34 presents baseline relationships for evaluating the drained friction angle of cohesionless soils. This table is based on data for relatively clean sands. Given this, selected values of ϕ' based on SPT N values should be reduced by 5° for clayey sands and the value from the table should be increased by 5° for gravelly sands.

Table 34. Relationship among relative density, SPT N value, and internal friction angle of cohesionless soils (after Meyerhof, 1956).

State of Packing	Relative Density (%)	Standard Penetration Resistance, N (blows/300 mm)	Friction angle, ϕ' (°)
Very loose	<20	<4	< 30
Loose	20-40	4-10	30-35
Compact	40-60	10-30	35-40
Dense	60-80	30-50	40-45
Very dense	>80	>50	>45

Note: N = 15 + (N' - 15) / 2 for N' > 15 in saturated very fine or silty sand, where N' = measured blow count and N = blow count corrected for dynamic pore pressure effects during the SPT.

Equation 72 is a derived correlation between ϕ' and normalized SPT resistance ($(N_1)_{60}$), where high-quality undisturbed frozen samples of natural sands were obtained that permitted direct measurements of ϕ' in triaxial cells (Hatanaka and Uchida, 1996). The data were obtained using an automatic trip hammer system where energy efficiency was reported as 78 percent. For an average state-of-practice with 60% efficiency in the U.S., the expression for peak ϕ' is given as:

$$\phi' = \sqrt{15.4(N_1)_{60}} + 20° \qquad \text{(Equation 72)}$$

The well-known correlation between N_{60} and ϕ' developed by Schmertmann (1975) is shown in figure 87. Results from this correlation tend to be somewhat conservative, especially for shallow depths (i.e., less than 2 m). The correlation shown in figure 87 can be approximated as:

$$\phi' \approx \tan^{-1}\left[N_{60} / \left(12.2 + 20.3\sigma'_{vo} / P_a\right)\right]^{0.34} \qquad \text{(Equation 73)}$$

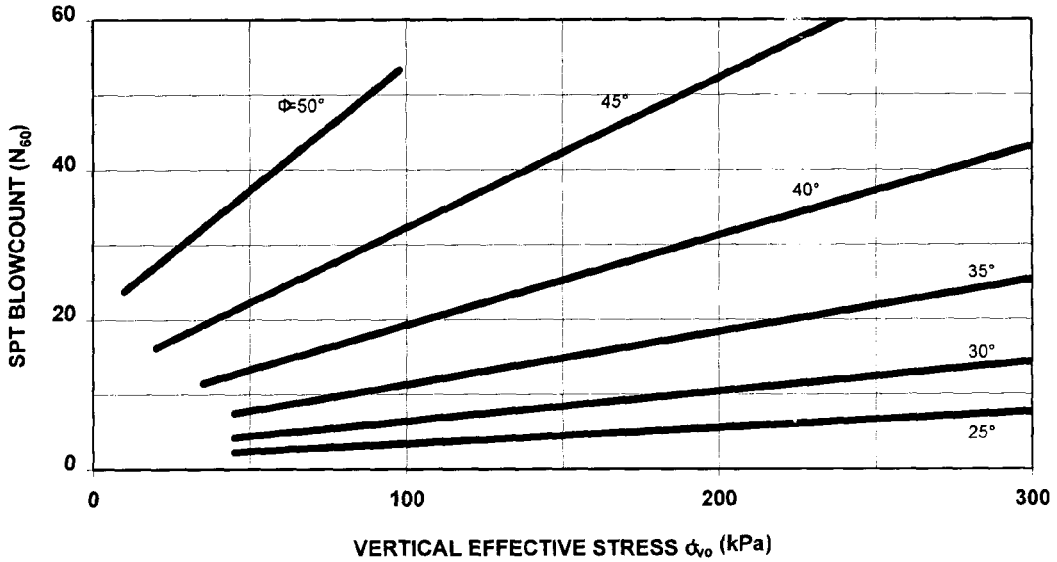

Figure 87. Correlation of ϕ' with SPT N_{60} in clean sands.

It is important to recognize that these correlations have been developed for relatively clean sands. Use of these correlations in, for example, micaceous sands is not recommended. The presence of mica in sand will tend to reduce the SPT blowcount significantly below that which would be measured for the same sand without mica. However, the actual friction angle of the clean sand and the micaceous sand may not be significantly different when measured in laboratory triaxial tests. Laboratory triaxial tests should be performed on silty sand soils where more exact values of ϕ' are required.

The SPT (and hence the correlations noted above) should not be used to estimate the drained friction angle of mostly gravel soil, unless the correlations are used conservatively or can be modified based on local experience. The size of gravel particles is often larger than the inner diameter of the split sampler used in the SPT test, thus it is likely that the SPT will overestimate the penetration resistance of a gravelly soil. In most cases, however, shear strengths of gravelly soils are sufficiently high for most engineering applications. Issues related to gravelly soils relate mostly to constraints associated with installation of driven piles and/or drilled shafts. However, in some highly seismic regions, it may be necessary to assess the liquefaction resistance of gravelly soils. In those cases, large penetration tests (LPT) and Becker penetration tests (BPT) may need to be performed.

Friction Angle Based on CPT

Bearing capacity theory is used to correlate ϕ' in sands to the measured point resistance in cone penetration testing. Robertson and Campanella (1983) developed the relationship between peak ϕ' and normalized cone tip resistance shown in figure 88. This may be approximated by:

$$\phi_{tc}' = \arctan[0.1 + 0.38\log(q_t / \sigma_{vo}')] \qquad \text{(Equation 74)}$$

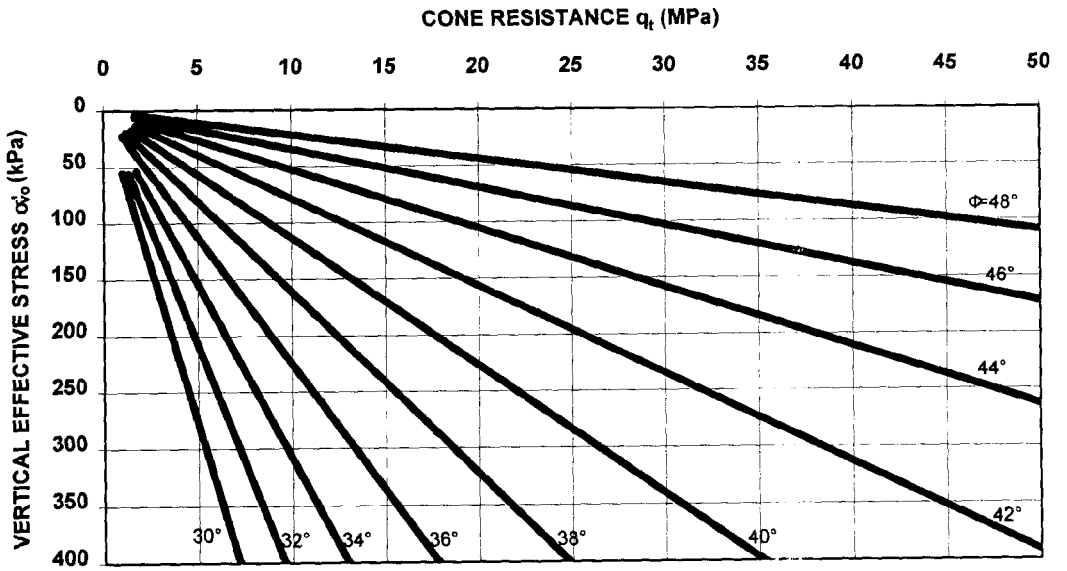

Figure 88. Correlation of ϕ' with normalized CPTq_t data in clean sands.

Friction Angle Based on DMT

Campanella and Robertson (1991) developed an equation relating the dilatometer horizontal stress index, K_D, to soil friction angle. This correlation is theoretically based as it considers the geometry of the dilatometer and an assumed soil failure surface around the dilatometer. Marchetti (1997) developed a lower bound envelope for ϕ' given by:

$$\phi' \approx 28° + 14.6 \log K_D - 2.1 \log^2 K_D \qquad \text{(Equation 75)}$$

This correlation is plotted in figure 89.

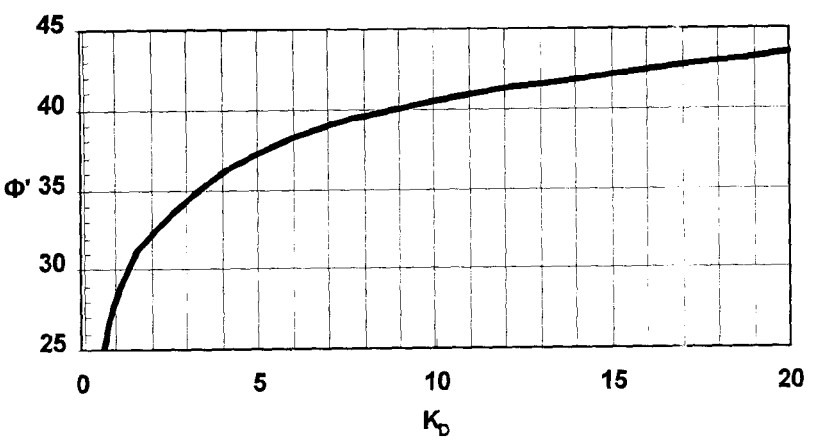

Figure 89. Correlation of ϕ' with the DMT K_D parameter for clean sands.

5.6.7 Selection of Total Stress Parameters (s_u) for Undrained Strength Design Analyses

For design analyses of short-term conditions in normally to lightly overconsolidated cohesive soils, the undrained shear strength, s_u, is commonly evaluated. A profile of s_u with depth should be developed at several locations across the site. Since undrained strength is not a unique property, profiles of undrained strength developed using different testing methods will be different. Typical practice on transportation projects is to develop profiles of s_u based on laboratory CU and UU testing and, for cases where undisturbed sampling is very difficult, field vane testing. Other in-situ methods have been presented which can also be used to develop a profile of s_u with depth. In this section, guidance on the development of undrained strength profiles is provided. A specific example of undrained strength profile development is provided in Soil Property Selection Example No. 1.

Specific issues that should be considered when developing a profile of undrained shear strength with depth are described below.

- Strength measurements from hand torvanes, pocket penetrometers, or unconfined compression tests should not be used solely to evaluate undrained shear strength for design analyses. Consolidated undrained triaxial tests with pore pressure measurements and in-situ tests should be used.

- All available undrained strength data should be plotted with depth. The type of test used to evaluate each undrained strength should be clearly identified. Known soil layering should be used so that trends in undrained strength data can be developed for each soil layer.

- Review data summaries for each laboratory strength test method. Moisture contents of specimens for strength testing should be compared to moisture contents of other samples at similar depths. Significant changes in moisture content will affect measured undrained strengths. Review Atterberg limits, grain size, and unit weight measurements to confirm soil layering.

- CU tests on normally to lightly overconsolidated samples that exhibit disturbance should contain at least one specimen consolidated to approximately at least 4 times σ_p' to permit extrapolation of the undrained shear strength at σ_p'.

- Undrained strengths from CU tests correspond to the effective consolidation pressure used in the test. This effective stress needs to be converted to the equivalent depth in the ground.

- A profile of σ_p' (or OCR) should be developed and used in evaluating undrained shear strength.

- Correlations for s_u based on in-situ test measurements (i.e., those based on table 33) should not be used for final design unless they have been calibrated to the specific soil profile under consideration.

A plot of an undrained strength profile should be developed with undrained strength on the x-axis and depth on the y-axis. Laboratory test data including CU and UU testing should be plotted at the correct depths. Typically, CU strengths will be greater than UU strengths, and this should be used to

judge the quality of the data. In-situ test data, which has been correlated to undrained strength, should be plotted at the depth where the measurement was taken. For strengths developed based on CPT, CPTu, and DMT, for which numerous measurements may have been taken, the data should be plotted as points without connecting the data with lines. This will facilitate visual identification of upper and lower bounds and anomalous data.

For intact clays (i.e., not fissured), the relationships developed for undrained strength (i.e., equation 70 should be plotted on the profile as well. The average effective stress friction angle from CU tests and the profile of preconsolidation stress is used to calculate the undrained strength using these relationships. This relationship has been developed from a database that includes over 100 clays and it can therefore be used as a means to evaluate potential data outliers. For example, strengths measured in CU tests should be higher than that for DSS. Therefore, the quality of the CU data can be judged by reviewing the overall trend in the CU data relative to the relationships based on the DSS, i.e., on average, the CU strengths should be higher. Also, a lower bound line can be drawn to represent the undrained shear strength assuming that the entire soil layer is normally consolidated (i.e., OCR = 1). This would be a line defined by $s_u=(0.5 \sin \phi') \sigma_{vo}'$. Data that fall below this line are likely to be anomalous and should not be included in the interpretation.

With all the data plotted, envelopes of undrained strength for design analyses should be developed. Also, the best-fit profile line should be developed using data corresponding to the likely range of stresses in the field. Undrained strength data corresponding to vertical effective stresses outside the range for the field application can be used for confirmation of the profile selected, but should not have equal weighting as for data points within the range of anticipated field stresses. It is noted that reported variations in undrained strength have been up to 40 percent (Duncan, 2000) meaning that typical standard variation in undrained strength may be equal to 40 percent of the average value. These variations are based on measurements of undrained strength using various testing methods for the same soil. Therefore, specific rules regarding the selection of a single profile line to represent undrained shear strength with depth cannot be developed. However, recognizing that undrained shear strength is a parameter used for limit state analyses (as compared to analyses of serviceability states), it is appropriate to develop an envelope for assumed worst credible case or critical case conditions. That is, analyses should be performed with a lower bound envelope to assure that calculated factors of safety are greater than 1.0. This lower bound envelope, however, needs to be developed for relevant data only; that is anomalous low values must be removed from the data set prior to developing this envelope. Unlike effective stress analysis wherein a lower bound friction angle can be selected with reasonable confidence (e.g., select a residual friction angle based on soil PI), the selection of lower bound undrained strength is much more difficult.

For heavily overconsolidated, fissured clays, the undrained strength in the field can be reduced by as much as 50 percent of the values obtained from laboratory testing because of the added macrofabric of cracks and fractures. When testing overconsolidated, fissured clays in the laboratory, this difference in measured strength can be minimized by testing samples with a maximum practical diameter (e.g., use full diameter samples from thin-wall tubes for UU testing). At relatively shallow depths, the effect of fissures on measured laboratory undrained strengths needs to be carefully considered since it is possible that overburden pressures in the field will not be large enough to close the fissures. At higher pressures, fissures may close and the undrained strength in the field will be closer to those measured in the laboratory. Due to the fissured nature of overconsolidated clays, which can permit relatively rapid local drainage at the level of the discontinuities in the clay (which,

in turn, may cause significant softening of the soil), it is generally difficult to define with any certainty the period of time during which the undrained strength of the clay may reliably be assumed to apply. Therefore, in overconsolidated, fissured clays, design analyses should be performed in terms of drained effective stress parameters, especially for cases where the clay soil is subject to unloading during the short-term (e.g., unloading due to soil removal at the base of an excavation or due to cut slope construction).

It is recognized, however, that certain state-of-the-practice design analyses for short-term conditions such as capacity evaluations of driven piles and drilled shafts are performed in terms of the undrained strength. Many of these design analyses are semi-empirical and based on successful design in these materials. Engineers involved in the design of geotechnical features in heavily overconsolidated, fissured materials should be cognizant of the fact that the short-term strength of these materials is typically much greater than the long-term drained strength. Design analyses should thus consider both cases.

5.6.8 Selection of Effective Stress Parameters (ϕ', c') for Design Analyses

Long-term effective stress strength parameters (c' and ϕ') of clays are best evaluated by slow consolidated drained direct shear box tests, consolidated drained triaxial compression tests, or consolidated undrained triaxial tests with pore pressure measurements. In laboratory tests, the rate of shearing should be sufficiently slow to ensure substantially complete dissipation of excess pore pressure in the drained tests or, in undrained tests, complete equalization of pore pressure throughout the specimen. Information on appropriate shearing rates has been provided in section 4.12.5.3. Laboratory tests should always be carried out to displacements sufficiently large to reach a stable, post-peak shear stress. As previously discussed, the selection of peak, fully-softened, or residual strength for design analyses must be made based on a careful review of the expected or tolerable displacements of the soil mass. Where pre-existing weak interfaces are present, direct shear methods should be used, if practical, to set up the sample so that the interface strength can be directly evaluated. Alternatively, soil material from within the shear zone should be sampled and reconstituted to the in-situ moisture content for shear testing.

The use of a cohesion intercept (c') for long-term analyses in natural materials must be carefully assessed. With continuing displacements, it is likely that the cohesion intercept value will decrease to zero for long-term conditions, especially for highly plastic clays.

The strength of granular strata can be assessed from penetration test data particularly the SPT, CPT, and DMT. Since laboratory testing on undisturbed samples of granular materials is impractical, it is necessary to rely on correlations to obtain the effective stress friction angle.

5.7 HYDRAULIC CONDUCTIVITY PROPERTIES OF SOIL

5.7.1 Introduction

The hydraulic conductivity of soil is important in the design of many transportation structures because it provides information related to the role that water is expected to have on the design, constructability, and performance of the structure. It is recognized that knowing what role water will

play (e.g., drained versus undrained, static versus flowing, etc.) is critical to understanding how the soil will behave.

Hydraulic conductivity data, whether obtained from the field or the laboratory, should be scrutinized due to test complexities (discussed in Section 4.12.5.4). These data should be considered in the context of the site geology and the method used to obtain the values. They are only as reliable as the method used to obtain them, keeping in mind that even excellent laboratory and field methodology may only provide values within an order of magnitude of actual conditions.

5.7.2 Laboratory Output/Data Reduction

The following parameters should be required in the laboratory output:

- Hydraulic conductivity recommendation;
- k versus head, k versus q, q_{out}/q_{in} information/plots;
- Sample dimensions (initial and final);
- Water content (initial and final);
- Sample weight (initial and final);
- Degree of saturation (initial and final);
- Permeameter type;
- Hydraulic gradient;
- Effective stress conditions;
- Temperature readings during the test period.

The resultant k value is meaningless without detailed knowledge of how the test was performed. These tests are difficult to perform accurately and results can be highly variable and highly dependent on laboratory conditions. The information listed above is essential and should be carefully analyzed to ensure that the test conditions were as close to field conditions as possible and that they match those conditions specified by the engineer. Special attention should be given to the possibility of sample disturbance, sidewall leakage, and other test errors that could affect the results. Trends in k and temperature during the test, gradients, stress conditions, and the degrees of saturation are the most important parameters to consider. Hydraulic conductivity values should have stabilized long before test termination, the gradients should be well below those listed in the ASTM D 5084 standard, stress conditions should match those from the zone of sample collection, and the degree of saturation should approach 100% (keeping in mind that it is impossible to obtain 100% saturation). Temperature changes during laboratory testing will affect the viscosity of water and, therefore, the resulting k values, so controlled laboratory tests conditions are essential.

The hydraulic conductivity data should be accompanied by Atterberg limits and grain size distribution information for correlation with field conditions and for textbook correlations/approximations of k. After receiving the laboratory data, the k values should be checked against the estimated values as discussed in the following section. If there is a major discrepancy (more than two orders of magnitude) this could be a sign of laboratory error, or possible anomalous soils.

5.7.3 Correlation Methods

Prior to reducing hydraulic conductivity data, hydraulic conductivities should be estimated using published charts, local data (if available), and correlations. Almost every soils, geology, and hydrogeology textbook contains charts of soil/rock type versus hydraulic conductivity. Figure 90 is a reprint of a chart created by Casagrande and later modified by Holtz and Kovacs (1981). This chart is useful because it provides information on appropriate laboratory conditions as well as hydraulic conductivity ranges for various soil types. Local data, available through the USDA Soil Conservation Service, USGS, state geologic survey, or local water supply district (if groundwater sources are used in the area), may provide the best initial estimate of k for the site area. Soil surveys will typically contain k values for all of the surficial soil types in the district; however, if subsurface information is required, the survey will provide little to no information.

Hazen's equation is the most common correlation equation used to estimate hydraulic conductivity for sands ($k \geq 10^{-3}$ cm/s). This equation is written as:

$$k = C(d_{10})^2 \qquad \text{(Equation 76)}$$

where: k is the hydraulic conductivity in cm/s;
C = coefficient ranging from 0.4 to 1.2 depending on sand size/sorting; and
d_{10} = effective grain size in mm at 10% passing by weight.

This equation is based solely on grain size and it requires input (d_{10}) from particle size distribution curves and the use of a coefficient estimated based on sand type (e.g., fine sand, poorly sorted, etc.). Hazen's equation should be used with caution since it only provides very approximate k estimates applicable only to clean sands (with less than 5% passing the No. 200 sieve) with d_{10} sizes between 0.1 and 3.0 mm (Holtz and Kovacs, 1981). Table 35 contains a comparison of Hazen's equation estimates with slug test information from an alluvial sand aquifer. One can see that in this deposit, the error ranged from slight to over one order of magnitude. The error would be expected to decrease as the sand becomes more uniform. Local knowledge of the soil conditions can allow site-specific values of C to be established.

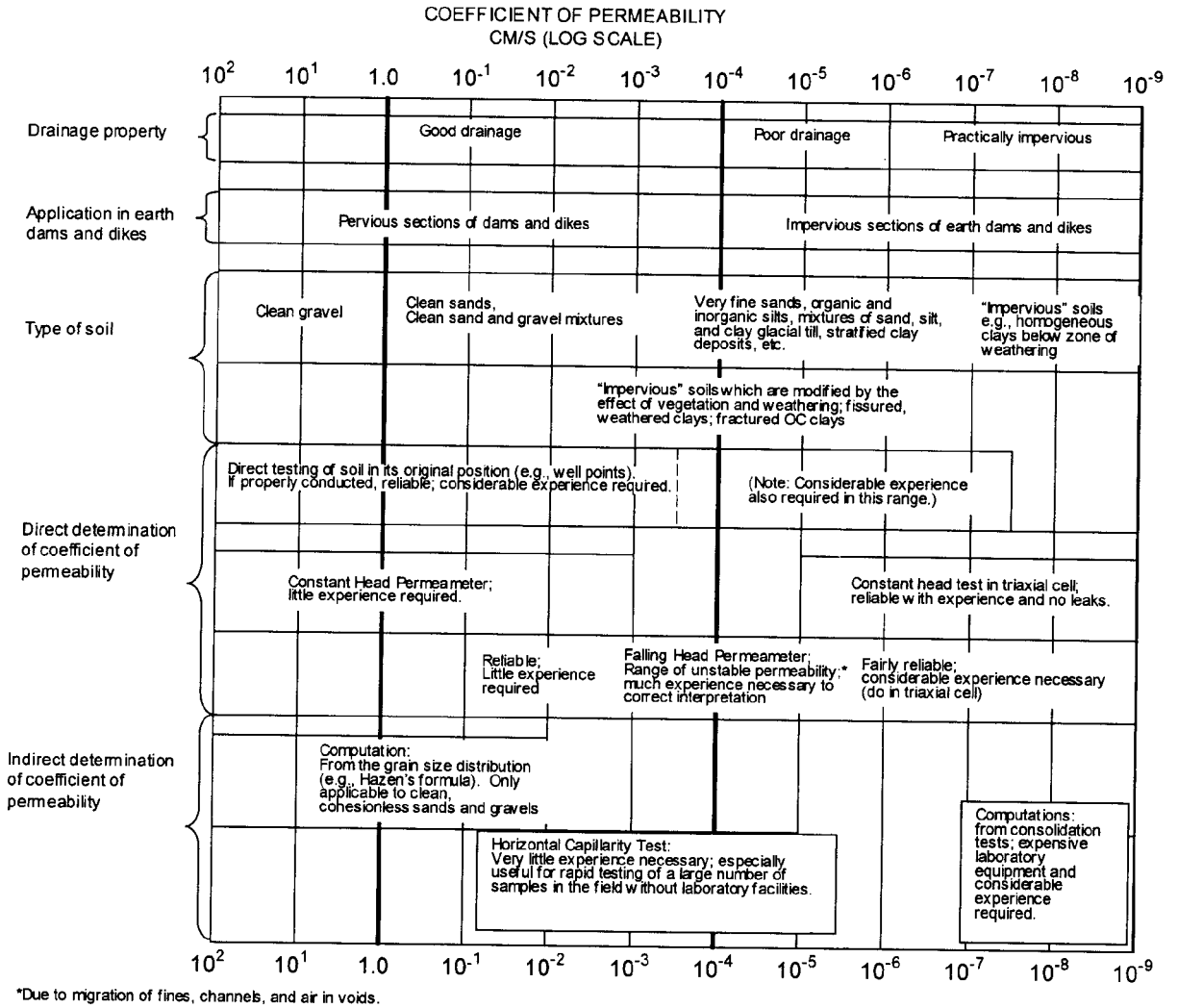

Figure 90. Range of hydraulic conductivity values based on soil type.

Another method of estimating hydraulic conductivity empirically through grain size was developed by GeoSyntec (1991) and is presented as Figure 91. As with Hazen's equation, grain size distribution information is necessary to develop the input parameter (i.e., d_{15}, grain size at 15% passing by weight) of the material. Using this value and the band of values corresponding to gradient and confining stress, a k value can be estimated. This method, as with other empirical methods, can only be used to provide an estimated value within 1 to 2 orders of magnitude of the in-situ condition. The lower the permeability and the higher the variability of grain size in the soil, the higher the error in using empirical relationships based on uniform particle distribution.

Table 35. Comparison of hydraulic conductivity from empirical and field methods.

Effective Particle Size, d_{10} (mm)	Coefficient, C (Hazen)	Hydraulic Conductivity (Hazen) (cm/s)	Log of k (Hazen)	Slug Test k Results (cm/s)	Log of k from Slug Test
0.8	1	6.4E-1	-0.194	4.3E-3	-2.367
0.3	1	9.0E-2	-1.046	1.3E-2	-1.886
0.9	1	8.1E-1	-0.092	2.2E-3	-2.658
1.3	1	1.7E0	0.230	1.2E-2	-1.921
2.0	1	4.0E0	0.602	1.6E-2	-1.796
0.3	1	9.0E-2	-1.046	6.9E-3	-2.161
0.8	1	6.4E-1	-0.194	1.8E-3	-2.745
0.5	1	2.5E-1	-0.602	2.0E-3	-2.699
	Average	**2.8E-1**	**5.0E-1**	**1.0E-2**	**9.4E-3**

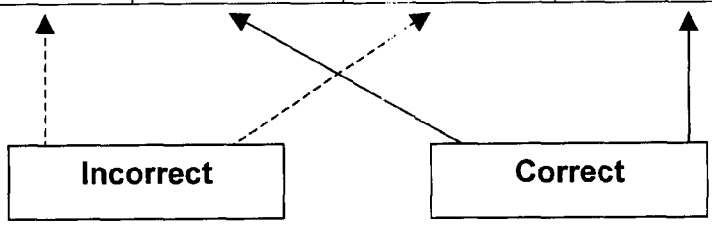

5.7.4 Interpretation Methods

As previously mentioned, hydraulic conductivity will vary across the site from point to point; however, it is important to separate potential error sources from actual field variations. Calculation of hydraulic conductivity from c_h interpretations using piezocone dissipation test data has been shown to be useful in silts and clays. These in-situ test results should be compared to values from the laboratory, but potential for flow anisotropy should be considered in this evaluation. The engineer should analyze the data collected during the field investigation (e.g., CPT and boring logs) paying close attention to: high permeability units/lenses within an overall low permeability unit; potential confining units (i.e., zones of low k overlying zones of high k); fractured zones; and other features which will: (1) result in varying k data across the site; (2) control groundwater flow; or (3) result in unexpected or anomalous data.

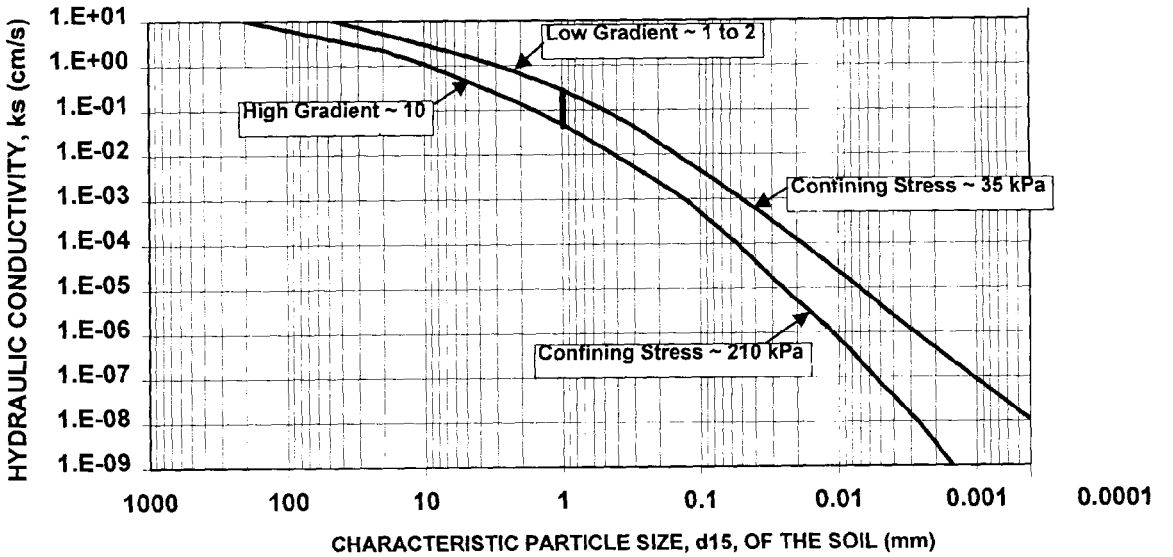

Figure 91. Range of hydraulic conductivity based on grain size (after GeoSyntec, 1991).

Considering the site geology, the laboratory and field data should be tabulated with other known data for the sample/test location and with depth, soil/rock type, grain size distribution, Atterberg limits, and water content. This table should also include important test information such as: stress conditions, gradients, and test method. Once this table is constructed it will be much easier to group like soil types and k values, to delineate distinct areas within the site, and to eliminate potentially erroneous data. Once these values have been grouped together and potentially erroneous values eliminated, it may be useful to compute an average value for each grouping. When averaging, the log of the hydraulic conductivity value must be taken before performing an arithmetic mean or incorrect results will be produced. First, the logarithm of each value should be taken. Second, an average value should be calculated from these logarithmic values. Finally, the antilog of this average value should be taken to calculate the average hydraulic conductivity value. Table 35 illustrates how to calculate the mean of the log of k data and compares this value with an incorrect direct arithmetic mean.

CHAPTER 6

INTERPRETATION OF ROCK PROPERTIES

6.1 INTRODUCTION

In chapter 4, laboratory and in-situ soil and rock tests were introduced. Chapter 5 focused on the interpretation of soil properties, starting with identification and classification of the material and proceeding through the interpretation of both routine and somewhat specialized laboratory and in-situ tests. The emphasis of this chapter is on rock properties. The type of tests described in this section range from relatively simple visual assessments to in-situ tests. There is, however, a conscious decision to place more emphasis on the visual assessment of rock, relative to the emphasis placed on the interpretation of laboratory and in-situ tests. Additionally, there is more emphasis placed herein on the visual assessment of rock than was devoted to the visual assessment of soil. The rationale for these two points of emphasis bears some introductory comments.

- *Why devote effort on visual observations, when laboratory and in-situ tests to assess specific properties are available?* In general, most soil is considered to behave as a continuous medium, although it is recognized that the soil is composed of discrete particles. From chapter 5, we know that the exception to this characterization is the behavior of highly over-consolidated clays that are often fractured. For these stiff and hard materials, the engineer must be careful to distinguish between the behavior of the stiff intact material and that of a "blocky" discontinuous matrix since the overall behavior of stiff soil is often governed by the discontinuities rather than by the intact "blocks". The behavior of rock can be considered to be an extreme example of the behavior of stiff soil; if the rock has discontinuities (e.g., fractures, bedding planes, joints, etc.), then the rock mass behavior will almost always be governed by the behavior of the discontinuities. Therefore, the orientation and characteristics (e.g., length, roughness, etc.) of the discontinuity, as well as the behavior of the material within the discontinuity (e.g., gouge, etc.) is critical to assessing the response of the rock mass to loading. Fortunately, there are several simple and inexpensive tests, as well as focused visual observations, that can be used to provide qualitative and quantitative information regarding the nature and extent of the discontinuities and the rock mass. In many cases, these visual observations are sufficient to provide accurate and adequate information for use in evaluating the engineering properties of the in-place rock mass.

- *Why devote more emphasis on visually assessing rock, compared to the effort to visually assess soil?* Again, it is noted that most soil is generally characterized as a relatively continuous medium. Visually assessing discrete soil particles may prove to be helpful, particularly with regards to angularity in sands or silt/clay distinctions in fine-grained soils. Laboratory and/or in-situ tests, however, are necessary to assess the response of the soil as a continuum. The rock counterpart to a soil continuum includes intact, non-fractured rock, relatively massive sedimentary rock that does not have weak bedding planes, and relatively massive, non-jointed igneous and metamorphic rocks. While these type rocks exist, it is with a much lower frequency than discontinuous or fractured rock masses of the same geologic origin. This is due in large part to the fact that even a few strategically located

discontinuities can control behavior of the rock mass. Because of the importance of the discontinuities in rock, and the fact that most rock is much more discontinuous than soil, emphasis is placed on visual assessment of the rock and the rock mass. Laboratory and in situ testing can be helpful in characterizing both discontinuous and intact rock.

6.2 ROCK MASS CLASSIFICATION

6.2.1 Description of Rock Masses

Standardized geologic mapping and logging procedures should be used for describing rock masses. The types of information collected will depend on site access, extent of rock outcrops, and the criticality of the proposed structure to be constructed on or in the rock mass. A method proposed by the International Society of Rock Mechanics (ISRM) (1981) provides standardized quantitative and qualitative information on rock masses. This and other rock mass classification systems are described in ASTM D5878. To introduce and explain the ISRM method, several figures and tables were prepared, primarily to provide a standardized definition of terms. Figure 92 provides an illustration of a rock mass and the 13 parameters that are included in a detailed rock description. Figure 93 shows how these parameters are divided into five categories. Table 36 provides a brief description of each of the terms. In addition to ISRM (1981), details on the use of this method to characterize rock masses are provided in Wyllie (1999) and FHWA-HI-99-007 (1998).

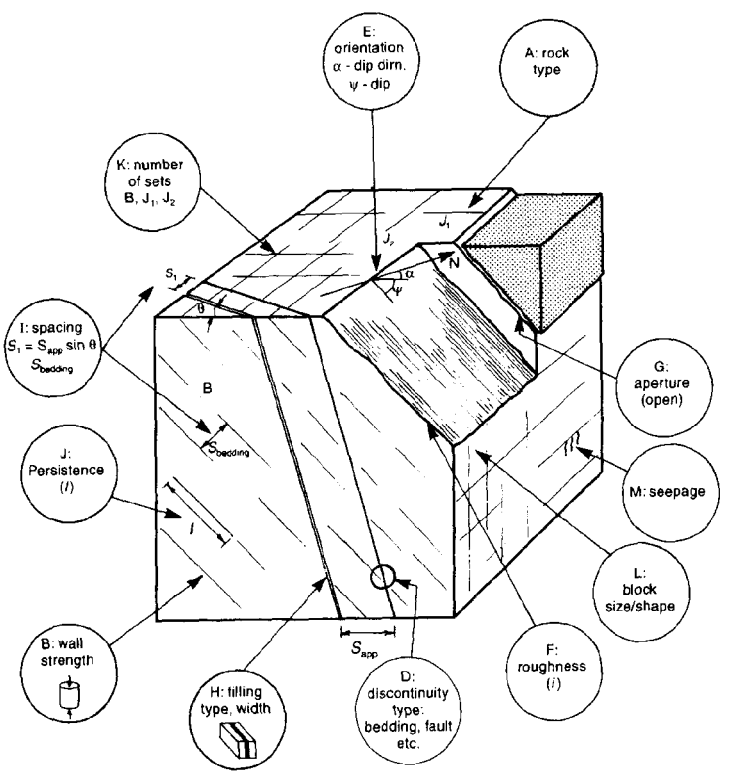

Figure 92. Illustration of geological mapping terms (after Wyllie, 1999, Foundations on Rock, Figure 4.4b, p. 101, E&FN Spon).

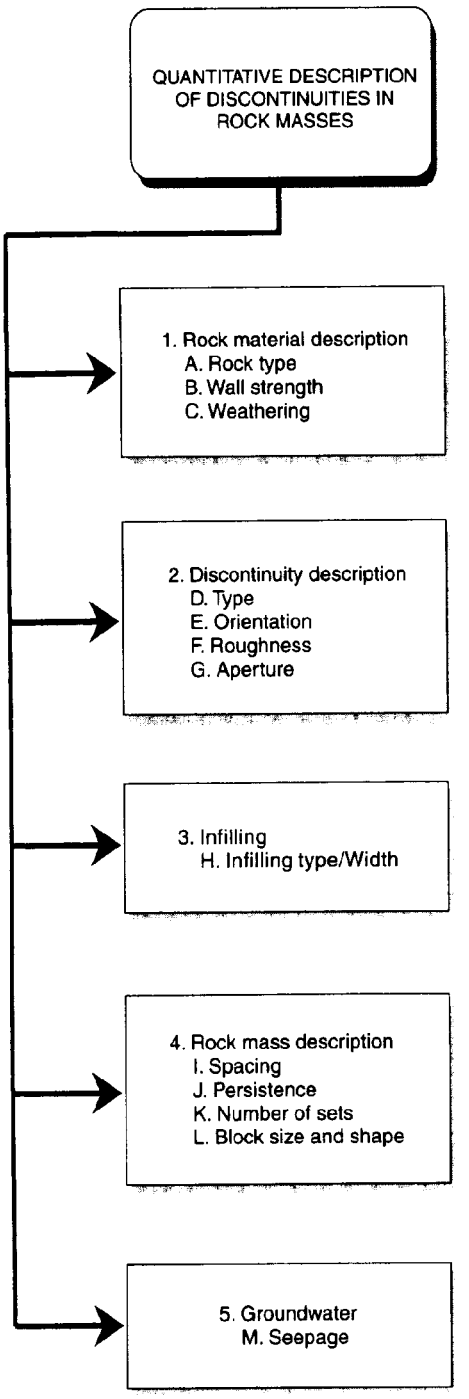

Figure 93. List of parameters and categories describing rock mass characteristics (after Wyllie, 1999).

Table 36. Description of geological mapping terms.

Term	Description
Rock Type	The rock type is defined by the origin of the rock (i.e., sedimentary, metamorphic, igneous), color (including whether light or dark minerals predominate), texture or fabric ranging from crystalline, granular, or glassy, and grain size ranging from boulders to silt/clay size particles.
Wall Strength	The compressive strength of the rock forming the walls of discontinuities will influence shear strength and deformability. Rock compressive strength categories and grade vary from extremely strong (> 250 MPa grade R6) to extremely weak (0.25 to 1 MPa grade R0) (see table 37).
Weathering	Reduction of rock strength due to weathering will reduce the shear strength of discontinuities as well as reduce the shear strength of the rock mass due to the reduced strength of the intact rock. Weathering categories and grades are summarized in table 38.
Discontinuity Type	The discontinuity type range from smooth tension joints of limited length to faults containing several centimeters of clay gouge and lengths of many kilometers. Discontinuity types include faults, bedding, foliation, joints, cleavage, and schistosity.
Discontinuity Orientation	The orientation of discontinuities is expressed as the dip and dip direction of the surface. Alternatively, the discontinuity can be represented by strike and dip. The dip of the discontinuity is the maximum angle of the plane to the horizontal (angle ψ in figure 92) and the dip direction is the direction of the horizontal trace of the line of dip, measured clockwise from north (angle α in figure 92).
Roughness	Roughness should be measured in the field on exposed surfaces with lengths of at least 2 m. The degree of roughness can be quantified in terms of the Joint Roughness Coefficient (JRC) as described in section 6.5.2.3. Wall roughness is an important component of shear strength, especially in the case of undisplaced and interlocked features (e.g., unfilled joints).
Aperture	Aperture is the perpendicular distance separating the adjacent rock walls of an open discontinuity (thereby distinguishing it from the width of a filled discontinuity), in which the space is air or is water filled. Categories of aperture range from cavernous (> 1 m) to very tight (< 0.1 mm).
Infilling Type and Width	Infilling is the term for material separating the adjacent walls of discontinuities such as fault gouge; the perpendicular distance between adjacent rock walls is termed the width of the filled discontinuity. Filled discontinuities can demonstrate a wide range of behavior and thus their affect on shear strength and deformability can vary widely.
Spacing	Discontinuity spacing can be mapped in rock faces and in drill core; spacing categories range from extremely wide (> 6000 mm) to very narrow (< 6 mm). The spacing of individual discontinuities has a strong influence on the mass permeability and seepage characteristics of the rock mass.
Persistence	Persistence is the measure of the continuous length or area of the discontinuity; persistence categories range from very high (> 20 m) to very low (< 1 m). This parameter is used to define the size of blocks and the length of potential sliding surfaces. Persistence is important in the evaluation of tension crack development behind the crest of a slope.
Number of Sets	The number of sets of discontinuities that intersect one another will influence the extent to which the rock mass can deform without failure of the intact rock. As the number of sets increases and the block sizes reduce, the greater the likelihood for blocks to rotate, translate, and crush under applied loads.
Block Size and Shape	The block size and shape are determined from the discontinuity spacing, persistence, and number of sets. Block shapes include blocky, tabular, shattered and columnar, while block size ranges from very large (> 8 m^3) to very small (< 0.0002 m^3).
Seepage	Observations of the seepage from discontinuities should be provided. Seepage quantities in unfilled discontinuities range from very tight and dry to continuous flow. Seepage quantities in filled discontinuities range from dry in heavily consolidated infillings to filling materials that are washed out completely and very high water pressures are experienced.

Table 37. Rock material strengths.

Grade	Description	Field Identification	Range of Uniaxial Compressive Strength (MPa)
R0	Extremely weak rock	Indented by thumbnail	0.25 – 1.0
R1	Very weak rock	Crumbles under firm blows with point of geological hammer; can be peeled by a pocket knife	1.0 – 5.0
R2	Weak rock	Can be peeled by a pocket knife with difficulty; shallow indentations made by firm blow with point of geological hammer	5.0 – 25
R3	Medium strong rock	Cannot be scraped or peeled with a pocket knife; specimen can be fractured with single firm blow of geological hammer	25 – 50
R4	Strong rock	Specimen requires more than one blow of geological hammer to cause fracture	50 – 100
R5	Very strong rock	Specimen requires many blows of geological hammer to cause fracture	100 – 250
R6	Extremely strong rock	Specimen can only be chipped with geological hammer	> 250

Table 38. Weathering grades.

Term	Description	Grade
Fresh	No visible sign of rock material weathering; slight discoloration on major discontinuity surfaces is possible	I
Slightly weathered	Discoloration indicates weathering of rock material and discontinuity surfaces. All the rock material may be discolored by weathering and the external surface may be somewhat weaker than in its fresh condition.	II
Moderately weathered	Less than half of the rock material is decomposed and/or disintegrated to a soil. Fresh or discolored rock is present either as a discontinuous framework or as corestones.	III
Highly weathered	More than half of the rock material is decomposed and/or disintegrated to a soil. Fresh or discolored rock is present either as a discontinuous framework or as corestones.	IV
Completely weathered	All rock material is decomposed and/or disintegrated to soil. The original mass structure is still largely intact.	V
Residual soil	All rock material is converted to soil. The mass structure and material fabric are destroyed but the apparent structure remains intact. There may be a large change in volume, but the soil has not been significantly transported.	VI

Using the terms described in table 36 and the first category in figure 93, a typical rock material description would be as follows (Wyllie, 1999):

slightly weathered, crystalline, gray, fine grained, medium strong basalt

An example of a rock mass description using table 36 and the four remaining categories in figure 93 would be as follows:

Columnar jointed basalt with vertical columns and one set of horizontal joints, spacing of vertical joints is very wide, spacing of horizontal joints wide, joint lengths are 3 to 5 m vertically, and 0.5 to 1 m horizontally; the discontinuity infilling is very soft clay with widths of 2 to 5 mm. The vertical columnar joints are smooth, while the horizontal joints are rough. No seepage observed.

6.2.2 Core Recovery and Rock Quality Designation

The easiest way to characterize the amount of material recovered during rock coring is to calculate "core recovery" as the amount (i.e. length) of recovered material divided by the total length of the core run (presented as a percentage). Rock Quality Designation (RQD) (ASTM D6032) is a modified core recovery percentage in which the lengths of all sound rock core pieces over 100 mm in length are summed and divided by the length of the core run. Pieces of core that are not hard and sound should not be included in the RQD evaluation even if they are at least 100 mm in length. The purpose of the soundness requirement is to downgrade rock quality where the rock has been altered and/or weakened by weathering. For the RQD evaluation, lengths must be measured along the centerline of the core. Figure 94 illustrates the correct procedure for calculating core recovery and RQD. Table 39 presents the correlation of RQD to rock quality.

The RQD is appropriate for use with all core sizes except for BQ and BX core with NX and NQ core size being optimal. Core breaks caused by the drilling process should be fitted together and counted as a single piece of sound core. Drilling breaks are usually evidenced by rough fresh surfaces, however for laminated rocks (i.e., rocks containing horizontally oriented fracture surfaces), it may be difficult to identify core breaks caused by drilling. In this case, the RQD should be estimated conservatively; for shear strength characterization it is conservative to not count the length near horizontal breaks whereas for estimates of rock blasting requirements, it is conservative to count the length near horizontal breaks.

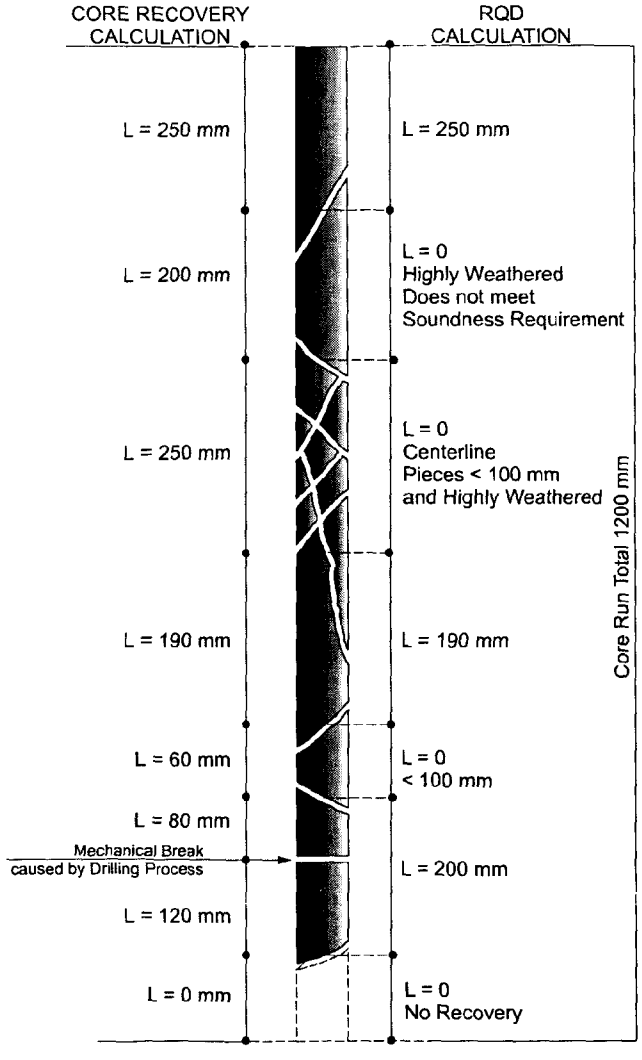

$$Core\,\text{Recovery}, CR = \frac{Total\,length\,of\,rock\,recovered}{Total\,core\,run\,length}$$

$$CR = \frac{(250+200+250+190+60+80+120)\,mm}{1{,}200\,mm}$$

$$CR = 96\%$$

$$RQD = \frac{\sum Length\,of\,sound\,pieces > 100\,mm}{Total\,core\,run\,length}$$

$$RQD = \frac{(250+190+200)\,mm}{1{,}200\,mm} * 100\%$$

$$RQD = 53\%$$

Figure 94. Calculation of core recovery and RQD.

6.2.3 CSIR Classification

The ISRM (1981) procedures, coupled with core recovery and RQD designations, provide vehicles for describing or characterizing rock and rock mass. A consistent method for rock mass classification is essential for evaluating rock properties used in design. The two most widely used rock classification systems were developed by the Council for Scientific and Industrial Research (CSIR) in South Africa (referred to as the "Q-rating system") and the Norwegian Geotechnical Institute (NGI) (referred to as the Geomechanics system). Both of these methods are described in detail in FHWA-HI-99-007 (1998). The CSIR classification system is the most widely used procedure in the US. Therefore, in this section an overview of the CSIR system is presented.

Table 39. Rock quality description based on RQD.

RQD Value	Description of Rock Quality
0-25 %	Very poor
25-50 %	Poor
50-75 %	Fair
75-90 %	Good
90-100 %	Excellent

The CSIR classification system considers the specific properties or conditions of the rock/rock mass, as well as an adjustment for the orientations of the joints. The following properties and conditions of the rock or rock mass are explicitly considered: (1) compressive strength of the intact rock (discussed in section 6.3); (2) RQD value; (3) joint spacing; (4) condition of the joints; and (5) groundwater conditions. As shown in table 40, each of these parameters is given a numerical rating based on the relative importance of the specific parameter on the behavior of the rock mass. This rating is adjusted to account for joint orientation depending on the favorability of the joint orientation for the specific project. The overall rating of the rock mass, termed the rock mass rating (RMR), is calculated as the sum of the individual ratings for each of the five parameters minus the adjustment for joint orientation (if applicable). Based on the final RMR, the rock mass is classified as: (1) Class I-very good rock; (2) Class II-good rock; (3) Class III-fair rock; (4) Class IV-poor rock; and (5) Class V-very poor rock. The RMR can be used to estimate rock mass deformation modulus and shear strength of the rock mass and can be an invaluable design aid when used appropriately.

Table 40. CSIR classification of jointed rock mass.

A. CLASSIFICATION PARAMETERS AND THEIR RATINGS

PARAMETER			RANGES OF VALUES						
1	Strength of intact rock material	Point load strength index	>8 MPa	4 to 8 Mpa	2 to 4 MPa	1 to 2 MPa	For this low range – uniaxial compressive test is preferred		
		Uniaxial compressive strength	>200 MPa	100 to 200 MPa	50 to 100 MPa	25 to 50 MPa	10 to 25 MPa	3 to 10 MPa	1 to 3 MPa
	Relative Rating		15	12	7	4	2	1	0
2	Drill core quality RQD		90% to 100%	75% to 90%	50% to 75%	25% to 50%	<25%		
	Relative Rating		20	17	13	8	3		
3	Spacing of joints		>3 m	1 to 3m	0.3 to 1 m	50 to 300 mm	<50mm		
	Relative Rating		30	25	20	10	5		
4	Condition of joints		Very rough surfaces Not continuous No separation Hard joint wall rock	Slightly rough surfaces Separation <1mm Hard joint wall rock	Slightly rough surfaces Separation <1mm Soft joint wall rock	Slickensided surfaces or Gouge <5 mm thick or Joints open 1 to 5 mm Continuous joints	Soft gouge >5 mm thick or Joints open >5 mm Continuous joints		
	Relative Rating		25	20	12	6	0		
5	Ground water	Inflow per 10 m tunnel length	None		<25 liters/min	25 to 125 liters/min	>125 liters/min		
		Ratio= joint water pressure/major principal stress	0		0.0 to 0.2	0.2 to 0.5	>0.5		
		General Conditions	Completely Dry		Moist only (interstitial water)	Water under moderate pressure	Severe water problems		
	Relative Rating		10		7	4	0		

B. RATING ADJUSTMENT FOR JOINT ORIENTATIONS

Strike and dip orientations of joints		Very favorable	Favorable	Fair	Unfavorable	Very Unfavorable
Ratings	Tunnels	0	-2	-5	-10	-12
	Foundations	0	-2	-7	-15	-25
	Slopes	0	-5	-25	-50	-60

C. ROCK MASS CLASSES DETERMINED FROM TOTAL RATINGS

RMR Rating	100 to 81	80 to 61	60 to 41	40 to 21	<20
Class No.	I	II	III	IV	V
Description	Very good rock	Good rock	Fair rock	Poor rock	Very poor rock

6.3 ROCK UNIAXIAL COMPRESSIVE STRENGTH

For the CSIR classification, as well as for several design applications, it is necessary to measure (or at least estimate) the uniaxial compressive strength of a rock core. The most reliable results for the uniaxial compressive strength of rock core are obtained when a series of uniaxial compressive strength calibration tests are carried out.

An estimate of the compressive strength of rock can be made using available correlation information based on the point load strength test. It has been found, on average, that the uniaxial compressive strength, σ_c, is about 20 to 25 (average is approximately 24) times the point load strength index. Tests on many different types of rock, however, show that the ratio can vary between 15 and 50, especially for anisotropic rocks. The point load strength test is not recommended for very weak rocks where the uniaxial compressive strength is less than approximately 25 MPa or where reasonably accurate values for compressive strength of intact rock core.

In the point load strength test, the fractured pieces of core should be examined after the point load strength test is completed. If a clean fracture runs from one loading point indentation to the other, the test results are considered acceptable. If the fracture runs across some other plane or if the loading points sink into the rock surface causing excessive crushing or deformation, the test result should be rejected (Hoek and Bray, 1977). When performing the point load strength test, information on the degree of weathering should be noted since the compressive strength of weathered material along the joint may be less than the uniaxial compressive strength.

If a uniaxial test is conducted in accordance with ASTM D2938, it is important to follow the preparation guidelines established in ASTM D4543. Most importantly, the specimen should be selected to provide a length/diameter ratio of at least 2 but less than 2.5 and the ends must be smooth, parallel and perpendicular to the long axis of the core. It is also noted that for a given rock mass, as the size of the tested rock core increases, the uniaxial compression strength decreases, due primarily to the fact that as the specimen size increases there is a higher likelihood of encountering discontinuities (albeit potentially small) in the rock core. An advantage of the point load strength test is that raw core can be used.

6.4 ROCK DEFORMATION MODULUS VALUES

6.4.1 Intact Rock Modulus

For certain design applications, it may be necessary (or desirable) to assess the deformation modulus of the rock core or the rock mass. The deformation modulus of intact rock, E_R, is evaluated by performing uniaxial compression tests (ASTM D3148) on pieces of rock core obtained from drilling using a diamond core barrel. The stress-strain behavior of the intact rock can be measured in the laboratory and plotted as shown in figure 95. The axial and diameter strain are measured using very sensitive deformation instruments or, more commonly, using direct bond strain gages. Microstrain is defined where:

$$\mu\varepsilon = \frac{\Delta \text{ original dimension}}{\text{original dimension}} \times 10^{-6} \qquad \text{(Equation 77)}$$

The plots in figure 95 show two cycles of a compression test on a sample of strong and stiff gneissic rock that exhibits approximately perfectly elastic behavior with no hysteresis and no permanent deformation at the level of test deformations.

The elastic constants calculated from the plots in figure 95 over the linear portion of the stress-strain curve include the Youngs modulus and Poisson ratio, and are calculated as follows (Wyllie, 1999):

Young's modulus = *Vertical stress/Vertical strain*
= 50.0 MPa / 610E – 6
= 82 GPa (11.9×10^6 psi)

Poisson's ratio = *Diametral strain/Vertical strain*
= 150E – 6 / 610E - 6
= 0.25

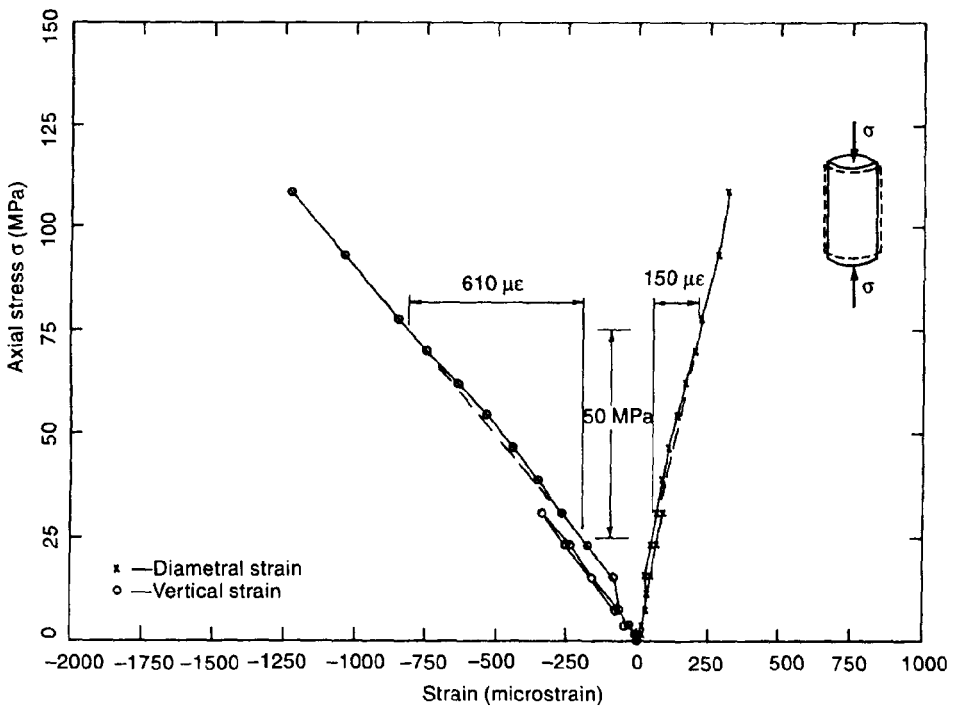

Figure 95. Axial and diametral stress-strain curves for intact rock tested in uniaxial compression (after Wyllie, 1999, Foundations on Rock, Figure 3.3, p. 52, E&FN Spon).

Table 41 shows the results of uniaxial compression tests carried out to determine the elastic constants of a variety of rock types (Lama and Vutukuri, 1978a, b). The Youngs modulus for intact rock is significantly larger than that for soil and typically varies between 0.1 to 100 GPa, but as can be seen from table 41, the values are rock formation specific. Calculated values of Poisson's ratio typically range from 0.25 to 0.4, but these too are often rock specific. Typically, the settlement of a rock foundation will be controlled by the deformation modulus corresponding to the overall rock mass (see section 6.4.2) and will not be controlled by the deformation modulus of intact rock. However, the appropriate rock mass deformation modulus for use in design can be evaluated using procedures which reduce the intact rock modulus based on simple parameters such as joint opening size, RQD, and/or RMR, as discussed subsequently.

Table 41. Typical elastic constants for intact rock (after Wyllie, 1999) (see Wyllie, 1999 for original references for tests).

Rock Type	Young's modulus GPa (psi × 10^6)	Poisson's Ratio	Reference
Andesite, Nevada	37.0 (5.5)	0.23	Brandon (1974)
Argillite, Alaska	68.0 (9.9)	0.22	Brandon (1974)
Basalt, Brazil	61.0 (8.8)	0.19	Ruiz (1966)
Chalk, USA	2.8 (0.4)	-	Underwood (1961)
Chert, Canada	95.2 (13.8)	0.22	Herget (1973)
Claystone, Canada	0.26 (0.04)	-	Brandon (1974)
Coal, USA	3.45 (0.5)	0.42	Ko and Gerstle (1976)
Diabase, Michigan	68.9 (10)	0.25	Wuerker (1956)
Dolomite, USA	51.7 (7.5)	0.29	Haimson and Fairhurst (1970)
Gneiss, Brazil	79.9 (11.6)	0.24	Ruiz (1966)
Granite, California	58.6 (8.5)	0.26	Michalopoulos and Triandafilidis (1976)
Limestone, USSR	53.9 (8.5)	0.32	Belikov (1967)
Salt, Ohio	28.5 (4.1)	0.22	Sellers (1970)
Sandstone, Germany	29.9 (4.3)	0.31	Van der Vlis (1970)
Shale, Japan	21.9 (3.2)	0.38	Kitahara *et al.* (1974)
Siltstone, Michigan	53.0 (7.7)	0.09	Parker and Scott (1964)
Tuff, Nevada	3.45 (0.5)	0.24	Cording (1967)

6.4.2 Rock Mass Modulus

6.4.2.1 Method Based On Rock Mass Rating

It is not possible to assess rock mass deformation characteristics in the laboratory since modulus values are highly dependent on the size of the sample. Bieniawski (1978) proposed a method of estimating the in situ rock mass modulus using the rock mass rating (RMR) previously described. The advantage of this approach is that RMR is evaluated from easily measured parameters (see table 40). It is explicitly noted that discontinuity orientation will have an affect on the rock mass modulus. For example, an unfavorable gouge-filled joint orientation with respect to settlement would be in a direction at right angles to the load direction resulting in closure of discontinuities and settlement whereas for rock slope stability analyses, an unfavorable orientation with respect to sliding would be in a direction parallel to the load direction or inclined and dipping towards an open face.

The empirical relationship between the RMR rating value and the in situ rock mass modulus is shown in figure 96. Based on a database review, the following equation for rock mass modulus, E_M, exhibiting a RMR > 50 was developed (Bieniawski, 1978):

$$E_M\,(GPa) = 2\,RMR - 100 \qquad \text{(Equation 78)}$$

Additional studies carried out on rock masses with RMR values ranging from approximately 20-85 resulted in the following modification (Serafim and Periera, 1983):

$$E_M\,(GPa) = 10^{(RMR-10)/40} \qquad \text{(Equation 79)}$$

For rock masses with a RMR greater than approximately 80 (i.e., "very good rock" according to the CSIR classification system), the value for E_M evaluated based on equation 79 should be compared to the deformation modulus of intact rock core as determined using ASTM D3148, and the lower value should be used for design calculations.

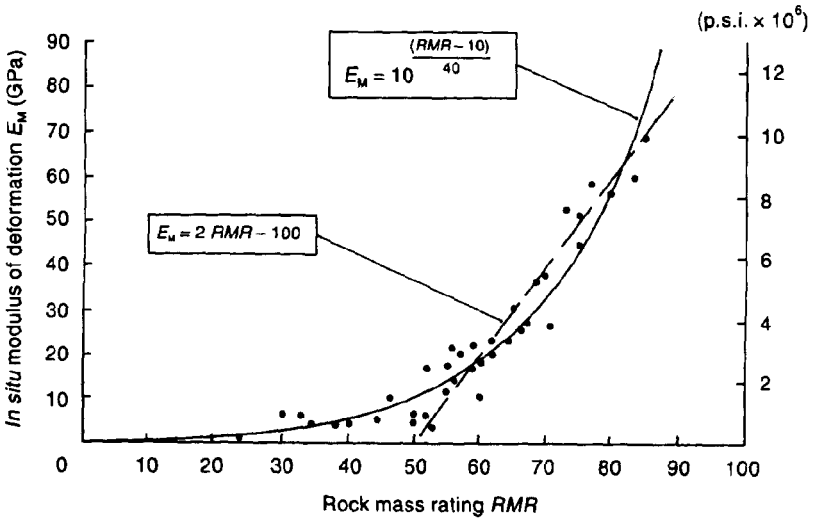

Figure 96. Relationship between in situ modulus and rock mass rating (after Bieniawski, 1978; Serafim and Pereira, 1983).

6.4.2.2 Method Based on RQD

An alternate empirical method for evaluating the in situ rock mass modulus has been developed by Carter and Kulhawy (1988) and is widely used in practice to establish reliable estimates. This method uses the RQD value, an estimate of the intact rock modulus, E_R, and a determination of whether the rock joints are open or closed to evaluate the rock mass modulus, E_M (see table 42). In using table 42, values intermediate between tabulated entry values may be obtained by linear interpolation. It is necessary to estimate E_R (see section 6.4.1) to establish a specific value of E_M.

Table 42. Estimation of E_M based on RQD (modified after Carter and Kulhawy, 1988).

RQD (in percent)	E_M/E_R	
	Closed Joints	Open Joints
100	1.00	0.60
70	0.70	0.10
50	0.15	0.10
20	0.05	0.05

6.4.2.3 Use of In situ Tests to Evaluate Rock Mass Modulus

The methods previously described for estimating the in situ rock mass modulus based on RMR and RQD can be used for typical foundation and rock slope applications on highway projects. For very critical structures such as dams and tunnels, it may be necessary to perform in situ tests to "directly" measure the in-situ rock mass modulus. In chapter 4, specific in situ tests were introduced for assessing rock mass modulus. In this section, the evaluation of the in situ rock mass modulus using the borehole dilatometer and borehole jack is described.

With all in situ tests there will be some disturbance of the rock, particularly where blasting must be used to prepare the site. The interpretation of the test should therefore recognize the potential for, and thus be able to assess the extent of this disturbance. Excavation of the foundation may also involve some disturbance to the rock and it is important to make an assessment of the degree of disturbance at the test site during testing compared with the likely condition at the foundation site at the time it is constructed.

Borehole Dilatometer

A typical borehole dilatometer curve for a test conducted in rock has been shown in figure 20. Using the borehole dilatometer, the shear modulus, G_d, and the modulus of elasticity, E_d, of the rock in the tested borehole are given by (ISRM, 1987):

$$G_d = k_R \frac{\pi L d^2}{\rho} \qquad \text{(Equation 80)}$$

$$E_d = 2(1+\nu_R)G_d \qquad \text{(Equation 81)}$$

where L is the length of the cell membrane; d is the diameter of the drill hole; ν_R is Poisson's ratio of the rock; and ρ is the pump constant defined as the fluid volume displaced per turn of pump wheel. The stiffness of rock over the length of the cell membrane, k_R is:

$$k_R = \frac{k_s k_T}{(k_s - k_T)} (MPa/turn) \qquad \text{(Equation 82)}$$

where k_s its is the stiffness of the hydraulic system and k_T is the stiffness of overall system plus rock (ratio D/C in figure 20). There are other versions of the borehole dilatometer that can be used and the details of these (as of the ISRM system) are beyond the scope of this document. It is, however, critical to note that when testing rock, several calibrations must be performed (see Wyllie, 1999).

- The k_R term is calculated from calibration of the hydraulic system and the results of a pressure-dilation test carried out in a calibration cylinder of known modulus. The stiffness of the hydraulic system, k_s, is calculated from the stiffness of the calibration cylinder and the slope of the calibration pressure-dilation curve, k_m (ratio B/A in figure 20).

- It is also necessary to make a correction for pressure losses due to the rigidity of the membrane. This is determined by inflating the dilatometer in the air without confinement to show the pressure required to inflate the membrane and the hydraulic system. It is usually necessary to "select" membranes to match the stiffness of the tested rock. For example, if a very stiff membrane is used to perform a test in soft rock, the calibration will dominate the field response.

- It is necessary to account for loss of volume in the hydraulic system that takes place in inflating and seating the membrane.

Should it be necessary to conduct borehole dilatometer tests, it will likely require the services of an organization with specific borehole dilatometer experience and the specialized equipment. It is important to request the specifics on the equipment and assure that the calibration tests are provided.

Borehole Jack

Figure 97 shows a typical pressure-displacement plot for a borehole jack test carried out in strong limestone. Details of the borehole jack test and methods are provided in ASTM D4971. For the condition of full contact between the borehole jack and the rock sidewall and for a rock Poisson's ratio of 0.25, the calculated in situ mass modulus, E_{calc} is given by

$$E_{calc} = \frac{1.15 \Delta Q_h}{(\Delta D / D)} \qquad \text{(Equation 83)}$$

where ΔQ_h is the increment in hydraulic pressure, ΔD is the change in hole diameter resulting from ΔQ_h, and D is the hole diameter. Equation 83 will vary depending on the assumed Poisson's ratio (see ASTM D4971 for modification based on Poisson's ratio values other than 0.25), however the effect of a different Poisson's ratio is relatively minor on the calculated value for E_{calc}. Using the data in figure 97 for the third loading cycle (for a pressure increment of 30 to 40 MPa), the measured diametral displacement is approximately 0.09 mm. With a hole diameter of 76.2 mm, equation 83 is used to calculate an E_{calc} of 9.7 GPa. For the borehole jack, the calculated value of rock modulus may need to be corrected to account for the variation in the ratio between the modulus of steel and the modulus of the intact rock. When the modulus of the steel is much greater than that of the intact rock, the correction factor is negligible because there is little deformation of the steel platens as the pressure is applied. However, when the intact rock modulus is high compared with the steel modulus, the modulus value calculated from the jack test is less than the "true" rock modulus and the "true" in situ mass modulus, E_{true} should be evaluated using figure 98. For a calculated modulus of 9.7 GPa, figure 98 indicates the E_{true} is approximately 12 GPa.

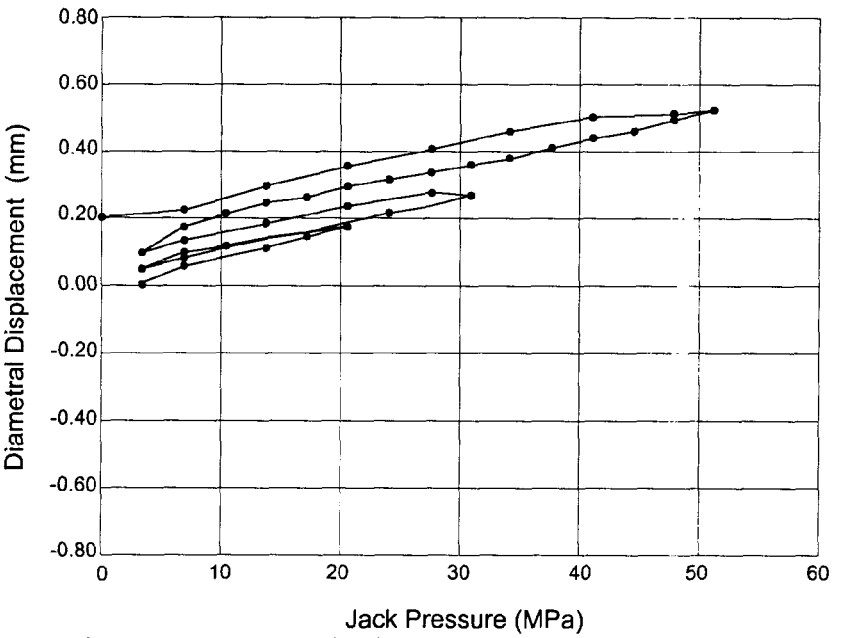

Figure 97. Pressure-displacement plot for borehole jack.

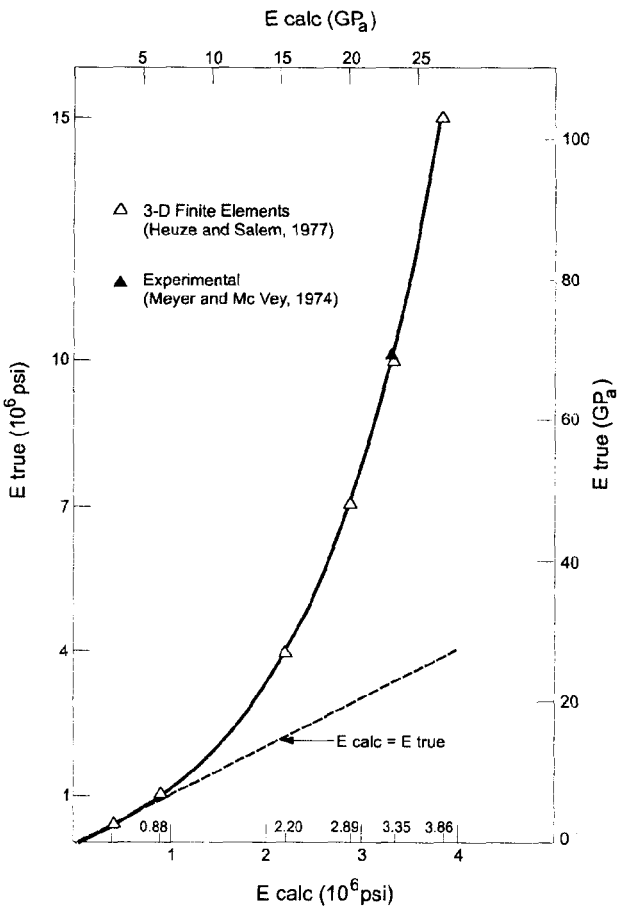

Figure 98. Curve of E_{true} versus E_{calc} (after ASTM D 4971).

6.4.3 Selection of Rock Deformation Modulus for Design

Various methods have been described for evaluating the deformation modulus in rock masses. For most highway design applications in which deformation evaluations are required, however, the empirical methods described based on either RMR or RQD can be used. As indicated, the use of in-situ test methods to evaluate a deformation modulus is typically only performed for critical or large structures such as major bridges or dams. Alternatively, if design analyses based on the use of either RMR or RQD result in predicted settlements that exceed target values for a particular foundation type, then it may be appropriate to perform in situ tests to develop a more accurate assessment of the in situ modulus. The most important consideration is to use the rock mass characteristics, not the characteristics of the intact rock core.

For shallow foundations, the average rock mass modulus over a depth equal to approximately 2 times the width of the foundation should be assessed. This can be done by measuring the intact rock modulus via uniaxial compression tests on samples of intact core from successive core samples and then evaluating the rock mass modulus based on table 42.

The selection of modulus values for a drilled shaft will depend on whether the shaft design is for end bearing only, side resistance only from a rock socket, or a combination of both. Many methods exist for evaluating deformations in drilled shafts and some are based on specific semi-empirical methods of evaluating rock mass modulus values based on the results of settlement data for previously constructed drilled shafts in particular rock types (see FHWA-IF-99-025, 1999). In general, however, it is recommended to use the procedures outlined in section 6.4.2 to obtain an estimate of the rock mass modulus. For drilled shafts with rock sockets in which load is carried in end-bearing and side resistance, an evaluation of the average rock mass deformation modulus around the rock socket and at the base of the shaft (at a depth of up to 2 times the diameter of the shaft below the base of the shaft) are required. Intact rock cores can be tested in uniaxial compression and then corrected to a rock mass modulus using table 42. The deformation modulus value can also be evaluated based on RMR ratings for rock near the shaft base and around the socket using figure 96.

6.5 ROCK SHEAR STRENGTH

6.5.1 Mohr-Coulomb Materials

For geotechnical design analyses, rock (i.e. intact rock and jointed rock masses) is generally assumed to be a Mohr-Coulomb material in which the shear strength of the rupture surface is expressed in terms of the cohesion intercept (c) and the friction angle (ϕ). When an effective normal stress σ' acts on the rupture surface, the shear stress (τ) developed is:

$$\tau = \sigma' \tan\phi + c \qquad \text{(Equation 84)}$$

Figure 99 illustrates the relationship between the typical strength parameters for five geological conditions. A description of these conditions is as follows:

- **Curve 1. Infilled discontinuity**: If the infilling is a weak clay or fault gouge, the friction angle of the infilling is likely to be low, and there may be some cohesion if the infilling is undisturbed. Alternatively, if the infilling is strong (e.g. calcite which produces a healed surface) then the cohesive strength and the friction angle may be significant.

- **Curve 2. Smooth discontinuity**: A smooth, clean discontinuity in the parent rock will have little or no cohesion, and the friction angle will be that of the parent rock. The friction angle of rock is related to the rock grain mineralogy and size; the friction angle is generally lower in fine-grained rocks than in coarse-grained rocks.

- **Curve 3. Rough discontinuity**: Clean, rough discontinuity surfaces will have little or no cohesion, and the friction angle will be made up of the rock material friction angle (ϕ), and a component related to the roughness, or asperities, of the surface (see section 6.5.2.3).

- **Curve 4. Fractured rock mass**: The shear strength of a fractured rock mass, in which the rupture surface lies partially on discontinuity surfaces and partially passes through intact rock, can be expressed as a curved envelope. At low normal stresses where individual fragments may move and rotate, the cohesion is low but the friction angle is high because the sliding surface is effectively rough and may involve non-frictional material. In addition, at the low normal stresses, the response may be dilative. At higher normal stresses, dilation is reduced and crushing of the rock fragments begins to take place and the friction angle reduces. The shape of the strength envelope is related to the degree of fracturing and the strength of the intact rock.

- **Curve 5. Weak intact rock**: The shear strength of weak, but intact, rock is governed by the combination of cohesion and parent rock friction. Some rock (e.g. tuff) comprises fine-grained material that has a low friction angle. However, due to its intact nature, the cohesion can be higher than that of a closely fractured well indurated rock.

In this section, a discussion of the shear strength behavior of infillings, smooth and rough discontinuities, and fractured rock masses are presented. Following this discussion, the methods commonly used to evaluate shear strength for these rock classes are presented. The direct shear testing method (laboratory or in situ) is commonly used to evaluate the shear strength of infillings and discontinuity surfaces. Shear strength for fractured rock masses is evaluated using back analysis methods or semi-empirically based on characterization information such as RMR and rock type.

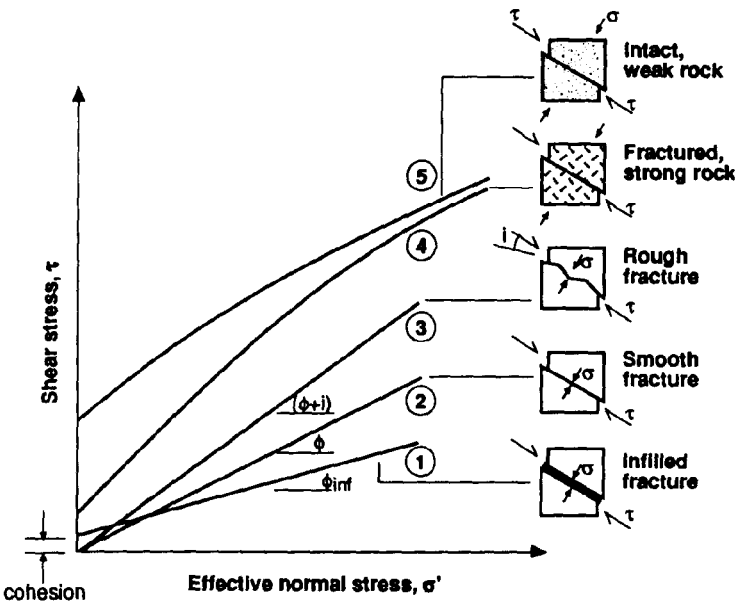

Figure 99. Relationships between shear stress and normal stress on rupture surface for five different geological conditions (TRB, 1996).

6.5.2 Shear Strength Of Discontinuities

6.5.2.1 General

If discontinuities are identified within a rock mass, it will be necessary to evaluate the friction angle and cohesion intercept along the potential rupture surface to perform design analyses. The investigation program should also obtain information on important fracture characteristics such as continuous length, surface roughness, thickness and characteristics of any infilling material, water occurrence, as well as the effect of water on the properties of the infilling. Shear strength properties of various discontinuity types are described in this section.

6.5.2.2 Friction Angle of Rock Surfaces

For a planar, clean (no infilling) discontinuity, the shear strength will be defined solely by the friction angle. The friction angle of the rock material is related to the size and shape of the grains exposed on the fracture surface and the rock mineralogy. Thus, a fine-grained rock and/or rock with a high mica content aligned parallel to the surface will tend to have a low friction angle, while a coarse-grained rock will have a high friction angle. Table 43 shows typical ranges of friction angles for a variety of rock types (Barton, 1973; Jaeger and Cook, 1976). The friction angles listed in table 43 should be used as a guideline only because actual values will likely vary from site to site, for a given rock type, and may vary slightly across a single site.

Table 43. Typical ranges of friction angles for a variety of rock types (after Barton, 1973; Jaeger and Cook, 1976).

Rock Class	Friction Angle Range[1]	Typical Rock Types
Low Friction	20 to 27°	Schists (high mica content), shale, marl
Medium Friction	27 to 34°	Sandstone, siltstone, chalk, gneiss, slate
High Friction	34 to 40°	Basalt, granite, limestone, conglomerate

Note: (1) Values assume no infilling and little relative movement between joint faces.

6.5.2.3 Surface Roughness

Surface irregularities or asperities produce interlock between discontinuity surfaces that increase the resistance to sliding (or shearing). Asperities can be considered as a series of saw teeth. When normal and shear forces are applied to a rock surface containing a clean, saw tooth fracture, the shear strength of the fracture surface is defined as follows:

$$\tau = \sigma' \tan(\phi + i) + c \qquad \text{(Equation 85)}$$

where i is the inclination of the saw teeth as shown in figure 100. This relationship shows that the effective friction angle of a rough surface is equal to the sum of the friction angle of the rock and the inclination of the asperities. Another way of viewing this increased strength due to asperities is that it requires work for the rock mass to dilate and move over the asperities.

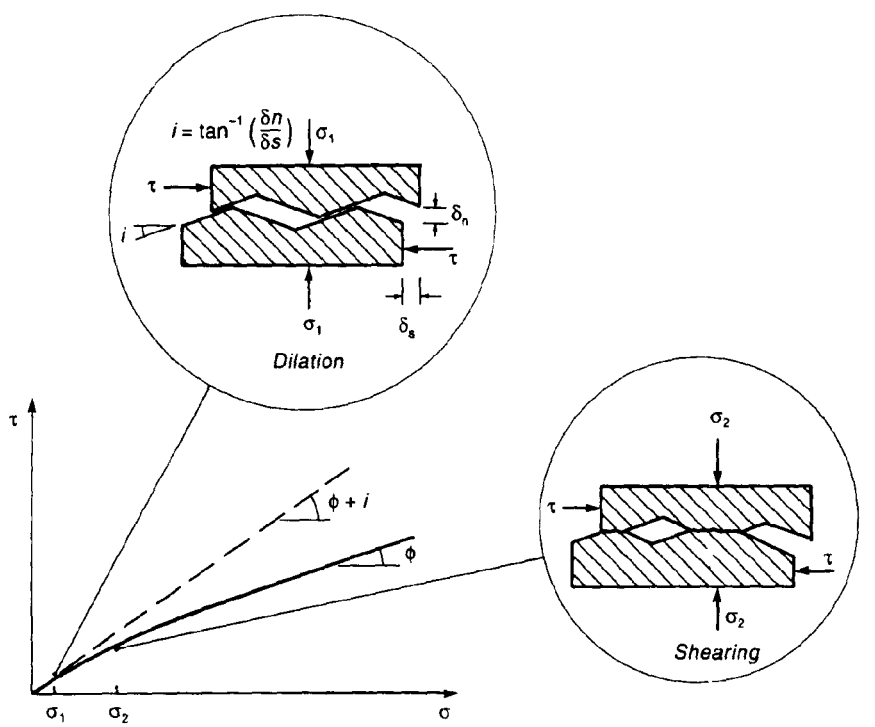

Figure 100. Effect of surface roughness and normal stress on the friction of a discontinuity surface (after Wyllie, 1999, Foundations on Rock, Figure 3.15, p. 70, E&FN Spon).

During shearing, the asperities can be sheared off, resulting in a reduction in the friction angle. With increasing stress levels, there is a transition from dilation to shearing. At this point, the degree to which the asperities are sheared off will depend on both the magnitude of the normal force in relation to the compressive strength of the rock on the fracture surface, and the displacement distance. A rough surface that is initially undisturbed and interlocked will have a friction angle of (ϕ + i), which represents the peak shear strength. With increasing normal stress and displacement, the asperities will be sheared off, and the friction angle will progressively reduce to a minimum value, or residual, friction angle of the rock, resulting in a curved failure envelope as shown in figure 100.

To quantify the relationship between the total friction angle (ϕ + i), the rock strength, and the normal stress acting on the rupture surface, Barton (1976) studied the shear strength behavior of artificially produced rough, clean "joints". The study showed that the shear strength of a rough rock surface can be defined by the following empirical equation

$$\tau = \sigma' \tan\left[\phi + JRC \log_{10}\left(JCS/\sigma'\right)\right] \qquad \text{(Equation 86)}$$

where: JRC= joint roughness coefficient; JCS = compressive strength of the rock adjacent to the fracture surface; and σ' = effective normal stress.

The roughness of the fracture surface is defined by the joint roughness coefficient, JRC. Barton carried out direct shear tests on a large number of natural discontinuities and calculated JRC values corresponding to the surface roughness of the different shear test specimens. From these tests a set of typical roughness profiles with specified JRC values were prepared (figure 101). By comparing a fracture surface with these standard profiles, the JRC value can be evaluated (Barton, 1976).

The term JRC $\log_{10}(JCS/\sigma')$ is equivalent to the inclination of the sawteeth or the roughness angle i in equation 85. At high stress levels when $JCS/\sigma' = 1$ and the asperities are sheared off, the term JRC $\log_{10}(JCS/\sigma')$ equals zero. At low stress levels, the ratio JCS/σ' becomes very large and the roughness component of the strength also becomes very large. In order that realistic values of the roughness component are used in design, the fracture surface (i.e. joint, etc.) should be visually inspected and the surface compared to the surfaces shown in figure 101. Regardless of the calculated values, for design the term (ϕ+i) should not exceed 50 degrees and the useful range for the ratio JCS/σ' is between 3 and 100. As more progressive displacement or relative movement occurs across the fracture surface, it should be recognized that the value (ϕ+i) reduces.

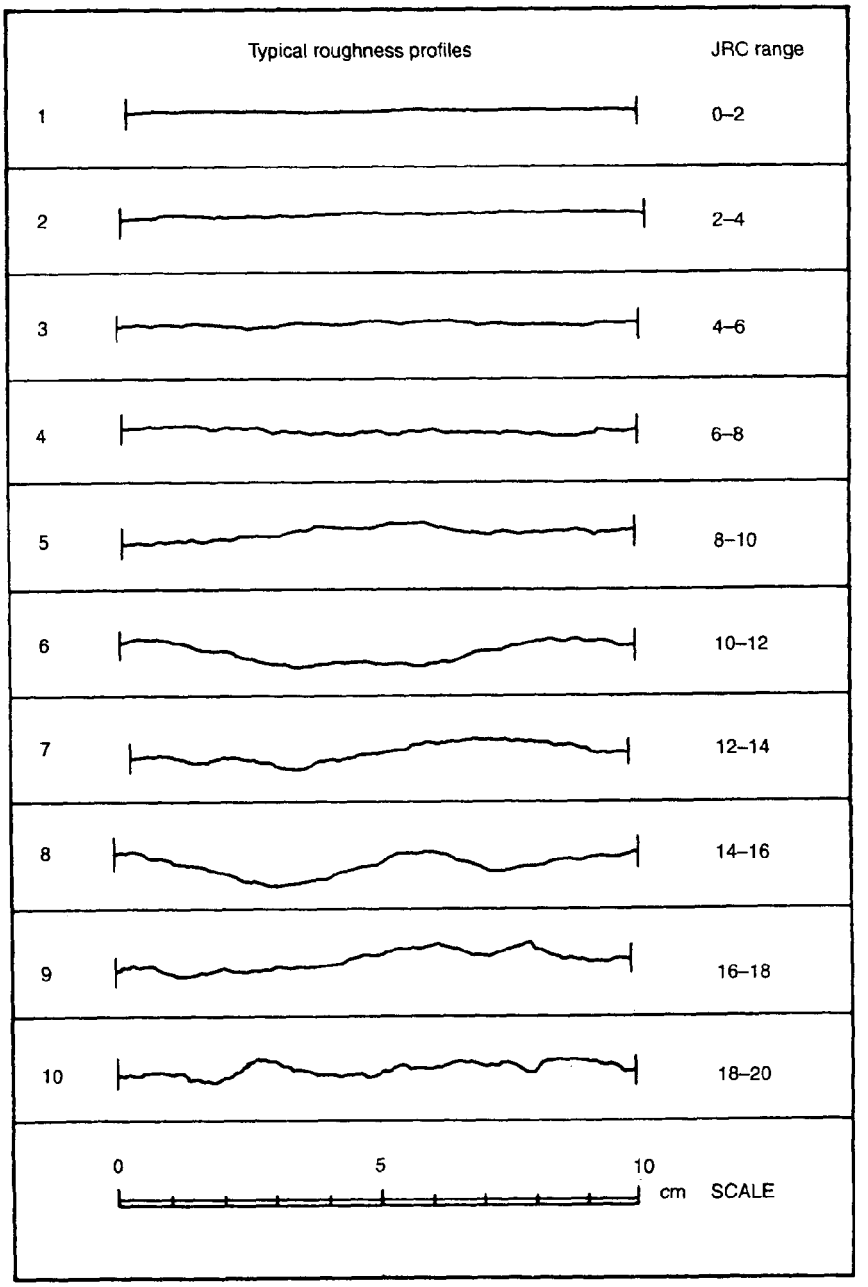

Figure 101. Definition of joint roughness coefficient, *JRC* (Barton, 1973).

6.5.2.4 Measurement of Surface Roughness

The method described in section 6.5.2.3 to evaluate the roughness angle (i) is typically used during preliminary design or where exposures of discontinuity surfaces are not available at the project site. If exposures of discontinuity surfaces on which sliding may occur are available at a project site, measurements can be made of the surface roughness. If the exposure is extensive, then the actual roughness angle (i) can be measured and used in equation 85 in evaluating the shear strength of the surface. Methods of making these measurements are beyond the scope of this document, but

information can be found in FHWA-HI-99-007 (1998) and Wyllie (1999). In critical cases, the joint surface can be exhumed and a laboratory direct shear test can be performed at the range of project-representative normal stresses to physically assess the strength of the rock along the fracture surface.

6.5.2.5 Discontinuity Infilling

If a discontinuity contains an infilling, the shear strength properties of the fracture will be influenced by the thickness and properties of the infilling. For example, for a relatively thick clay-filled fault zone in granite, the clay and not the granite would control the shear strength of the discontinuity; if the gouge in fairly thin and the granite surfaces are in contact along much of the fracture, the strength value will be intermediate between that of the parent rock plus asperities and the gouge material. In the case of a healed, calcite-filled fracture, a high cohesion would be used in design if the discontinuity remained healed after any construction-induced disturbance. With respect to the thickness of an infilling, if it is more than about 25 to 50 percent of the amplitude of the asperities, there will be little or no rock-to-rock contact, and the shear strength properties of the fracture will be controlled by the shear strength properties of the infilling (Goodman, 1970).

Infillings are generally divided into the following two groups:

- **Clays** – For montmorillonite and bentonitic clays, and clays encountered during coal mining, tests have been conducted that demonstrate friction angles ranging from about 8 to 20 degrees and cohesion intercept values ranging from 0 to about 200 kPa.

- **Faults, shears and breccias** – For these rocks, the material formed in fault zones and shears in rocks such as granite, diorite, basalt, and limestone will typically contain clay as well as granular fragments. The gouge materials associated with the rock types typically have friction angles ranging from about 25 to 45 degrees, and cohesion intercept values ranging from 0 to about 100 kPa. Fault gouge derived from coarse-grained rocks such as granites tend to have higher friction angles than those from fine-grained rocks such as limestones.

As part of a Barton (1976) study, it was found that the residual friction angle of filled discontinuities was about 2 to 4 degrees less than the peak friction angle, while the residual cohesion intercept was essentially zero.

Filled discontinuities can be divided into two general categories, depending on whether there has been previous displacement of the discontinuity (Barton, 1974). These categories are further subdivided into either normally-consolidated (N-C) or over-consolidated (O-C) materials (figure 102):

- **Recently displaced discontinuities** - These types of discontinuities include faults, shear zones, clay mylonites, and bedding-surface slips. In faults and shear zones, the infilling is formed by the shearing process which may have occurred many times and produced considerable displacement. The gouge formed in this process may include both clay-size particles, and breccia with the particle orientation and striations of the breccia aligned parallel to the direction of shearing. In contrast, the mylonites and bedding-surface slips are discontinuities that were originally clay bearing, and along which slip occurred during

folding or sliding. For these types of discontinuities their shear strength will likely be at or close to the residual strength (figure 102, graph I).

- **Undisplaced discontinuities** - Infilled discontinuities that have undergone no previous displacement include igneous and metamorphic rocks that have weathered along the discontinuity to form a clay layer. For example, diabase usually weathers to amphibolite and eventually to clay. Other undisplaced discontinuities include thin beds of clay and weak shales that are found with sandstone in interbedded sedimentary formations. Hydrothermal alteration may form infillings that can include low strength materials such as montmorillonite, and high strength materials such as quartz and calcite.

The infillings of undisplaced discontinuities can be divided into normally consolidated (N-C) and overconsolidated (O-C) materials that have significant differences in peak strength values. This strength difference is illustrated on figure 102 in graphs II and III. While the peak shear strength of over-consolidated clay infillings may be high, there can be a significant loss of strength due to softening, swelling, and pore pressure changes on unloading. Unloading occurs when rock is excavated for a slope or foundation, for example. Strength loss also occurs on displacement in brittle materials such as calcite.

For these conditions, it is important that the design assess the type of infilling and the degree of potential displacement along the discontinuity. As shown in table 44, the effects of the type of infilling and parent rock can have a significant effect on strength parameters.

6.5.2.6. Effect of Water on Shear Strength

The most significant effect of ground water on slope stability is the reduction in the effective normal stress produced by water pressures acting within the slope. A reduction in the effective normal stress results in a corresponding reduction in the shear strength of the rupture surface. Generally, the strength properties of rock are the same whether they are wet or dry; however some rocks, such as shales containing swelling clay, exhibit a loss of strength in the presence of water. Therefore, it is necessary to assess whether the infilling material is adversely affected by the occurrence of water. To this end, it is important to note that in some cases the in situ condition has tight and relatively dry fractures. However, due to construction, there could be sufficient movement to allow a pathway for water to become introduced to the rock and the rock infill material.

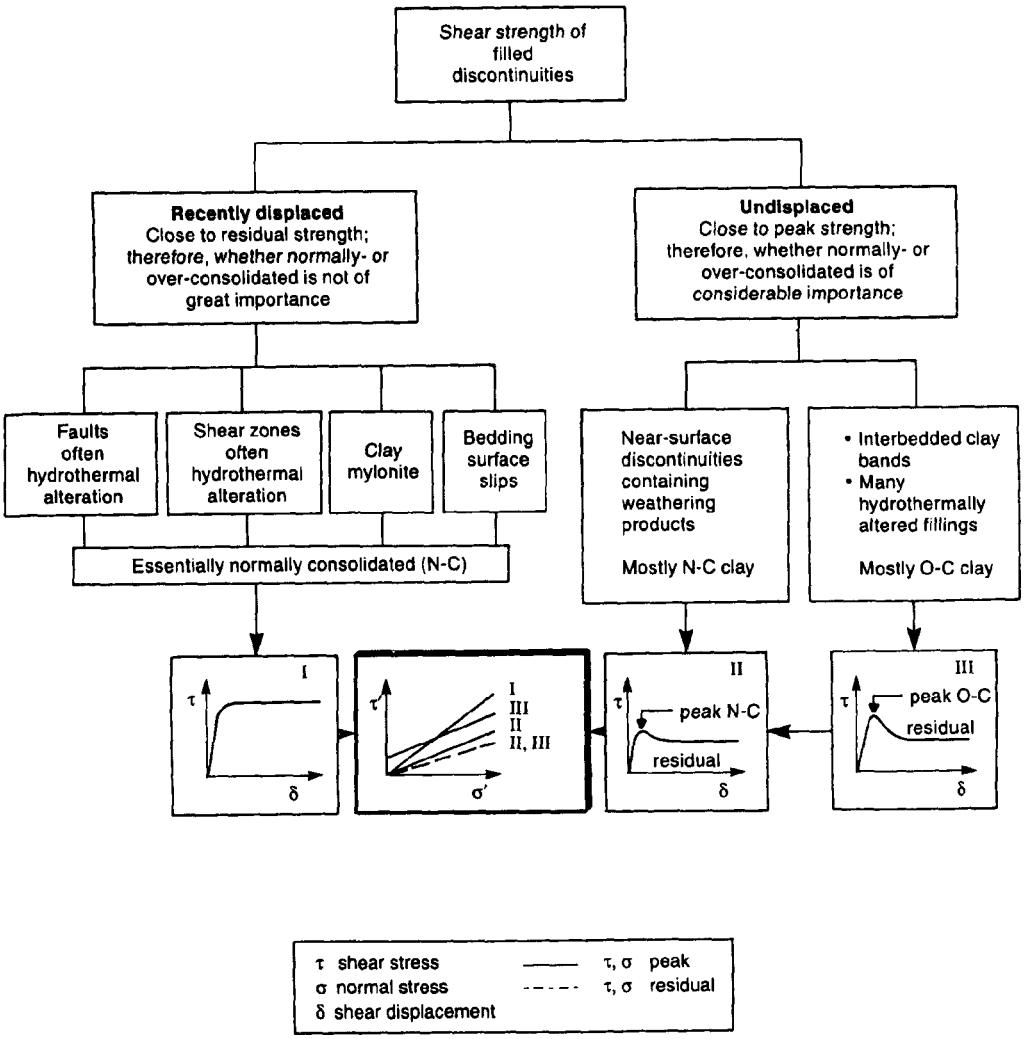

Figure 102. Simplified division of filled discontinuities into displaced and undisplaced, and NC and OC categories (after Wyllie, 1999, Foundations on Rock, Figure 3.18, p. 73, E&FN Spon).

Table 44. Shear strength of filled discontinuities (modified after Hoek and Bray, 1977) (Note: missing data implies shear strength not reported in original table; see Hoek and Bray, 1977 for references for testing data).

Rock Type	Description	Peak Strength		Residual Strength	
		c′ (kPa)	ϕ′	c′ (kPa)	ϕ′
Igneous Rocks					
Basalt	Clayey basaltic breccia, wide variation from clay to basalt content	240	42		
Diorite	Clay gouge (2 percent clay, PI=17)	0	26.5		
Granite	Clay-filled faults	0 to 100	24 to 45		
	Weakened with sandy-loam fault filling	50	40		
	Tectonic shear zones, schistose and broken granites, disintegrated rock and gouge	242	42		
Metamorphic Rocks					
Schists, quartzites, and siliceous schists	10- to 15-cm thick clay filling	30 to 80	32		
	Stratification with thin clay	610 to 740	41		
	Stratification with thick clay	380	31		
Slates	Finely laminated and altered	50	33		
Sedimentary Rocks					
Dolomite	Altered shale bed, approximately 15-cm thick	41	14.5	22	17
Limestone	6 mm clay layer			0	13
Limestone, marl, and lignites	Interbedded lignite layers	80	38		
	lignite/marl contact	100	10		
Limestone	Marlaceous joints, 2-mm thick	0	25	0	15 to 24
Sandstone (Graywacke)	1 to 2-mm thick clay in bedding layer			0	21
Strata containing coal	Clay mylonite seams, 1 to 2.5 cm thick	11 to 13	16	0	11 to 11.5
Lignite	Layer between lignite and underlying clay	14 to 30	15 to 17.5		

Table 44. Shear strength of filled discontinuities (modified after Hoek and Bray, 1977) (Note: missing data implies shear strength not reported in original table; see Hoek and Bray, 1977 for references for testing data).

Rock Type	Description	Peak Strength		Residual Strength	
		c′ (kPa)	ϕ′	c′ (kPa)	ϕ′
Sedimentary Rocks (clays and shales)					
Bentonite	Bentonite seam in chalk	15	7.5		
	Thin layers	90 to 120	12 to 17		
	Triaxial tests	60 to 100	9 to 13		
Bentonitic shale	Triaxial tests	0 to 270	8.5 to 29		
	Direct shear tests			30	8.5
Clays	Overconsolidated slips, joints, and minor shears	0 to 180	12 to 18.5	0 to 3	10.5 to 16
Clay Shale	Triaxial tests	60	32		
Clay Shale	Stratification surfaces			0	19.5
Montmorillonite Clay	Montmorillonite	360	14	80	11
	8 cm seams of montmorillonite clay in chalk	16 to 20	7.5 to 11.5		

6.5.2.7 Laboratory Direct Shear Testing

In a laboratory direct shear test on rock, the measured friction angle is the sum of the friction angle of the rock (ϕ), and the roughness of the surface (i) at each normal stress level. The roughness of the surface is calculated from the plots of shear and normal displacement (δs and δn, respectively, on figure 103(a) as follows:

$$i = \tan^{-1}\left(\frac{\delta n}{\delta s}\right) \qquad \text{(Equation 87)}$$

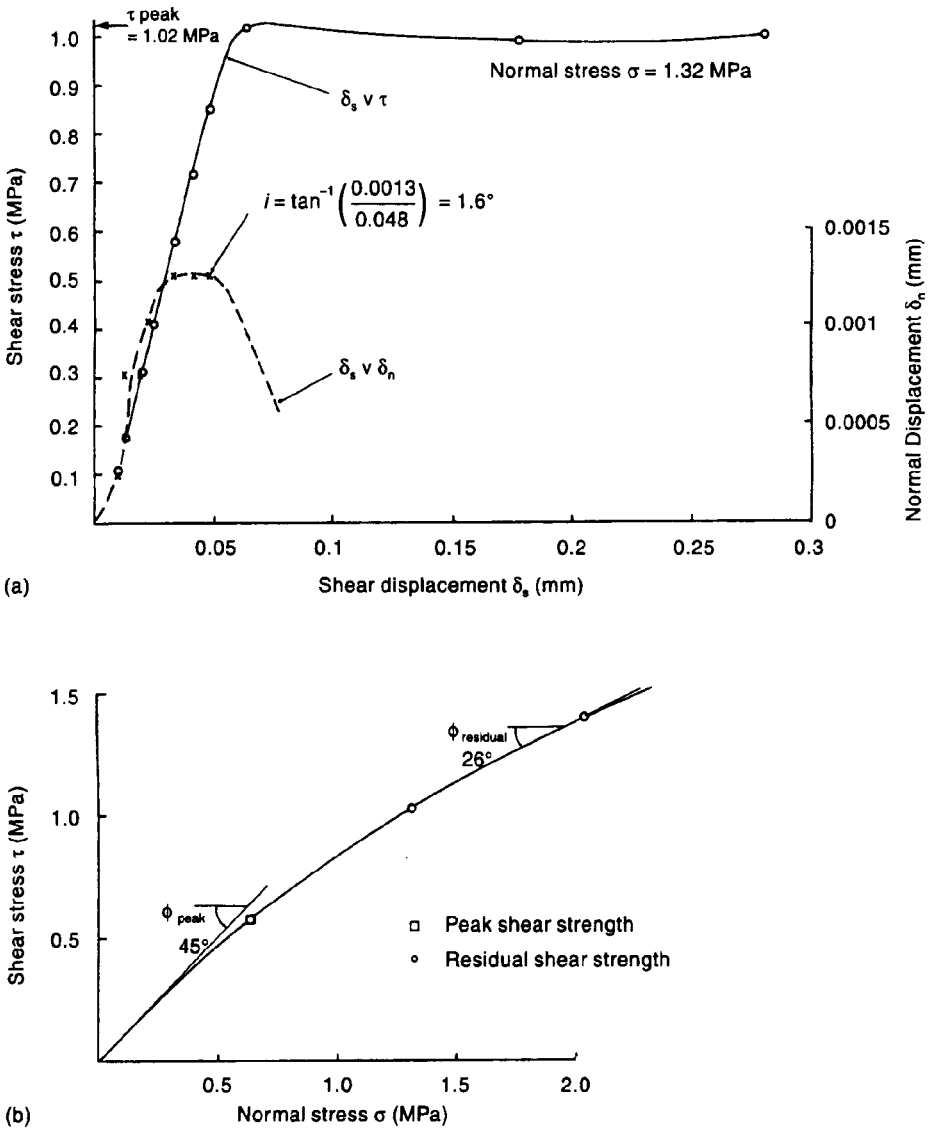

Figure 103. Results of direct shear test of filled discontinuity showing measurements of shear strength and roughness (after Wyllie, 1999, Foundations on Rock, Figure 3.20, p. 75, E&FN Spon).

This value of *i* is the shear strength component due to dilation of the rock upon shear. This value is subtracted from the friction angle calculated from the plot of shear and normal stresses at failure (considering peak conditions) to obtain the friction angle of the rock. For example, figure 103(a) indicates that the peak strength is 1.02 MPa. For a normal stress of 1.32 MPa, this results in a friction angle of 37.7°. Therefore, for a dilation angle of 1.6°, the friction angle of the parent rock is 36.1°. This friction angle is actually an "instantaneous" friction angle and represents the tangent to the strength envelope at a normal stress of 1.32 MPa.

In laboratory direct shear testing on rock, it is typical to test each sample at a minimum of three normal stress levels, with the sample being reset to its original position between tests. When the tests are run at progressively higher normal stress levels, the total friction angle of the surface will reduce with each test if the asperities are progressively sheared. The maximum design load should be considered when establishing the normal stresses as used in the test.

It can be difficult to measure the cohesion of a surface with the direct shear test. For cases where the cohesion is very low, it may not be possible to obtain an undisturbed sample so the cohesion may be reduced or lost during sampling. If the cohesion is high and the sample is intact, the material holding the sample will have to be stronger than the infilling material if the sample is to shear. Where it is important that the cohesion of a weak infilling be measured, an in situ direct shear test of the undisturbed material may be required.

6.5.3 Shear Strength Of Fractured Rock Masses

6.5.3.1 General

A rupture surface in fractured rock for which there is no distinct discontinuity surface comprises both natural discontinuities aligned on the rupture surface, together with some shear failure through intact rock. It is difficult and expensive to sample and test large samples of fractured rock, therefore, two empirical methods of evaluating the friction angle and cohesion intercept of fractured rock masses have been developed and are described in this section. In both methods, it is necessary to categorize the rock mass in terms of both the intact rock strength and the characteristics of the discontinuities. It is advisable to compare the strength values obtained by both methods to improve the reliability of values used in design.

6.5.3.2 Strength Determination by Back Analysis of Failures

The most reliable method of evaluating the strength of a rock mass is to back analyze a failed, or failing, slope. This involves carrying out a stability analysis with the factor of safety set at 1.0 and using available information on the position of the rupture surface, the groundwater conditions at the time of failure and any external forces such as foundation loads and earthquake motion, if applicable. Additional information on performing back analyses as a means to evaluate fractured rock mass shear strength is provided in FHWA-HI-99-007 (1998).

6.5.3.3 Hoek-Brown Strength Criteria for Fractured Rock Masses

The shear strength of fractured rock masses can also be evaluated using the method developed by Hoek (1983) and Hoek and Brown (1988, 1997) in which the shear strength is represented as a curved envelope (figure 104). The three parameters defining the curved strength envelope of the fractured rock mass are the uniaxial compressive strength of the intact rock, σ_c, and two dimensionless constants m and s. The values of m and s are defined in table 45. The constants m and s depend on the rock type and the degrees of fracturing of the rock mass. In table 45, rock types are grouped into five classes depending on the grain size and crystal structure. The six qualities of the rock mass are defined in table 45 either by the brief descriptions of the geology or by rock mass rating (RMR) that assign point scores to a number of characteristics of the rock mass (see table 45).

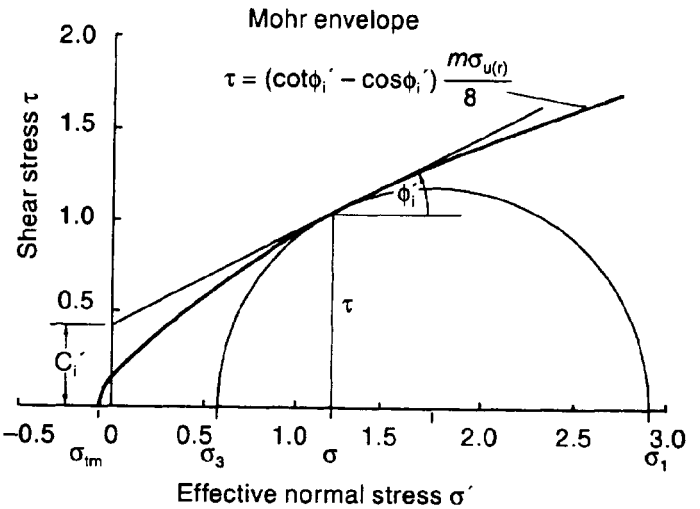

Figure 104. Typical curved shear strength envelope defined by Hoek-Brown theory for rock mass strength (Hoek, 1983).

The equation for the curved shear strength envelope is:

$$\tau = (\cot\phi_i' - \cos\phi_i')\frac{m\sigma_c}{8} \qquad \text{(Equation 88)}$$

where τ is the shear stress at failure, σ_c is the uniaxial compressive strength of the intact rock and ϕ_i' is the instantaneous friction angle at given values of τ and σ'. The value of ϕ_i' is the inclination of the tangent to the Mohr failure envelope at the point (σ', τ) as shown in figure 104 and is given by:

$$\phi_i' = \tan^{-1}\left(4h\cos^2\left[30 + 0.33\sin^{-1}(h^{-3/2})\right] - 1\right)^{-1/2} \qquad \text{(Equation 89)}$$

where

$$h = 1 + \frac{16(m\sigma' + s\sigma_c)}{3m^2\sigma_c} \qquad \text{(Equation 90)}$$

The instantaneous cohesion (c_i') is the intercept of the line defining the friction angle on the shear stress axis and is given by:

$$c_i' = \tau - \sigma' \tan \phi_i' \qquad \text{Equation (91)}$$

Table 45. Approximate relationship between rock-mass quality and material constants used in defining nonlinear strength (Hoek and Brown, 1988).

Empirical failure criterion $\sigma'_1 = \sigma'_3 + (m\sigma_c \sigma'_3 + s\sigma_c^2)^{1/2}$ σ'_1 = major principal effective stress σ'_3 = minor principal effective stress σ_C = uniaxial compressive strength of intact rock, and *m* and *s* are empirical constants Rock Quality		CARBONATE ROCKS WITH WELL DEVELOPED CRYSTAL CLEAVAGE – *dolomite, limestone and marble*	LITHIFIED ARGRILLACEOUS ROCKS – *mudstone, siltstone, shale and slate (normal to cleavage)*	ARENACEOUS ROCKS WITH STRONG CRYSTALS AND POORLY DEVELOPED CRYSTAL CLEAVAGE – *sandstone and quartzite*	FINE GRAINED POLYMINERALLIC IGNEOUS CRYSTALLINE ROCKS – *andesite, dolerite, diabase and rhyolite*	COARSE GRAINED POLYMINERALLIC IGNEOUS & METAMORPHIC CRYSTALLINE ROCKS – *amphibolite, gabbro gneiss, granite, norite, quartz-diorite*
INTACT ROCK SAMPLES Laboratory size specimens free from discontinuities CSIR rating(1): RMR = 100	m s	7.00 1.00	10.00 1.00	15.00 1.00	17.00 1.00	25.00 1.00
VERY GOOD QUALITY ROCK MASS Tightly interlocking undisturbed rock with unweathered joints at 1 to 3 m CSIR rating: RMR = 85	m s	2.40 0.082	3.43 0.082	5.14 0.082	5.82 0.082	8.567 0.082
GOOD QUALITY ROCK MASS Fresh to slightly weathered rock, slightly disturbed with joints at 1 to 3 m CSIR rating: RMR = 65	m s	0.575 0.00293	0.821 0.00293	1.231 0.00293	1.395 0.00293	2.052 0.00293
FAIR QUALITY ROCK MASS Several sets of moderately weathered joints spaced at 0.3 to 1 m CSIR rating: RMR = 44	m s	0.128 0.00009	0.183 0.00009	0.275 0.00009	0.311 0.00009	0.458 0.00009
POOR QUALITY ROCK MASS Numerous weathered joints at 30-500 mm; some gouge. Clean compacted waste rock. CSIR rating: RMR = 23	m s	0.029 0.000003	0.041 0.000003	0.061 0.000003	0.069 0.000003	0.102 0.000003
VERY POOR QUALITY ROCK MASS Numerous heavily weathered joints spaced < 50 mm with gouge. Waste rock with fines. CSIR rating: RMR = 3	m s	0.007 0.0000001	0.010 0.0000001	0.015 0.0000001	0.017 0.0000001	0.025 0.0000001

Notes: (1) CSIR = Council of Scientific and Industrial Research (Bieniawski, 1974 and table 40).

The features of the curved shear strength envelope are that, at low normal stress levels, the blocks of rock are interlocked and the instantaneous friction angle is high, whereas at higher normal stress levels, shearing of the rock is initiated with the result that the friction angle reduces. The instantaneous cohesion progressively increases in direct proportion to the normal stress as a result of the greater confinement and interlock of the rock mass.

The procedure for using the curved strength envelopes in a stability analysis is first to evaluate the range of effective normal stresses acting along a potential rupture surface in the slope, and second to calculate the instantaneous cohesion values and friction angles (c_i', ϕ_i') in this stress range. The stability analysis is carried out in a traditional stability calculation, except that values of c_i' and ϕ_i' are used corresponding to the variation in normal stress along the sliding surface. Many commercial limit equilibrium stability analysis programs enable the user to input the actual shear stress-normal stress curve when performing the analysis.

Figure 105 illustrates the application of the information in table 45 for three different conditions. These curves cover the range from very poor quality rock mass to very good quality rock mass. Table 46 shows values for the parameters used to develop figure 105. The reader of this document can verify the correct implementation of equations 88 to 91 by comparing to values on table 46.

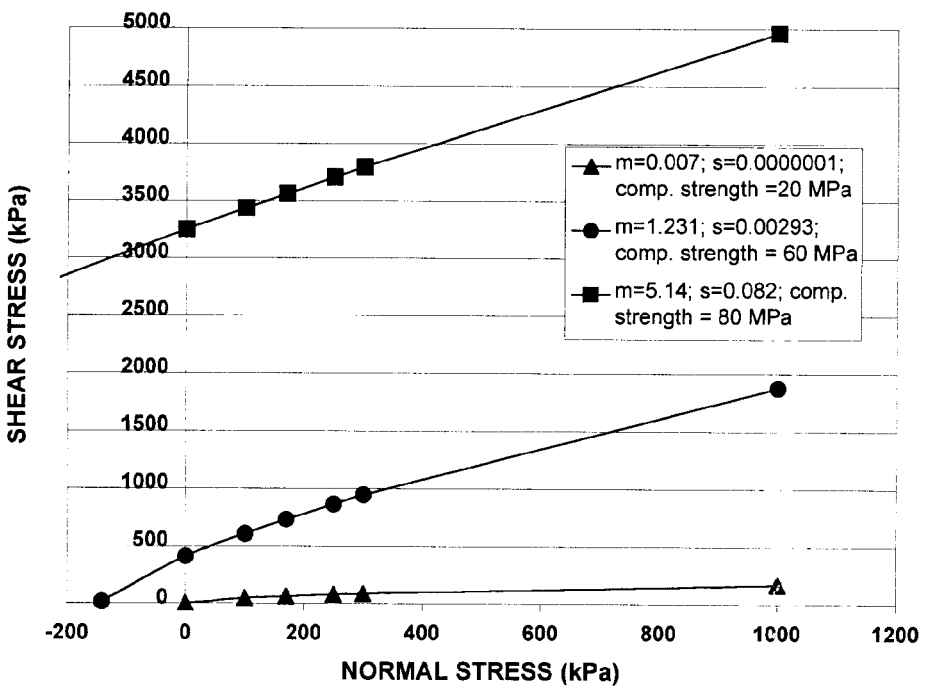

Figure 105. Illustration of use of nonlinear shear strength for three fractured rock mass types.

Table 46. Parameters used to develop strength envelopes in figure 105.

	Curve 1 m=0.007; s=0.0000001; σ_c=20 MPa				Curve 2 m=1.231; s=0.00293; σ_c=60 MPa				Curve 3 m=5.14; s=0.082; σ_c=80 MPa			
σ' (kPa)	h	ϕ'_i	c'_i (kPa)	τ (kPa)	h	ϕ'_i	c'_i (kPa)	τ (kPa)	h	ϕ'_i	c'_i (kPa)	τ (kPa)
-1,000	-	-	-	-	-	-	-	-	1.004	70.5	3,868	1,049
-500	-	-	-	-	-	-	-	-	1.010	65.0	3,326	2,254
0	1.011	64.5	0.8	0.8	1.010	64.8	412.0	412.0	1.017	61.9	3,250	3,250
100	4.820	15.5	18.2	46.1	1.017	61.5	424.8	608.9	1.018	61.4	3,252	3,435
170	7.487	12.3	26.1	63.2	1.023	59.8	441.5	733.1	1.019	61.0	3,255	3,562
250	10.535	10.3	33.6	79.0	1.028	58.1	463.8	865.8	1.020	60.7	3,261	3,705
300	12.439	9.5	37.7	87.7	1.032	57.2	478.6	944.8	1.020	60.4	3,265	3,794
1,000	39.106	5.3	78.4	171.2	1.083	49.6	699.9	1874.6	1.030	57.8	3,373	4,963

6.5.4 Selection of Rock Shear Strength for Design

This section provides a summary of the information presented on the evaluation of shear strength for discontinuities, infillings, and fractured rock masses and some basic recommendations on selection of shear strength for design.

Smooth Discontinuity

As discussed, the shear strength for a smooth discontinuity is represented by a friction angle of the parent rock material. To evaluate the friction angle of this type of discontinuity surface for design, direct shear tests on samples can be performed. Samples can be formed in the laboratory by cutting samples of intact core. The range of typical friction angles provided in table 43 should be used in evaluating measured values.

Rough Discontinuity

The shear strength of a discontinuity surface is related to the roughness of the discontinuity. The magnitude of additional strength resulting from roughness for a given normal load will depend on the roughness profile and the compressive strength of the joint wall. The term JRC $\log_{10}$(JCS/σ') can be used to obtain an estimate of the joint roughness angle, i, for cases where the normal stresses for design are within the range of 1 to 30 percent of the joint compressive strength. These stress ranges are common for many rock slopes. For values less than 1 percent or greater than 30 percent, this procedure is not valid. As previously noted, the maximum value for (ϕ+i) should be 50° and the minimum value is simply the friction angle of the intact rock corresponding to stress and deformation levels sufficiently large to have sheared through all asperities (i.e., zero dilation). A typical value for the basic rock friction (i.e., for a smooth discontinuity) is 30°.

It is noted that for very critical structures, it may be necessary to perform in situ direct shear tests to estimate the shear strength of a discontinuity surface (regardless of whether the surface is smooth, rough, or infilled). Moreover, designers should recognize that accurate measurement of the roughness angle is difficult. Therefore, if design analyses indicate that a relatively large, although seemingly achievable, value for i is required to demonstrate a stable slope (or other structure), than more detailed field measurements of surface roughness (as compared to that obtained using figure 100) are necessary to confirm the value for *i*. For these critical cases, additional effort should be expended to assess the orientation of the discontinuity in relation to design conditions.

Infillings

When a major discontinuity with a significant thickness of filling is encountered in a rock mass in which a slope is to be excavated or where the discontinuity is adversely dipping, the designer should assume that shear failure would occur through this material. Figure 102 presents a general method of characterizing joint fillings according to whether the filling material is undisplaced or displaced and whether the filling material is normally consolidated or overconsolidated. For fillings that are displaced, it should be assumed that the material is at or near residual strength conditions in the field. The residual strength of the material can be evaluated in the laboratory using a direct shear-testing device in which samples of the filling material are reconstituted into the direct shear-testing device at the in situ moisture content. If the filling is judged to be undisplaced, then the designer needs to evaluate whether the proposed structure can be expected to undergo minimal deformations such that the peak strength of the infilling can be used in design. If it becomes critical to evaluate the peak strength of the infilling (including both friction angle and cohesion intercept), it will likely be necessary to perform laboratory or in situ direct shear tests of the infilling material. If laboratory testing is selected, great care must be exercised in obtaining samples for testing. The sample halves should not be displaced relative to each other and the samples should be sealed after collection to minimize moisture losses.

Fractured Rock Masses

In conditions where a fractured rock mass can be described using the RMR, the shear strength can be evaluated using equations 88 to 91. In all cases, however, and for shear strength considerations for smooth discontinuities, rough discontinuities, infillings, and weak rock, the designer should perform a detailed review of previous reports on shear strength evaluations performed in similar geologic environments. Also, the design engineer should perform a sensitivity study to evaluate whether small changes in shear strength (i.e., friction angle, cohesion intercept, roughness angle) result in relatively large changes in a calculated factor of safety. If this is the case, it may be prudent to reevaluate the investigation and testing program and perform high quality laboratory and/or in situ tests.

CHAPTER 7

INTERPRETATION OF PROPERTIES FOR SPECIAL MATERIALS

7.1 INTRODUCTION

This section of the document provides information on the evaluation of properties for several "special" soil and rock deposits that may be encountered on typical transportation projects. The special deposits discussed in this section include: (1) loess; (2) expansive soils; (3) organic soils and peat; (4) colluvium and talus; (5) shales and degradable materials; (6) cemented sands; (7) sensitive clays; and (8) partially saturated soils. A summary of sampling/testing difficulties and engineering characteristics associated with these materials is provided in table 47. The remainder of this chapter provides specific guidance on the evaluation of index and engineering properties for these special materials.

The laboratory and in-situ test methods described previously can be used for the special deposits described herein, subject to various practical limitations. These limitations may include difficulty in obtaining "undisturbed" samples for laboratory testing and problems associated with laboratory testing of partially saturated soils. Because the methods described in chapter 5 generally can be modified to evaluate properties for the special materials discussed herein, the most important aspect of property characterization in these special materials is the ability to identify them.

Table 47. Summary of sampling difficulties and engineering characteristics of special materials.

Soil Description	Soil Identification	Sampling and Testing Difficulties	Engineering Characteristics
Loess and Collapsible Soils	wind-blown sand, silt, and clay with weak binder (loess); silty clays exhibiting loose structure and weak interparticle bonds (collapsible soils)	low moisture content and unit weight, low SPT N values, sensitive structure that may collapse during undisturbed sampling, in-situ testing using CPT and DMT good for in-situ properties	erodible, irrecoverable collapse upon inundation, need to assess material characteristics at design moisture contents
Expansive Soils	clay-rich soils in arid and semi-arid regions that are subject to wet/dry and freeze/thaw cycles resulting in deep desiccation cracking	low moisture content when dry and heavily fissured; difficult to obtain undisturbed sample	undergoes significant recoverable volume changes (both shrinkage and swelling) when moisture content changes; need to assess range of moisture content variation and depth of seasonal moisture content change for design
Organic Soils and Peat	high moisture content relative to plasticity and fibrous texture; high loss of mass upon heating above 440°C	samples may be very soft and fibrous and difficult to recover; in-situ test may over estimate strength due to fibrous nature of material	highly compressible and subject to high secondary compression; potentially corrosive

Table 47. Summary of sampling difficulties and engineering characteristics of special materials (continued).

Soil Description	Soil Identification	Sampling and Testing Difficulties	Engineering Characteristics
Colluvium and Talus	weathered materials that migrate and accumulate on the sides and at the toe of slopes; fine grained material with rock fragments (colluvium); coarse grained material with boulders (talus)	Colluvium: thin lenses of material likely; rock fragments make sampling difficult; test pits and trenches helpful Talus: boulders preclude invasive investigation techniques; geophysical techniques including Spectral Analysis of Surface Waves (SASW) can be used to evaluate talus thickness	Colluvium: can form thin weak layer that influences slope stability; water accumulates at colluvium/rock interface Talus: in-situ material may exist near angle of repose (i.e., FOS=1)
Shale and other Degradable Materials	poorly indurated shale, claystone and mudstone that degrades to the parent soil material upon contact with water and air	in-situ materials may be rock-like and difficult to sample, requiring rock drilling equipment; water introduced during drilling may initiate degradation	material used as rockfill may unexpectedly degrade upon contact with water; slope stability will progressively decrease
Cemented Sands	sandy soil with salt or calcareous bonding at points of grain-to-grain contact; cementing agent may be soluble or insoluble	high blow counts make material appear as dense sand; penetration tests meet refusal; rock coring equipment may be necessary, but water may cause dissolution of binder	soil is brittle and appears to be very strong; potential for collapse or failure if binder is soluble; long-term strength may degrade to that of uncemented sand
Sensitive Clays	marine deposit generally consisting of silty, low-plasticity clays that have been leached of salt resulting in metastable structure	metastable structure makes undisturbed sampling difficult; may require special foil sampler	in-situ soils can collapse with little or no warning due to inherent metastable structure
Partially Saturated Soils	almost all in-situ soils that exist above the groundwater table	partially saturated soils are generally stronger than saturated soils and present no special sampling difficulties as a result of partial saturation; some soils may be brittle at natural moisture contact; in-situ testing may be helpful in establishing existing properties but uncertain drainage conditions during in-situ tests make property evaluation difficult	these soils exist naturally but in-situ strengths may be significantly different than laboratory strengths because lab tests rely on saturated specimens; in-situ tests results may not be applicable for design conditions

7.2 LOESS

7.2.1 Identification of Loess

Collapsible soils generally classify as soils that undergo a relatively significant and sudden decrease in volume when water is introduced. Types of collapsible soil include: (1) loose man-made fills; (2) colluvium (discussed subsequently in section 7.5); and (3) loess. Collapsible soils usually exist in the ground at relatively low values of dry unit weight and moisture content. At these conditions the materials are moderately strong and exhibit a slight but characteristic apparent cohesion. In their natural state, such soils can support moderate loads and undergo relatively small settlements. Upon wetting, however, the cohesion in the soil is lost and large settlements can occur even if the loading remains constant. If subsurface exploration results indicate the presence of collapsible soils, then laboratory testing of undisturbed samples (discussed subsequently) should be performed to quantify the magnitude of volume reduction upon wetting. In this section, the engineering properties of loess are specifically described, although other collapsible soils can be expected to behave similarly.

Loess, which is common in the central U.S. as well as portions of Washington, Oregon, Idaho, and Alaska, is a uniform cohesive wind-blown (i.e., aeolian) soil consisting primarily of silt-sized particles. The apparent cohesion of the material is the result of calcareous clay binder that holds the silt particles together. The clay coating and wind blown formation create a very loose soil structure with little true particle-to-particle contact especially at low confining pressures. For loess (as well as for man-made fills), relatively low SPT N values can be used as an indicator of the potential for collapse. The engineering behavior of loess is affected by whether the loess is sandy, silty, or clayey. Silty loess is characterized as being extremely erodible; sandy and clayey loess are collapsible but are much less erodible than silty loess. Hydrometer testing should be performed on the material passing a No. 200 sieve to evaluate the quantity of sand, silt and clay.

7.2.2 Issues Related to Subsurface Exploration in Loess

Typical drilling and disturbed sampling procedures can be used to obtain loess samples for laboratory sieve analysis, hydrometer, soil classification, and Atterberg limits testing. In regions of the U.S. where loess is present, engineers have developed design charts for cut slopes in loess. These charts are used for relatively low-height cut slopes; however, for designs involving high cut slopes, undisturbed samples should be collected for laboratory strength and consolidation testing. Because of the collapsible nature of loess, it is absolutely critical to use sampling and sample handling procedures that minimize disturbance. Such procedures have been discussed in chapter 4. Oftentimes, critical potential failure surfaces for slope stability analyses are relatively shallow for soils exhibiting relatively small cohesion intercepts such as loess. It is therefore important to accurately characterize the shear strength of the loess at relatively shallow depths. For samples to be collected at shallow depths, it may be prudent to obtain block samples from trenches or test pits.

The shear strength of loess is greatly affected by the degree of saturation of the soil. Therefore, it is essential to develop an accurate estimate of the position of the depth to groundwater and to assess whether the degree of saturation for the deposit will likely change during the design life (i.e., will

there be a change in the position of the groundwater table). If the loess may eventually become saturated, it is explicitly noted that in-situ tests results alone should not be used to develop design parameters. Typical in-situ testing procedures including the SPT, CPT, and DMT can be used to assess the current shear strength properties of the soil deposit only if the current state will be maintained during the project design life. Additionally, in-situ testing procedures should only be used to assess shear strength properties if the results are correlated to laboratory strength tests performed on samples at similar moisture contents and saturation conditions.

7.2.3 Laboratory Strength Testing of Loess

A common issue related to loess (and all soils that are partially saturated), is that the shear strength at low confining pressures, derived primarily by a cohesion intercept, is greatly affected by the moisture content (and saturation condition) of the sample. Saturation of the loess material "softens" the calcareous clay binder and greatly decreases strength. This, in turn, may lead to slope instability and accelerated erosion. Prior to performing laboratory shear strength tests, a critical assessment of the expected saturation conditions of the loess soil for the projected design life must be considered. The saturation condition will be affected by the location of the groundwater table and surface drainage measures. It is conservative to perform CIU triaxial tests on saturated loess samples and use the calculated undrained strength parameters for stability analyses.

7.2.4 Evaluation of Collapse Potential

In addition to potential strength loss due to saturation, loess (and other collapsible soils) can undergo volume change due to collapse of the soil structure when the sample becomes inundated. For situations in which it is necessary to construct a facility in and around collapsible soils such as loess, it is of primary importance to estimate the magnitude of potential collapse that may occur if the soil becomes wetted. To do this, a one-dimensional collapse potential test can be performed in an oedometer on undisturbed or recompacted samples according to ASTM D 5333, "*Standard Test Method for Measurement of Collapse Potential of Soils*". For this test, a sample is placed in an oedometer and the vertical pressure on the sample is increased to the anticipated final loading in the field. At this load level, water is introduced to the sample and the resulting deformation due to collapse is recorded. The percent collapse (%C) is defined as:

$$\%C = \frac{100\,\Delta H_c}{H_o} \qquad \text{(Equation 92)}$$

where ΔH_c is change in height upon wetting and H_o is the initial height of the specimen. For a soil layer with a given thickness, H, the settlement due to collapse, $s_{collapse}$, may be calculated as:

$$s_{collapse} = \frac{(\%C)}{100(H)} \qquad \text{(Equation 93)}$$

The collapse potential (CP) is calculated as the percent collapse (%C) of a soil specimen subjected to a total load of 200 kPa as measured using ASTM D 5333. The CP is an index value used to compare the susceptibility of collapse for various soils. Table 48 provides a relative indication of the degree of severity for various values of CP.

Table 48. Qualitative assessment of collapse potential (after ASTM D 5333).

Collapse Potential (CP)	Severity of Problem
0	None
0.1 to 2%	Slight
2.1 to 6%	Moderate
6.1 to 10%	Moderately Severe
>10%	Severe

7.3 EXPANSIVE SOILS

7.3.1 Identification of Expansive Soils

Expansive soils are typically clayey soils that undergo large volume changes in direct response to moisture changes in the soil. Unlike collapsible soils, expansive soils tend to increase in volume (i.e., swell) as the moisture content of the soil is increased and decrease in volume (i.e., shrink) as the moisture content of the soil is decreased. Although the expansion potential of a soil can be related to many factors (e.g., soil structure and fabric, environmental conditions, etc.), it is primarily controlled by the clay mineralogy. Soils that contain low-plasticity kaolinite will tend to exhibit a lower shrink/swell potential than soils containing high-plasticity montmorillonite. Expansive soils are found throughout the U.S., however, damage caused by expansive clays is most prevalent in California, Wyoming, Colorado, and Texas where the climate is considered to be semi-arid and periods of intense rainfall are followed by long periods of drought. This pattern of wet and dry cycles results in periods of extensive near-surface drying and desiccation crack formation. During intense precipitation, water is added to the deep cracks permitting the soil to swell; upon drying, the soil will shrink. This weather pattern results in cycles of swelling and shrinking that can be detrimental to the performance of pavements, slabs on-grade, and retaining walls.

Deep-seated volume changes in expansive soils are rare. More common are volume changes within the upper few meters of a soil deposit. These upper few meters are more likely to be affected by seasonal moisture content changes due to climatic changes. The zone over which volume changes are most likely to occur is defined as the active zone. The active zone can be evaluated by plotting the moisture content with depth for samples taken during the wet season and for samples taken during the dry season. The depth at which the moisture content becomes nearly constant is the limit of the active zone depth (which is also referred to as the depth of seasonal moisture change). The active zone is an important consideration in foundation design. In the design of piles or drilled shafts, it is important to recognize that full side friction resistance may not be realized in this zone.

As the soil undergoes cycles of shrinking and swelling, it may lose contact with the pile or shaft. Alternatively, as the soil swells, it may impose significant uplift pressures on the foundation element.

In the field, the presence of surface desiccation cracks and/or fissures in a clay deposit is an indication of expansion potential. Experience has indicated that the most problematic expansive near-surface soils are typically highly plastic, stiff, fissured overconsolidated clays. To identify expansive soils in the laboratory, several classification methods have been developed. Currently, there is not a standard classification procedure; different methods are used in various locations across the U.S. Typically, methods include the use of Atterberg Limits and/or clay soil percentage to qualitatively describe a soil as having low, medium, high, or very high expansion potential. Generally, soils with a plasticity index less than 15 percent will not exhibit expansive behavior. For soils with a plasticity index greater than 15 percent, the clay content of the soil should be evaluated in addition to the Atterberg Limits. Figure 106 shows the swelling potential of a remolded soil as related to the soil activity and clay fraction. For the purposes of evaluating expansion potential of a soil, activity can be defined as:

$$\text{Activity (A)} = \frac{\text{Plasticity Index (PI)}}{\text{Clay Fraction (CF)}} \qquad \text{(Equation 94)}$$

where CF is the clay fraction that corresponds to the percentage of particles exhibiting an equivalent diameter (d_s)<0.002 mm as calculated from a hydrometer test performed in accordance with ASTM D422, *Standard Test Method for Particle Size Analysis of Soils.*

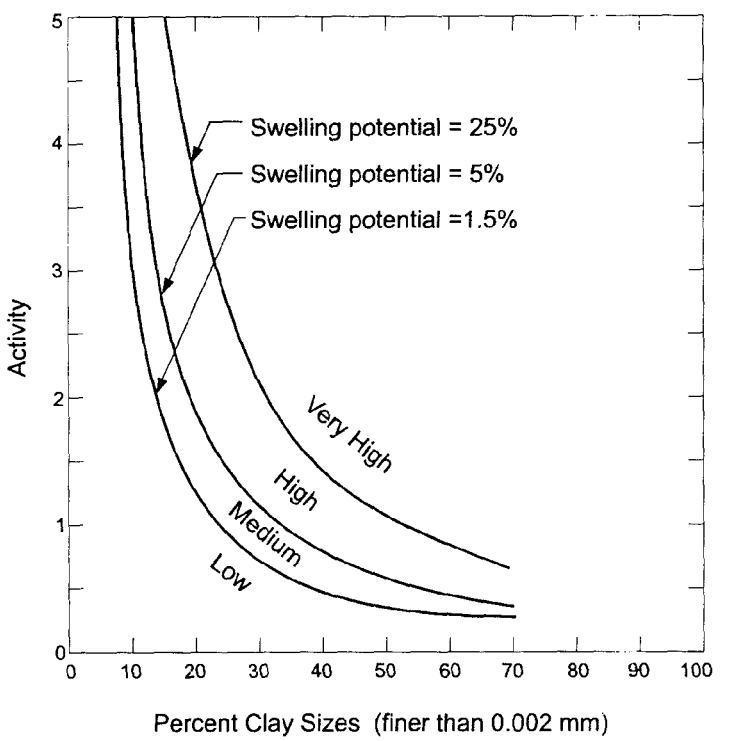

Figure 106. Classification chart for swelling potential (after Seed et al., 1962)

Figure 107 relates expansion potential to liquid limit and in-situ dry density based on the experience of the U.S. Bureau of Reclamation. Additional tests for the qualitative assessment of expansion potential include percent swell calculated from the California Bearing Ratio (CBR) test (ASTM D4429), the free swell test, and the expansion index test. These tests and others are discussed in Chen (1988) and Nelson and Miller (1992). Such correlations are semi-empirical and should only be used for an initial assessment of the expansion potential of a soil. If any of the above tests indicate a potentially expansive soil, laboratory testing, as described in the next section, should be conducted on undisturbed samples to assess the potential swelling pressures of the material.

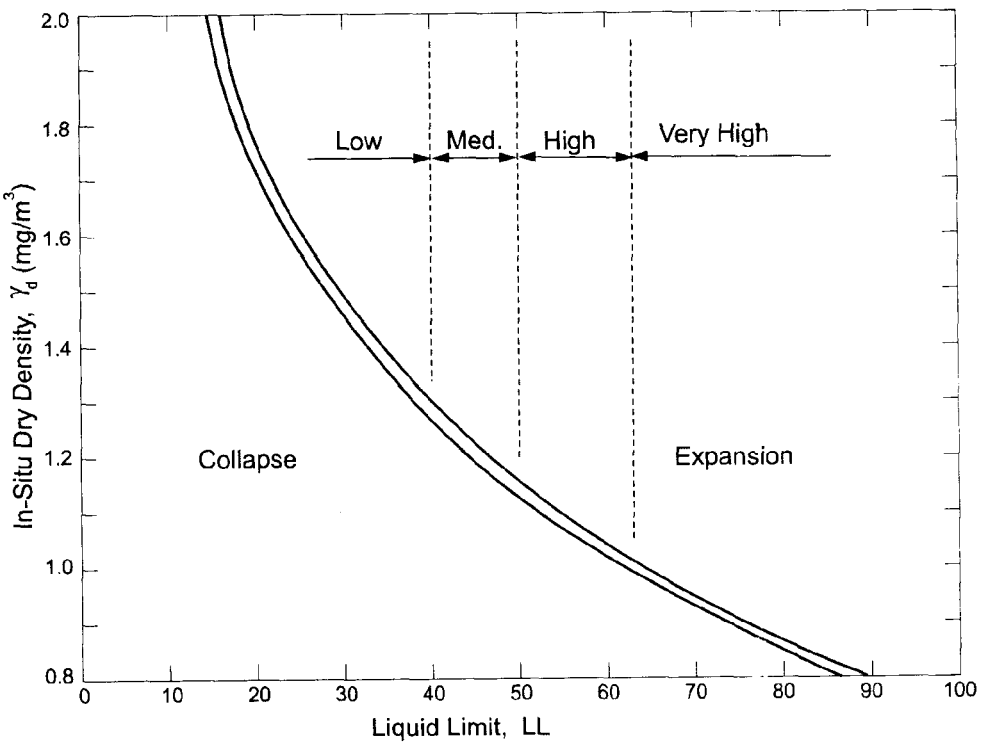

Figure 107. Guide to collapsibility, compressibility, and expansion based on in-situ dry density and liquid limit (after Mitchell and Gardner, 1975 and Gibbs, 1969)

7.3.2 Evaluation of Expansion (Swell) Potential

For situations in which it is necessary to construct a facility in and around expansive soils, it will be necessary to estimate the magnitude of swell (i.e., surface heave) and the corresponding swelling pressures that may occur if the soil becomes wetted. A one-dimensional swell potential test can be performed in an oedometer on undisturbed or recompacted samples according to AASHTO T256 or ASTM D4546, "*Standard Test Method for One-Dimensional Swell or Settlement Potential of Cohesive Soils*". In this test, the swell potential is evaluated by observing and measuring the swell of a laterally confined specimen when it is surcharged and flooded with water. Alternatively, after the

specimen is inundated, the height of the specimen is kept constant by adding load. The swelling pressure is then defined as the vertical stress necessary to maintain zero volume change. Swelling pressures in some expansive soils may be relatively large such that the loads imposed from lightweight structures or pavements do little to counteract swelling (heave).

The use of the one-dimensional swell potential test to evaluate in-situ swell potential of natural and compacted clay soils has limitations including:

- Lateral swell and lateral confining pressure are not simulated in the laboratory. The calculated magnitude of swell in the vertical direction may not be a reliable estimate of soil expansion for structures which are not confined laterally (e.g., bridge abutments);

- The rate of swell calculated in the laboratory will not likely be indicative of rates of swell experienced in the field. Laboratory tests cannot simulate the actual availability of water in the field.

- Long-term swell may be significant for some soils and should be added to primary swell, especially if the design is anticipated to have long-term access to water.

7.3.3 Shear Strength Evaluation of Expansive Soils

As noted previously, potentially problematic expansive soils are located near the ground surface and are heavily overconsolidated. These soils usually contain montmorillonite or other highly plastic mineral and have natural moisture contents equal or less than the plastic limit of the soil. Practically speaking, the shear strength of these materials is relatively high and therefore presents no major concerns relative to, for example, shallow foundation bearing capacity or embankment slope stability. However, if active controls are not incorporated into the design to minimize the potential for large moisture changes and subsequent expansion, then laboratory strength testing needs to be performed for the most critical saturation condition the soil is expected to incur in the field. If the near-surface soils will undergo relatively large seasonal changes in moisture content, then shear strength testing should be performed on specimens at the anticipated highest moisture content. Less conservative shear strength assessments (i.e., shear strengths corresponding to moisture contents other than the highest anticipated) can be used for cases where active measures are incorporated into the design to assure that a reasonably constant moisture content is maintained in the field.

7.4 ORGANIC SOILS AND PEAT

7.4.1 Introduction

Organic soils (i.e., organic clays and organic silts) present similar engineering challenges as soft silts and clays, including low undrained shear strengths and high compressibility. In addition, organic silts and clays undergo significant secondary (or creep) deformations. Such long-term, continuous deformation can present significant maintenance issues for embankments and other structures that may be founded over such materials. Like other organic soils, peats also undergo significant

secondary deformations. In this section, the identification and classification of organic soils and peats are discussed along with information on evaluating shear strength and compression properties for these materials.

7.4.2 Identification of Organic Soils and Peat

Organic soils and peats are evidenced during subsurface exploration based on the presence of decaying vegetative matter and a strong odor. Typically, the materials are greenish, dark gray, or black in color and can have very fibrous structures with wood fragments and plant remains. Disturbed sampling techniques (e.g., auger cuttings that are brought to the surface) are used to provide a visual confirmation of the organic material. In-situ testing can also be used to identify subsurface layers of organic material. For example, these materials can be identified using the CPT by low cone tip resistance and relatively high friction ratios (see figure 38). Classification charts for the CPTu (figure 39) and the DMT (figure 43) have also been developed to identify organic materials and peat. However, it is recommended that disturbed samples be obtained to correlate CPT, CPTu, and DMT readings as it may be difficult to rely solely on in-situ testing. Oftentimes, clayey soils and organic soils do not have significantly different sounding information (i.e., stiffer organic soils will be classified as clays using the DMT classification charts).

Samples of soil layers noted as organic on a boring log should be tested in the laboratory to evaluate the percentage of organic matter. The non-organic portion of the sample will control the engineering behavior of soils when the organic content is less than approximately 20 percent (Arman, 1970). Organic content is evaluated in the laboratory using one of several methods available in AASHTO T194 and ASTM D 2974, "*Standard Test Method for Moisture, Ash, and Organic Matter of Peat Material and Other Organic Soils.*" In this test, a sample of the material is dried, weighed, and then heated at high temperature. After cooling, the sample is reweighed and the loss of mass is calculated. After heating, ash is left over; therefore, organic content is equal to $100\text{-}A_c$ where A_c is the percentage of ash. The liquid limit test can also be used as a qualitative index of organic matter by comparing the liquid limit value for a sample that was dried before testing to the liquid limit value for a sample that was not dried. If the liquid limit of the sample that was dried is less than 75 percent of the value of the liquid limit for the sample that was not dried then the soil may be classified as organic.

Landva et al. (1983) developed a system for classifying organic soils and peats. In this system, peats and organic soils are divided into four groups: (1) peats (Pt); (2) peaty organic soils (PtO); (3) organic soils (O); and (4) silts and clays with organic content (MO and CO, respectively). Table 49 summarizes the typical ranges of the properties used in this classification system.

Table 49. Organic soils and peat classification properties (after Landva et al., 1983).

Material	A_c	Moisture Content (w_n)	Specific Gravity (G_s)	Fiber Content
Pt	<20%	>500%	< 1.7	> 50%
PtO	20 - 40%	150 - 800%	1.6 – 1.9	<50%
O	40 - 95%	100 – 500%	> 1.7	Insignificant
MO, CO	95 - 99%	<100%	> 2.4	None

7.4.3 Issues Related to Subsurface Exploration and Sampling of Organic Soils and Peat

Organic soils and non-fibrous peats can be very weak and compressible due to a high moisture content and large void ratio. Like most soft clays, it can be difficult to obtain undisturbed samples of organic soils for laboratory performance testing. Thin walled fixed piston samplers are most suitable for undisturbed sampling of organic soils. Undisturbed sampling in fibrous peats, however, is very difficult due to the likely compression of the peat fibers during sampler advancement. Where undisturbed sampling with piston samplers is attempted, it is critical that the sampler have a sharp edge. If possible, fibrous peats should be sampled using block-sampling techniques.

Engineering properties of peats and organic soils can vary significantly both spatially and with depth. Samples obtained within a few feet of each other may exhibit vastly different behaviors during loading. Therefore, subsurface investigations that encounter organic soils and peats should involve more sampling and testing as compared to inorganic soils to adequately characterize the materials.

7.4.4 Shear Strength of Organic Soils and Peats

Like all soils, the shear strength of organic soils is directly related to the effective stress in the ground and stress history of the deposit. Since organic soils are relatively lightweight (i.e., low dry density), saturated, and have no significant stress history, their strengths are usually very low. Where good quality undisturbed samples can be obtained, laboratory triaxial strength testing should be performed to obtain undrained shear strength information for design. Like most clayey soils, organic soils typically have very low hydraulic conductivities, therefore the assumption of undrained failure imposed by the CPT, CPTu, and VST allow for the use of these in-situ testing devices as a means to correlate undrained shear strength. The relationships given in table 33 for these in-situ tests can be used for testing in organic soils. The various factors (i.e., N_k, μ) should be developed based on site-specific data and laboratory triaxial data for a few samples. Correlations based on cone tip resistance may be difficult to use since it is likely that the tip resistance in organic soils will be extremely low, thus requiring high resolution load cells.

In using the vane shear test in organic soils, it is noted that the time to failure in the test will have an impact on the measured vane shear strength. Also, organic soils may possess enough fibers to act as localized reinforcement and lead to vane shear strengths that are too high. For these reasons, use of the equation $s_u=\mu s_{u(VST)}$ may overestimate the undrained strength of the organic clay or silt. Because of fiber content, the vane shear test is inappropriate for relatively high fiber organic soils and for fibrous peats. Moreover, due to the fibrous nature of such soils, hydraulic conductivities are relatively large (compared to silts and clays), and the appropriate shear strength for design may be more appropriately defined using drained strength parameters, as discussed below.

In fibrous peats, the fibers tend to act as tensile reinforcement in the soil. Therefore, the strength behavior is almost entirely frictional with large friction angles (i.e., greater than 35°). However, the shearing resistance varies significantly depending on the orientation of the failure plane relative to the general alignment of the fibers. Generally, the fibers are oriented horizontally. Therefore, failure planes in triaxial test samples may intersect the fibers resulting in high shear strengths. It is also noted that peat samples may require significant deformations (i.e., greater than 20 percent axial strain in drained laboratory triaxial tests) to mobilize the full strength of the material. This needs to be considered in stability analysis so that the mobilized strength for the analysis is consistent with the expected level of deformation.

7.4.5 Compressibility of Organic Soils and Peats

If a shallow foundation is to be constructed in and around an area with a near-surface deposit of organic soil or peat, the layer will likely be excavated and replaced prior to foundation construction. For embankments and foundations that are constructed over organic soil or peat layers, primary settlement will occur over a relatively short time (i.e., within a few days or months), and the majority of the total settlements will result from the long-term secondary compression of these soils. Therefore, secondary settlement will be the dominant component of settlement during the design life of the structure and should be evaluated as presented in section 5.4.2.7.

Because of high in-situ void ratios, organic soils and peats will have high C_c values (i.e., >1). Figure 108 can be used to estimate C_c values for clays, silts, and peats based on in-situ moisture content. As discussed in chapter 5, C_α/C_c for organic silts and clays is approximately 0.05 ± 0.01 and for peats, the value is approximately 0.06 ± 0.01, the highest value for geotechnical materials (Mesri et al., 1997). It is noted that standard one-dimensional oedometer tests and interpretation methods (as described in chapter 5) are used to evaluate C_c and C_α in organic soils and peats. In peaty soils, it may be difficult to identify the time to the end of primary consolidation, t_p, since the transition from primary to secondary compression is not easily identified using standard interpretation methods. However, reasonably accurate estimates of C_α can still be made. The maximum vertical effective stress in the ground needs to be assessed so that a reasonably conservative estimate of secondary compression can be assessed. Like other soils, organic soils and peats will show an increase in C_α for stress levels just in excess of the preconsolidation stress, σ_p'. It is therefore important to perform laboratory oedometer tests on organic soils and peats to stress levels greater than σ_p'. Calculated values of C_α will likely decrease for stress levels significantly greater than σ_p', so tests should be performed to sufficiently high loads to ensure that the maximum value for C_α is calculated.

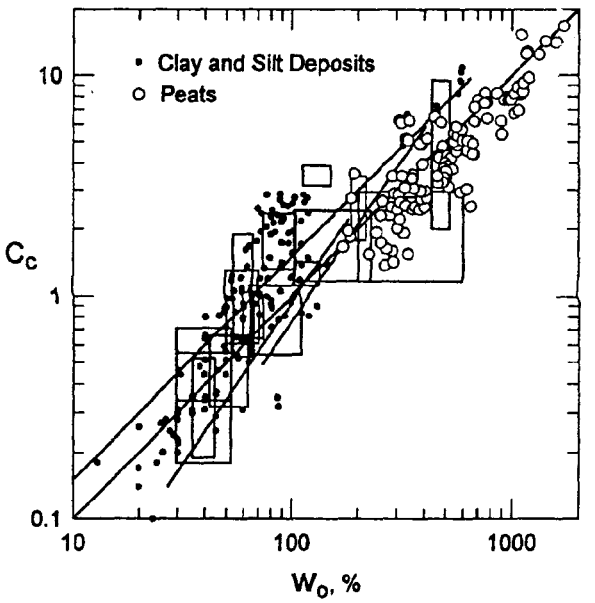

Figure 108. Values of natural water content and compression index for peats, clays, and silts (after Mesri, Stark, Ajlouni, and Chen, 1997).

7.5 COLLUVIUM AND TALUS

7.5.1 Identification of Colluvium and Talus

Colluvium (colluvial soil) and talus are generally relatively loose deposits found near the base of slopes and may accumulate in valleys, swales, or other low-lying topographic features. Colluvial soils generally result from a two-stage process of: (1) in place weathering of the parent rock; and (2) subsequent migration downslope primarily by gravity through creep. Colluvium commonly consists of rock fragments in a heterogeneous clayey to sandy matrix. Talus, like colluvium, also accumulates at the base of slopes, but generally consists of the mechanically weathered granular component of the parent rock. Talus slopes are commonly characterized as well-graded boulders to sand- or silt-sized particles. In general, colluvium occurs in temperate and humid environments while talus predominantly occurs in arid and semi-arid regions. The characteristics of the parent bedrock and the climate in which the weathering and migration/transportation take place determine the characteristics of the colluvium and talus deposits.

Accumulations of colluvium and talus on the sideslopes and at the base of sideslopes are often associated with slope stability problems. To route transportation passageways, cut slopes often have to be made in colluvium and talus deposits located near the base of a slope. In many cases, the cut slope often exposes the colluvium/talus material. Because these materials typically form by migration and sliding along the slope, they are often only marginally stable in their natural state. Therefore, the cut slopes made in these deposits tend to disrupt the natural equilibrium, thus requiring aggressive monitoring and maintenance.

7.5.2 Issues Related to Subsurface Exploration and Testing in Colluvium

Typical drilling and sampling techniques can be utilized in colluvium to obtain samples for evaluating the physical characteristics of the material, provided it consists primarily of fine-grained particles. In some cases, colluvium exists as a massive deposit upward of 5 meters in thickness, while in other cases, the colluvium may occur as only a relatively thin (i.e., <1-m thick) weathered zone. In cases where the colluvial material occurs as only relatively thin lenses within a soil stratum and is highly weathered, it is easy to drill through the material and not realize its presence. Drilling and sampling in colluvial soils with large rock fragments can prove to be difficult. In addition to the above concerns, potential access problems due to relatively steep slopes and marginal stability and safety concerns typically make drilling and sampling in colluvium relatively difficult and expensive.

Test pits and trenches represent economical alternative exploration methods for colluvium. This approach allows visual observation of the subsurface conditions in these materials. Test pits and trenches are typically backhoe-excavated; however, shallow hand-excavated test pits can provide subsurface data in inaccessible areas. Undisturbed block samples of colluvium can be cut from the sidewalls of the test pits and trenches. In cases where rock fragments do not preclude sampling, the colluvium may be sampled by manually advancing (i.e., pushing or driving) Shelby tubes or other types of sampling tubes from the sidewalls of the test pit. Test pits and trenches can also be used to evaluate the depth to bedrock and the groundwater conditions within the colluvium.

Inclinometers and piezometers can be used as another means to characterize the engineering performance of in-situ colluvium deposits. Inclinometers socketed into underlying bedrock can be used to assess whether the colluvium is actively creeping down the slope. The measured displacements provide an indication of the relative stability of the colluvial soil slope. Piezometers installed at various depths within the colluvium, especially at the colluvium/bedrock interface, provide vital information regarding the groundwater conditions within the colluvium. It is common that the colluvium/rock interface provides a shallow aquitard that allows water to accumulate in the colluvium at the interface. This water can foster the further degradation of the parent rock (particularly if the underlying rock is poorly indurated shale and/or mudstone) and may cause seepage to occur along the interface. Both of these factors tend to reduce stability of the colluvium veneer along the slope.

7.5.3 Issues Related to Subsurface Exploration and Testing in Talus

Because the materials in talus slopes includes particles that range from silt and sand to boulders, site exploration is extremely difficult. Although individual samples of talus components may be recovered, they are often of little use because these small samples are indicative of only the matrix component of the talus, and are not at all representative of the mass itself. Thus, characterizing the global behavior or global properties is extremely difficult when using conventional drilling and sampling equipment. Similarly, any in-situ test requiring penetration is not useful because the penetration would likely meet refusal on a large rock/boulder.

The occurrence of talus can probably best be identified by the use of aerial photographs and site reconnaissance. Site subsurface characterization is probably best performed by geophysical methods that are non-invasive (e.g., SASW). In most cases, foundation support will need to be achieved in competent rock below the talus material. For this reason, geophysical techniques that can identify the depth to competent rock are particularly useful, especially where characterization over great lengths is required.

7.5.4 Compressibility of Colluvium and Talus

The compressibility of the colluvial soils can generally be assessed in the laboratory using the standard oedeometer test, provided that undisturbed samples can be obtained in the field. Additionally, settlements for these materials can be calculated based on the results of geophysical tests and the use of elastic theory as discussed in section 5.5. The shear wave velocity can be obtained from geophysical testing and provides a reliable means of evaluating the small strain shear modulus of a soil.

Talus often exists in-situ as a loose mixture of granular material and boulders that may experience settlements during construction. Compression properties are difficult to assess due to the "scale" of the materials (i.e., large boulders to fine-grained soils) and the heterogeneity of the material (i.e., large rocks and large void spaces). The void spaces create the potential for large concrete over pours and/or lost grout in the construction of drilled shafts and anchors. Therefore, the assumed side friction capacity of the design may not be realized. Because of this and the compression potential of the material, foundation systems should not be designed to derive resistance from talus materials and should, instead, be founded in competent material below the talus.

7.5.5 Shear Strength of Colluvium and Talus

Shear strength of colluvium can be assessed from laboratory tests on undisturbed samples. In some cases, however, the colluvium is relatively strong and it is instead the colluvial material and potentially weathered rock at the colluvial soil/rock interface that represents the weakest material and where the greatest potential for sliding instability exists. As mentioned previously, water may accumulate at the colluvium/rock interface, weakening the soil and rock materials at this interface.

The shear strength of the material at the colluvium/rock interface can be evaluated by performing laboratory direct shear tests on remolded samples of the material at the expected in-situ moisture content. In the test, residual conditions should be evaluated, especially if there is a potential that the material had been previously displaced as a result of landsliding or creep. Figure 76 can be used to make preliminary estimates of the drained residual friction angle.

A reliable method to evaluate the strength of both colluvium and talus is to back analyze a failed or failing slope in close proximity to the project location. For talus materials, because of sampling difficulties, back analysis is often the only method for evaluating shear strength. Back analyses involve performing stability analyses where the values of the cohesion intercept and friction angle

are modified to achieve a factor of safety of 1.0. This method for determining shear strengths is only accurate if a thorough assessment of the slope geometry and groundwater table are made. Additionally, the depth to competent rock and the location of a known or anticipated slip surface should be assessed via borings or by geophysical methods.

7.6 SHALES AND DEGRADABLE MATERIALS

7.6.1 Identification of Degradable Materials

On many transportation projects, construction activities involve the use of potentially degradable materials. Additionally, in many parts of the U.S., foundations are commonly built on these materials. Although the material may, at first, exhibit rock-like characteristics, it has the potential to degrade to soil-size particles. The gradual but ultimate degradation of the rock to the original parent soil material can occur within minutes or after several years of exposure to air and/or water. Shale, the most common member of this family of materials, can generically be considered to include claystone, siltstone, and mudstone.

In many parts of the U.S., high-quality granular material is not locally available for use as borrow material in the construction of earth embankments and/or rockfill. As a result, degradable materials that, at first, appear to be competent granular materials are used. However, once in contact with water, these materials may degrade causing problems and/or failures during the service life of the structure. Foundations built on these materials are also at risk for failure. Drilling and other construction activities often introduce water, initiating the degradation process. Deep foundations, especially rock-socketed drilled shafts, which may be designed considering intimate contact with and support from the rock interface may fail as the materials degrade and contact is lost. Additionally, highway cuts are often excavated in degradable rock. The exposure of the cut to atmospheric conditions may result in significant degradation during the service life of the cut slope.

Many rock types are prone to degradation when exposed to the cyclic wet/dry and freeze/thaw weathering processes. Rock types that are particularly susceptible to degradation due to these processes are poorly indurated shale and claystone exhibiting high clay content. The degradation can take the form of swelling, weakening, and ultimately disintegration. The effect of degradation on slope stability can range from surficial sloughing and gradual retreat of the face, to catastrophic slope failures resulting from the significant loss of strength. In sedimentary rock formations comprising alternating beds of resistant sandstone and relatively degradable shale, the weathering process can develop overhangs in the sandstone and produce a rockfall hazard. In shallow foundations, the assumed bearing capacity of the material may decrease as the foundation material degrades resulting in settlements and/or foundation failures. In deep foundations, as discussed above, the assumed end bearing and/or side friction may decrease over time.

When potentially degradable materials are encountered, it is essential to establish the anticipated competency of the materials over the service life of the project. An assessment of the time required for significant degradation relative to the service life of the structure should be evaluated. Commonly, the point load test, the slake durability test, and the jar slake test are used to make this

assessment. Classification systems and index values have also been developed for identifying the behavior of shales (see chapter 21 of TRB, 1996).

7.6.2 Slake Durability Test

A simple index test to assess the tendency of rock to weather and degrade is the slake durability test, ASTM D4644, *"Standard Test Method for Slake Durability of Shales and Similar Weak Rocks"*. The test procedure includes placing the sample in a 2 mm square wire mesh drum and drying it in an oven to constant weight at 110°C. The test sample should consist of ten representative, intact, approximately equidimensional fragments weighing 40 to 60 grams each. The wire mesh drum is then partially submerged in water and rotated at 20 revolutions per minute for a period of 10 minutes. The drum and its contents are then dried a second time and the loss of weight is recorded. The test cycle is then repeated a second time and the slake durability index, I_D, is calculated as the ratio (reported as a percent) of final to initial dry weights of the sample. Earlier versions of this test (and some classification index systems) included up to five wet/dry cycles. The slake durability index is usually combined with other indices to formally assess rock durability. In general, a high slake durability index indicates that the rock is not particularly susceptible to degradation when exposed. For highly degradable rocks (i.e., a low I_d), it is useful to carry out soil classification tests such as Atterberg limits and X-ray diffraction tests to identify clay mineral types and evaluate if swelling clays (e.g., montmorillonites) are present and responsible for the degradation.

7.6.3 Jar Slake Test

Like the slake durability test, the jar slake test requires that pieces of the rock be immersed in water and that evidence of degradation be noted. This test is somewhat easier and less quantitative than the slake durability test. The procedure for the jar slake test for shale materials is summarized as follows (TRB, 1996):

- A piece of oven-dried shale is immersed in enough water to cover it by 15 mm.
- After immersion, the piece is observed continuously for the first 10 minutes, followed by an additional 20 minutes of discontinuous, but careful, monitoring. If a reaction between the water and the rock is to occur, it will usually occur during this time period. A final observation of the condition of the rock is made after 24 hours.
- Based on the visual observations, the Jar Slake Index, I_J, is established using the criteria described in table 50.

Table 50. Evaluation of jar slake index, I_J.

Jar Slake Index, I_J	General behavior during test
1	Degrades rapidly to a pile of flakes or mud
2	Breaks rapidly and/or forms many chips
3	Breaks slowly and/or forms few chips
4	Breaks rapidly and/or develops several fractures
5	Breaks slowly and/or develops few fractures
6	No change

Like the slake durability index, the jar slake index is commonly used in combination with other indices to systematically classify the durability of the rock. This is described in section 7.6.5.

7.6.4 Point-Load Test

The point load test was initially developed to estimate the compressive strength of rock in which both rock core samples and fractured rock can be tested. However, because the testing equipment is portable and the test itself is inexpensive, the point load test is also used to assess the degradation potential of materials such as shales. The test is conducted by compressing a piece of rock to failure between two points on cone-shaped platens. Each of the cone points has a 5-mm radius of curvature and the cone bodies themselves include a 60° apex angle. The point load strength, I_s is calculated as:

$$I_s = \frac{P}{D^2} \qquad \text{(Equation 95)}$$

where P is the point load breaking strength and D is the distance between the platens (i.e., the approximate diameter of the rock). Details of this test are provided in FHWA HI-99-007 (1998) and in Section 4.13.2. Using the point load strength, the material can be classified as durable and strong for $I_S > 6$ MPa, conditionally durable for 2 MPa $< I_S < 6$ MPa, or non-durable and weak for $I_S < 2$ MPa (after Welsh et al., 1991). Because the point load test was not specifically developed for estimating the degradation potential of shales, it should only be used to make preliminary assessments of degradation potential. If the test indicates a potential for degradation, further testing should be conducted in the laboratory using the methods discussed previously.

7.6.5 Use of Shale Material

The laboratory and field index tests described above can be used to assess whether a shale (or other potentially degradable material) may be considered to be rockfill, soil, or as intermediate material between soil and rockfill. Intermediate materials are considered to be non-durable materials and

need to be conditioned to be soil-like prior to use as a construction material. Strohm et al. (1978) developed the criteria presented in table 51 based on values of I_D and I_J. Other shale rating systems and rock durability classification criteria are available to assist the designer.

Table 51. Criteria for rockfill materials (after Strohm et al., 1978).

Slake Durability Index, I_D	Jar Slake Index, I_J	Category
>90	=6	Durable rockfill materials, if minus gravel-sized fraction is less than 20 to 30 percent
60 to 90	3 to 5	Hard, Non-durable intermediate material
<60	≤2	Soft, non-durable materials treated as soil

7.7 CEMENTED SANDS

7.7.1 Identification of Cemented Sands

Cemented sands are naturally occurring granular materials that have a cementing material either in the void space between individual grains or at the points of grain-to-grain contact. The result of the cementing action is that the sand exhibits a true cohesion (i.e., a component of shear strength that is independent of confining pressure). As a result, cemented sands are usually "stronger" than uncemented sands. This increased strength, however, presents several problematic characteristics: (1) the cementing agent may be so weak that it is destroyed during sampling, thus resulting in a poor characterization of the in-situ deposit; (2) the cementing agent may be soluble or extremely weak, such that the cohesion cannot be relied upon for long-term design conditions; and (3) at failure, the cemented sand exhibits a brittle load-deformation response that explicitly must be recognized.

The primary consequence of cementation is to increase strength and reduce compressibility relative to uncemented materials. Thus, from this perspective, it is recognized that cementation improves the engineering characteristics of the deposit. Weakly cemented sands can form due to grain-to-grain point-contact welding as a result of aging or from a clay-silt binder that accompanies a wind-blown dune deposit. At the other extreme, the cemented sand can be characterized as weak sandstone, where a carbonate bond may occur at the grain contacts. Regardless of the method of origin, cementation results in stiff, but brittle, load-deformation behavior. Such behavior must be carefully assessed when evaluating shear strength for design, as discussed subsequently.

7.7.2 Issues Related to Subsurface Exploration and Testing in Cemented Sands

Cemented sands often present sampling difficulties. If the materials are weakly cemented, the cemented structure might not be recognized when conventional soil sampling techniques are attempted. In these cases, the SPT blow counts may appear to be uncharacteristically high, but the recovered materials may appear to be uncemented. This is because the relatively weak cementing materials can be easily disrupted during drilling and cemented sand, while relatively weak, may be sufficient enough to preclude sampling using Shelby tubes. In both of these cases, the driving/pushing resistance is mistakenly interpreted as being characteristic of dense uncemented sands. At low working stress levels, this mischaracterization may be conservative; but at high working stresses, a dense sand may, in fact be stronger than a loose cemented sand, resulting in unconservative estimates of strength. At the other extreme, if the subsurface materials are characterized as soft rocks, conventional rock sampling/coring techniques may result in very poor (if any) sample recovery, due to the disturbance induced by the drilling equipment and the effects of water on the cemented structure.

It is often possible to correctly identify and characterize cemented sands through careful observation during field reconnaissance, drilling, and sampling. The easiest technique to correctly identify cemented materials is to visually observe an exposed excavation or natural cut (e.g., stream bank erosion) in the material. For shallow deposits, test pits permit observation of the material and allow access for recovery of a block sample. For deep deposits, the following two techniques can be employed by the field engineer or geologist: (1) carefully observe the recovered cuttings and attempt to recover small pieces of the cemented materials that are returned within the matrix of uncemented sands; and (2) be observant of the potential reasons for "anomalous" behavior during drilling and sampling (e.g., uncharacteristically high blow counts during soil sampling, poor core recovery despite relatively uniform moderate drilling resistance, etc.). In some cases, double coring techniques employing Pitcher barrel samplers (soils) and Dennison samplers (rock) can be used to provide representative samples of deep deposits for visual characterization of the cemented nature of the material.

With regards to laboratory testing, it is necessary to be extremely careful when extruding and handling the cemented materials. The relatively weak and brittle cementing agent can yield to even gentle fingertip pressure during handling and trimming. If possible, the recovered cemented materials should not be trimmed, but rather tested at the as-recovered diameter. For recovered block samples, the material should be carefully "shaved" in the laboratory to obtain a specimen suitable for testing.

7.7.3 Interpretation of Laboratory and Field Testing Results in Cemented Sands

As mentioned previously, an indicator of cemented sands is uncharacteristic or unanticipated behavior. Specifically, unusually high blow counts and/or poor recovery are characteristics of cemented sands. There are, however, several other reasons for high blow counts and poor recovery, so these by themselves cannot be taken as reliable indicators of the presence of cemented sands. If sufficient materials are recovered to allow laboratory testing, index tests and performance tests can

reliably identify the existence and the character of the cemented material. In the case of index tests, a simple unit weight determination on an undisturbed specimen can quickly and reliably identify whether the material is as dense as the high blowcount response would indicate. It may be possible to either immerse a sample in water or simply add water to a piece of the intact sample to assess whether the cementing agent is soluble or if the material softens when inundated with water. If either of these responses is identified, a careful assessment must be made of whether the service conditions will result in the introduction of (and the effect of) water.

If specific strength/deformation characteristics are needed, laboratory triaxial shear or direct shear testing is recommended. Because of the sensitive and brittle nature of the cementing materials these tests must be carefully conducted and interpreted. It is important that representative samples be selected for laboratory testing, because one of the effects of sample disturbance is that only the strongest materials may survive the drilling/sampling process. Block sampling has been shown to be an effective technique for obtaining samples of cemented sands suitable for laboratory testing. In-situ testing using a pressuremeter has also been used effectively to provide quantitative strength and stiffness information. Other in-situ testing techniques, specifically the SPT and dilatometer, provide useful qualitative results, but must be calibrated to specific site/material conditions to provide quantitative information.

The load versus deformation response of cemented sands must also be reviewed from the perspective of the brittle character of the material. At low confining pressures, the response due to cementation will dominate the frictional response. This results in an initial stiff response due to the cementation, followed by a strain softening response associated with the frictional characteristics of the sand after rupture of the cementing bonds. As the confining pressure increases for a specific degree of cementation, the difference between the peak and post-peak strengths decrease. At the limit at high confining pressures, it is possible that application of the confining pressure may result is disruption of cementing bonds, resulting in a load-deformation response that is consistent with that of an uncemented sand. The lesson from this general response characteristic is that the range of test confining pressures must be carefully selected to match the anticipated service conditions. Additionally, because the cementing bonds can be disrupted at low strains, the anticipated strains under the anticipated working stress should be assessed to allow the engineer to decide whether the peak (i.e., cemented) or the large-displacement (i.e., uncemented) strengths should be used in design. As an example, large-displacement pile driven into calcium carbonate sands will likely exhibit frictional capacities significantly less than that which would be predicted based on peak strengths derived from undisturbed samples. Driving piles can destroy bonds and disrupt the delicate structure of the cemented material (see Focht, 1994).

7.8 SENSITIVE CLAYS

7.8.1 Identification of Sensitive Clays

Most geotechnical engineers are aware of the strain softening response (i.e., a peak strength followed by a reduction in strength with ongoing deformation) of soils under drained loading. In general, over-consolidated clays, dense sands, and most soils tested under low confining pressures tend to

exhibit a strain softening response under drained loading conditions. This behavior is due to the dilation (i.e., positive volume change) characteristic of these materials. For these soils under undrained loading conditions the strain softening behavior generally is not observed, due primarily to the generation of negative pore water pressure that prohibits the increase in volume. In two notable soils, however, there is a post-peak reduction in the undrained strength: (1) extremely loose sands; and (2) sensitive clays. Extremely loose sands that tend to strain soften can be subject to catastrophic static liquefaction. Fortunately, the natural occurrence of these materials is very rare, as they are usually associated with hydraulically filled structures. Sensitive clays, while naturally occurring, are generally confined to specific geographic regions of the world where there was extensive glaciation followed by isostatic uplift. The strain softening response in undrained shear loading for both loose hydraulically placed sands and sensitive clays are attributed to their unique metastable structure. Because strain-softening loose sands rarely are encountered, and are almost never encountered as part of highway construction, additional discussion is not provided for these materials. Sensitive clays, while confined to specific geographically regions, warrant a brief discussion in this document.

The metastable structure of sensitive clays is established when relatively low plasticity clays are deposited in brackish (i.e., salty) waters in a flocculated particle orientation. The resulting high void ratio soil structure, due to the edge-to-face alignment of the clay plates, is stable although the soils in the deposit have high natural moisture content and a moderately high liquidity index. In this state, the clay is weak, but not likely sensitive. The sensitive characteristics are introduced when fresh water is leached through the uplifted deposit, replacing the brackish water with the fresh water. As a result of the replacement with fresh water, the electro-chemical interaction between clay plates is altered to the point where the Atterberg limits reduce and the liquidity index increases. In this state, the clay "favors" a dispersed soil structure; however, the existing flocculated structure is maintained until some mechanical action causes a disruption of the structure (i.e., the peak strength is mobilized). Because the disturbed clay now prefers a dispersed soil structure, there is a significant reduction in the post-peak shear strength due to the large amount of unbound pore water associated with the dispersed soil structure.

7.8.2 Issues Related to Subsurface Exploration and Testing in Sensitive Clays

Sampling and laboratory testing of sensitive clays is extremely difficult, primarily because the disturbance typical of conventional sampling and testing techniques may be sufficient to disrupt the in-situ soil structure. Essentially, this disturbance has the effect of mobilizing the peak strength of the material. In the extreme case of the glacial quick clays, the in-situ material may currently exist at a liquidity index that is greater than unity (i.e., the in-situ moisture content is greater than the liquid limit). Therefore, if the sample is disturbed to a degree sufficient to disrupt the in-situ soil structure, the once-solid soil will behave as a viscous liquid.

When sampling and testing sensitive soils, extreme care must be exercised to minimize the potential for disrupting the in-situ soil structure. Conventional thin-walled tube samplers that are deployed rapidly may be appropriate for moderately sensitive materials. In some cases, using samplers larger than the conventional 3-inch diameter Shelby tubes will provide better recovery of less disturbed

material. Regardless of the sample size, rapid sampler deployment has been shown to be effective at minimizing disturbance induced by friction along the walls of the sampler. In very sensitive soils, specially developed samplers that rely on foil liners to encapsulate the samples are used. This equipment is specialized, but may be common in areas of the country where sensitive clays are encountered (e.g., the northeastern seaboard, St. Lawrence Seaway valley, etc.). For shallow deposits, excavation of block samples is an excellent alternative. The key to laboratory testing follows the guidelines from field sampling, that is, handle the material with extreme care. The samples should not be trimmed to a smaller diameter. It is best to extrude the sample directly onto the testing pedestal and provide confinement using a thin membrane.

Field testing in sensitive soils using a field vane is an excellent alternative (or compliment) to laboratory testing. Local experience has been developed in parts of the country where sensitive soils are common. Specifically, the size of the vane and the methods for deployment should be matched to the strength of the material. One of the advantages of this type of field testing is that the equipment can be extremely portable and easy to hand-deploy over sensitive (or very soft) materials. Similarly, there are encouraging results from other types of in-situ tests, specifically the piezocone penetrometer (CPTu) and flat-plate dilatometer (DMT), conducted in soft and/or sensitive soils. The key to testing using these devices is to match the resolution of the testing equipment (i.e., capacity of load cells, membrane stiffness calibration, etc.) to the anticipated strength of the tested materials.

7.8.3 Interpretation of Laboratory and Field Testing Results in Sensitive Soils

Regarding the interpretation of the laboratory and field tests conducted on or in soft and/or sensitive soils, it is important to recognize that the stress-strain behavior of the soil is a function of the soil structure, and that the structure can potentially change during the test. In the cases of both consolidation and shear testing, the change in structure can result in the apparent "collapse" of the initial structure, meaning that there are two distinct and different regions of behavior associated with the pre-collapse and the post-collapse structure. When interpreting the test results, it is important to recognize whether a structure change occurred during the test. For example, in moderately sensitive materials, the specimen may have been sufficiently disturbed to mobilize the peak strength prior to conducting the laboratory test. In these cases, the laboratory test results will need to be associated with a post-peak response. It is explicitly noted that because of the structure-specific test results, most results of laboratory tests on sensitive soils cannot be normalized. Any test that requires confinement or testing above the in-situ state of stress is prone to initiate irreversible structural changes in the soil. For these reasons, it is recommended that field vane shear tests always be conducted in soft and/or sensitive soils. This test has been widely used throughout the world and can be modified for almost any soft soil condition. In addition, the test can be readily used to assess sensitivity because the peak- and post-peak strengths are explicitly provided.

7.9 PARTIALLLY SATURATED SOILS

7.9.1 Identification of Partially Saturated Soils

There has been a recent interest in understanding the behavior of partially saturated (aka "unsaturated") soils. This interest generally focuses on the relative roles of pore water and pore air pressures in determining the behavior of soil. The profession has learned from this focused interest that the roles of the pore fluids can change and are dependent on the relative moisture content of the tested material. The implications from these studies is that it may be difficult, if not impossible, to assess the stress-strain behavior of partially saturated soils using only the results of tests conducted on saturated specimens. This is important because: (1) almost all laboratory tests for strength and compressibility are conducted on saturated soil specimens; and (2) the majority of soils that occur in nature are not completely saturated. It is recognized that sands, silts and clays obtained from below (and in many cases above) the water table are nearly saturated. In addition, for most of these soils, the effect of partial saturation is to stiffen and strengthen the tested material. The degree of stiffness/strength change is inversely related to the degree of saturation, with the low saturation specimens showing the largest differences. Therefore, relying on the results of tests conducted on saturated soil specimens to assess the properties of their in-situ unsaturated condition generally provides a conservative assessment of the materials strength and compressibility relative to the properties of the in-situ material.

Relative to this section of the document, it can be argued that unsaturated soils are not really "unique" or "special". What is important is that when attempting to assess performance in comparison to design, it is important to recognize that the in-situ strength and compressibility of unsaturated soils will likely differ from the properties that were used in the design. Because the saturated soil response will likely represent a worst-case representation of field conditions, it is entirely reasonable that the design parameters be developed based on saturated soil conditions.

7.9.2 Sampling and Testing Partially Saturated Soils

Since most in-situ soils exist in an unsaturated condition, conventional sampling and specimen preparation procedures specifically recognize the characteristics of unsaturated soils. In general, the air component of the pore volume interacts with the pore water to form menisci between the solid soil particles. The surface tension resulting from this interaction essentially increases the relative confinement on the sample. This, in turn, explains why soil specimens that are usually thought to be "cohesionless" can be collected in the field and will remain intact. Sampling partially saturated soils can be extremely difficult when the natural materials exist at a low degree of saturation (i.e., typically less than 50 percent). In this state, the surface tension is very large but the available water is so widely distributed that the natural material can be extremely brittle. In a sandy material the material is subject to "collapse" from even the slightest disturbance during sampling or material handling. In cohesive soils, the material may become too hard to effectively sample using a thin-walled sampler. This is often the case of colluvial or residual soil materials. In the cases where sampling is difficult and the deposit is shallow, block sampling and test pit exploration can prove to be very helpful.

7.9.3 Interpretation of Laboratory and Field Testing Results of Partially Saturated Soils

In general, soils should be tested in their unsaturated state. Most laboratory tests are conducted on saturated specimens to accommodate the measurement of either the excess pore pressure (undrained) or volume change (drained) characteristics of the soil. For tests that are conducted on partially saturated specimens, it is explicitly noted that the measurement of excess pore pressure and volume change is difficult because there will be a differential pressure in the two pore fluids, depending on the rate of testing, the type of soil, and the degree of saturation. As a result, total stress tests are generally conducted wherein the pore pressure/volume change characteristics are explicitly not measured. In interpreting the results from these tests, it should be noted that the effect of the air/water menisci is to provide a negative pore pressure and thus a potentially significant effective confining pressure. The result of this will be that the material is stronger and stiffer than would be anticipated for a saturated material, particularly in a condition where no (or very little) confining pressure is externally applied. From the interpretation of strength properties perspective, this means that the material will exhibit an apparent cohesion intercept and an unconfined compressive strength. In some cases, it may be appropriate to use these apparent strengths in design, particularly for short-term loading conditions or in cases where the material will likely never become saturated.

In the case of the interpretation of field tests, it must be explicitly recognized that the natural materials are unsaturated and that the measured response will represent the actual strength/stiffness of the material in the in-situ condition. Because many interpretation procedures explicitly assume saturated conditions, the interpreted in-situ properties may be significantly stronger/stiffer than would be anticipated based on simple index tests and visual classification of the materials. In these cases, the test result is reporting the actual response and behavior of the material. The potential shortcoming is the inability of the conventional interpretation techniques to distinguish the influence of partial saturation.

CHAPTER 8

APPLYING JUDGEMENT IN SELECTING SOIL AND ROCK PROPERTIES FOR DESIGN

8.1 INTRODUCTION

The reader is referred back to the flow chart presented in chapter 2, with a specific charge to review the flow chart in the context of what information and guidance was provided in chapters 3 through 7 of this document. In these sections, several "how to" recommendations were made relative to the measurement and assessment of soil and rock properties. These aspects included recommendations for planning and executing a subsurface investigation, selecting drilling and sampling techniques, selecting sampling intervals and number of samples, developing the field and laboratory testing programs, and conducting and interpreting the field and laboratory tests. Recommendations have been made regarding which laboratory and in-situ tests are appropriate for obtaining specific soil and rock properties that may be needed in design. Finally, in chapters 5 and 6, recommendations were made regarding the interpretation of the laboratory and field tests. Notice that at this point, the reader should be near the end of the flow chart, and specifically at the step identified as *Select Material Properties and Finalize Subsurface Model.* At this point, two potentially significant questions are raised. Specifically, what should the engineer do if during the material property selection process it is found that: (1) there are inconsistencies between the results of selected tests; or (2) there is a significant variability in a selected parameter within the assumed relatively "uniform" subsurface model? To resolve these two issues, the engineer should carefully scrutinize the available data, assess the application where these data are needed, and ultimately apply judgment to select the appropriate value(s) considered for the design. From the early days as students in the introductory geotechnical engineering classroom, the term "judgment" has been used to describe how the geotechnical engineer makes decisions. While it is difficult to describe how to apply judgment or how to define what is "good" or "bad" judgment, this section will address the steps that should be followed to in making a judgment in response to the two previously posed questions.

8.2 RESOLVING INCONSISTENCIES BETWEEN TEST RESULTS

One of the goals of this document has been to make recommendations regarding the type of tests to conduct for a given application or for a specific soil/rock property. In many cases, multiple tests/resources were identified to assist the engineer in obtaining the needed information. Inevitably, because of the inherent variability of the soil deposit itself, the variations due to laboratory and field testing conditions, and the variation inherent in engineering property correlations, the calculated/estimated results will not be entirely consistent. Typical common examples of scenarios where inconsistent data are generated include: (1) SPT blow counts that are conducted across the entire site to correlate specific properties for the type of encountered soil and a limited number of index and/or performance tests conducted on a few "representative' samples; and (2) field vane shear test (VST) to provide a nearly continuous undrained strength profile versus depth at a project site and a few "high quality" unconsolidated undrained (UU) triaxial shear tests, again on recovered

representative samples. The following provides a step-by-step summary of how the engineer may resolve these differences.

1. *Data Validation:* Assess the field and the laboratory test results to determine whether the reported test results are accurate and are recorded correctly for the appropriate material. Disregard (or at least downplay) potentially questionable results.

2. *Historical Comparison:* Assess results with respect to anticipated results based on site and/or regional history. If the new results are inconsistent with a wealth of site/regional data, it will be necessary to assess whether the new data are anomalous or whether the new site conditions are anomalous.

3. *Performance Comparison:* Assess results with respect to historic performance of structures at the site or within the region, if possible. For example, if settlements at adjacent structures or wall movements have been recorded historically, it may be possible to back-calculate actual in-situ soil properties. These can then be compared to the measured/correlated properties that are in question.

4. *Correlation Calibration:* Develop site-specific correlations using the new field and laboratory data. Assess whether this correlation is within the range of variability typically associated with the correlation based on previous historic data used to develop the generic correlation.

5. *Assess Influence of Test Complexity:* Assess results from the perspective of the tests themselves. Some tests may be easy to conduct and calibrate, but provide data of a "general" character (e.g., Atterberg limits) while other tests are complex and subject to operator influences, yet provide "specific" test results (e.g., stress path triaxial tests). It may be found that certain tests consistently provide high (or low) values compared to the anticipated results. Alternatively, certain field tests may be assumed to be undrained, when in fact the test duration allows drainage.

The ultimate goal of this activity is to confirm that the data are valid for the test considered. In many cases, after considering all of these steps, it may be found that the actual anticipated range of properties is much less than originally reported. However, it is also common to find that the results of this step will indicate that all of the data are apparently valid and, thus, the material at the site is inherently variable; this by itself is a significant finding. The net outcome of this step is to provide a summary of valid data that is representative of the soils at the site. The fact that these data may be variable is discussed subsequently.

8.3 ESTIMATING VARIABILITY OF SELECTED PARAMETERS

In the previous section, it was noted that variability (or uncertainty) may be characteristic of the material or of the soil deposit, and the variability includes the combination of both inherent material variability and testing variability. Just as judgment was used to assess data quality and accuracy, it is necessary to apply similar judgment to estimate the variability for each of the selected parameters that will be considered in the design. There are several techniques to estimate this variability.

1. *Experience:* In some cases the engineer may have accumulated extensive experience in the region that it is possible to accurately select an average, typical or design value for the selected parameter, as well as the appropriate variability for the parameter.

2. *Statistics:* If the engineer has extensive experience in a region, there may be sufficient data to formally establish the average value and the variability (i.e., mean and standard deviation) for the specific design parameter.

3. *Published Values for Variability:* It has been found that engineers can estimate average values for specific parameters with a relatively high degree of accuracy, if sufficient data are presented. Unfortunately, it has also been found that engineers typically believe that there is less variability in these soil parameters than the data actually support. In recognition of these phenomena, Duncan (2000) prepared a table that presents an accumulation of experience regarding the coefficient of variation for several soil parameters. The values for the coefficient of variation (defined as the standard deviation divided by the average value) suggested by Duncan are presented in table 52.

4. *Establish Best-Case and Worst-Case Scenarios:* Once again, relying on the experience of the engineer, it may be possible to establish not only the average value for a selected parameter, but also an "absolute" upper-bound and a lower-bound (i.e., best-case and worst-case) estimate for the parameter. Once these extreme values are defined, it is possible to utilize the "three-sigma rule" as described in Duncan (2000) to define the highest conceivable value (HCV) and the lowest conceivable value (LCV) for the parameter. It can be shown that 99.73 percent of the data for the specific parameter value will be within the range of the HCV and the LCV. Therefore, these values can be used to assess the standard deviation and thus the coefficient of variation. Soil Property Selection Example No. 2 illustrates the use of the "three-sigma rule" and the LCV and HCV.

The outcome of this step is to provide a best estimate of the specific parameter and a quantifiable measure of anticipated variability of the parameter. Regardless of the procedures used to formally estimate the variability of the selected parameter, it is important to review information from the previous section to confirm that the coefficient of variability resulting from this step encompasses the actual variability for the parameter as measured (or estimated) from the data. In the unlikely event that the variability resulting from section 8.2 is higher than the values resulting from calculations in section 8.3, it is likely that distinct material differences at the site exist, rather than simply inherent material variations.

8.4 FINAL SELECTION OF DESIGN PARAMETERS

A combination of judgment, experience, and actual data were used to assess the validity of the data and the anticipated variability of the data that are needed for design. This final step again involves judgment and the use of information from the previous two sections to select the appropriate design parameters. Using information provided from section 8.2 (and hopefully section 8.3), there are three approaches to this final selection.

Table 52. Values of coefficient of variation, V, for geotechncial properties and in situ tests (after Duncan, 2000) (see Duncan, 2000 for original references on reported values of V).

Measured or interpreted parameter value	**Coefficient of Variation, V (%)**
Unit weight, γ	3 to 7 %
Buoyant unit weight, γ_b	0 to 10 %
Effective stress friction angle, ϕ'	2 to 13 %
Undrained shear strength, s_u	13 to 40 %
Undrained strength ratio (s_u/σ_v')	5 to 15 %
Compression index, C_c	10 to 37 %
Preconsolidation stress, σ_p'	10 to 35 %
Hydraulic conductivity of saturated clay, k	68 to 90 %
Hydraulic conductivity of partly-saturated clay, k	130 to 240 %
Coefficient of consolidation, c_v	33 to 68 %
Standard penetration blowcount, N	15 to 45 %
Electric cone penetration test, q_c	5 to 15 %
Mechanical cone penetration test, q_c	15 to 37 %
Vane shear test undrained strength, s_{uVST}	10 to 20 %

1. *Semi-Deterministic:* The engineer may simply estimate the design value by some form of judgment based on experience. For example, the undrained strength profile could be established by using the average of the field VST and the lab UU test results. The engineer may not use the UU test results for samples at significant depths. Similarly, the compression index for a clayey sand could be established based on historical regional correlations to SPT results. This selected value could be used in the requisite calculations to assess the design factor of safety (or the anticipated settlements). If acceptable performance is calculated (e.g., global calculated factor of safety (FOS) greater than 1.5 or total calculated settlements of less than 1 inch), the engineer may conclude that the design is complete. This approach has been adopted by many but is not recommended because it does not account for the heretofore described inherent variability of the selected parameters. Additionally, and probably most importantly, this procedure potentially allows the design engineer to use the rule-of-thumb or the experience of others without first-hand knowledge of the limitations and assumptions inherent to the assumptions.

2. *Statistics and Sensitivity Analyses:* The engineer can use experience to assess the average value for the selected parameter, but explicitly also considers a reduced estimate of this value for design. For example, using the coefficient of variability resulting from section 8.3, the engineer may also select a reduced estimate (e.g., the mean value minus 1 standard deviation ...aka "mean minus 1 sigma") for consideration in design. By conducting

analyses at these two potential values, an assessment is made of the sensitivity of the analysis results to a range of potential design values. If these analyses indicate that acceptable results are provided and that the analyses are not particularly sensitive to the selected parameters, the engineer may be comfortable with concluding the analyses. If, on the other hand, the engineer determines that the calculation results are marginal or that the results are sensitive to the selected parameter, additional data review and parameter selection are warranted. If the engineer is experienced, this technique can be quite effective, particularly when it can be shown that additional analyses are not warranted. One potential disadvantage of this method is that "experience" can be used to selectively use parameters that provide the desired calculation result.

3. *Probabilistic Analyses:* The previously referenced paper by Duncan (2000) presents an approach that explicitly combines variability in the design calculations and concepts of probability to estimate the potential for failure (or poor performance). Although not described in detail in this document, the technique involves the following three steps: (1) perform calculations (e.g., slope stability or settlement calculations) explicitly using the HCV and LCV values previously identified for each significant parameter or property; (2) use the results of these calculations to establish the variability of the calculation results to the selected parameter values; and (3) use the calculated variability to assess the probability of failure. The authors believe that, in time, this procedure (or something similar) will be incorporated into conventional practice, particularly in cases where highly variable properties are encountered and extensive investigation and testing are the only other techniques available to assess the values of the parameters.

Regardless of the technique used to select the specific design value (or range of design values), the engineer will be provided with a measure of the calculated performance. The advantages of the first technique are that it is relatively simple and likely follows traditional practice. The latter two approaches incorporate a formal assessment of the variability in the calculation results to variations in material parameter selection. The authors believe that each of these approaches has merit and is appropriate under certain design conditions. Semi-deterministic techniques are recommended to be used only when the individual engineer has extensive experience in the project area and with the materials involved in the design. In this case, experience is extensively relied upon and should only be considered for non-critical applications. The use of statistics and sensitivity analyses should generally be considered the minimum practice. For this case, the engineer should be experienced with the materials and the application so that an interpretation of the sensitivity studies can be effectively understood. Ideally, the calculations can be considered complete when the calculation results are shown to be relatively insensitive to the anticipated variation in the selected parameter. Probabilistic techniques should be considered whenever the variability in the parameters is large or where the consequence of failure is high, and when the costs of acquiring additional confirming data are large.

REFERENCES

American Association of State Highway and Transportation Officials (AASHTO) (1986). "Standard Specifications for Transportation Materials and Methods of Sampling and Testing, Part I, Specifications, 14th ed." AASHTO, Washington, D.C.

AASHTO (1988). "Manual on Subsurface Investigations." Washington, D.C.

AASHTO (1992). "Standard Specifications for Transportation Materials and Methods of Sampling and Testing, Part II, Tests." Washington, D.C.

AASHTO (1996). "Standard Specifications for Highway Bridges, 16th Edition." Washington, D.C.

Aas, G., Lacasse, S., Lunne, I., and Hoek, K. (1986). "Use of In-Situ Tests for Foundation Designs in Clay." Proceedings, In Situ '86, ASCE, pp. 1-30.

Arman, A. (1970). "Engineering Classification of Organic Soils." Highway Research Record No. 310, National Academy of Sciences, Washington, D.C., pp. 75-89.

ASTM (1997). Annual Book of ASTM Standards. American Society for Testing and Materials, Philadelphia, Penn.

ASTM (1988). Vane Shear Strength Testing in Soils: Field and Laboratory Studies, ASTM STP 1014, 378 pp.

Azzouz, A.S., Krizek, R.J., and Corotis, R.B. (1976). "Regression Analysis of Soil Compressibility." Soils and Foundations, Vol. 16, No. 2, pp. 19-29.

Baguelin, F., Jezequel, J.F., Mee, E.L., and Mehaute, A.E. (1972). "Expansion of Cylindrical Probes in Cohesive Soils." Journal of the Soil Mechanics and Foundation Division, ASCE, Vol. 98, SM11, pp. 1129-1142.

Bardet, J.P. (1997). Experimental Soil Mechanics. Prentice Hall, New Jersey, 584 pp.

Barksdale, R.D., Ferry, C.T., and Lawrence, J.D. (1986). "Residual Soil Settlement from Pressuremeter Moduli." Proceedings, In Situ '86, ASCE, Geotechnical Special Publication No. 6, Blacksburg, VA, pp. 447-461.

Barton, N.R. (1973). "Review of a New Shear Strength Criteria for Rock Joints." Engineering Geology, Vol. 7, pp. 189-236.

Barton, N.R. (1974). "Review of the Shear Strength of Filled Discontinuities." Norwegian Geotechnical Institute, Publication No. 105.

Barton, N.R. (1976). "The Shear Strength of Rock and Rock Joints." Engineering Geology, Vol. 7, Elsevier Science Publishing Company, Inc., New York, N.Y., pp. 287-332.

Becker, D.E., Crooks, J.H.A., Been, K. and Jefferies, M.G. (1987). "Work as a Criterion for Determining In-Situ and Yield Stresses in Clays." Canadian Geotechnical Journal, Vol. 24, No. 4, pp. 549-564.

Bieniawski, Z.T. (1974). "Geomechanics Classification of Rock Masses and its Application in Tunnelling." Proceedings of the 3rd International Congress on Rock Mechanics, Denver, Vol. 2, No. 2, pp. 27-32.

Bieniawski, Z.T. (1978). "Determining Rock Mass Deformability: Experience from Case Histories." International Journal of Rock Mechanics, Mineral Science, and Geomechanics, Abstract. Vol. 15, pp. 237-247.

Bolton, M.D. (1986). "The Strength and Dilatancy of Sands." Geotechnique, Vol. 36, No. 1, pp. 65-78.

Burns, S.E., and Mayne, P.W. (1996). "Small- and High-Strain Measurements of In-Situ Soil Properties Using the Seismic Cone Pentrometer." Transportation Research Record 1548, National Academy Press, Washington. D.C., pp. 81-88.

Campanella, R.G. (1994). "Field Methods for Dynamic Geotechnical Testing: An Overview of Capabilities and Needs." Dynamic Geotechnical Testing II, Special Technical Publication No. 1213, ASTM, Philadelphia, PA, pp. 3-23.

Campanella, R.G., and Robertson, P.K. (1991). "Use and Interpretation of a Research Dilatometer." Canadian Geotechnical Journal, Vol. 28, No. 1, pp. 113-126.

Carter, J.P. and Kulhawy, F.H. (1988). "Analysis and Design of Drilled Shaft Foundations Socketed into Rock." Final Report, Project 1493-4, EPRI EL-5918, Cornell University, Ithica, NY.

Chandler, R.J. (1988). "The In-Situ Measurement of the Undrained Shear Strength of Clays Using the Field Vane." Vane Shear Strength Testing in Soils: Field and Laboratory Studies, ASTM, Special Publication No. 1014, Philadelphia, PA, pp. 13-44.

Chen, F.H. (1988). Foundations on Expansive Soils. Elsevier Science Publishing Company, Inc., New York, N.Y., 463 pp.

Clarke, B.G. (1995). Pressuremeters in Geotechnical Design, Blackie Academic & Professional, 364 pp.

Day, R.W. (1999). Geotechnical and Foundation Engineering. McGraw-Hill, New York, N.Y.

Deere, D.U., and Patton, F.D. (1971). "Slope Stability in Residual Soils." Proceedings, Fourth Pan American Conference on Soil Mechanics and Foundation Engineering, San Juan, 87 pp.

Duncan, J.M. (2000). "Factors of Safety and Reliability in Geotechnical Engineering." Journal of Geotechnical and Geoenvironmental Engineering, Vol. 126, No. 4, pp. 307-316.

FHWA/RD-86/185 (1987). Spread Footings for Highway Bridges. Federal Highway Administration, U.S. Department of Transportation.

FHWA-IP-89-008 (1989). The Pressuremeter Test for Highway Applications. Federal Highway Administration, U.S. Department of Transportation.

FHWA-SA-92-045 (1993). EMBANK: A Microcomputer Program to Determine One-Dimensional Compression Settlement Due to Embankment Loads. Federal Highway Administration, U.S. Department of Transportation.

FHWA-SA-94-005 (1994). Advanced Technologies for Soil Slope Stability. Federal Highway Administration, U.S. Department of Transportation.

FHWA-HI-97-013 (1996). Design and Construction of Driven Pile Foundations. Federal Highway Administration, U.S. Department of Transportation.

FHWA-HI-97-021 (1997). Subsurface Investigations: Training Course in Geotechnical and Foundation Engineering. Federal Highway Administration, U.S. Department of Transportation.

FHWA-HI-99-007 (1998). Rock Slopes: Reference Manual. National Highways Institute, Federal Highway Administration, U.S. Department of Transportation.

FHWA-IF-99-025 (1999). Drilled Shafts: Construction Procedures and Design Methods. Federal Highway Administration, U.S. Department of Transportation.

FHWA-SA-97-076 (1997). Geotechnical Engineering Circular No. 3, Design Guidance: Geotechnical Earthquake Engineering for Highways, Volume I – Design Principles. Federal Highway Administration, U.S. Department of Transportation.

Finno, R.J. and Chung, C.K. (1992). "Stress-Strain-Strength Responses of Compressible Chicago Glacial Clays," Journal of Geotechnical Engineering, Volume 118, No 10, pp. 1607-1625.

Focht, J.A. (1994). "Lessons Learned from Missed Predictions" ASCE Journal of Geotechnical Engineering, Vol. 120, No. 10, pp. 1651-1683.

GeoSyntec Consultants, Inc. (1991). Geotextile Filter Design Manual.

Gibbs, H.J. (1969). "Discussion, Proceedings of the Specialty Session No. 3 on Expansive Soils and Moisture Movement in Partly Saturated Soils." Seventh International Conference on Soil Mechanics and Foundation Engineering, Mexico City, Mexico.

Giroud, J.P. (1968). "Settlement of an Embankment Resting on a Semi-Infinite Elastic Soil." Highway Research Record No. 223, pp. 813-831.

Goodman, R.E. (1970). "The Deformability of Joints. In Determination of the In-Situ Modulus of Deformation of Rock." ASTM, Special Technical Publication, No. 477, pp. 174-196.

Handy, R.L., Remmes, B., Moldt, S., Lutenegger, A.J., and Trott, G. (1982). "In-situ Stress Determination by Iowa Stepped Blade." ASCE Journal of Geotechnical Engineering, Vol. 108, No. GT11, pp. 1405-1422.

Harr, M.E. (1966). Foundations of Theoretical Soil Mechanics, McGraw-Hill Book Company, New York, 381 pp.

Hatanaka, M., and Uchida, A. (1996). "Empirical Correlation Between Penetration Resistance and Internal Friction Angle of Sandy Soils." Soils and Foundations, Vol. 36, No. 4, pp. 1-9.

Head, K.H. (1986). Manual of Soil Laboratory Testing, Vol. 3: Effective Stress Tests. John Wiley & Sons, New York, NY.

Hoek, E. (1983). "Strength of Jointed Rock Masses." Geotechnique, Vol. 33, No. 3, pp. 187-223.

Hoek, E., and Bray, J.W. (1977). Rock Slope Engineering. Institution of Mining and Metallurgy, London, U.K.

Hoek, E., and Brown, E.T. (1988). "The Hoek-Brown Failure Criterion – a 1988 Update." Proceedings, 15th Canadian Rock Mechanics Symposium, Toronto, Canada.

Hoek, E., and Brown, E.T. (1997). "Practical Estimates of Rock Mass Strength." International Journal of Rock Mechanics and Mining Sciences, (available at http://www.rocscience.com/)

Holtz, R.D. and Kovacs, W.D. (1981). An Introduction to Geotechnical Engineering. Prentice-Hall Inc., Englewood Cliffs, New Jersey, 733 pp.

ISRM (1981). "Suggested Methods for the Quantitative Description of Discontinuities in Rock Masses." Pergamon Press, UK.

ISRM (1987). "Suggested Methods for Deformability Determination Using a Flexible Dilatometer." International Journal of Rock Mechanics, Mineral Science, and Geomechanics, Abstract, Volume 24, Number 2, pp. 123-134.

Jaeger, J.C., and Cook, N.G.W. (1976). Fundamentals of Rock Mechanics. Chapman & Hall, London, U.K., 99 pp.

Jamiolkowski, M., Ladd, C.C., Germaine, J. and Lancellotta, R. (1985). "New Developments in Field and Lab Testing of Soils." Proceedings, 11th International Conference on Soil Mechanics and Foundations Engineering, Vol. 1, San Francisco, CA, pp. 57-154.

Jamiolkowski, M., Lancellotta, R., LoPresti, D.C.F., and Pallara, O. (1994). "Stiffness of Toyoura Sand at Small and Intermediate Strain." Proceedings, 13th International Conference on Soil Mechanics & Foundation Engineering, Vol. 3, New Delhi, India, 169-173.

Kates, G. (1996). "Development and Implementation of a Seismic Flat Dilatometer Test for Small- and High- Strain Soil Properties." M.S. Thesis, School of Civil and Environmental Engineering, Georgia Institute of Technology, Atlanta, 173 pp.

Keaveny, J.M. and Mitchell, J.K. (1986). "Strength of Fine-Grained Soils using the Piezocone." Use of In-Situ Tests in Geotechnical Engineering, Geotechnical Special Publication No. 6, ASCE, New York, N.Y., pp. 668-685.

Koutsoftas, D. and Ladd, C.C. (1985). "Design Strengths for Offshore Clay." ASCE Journal of Geotechnical Engineering, Vol. 111, No. 3, pp. 337-356.

Kulhawy, F.H., and Mayne, P.W. (1990). Manual on Estimating Soil Properties for Foundation Design. Report EL-6800, Electric Power Research Institute, Palo Alta, CA, August, 306 pp.

Lacasse, S., and Lunne, T. (1988). "Calibration of Dilatometer Correlations." Proceedings, First International Symposium on Penetration Testing, Vol. X.

Ladd, C.C. and Lambe, T.W. (1963). "The Strength of Undisturbed Clay Determined from Undrained Tests." *Laboratory Shear Testing of Soils*, ASTM Special Technical Publication No. 361, pp. 342-371.

Ladd, C.C. (1991). "Stability Evaluation During Staged Construction." ASCE Journal of Geotechnical Engineering, Vol. 117, No. 4, pp. 540-615.

Lama, R.D., and Vutukuri, V.S. (1978a). Handbook on the Mechanical Properties of Rock, Vol. I. Trans Tech Publications, Claustal, Germany, pp. 87-138.

Lama, R.D., and Vutukuri, V.S. (1978b). Handbook on the Mechanical Properties of Rock, Vol. II. Trans Tech Publications, Claustal, Germany, pp. 105-148.

Lambe, T.W., and Whitman, R.V. (1969). Soil Mechanics. John Wiley & Sons, New York, N.Y., 553 pp.

Landva, A.O., Korpijaakko, E.O., and Pheeney, P.E. (1983). "Geotechnical Classification of Peats and Organic Soils." Testing of Peats and Organic Soils, ASTM, Special Technical Publication No. 820, P.M. Jarrett, Ed., American Society for Testing and Materials, pp. 37-51.

Larsson, R. (1980). "Undrained Shear Strength in Stability Calculations of Embankments." Canadian Geotechnical Journal, Vol. 17, No. 4, pp. 591-602.

Liao, S.S., and Whitman, R.V. (1986). "Overburden Correction Factors for SPT in Sand." Journal of Geotechnical Engineering, ASCE, Vol. 112, No. 3, pp. 373-377.

Lowe, J., III, Jona, E., and Obrician, V. (1969). "Controlled Gradient Consolidation Test." Journal of Soil Mechanics Foundation Engineering Division, ASCE, Vol. 95, No. SM1, pp. 77-98.

Lunne, T., Robertson, P.K., and Powell, J.J.M. (1997). Cone Penetration Testing in Geotechnical Practice. Blackie Academic, Chapman Hall, London, 312 pp.

Marchetti, S. (1980). "In-Situ Tests by Flat Dilatometer." ASCE Journal of Geotechnical Engineering, Vol. 106, No. GT3, pp. 299-324.

Marchetti, S. (1997). "The Flat Dilatometer: Design Applications." Proceedings, 3rd International Geotechnical Engineering Conference, Soil Mechanics and Foundations Research Laboratory, Cairo University, Egypt, pp. 421-448.

Marchetti, S., and Crapps, D.K. (1981). Flat Dilatometer Manual, GPE, Inc., Gainesville, Florida.

Martin, R.E. (1977). "Estimating Foundation Settlements in Residual Soils." Journal of the Geotechnical Engineering Division, ASCE, Vol. 103, No. GT3, pp. 197-212.

Martin, G.K., and Mayne, P.W. (1998). "Seismic Flat Dilatometer Tests in Piedmont Residuum." Proceedings, International Conference on Site Characterization, Vol. 2, Balkema, Rotterdam, pp. 837-843.

Mayne, P.W. (1988). "Determining OCR in Clays from Laboratory Strength." ASCE Journal of Geotechnical Engineering, Vol. 114, No. 1, pp. 76-92.

Mayne, P.W., and Frost, D.D. (1988). "Dilatometer Experience in Washington, D.C., and Vicinity." Transportation Research Record 1169, National Academy Press, Washington, D.C., pp. 16-23.

Mayne, P.W., and Kemper, J.B. (1988). "Profiling OCR in Stiff Clays by CPT and SPT." ASTM Geotechnical Testing Journal, Vol. 11, No. 2, pp. 139-147.

Mayne, P.W. and Bachus, R.C. (1989). "Penetration Pore Pressures in Clay by CPTU, DMT, and SBP." Proceedings, 12th International Conference on Soil Mechanics and Foundation Engineering, Vol. 1, Rio de Janeiro, A.A. Balkema, Rotterdam, pp. 291-294.

Mayne, P.W. and Poulos, H.G. (1999). "Approximate Displacement Influence Factors for Elastic Shallow Foundations." Journal of Geotechnical and Geoenvironmental Engineering, Vol. 125, No. 6, pp. 453-460.

Mayne, P.W., Schneider, J.A. and Martin, G.K. (1999). "Small- and Large-Strain Soil Properties from Seismic Flat Dilatometer Tests." Proceedings, Pre-Failure Deformation Characteristics of Geomaterials, Vol. 1, Balkema, Rotterdam, pp. 419-426.

Mesri, G., and Abdel-Ghaffar, M.E.M. (1993). "Cohesion Intercept in Effective Stress Stability Analysis." Journal of Geotechnical Engineering, Vol. 119, No. 8, pp. 1229-1249.

Mesri, G., Stark, T.D., Ajlouni, M.A., and Chen, C.S. (1997). "Secondary Compression of Peat With or Without Surcharging." Journal of Geotechnical Engineering, Vol. 123, No. 5, pp. 411-421.

Meyerhof, G.G. (1951). "The Ultimate Bearing Capacity of Foundations." Geotechnique Vol. 2, pp. 301-332.

Mitchell, J.K. and Gardner, W.S. (1975). "In Situ Measurement of Volume Change Characteristics." State-of-the-Art Report, Proceedings, ASCE Specialty Conference on In Situ Measurement of Soil Properties, Raleigh, North Carolina, Vol. II, 333 pp.

NAVFAC (1982). "Foundations and Earth Structures Design Manual 7.2." Department of the Navy, Alexandria, Virginia.

Nelson, J.D. and Miller, Debora, J. (1992). Expansive Soils: Problems and Practices in Foundation and Pavement Engineering. John Wiley and Sons, Inc., New York, N.Y., 259 pp.

Poulos, H.G., and Davis, E.H. (1974). Elastic Solutions for Soil and Rock Mechanics. John Wiley & Sons, Inc., New York, N.Y., 410 pp.

Powell, J.J.M. and Quarterman, R.S.T. (1988). Penetration Testing 1988, ISOPT-1, De Ruiter (ed.), Balkema, Rotterdam, pp. 903-909.

Robertson, P.K., and Campanella, R.G. (1983). "Interpretation of Cone Penetration Tests." Canadian Geotechnical Journal, Vol. 20, No. 4, pp. 718-754.

Robertson, P.K., Campanella, R.G., Gillespie, D., and Greig, J. (1986). "Use of Piezomenter Cone Data, Use of In-Situ Tests in Geotechnical Engineering." ASCE Geotechnical Special Publication No. 6, pp. 1263-1280.

Saint Simon, P.G.R., Solymar, Z.V., and Thompson, W.J. (1979). "Damsite Investigation in Soft Rocks of Peace River Valley, Alberta, Canada." Proceedings, 4th International Conference on Rock Mechanics, Montreux, Vol. 2, pp. 553-560.

Schofield, A.N., and Wroth, C.P. (1968). Critical State Soil Mechanics. McGraw-Hill, London, U.K., 310 pp.

Schmertmann, J.H. (1970). "Static Cone to Compute Static Settlement Over Sand." Journal of the Soil Mechanics and Foundations Division, ASCE, Vol. 96, No. SM3, pp. 1011-1043.

Schmertmann, J.H. (1975). "Measurement of In-Situ Shear Strength." Proceedings, ASCE Conference on In-Situ Measurement of Soil Properties, Vol. 2., Raleigh, N.C., pp. 57-138.

Schmertmann, J.H. (1986). "Suggested Method for Performing the Flat Dilatometer Test." Geotechnical Testing Journal, Vol. 9, No. 2, pp. 93-101.

Schmertmann, J.H. (1991). DMT Digest No. 12, GPE, Inc. Gainesville, FL

Seed, H.B., Woodward, R.J., and Lundgren, R. (1962). "Prediction of Swelling Potential for Compacted Clays." Journal of Soil Mechanics and Foundations Division, ASCE, Vol. 88, No. 3, pp. 53-87.

Serafim, J.L., and Pereira, J.P. (1983). "Considerations of the Geomechanics Classification of Bieniawski." Proceedings of the International Symposium of Engineering Geology and Underground Construction, Lisbon, pp. 1133-1144.

Skempton, A.W. (1953). "The Collodial Activity of Clays." Proceedings, Third International Conference on Soil Mechanics and Foundation Engineering, Vol. I, pp. 57-61.

Skempton, A.W. (1986). "SPT Procedures and the Effects in Sands of Overburden Pressure, Relative Density, Particle Size, Aging, and Overconsolidation." Geotechnique, Vol. 36, No. 3, pp. 425-447.

Sowers, G.F. (1963). "Engineering Properties of Residual Soils Derived from Igneous and Metamorphic Rocks." Proceedings, Second Pan-American Conference on Soil Mechanics and Foundation Engineering, Vol. 1, Associacao Brasileira de Mechanica dos Solos, Brasil, pp. 39-62.

Sowers, G.F., and Richardson, T. (1983). "Residual Soils of the Piedmont and Blue Ridge." Transportation Research Record 919, Transportation Research Board, National Academy Press, Washington, D.C., pp. 10-16.

Stark, T.D., and Eid, H.T. (1994). "Drained Residual Strength of Cohesive Soils." Journal of Geotechnical Engineering, Vol. 120, No. 5, pp. 856-871.

Strohm, W.E., Jr., Bragg, G.H., Jr., and Zeigler, T.H. (1978). "Technical Guidelines (Report FHWA-RD-78-141)." Design and Construction of Compacted Shale Embankments, U.S. Department of Transportation, Vol. 4, 154 pp.

Stroud, M.A. (1974). "The Standard Penetration Test in Insensitive Clays and Soft Rocks." Proceedings, European Symposium on Penetration Testing, Vol. 2.2, Stockholm, Sweden, pp. 367-375.

Stroud, M.A. (1989). "Standard Penetration Test: Introduction Part 2." Penetration Testing in the U.K., Thomas Telford, London, pp. 29-50.

Tavenas, F.A., Blanchette, G., Leroueil, S., Roy, M. and LaRochelle, P. (1975). "Difficulties in the In Situ Determination of K_o in Soft Sensitive Clays." Proceedings, In-Situ Measurement of Soil Properties, Vol. I, ASCE, Raleigh, North Carolina, pp. 450-476.

Tavenas, F., Leroueil, S., and Roy, M. (1982). "The Piezocone Test in Clays: Use and Limitations." Proceedings, 2nd European Symposium on Penetration Testing, Vol. 2, Amsterdam, 889-894. A.A. Balkema, Rotterdam.

Teh, C.I. and Houlsby, G.T. (1991). "An Analytical Study of the Cone Penetration Test in Clay." Geotechnique, Vol. 41, No.1, pp. 17-34.

Terzaghi, K., and Peck, R.G. (1967). Soil Mechanics in Engineering Practice. John Wiley & Sons, Inc., New York, N.Y.

Terzaghi, K., Peck, R.G., and Mesri, G. (1996). Soil Mechanics in Engineering Practice, John Wiley & Sons, Inc., New York, N.Y., pp. 549.

Transportation Research Board (TRB) (1996). Landslides: Investigation and Mitigation, Special Report 247. National Academy Press, Washington D.C., 674 pp.

Vesic, A.S. (1977). "Design of Pile Foundations." Synthesis of Highway Practice 42, Transportation Research Board, Washington, D.C., 68 pp.

Vinson, J., and Brown, D.A. (1997). "Site Characterization of the Spring Villa Geotechnical Test Site and a Comparison of Strength and Stiffness Parameters for a Piedmont Residual Soil." Report No. IR-97-04, Highway Research Center, Harbert Engineering Center, Auburn University, AL, 385 pp.

Welsh, R.A. Jr., Vallejo, L.E., Lovell, L.W., and Robinson, M.K. (1991). "The U.S. Office of Surface Mining (OSM) Proposed Strength-Durability Classification System." Proceedings, Symposium on Detection of and Construction at the Soil/Rock Interface, W.F. Kane and B. Amadei, Eds., ASCE Geotechnical Special Publication No. 28, American Society of Civil Engineers, New York, N.Y.

Windle, D., and Wroth, C.P. (1977). "In Situ Measurement of the Properties of Stiff Clays." Proceedings, 9th International Conference on Soil Mechanics and Foundation Engineering, Tokyo, Japan, pp. 347-352.

Wood, D.M. (1990). Soil Behavior and Critical State Soil Mechanics. Cambridge University Press, U.K., 462 pp.

Woods, R.G. (1994). "Laboratory Measurement of Dynamic Soil Properties." Dynamic Geotechnical Testing II, ASTM, Special Technical Publication No. 1213, Philadelphia, PA, 165-190.

Wroth, C.P. (1984). "The Interpretation of In-Situ Soil Tests." Rankine Lecture, Geotechnique, Vol. 34, No. 4, pp. 449-489.

Wyllie, D.C. (1999). Foundations on Rock. Routledge, New York, N.Y., 401 pp.

APPENDIX A

SOIL AND ROCK PROPERTY SELECTION EXAMPLES

OVERVIEW

Soil and rock property selection examples are provided in this section. The purpose of these examples is to illustrate the application of the methods and procedures described in chapters 1 through 8 of this GEC. For each example, a different soil profile is used. Table A-1 provides a summary of the examples included in this section along with a list of the particular properties and parameters that are evaluated. It is noted that the methods used to evaluate certain properties and/or parameters do not necessarily vary significantly depending on the specific soil profile. For example, the methods and techniques used to evaluate subsurface stratigraphy from SPT and disturbed sample information and in-situ testing data does not vary significantly in soft cohesive soils and heavily overconsolidated soils. For this reason, the first two examples have been developed to be comprehensive with respect to evaluating all potentially relevant properties and parameters. The remaining example focuses on the evaluation of properties and parameters that are considered to be unique to the particular soil profile.

Table A-1. Summary of soil property selection examples.

Example No.	Subsurface Profile	Properties and Parameters Evaluated
1	Soft to Medium Clay and Overconsolidated Clay Crust	• Development of a Subsurface Profile (soil type, w_n, LL, PL, PI, LI, γ_{tot}, γ_{dry}) • Stress History (σ_p') • Deformation Parameters (C_c, $C_{c\varepsilon}$, C_r, C_α) • Time Rate of Consolidation (c_v, c_h) • In-Situ Horizontal Stresses (K_o) • Undrained Shear Strength ($s_{u,UU}$, $s_{u,CIUC}$, $s_{u,VST}$, $s_{u,CPT}$, $s_{u,CPTu}$, $s_{u,DMT}$)
2	Piedmont Residual Soil, Weathered Rock, and Rock	• Development of a Subsurface Profile (soil type, GSD, w_n, LL, PL, PI, LI, γ_{dry}) • Deformation Parameters (E_{PMT}, E_{DMT}) • Drained Strength (c', ϕ')
3	Heavily overconsolidated clays	• Development of a Subsurface Profile (soil type, w_n, LL, PL, PI, LI, γ_{tot}, γ_{dry}) • Stress History (σ_p') • Deformation Parameters (C_c, $C_{c\varepsilon}$) • In-Situ Horizontal Stresses (K_o) • Undrained Strength Properties • Swell Potential

SOIL AND ROCK PROPERTY SELECTION EXAMPLE NO. 1

Soft to medium clay and overconsolidated clay crust

INTRODUCTION

The purpose of this example is to describe procedures and interpretation methods available in current practice for evaluating soil properties and parameters for soft to medium clays that may include overconsolidated clay crusts. Additionally, guidelines for sampling, testing, and property selection will be discussed. This example covers properties necessary for design on soft clay including: (1) subsurface stratigraphy (i.e., soil layering and groundwater levels); (2) in-situ stress state; (3) shear strength; and (4) consolidation. Various laboratory and in-situ testing devices may be used to evaluate clay soil properties. Several methods are presented for each property to demonstrate the utility and limitations of each and the rationale is provided to evaluate a particular property value for design when multiple values from several tests are recorded. This information may also be used by design engineers to plan an appropriately scoped subsurface investigation program.

In developing this example, it is assumed that the engineer has reviewed engineering reports, boring logs, and other sources of information on the local geology for the area to be investigated. The data used for this example are from projects, located in the vicinity of the Connecticut River Valley of western Massachusetts. Subsurface soils in this area include an overconsolidated clay crust overlying a thick layer of soft to medium clay with silt and sand varves. The general subsurface stratigraphy consists of 1 m of fill soil overlying a thick deposit of Connecticut Valley varved clay. Below the varved clay are dense silt deposits overlying bedrock. The thickness of individual silt or clay varves is typically approximately 2 to 8 mm and the varves are generally horizontally oriented. The upper 5 m of the varved clay deposit is overconsolidated because of surface erosion, desiccation, and seasonal groundwater level fluctuations. Below this weathered crust the soils become soft and near normally consolidated with increasing depth. For this example, the ground water table is located approximately 1 m below the ground surface.

DATA REQUIREMENTS

A detailed review of existing geotechnical data for the site will likely reveal information on subsurface stratigraphy and engineering properties of the soil similar to that information provided in the Introduction. For this site, it is likely that structural foundations required to support relatively large loads would consist of deep foundation elements (e.g., driven piles, drilled shafts) founded on or within the dense soil/rock layers below the varved clays. Relatively small loads may be able to be supported by a structural element founded within the upper overconsolidated clay crust. Table 1 provides information on analysis requirements, soil properties, and laboratory and field-testing required to perform a design for specific geotechnical applications that may be constructed on the soil profile used for this example as well as other subsurface profiles. This table provides a link between design applications and engineering properties required for design and constructability assessments.

SUBSURFACE EXPLORATION AND TESTING PROGRAM

A subsurface exploration and testing program for a soft to medium clay site including the number, location, and depth of borings, test pits, and hand augers, and number, location, and depth of disturbed and undisturbed samples will depend on factors which range from the specific design application, local geology, and the performance requirements for the design application.

For this site, basic soil data (e.g., visual identification, classification, and index tests) obtained using disturbed split spoon samples and SPT blowcount values may be sufficient to develop a subsurface profile to be used for design analyses. Using these methods would likely require continuous sampling in the upper reaches of the subsurface to discern the transition from the crust to the softer clay soils. This transition could also be accurately evaluated using cone penetration testing and /or dilatometer testing. However, since split barrel samples obtained during a SPT cannot provide specimens suitable for performance-evaluation testing, and the SPT blowcount values cannot be used to assess shear strength or compressibility properties of clayey soils for final design, other in-situ and laboratory tests are required. Therefore, in-situ testing methods combined with laboratory tests on specimens from high quality undisturbed samples are necessary to develop design parameters

For most applications involving relatively soft cohesive soils, it is necessary to develop shear strength and compressibility parameters to be used for design. These parameters should be evaluated using laboratory testing methods and high quality undisturbed cohesive soil samples. Procedures for obtaining undisturbed soil samples have been described in chapter 4 of this document. It may be necessary or preferable to use in-situ testing devices to obtain data to complement the laboratory testing, especially if the project site is relatively large, if the project schedule is critical, if the soil deposit is highly stratified or has a highly developed macrofabric (e.g., an overconsolidated clay crust), or if it is difficult to obtain undisturbed samples. Local correlations between fundamental properties and in-situ test parameters are desirable, but global correlations confirmed with site specific laboratory test data may be equally appropriate.

DEVELOPMENT OF SUBSURFACE PROFILE FOR DESIGN

General

In this example, data collected from the SPT with recovery of disturbed samples, electric cone penetration test (CPT), piezocone penetration test (CPTu), and flat plate dilatometer test (DMT) are used to develop a subsurface profile for the site. When using CPT, CPTu, and DMT data, derived parameters are calculated and incorporated into empirical classification charts. The soil profiles developed from each test method are compared and a single subsurface profile is developed.

Use of SPT and Disturbed Sampling

A boring log for the site is shown on figure A-1. A review of all available boring logs indicates that the subsurface profile consists of up to 5 m of relatively stiff varved clay and varved silt. Below this is a layer of soft varved clay that varies in thickness from 16 to 29 m. Below the varved clay is a layer of very stiff to hard varved silt.

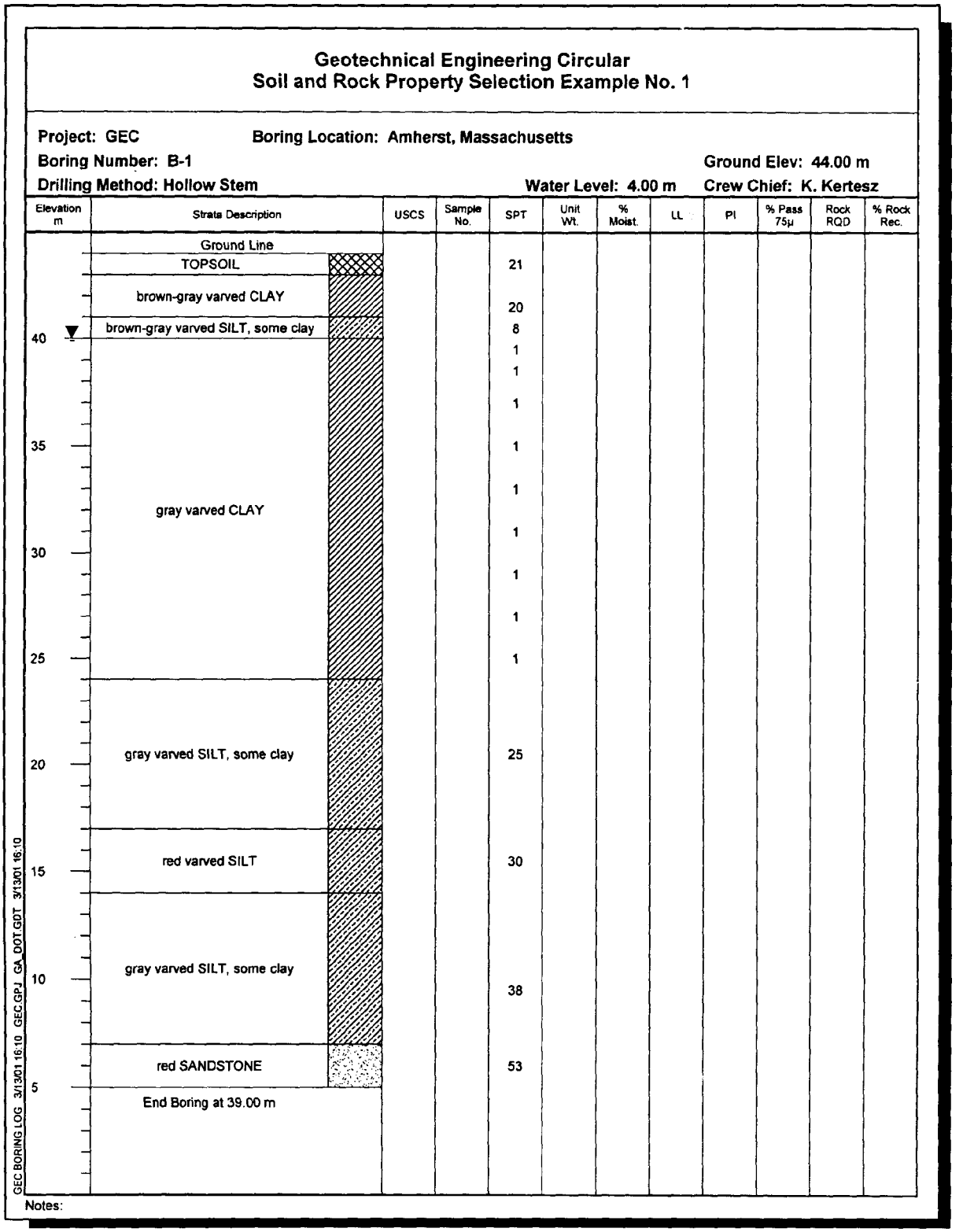

Figure A-1. Boring log B1.

The interpreted soil profile based on SPT data, visual identification and laboratory soil classification, and index testing of disturbed samples indicates two primary soil layers, Layer A and Layer B. Since this example focuses on overconsolidated crusts and soft to medium clays, the dense silt and bedrock below the soft varved clay are not considered further in this example. For clayey and silty soils, consistency can be evaluated using SPT blowcount (N) values (see table 23) and comparison of natural moisture content (w_n) to Atterberg Limits using the Liquidity Index (LI).

A summary of SPT N values, index test results, and calculated LI values are provided in figure A-2 for three borings (B1, B2, and B3). Interpretation of soil layers A and B is described below.

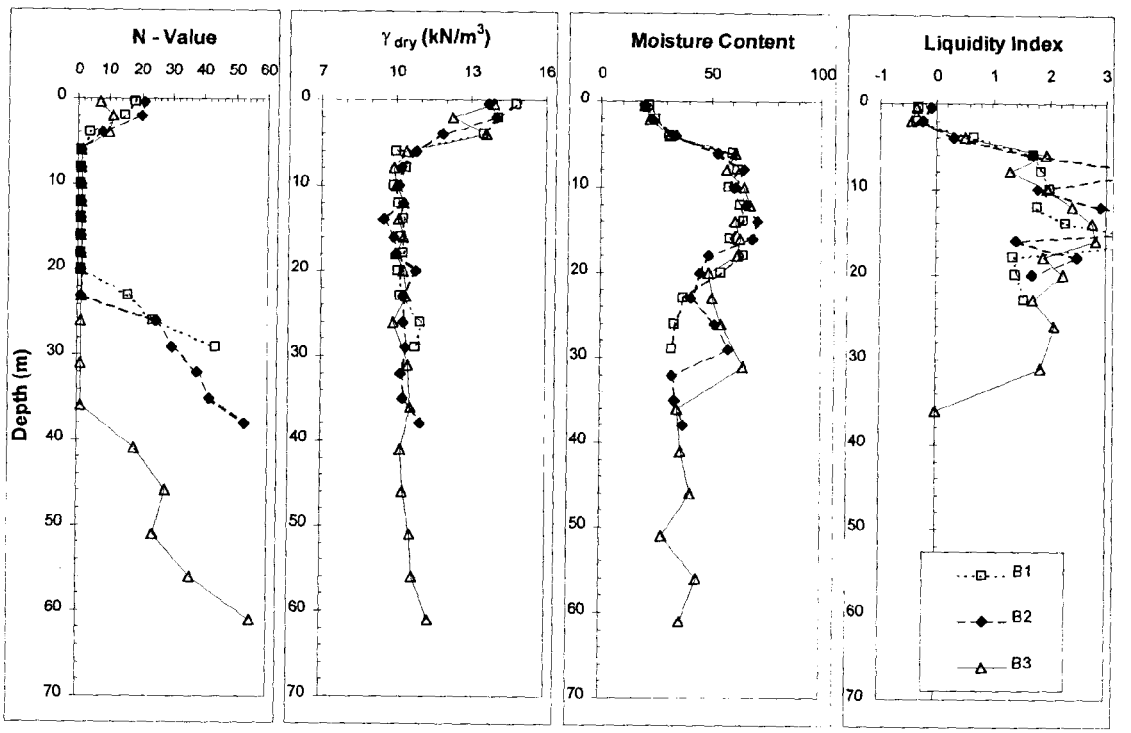

Figure A-2. Summary data for samples from Borings B1, B2, and B3.

Layer A

Layer A is located between the ground surface and a depth of 5 m. SPT N values for the three borings range from 6 to 21 blows/300 mm over this 5-m depth range indicating a medium stiff to stiff soil. Liquidity indices increase from approximately –0.5 for the upper 1 m to approximately 0.7 at a depth of 4 m. These data indicate that the upper varved clay and varved silt crust is overconsolidated. Values of LI approach 1 at a depth of 5 m. Liquidity indices less than approximately 0.7 generally indicate that the soil is overconsolidated.

Layer B

Layer B is located below a depth of approximately 5 m. This layer is a very soft varved clay based on SPT N values (0 to 1 blows/300 mm) and on visual identification of disturbed samples. This layer extends to various depths in each boring. Atterberg limits data indicate that the material is a low plasticity silt. Grain size information for samples collected in Boring B1 indicate that the soil is

a silty clay to clayey silt. Note that the Atterberg limits testing was performed on a bulk specimen and that the Atterberg limits data for individual clay and silt varves would likely vary. The calculated LI is greater than one indicating that the soil is normally consolidated to lightly overconsolidated.

CPT Stratigraphy

Measurements of CPT tip resistance (q_t), sleeve friction (f_s), and calculated friction ratio can be used to identify major stratigraphy changes in soil profiles. A CPT record for the example soil is shown on figure A-3. The profile shown for the two-layer system discussed previously (i.e., Layer A and Layer B) reveals additional subtle signatures of the layer, specifically the transition into and between these two major layers. Four layers (A1, A2, B1, and B2) are shown in figure A-3 and the interpretation of these layers is discussed subsequently. Individual measurements of q_t and friction ratio are plotted on the classification chart (figure A-4). With reference to figure A-4, it is noted that tip resistance values less than 5 MPa are indicative of clayey and silty materials, while tip resistance values greater than 10 MPa are associated with sandy materials. Soil layers with tip resistance values between 5 MPa and 10 MPa range from loose sands or silt mixtures to overconsolidated clays. Tip resistance values for the example soil deposit are less than 5 MPa, indicating that the interpreted soil layering is a result of soil stiffness variation in clayey or silty material rather than a change in soil type. Table A-2 summarizes results of the CPT subsurface profile interpretation.

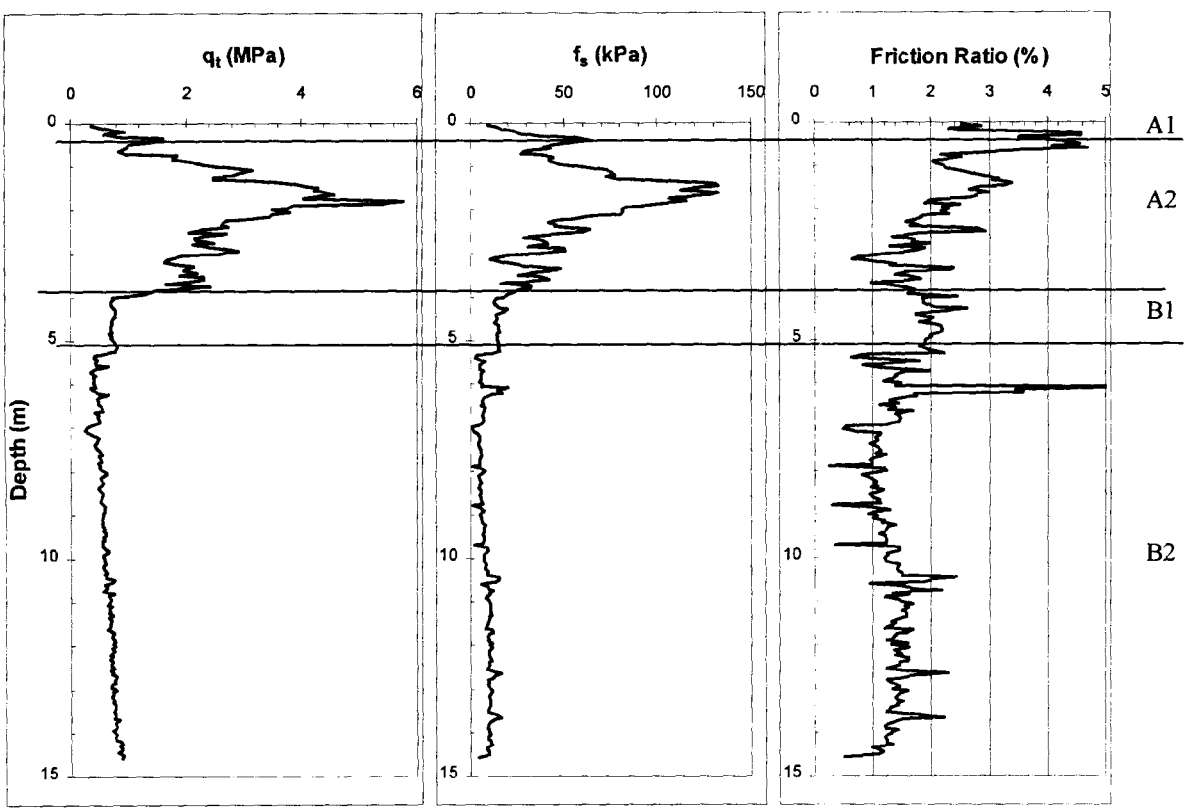

Figure A-3. Subsurface soil layering based on CPT data and friction ratio.

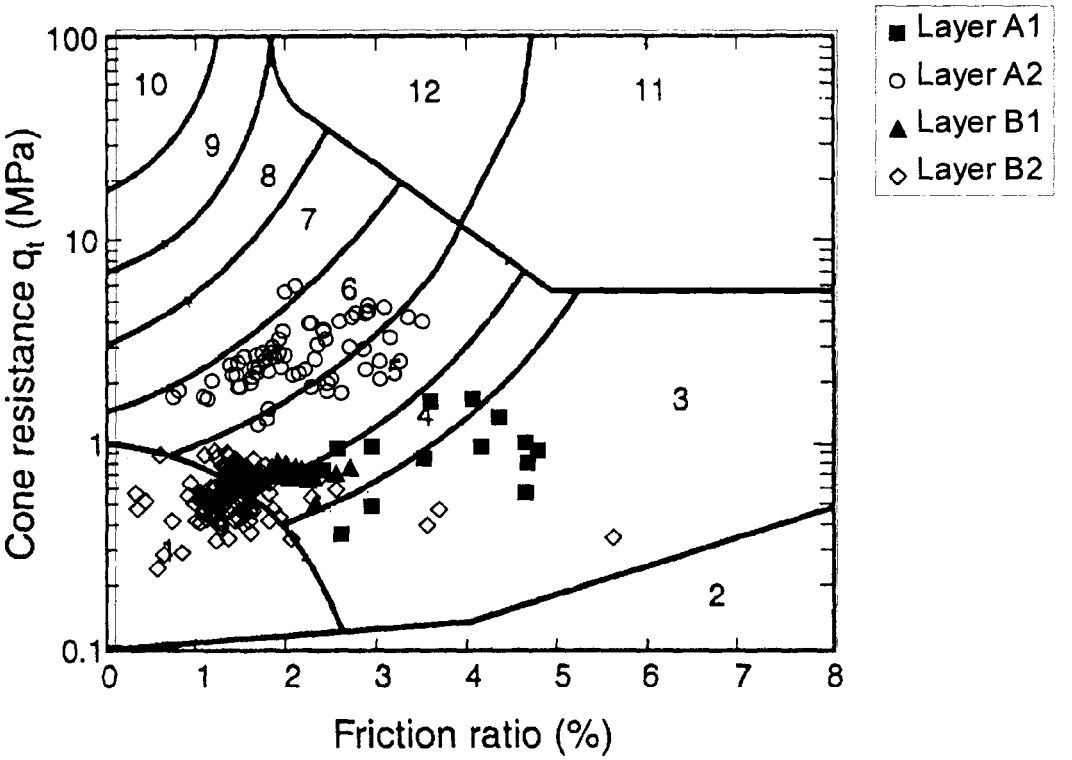

Figure A-4. Classification of soil type based on q_t and friction ratio.

Table A-2. Summary of CPT subsurface profile interpretation.

Layer	Depth Range (m)	q_t-FR zones	Classification
A1	0-0.7	3, 4	Silty clay
A2	0.7-3.95	5, 6, 7	Clayey silt
B1	3.95-5.25	4, 5	Silty clay
B2	5.25 to top of dense silt layer	1,3 ,4, 5	Clay

CPTu Stratigraphy

The piezocone provides the same information as the electric cone but also provides readings of penetration pore pressure with depth. The calculated pore pressure parameter (i.e., $B_q=(u_2-u_o)/(q_t-\sigma_{vo})$) provides information that is used for stratigraphy profiling. Determination of stratigraphy in this section will concentrate on information obtained from the u_2 penetration porewater pressure and B_q parameter. Five layers are shown in figure A-5, as interpreted using q_t, friction ratio, u_2, and the calculated B_q parameter. Individual measurements of B_q and q_t are plotted on the Robertson et al. (1986) classification chart (figure A-6). Table A-3 summarizes the results of the CPTu subsurface profile interpretation.

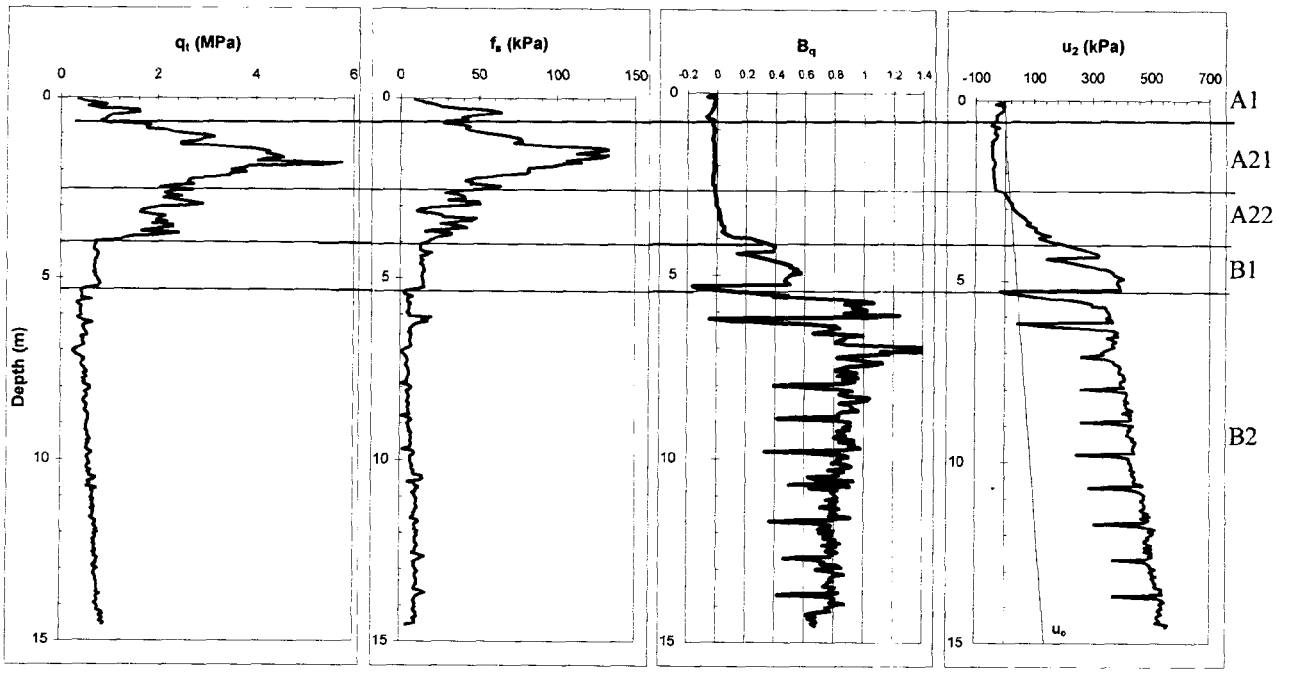

Figure A-5. Subsurface soil layering based on CPTu data, friction ratio, and B_q parameter.

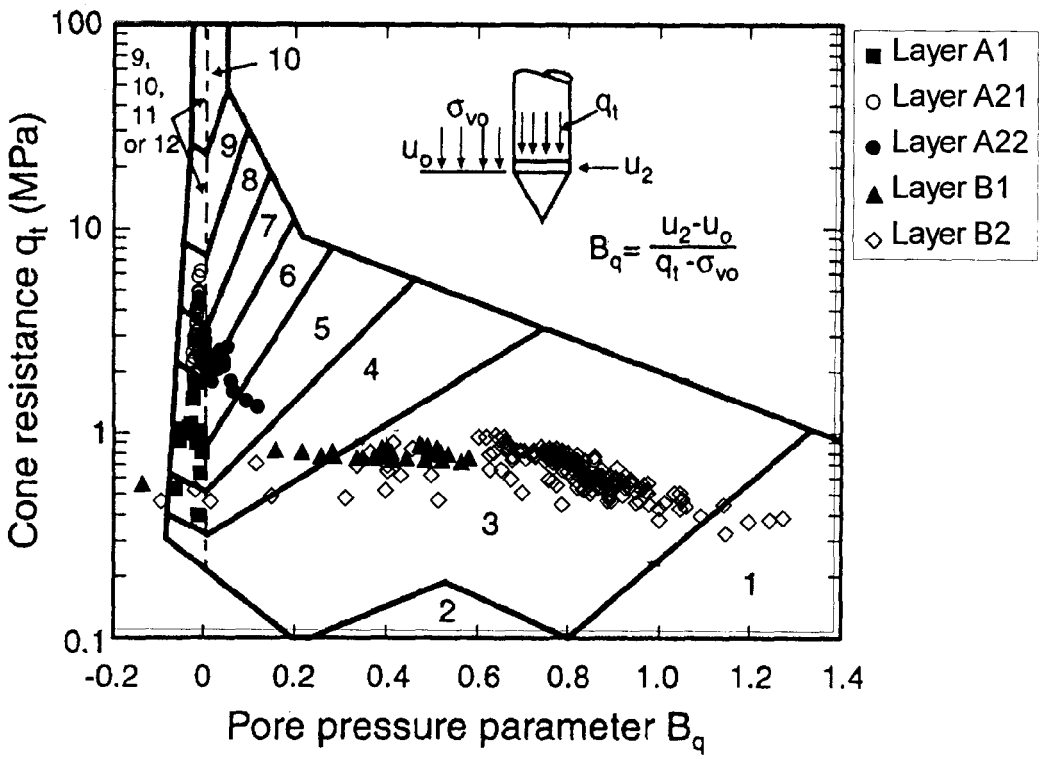

Figure A-6. Classification of soil type based on q_t and B_q.

Table A-3. Summary of CPTu subsurface profile interpretation.

Layer	Depth Range (m)	Q_t-FR zones	B_q-FR zones	Classification
A1	0-0.7	3, 4		Silty clay
A21	0.7-2.65	5, 6, 7	6, 7, 8	Clayey silt
A22	2.65-3.95	5, 6	5, 6	Clayey silt
B1	3.95-5.25	4, 5	3, 4	Silty clay
B2	5.25 to top of dense silt layer	1,3 ,4, 5	1,3 , 4	Clay

For this example, the data obtained from penetration pore pressure using the piezocone were used to further delineate soil layer A2 between a depth of 0.7 and 3.95 m. This layer is further delineated and referred to as Layers A21 and A22. Additional discussion on the characterization of these layers is provided below.

Layer A21

Layer A21 exhibits tip resistance typical of a stiff clay to a very loose silty sand (3 to 4 MPa). Data points primarily plot in zones 5 through 7 of the q_t-FR and q_t-B_q classification charts. While this layer classifies as a clayey silt to a sandy silt, further review of the raw u_2 pore pressure data indicates that the layer is an overconsolidated clay. The u_2 pore pressure readings are about -50 kPa. Negative pore pressures may be measured in dense sands, however, the measured tip resistance in this layer is less than about 5 MPa, which, as previously noted, is indicative of silty and clayey materials.

Layer A22

During a cone test, there is a slight delay in penetration while a cone rod is added at 1-m intervals. For sandy materials, rapid dissipation of penetration pore pressures is noted during these brief delays. Although Layer A22 may exhibit behavior of a sandy silt (Zone 6), the rapid dissipation of pore pressure during rod breaks was not apparent, indicating that the layer may be more representative of a silt.

Stratigraphy based on DMT Data

Like the CPT, empirical charts that incorporate index parameters based on testing device measurements are used for soil classification from DMT data. Figure A-7 shows raw DMT data and derived indices (i.e., I_D, E_D, K_D) along with five interpreted soil layers for the example soil profile. Figure A-8 shows the material index values, I_D, and dilatometer modulus values, E_D, within each layer plotted on a soil classification chart developed by Marchetti & Crapps (1981). The layering that was delineated using the DMT matches closely that evaluated based on the CPTu data. The same layer designators are used for the DMT data as was used for the CPTu data.

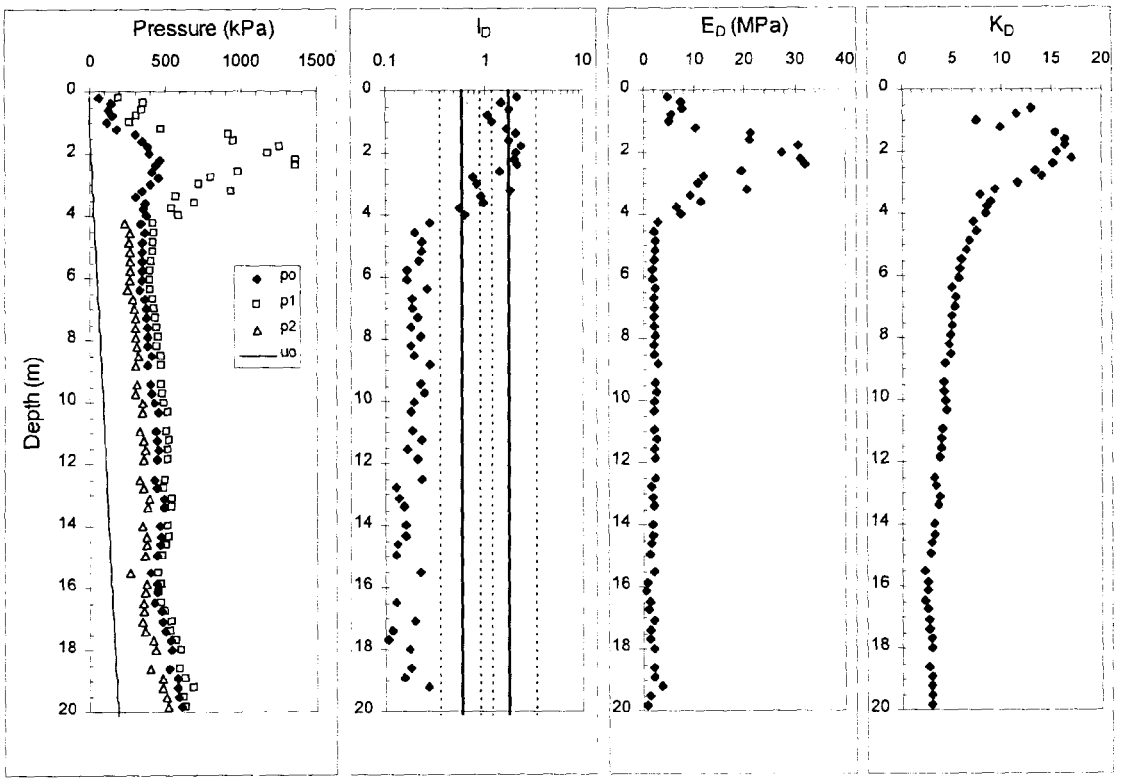

Figure A-7. Subsurface soil layering based on DMT index values.

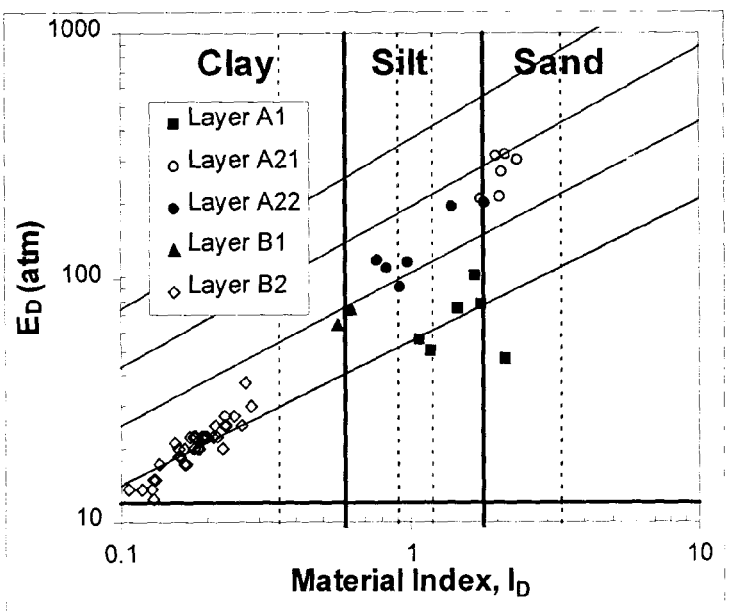

Figure A-8. Classification and consistency of soil layers based on DMT data.

Layer A1

Layer A1 extends to 1.2 m below the ground surface and is classified as compressible silt to sandy silt based on figure A-8. The boundary between Layer A1 and Layer A21 is noted by the increase in E_D (see figure A-7).

Layer A21

Layer A21 is located at depths between depths of 1.2 m and 2.4 m, and is classified as a medium rigidity silty sand based on figure A-8. High values of overconsolidation ratio (OCR) are associated with high K_D values. Since the crust is variable and has a high silt content with the potential for some sand (see figure A-2 for Boring B1), this layer is classified as an overconsolidated sandy silt. The boundary between Layer A21 and Layer A22 is evidenced by a decrease in I_D, E_D, and K_D.

Layer A22

Layer A22 is located at depths between 2.4 m and 3.6 m. This layer classifies as a medium dense silt. Since the K_D value is still high in this layer, it is likely that the layer is overconsolidated. The layer is classified as an overconsolidated silt. The boundary between layer A22 and Layer B1 is evidenced by a decrease in I_D, E_D, and K_D.

Layer B1

Layer B1 is located at depths between 3.6 m and 4.0 m. Based on figure A-8, this layer classifies as a medium consistency silty clay to clayey silt. The K_D value is greater than 5, which is indicative of a slightly overconsolidated material. This layer is classified as a slightly overconsolidated varved silty clay to clayey silt. The boundary between layer B1 and Layer B2 is evidenced by a decrease in I_D, E_D, and K_D.

Layer B2

Layer B2 is located at depths greater than 4 m to the end of the sounding (20 m). This layer classifies as a soft clay based on figure A-8.

Summary

Results indicate that the primary difference between the methods presented is in the resolution of the thickness and soil behavioral characteristics of the upper overconsolidated clay crust. The most detail is provided by the CPTu and DMT, followed by the CPT and SPT with disturbed sampling. Any one of these methods, however, provides sufficient detail to develop a subsurface profile for use in most geotechnical design analyses. It is likely that for settlement and stability analyses, it would only be necessary to perform analyses assuming a two-layer system, that being an overconsolidated clay crust overlying soft clay. Where detailed stratigraphic profiling is required (e.g., identification of liquefiable materials or slip surface), the CPTu, CPT, or DMT are relatively fast and inexpensive as compared to continuous sampling.

BASELINE DATA COLLECTION AND INTERPRETATION

Index Data Interpretation

In addition to data collected as part of the field investigation, the following laboratory data should be collected for disturbed and undisturbed soil samples: (1) natural moisture content; (2) visual identification; (3) dry unit weight; and (4) Atterberg limits. A summary of these data has been provided on figure A-2 for Boring B1, B2, and B3.

Calculation of Overburden Stresses

The vertical effective stress in the ground, σ_{vo}', is illustrated graphically by plotting effective stress with depth. This diagram is sometimes referred to as a "P_o diagram". Pressure diagrams are shown for boring location B1 in figure A-9. This diagram also shows calculated total stresses and pore pressures in the ground. The ground water table is located approximately 1 m below the ground surface.

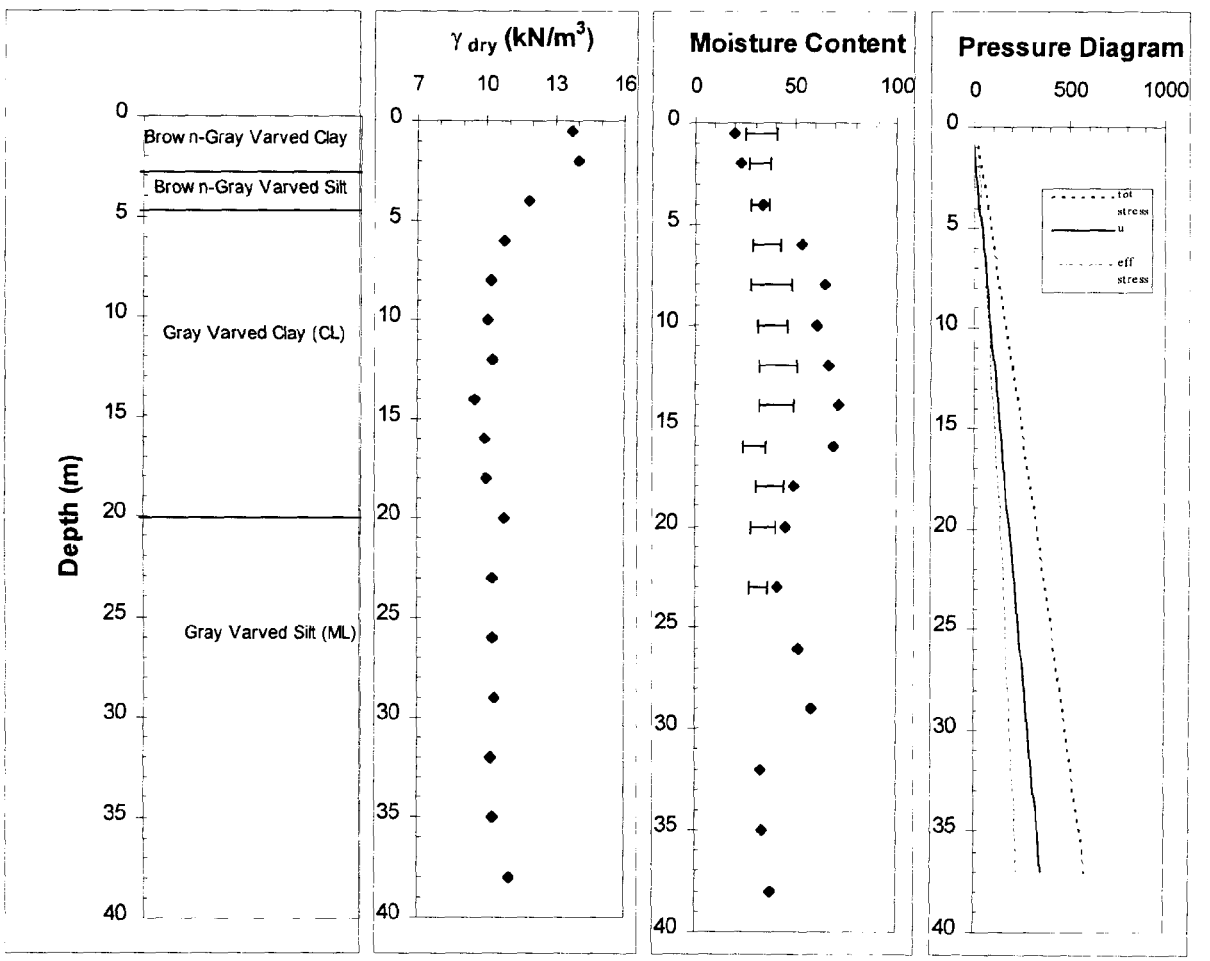

Figure A-9. Index properties and "P_o diagram" for Boring B1.

To develop the diagram for the example soil profile, the average total unit weight of each soil layer in the profile was evaluated using laboratory results. For each layer, the total unit weight (γ_t) was calculated using laboratory-measured dry unit weight (γ_d) and natural moisture content (w_n) values according to the equation:

$$\gamma_t = \gamma_d (1 + w_n) \qquad \text{(Equation A-1)}$$

For the example profile, it is sufficient to evaluate an average total unit weight value for the upper crust layer and the lower soft varved clay layer. Typically, scatter in unit weight data is small and average values can be used for design analyses. Using the information in figure A-2, the average total unit weight for the upper crust layer is 17 kN/m^3, and the average unit weight for the lower soft varved clay layer is 16.3 kN/m^3. These values were used to develop the P_o diagram.

CONSOLIDATION PROPERTIES OF SOIL

Overview

In this section, laboratory and in-situ testing methods to evaluate consolidation properties are presented. These properties relate to primary and secondary consolidation of clayey soils. First-order predictors (e.g., correlations to simple index properties) for consolidation properties are presented as well as more detailed methods for evaluating site-specific design properties.

Selection of Undisturbed Samples for Laboratory Consolidation Tests

Information on subsurface stratigraphy and basic index properties should be used to select the number and depths of undisturbed samples for laboratory consolidation testing. The number of samples should be selected to facilitate the development of a profile of preconsolidation stress, σ_p', with depth. For the example profile, at least two consolidation tests should be performed for the soils in the crust layer (between approximately 1 and 5 m), one test just below the transition depth from the crust to the underlying varved clay (at approximate depth of 5 to 6 m) and then at 3 to 5-m intervals within the varved clay deposit.

Evaluation of Preconsolidation Stress from Laboratory Testing

Standard one-dimensional consolidation tests (ASTM D2435) were performed on specimens from undisturbed tube samples at the approximate depths noted above. During sampling, transportation, extrusion, and trimming, samples must be carefully handled to prevent disturbance. For the consolidation test results presented here, it is assumed that the test has been performed over the required range of vertical stresses. These vertical stresses should be selected based on the specific loads imparted to the soil for the project conditions.

Typically, testing will incorporate a loading schedule with a load increment ratio (LIR) of one (1). This implies that each successive load is twice as large as the previous load. To obtain quality data, the engineer should estimate the σ_p'. With σ_p' estimated, smaller load increments can be specified

for stress levels near σ_p'. This will facilitate a more accurate assessment of the σ_p'. It is recommended that an unload-reload cycle be performed just before σ_p and recompression behavior be evaluated from this as opposed to using the initial portion of the consolidation curve up to σ_p'.

Figure A-10 shows the evaluation of σ'_p for a specimen using the Casagrande method and figure A-11 shows the evaluation of σ'_p for the same specimen using the strain energy method. Results summarized in table A-4 indicate that σ'_p values calculated from the strain energy method are at least equal to those calculated from the Casagrande method. Also shown on table A-4 are measures of sample disturbance using the sampling disturbance index described in chapter 4. Results show that where disturbance measures indicate that the sample is relatively undisturbed (i.e., rankings of VG or AT), that the Casagrande σ'_p is no less than 90 percent of the σ'_p value from the strain-energy method. Where the disturbance measures indicate that the sample is likely to be disturbed (i.e., ranking of DT), then the Casagrande σ'_p value was as low as 75 percent of the strain-energy value. Where disturbance is relatively large, graphical techniques such as Schmertmann's method (see Holtz and Kovacs, 1981) may be used to develop a "field-corrected" consolidation curve. Alternatively, the observations from this example support the recommendation to use the strain-energy method for all evaluations, especially when sample disturbance is notable.

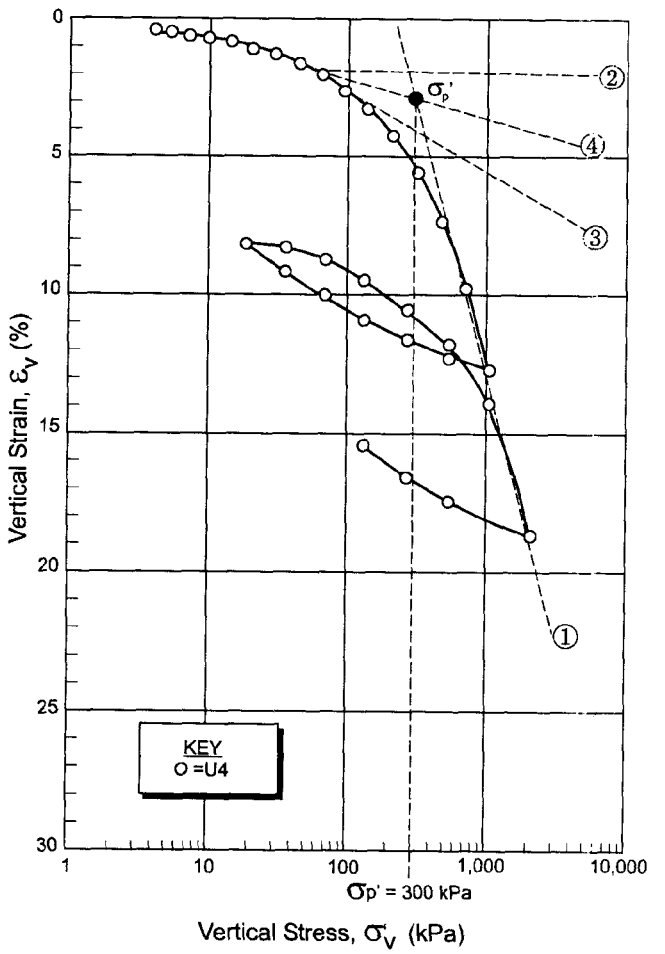

Figure A-10. Evaluation of σ_p' using the Casagrande method.

Table A-4. Summary of laboratory testing on varved clay samples.

Test #	Block #	Depth	w_n	LL	PI	ρ_{dry}	e_o	σ_{vo}'	σ_p'	σ_p'	OCR	OCR	ε at	SQR	$C_{c\varepsilon}$	C_c	$C_{r\varepsilon}$	C_r
		(m)						(kPa)	Casa	SE	Casa	SE	σ_{vo}'					
-	-	1.52	23	37.4	11.1	-	0.667	14.7	160	170	10.9	11.6	0.1	VG	0.064	0.11	0.006	0.01
137	F1-T1-E3	2.72	39	44	13.6	1.31	1.21	39.1	250	-	6.4	-	1.5	DT	0.16	0.35	0.03	0.07
138	F1-T1-E3	2.72	38.3	44	13.6	1.31	1.21	39.1	280	-	7.2	-	1.1	DT	0.13	0.29	0.03	0.07
-	-	2.72	39	44	13.6	-	1.131	39.1	300	320	7.7	8.2	1.4	DT	0.192	0.41	0.028	0.06
-	-	3.05	33	37.4	9.9	-	0.957	50.1	220	265	4.4	5.3	2.6	DT	0.215	0.42	0.012	0.02
120	F1-T3-E1	3.3	41.2	46.4	16.5	1.32	1.20	43.8	330	-	7.5	-	1.0	AT	0.17	0.37	0.03	0.07
121	F1-T3-E1	3.3	38.4	46.4	16.5	1.32	1.20	43.8	420	-	9.6	-	0.8	AT	0.15	0.33	0.03	0.07
140	F1-T5-E1	4.27	42.4	42.5	13	1.19	1.44	50.7	250	-	4.9	-	1.0	AT	0.21	0.51	0.04	0.10
139	F1-T5-E1	4.27	46.7	42.5	13	1.19	1.44	50.7	260	-	5.1	-	1.4	DT	0.19	0.46	0.03	0.07
141	F1-T7-E1	5.26	49.4	40	11.9	1.13	1.57	57.8	170	-	2.9	-	1.3	AT	0.21	0.54	0.04	0.10
142	F1-T7-E1	5.26	48.9	40	11.9	1.13	1.57	57.8	150	-	2.6	-	2.2	AT	0.16	0.41	0.03	0.08
-	-	6.1	60	46	17.5	-	1.74	59.1	200	175	3.4	3.0	1.1	DT	0.221	0.61	0.023	0.06
144	F1-T9-E1	6.3	56	45.9	17.5	1.08	1.69	65.1	135	-	2.1	-	1.1	AT	0.21	0.56	0.04	0.11
143	F1-T9-E1	6.3	59.8	45.9	17.5	1.08	1.69	65.1	135	-	2.1	-	0.9	VG	0.17	0.46	0.03	0.08
-	-	6.3	56	45.9	17.5	-	1.624	65.1	125	135	1.9	2.1	1.0	VG	0.22	0.58	0.045	0.12
145	F1-T11-E1	7.34	52.9	44.7	12.8	1.16	1.50	71.9	155	-	2.2	-	1.9	AT	0.22	0.55	0.04	0.10
146	F1-T11-E1	7.34	46.7	44.7	12.8	1.16	1.50	71.9	140	-	1.9	-	2.2	AT	0.15	0.38	0.03	0.08
117	F1-T13-E1	8.61	61	49.8	18.2	1.07	1.71	80.2	160	-	2.0	-	2.7	AT	0.19	0.51	0.02	0.05
147	F1-T13-E1	8.61	57.2	49.8	18.2	1.07	1.71	80.2	135	-	1.7	-	2.4	AT	0.21	0.57	0.04	0.11
-	-	9.14	63.4	47	16.9	-	1.839	78.9	120	160	1.5	2.0	3.7	AT	0.185	0.53	0.024	0.07
-	-	10.67	59.2	50	20.3	-	1.717	91.1	105	-	1.2	-	6.0	DT	0.196	0.53	0.016	0.04
-	-	12.19	65	49.2	18.7	-	1.885	103.4	111	-	1.1	-	6.2	DT	0.169	0.49	0.023	0.07
-	-	18.29	43	44.4	14.5	-	1.247	128.9	120	120	0.9	0.9	6	DT	0.258	0.58	0.038	0.09
-	-	21.3	39.9	-	NP	-	1.157	161.3	160.2	-	1.0	-	5.05	DT	0.049	0.11	0.005	0.01
-	-	24.38	56.1	-	NP	-	1.627	194.4	250	-	1.3	-	10.5	DT	0.185	0.48	0.025	0.07
-	-	27.43	32	-	NP	-	0.928	223.9	205	260	0.9	1.2	4.2	DT	0.084	0.16	0.009	0.02

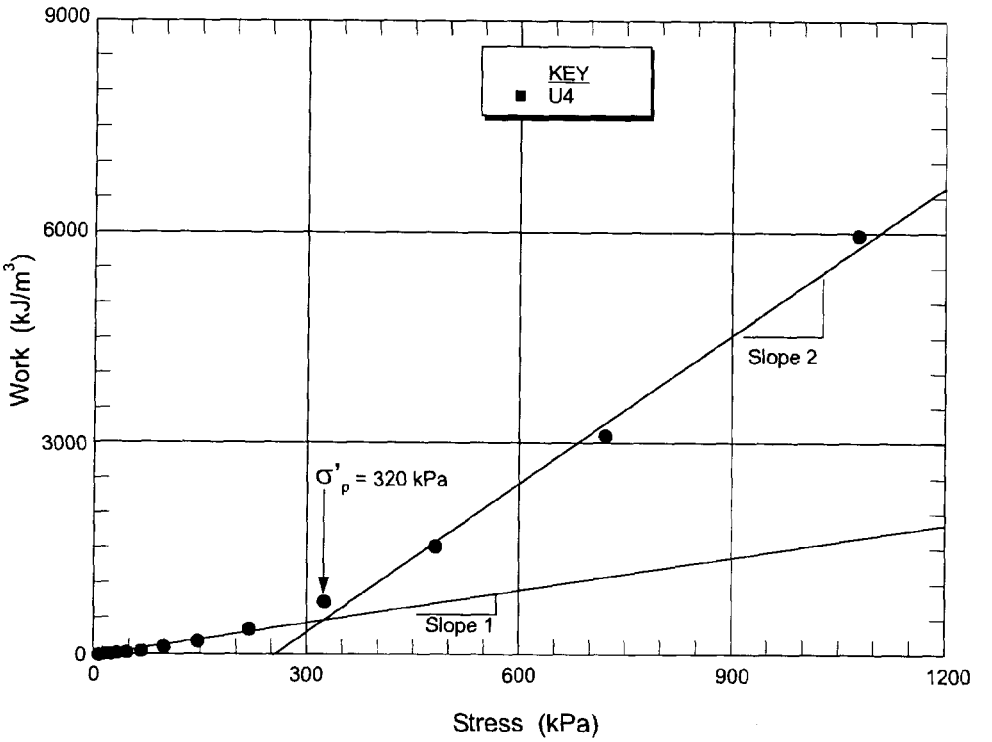

Figure A-11. Evaluation of σ_p' using the strain energy method.

In-Situ Test Methods to Evaluate σ'_p

In this section, estimates of σ'_p using in-situ testing methods are presented. Recommended specific equations are as follows:

Cone Penetration Test:	$\sigma_p' = 0.33\ (q_T - \sigma_{vo})$	(Equation A-2)
Type 2 Piezocone (shoulder element):	$\sigma_p' = 0.53\ (u_2 - u_o)$	(Equation A-3)
Flat (Plate) Dilatometer Test:	$\sigma_p' = 0.51\ (p_0 - u_o)$	(Equation A-4)
Field Vane Test:	$\sigma_p' = 3.54\ (s_{u,VST})$	(Equation A-5)

Figure A-12 shows a profile of σ_p' based on the aforementioned correlations for in-situ tests and the profile presented previously. Also shown on this figure are the results of the laboratory oedometer tests.

Calculated values of σ_p' compare favorably to the values obtained from the laboratory testing, except as noted subsequently.

- Since the piezocone with a shoulder element (i.e., $CPTu_2$) measures negative penetration pore water pressures in the upper 4 m, the correlation for σ_p' is not valid in this region.
- Each correlation tends to underpredict values of σ_p' for stiff fissured clays. The use of these correlations for stiff fissured clays is therefore conservative.

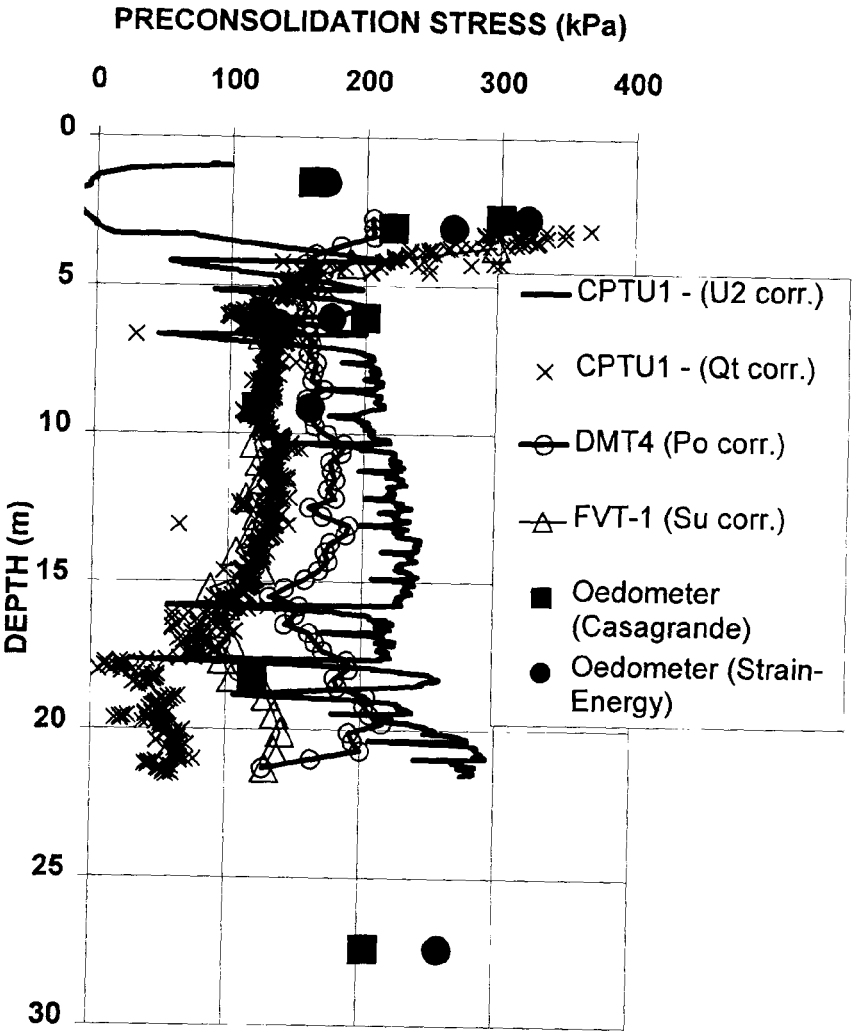

Figure A-12. Profile of σ_p' based on correlations with in-situ testing devices.

In figure A-12, the average trend line using equations A-2 through A-5 is plotted. For each of these correlations, the standard deviation (SD) is approximately 100 kPa (see figures 53, 55, 56, and 58 for SD values). The results in figure A-12 indicate that the proposed first-order correlation for σ_p' which is based on a large database of clay soil sites, is appropriate for the varved clay soils of this site. For each test device, the resulting correlated σ_p' value was within ±1 SD of a profile drawn through the laboratory testing results.

The utility of both in-situ testing devices and laboratory oedometer testing could be realized for a reasonably large project where several boring locations would be required. If, for example, a project required twenty geotechnical test borings to achieve appropriate coverage for comprehensive characterization, it likely would be faster and more cost-effective to replace borings with additional locations for in-situ testing such as CPT or DMT. In addition, as shown previously, additional data such as stratigraphic profiling can be provided. By comparing laboratory-measured σ_p' values with an in-situ testing device result, the correlations previously described could be easily adjusted to more closely match the laboratory-measured results for σ_p'. The value of the in-situ testing device is that comparisons of in-situ testing results from additional locations could be compared to that of the baseline location to verify similar conditions. If trends in the data were similar, but correlated σ_p' values were higher than those from the baseline, then this information could be used to justify a different σ_p' profile with depth at the other location. If trends in the data were very different, then additional geotechnical borings and undisturbed sampling could be performed at that location and additional laboratory consolidation tests performed.

Evaluation of C_c and C_r

Overview

Compression parameters C_c and C_r can be interpreted by correlation or by direct laboratory-measurement. The value of C_c is evaluated by drawing a best-fit tangent line to data on an e-log σ'_{vc} representation of consolidation data along the virgin (i.e., part of curve where stresses are greater than σ'_p) portion of the curve. The modified compression index, $C_{c\varepsilon}$, is evaluated similarly on a plot of ε_v-log σ'_{vc}. An example evaluation of $C_{c\varepsilon}$ for the example soil profile is shown on figure A-13.

Data Interpretation

Numerous correlations relating simple soil index properties (e.g., LL, w_n) to C_c and $C_{c\varepsilon}$ are available in the literature for silts and clays. These correlations are often used for first-order predictions of settlements, but should not be relied upon for final design, unless the correlation has been developed using site-specific laboratory consolidation test data. For most clays, values of $C_{c\varepsilon}$ tend to increase with increasing moisture contents, however, significant scatter exists for the data. Several empirical correlations are shown in figure A-14 along with actual data from the example soil profile. A review of figure A-14 indicates that correlations proposed by Terzaghi and Peck (1967) and Lambe and Whitman (1969) generally underpredict compression parameter values (i.e., C_c or $C_{c\varepsilon}$) as compared to laboratory-measured values. On average, the correlation developed by Azzouz et al. (1976) for Chicago clays provides a reasonable approximation of C_c.

It is interesting to note that the correlation developed for Hackensack Valley varved clays, which should be more representative for the example varved clay deposit, on average, overpredicts laboratory-measured $C_{c\varepsilon}$ values. Figure A-15 shows the results of an extensive investigation of the Connecticut Valley varved clays. This figure depicts the large scatter that exists in $C_{c\varepsilon}$ data for this deposit. Figures A-14 and A-15 demonstrate that significant uncertainty may exist when using published correlations for clay compression indices to perform design calculations.

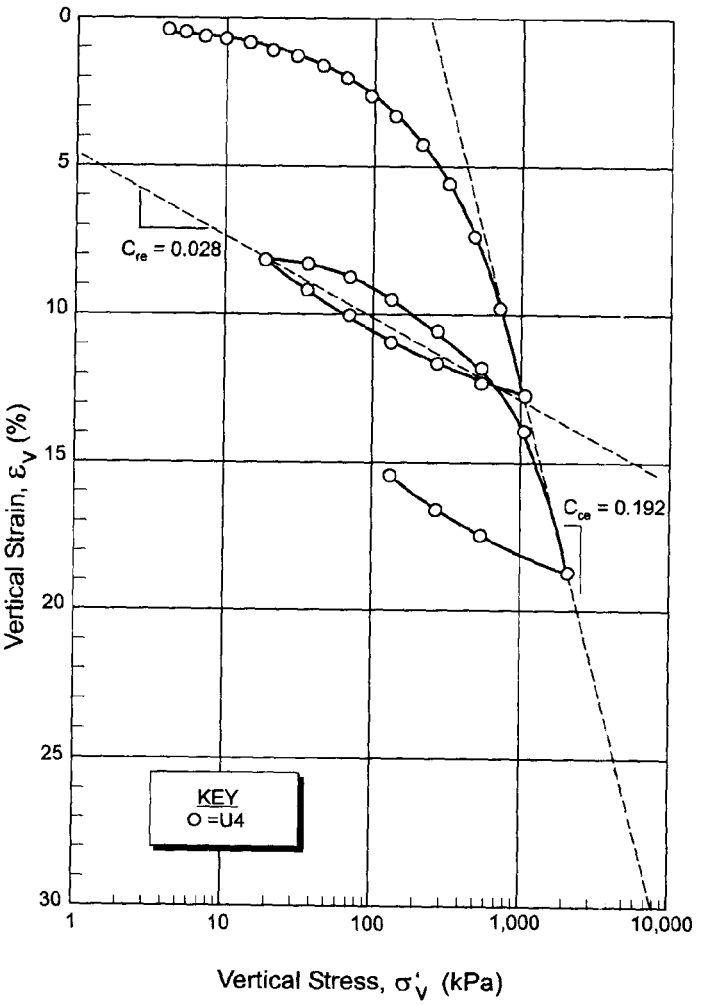

Figure A-13. Sample graphical evaluation for $C_{c\varepsilon}$ and $C_{r\varepsilon}$.

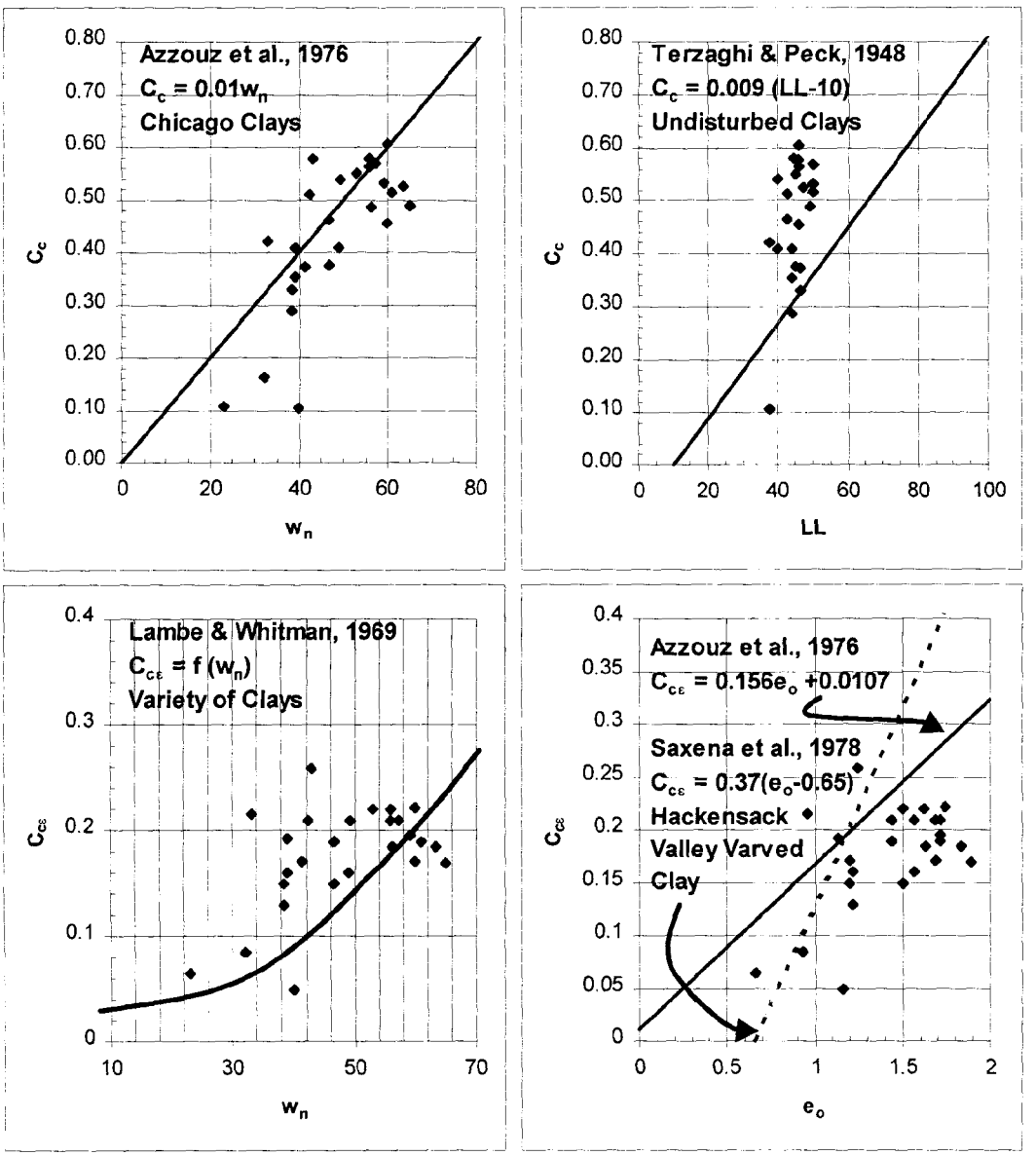

Figure A-14. Empirical correlations of C_c and $C_{c\varepsilon}$.

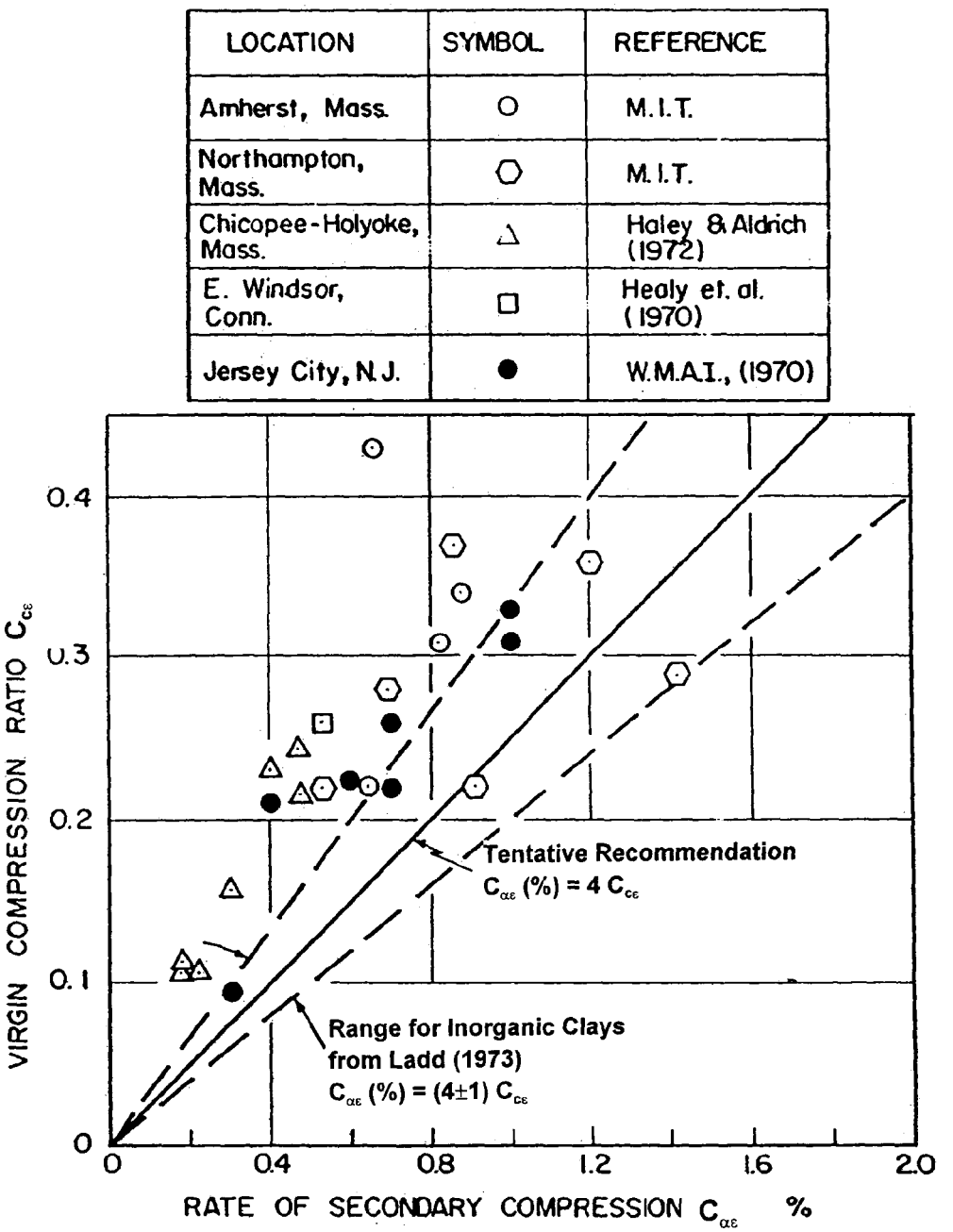

Figure A-15. Secondary compression results for Connecticut Valley varved clays investigation.

Figure A-16 shows the laboratory-measured $C_{c\varepsilon}$ versus depth. For the varved clay, $C_{c\varepsilon}$ ranges from 0.07 to 0.22 with an average value of 0.19. Interpreting a value for design should be based on a rational assessment of the data. The objective is to assign a $C_{c\varepsilon}$ value to each behaviorally different subsurface layer or to assign some representative value for the entire subsurface. Assessments to be made in evaluating the $C_{c\varepsilon}$ data include: (1) depth ranges where the material is more silty or sandy as compared to other depth ranges; (2) depth of transition from crust layer to underlying varved clay deposit; and (3) assessment of sampling disturbance.

The variability in $C_{c\varepsilon}$ as shown in figure A-16 is likely the result of: (i) some samples being more disturbed than others; and (ii) the possibility that, due to the varved nature of the deposit, there is relatively significant variation between samples as to the amount of silt, sand, and clay. Lower values of $C_{c\varepsilon}$ would be expected for samples that contain higher amounts of silt and sand as compared to those with a higher percentage of clay.

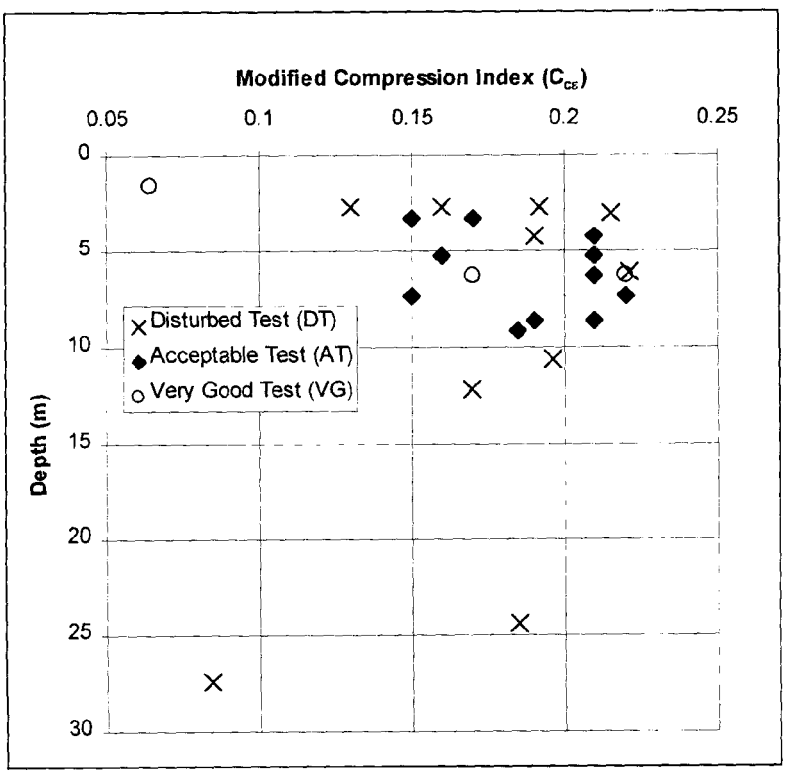

Figure A-16. Laboratory-measured $C_{c\varepsilon}$ vs. depth.

It is inferred from the calculated sample disturbance indices for samples from the overconsolidated clay crust (i.e., depths less than approximately 4 m), that 5 of the 9 tests are designated as disturbed. This is likely due to the fissured nature of this material and that relatively large volume changes may have occurred during the initial portion of the test to close the fissures. It appears as though the single value of $C_{c\varepsilon}$ = 0.07 at 1.5 m may be an outlying data point. For the normally consolidated to lightly overconsolidated portion of the profile (i.e., for depths greater than approximately 4 m), the vast majority (9 out of 10) of the samples between a depth of 4 and 8.6 m are designated as acceptable to very good with respect to the sample disturbance index. For this depth range, $C_{c\varepsilon}$

ranges from 0.15 to 0.22 with an average value of 0.20. The three samples below a depth of 8.5 m were designated as disturbed and have an average $C_{c\varepsilon}$ of 0.18. The sample at a depth of 27.5 m was mostly silt and not considered to be representative of the varved clay.

Since the varved clay deposit is "consistently heterogeneous" in that the profile contains thin layers of silt and clay, it is appropriate to use an average value for $C_{c\varepsilon}$ for design settlement analyses. Based on this, a value of 0.20 is appropriate for $C_{c\varepsilon}$ for the entire profile. The average recompression ratio is 0.03 ± 0.01. For design, it would be reasonable to select a value for design of 0.04 for the entire varved clay and varved silt profile.

Laboratory Evaluation of c_v

Figure A-17 shows a plot of calculated c_v values for reload and virgin compression for five varved clay samples tested in one-dimensional compression. The c_v values are plotted as a function of normalized stress that is defined as σ_{vc}'/σ_p', where σ_{vo}' is the vertical effective stress in the ground at the depth where the sample was taken. Each sample exhibits the same trend of c_v significantly reducing for load levels in the normally consolidated range (i.e., for $\sigma_{vc}'/\sigma_p'>1$). Scatter in the overconsolidated range is typical and may result from the following: (1) consolidation occurs quite rapidly at these load levels making the determination of the time for the end of primary consolidation difficult; and (2) in very stiff clays, fissures may exist at low stress levels which will affect drainage rates. Some of the inherent variability associated with evaluation of this parameter can be minimized by concentrating the interpretation on values corresponding to a reload cycle and to values associated with virgin compression. Values from initial loading should not be used due to inevitable sample disturbance effects. Data from a reload cycle is likely more representative of the "field curve".

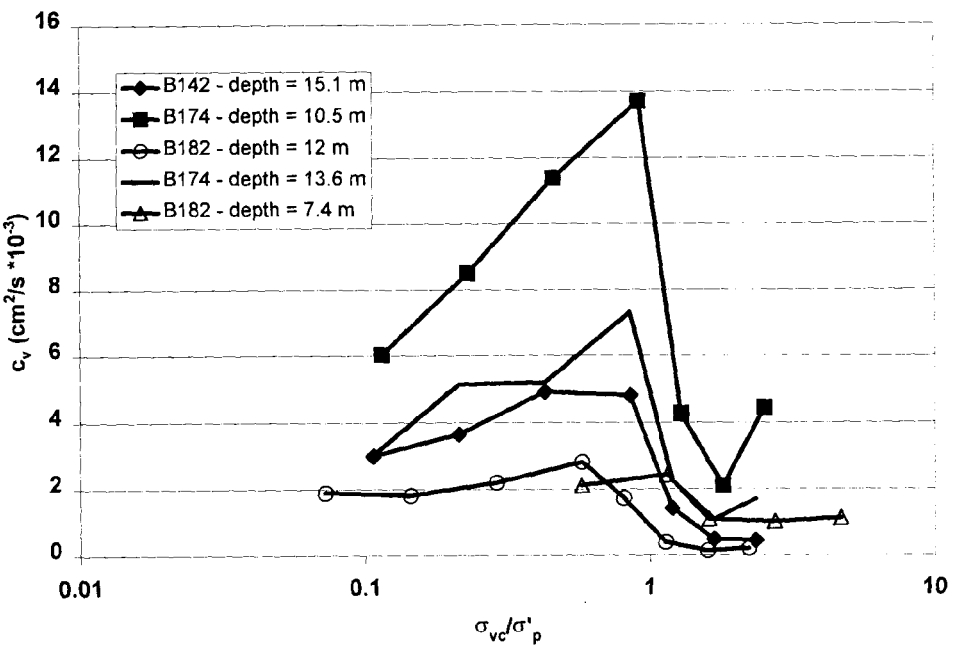

Figure A-17. c_v values from laboratory consolidation tests.

A rational approach to selecting a c_v value would include first assessing whether the applied loads are sufficiently high to consolidate the compressible layer to stress levels beyond σ_p'. If stress levels after consolidation are below approximately $0.8\sigma_p'$, an average c_v value associated with stress levels below $0.8\sigma_p'$ should be used for design. If the compressible layer will consolidate to stress levels in excess of σ_p' or greater than $0.8\sigma_p'$ as described here, then the average c_v value for the range of stresses from σ_p' to the final vertical effective stress in the ground should be used. This value, however, should not exceed the average value obtained for the overconsolidated stress range (i.e., less than $0.8\sigma_p'$).

The data shown in figure A-17 indicate that measured c_v values for the sample from B174 at a depth of 10.5 m are greater than those for the other four samples, although the difference is much less in the normally consolidated range. This may be due to more silt in the sample as compared to other samples, however, such scatter can be expected even for similar deposits due to the evaluation method used to obtain c_v. These data indicate that a reasonable average value for the normally consolidated range is 0.0008 cm^2/s and, for the overconsolidated range, a value of 0.003 cm^2/s is reasonable.

Evaluation of c_h from CPTu Dissipation Data

In this section, dissipation test results from piezocone testing are used to estimate the horizontal coefficient of consolidation, c_h, in the varved clay profile at two different depths in the deposit. To perform a dissipation test, cone penetration is paused at a test depth and pore pressures are recorded with time. Pore pressure dissipation curves for the two dissipation tests are shown on figure A-18. The procedures used to evaluate c_h have been provided in section 5.4.4.

To calculate c_h using a piezocone, the modified time factor, T* must be evaluated. The parameter T* is related to the degree of consolidation, U. Values of T* are presented in section 5.4.4 (see table 27) for various stages of dissipation. The parameter U has been defined in equation 47. Figure A-19 shows normalized excess pore pressure curves for the two dissipation tests.

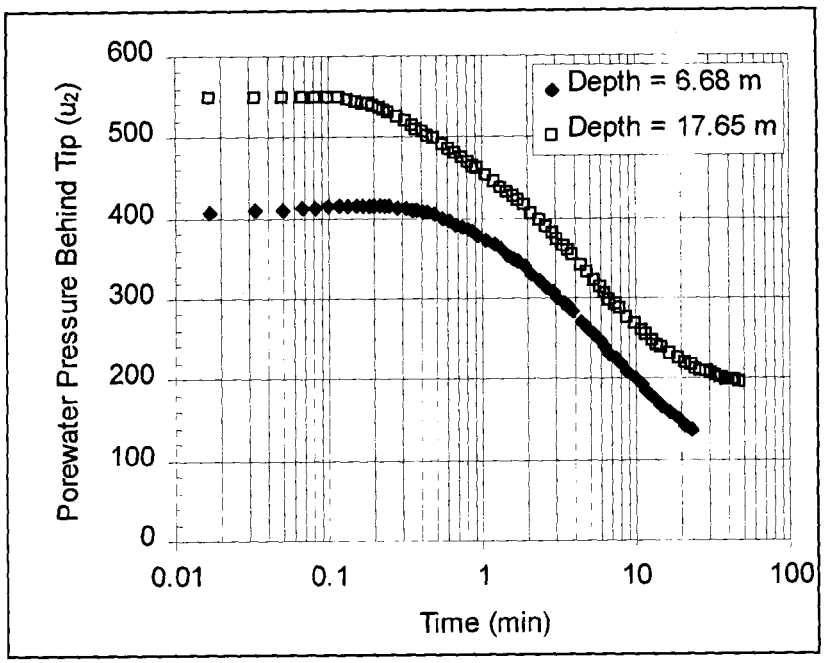

Figure A-18. $CPTu_2$ pore pressure dissipation curves.

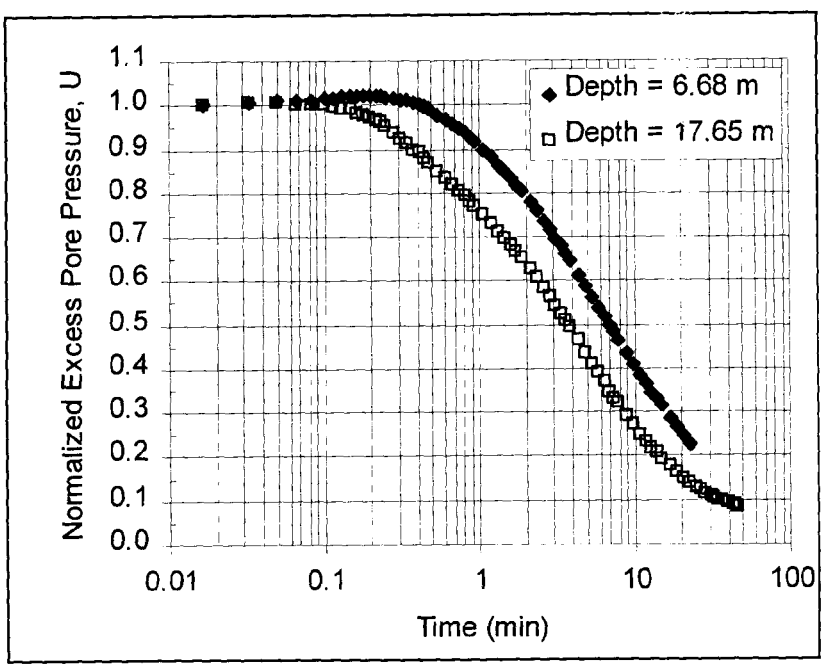

Figure A-19. Normalized $CPTu_2$ dissipation curves

The parameters used for this example to evaluate c_h are shown in table A-5. A standard cone with a projected tip area of 10 cm^2 and a diameter of 35.6 mm was used in the evaluation. Tables A-6 and A-7 present calculations of c_h at various degrees of consolidation using normalized curves for the two depths presented above. Values for c_h can be estimated for various degrees of consolidation,

however, evaluations for design should be made based on a degree of consolidation of at least 50 percent. The parameter c_h is calculated according to the following:

$$c_h = \frac{T^*\left(a^2\sqrt{I_r}\right)}{t} \qquad \text{(Equation A-6)}$$

Table A-5. Parameters used for analysis of dissipation data.

Depth (m)	Filter Location	Cone Radius, a (cm)	Plasticity Index (PI)	OCR	Rigidity Index, I_r (figure 60)
6.68	u_2	1.78	10	2	230
17.65	u_2	1.78	15	1	210

Table A-6. Evaluation of c_h from CPTu_2 dissipation data at 6.68 m

Normalized Excess Pore Pressure, U	T* for u_2 element location	Cone Radius, a (cm)	Square Root of Rigidity Index, $\sqrt{I_r}$	Time to Normalized Excess Pore Pressure, U (min)	c_h (cm^2/s)*10^{-3}
0.8	0.038	1.78	15.2	1.9	16
0.7	0.078	1.78	15.2	3.1	20
0.6	0.142	1.78	15.2	4.6	25
0.5	0.245	1.78	15.2	6.9	29
0.4	0.439	1.78	15.2	10.4	34
0.3	0.804	1.78	15.2	15.9	41
0.2	1.60	1.78	15.2	26	49

Table A-7. Evaluation of c_h from CPTu_2 dissipation data at 17.65 m

Normalized Excess Pore Pressure, U	T* for u_2 element location	Cone Radius, a (cm)	Square Root of Rigidity Index, $\sqrt{I_r}$	Time to Normalized Excess Pore Pressure, U (min)	c_h (cm^2/s)*10^{-3}
0.8	0.038	1.78	14.5	0.75	39
0.7	0.078	1.78	14.5	1.4	43
0.6	0.142	1.78	14.5	2.4	45
0.5	0.245	1.78	14.5	3.8	49
0.4	0.439	1.78	14.5	5.6	60
0.3	0.804	1.78	14.5	8.5	72
0.2	1.60	1.78	14.5	13.9	88

A comparison of the c_h values reported in tables A-6 and A-7 to the c_v values from figure A-17 for laboratory testing on varved clay samples indicates that the horizontal coefficient of consolidation may be on the order of 50 times greater than the vertical coefficient of consolidation. Typically, c_h is greater than c_v in clays due to the presence of localized pockets of higher permeability material. In the case of varved clays, this affect is magnified due to the continuous nature of the silt and sand varves.

The selection of an appropriate value for a coefficient of consolidation (i.e., c_v or c_h) will depend on the design application. For large area fills (i.e., where the width of the loaded area is greater than say 2 times the thickness of the cohesive soil deposit), a c_v value should be used. Where wick drains are used or for the evaluation of pile driving induced pore pressures, a c_h value should be used. For each specific design, the engineer should evaluate the drainage distances and likely direction of consolidation water flow and select a c_v, c_h, or intermediate value accordingly. Alternatively, the best assessment of time rate of settlement (or time for consolidation) can be achieved using piezometers.

Evaluation of C_α

In geotechnical design analyses, it is assumed that secondary settlement occurs after primary consolidation is completed. As noted earlier, secondary compression settlements may be relatively large for organic soils. For the soil profile used in this example, secondary compression settlements would be expected to be insignificant for typical highway projects since the soils are not organic. However, the procedures to calculate $C_{\alpha\varepsilon}$ are the same regardless of the soil type. This example demonstrates the evaluation and interpretation of $C_{\alpha\varepsilon}$.

Figure A-20 shows calculated values of $C_{\alpha\varepsilon}$ versus σ_{vc}'/σ_p' for reload and virgin compression for the same five consolidation tests discussed in the section of this example on laboratory evaluation of c_v. For each load increment, the time to complete primary consolidation was evaluated and $C_{\alpha\varepsilon}$ was evaluated over a period after primary consolidation was completed. This plot indicates that values of $C_{\alpha\varepsilon}$ are affected by stress history in that maximum values for $C_{\alpha\varepsilon}$ are evaluated for stress levels greater than the preconsolidation stress (i.e., at stresses corresponding to virgin compression). Therefore, to assess a value of $C_{\alpha\varepsilon}$ to be used for design analyses, the final effective stress in the ground after primary consolidation is completed should be evaluated. If the final effective stress is less than approximately $0.8\sigma_p'$, then an average value of $C_{\alpha\varepsilon}$ evaluated in the overconsolidated range may be used for design. If final effective stresses in the ground exceed σ_p', then it is conservative to select $C_{\alpha\varepsilon}$ value corresponding to stresses in the range of 1 to 2 times σ_p'.

For normally consolidated soils, the ratio of the coefficient of secondary compression to the compression index ($C_\alpha/C_c = C_{\alpha\varepsilon}/C_{c\varepsilon}$) is relatively constant for a given soil. On average, the value of $C_{\alpha\varepsilon}/C_{c\varepsilon}$ is 0.04 ± 0.01 for inorganic clays and silts. This value may be used to assess the values from the laboratory tests. Figure A-21 shows a plot of $C_{\alpha\varepsilon}$ versus $C_{c\varepsilon}$ for the five consolidation tests. The values of $C_{c\varepsilon}$ were obtained from the laboratory consolidation curves (not provided herein) and are representative of the slope of the strain vs. log σ_{vc}' curve at each stress level. The average $C_{c\varepsilon}$ value from the five consolidation tests is 0.35. The results indicate a range for $C_{\alpha\varepsilon}/C_{c\varepsilon}$ from 0.02 to 0.04. This range of values is, on average, slightly less than that reported in the literature for inorganic clays and silts. It is noted that for samples that are disturbed, laboratory-measured values of C_α (or

$C_{\alpha\varepsilon}$) may be underestimated in the normally consolidated range as compared to results from high-quality undisturbed samples. For design, an average value corresponding to $C_{\alpha\varepsilon}/C_{c\varepsilon}$ = 0.03 for an average $C_{c\varepsilon}$ = 0.35 could be used, i.e., $C_{\alpha\varepsilon}$=1.05 (say 1 percent). This value is consistent with the range shown in figure A-20 for $C_{\alpha\varepsilon}$ values in the range for $\sigma_{vc}'/\sigma_p' > 1$.

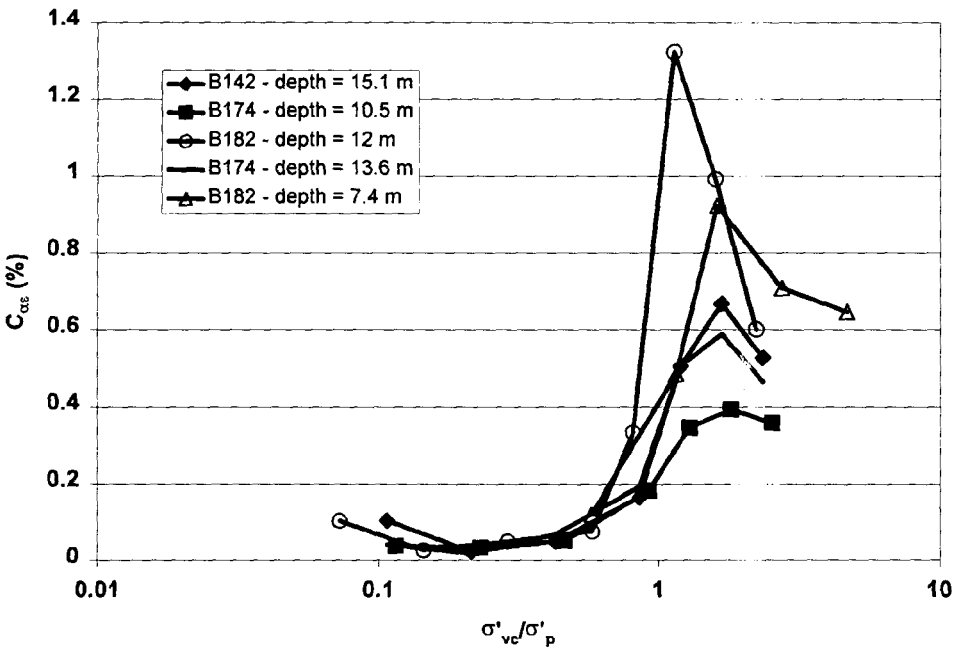

Figure A-20. $C_{\alpha\varepsilon}$ values from laboratory consolidation tests.

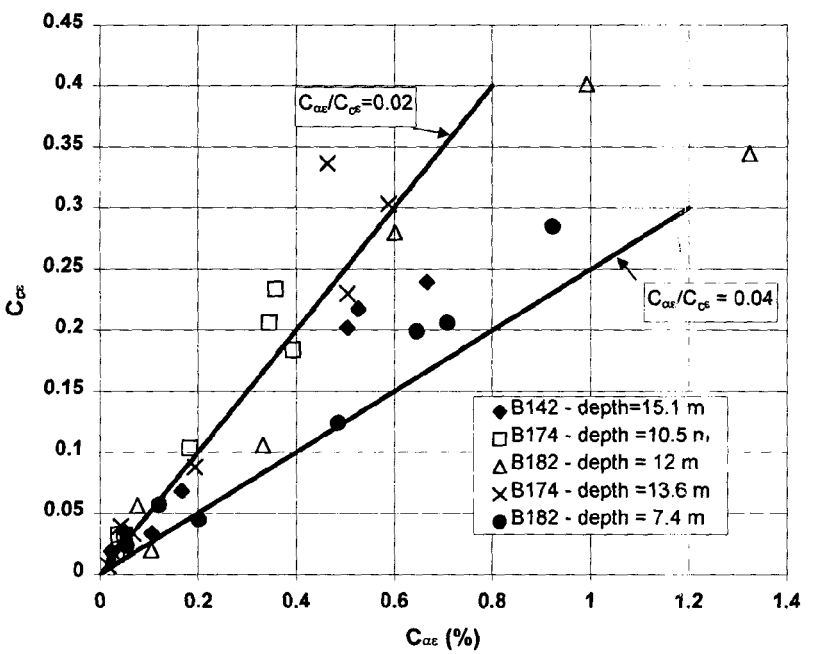

Figure A-21. Comparison of $C_{\alpha\varepsilon}$ and $C_{c\varepsilon}$ for laboratory consolidation tests.

EVALUATION OF IN-SITU HORIZONTAL STRESSES

For overconsolidated soils (clays, silts, sands, and gravels), K_o can be calculated according to the following equation:

$$K_o = (1 - \sin\phi')OCR^{\sin\phi'} \qquad \text{(Equation A-7)}$$

Using results from undrained triaxial compression tests and one-dimensional consolidation tests, values of ϕ' and OCR for the example soil profile can be substituted into equation A-7 to develop a profile of K_o with depth. This profile is shown on figure A-22. Also shown on this figure are profiles of K_o with depth based on in-situ testing devices. To develop these profiles using in-situ test data, the preconsolidation stress was calculated at each measurement point using equations A-2 through A-5 for estimating preconsolidation stress from measured in-situ testing device parameters. From this, the OCR value was calculated and K_o was evaluated using equation A-7.

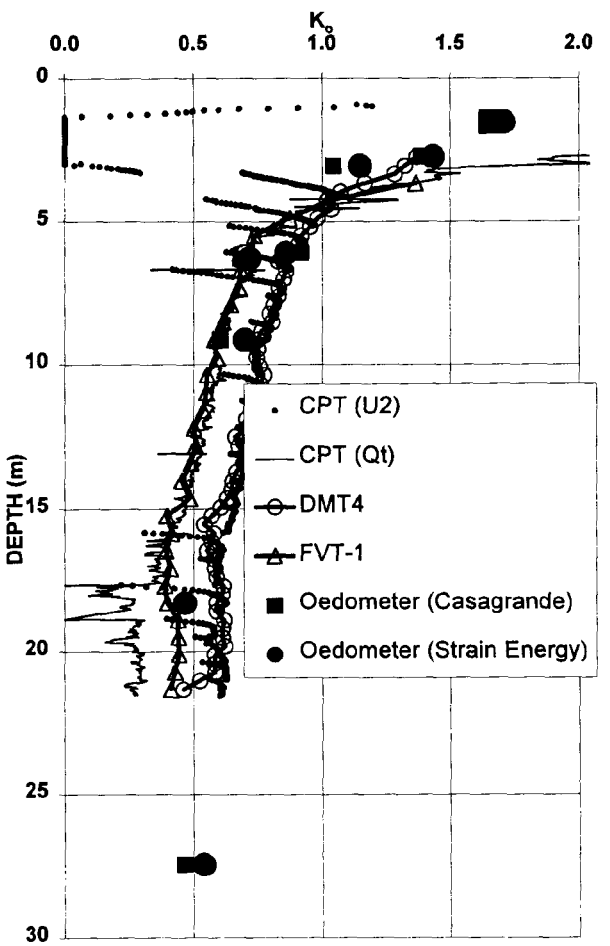

Figure A-22. K_o value calculated using in-situ testing devices.

For the soft normally to lightly overconsolidated clay layer, which exists below approximately a depth of 5 m, all methods provide reasonable values of K_o. The maximum difference between any two calculated K_o values at any depth is approximately 0.2. It is noted that the variation is caused by differences in calculated values of preconsolidation stress (and thus OCR). This variation should not result in a significant effect on design calculations that require estimates of K_o in soft to medium clays.

The methods described in this section for evaluating K_o are well-suited for evaluations in normally to lightly overconsolidated clay soils and for intact (i.e., non-fissured) overconsolidated soils. In addition, the use of the in-situ testing method correlations likely results in lower values of K_o than actual values. Whether or not values that are less than actual values for K_o are conservative or unconservative needs to be evaluated based on the specific design application. Where a more accurate assessment of K_o is required for design, it is recommended that either laboratory triaxial tests on undisturbed samples subjected to K_o consolidation or in-situ self-boring pressuremeter testing be performed.

UNDRAINED SHEAR STRENGTH

Overview

The evaluation of undrained shear strength, s_u, for the soft to medium varved clay deposit is provided in this section. Specifically, laboratory strength data from CIUC and UU testing as well as derived s_u values from CPT, CPTu, DMT, and VST are presented. Based on these data, a recommended undrained strength profile is developed.

Baseline Data for Undrained Strength Evaluation

The methods presented in chapter 5 indicate that the preconsolidation stress profile should be developed for a cohesive deposit and that this information is useful in evaluating undrained strength. For this section of the example, the profile of preconsolidation stress shown in figure A-23 is used. Also shown on this figure is a plot of the vertical effective stress with depth (i.e., the "P_o diagram").

Undrained Shear Strength Evaluation from Laboratory Shear Strength Tests

Table A-8 shows a summary of the triaxial tests (UU and CU) performed and the results of this testing. For the CU tests, the isotropic consolidation stress used was selected to be equal to the vertical effective stress in the ground. Therefore, the undrained strength measured in the CU tests corresponds to the depth at which the sample was taken. Example stress-strain and pore pressure-strain curves are shown below for a UU and CU test.

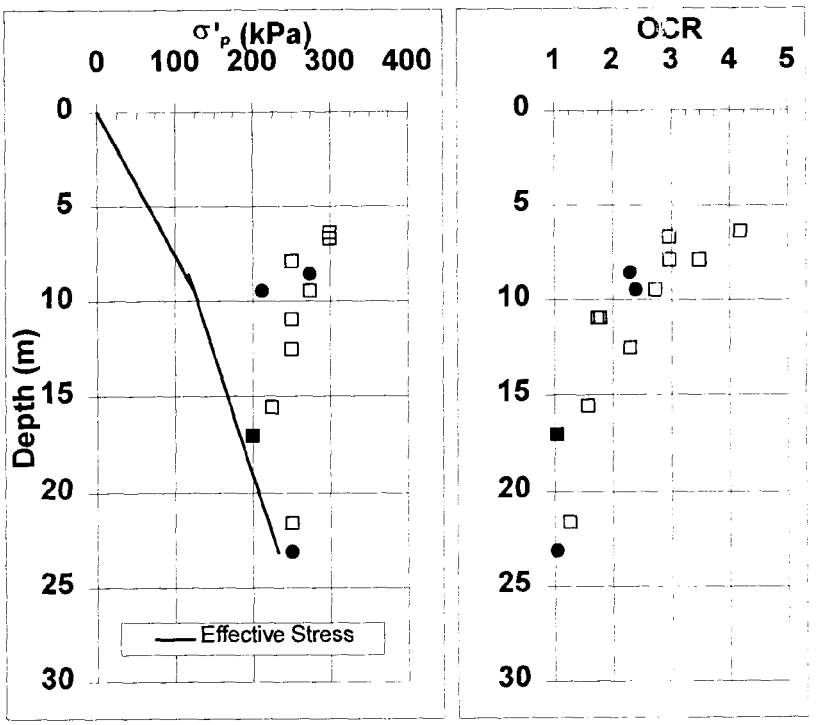

Figure A-23. P_o diagram developed from 1-D consolidation data.

Table A-8. Summary of triaxial test data.

Boring	Sample	Test No.	Test Type	Depth (m)	w (%)	LL	PI	γ_{dry}	Cell Stress (kPa)	Peak s. (kPa)	Δu_f (kPa)	σ_p' (kPa)	OCR	ϕ'
S-43	UP-1C	R-1	CIUC	8.5	41.4	46	21	12.9	119.6	62.8	56.4	275	2.30	31.3
S-52	UP-3B	R-4	CIUC	9.4	52.5	56	30	11.4	88.3	44.1	47.1	212	2.40	30.8
S-43	UP-4C	R-2	CIUC	17.1	51.6	52	25	11.6	191.2	70.6	109.8	200	1.05	28.6
S-43	UP-6C	R-3	CIUC	23.2	49.2	52	26	11.9	239.3	77.5	147.1	250	1.04	27.5
BR-35	UP-1	Q-14	UU	6.4	53.3	56	29	11.1	71.6	27.5	NA	300	4.2	NA
S-52	UP-2	Q-9	UU	6.4	52.3	60	32	11.1	59.8	44.1	NA	300	5.0	NA
S-56	UP-2	Q-8	UU	6.4	48.7	49	25	11.7	71.6	33.3	NA	300	4.2	NA
BR-16	UP-1	Q-1	UU	6.7	44.9	51	25	12.1	100.0	34.3	NA	300	3.0	NA
BR-24	UP-1	Q-6	UU	7.9	59.4	60	33	10.3	71.6	27.5	NA	250	3.5	NA
BR-8	UP-1	Q-12	UU	7.9	51.6	50	25	11.1	83.4	34.3	NA	250	3.0	NA
BR-11	UP-1	Q-7	UU	9.4	52.3	50	25	11.1	100.0	37.3	NA	275	2.7	NA
BR-16	UP-2	Q-2	UU	11.0	54.6	53	27	10.9	139.3	34.3	NA	250	1.8	NA
S-43	UP-2	Q-4	UU	11.0	48.1	52	25	11.9	143.2	42.2	NA	250	1.7	NA
S-52	UP-4	Q-10	UU	12.5	47.6	45	21	11.7	107.9	31.4	NA	250	2.3	NA
BR-35	UP-4	Q-15	UU	15.5	51.5	48	23	11.1	143.2	19.6	NA	225	1.6	NA
S-43	UP-4	Q-5	UU	17.1	51.6	52	25	11.3	191.2	32.4	NA	200	1.0	NA
BR-11	UP-3	Q-11	UU	21.6	41.7	39	17	12.6	196.1	39.2	NA	250	1.3	NA

Laboratory Shear Strength Testing

Unconsolidated Undrained (UU) Triaxial Test

Unconsolidated Undrained (UU) tests were performed on samples of a Connecticut valley varved clay associated with a highway project in Connecticut. A stress–strain strain curve from an unconsolidated undrained test is presented in Figure A-24 (a). The undrained shear strength from this test would be half the maximum principal stress difference, $\Delta\sigma_{max}$. For this test $\Delta\sigma_{max}$ = 160.8 kPa, so the undrained shear strength from this UU test is 80.4 kPa.

Since shear strength will vary for different test types, it is best to designate the shear strength using the acronym for the associated laboratory or field test. For the unconsolidated undrained (UU) test, the undrained shear strength is designated $s_{u,\,UU}$.

Total stress paths can be presented for an unconsolidated undrained test with the total stress state variables q and p defined as:

$$q = \frac{(\sigma_1 - \sigma_3)}{2} \quad \text{and} \quad p = \frac{(\sigma_1 + \sigma_3)}{2} \qquad \text{(Equation A-8)}$$

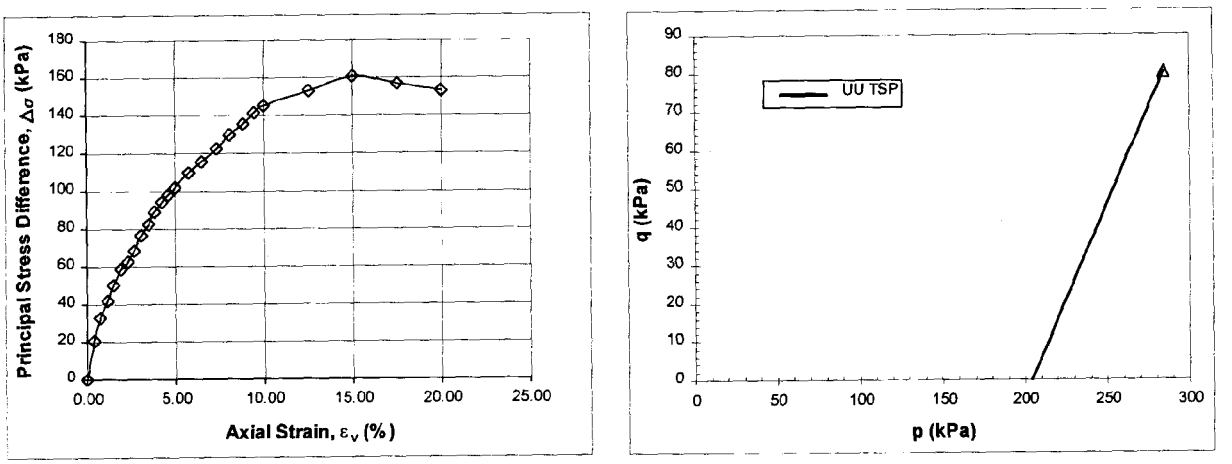

Figure A-24. Stress – strain curve and stress path for a UU test on Connecticut Valley varved clay specimen.

A total stress path for a UU test is presented in figure A-24 (b). Since q is equal to the principal stress difference divided by 2, it can be seen in figure A-24 (b) that the failure point from the stress path plot is equal to the undrained shear strength, $s_{u,\,UU}$ = 80.4 kPa.

Isotropically Consolidated Undrained Compression (CIUC) Triaxial Test

Isotropically consolidated undrained compression (CIUC) triaxial tests with pore pressure measurements were also performed on samples of the Connecticut valley varved clay. For a triaxial compression test, the undrained shear strength will be determined as half the maximum principal stress difference, $\Delta\sigma_{max}$. Figure A-25 (a) shows a stress strain curve from a CIUC test of Connecticut

valley varved clay. For this test $\Delta\sigma_{max}$ = 160.7 kPa, so the undrained shear strength from this CIUC test is 80.4 kPa. For the isotropically consolidated undrained compression (CIUC) test, the

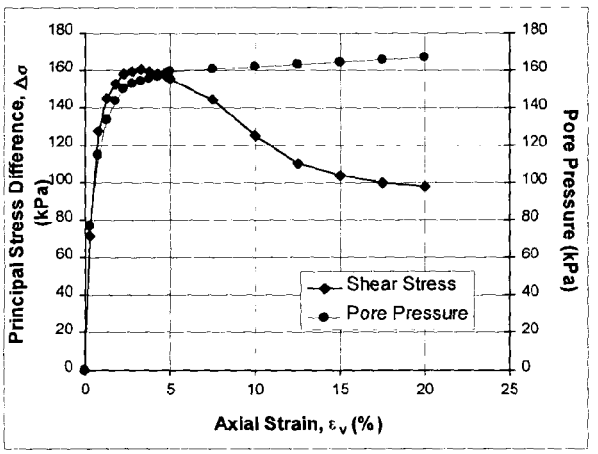

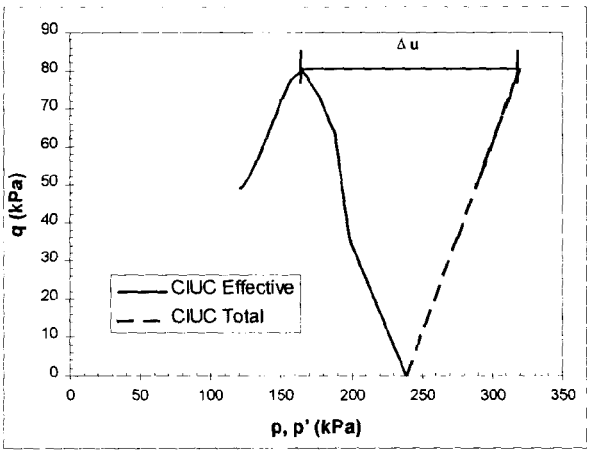

undrained shear strength is designated $s_{u,\,CIUC}$.

Figure A-25. (a) Stress – strain curve and stress path for a CIUC test on a Connecticut Valley varved clay specimen.

The total and effective stress paths for this CIUC test are shown in Figure A-25 (b). The effective stress path variable, p′, is equal to:

$$p' = p - \Delta u \qquad \text{(Equation A-9)}$$

The horizontal difference between the total and effective stress paths is the change in pore pressure (Δu) induced by the shearing of the soil and the triaxial test.

Drained Strength Evaluation

Data from the CIUC tests was used to estimate the drained friction angle, ϕ'. To define the failure envelope, values for p′ and q at failure were plotted. Figure A-26 shows the effective stress failure points for the CIUC tests, and the interpreted failure envelope.

The failure envelope exhibits a break at about p′=120 kPa. Therefore, a friction angle of 31° is calculated for the low stress range and a friction angle of 18.2° with an effective cohesion intercept of 26 kPa is calculated for stress ranges higher than p′ = 120 kPa.

Summary of Laboratory Shear Strength Testing Results and Design Shear Strength Profile

Figure A-27 shows a plot of undrained strength vs. vertical effective stress for the UU and CU results. Included on this figure is the relationship given by equation 68 and 70. Recall that equation 68 derived for the direct simple shear mode was developed based on a large database of shear strength testing in clays. This relationship uses the preconsolidation stress profile shown in figure

A-23 to evaluate OCR and a drained friction angle of 18.2 degrees. The drained friction angle that should be used for the database approach (i.e., equation 70) should correspond to the direct simple shear mode. For most soils, there will only be a minor difference between the drained friction angle from a TXC test and a DSS test. However, because of the horizontal stratification of the varved clay deposit, the friction angle from DSS loading will be significantly lower than that from TXC. Available data in the literature indicates that ϕ' for the DSS mode for varved clays is on the order of 16 to 20 degrees. Therefore, the interpreted value of 18.2 degrees was used herein. Figure A-28 shows a plot of s_u/σ_{vo}' vs. OCR. This plot indicates that the laboratory strength test measurements (both UU and CU) indicate that the soil can be characterized using a relationship similar to equation 70.

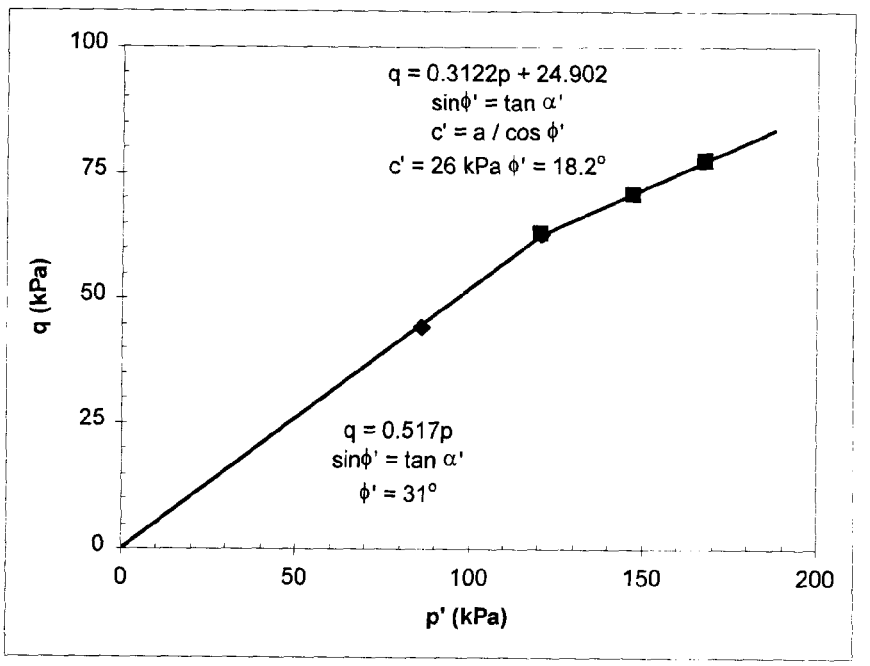

Figure A-26. Effective stress properties from CIUC test data.

The results from UU tests are consistently below those from CU testing and from equation 68. Based on laboratory testing alone, it appears as though an average profile line between the UU and CU strengths would be appropriate, but perhaps still on high side. The results of CU and UU testing for varved materials needs to be carefully considered relative to the design application. Because of the horizontal stratification of varved materials, it is likely that the lowest shear strength would be associated with shearing in a near-horizontal direction. Therefore, failure surfaces that develop in UU and CU tests may not be consistent with potential critical conditions for field applications. For this reason, it may be necessary to perform direct simple shear testing for projects involving varved clays and potentially marginal stability conditions.

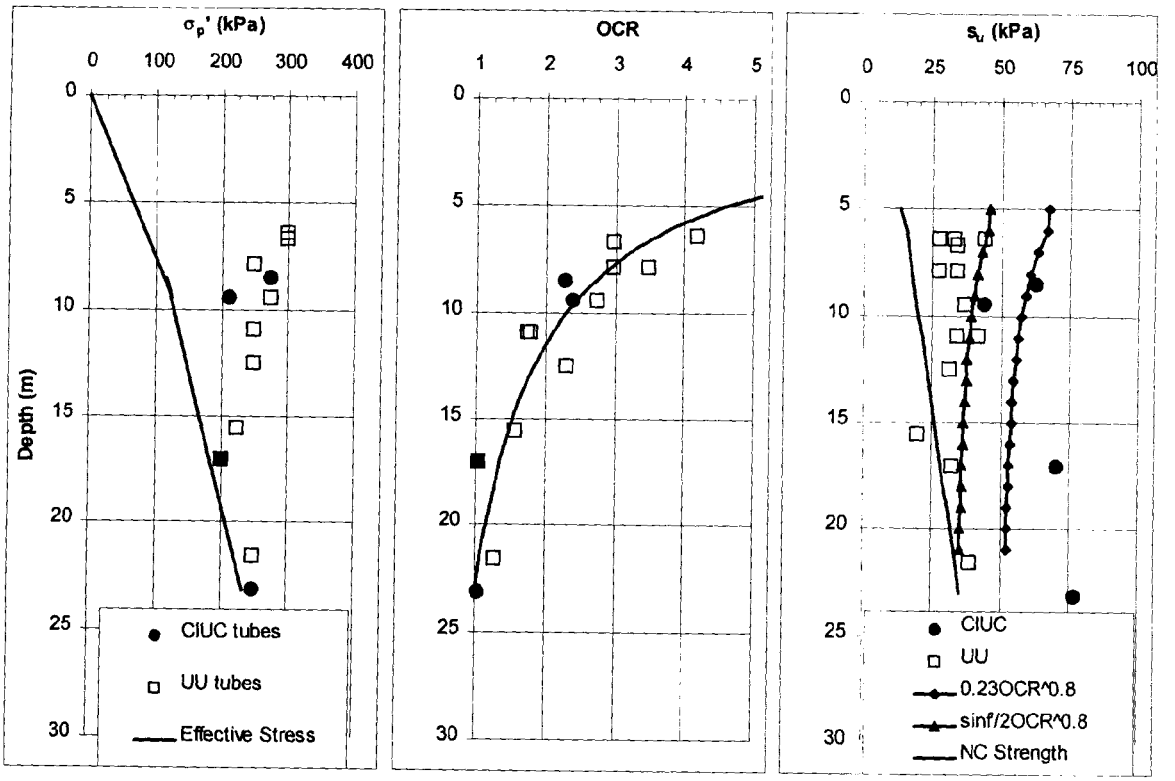

Figure A-27. P_o diagram with OCR and s_u vs. depth.

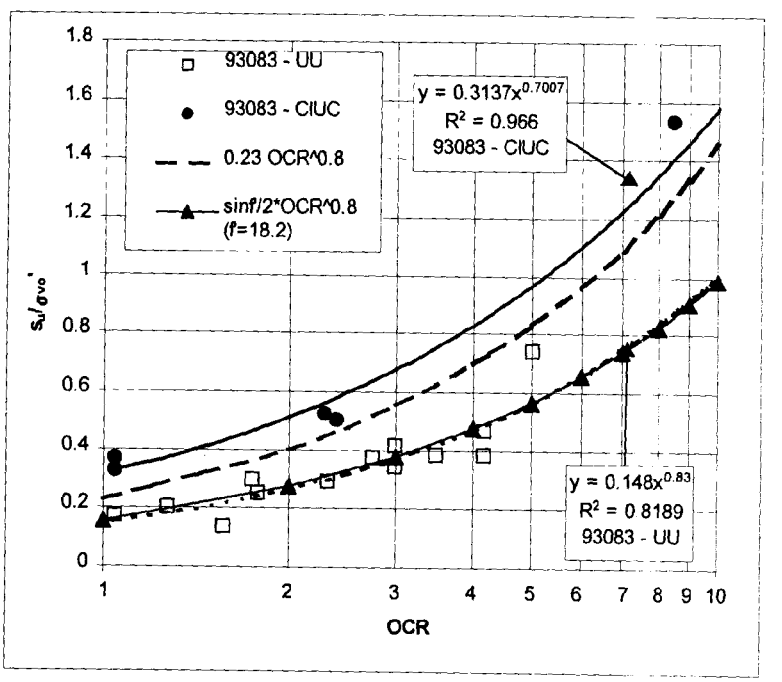

Figure A-28. Normalized strength property relationships for various shear modes.

As previously discussed in chapter 5, the DSS is considered to represent an average condition between compression and extension loading and one which is applicable to most stability and bearing capacity evaluations. For most soils, the trend in strength is s_u(compression) > s_u (DSS) > s_u (extension). However, for varved clay soils, the DSS mode represents the most critical (i.e., lowest) undrained strength because shearing occurs parallel to the varves. Therefore, a design shear strength envelope (which is intended to reflect the average undrained shear strength) for a varved clay deposit should be representative of an average between direct simple shear and compression. Therefore, based on figure A-27, it would be reasonable to assign a constant value of about 45 kPa for the undrained strength over a depth of 5 to 23 m.

STRENGTH EVALUATION FROM IN-SITU TESTS

Overview

The use of in-situ tests for evaluating undrained shear strength is presented in this section. In-situ test data used herein were obtained for a soft to medium varved clay deposit located near Amherst, Massachusetts. Relationships between in-situ test parameters and undrained strength have been summarized in table 33. The relationships presented in table 33 can be used for first-order evaluations of undrained strength. As discussed in section 5.6.5, for some in-situ testing devices, available correlations relate an in-situ testing parameter to a particular undrained strength that corresponds to a mode of shear. Herein, the direct simple shear mode is used.

As discussed in section 5.6.5, the recommended approach to using in-situ test data to evaluate undrained shear strength for design is to use the data to develop a profile of σ_p' (and thus OCR) using the relationships provided in section 5.4.3 (i.e., equations 41 through 46). From the OCR profile, an undrained strength profile can be developed using equation 68 or 70. This method is also illustrated in this section.

Vane Shear Test

A summary of vane shear testing results is shown in table A-9. At each testing depth, the maximum torque, T_{max}, required to turn the vane device was recorded. The undrained strength corresponding to peak conditions from the vane $s_{u(VST)}$ is calculated as:

$$s_{u(VST)} = \frac{6T_{max}}{7\pi D^3} \qquad \text{(Equation A-10)}$$

where D is the diameter of the vane which equals 5.1 cm for these tests. The average plasticity index (PI) of the soil is less than 20 indicating that the reduction factor, μ, can be assumed to equal 1.0.

Table A-9. Vane shear data.

Depth (m)	Vane Diameter, D (cm)	Vane Height (cm)	Torque (Nm)	$s_{u,VST}$ (kPa)
3.66	5.08	10.16	40.3	83.8
4.27	5.08	10.16	25.7	53.5
4.88	5.08	10.16	20.9	43.6
5.49	5.08	10.16	16.4	34.1
6.1	5.08	10.16	17.4	36.3
6.71	5.08	10.16	16.8	34.9
7.32	5.08	10.16	17.6	36.7
7.92	5.08	10.16	17.2	35.9
8.53	5.08	10.16	16.7	34.7
9.14	5.08	10.16	16.0	33.3
9.75	5.08	10.16	17.4	36.3
10.36	5.08	10.16	16.1	33.6
10.97	5.08	10.16	16.7	34.8
11.58	5.08	10.16	16.9	35.2
12.19	5.08	10.16	15.4	32
12.8	5.08	10.16	16.5	34.4
13.41	5.08	10.16	16.0	33.3
14.02	5.08	10.16	14.5	30.1
14.63	5.08	10.16	17.0	35.4
15.24	5.08	10.16	11.9	24.8

Note: $\mu = 1$ for all test depths

Piezocone Penetration Test (CPTu)

Results of a piezocone sounding were use to evaluate undrained strength according to the following correlations:

$$s_{u(CPT)} = \frac{q_t - \sigma_{vo}}{N_k} \qquad \text{(Equation A-11)}$$

$$s_{u(CPT_u)} = \frac{u_m - u_o}{N_{\Delta um}} \qquad \text{(Equation A-12)}$$

The correlation for $s_{u(CPT)}$ can be compared to the DSS mode of shear with an assumed N_k value of 15 (see table 33). The piezocone used was a type 2 (indicating that the filter element is located at the shoulder of the penetrometer). The correlation for $s_{u(CPTu)}$ can be compared to the vane shear testing device using a $N_{\Delta um}$ factor equal to 7.9 (see table 33).

Flat Plate Dilatometer (DMT)

A DMT was performed in the varved clay deposit as well. According to table 33, the K_D parameter from a DMT can be correlated to undrained strength (for the DSS mode of shear) according to:

$$s_{u(DMT)} = 0.14\sigma_{vo}'(0.5K_D)^{1.25} \qquad \text{(Equation A-13)}$$

Comparison of Undrained Strength Results using In-situ Tests

Calculated undrained shear strengths from the correlations for VST, CPT, CPTu, and DMT are compared to laboratory DSS tests. The DSS test results were obtained for varved clay soils from the Amherst site. A review of figure A-29 (a) and (b) indicates the following:

- The undrained shear strength estimated using the VST is approximately 50 percent greater than the laboratory DSS undrained strengths. Undrained strengths measured using the VST are typically greater than those from DSS tests.

- The use of N_K equal to 15 results in good agreements to the laboratory DSS data for depths greater than 4 m. At depths less than 4 m, the clay crust is fissured and it is likely that partial drainage occurs. Since the cone factor is based on analyses that consider undrained conditions, significant error, as is seen here, can be expected when using such a correlation in a soil that behaves in a partially drained manner during penetration of the penetrometer.

- Use of a piezocone pore pressure factor $N_{\Delta um} = 7.9$ results in calculated undrained strengths that are up to 50 percent greater than the laboratory DSS. This is likely due to the fact that the piezocone pore pressure factor of 7.9 is based on a database in which piezocone results are calibrated to vane shear test results. Drops in s_u at 1-m intervals correspond to dissipation of penetration prorewater pressure at pauses in penetration. These pauses are necessary for addition of rods to advance the penetrometer.

- The DMT data matches laboratory DSS test data reasonably well.

As previously noted, in-situ data can be correlated to σ_p' for use in equation 70. Figure A-29 shows calculated profiles of undrained strength for the CPT, CPTu, DMT, and VST. Equations A-2, A-3, A-4, and A-5 were used to evaluate σ_p' and the undrained strength was calculated according to

$$s_u = \frac{\sin\phi'}{2} OCR^{0.8} \cdot (\sigma_{vo}') \qquad \text{(Equation A-14)}$$

When compared to figures A-29(a) and A-29(b), the use of equation A-14 results in better agreement to the laboratory DSS for VST and CPTu and slightly better agreement for the CPT.

little to no residual soil structure remaining. These layers are typically on the order of 1 meter thick in the Piedmont province, but may be thicker in tropical residual soils. The saprolite horizon (II) consists of highly variable, highly anisotropic materials, reflecting the structure of the original parent rock. This layer is composed of silty sands and sandy silts which may contain some mica. The presence of mica will lead to an increased void ratio and significantly affect the engineering properties of the material. Relic fractures and joints of the parent rock are maintained in the soil structure, as well as slickensided planes of weakness. The depth to and thickness of the partially weatherd rock zone is highly variable. More weathering typically occurs along fractures, and new fractures open as weathering continues. This will lead to alternating hard weathered rock and soft weathered soil zones until competent rock is reached. For classification purposes of residual soil profiles, competent rock is defined as material having a RQD greater than 75 percent.

SUBSURFACE EXPLORATION AND TESTING PROGRAM

A subsurface exploration in residual soils will be primarily concerned with estimating the extent of zones within the weathering profile. The thickness and variability of the saprolite layer will be of concern for most design problems, and the depth to weathered rock and depth to competent rock may be of concern depending upon the project specifications and local geology. Generally, SPTs on 1.5-m intervals can provide information on the thickness of the layers, and depth to weathered bedrock. Rock coring should be used to confirm competent bedrock, when depth to and consistency of rock is a design parameter. Experience using in-situ tests, such as the PMT, CPT, CPTu, and DMT, have shown their applicability to design problems in Piedmont residual soils. The CPT and CPTu can provide additional information that can be used to develop a more detailed subsurface profile. Based on previous local experience, the PMT and DMT can be used to provide estimates of in-situ elastic deformation properties.

DEVELOPMENT OF SUBSURFACE SOIL PROFILE FOR DESIGN

General

At the west-central Alabama site, in-situ test methods were used to develop a subsurface profile. This section provides information on soil profiles developed from drilling and sampling information, piezocone data, and flat plate DMT data. SPT's are performed at 1.5-m intervals, CPTu data is available every 5 cm, and the flat dilatometer tests were performed every 30 cm at this site. Results from series of each test type are considered individually within separate subsections.

Use of SPT and Disturbed Sampling

A geotechnical boring with Standard Penetration Testing at the site is shown on figure A-31. Eight borings were performed at the site, SPTs were performed in four of the borings and the other borings were primarily used to collect Shelby Tube samples. The investigation was performed to assess soil conditions for installation and testing of 12-m long drilled shafts, thus borings significantly deeper than 12 m are not available at this site. The water table varies from 2 to 5 meters below ground surface.

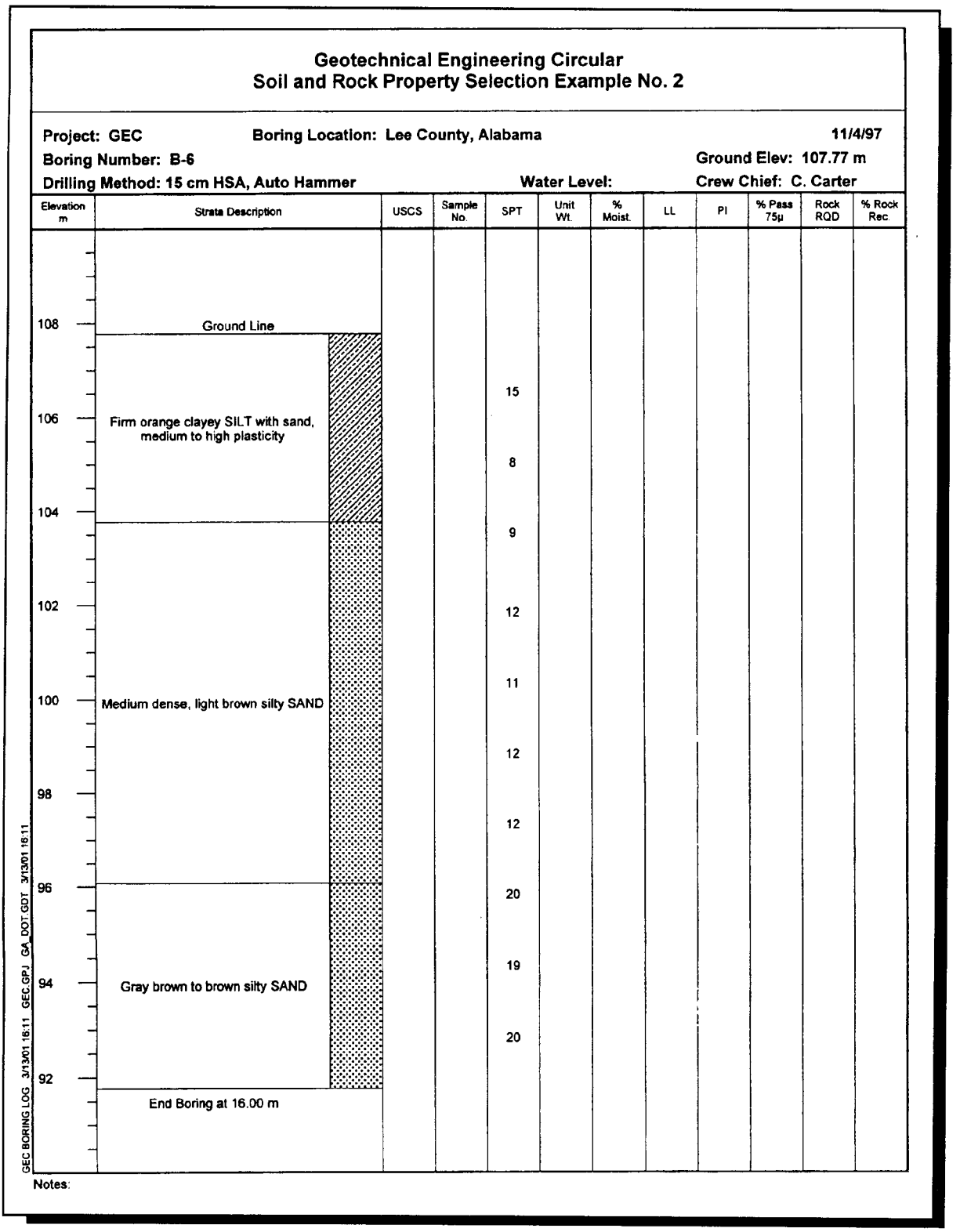

Figure A-31. Boring log for Alabama site.

Index testing and SPT N-values are presented in figure A-32. Index tests results are summarized in table A-10. A CME automatic hammer was used to perform the SPTs, with an assumed energy efficiency of 90 percent. The energy efficiency should be calibrated periodically in accordance with ASTM D4633, and efficiency values should be obtained from the drilling subcontractor. The dry density of the soil ranges from 13 to 17 kN/m^3, with a majority of the data around 15 kN/m^3. Low dry unit weight values, and thus high void ratios, may indicate the presence of mica. This will significantly affect compressibility properties of the soils, and thus the presence of mica based on visual identification should be noted in the boring logs as well as in laboratory data sheets.

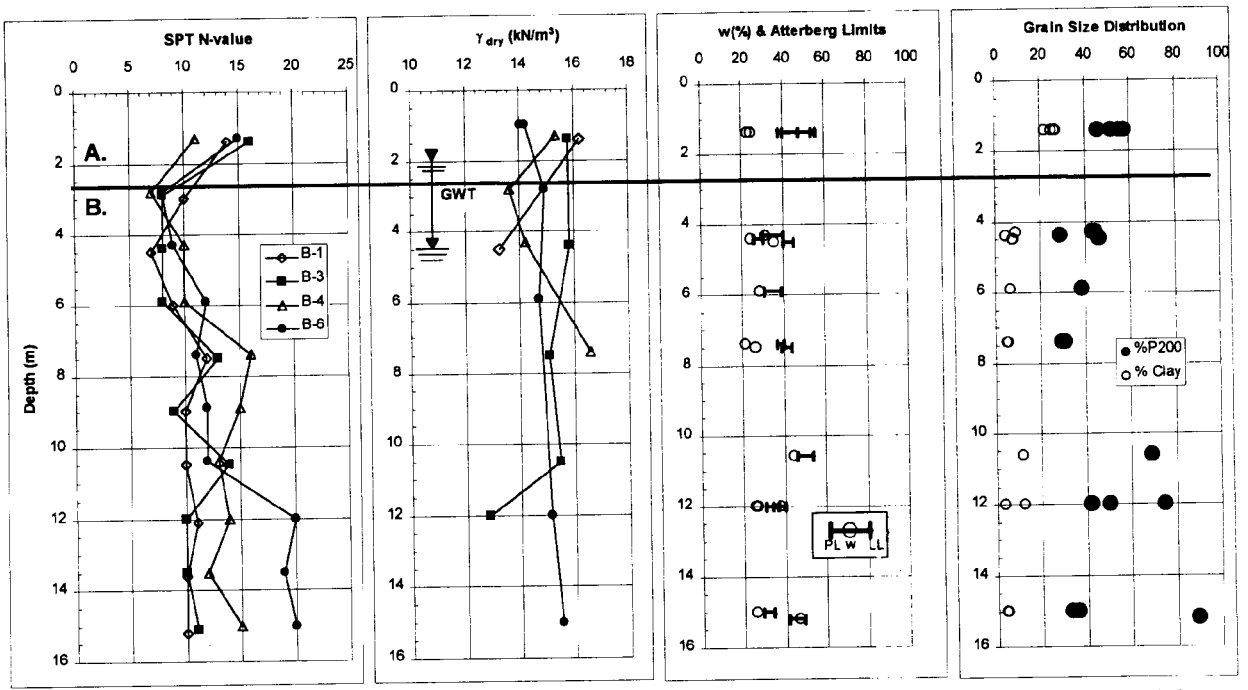

Figure A-32. Summary index test data for samples from borings B-1, B-3, B-4, and B-6 at Alabama site.

From hydrometer analyses, the clay content (finer than 0.002 mm) ranges from up to 30 percent clay in the upper 3 meters and below 15 percent clay for the remaining depth. The tested samples show between 27 and 85 percent fines (passing No. 200 sieve) from mechanical grain size analyses. Since the mean grain size for Piedmont soils is near the opening size for the U.S. No. 200 sieve (0.075 mm), it appears as if there is significant variability in the fines content. The soil acts as a dual symbol material, (SM-ML) exhibiting characteristics of fine-grained soils (undrained behavior) and coarse-grained soils (drained) when subject to different types of loading. For most transportation projects, loading conditions in the Piedmont province will occur under drained conditions.

While Atterberg limits data were obtained for several samples, about 50 percent of the samples tested at the site classified as non-plastic.

Table A-10. Index properties of Piedmont soils at the Alabama site.

Boring	Depth (m)	% Sand	% Silt	% Clay	% Fines	LL	PL	PI	MC (%)	LI
B1	1.4	53.7	21	25.3	46.3	48	38	10	22.9	-1.51
B1	1.4	47.5	30.2	22.3	52.5	48	38	10	22.9	-1.51
B3	1.4	42.2	31	26.8	57.8	54	40	14	24.5	-1.11
B3	1.4	44	28.6	27.4	56	56	40	16	24.5	-0.97
B4	4.3	57.1	33.6	9.3	42.9	40	30	10	31.1	0.11
B4	4.3	55.3	35.8	8.9	44.7	40	30	10	31.1	0.11
B3	4.4	71.3	24.2	4.5	28.7	30	26	4	24.3	-0.43
B1	4.5	53.8	38.3	7.9	46.2	45	40	5	35.8	-0.84
B1	4.5	53.2	39	7.8	46.8	45	40	5	35.8	-0.84
B6	5.9	61.2	32.3	6.5	38.8	39	31	8	28.8	-0.28
B4	7.4	70.6	23.8	5.6	29.4	40	37	3	21.6	-5.13
B4	7.4	68.8	25.9	5.3	31.2	40	37	3	21.6	-5.13
B1	7.5	15.2	-	-	84.8	44	39	5	26.4	-2.52
B1	10.6	30.9	57.2	11.9	69.1	54	46	8	44.6	-0.18
B3	12	50	38	12	50	40	36	4	38.1	0.53
B4	12	25.4	-	-	74.6	37	31	6	25.9	-0.85
B6	12	58.4	37.9	3.7	41.6	37	34	3	27.1	-2.30
B6	12	57.9	38.4	3.7	42.1	37	34	3	27.1	-2.30
B6	15	66.9	28.4	4.7	33.1	34	29	5	25.6	-0.68
B6	15	64.2	31.5	4.3	35.8	34	29	5	25.6	-0.68
B1	15.2	10.5	-	-	89.5	49	41	8	46.9	0.74
Average	-	49.3	28.8	16.4	50.7	40.56	33.96	6.6	28.4	-1.07

LL = Liquid Limit; PL =Plastic Limit; PI = Plasticity Index; MC = Moisture Content; LI = Liquidity Index

A review of all boring logs and laboratory index test data at the site show about 3 to 4 meters of sandy silt with clay over silty sand. These two zones are labeled A and B in figure A-32. Since this site is located at the southwest end of the Piedmont, additional heat and humidity of the subtropical environment coupled with the rise and fall of the near surface water table have led to increased weathering and desiccation of the near surface soils. The increased weathering results in a higher clay content, while the desiccation resulted in higher N-values. Dry unit weight values were typically between 14 and 16 kN/m^3, but values were as low as 13 kN/m^3 and as high as 16.8 kN/m^3. This variation in unit weight may have been induced by the weathering profile, may be indicative of a localized softer zone, may have resulted from samples taken on a relic fissure, or may have resulted from disturbance during sampling and testing. The assessment of potential thin zones of soft soils by use of conventional drilling and sampling methods is difficult in the Piedmont, since layers may be missed during the investigation. Sample disturbance is likely, which may affect the outcome and interpretations of laboratory test data.

Stratigraphy from CPTu Data

Figure A-33 presents the tip resistance (q_t), sleeve friction (f_s), friction ratio (FR = $f_s/q_t \cdot 100$), and penetration pore pressure measured behind the tip (u_2) with depth for two CPTu soundings at the Alabama site. The interpreted layering profile and differences between the measured signatures for the two different soundings (signature 1 and signature 2) are discussed with respect to an interpreted weathering profile. Figure A-34 shows CPTu data for one sounding (signature 1) from the Alabama site presented on the Robertson et al. (1986) soil behavior type charts.

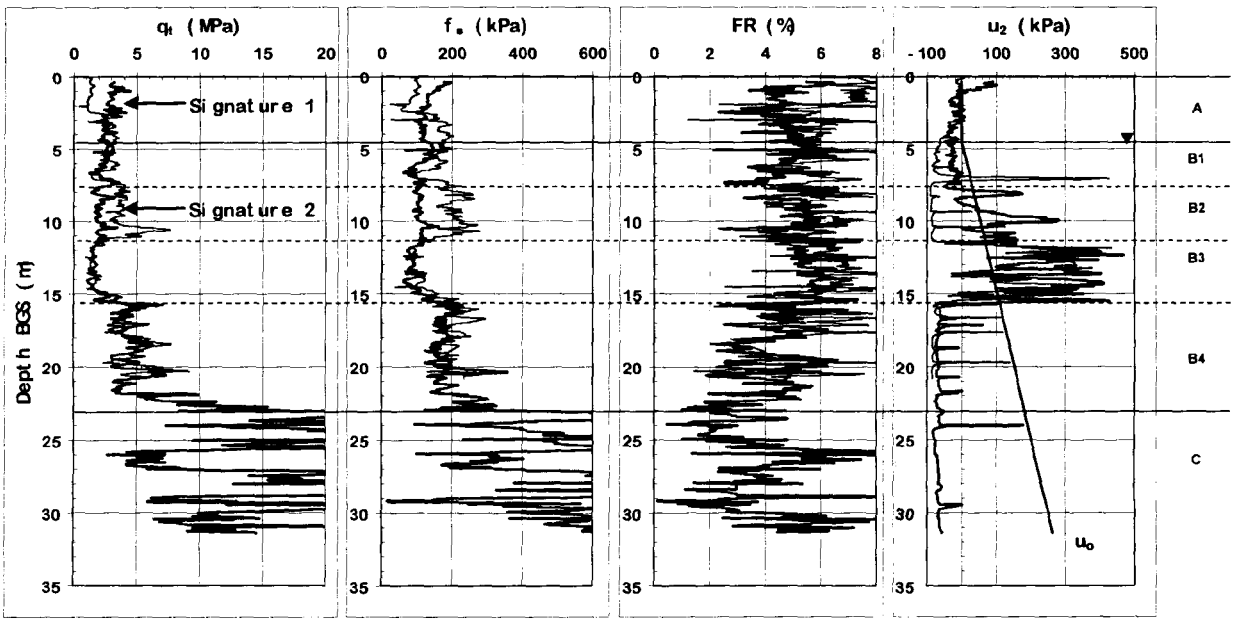

Figure A-33. Subsurface layering based on CPTu data.

Two primary layers (A and B) are selected in the upper 15 meters of the profile. Based on differences in cone signature, Layer B is divided into four subsections (B1, B2, B3, B4). Below 21 to 23 meters, the Layer C is distinguished based on the piezocone signature. The pore pressure (u_2) and tip resistance (q_t) response tend to control the selected stratigraphy, while the friction ratio (FR) displays a range of soil response from sand to clay. Table A-11 summarizes the results of the CPTu profile interpretation for signature 1.

Layer A

Layer A is designated as a desiccated zone of partially-saturated soils. The u_2 pore pressure response is around zero, but may be positive or negative. These varying conditions may be an indication of current degree of saturation, depending upon the humidity, infiltration, and prior rainfall around the time of testing. Since this layer is a partially saturated zone, the pore pressure response will not be used for classification purposes. Tip resistance and sleeve friction values have parallel responses, increasing and decreasing at similar depths within the layer. Signature 2 initially has a lower tip resistance (about 1.2 MPa) and higher friction ratio (about 7) than signature 1, but the two signatures converge at 2.5 meters with a tip resistance around 2.7 MPa and a friction ratio

around 5. The difference in these two signatures is likely indicative of differential near-surface weathering. While this layer covers 4 zones of the classification chart presented in figure A-34, the average response indicates a silty clay to clay with the variation in the response indicating the presence of some sand.

Table A-11. Summary of CPTu subsurface profile interpretation.

Layer	Depth Range (m)	$q_t - FR$ zones (Robertson et al., 1986)	$q_t - B_q$ zones	Soil Behavior Type Classification	Residual Soil Weathering Horizon
A	0 to 4.5	3,4,5,6	-	Clayey silt to silty clay with sand	Horizon IA/IB
B1	4.5 to 7.75	3,4,5,6	6,7	Clayey silt to silty clay with sand	Saprolite
B2[1]	7.75 to 11.5	3,4,5	5,6,7	Clayey silt to silty clay with sand	Variable Saprolite, some softer material
B3[1]	11.5 to 15.6	3,4	4,5,6	Silty clay to clay with sand	Softer Saprolite
B4	15.6 to 23	3,4,5,6,7,8,11	7,8	Silty sand with sand	Denser Saprolite
C	23 +	3,4,5,6,7,8,9, 11,12	8,9,10	Alternating seams of silty sand with sand and gravel (rock fragments) and clayey silt to sandy silt with clay	Partially Weathered Rock

[1] While zone B2 and B3 have similar soil behavior types and residual soils horizons, they are primarily separated to discuss differences between cone signature 1 and cone signature 2.

Layer B

Variation in the upper weathered soil portion of the profile is inferred from the two cone signatures between 4.5 and approximately 22 meters depth.

Layer B1

This sublayer generally has a similar response for both cone signatures with a tip resistance around 2.6 MPa, a friction ratio around 5, and negative u_2 penetration pore water pressures up to about negative 100 kPa. Penetration pore pressures greater than negative 100 kPa (negative 1 atmosphere) have not been reported for any soil type, and it its believed that a limiting negative pore pressure is a function of cavitation of the porewater at about negative one atmosphere.

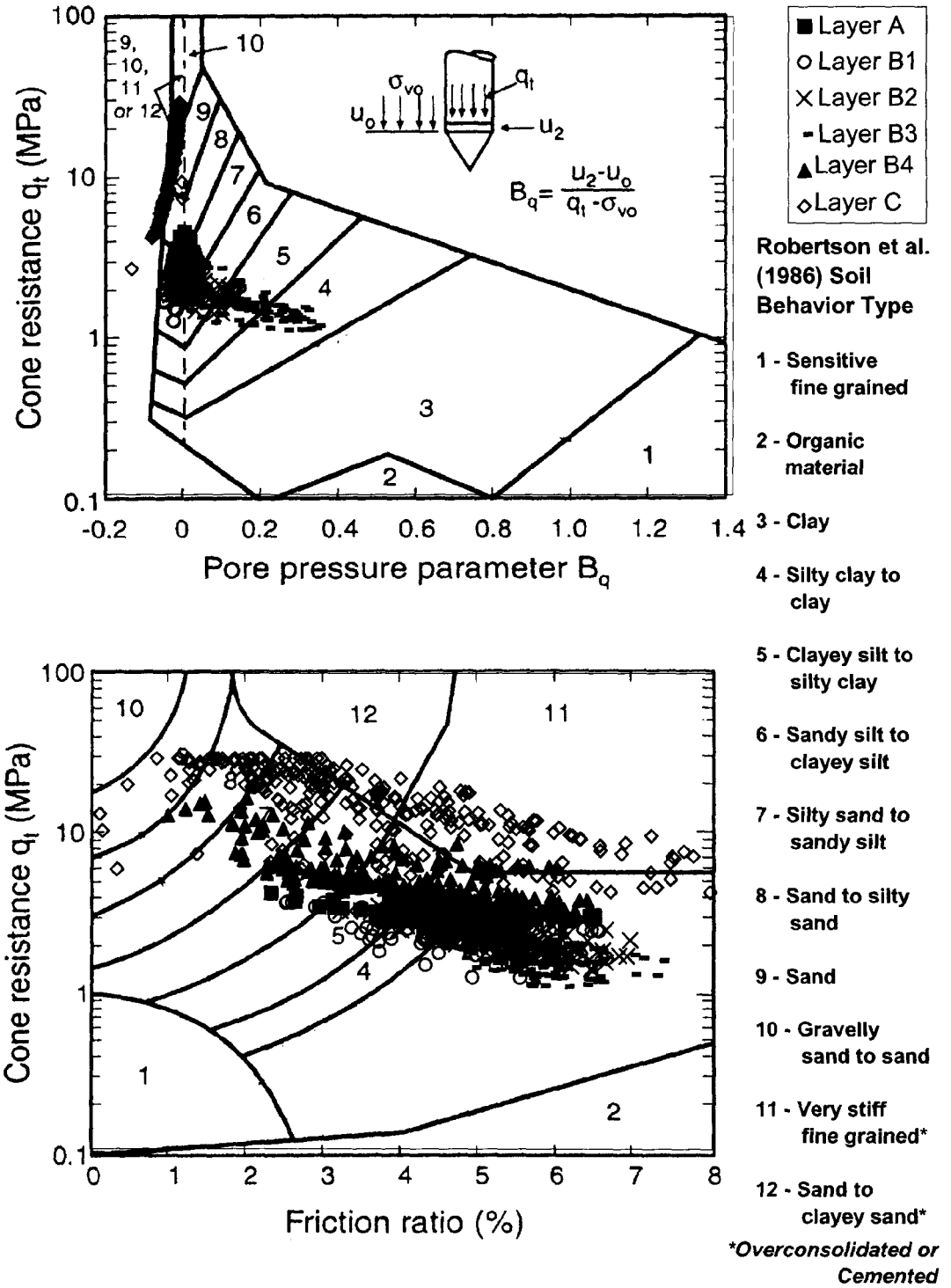

Figure A-34. Soil classification charts with CPTu data from Alabama site (signature 1).

Layer B2

Layer B2 shows quite a different response for all 3 piezocone parameters when signature 1 is compared to signature 2. Signature 1 has a q_t of about 2 MPa, f_s of about 100 kPa, FR of about 5, and positive u_2 penetration porewater pressures up to about 300 kPa. Signature 2 has a q_t of about 4 MPa, f_s of about 200 kPa, FR of about 5, and u_2 penetration porewater pressures of about negative 80 kPa. The contrasts in this layer are interesting in that the tip resistance and sleeve friction values are proportionally higher in signature 2 when compared to signature 1, and the u_2 penetration porewater pressures are negative in the stiffer soils (signature 2) and mostly positive in the softer soils (signature 1). The transition from negative to positive u_2 penetration porewater pressures is likely indicative of transition from a dense dilative sandy silt material to a looser more clayey silt.

Layer B3

Layer B3 shows the convergence of signatures 1 and 2 to q_t values of about 2 MPa, f_s of about 100 kPa, FR of about 5, and positive u_2 penetration porewater pressures up to about 500 kPa. At both test locations a softer clayey silt has been encountered.

Layer B4

At a depth of about 15.6 meters the tip resistance and sleeve friction values increase to about 4.7 MPa and 200 kPa, respectively, yielding a friction ratio between 4 and 4.5. The u_2 penetration porewater pressures become negative again in this layer. Due to the higher tip resistance and negative u_2 penetration porewater pressures, it is inferred that this layer consists of a dense silty sand.

Layer C

The transition into Layer C is not abrupt, and likely occurs between 21 and 23 meters depth in this profile. The cone test that produced signature 2 met refusal at about 21 meters, while the cone test that produced signature 1 was continued until about 32 meters. According to table A-11, Layer C classifies as every soil behavior type except sensitive fine grained, organic material, or gravelly sand. While this may seem prohibitive to classification of the layer, the soil layer becomes obvious when you consider the residual soil weathering profile. Alternating layers of very stiff material ($q_t \approx$ 20+ MPa) and softer zones ($q_t \approx$ 5 to 15 MPa) are indicative of the partially weathered rock horizon. The u_2 penetration pore pressures are still negative, showing no change from the saprolite horizon. The friction ratio values are still variable, but on average are lower in the very stiff soils and higher in the soft zones.

The depth to competent rock is quite variable in the Piedmont. Cone penetration testing through weathered rock is difficult and may require termination of a sounding before competent rock is confirmed, due to inclination, and overstressing of load cells. For design problems where depth to rock is important, it should be ensured that rock is reached rather than an intermediate layer within the partially weathered rock zone. Rock coring of at least 1.5 m is recommended to accompany CPT and CPTu investigations in residual soils where depth to competent rock is needed.

Stratigraphy from DMT Data

Figure A-35 shows the results of four DMTs performed at the Alabama site with the open symbols representing the p_0 lift-off pressure and closed symbols representing the p_1 expansion pressure. In figure A-36, the index parameters I_D and E_D are used to estimate classification and consistency.

The material index, I_D, indicates that the site is primarily clayey silts and silts. One of the soundings also indicates the possibility of thin clayey seams at 5.5 and 10.5 meters. While the material index is uniform throughout the site, the increase in the horizontal stress index parameter, K_D, is used to separate a stiff overconsolidated crust at depths above about 3.5 meters. This crust is labeled Layer A, while the underlying soils are labeled Layer B. It is inferred from figure A-36 that the clayey silts, silts, and sandy silts are of medium dense to dense consistency.

Summary

Similar soil profiles were developed in the upper 16 meters using the SPT, CPTu, or DMT. A stiff desiccated crust exists up to around 2.75 to 4.5 meters, which is underlain by silty sands to sandy silt with some clay to 16 meters. Using data from the piezocone penetrometer, the saprolite profile was interpreted to continue to about 22 meters where it transitioned to partially weathered rock to the end of the sounding at 32 meters. The distinction between partially weathered rock and competent bedrock cannot be confirmed using the cone penetrometer. The CPTu provided the most detail for evaluating site stratigraphy. The u_2 penetration porewater pressure measurements provided additional insight into the weathering profile where conventional laboratory index tests did not show distinct differences in soil type. The potential for significant variability in the weathering profile can be addressed with piezocone testing, since the CPTu can provide rapid and inexpensive profiling of a site when compared to traditional drilling. While the piezocone provided good resolution of layering and changes in the weathering profile, companion drilling, sampling, and visual classification are recommended so the engineer can get a better idea of important defects and features. These may include mica content, the presence of original rock structure, and slickensided planes of weakness in the soil matrix.

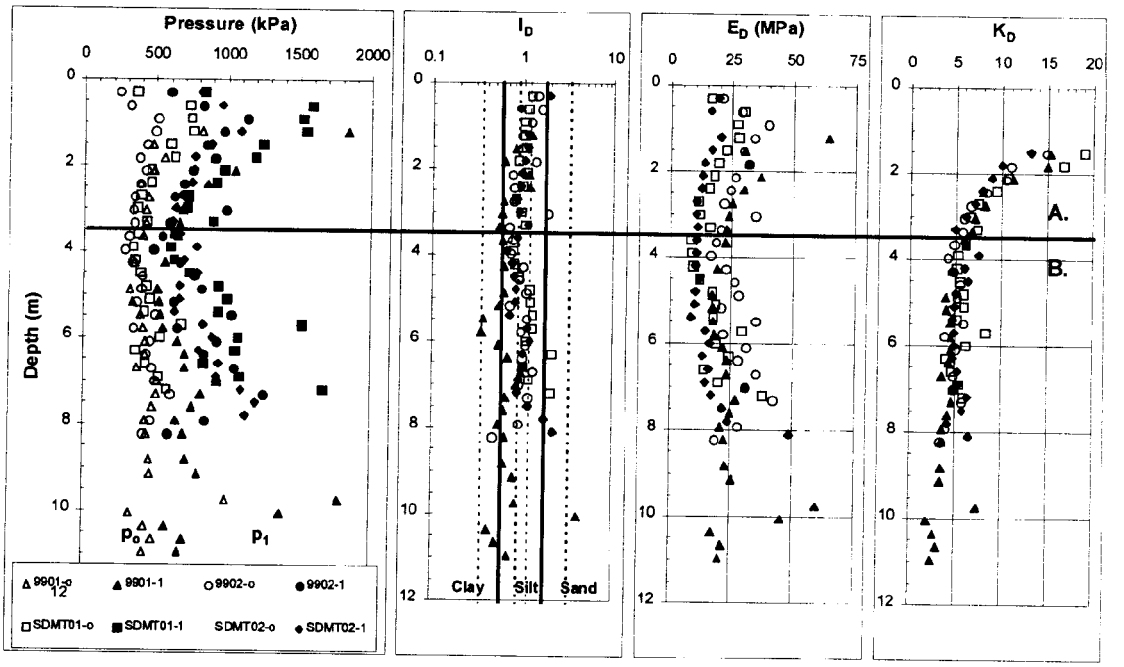

Figure A-35. Soil stratigraphy from DMT index values.

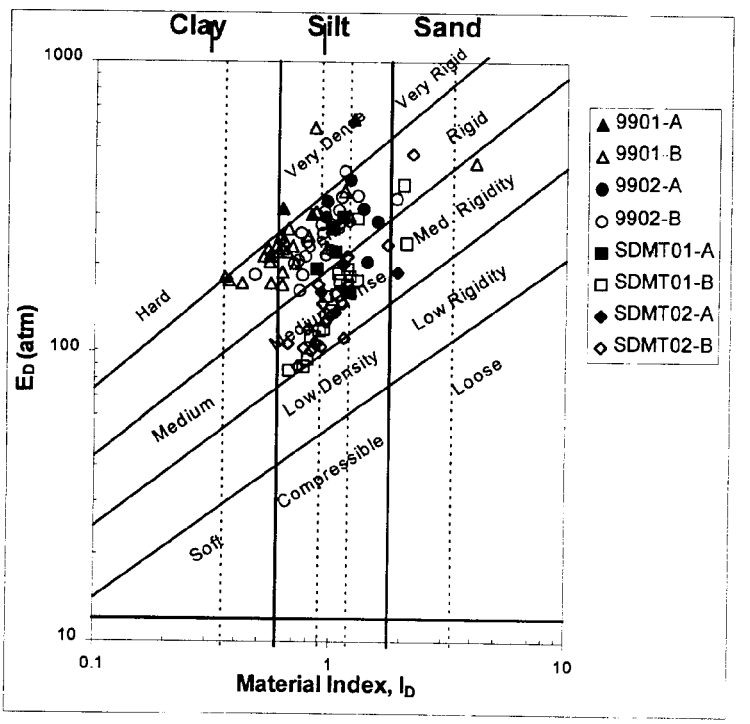

Figure A-36. Classification and consistency of soil at Alabama site based on DMT data.

RELATIONSHIP BETWEEN SPT N VALUES AND IN-SITU TEST PARAMETERS

Substantial design and experience in residual soils of the Piedmont province have been based on SPT blow counts. This example presents strength and compression properties derived from the SPT as well as other in-situ tests. This section provides correlation between the SPT N-value and other in-situ test reference parameters, such as CPT tip resistance, q_t. Due to the large amount of scatter in correlations between N-value and other in-situ test resistance parameters, it is not recommended to use these correlations directly in design. Rather, these correlations are presented as a reference so that the engineer with many years of design experience with the SPT can get a feel for other in-situ test parameters. Assessment of engineering properties using individual in-situ and laboratory tests will be presented in the following sections.

Figure A-37 provides a correlation which relates the ratio of cone tip resistance to N-value as a function of mean particle size, D_{50} (Kulhawy & Mayne, 1990). The soils at the Alabama site with a higher fines content plot with q_c/N values between 1 and 2, while the more granular material ($D_{50} \geq$ 0.075 mm) plot with q_c/N ratios of between 2 and 4. These data are in agreement with previously proposed correlations, and thus first order data quality seems acceptable.

Figure A-38 compares dilatometer modulus, E_D, corresponding to a factor of safety of 3 (i.e., back-calculations corresponding to working load levels) to N-value using a correlation presented in Mayne & Frost (1988). Data from the Alabama site as well as data from additional sites in the Piedmont province are included for comparison to the proposed trend. The Alabama data follow the previously proposed trend and matches well with the additional data provided. The first order quality of the DMT data appears to be reasonable.

Figure A-39 compares the initial elastic modulus from pressuremeter tests to N-value using a correlation for Piedmont soils presented in Martin (1977). Menard prebored pressuremeter initial elastic modulus data from the Alabama site is evaluated along with cone pressuremeter (CPM) unload-reload (U-R) modulus data from the Alabama site. The initial modulus values from the Menard PMTs fit within the range of uncertainty of the Martin (1977) correlation, but the U-R modulus from the CPM is one to two orders of magnitude higher than expected. This is likely due to disturbance inherent in the CPM test as well as possible additional errors in test procedure that will be discussed in a latter section on deformation data from the PMT.

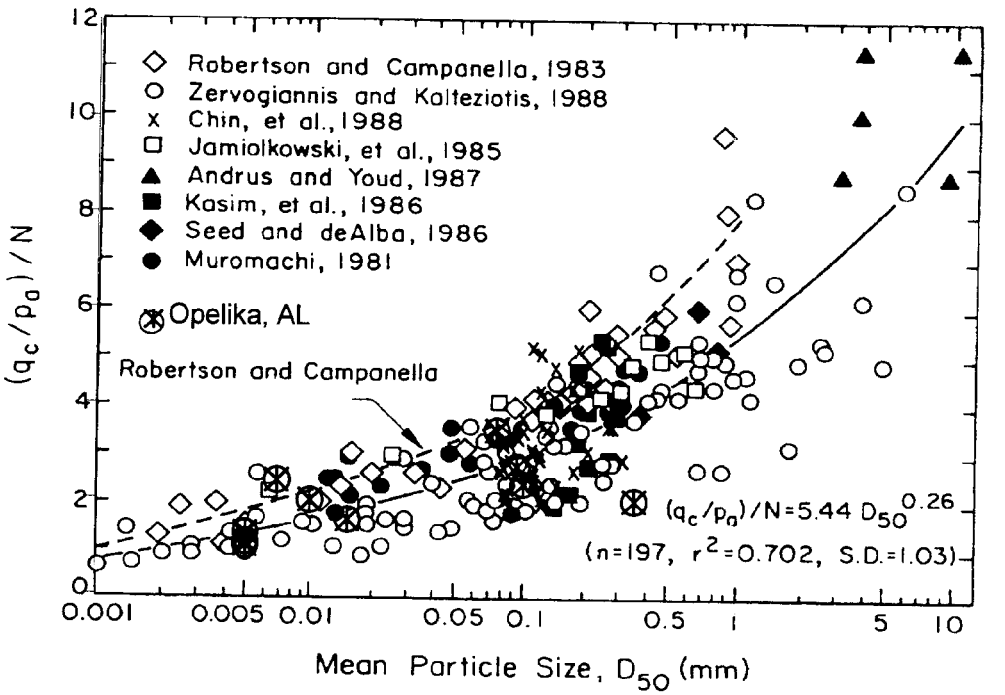

Figure A-37. Comparison of Alabama site data to published trend between CPT tip resistance and N-value as a function of mean grain size (Kulhawy & Mayne, 1990).

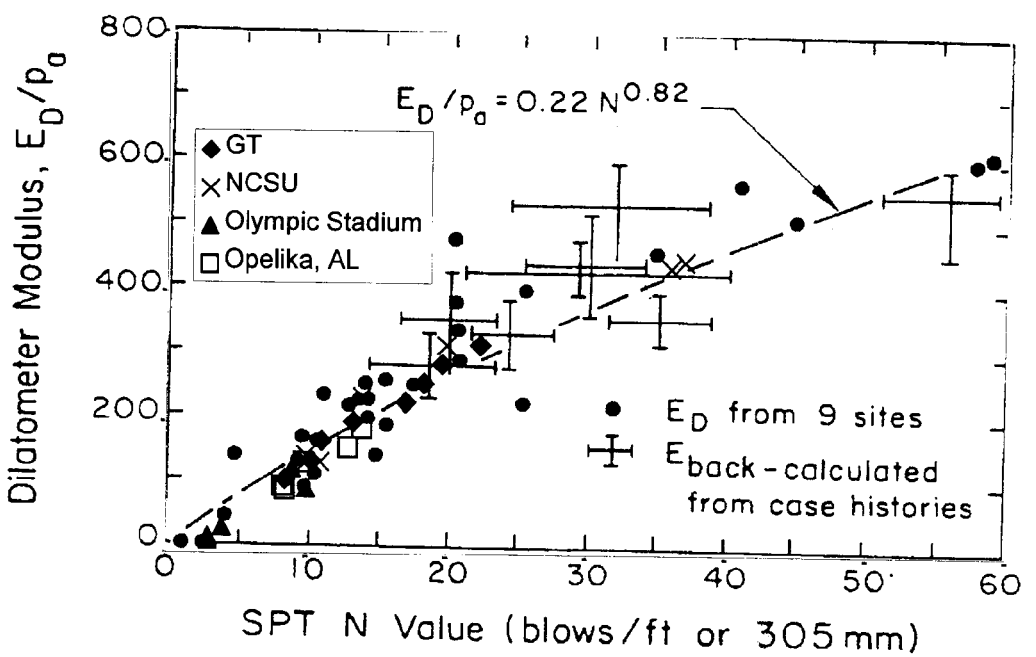

Figure A-38. Comparison of Opelika, Alabama data to published trend between dilatometer modulus and N-value in Piedmont sandy silts (Mayne & Frost, 1988).

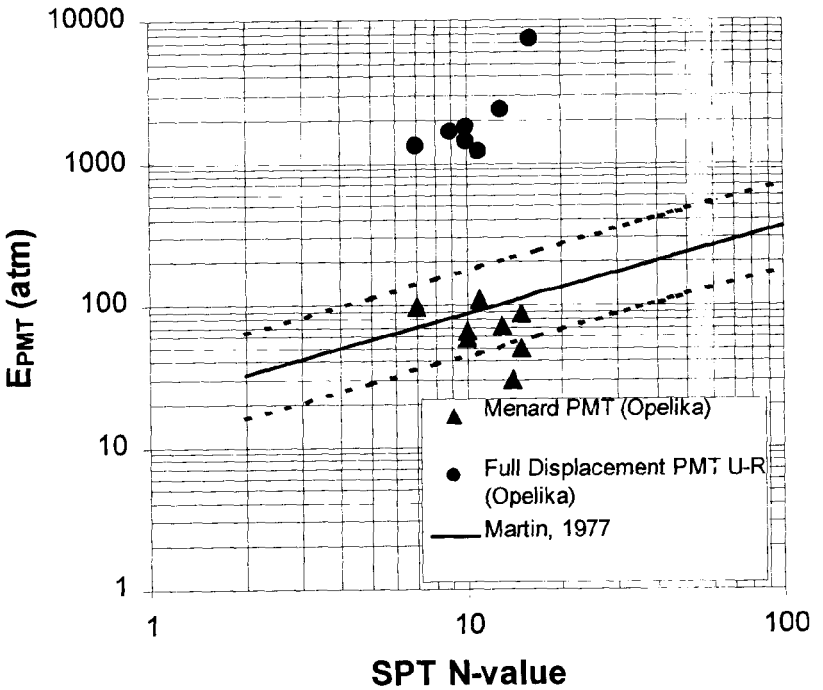

Figure A-39. Comparison of Opelika, Alabama data to published trends between PMT modulus and N-Value in Piedmont soils (Martin, 1977).

DEFORMATION CHARACTERISTICS OF RESIDUAL SOILS

General

While compression properties from laboratory oedometer tests are commonly used to assess settlements for clayey soils, the elastic modulus is typically used to calculate settlements in granular soils. Residual soils are intermediate and thus oedometer test results and methods relying on elastic modulus values are used in practice to evaluate settlements in residual soils. Oedometer test results for the soils at the Alabama site are presented in this section and information on potential errors and limitations in estimating settlements of residual soils based on oedometer tests are presented.

Information on evaluating an elastic modulus in residual soils using various in-situ tests is presented in this section. Elastic moduli calculated from pressuremeter test (PMT) data and flat plate dilatometer test (DMT) data, as well as interpreted from shear wave velocity data are presented.

Evaluation of Compression Properties from Laboratory Oedometer Tests

Laboratory consolidation test results for residual soils are affected by the high sand and silt content, as well as disturbance that typically occurs during sampling, extraction, and trimming of the specimens. Most conventional consolidation curves for residual soil are generally rounded due to disturbance. Predicted settlements using conventional consolidation curves for Piedmont residual soils are usually 1.25 to 1.5 times greater than actual measured values. This overprediction of settlement may result in the use of deep foundation systems where shallow foundations could have

been used. One-dimensional consolidation curves for specimens from the Alabama site are shown in figure A-40(a). The strain energy method is used to evaluate the preconsolidation stress since it can lead to a less ambiguous estimation of preconsolidation stress from oedometer tests on residual soils, as shown in figure A-40(b). Data from laboratory oedometer tests on Piedmont residual soils at the Alabama site are shown in table A-12.

Sample disturbance was evaluated using the procedures outlined in chapter 4, and results are presented in table A-12. The strain levels to reach in-situ vertical effective stress indicate that all specimens were likely to be disturbed. The curves never reached a truly linear virgin compression line, increasing the difficulty in selecting a preconsolidation stress from the test data. Unload-reload cycles performed immediately before the anticipated preconsolidation stress will result in a more accurate evaluation of the recompression index.

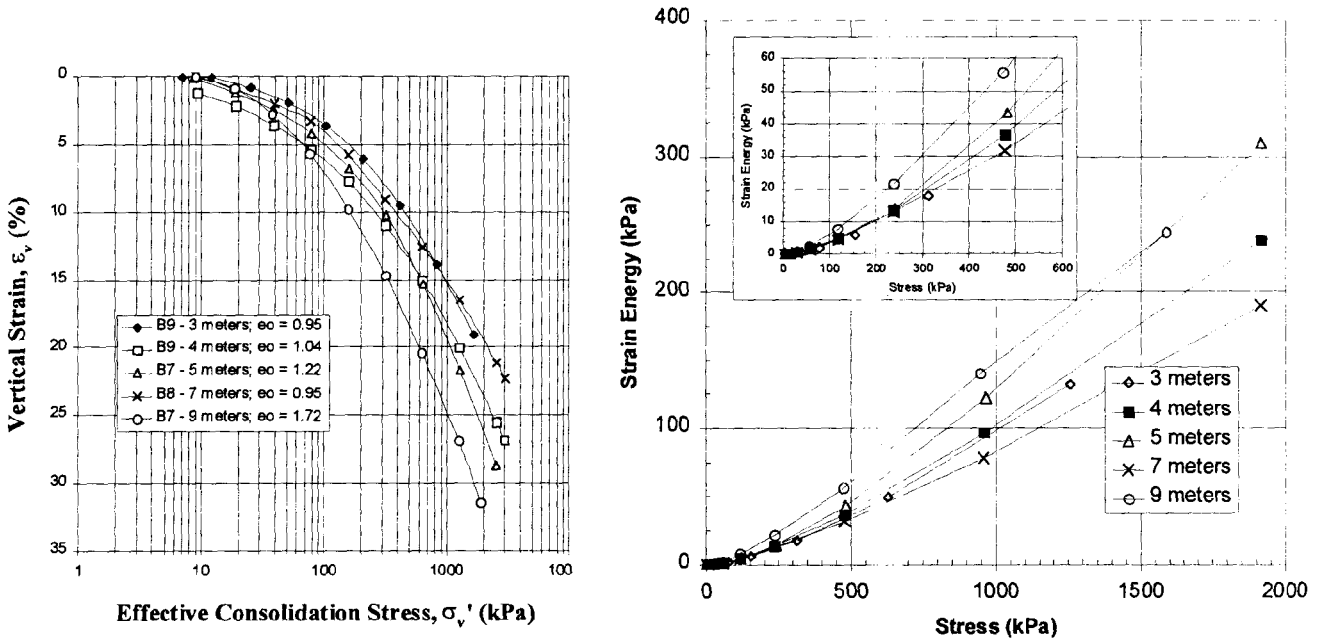

Figure A-40. Laboratory 1-D consolidation curves
(a) Stress – Strain; (b) Stress – Strain Energy

Table A-12. Summary of oedometer testing on Piedmont residual soils.

Boring	Depth (m)	LL	PI	w_n (%)	e_o	σ_{vo}' (kPa)	Casagrande σ_p' (kPa)	Casagrande OCR	Strain Energy σ_p' (kPa)	Strain Energy OCR	Strain to σ_{vo}' (%)	Sample Quality[1]
B9	3	37	10	30.2	0.95	62.2	200	3.2	375	6.0	2.0	DT
B9	4	39	12	27.2	1.04	79.8	190	2.4	400	5.0	5.4	DT
B7	5	28	4	32.8	1.22	88.5	220	2.5	375	4.2	4.4	DT
B8	7	-	NP	25.4	0.95	104.4	215	2.1	250	2.4	4.0	DT
B7	9	-	NP	45.3	1.72	122.2	100	< 1	155	1.3	8.3	DT

[1] Evaluated using estimated OCR and strain at in-situ vertical effective stress; DT – Disturbed test

In the next sections, calculations of elastic modulus are presented for various in-situ testing methods. In order to compare those values to values obtained from consolidation data, typical recompression parameters can be used to calculate an elastic modulus. For example, using the consolidation data for Boring B9 at 4 meters results in a value of $C_{r\varepsilon}$ of about 0.05. The elastic modulus can be calculated as:

$$E = \frac{2.3\sigma'_v}{C_{r\varepsilon}}\left[\frac{(1+\nu)(1-2\nu)}{(1-\nu)}\right] \qquad \text{(Equation A-15)}$$

Using a vertical effective stress of 100 kPa and a Poisson's ratio of 0.1, results in a calculated elastic modulus, E, of 4,500 kPa.

Elastic Modulus from Pressuremeter Data

The pressuremeter elastic modulus estimated from the applied stress – volume curve can be used for elastic settlement analysis as outlined in FHWA-IP-89-008 (1989). Settlement analyses for Piedmont residual soils based on elastic modulus values from pressuremeter testing have been shown to be more accurate than those based on conventional settlement analyses using compression properties from laboratory oedometer testing. Menard pressuremeter data from the Alabama site are shown in figure A-41 and full displacement pressuremeter data from the same site is shown in figure A-42. Data summaries are provided in tables A-13 and A-14.

The calculation of the pressuremeter elastic modulus has been presented in section 4.7. Using the applied stress – probe volume curve at 8 m in boring B-5, the elastic modulus is calculated as:

$$E_P = 2(1+\nu)(V_0+V_m)\frac{\Delta P}{\Delta V} = 2(1+0.33)(790cm^3+202.5cm^3)\frac{(500-150)kPa}{(295-110)cm^3} = 4{,}995\,kPa \qquad \text{(Equation A-16)}$$

where ν is the Poison ratio taken as 0.33, V_o is the initial volume of the probe, V_m is the mean volume of the probe over the stress range of consideration (i.e., (110 cm^3 + 295 cm^3)/2 = 202.5 cm^3), and ΔP / ΔV is the slope of the linear portion of the stress – volume curve (between p_o and p_f or p_u and p_r).

Table A-13. Test data and calculated elastic modulus from Menard PMT data at the Alabama site.

Boring	Depth (m)	p_o (kPa)	p_f (kPa)	p_L (kPa)	Δp (kPa)	ΔV (cm^3)	V_o (cm^3)	V_m (cm^3)	E_P (kPa)
B-5	1	64	436	NA	372	91	790	234.5	11,140
B-5	2	95	341	NA	246	71	790	267.5	9,746
B-5	4	151	410	NA	259	142	790	414	5,841
B-5	6	169	600	NA	431	190	790	314	6,662
B-5	8	150	500	NA	350	185	790	202.5	4,995
B-5	10	255	537	NA	282	100	790	160	7,126
B-5	12	246	573	NA	327	277	790	179	3,043
B-5	15	475	874	NA	399	142	790	396.5	8,868

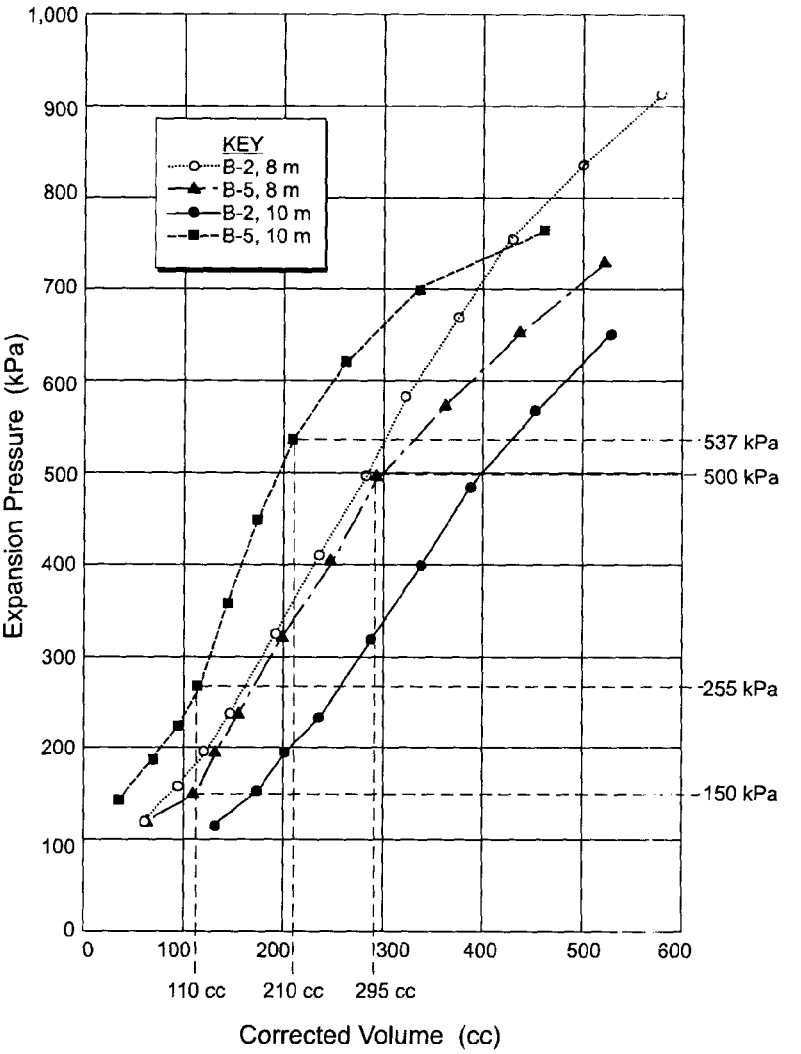

Figure A-41. Menard pressuremeter data for the Alabama site.

Table A-14. Test data and calculated unload-reload elastic modulus from full displacement PMT data (C-41) at the Alabama site.

Depth (m)	p_u (kPa)	p_r (kPa)	p_L (kPa)	Δp (kPa)	ΔV (cm^3)	V_o (cm^3)	V_c (cm^3)	V_m (cm^3)	E_{u-r} (kPa)	E_{u-r}/E_P
1	97.8	617.4	940	519.6	2.7	192	34.67	14.15	123,276	11
2	117	584	800	467	1.8	192	34.67	15	166,782	17
3	137	610	900	473	2.3	192	34.67	15.25	132,339	NA
4	136	526	740	390	1.4	192	34.67	14.9	179,003	31
6	127	486	782	359	1.6	192	34.67	16.1	144,894	22
8	72	645	1000	573	0.5	192	34.67	15.05	736,850	148
10	113	900	1600	787	2.1	192	34.67	12.65	238,570	33

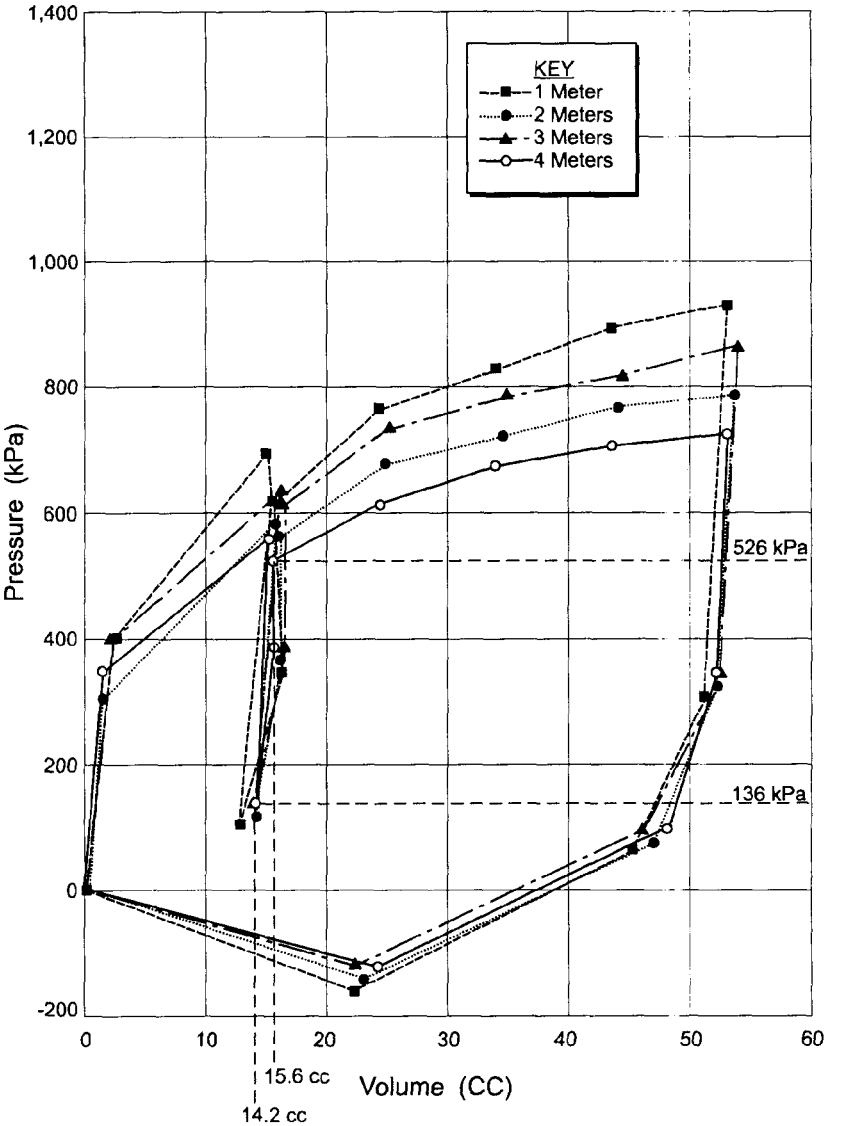

Figure A-42. Full displacement pressuremeter data for the Alabama site.

The data presented in tables A-13 and A-14 indicate that the initial modulus data from the PMT (i.e., E_p) is over an order of magnitude lower than the unload-reload modulus (i.e., E_{u-r}) from the full displacement pressuremeter. This result is likely caused by the following: (1) disturbance during preparation of the borehole for the Menard pressuremeter tests; and (2) the lack of a creep stage during the full displacement pressuremeter tests.

The correlation presented in figure A-39 can be used to evaluate the elastic modulus values obtained from the two different methods of pressuremeter testing. This figure indicates that the E_p values obtained are in good agreement with the Martin (1977) correlation and the E_{u-r} values are excessively high. It is noted that the Martin (1977) correlation used the initial elastic modulus from prebored pressuremeter data, and thus disturbance during borehole preparation likely led to a lower

slope of the expansion pressure curve, and thus a lower value of the initial pressuremeter elastic modulus. This disturbance and low elastic modulus from Menard PMT data was also likely at the Alabama site. To account for this disturbance, at least one unload-reload curve should be performed. Below the yield stress (p_f) the soil will generally act elastically, and after p_F the unload-reload elastic modulus will gradually decrease with increasing strain. It is good practice to perform the unload-reload curve near the anticipated yield stress (p_F) to estimate the maximum elastic modulus.

Very high unload-reload elastic modulus values were calculated from full displacement pressuremeter data. Typically the unload-reload modulus in Piedmont soils will be 2 to 4 times greater than the initial pressuremeter modulus, but the ratio of E_{u-r} to E_p presented in table A-14 varied from 11 to 148. High modulus values from full displacement pressuremeter data are likely due to disturbance from insertion of the probe as well as the lack of a creep test prior to performing the unload-reload loop.

From the test data presented, the pressuremeter elastic moduli produced by the Menard test would be recommended for design. Values from the full displacement pressuremeter tests appear unconservatively high. The pressuremeter modulus – SPT N-value correlation for Piedmont data (figure A-39) was used to identify potentially erroneous data. It is recommended that creep tests and unload–reload curves be performed for future investigations.

Elastic Modulus from DMT Data

As described in section 5.5, the selection of an elastic modulus for use in deformation analyses depends on the soil stress level. That is for designs with very high factors of safety, it is likely that the initial small-strain modulus could be used whereas for more typical factors of safety some reduced value of the initial modulus is appropriate for settlement analyses. For most designs, the elastic modulus corresponding to 25 percent of failure stress, E_{25}, may be used. In Piedmont residual soils, the use of the dilatometer modulus, E_D, as equal to E_{25} has been shown to provide reasonably accurate predictions of settlement (Mayne & Frost, 1988). Dilatometer modulus values from this investigation resemble previously proposed correlations to SPT N-value as shown in figure A-38. Figure A-43 compares the dilatometer elastic modulus, E_D, to the pressuremeter elastic modulus, E_p.

Figure A-43 indicates that the dilatometer modulus is 2 to 5 times greater than the initial elastic modulus from the PMT with an overall average value of E_d = 21,200 kPa (210 atm). Since unload-reload tests were not performed during the Menard pressuremeter tests, it is anticipated that the reported pressuremeter modulus values are low and that modulus values based on unload-reload tests would be more representative of the elastic modulus of the soil. It is anticipated that a properly performed unload-reload cycle after a creep test would yield a pressuremeter modulus that is 2 to 4 times greater than that reported. Therefore, for elastic settlement calculations using the available data from the Alabama site, the DMT modulus, E_D, could be used directly in calculations provided that working stress levels are consistent with a mobilized soil strength of about 25 percent.

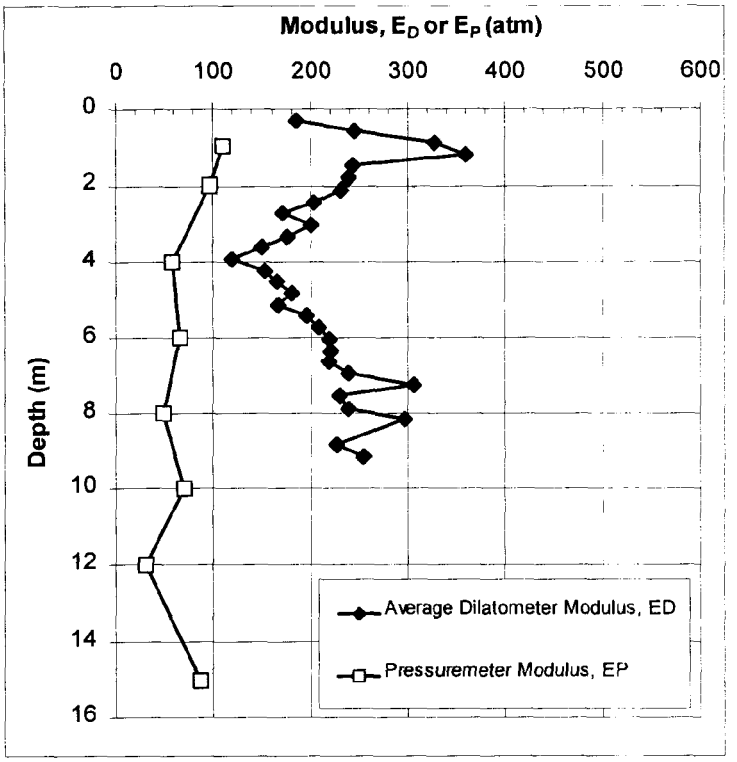

Figure A-43. Dilatometer modulus E_D compared to pressuremeter modulus, E_P

Elastic Modulus from Shear Wave Velocity Data

As discussed in section 5.5, the initial elastic modulus can also be calculated from shear wave velocity data and reduced to an appropriate value consistent with anticipated working stress levels for the design. Shear wave velocity, interpreted mass density, and elastic modulus profiles for the Alabama site are shown in figure A-44. The shear wave velocity was recorded using a seismic piezocone and the mass density was estimated using a correlation to shear wave velocity, V_s, (in m/s) and depth, z, (in m) as presented in Mayne et al. (1999):

$$\rho_t \approx 1 + \frac{1}{0.614 + 58.7(\log z + 1.095)/V_s} \qquad \text{(Equation A-17)}$$

Laboratory values of mass density are also shown on figure A-44, and agree well with the correlation in equation A-17.

The initial elastic modulus is calculated using equations 51 and 52. As discussed for the DMT elastic modulus, the use of E as equal to E_{25} for design purposes has been shown to be reasonable in Piedmont soils. The associated strain level corresponds to a factor of safety value, where $FS=1/(q/q_u)$, equal to 4 and a modulus ratio of:

$$\frac{E}{E_o} = 1 - \left(\frac{q}{q_u}\right)^{0.3} = 1 - (0.25)^{0.3} = 0.34 \qquad \text{(Equation A-18)}$$

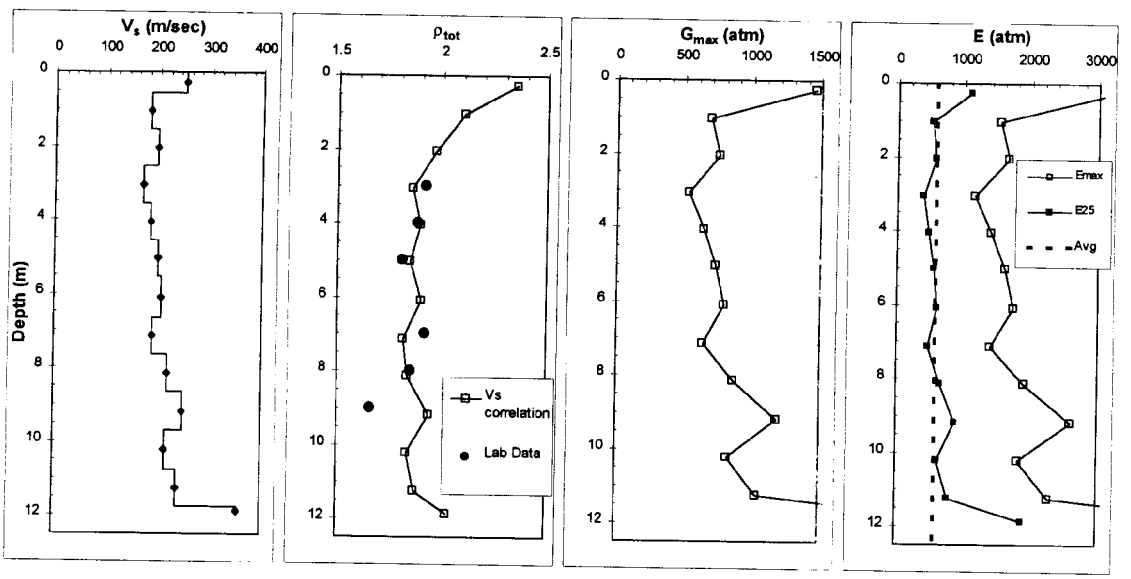

Figure A-44. Calculation of elastic modulus from shear wave velocity data.

For the profile shown in figure A-44, the average shear wave velocity to a depth of about 12 m is 204 m/s. Using equation A-17, an average shear wave velocity of 204 m/s, and an average depth of 6 m, the estimated total mass density, ρ_{tot}, is 1.87. From equation 52, the average maximum shear modulus would equal, $G_o = \rho_{tot} \cdot V_s^2 = 1.87\ (204)^2 = 77{,}822$ kPa = 77.8 MPa. To convert between the small strain shear modulus and small strain elastic modulus, equation 51 is used with a Poisson ratio (ν) equal to 0.1, $E_o = 2 \cdot G_o \cdot (1+\nu) = 2 \cdot 77{,}822$ kPa $\cdot$ (1+0.1) = 171,208 kPa = 171 MPa. As shown in equation A-18, the E/E_o reduction value associated with a FS equal to 4 (E_{25}) is 0.34, yielding E_{25} = $0.34 \cdot E_o = 0.34 \cdot 171{,}208$ kPa = 58,210 kPa = 58 MPa.

The appropriate E value can also be calculated directly from shear wave velocity using equation 54:

$$E_s = 0.34 \cdot 2 \cdot 1.87 \cdot 204^2 \cdot (1 + 0.1) = 58{,}210\,kPa = 58\,MPa = 573\,atm \qquad \text{(Equation A-19)}$$

This value is about 2.7 times greater than the E_{25} value calculated from the DMT. Since Piedmont soils are considered to be structured due to the relict bonding and features of the parent rock, it can be assumed that the small strain shear wave velocity measurements would capture the effects of these structural features whereas the DMT and PMT would cause some disturbance. It is noted that if a FS value of 2.5 (i.e., mobilized strength corresponding to 40 percent of the ultimate strength) was used for design, the associated E/E_u reduction factor would be 0.24, and the E_{40} value would be about 41,089 kPa.

Summary

Calculations of compression properties for Piedmont residual soils have been presented based on laboratory oedometer tests, Menard pressuremeter, full-displacement pressuremeter, and the DMT. Shear wave velocity data has also been used. Table A-15 shows a summary table of the average elastic modulus values measured (or evaluated) based on these tests.

Table A-15. Summary of elastic modulus values from various tests.

Test Type	Elastic Modulus (kPa)
Laboratory oedometer	4,500
Menard pressuremeter	7,585
Full-displacement pressuremeter	>100,000
Dilatometer	21,200
Shear Wave Velocity correlation	58,210 (E_{25}) 41,089 (E_{40})
SPT N correlation (see table 29) E_s=700 $(N_1)_{60}$	10,500

As previously discussed, modulus values from the full-displacement pressuremeter are clearly too large for the reasons discussed. It is important to note that modulus values from laboratory oedometer tests and from a correlation using SPT N values underestimates the modulus (relative to other tests) by a factor of 2 to greater than 10. Moreover, where settlements are critical, it can be seen that more sophisticated methods such as the DMT, PMT, or shear-wave velocity evaluations may be warranted. Perhaps more importantly, this assessment of compression properties demonstrates the importance of using high-quality undisturbed samples for laboratory testing. Where it is clear that obtaining undisturbed samples will be difficult and impractical, consideration should be given to performing appropriate in-situ testing.

STRENGTH CHARACTERISTICS OF PIEDMONT RESIDUAL SOILS

General

Selection of design strength properties in residual soils is particularly difficult due to the intermediate drainage conditions, as well as potential variability in the weathering profile and presence of slickensided planes of weakness. In-situ penetration tests in silty and clayey materials are typically undrained. In some cases in Piedmont residual soils, dissipation of excess penetration pore pressures occur within 1 to 3 minutes of paused penetration indicating partially drained conditions. Therefore, correlations between in-situ test parameters and either undrained strength or drained strength parameters are not appropriate. Additionally, the presence of mica may significantly reduce SPT blowcounts and could affect other in-situ test parameters to varying degrees, but will not reduce the effective stress friction angle to the same degree. In summary though, due to the relatively high hydraulic conductivity values of residual soils, most loading

conditions associated with typical transportation construction activities will occur over such a time period that the prevailing drainage condition in the residual soil is drained. Analysis of data for this example is therefore referenced to the drained condition.

In this example, laboratory strength characteristics of Piedmont soils are evaluated using isotropically consolidated undrained triaxial compression tests with pore pressure measurements (CIUC). Correlations between strength parameters and in-situ test parameters are compared to the Alabama site laboratory data and recommendations for design strength values are presented.

Summary of CIUC Test Data

Fifteen CIUC triaxial tests were performed on nominally undisturbed Shelby tube samples from the Alabama site. A typical stress-strain curve and pore pressure-strain curve for two specimens are shown in figure A-45 and detailed testing data for specimen B2-1-1 during the shearing portion of the test are provided in table A-16. Triaxial test summary information is presented in table A-17.

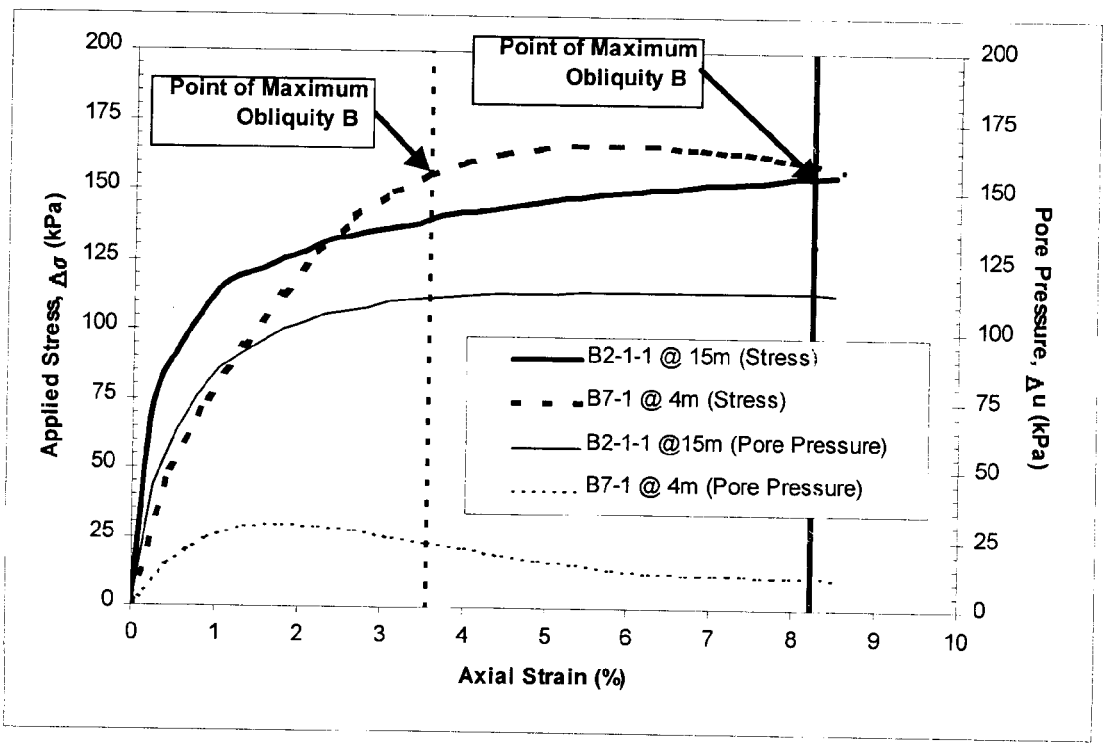

Figure A-45. Stress-strain curve for CIUC tests on samples B2-1-1 at 15 m and B7-1 at 4 m.

Failure was defined at the point of maximum obliquity. The point of maximum obliquity occurs when the ratio of σ_1' to σ_3' is a maximum. For test B2-1-1, the point of maximum obliquity occurs at an axial strain of approximately 8.2%, and the obliquity value corresponding to that strain level is:

$$\frac{\sigma_1'}{\sigma_3'} = \frac{(\sigma_1 - \Delta u)}{(\sigma_3 - \Delta u)} = \frac{(326.2 - 114.46)}{(171.02 - 114.46)} = 3.744 \qquad \text{(Equation A-20)}$$

where σ_3 is the minor principal stress (which is equal to the consolidation stress in a CIUC test), σ_1 is the major principal stress (which is equal to the applied vertical stress in a CIUC test), the prime (') sign indicates effective stress which requires the subtraction of excess pore pressure, Δu, from each principal stress. While the point of maximum obliquity may occur near the end of the test, as shown for specimen B2-1-1 in figure A-45, it may also occur earlier in the test, as shown for specimen B7-1 in figure A-45. This point is easy to find when using a spreadsheet application for data analysis, as shown in table A-16.

Table A-16. Stress-strain data for specimen B2-1-1 at 15 m.

Axial Deflect. (cm)	Axial Strain, ε_v (%)	Axial Load (N)	Corrected Area (cm^2)	$\Delta\sigma$ (kPa)	σ_3 (kPa)	σ_1 (kPa)	Δu (kPa)	p (kPa)	p' (kPa)	q (kPa)	(σ_1'/σ_3')
0.000	0.00	0.0	39.2	0.0	171.0	171.0	0.0	171.0	171.0	0.0	1.000
0.036	0.26	289.1	39.3	73.5	171.0	244.5	44.1	207.8	163.6	36.7	1.579
0.071	0.51	359.9	39.4	91.2	171.0	262.3	62.7	216.6	153.9	45.6	1.843
0.107	0.77	409.7	39.5	103.6	171.0	274.6	75.8	222.8	147.0	51.8	2.089
0.142	1.02	452.8	39.6	114.2	171.0	285.2	85.5	228.1	142.6	57.1	2.336
0.178	1.28	472.8	39.7	119.0	171.0	290.0	91.0	230.5	139.5	59.5	2.487
0.213	1.54	485.7	39.9	121.9	171.0	292.9	95.8	232.0	136.1	60.9	2.621
0.249	1.79	500.4	40.0	125.2	171.0	296.3	100.0	233.6	133.7	62.6	2.763
0.284	2.05	512.4	40.1	127.9	171.0	298.9	102.7	235.0	132.2	64.0	2.873
0.320	2.30	527.1	40.2	131.2	171.0	302.3	105.5	236.6	131.1	65.6	3.003
0.356	2.56	536.5	40.3	133.2	171.0	304.2	106.9	237.6	130.8	66.6	3.077
0.391	2.82	544.9	40.4	135.0	171.0	306.0	108.3	238.5	130.2	67.5	3.150
0.427	3.07	552.5	40.5	136.5	171.0	307.5	110.3	239.3	128.9	68.2	3.248
0.462	3.33	558.3	40.6	137.5	171.0	308.6	111.0	239.8	128.8	68.8	3.292
0.498	3.59	567.6	40.7	139.5	171.0	310.5	111.7	240.8	129.1	69.7	3.351
0.533	3.84	575.6	40.8	141.1	171.0	312.1	112.4	241.5	129.2	70.5	3.406
0.569	4.10	581.8	40.9	142.2	171.0	313.2	113.1	242.1	129.0	71.1	3.454
0.605	4.35	586.7	41.0	143.0	171.0	314.0	113.8	242.5	128.8	71.5	3.498
0.640	4.61	594.7	41.1	144.6	171.0	315.6	113.8	243.3	129.5	72.3	3.525
0.676	4.87	600.5	41.2	145.6	171.0	316.6	113.8	243.8	130.0	72.8	3.543
0.711	5.12	606.7	41.4	146.7	171.0	317.7	113.8	244.4	130.6	73.4	3.562
0.747	5.38	613.0	41.5	147.8	171.0	318.8	114.5	244.9	130.5	73.9	3.613
0.782	5.63	618.3	41.6	148.7	171.0	319.7	114.5	245.4	130.9	74.3	3.629
0.818	5.89	622.8	41.7	149.4	171.0	320.4	114.5	245.7	131.2	74.7	3.641
0.853	6.15	627.6	41.8	150.1	171.0	321.1	114.5	246.1	131.6	75.1	3.654
0.889	6.40	632.5	41.9	150.9	171.0	321.9	114.5	246.5	132.0	75.4	3.668
0.925	6.66	636.1	42.0	151.3	171.0	322.3	114.5	246.7	132.2	75.7	3.675
0.965	6.95	641.9	42.2	152.2	171.0	323.2	114.5	247.1	132.7	76.1	3.691
1.001	7.21	644.5	42.3	152.4	171.0	323.4	114.5	247.2	132.8	76.2	3.695
1.036	7.46	649.9	42.4	153.3	171.0	324.3	114.5	247.7	133.2	76.6	3.710
1.072	7.72	653.9	42.5	153.8	171.02	324.8	114.46	247.9	133.5	76.9	3.719
1.107	7.98	659.7	42.6	154.7	171.02	325.7	114.46	248.4	133.9	77.4	3.735
1.143	8.23	663.7	42.8	155.2	171.02	326.2	114.46	248.6	134.2	77.6	3.744
1.179	8.49	667.7	42.9	155.7	171.02	326.7	113.77	248.9	135.1	77.9	3.720

Notes: The highlighted point refers to the maximum principal stress ratio, and thus failure at maximum obliquity.

Failure Envelopes and Design Strength

Table A-17 provides a summary of the results of the CIUC triaxial tests conducted. The table contains parameters at failure, including strain ($\varepsilon_{v,ff}$), excess pore pressure (Δu_{ff}), Skempton's pore pressure parameter (A_{ff}), the stress path parameters (p, p', and q), and the secant effective stress friction angle (ϕ'). For example, Skempton's A_{ff} parameter for specimen B5-1 at 4 m shown in table A-17 was calculated as:

$$A_{ff} = \frac{\Delta u - \Delta\sigma_3}{\Delta\sigma_1 - \Delta\sigma_3} = \frac{33.4\,kPa - 0\,kPa}{158.2\,kPa - 0\,kPa} = 0.21 \qquad \text{(Equation A-21)}$$

The stress path parameters for specimen B5-2-2 at 15 m shown in table A-17 were calculated as:

$$p = \frac{(\sigma_1 + \sigma_3)}{2} = \frac{(917.6\,kPa + 413.7\,kPa)}{2} = 665.65\,kPa \qquad \text{(Equation A-22)}$$

$$p' = p - u = 665.65\,kPa - 198.6\,kPa = 467.1\,kPa \qquad \text{(Equation A-23)}$$

$$q = \frac{(\sigma_1 - \sigma_3)}{2} = \frac{(917.6\,kPa - 413.7\,kPa)}{2} = 251.95\,kPa \qquad \text{(Equation A-24)}$$

The effective stress path is shown on figure A-46.

Table A-17. Strength properties from CIUC triaxial tests on Piedmont soils from the Alabama site.

Boring	Depth (m)	σ_{3C}' (kPa)	$\Delta\sigma_{ff}$ (kPa)	$\sigma_{1,ff}$ (kPa)	$\varepsilon_{v,ff}$ (%)	Δu_{ff} (kPa)	A_{ff}	p (kPa)	p' (kPa)	q (kPa)	Secant ϕ' (deg)
B5-1	4	52.3	158.2	210.5	13.8	33.4	0.21	131.4	98.0	79.1	53.8
B7-1	4	84.8	155.8	240.6	3.6	23.4	0.15	162.7	139.3	77.9	34.0
B7-2	4	162.0	188.0	350.0	6.8	62.1	0.33	256.0	193.9	94.0	29.0
B7-1	6	179.3	248.5	427.7	4.4	108.4	0.44	303.5	195.1	124.2	39.6
B8-2	6	179.3	248.5	427.7	4.7	108.4	0.44	303.5	195.1	124.2	39.6
B7-2-1	8	206.8	233.9	440.7	4.0	136.9	0.59	323.7	186.8	116.9	38.8
B7-2-2	8	310.3	351.9	662.2	10.7	201.5	0.57	486.3	284.7	176.0	38.2
B7-1	10	120.7	183.3	303.9	4.1	72.6	0.40	212.3	139.7	91.6	41.0
B7-2	10	241.3	313.8	555.1	9.3	159.2	0.51	398.2	239.0	156.9	41.0
B2-1	12	115.6	116.5	232.1	15.0	46.9	0.40	173.9	127.0	58.3	27.3
B2-6	12	115.6	105.0	220.6	8.2	54.5	0.52	168.1	113.6	52.5	27.5
B5-1	12	127.2	174.2	301.4	7.3	46.3	0.27	214.3	168.0	87.1	31.2
B5-2	12	102.0	116.4	218.4	5.0	47.2	0.41	160.2	113.0	58.2	31.0
B2-1-1	15	171.0	155.2	326.2	8.2	114.5	0.74	248.6	134.2	77.6	35.3
B5-2-2	15	413.7	503.9	917.6	2.9	198.6	0.39	665.6	467.1	251.9	32.6

Notes: The subscript ff refers to measurement made at failure. Failure is defined as the point of maximum obliquity.

The secant effective stress friction angle for specimen B7-2-2 at 8 m is calculated as:

$$\phi' = \arcsin(\tan\psi') = \arcsin\left(\frac{q}{p'}\right) = \arcsin\left(\frac{176}{284.7}\right) = 38.2^{o} \qquad \text{(Equation A-25)}$$

Figure A-47 shows a range of effective stress failure envelopes for the data. The trend line shown in this figure was developed assuming the effective stress cohesion intercept is zero. A regression analysis was also performed (although not shown) to evaluate the best-fit cohesion intercept. This analysis resulted in ϕ'=33.8° and c'=4.9 kPa. Based on this, it does not appear that there is a significant cohesion intercept in the laboratory specimens tested from this site. Since the cohesion intercept is fairly insignificant, the effective stress shear strength properties of the soil at this site will be modeled solely using a friction angle of 35.2° based on regression analyses.

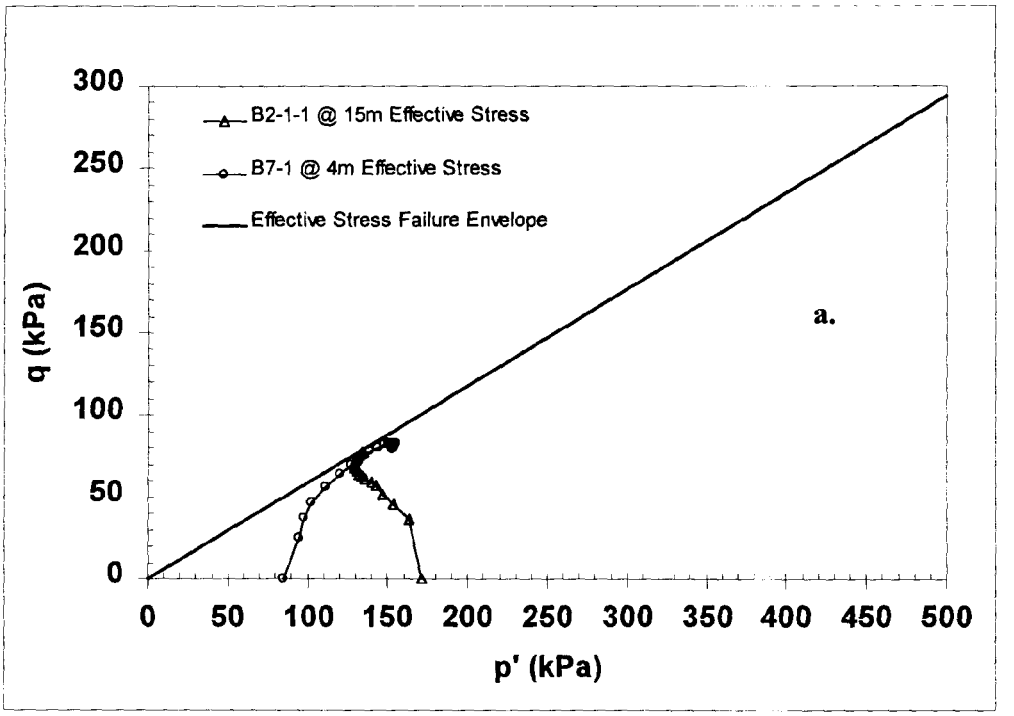

Figure A-46. Effective stress paths for CIUC tests shown in figure A-45.

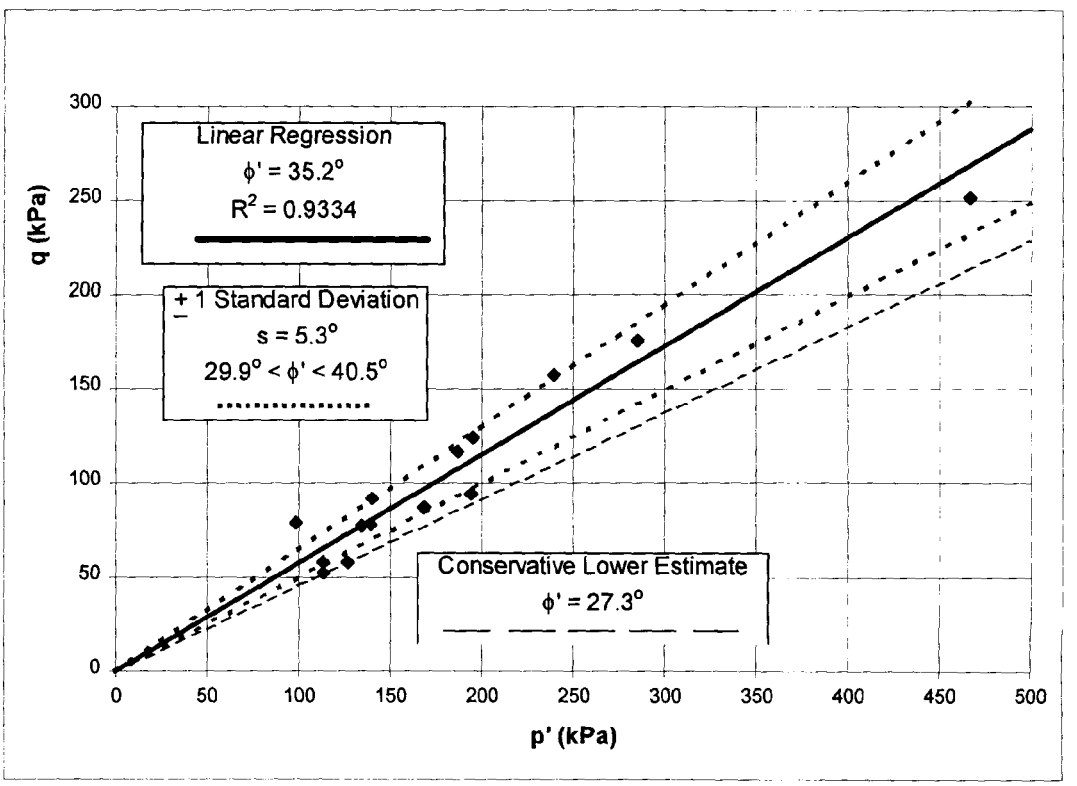

Figure A-47. Effective stress failure envelopes based on triaxial test data.

Statistical Analysis of Strength Data

In this section, a more detailed assessment of the laboratory strength data is presented. Basic statistical measures and statistical analyses are illustrated using the laboratory strength data.

Review of the individual data points in figure A-47 indicates that the effective stress failure envelope from linear regression of the data points (i.e., $\phi'=35.2°$) may be unconservative at effective stresses greater than 300 kPa. In addition, the scatter of the data suggests that it may not be prudent to adopt the average friction angle for design analyses without also performing design analyses with a more conservative representation of the effective stress friction angle.

To assess the laboratory strength data further, the standard deviation in the secant friction angle data was calculated. For this calculation, the mean effective stress friction angle ($\bar{\phi}'_i$) was taken as 35.2° from the linear regression. Since the measured data is actually the slope of the failure envelope given by tan ψ', the mean of sin ϕ'=tan ψ' ($\bar{x}_i$) was used. This value was calculated as 0.5764. The number of samples (n) is 15. The standard deviation of sin ϕ' was calculated as:

$$s = \sqrt{\frac{\sum_{i=1}^{n}(x_i - \bar{x}_i)^2}{n-1}} = \sqrt{\frac{\sum_{i=1}^{n}(x_i - 0.5764)^2}{15-1}} = \sqrt{\frac{0.122}{14}} = 0.0934 \qquad \text{(Equation A-26)}$$

To determine the standard deviation of ϕ', the arcsine (s) was calculated to be 5.3°. The effective stress friction angle of this material is likely between the average (35.2°) and $\pm$ one standard deviation, resulting in an effective stress friction angle between 29.9 and 40.5 degrees. The average and the average $\pm$ one standard deviation are plotted on figure A-47. The average minus 1 standard deviation contains the data at high effective stresses, but does not adequately encompass the scatter at effective stresses around 100 kPa to 200 kPa. To account for scatter at lower effective stresses, a conservative lower estimate of 27.3 degrees is also shown in figure A-47. This statistical analysis is useful since it provides a rational approach to develop conservative design properties. That is, for this laboratory data, it would be appropriate to confidently select a friction angle of 29.9° as lower bound value for design.

The statistical analysis performed above was possible due to the relatively large size of an available database of friction angle data (i.e., 15 triaxial tests). It is possible, however, to assess the statistical variability of the friction angle of a soil (or other properties) without a relatively significant database. Published values of the coefficient of variation, V, defined as the standard deviation divided by the average value, are available for various soil properties (see Duncan, 2000 and table 52) and these can be used to facilitate a simple statistical analysis without requiring significant amounts of data. For example, table 52 indicates that the coefficient of variation for soil effective stress friction angle is estimated at 2 to 13 percent, and thus the standard deviation estimated from this laboratory data would be between:

$$s = V \cdot \bar{\phi}' = 0.02 \cdot 35.2^o = 0.7^o \qquad \text{(Equation A-27)}$$

$$s = V \cdot \overline{\phi'} = 0.13 \cdot 35.21^{o} = 4.6^{o} \qquad \text{(Equation A-28)}$$

From this calculation, it is evident that the calculated standard deviation from laboratory tests on Piedmont soils from the Alabama site is actually slightly greater than a maximum standard deviation calculated using V=13 percent.

A third method for assessing standard deviation from minimal laboratory or field test results uses the three-sigma rule (Duncan, 2000). The three-sigma rule says that 99 73 percent of all values of a normally distributed parameter fall within three standard deviations of the mean. Therefore, if HCV = highest conceivable value of the parameter and LCV = lowest conceivable value of the parameter, these are approximately three standard deviations above and below the average value. The standard deviation can then be estimated from:

$$s = \frac{HCV - LCV}{6} \qquad \text{(Equation A-29)}$$

Using secant effective stress friction angle laboratory data from this example and assuming that the maximum and minimum values for the friction angle represent the HCV and the LCV, respectively, results in:

$$s = \frac{HCV - LCV}{6} = \frac{53.8^{o} - 27.3^{o}}{6} = 4.4^{o} \qquad \text{(Equation A-30)}$$

This leads to a coefficient of variation of:

$$V = \frac{s}{\overline{\phi'}} = \frac{4.4}{35.2} = 0.125 = 13\% \qquad \text{(Equation A-31)}$$

This value for the coefficient of variation is in good agreement with published values and with the value estimated from all the laboratory data. Difficulties in assessment of the coefficient of variation from the three-sigma rule lie in the estimation of the highest and lowest conceivable value. The HCV and LCV are typically underestimated, and would likely have been underestimated in this case if the large amount of laboratory data were not available.

Shear Strength based on Correlation to In-Situ Test Parameters

Correlations for the SPT, CPT, and DMT are compared to a best-fit linear regression effective stress friction angle failure envelope in figure A-48. The following correlations between in-situ test parameters and effective stress friction angle are recommended for clean sands, but are used herein for Piedmont residual silty sands to demonstrate potential errors associated with applying correlations incorrectly.

Standard Penetration Test: $\phi' = [15.4 \cdot (N_1)_{60}]^{0.5} + 20^{o}$ (Equation A-32)

Cone Penetration Test: $\phi' = 17.6^{o} + 11.0 \cdot \log [(q_c/p_a)/(\sigma_{vo}'/p_a)^{0.5}]$ (Equation A-33)

Flat Dilatometer Test: $\phi' = 28^{o} + 14.6 \cdot \log K_D - 2.1 \cdot \log^2 K_D$ (Equation A-34)

The applicability of these correlations are difficult to assess since: (1) residual soils are not clean sands, and in-situ test parameters are likely effected to some degree by fines content as well as mica content; (2) there is significant variability in residual soil deposits, so in-situ test data may not be directly comparable to the laboratory test data at equal depths; and (3) the penetration may be undrained, partially drained, or drained. Figure A-48 shows friction angle from laboratory data compared to friction angle estimated from in-situ test data using the equations presented above. Adjacent to the friction angle plot is the profile of u_2 penetration porewater pressure with depth.

From CIUC triaxial test data shown in figure A-48, the friction angle is estimated to be 35.2 degrees using best-fit linear regression. Tests were performed at depths of 4, 6, 8, 10, 12, and 15 m. Above 3 to 4 m, the soil consists of an overconsolidated partially saturated crust with higher fines content as compared to the soil at greater depth, thus the correlations will not be discussed for material from the ground surface to a depth of 4 m. It is noted, however, that the correlated effective stress friction angles approach high values at low depths.

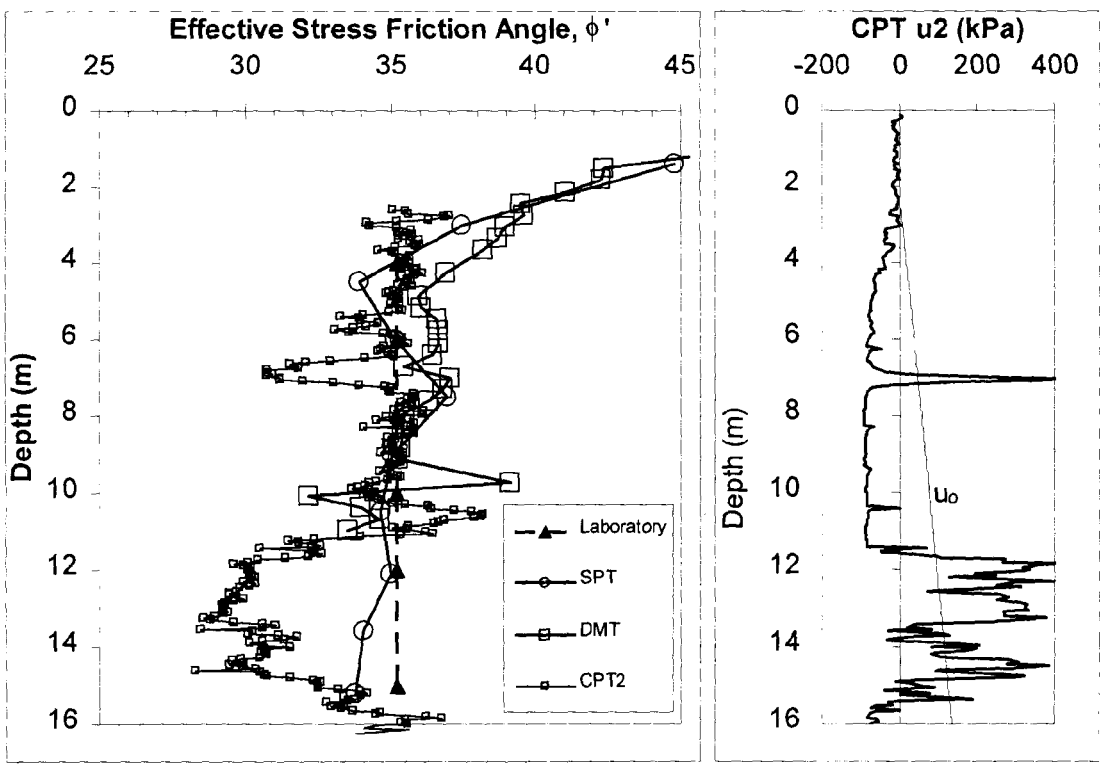

Figure A-48. Estimate of effective stress friction angle at Alabama site using in-situ test data.

Effective stress friction angle estimated from SPT $(N_1)_{60}$ values using the Hatanaka & Uchida correlation slightly underestimate the laboratory friction angle value by about 1 degree until about 12 to 16 m where the ϕ' values are underpredicted by about 2 to 3 degrees. While the correlation seems to work well, the effects of fines content and mica content on this correlation are unknown and it is likely that the good agreement is due to compensating errors. The energy efficiency of the automatic hammer was assumed to be 90 percent, but may have varied from 50 to 90 percent. The variation in

energy efficiency alone would result in a reduction of up to about 4 degrees of the estimated friction angle. This shows that while correlations of effective stress friction angle of clean sands using SPT $(N_1)_{60}$ data from Piedmont soils at the Alabama site match well, the correlation is sensitive to the energy efficiency of the SPT hammer which adds considerable uncertainty. There is little confidence in the use of this clean sand correlation in Piedmont soils without site-specific laboratory confirmation.

Results from the correlation between CPT tip resistance and effective stress friction angle of clean sands slightly underpredicts laboratory CIUC data by about 1 degree for a majority of the sounding, but may underpredict ϕ' by about 6 degrees or more. It is noted that sharp differences in estimated effective stress friction angle from CPT data and laboratory values occur where the u_2 penetration porewater pressure switches from negative to positive. The positive u_2 penetration porewater pressures are coupled with a reduction in tip resistance that leads to the reduction in estimated friction angle. Since the zone of positive excess (greater than hydrostatic) penetration porewater pressures is indicative of partially undrained penetration, the tip resistance in those zones is likely not a function of effective stress friction angle and the correlation between tip resistance and effective stress friction angle is not valid for these zones. Additionally, fines and mica content will affect CPT tip resistance. Therefore, the good agreement between the tip resistance-ϕ' correlation in the upper 10 meters may be a result of compensating errors.

Effective stress friction angle estimated from correlations to DMT K_D parameter match well with ϕ' from laboratory CIUC tests. Since the DMTs are performed at pauses in penetration, testing under essentially drained conditions is possible. The DMT-ϕ' correlation is anticipated to be a lower bound relationship, and ϕ' estimates from DMT data match well from 4 to 8 meters and slightly underpredicts the friction angle from 8 to 12 m. Once again, the effect of drainage conditions and fines/mica content on the estimated friction angle has not been verified for DMT testing in residual soils.

Recommended Drained Strength for Design

For strength characterization, it is recommended to perform laboratory tests at a range of confining stresses that encompass the design loads. Due to the inherent variability of Piedmont soils, upper and lower bound values of effective stress friction angle should be evaluated along with a best estimation of friction angle. If sufficient data is not available to assess the standard deviation of the friction angle, then published coefficient of variation values can be used to estimate the standard deviation from the average friction angle.

Selection of an appropriate failure envelope for design from laboratory data has been discussed in previous sections, along with statistical variability in friction angle. While correlations between ϕ' and in-situ test parameters show good agreement at some locations, the variability in the soil profile and uncertainty in the effects on test readings due to fines and mica content may lead to acceptable agreement due to compensating errors.

PROPERTIES OF WEATHERED ROCK AND ROCK

In this section, information and property evaluation for weathered rock and rock commonly found in the Piedmont province is presented. Rock core information and laboratory testing data are from a project site located in Atlanta, Georgia.

Stratigraphy Information

Figure A-49 shows a rock core log from a depth of 17 to 57 ft (5.2 to 17.4 m). The overburden soils at this site (not depicted on the log shown on figure A-49) consist primarily of silty sands (SM) underlain by partially weathered rock. For this project, partially weathered rock was defined as material which exhibits SPT N values greater than 100-blows/300 mm. The partially weathered rock is a transition zone from the overburden (residual) soils to the underlying sound rock. A 3-ft (1-m) thick layer of partially weathered rock was encountered at a depth of 14 ft below the ground surface. Below the partially weathered rock, is gneiss. A review of the log indicates very good core recovery and high RQD values (greater than 90 percent) indicating excellent rock.

Rock Strength and Deformation Properties

Figure A-50 and A-51 show the results of unconfined compression strength tests on rock core from this boring. These samples are taken from depths of 18 ft (just below the partially weathered rock) and 40 ft. The stress-strain curve for the sample at 18 ft shows a common feature of laboratory compression testing on rocks that are fractured, that being an initial response that is "softer" than the subsequent response. This is due to the initial compression of the joints. The unconfined compressive strength of these samples is given on the data sheets. A deformation modulus was calculated (see figures A-50 and A-51) for each sample. The sample at 18 ft has a modulus of 16.1 GPa and the sample at 40 ft has a modulus of 22.1 GPa.

Figure A-52 shows the results of a laboratory direct shear test on a rock joint. This joint is relatively planar (i.e., smooth) and is filled with soil material. For this testing, two normal stress levels were selected, 4.3 ksf (206 kPa) and 8.6 ksf (412 kPa). For this test series, the sample was sheared at one confining stress until both peak and residual strength had been reached. For subsequent confining stresses, shearing was carried out to a residual shear strength value. Measured friction angles are shown on figure A-52. The irregular (as compared to soils) shear stress-deformation curve results from the opening and closing of the joint as the sample is sheared.

ROCK CORE LOG

Date 2/6/01

ROUTE GEC No. 5 DESCRIPTION Core Boring Record LOGGED BY

SECTION LOCATION

COUNTY Fulton CORING METHOD Rotary core with water flush

STRUCT. NO.
Station

CORING BARREL TYPE & SIZE NX Diamond Bit

Core Diameter 1.875 in
Top of Rock Elev. 1056 ft
Begin Core Elev. 1056 ft

BORING NO. NC-122
Station
Offset
Ground Surface Elev. 1083.00 ft

		DEPTH (ft)	CORE (#)	RECOVERY (%)	R.Q.D. (%)
Hard to very hard, light gray and gray, biotite muscovite gneiss	1056.00		R-1	79	63
		20	R-2	100	100
			R-3	100	100
		25	R-4	100	100
Hard to very hard, gray-green, biotite, amphibole (hornblende) gneiss	1045.00	30	R-5	89	89
			R-6	100	100
		35			

Figure A-49. Rock core log (page 1 of 2).

ROCK CORE LOG

Date 2/6/01

ROUTE GEC No. 5 DESCRIPTION Core Boring Record LOGGED BY

SECTION LOCATION

COUNTY Fulton CORING METHOD Rotary core with water flush

STRUCT. NO.
Station

CORING BARREL TYPE & SIZE NX Diamond Bit

Core Diameter 1.875 in
Top of Rock Elev. 1056 ft
Begin Core Elev. 1056 ft

BORING NO. NC-122
Station
Offset
Ground Surface Elev. 1083.00 ft

	DEPTH (ft)	CORE (#)	RECOVERY (%)	R.Q.D. (%)
Hard to very hard, gray-green, biotite, amphibole (hornblende) gneiss *(continued)*				
		R-7	100	100
	40			
1031.00				
Hard to very hard, dark gray and green, biotite, amphibole (hornblende) gneiss				
		R-8	100	100
	45			
1023.80		R-9	100	100
Very hard, dark gray and green, biotite, amphibole (hornblende) gneiss				
	50			
		R-10	100	100
	55			
1016.00				
Coring Terminated				

Figure A-49. Rock core log (page 2 of 2).

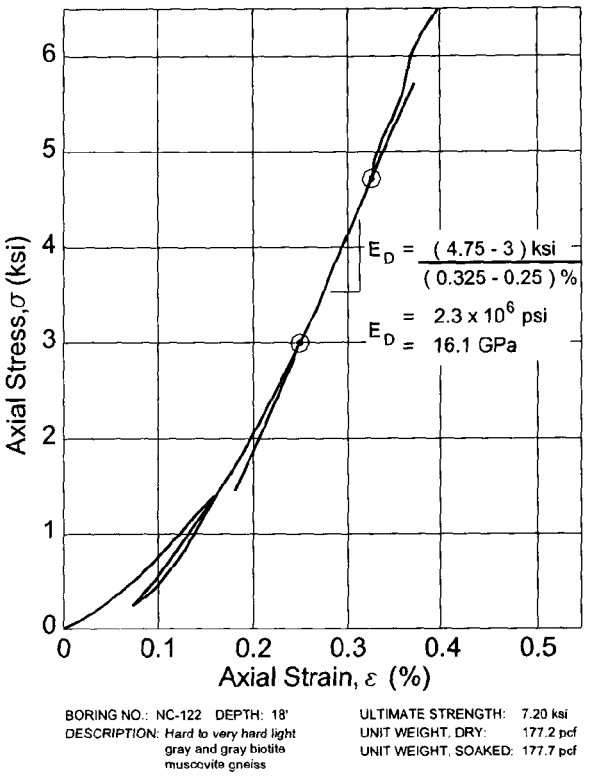

Figure A-50. Unconfined compression test results (sample depth 18 ft).

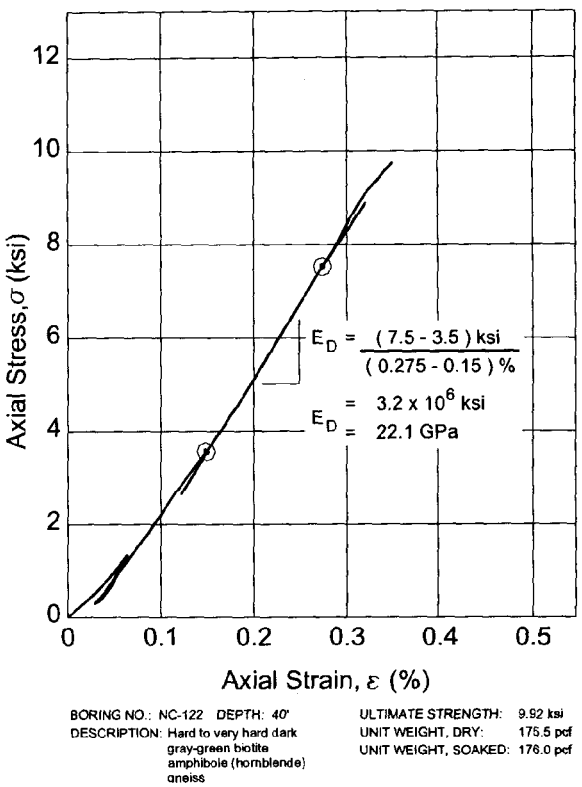

Figure A-51. Unconfined compression test results (sample depth 40 ft).

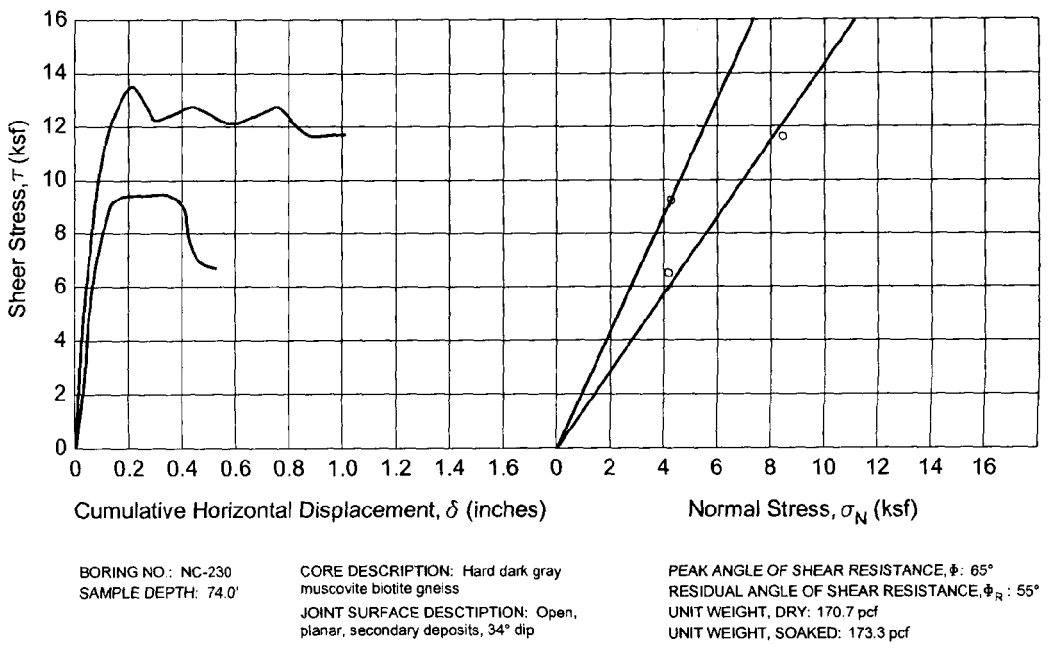

Figure A-52. Direct shear test results on rock joint (sample depth 74 ft).

SOIL AND ROCK PROPERTY SELECTION EXAMPLE NO. 3

Heavily overconsolidated clays

INTRODUCTION

This example problem describes procedures and interpretation methods for evaluating properties for heavily overconsolidated clays. Specifically, this problem focuses on: (1) subsurface profile development from laboratory and in-situ test results; (2) consolidation parameters; (3) in-situ stress state (i.e., K_o); (4) undrained shear strength; and (5) swell potential. The evaluation procedures for properties of overconsolidated clays such as subsurface profile, consolidation, in-situ stress state, and shear strength are similar to those previously described in Property Selection Example Nos. 1 and 2. In this Property Selection Example, issues specifically relevant to the evaluation of these properties as they relate to heavily overconsolidated materials are highlighted. The reader is referred to the previous example problems for more detail on the baseline procedures for property evaluation.

The project site is located near Houston, Texas. The subsurface soils at the Site consist primarily of clays that have been preconsolidated throughout their thickness as a result of dessication. Thin seams of fine sand and silt are also present throughout the soil profile. The depth to groundwater is approximately 2 m. The clayey soils of this region have a complex structure including joints, fissures, and silt and sand seams.

The subsurface stratigraphy at the Site consists of the upper "Beaumont" formation to a depth of approximately 8-12 m and the lower "Montgomery" formation with a reported thickness of approximately 150 m. The Beaumont formation comprises primarily stiff plastic clays with thin seams of sand and silt, while the Montgomery formation comprises stiff clays of lower plasticity with more silt and sand layers. Available geologic information indicates that the surface of the Montgomery formation became highly weathered before deposition of the Beaumont, and consequently much of the clay was leached from the surface. As a result, a significant silt and sand region exists at the Beaumont/Montgomery interface and the transition is typically readily apparent in both laboratory and in-situ tests. The soils in this region are highly variable due to depositional history (location relative to a distributary channel) resulting in highly variable engineering properties across the Site.

SUBSURFACE EXPLORATION AND TESTING PROGRAM

A basic description of the subsurface stratigraphy at the Site was evaluated from SPT blow count values and soil index data collected from disturbed split spoon samples across the Site. In-situ testing including CPTu, DMT, and self-boring pressuremeter (SBPMT) results are also provided. Undisturbed samples for laboratory consolidation and strength testing were obtained from thin-walled Shelby tubes.

DEVELOPMENT OF A SUBSURFACE PROFILE FOR DESIGN

As discussed in the previous example problems, methods commonly employed to determine the subsurface profile include the SPT, CPTu, and the DMT. In this example, data collected from each of these tests are presented and compiled to develop a subsurface profile.

Use of SPT and Disturbed Sampling

Figure A-53 shows a boring log for the Site. The log indicates an 8 m thick layer of stiff to very stiff clay overlying about 1 m of silty clay. Below this, there is an 11-m thick layer of stiff clay with sand and clayey silts. The log indicates a definitive transition at approximately a depth of 8 m where SPT blowcounts decrease from 18 to 7 within 1.5 meters. Correlation with SPT blowcount values indicates that the clayey soils are medium stiff to very stiff clays and silts.

Index test results are included in figure A-54. These results indicate that the total unit weight is approximately constant within the Beaumont and Montgomery layer with average values of 19.9 kN/m^3 (Beaumont) and 20.7 kN/m^3 (Montgomery). The moisture content is typically around 20 percent with a decrease at the Beaumont/Montgomery interface. In the Beaumont formation, moisture contents are, overall, very close to the plastic limit of the soil indicating that the soils in this formation are heavily overconsolidated. Soils within the Beaumont are much more plastic than the Montgomery as shown in the plasticity chart (figure A-55).

Table A-18 provides a detailed assessment of the stratigraphy based on the boring information and index testing results. Six individual layers are identified based on this information. This layering is used to evaluate results from CPT, CPTu, and DMT in the following sections.

Table A-18. Soil stratigraphy from SPT and classification testing.

Layer ID[1]	Depth (m)	Classification and Description
1	0 – 3	Very stiff clay of varying plasticity (CL-CH).
2	3 - 7	Stiff to very stiff clay of high plasticity (CH). Highly plastic soils with liquid limits greater than 50.
3	7 - 8.5	Medium Stiff Silty Clay (CL). Transition zone from Beaumont to Montgomery. Moisture content and plasticity decreases.
4	8.5 - 14	Stiff to very stiff sandy clay with sand pockets (CL). N values increase. Soils less plastic with lower moisture content than the Beaumont soils.
5	14 - 18	Dense silt with clayey silt and sand layers (ML). Soil layer is sandier as indicated by higher blowcounts and less plastic soils.
6	18 - ?	Stiff clay (CL).

[1]The Layer ID numbers in table will correspond to the Layer ID numbers for CPTu and DMT results to be discussed subsequently.

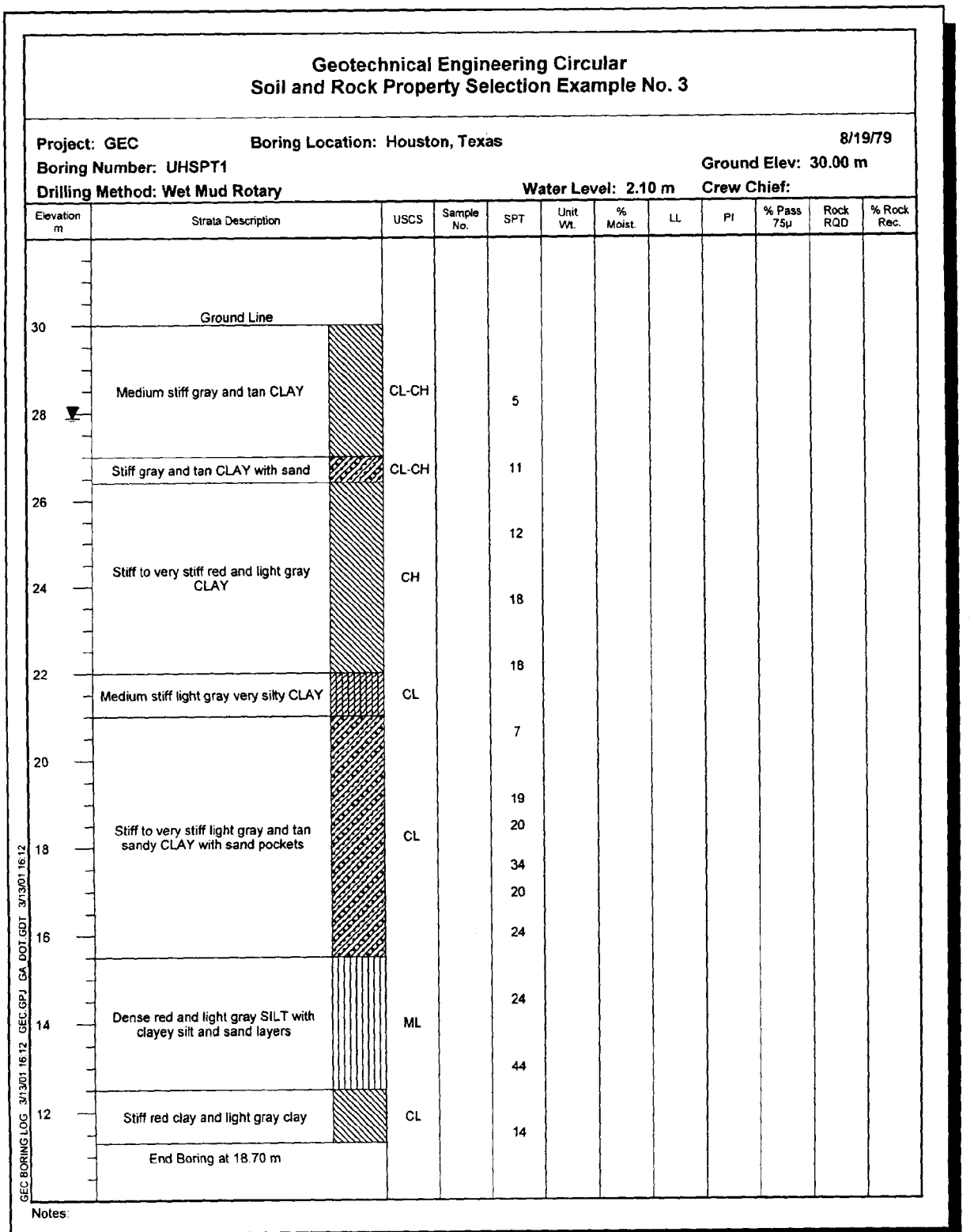

Figure A-53. Boring Log UHSPT1

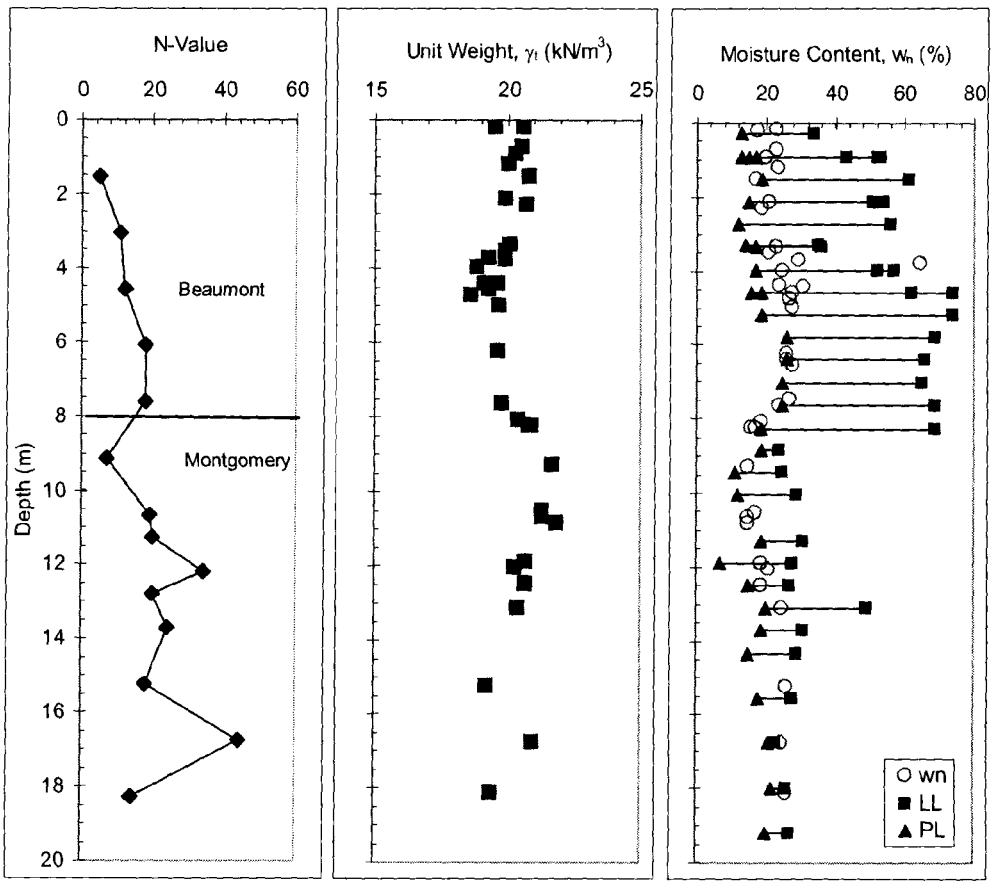

Figure A-54. Summary test data from samples across site.

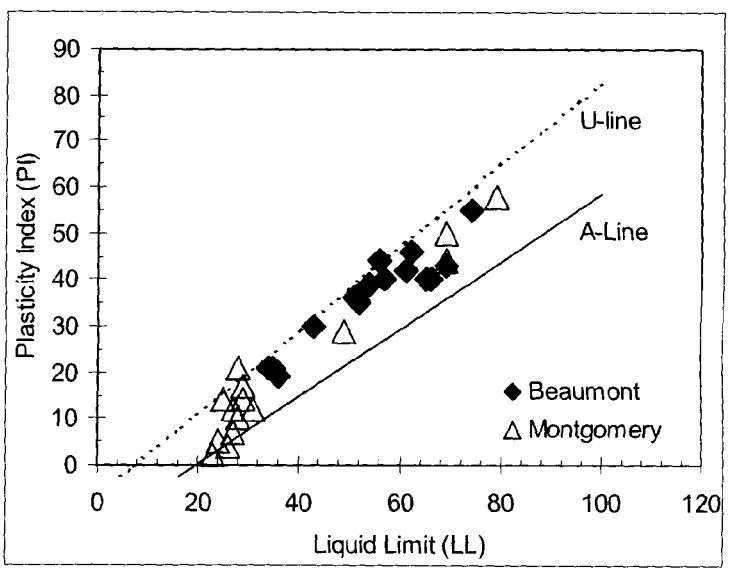

Figure A-55. Atterberg limits results for soil samples.

Stratigraphy from CPTu Data

Three CPTu soundings designated UHDU1, UHDU2, and UHDU3 are shown in figure A-56. For UHDU1 and UHDU3, pore pressures were measured on the sleeve just behind the cone tip (u_2), and for UHDU2, pore pressures were measured at the cone tip (u_1). The six layer designations previously developed based on boring log information (see table A-18) are used in the subsurface characterization based on CPTu measurements.

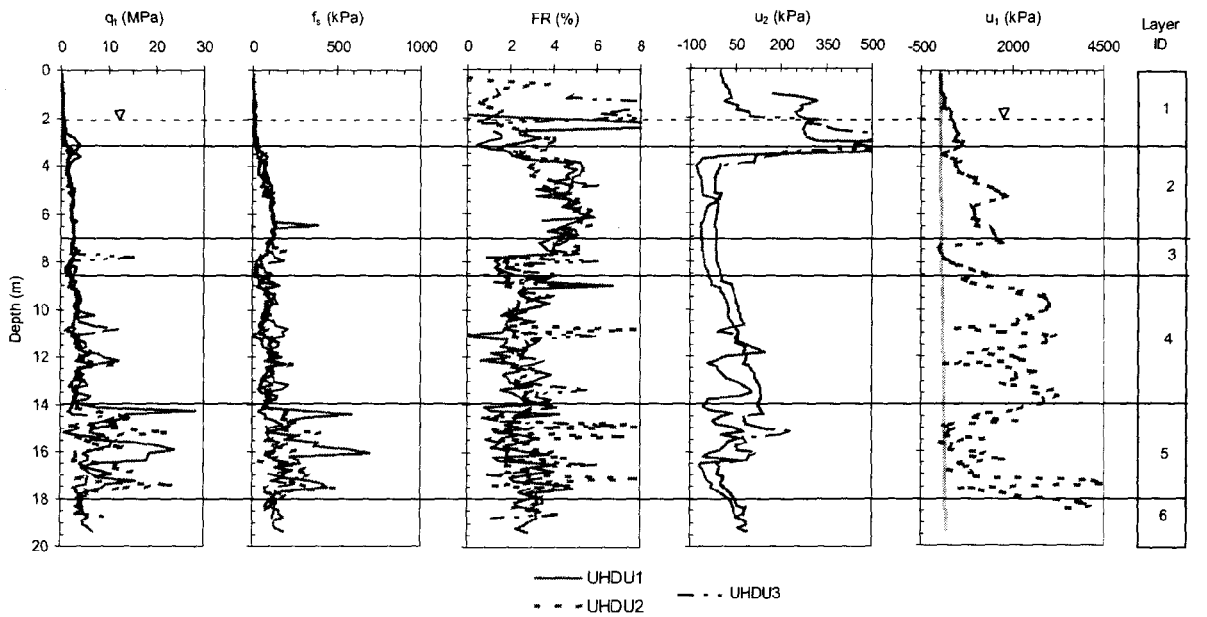

Figure A-56. Results of CPT measurements at site.

Based on a review of the CPTu data, the following interpretations can be made:

- A transition from Layer 1 to Layer 2 can be inferred from the significant reduction in pore pressure in the u_2 measurement. These negative pore pressure values indicate that this layer (Layer 2) is overconsolidated.
- The transition between Layer 2 and Layer 3 can be inferred by an overall reduction in friction ratio and a significant decrease in penetration pore pressure (u_1). This indicates that Layer 3 is more silty and/or sandy than the more clayey Layer 1.
- Layer 4 is clearly evidenced for the depth range of 8.5 to 14 m by a slight increase in the q_t with depth. The increase in q_t coupled with a slight decrease in FR indicates that Layer 4 is siltier than Layer 3 as shown in the classification charts presented in figure A-57. Also, the q_t response is more variable than for previous depth increments indicating the presence of harder silt or sand seams within the silty clay to clayey silt layer.
- Below 14 m the increase in q_t is consistent with the increase in blowcounts shown in the SPT and indicates sandy silt to sand. The spikes in the q_t response showing increases correlate to similar spikes showing decreased penetration pore pressures, thus indicating sandier seams.

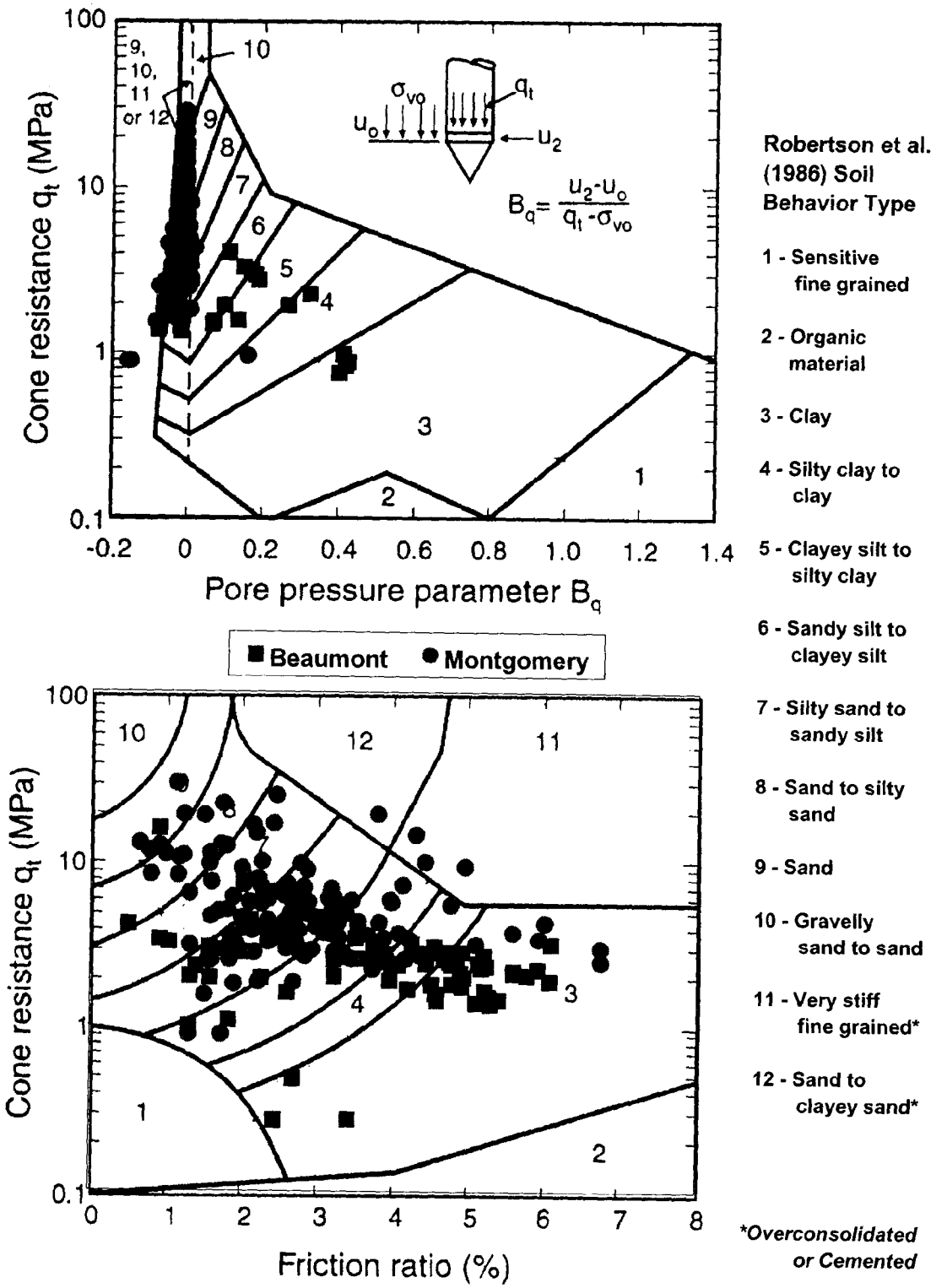

Figure A-57. Classification of soils using CPT derived parameters.

Stratigraphy from DMT Data

Figure A-58 shows the results of four DMTs performed at the Houston site. In figure A-59, the index parameters I_D and E_D are used to estimate classification and consistency.

The material index, I_D, indicates that the site soils range from silty clays to silty sands. Soils closer to and within the "sand" classification are primarily within the thin sand and silt seams of the Montgomery formation. Borderline points (i.e., at the sand/silt transition around $I_D = 2$) are near the Beaumont/Montgomery interface at a depth of approximately 8 m.

Overall, the E_D parameter increases with depth indicating that the Montgomery formation is stiffer than the Beaumont formation. Above 8 m, different soundings show relatively similar results. Below 8 m, sounding results are much more variable. This is consistent in that the Montgomery formation is known to be more variable (i.e., more silt and sand content/seams within clayey matrix).

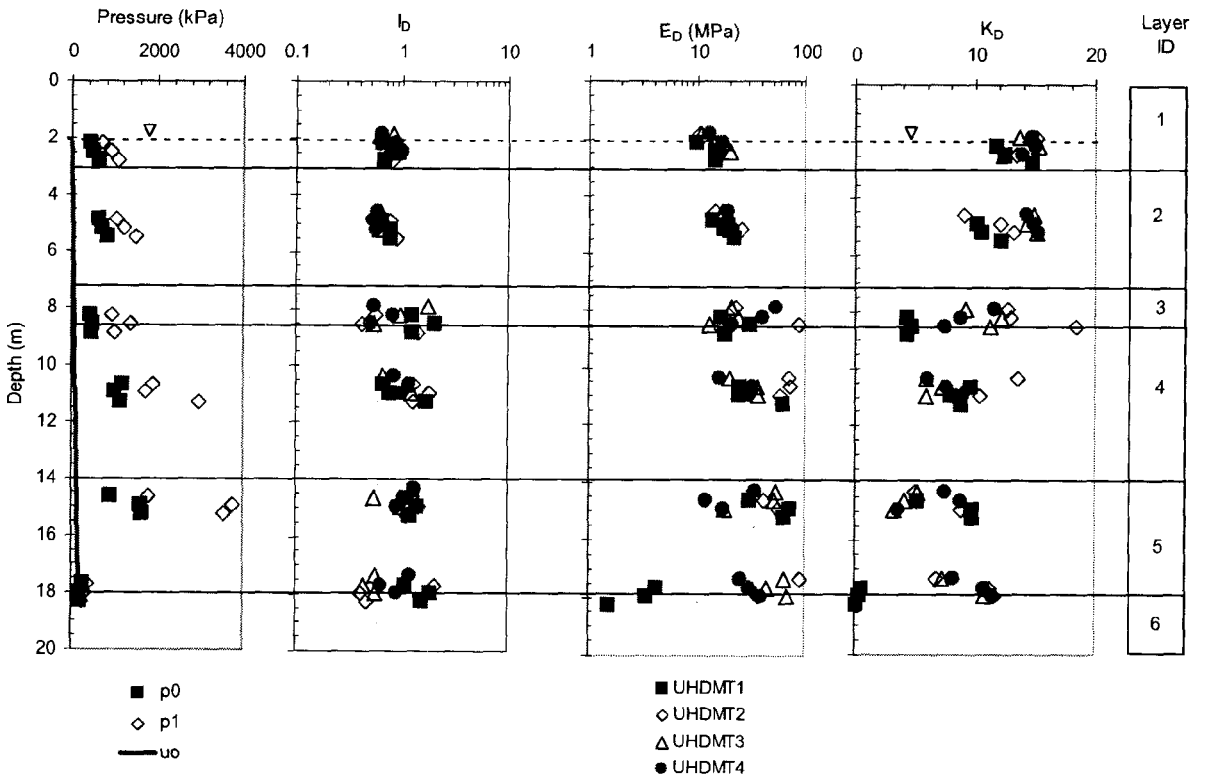

Figure A-58. Results of DMT measurements at site.

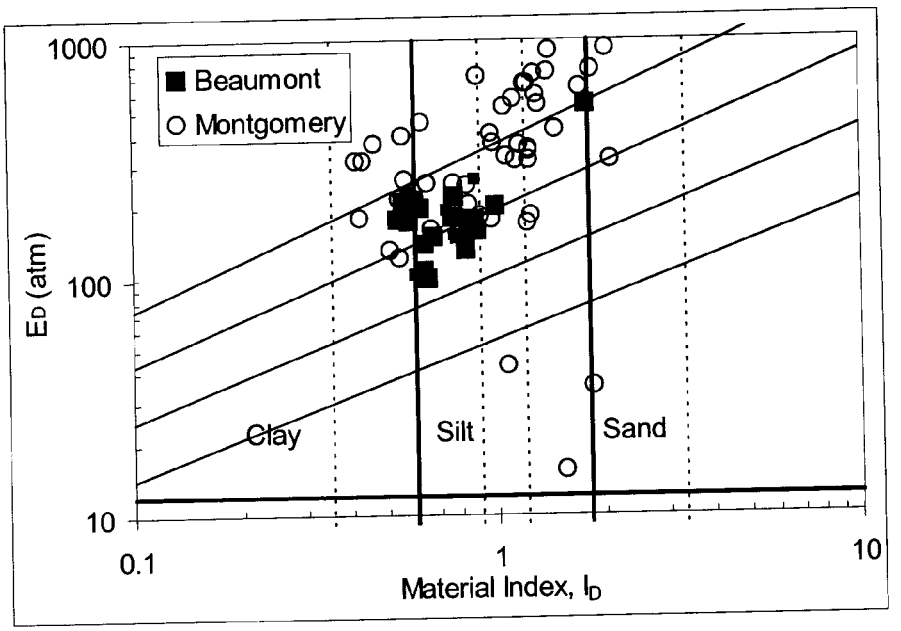

Figure A-59. Classification of soils using DMT derived parameters.

CONSOLIDATION TEST RESULTS

Laboratory one-dimensional consolidation tests were performed on four samples at various depths. The results of the testing are summarized in table A-19. Figure A-60 shows the determination of $C_{c\varepsilon}$, $C_{r\varepsilon}$, and σ_p' for a sample from a depth of 7 m.

Table A-19. Summary of oedometer testing on heavily overconsolidated clays.

Boring	Depth (m)	γ_d (kN/m^3)	σ_{vo}' (kPa)	σ_p' (kPa)	OCR	$C_{c\varepsilon}$	$C_{r\varepsilon}$	Strain to σ'_{vo} (%)	Sample Quality
UHS2	2.9	16.5	56	400	7.1	0.19	0.02	0.4	Very Good
UHS2	7.0	14.6	97	1,200	12.4	0.18	0.03	1.5	Acceptable
UHS3	10.1	18.5	128	250	2.0	0.06	0.01	1.0	Acceptable
UHS2	11.3	17.6	140	650	4.6	0.08	0.01	2.0	Disturbed
UHS2	14.3	16.9	171	1000	5.8	0.10	0.01	1.2	Acceptable

Notc: Preconsolidation stress was calculated using the Stain Energy Method.

Compression Parameters

Based on these data, a $C_{c\varepsilon}$ for design of 0.20 is appropriate for the Beaumont layer and 0.10 is appropriate for the Montgomery layer. This difference in compression index is consistent with the fact that the Montgomery formation is sandier than the Beaumont formation. As can be seen from figure A-60, these clayey soils undergo significant rebound (or swelling) upon unloading. For this reason, the practice of loading the soil to just before the preconsolidation stress and then unloading and using information from the unload-reload cycle to obtain a recompression index is likely to be conservative because of the significant swelling that occurs during unloading.

Also, if significant swelling is allowed to occur, particularly at low stress levels, then this swelling may cause the soil to become significantly destructured as compared to the in-situ material. In this case, if the soil is then reloaded into the virgin compression region, the interpreted value of $C_{c\varepsilon}$ may not be representative for design calculations. In other words, if the design will only include compressive loadings and consolidation and no unload cycles, then the value for $C_{c\varepsilon}$ obtained in the laboratory for a soil that has been subjected to swelling may not be representative. This issue should be considered when developing a laboratory consolidation-testing program.

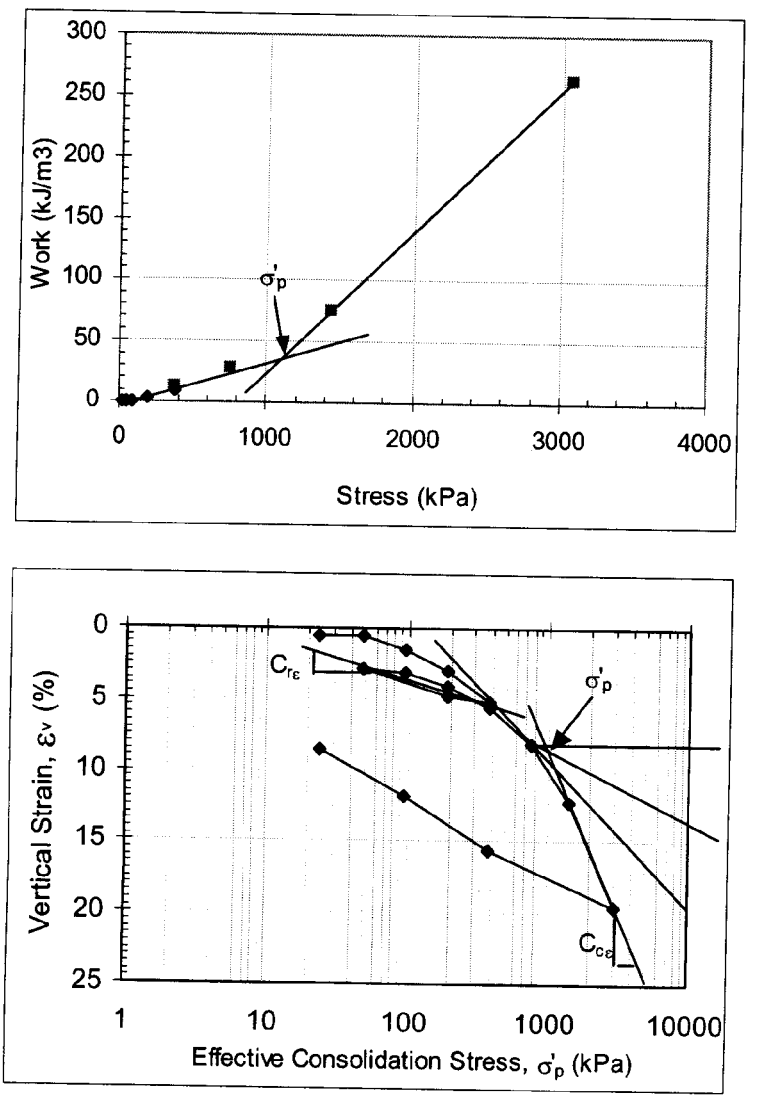

Figure A-60. Evaluation of $C_{c\varepsilon}$, $C_{r\varepsilon}$, and σ_p' using oedometer test results for sample at depth of 7 m.

Preconsolidation Stress

Figure A-61 summarizes the results of the evaluation of preconsolidation stresses from laboratory oedometer testing (using the Strain Energy approach) and from correlations to in-situ testing parameters. These data indicate that the DMT data closely matches the preconsolidation stresses

evaluated based on laboratory oedometer tests. These data also indicate a somewhat typical result for overconsolidated deposits, that being higher OCR values at shallower depths. Also, the data indicate that the deposit is still overconsolidated at depths of up to 14 m.

Significant scatter is apparent in the CPTu correlations due to the presence of sandy and silty layers and seams. It is noted, however, that if the CPTu data from depths less than 2 m (above the ground water table and where desiccation effects are most prevalent) and from depths greater than 8 m are omitted, the CPTu correlation for σ_p' tends to envelope the values obtained from the DMT and oedometer with an average OCR over this depth range of about 6 to 8. At depths greater than 8 m (i.e., the Montgomery formation), the CPTu correlations consistently overpredict OCR values relative to the DMT and oedometer test results. Based on CPTu classification, the soils in the Montgomery formation have tip resistances on the order of 2 to 5 MPa and a friction ratio of about 3 indicating a more silty and sandier material. The correlations are not appropriate for estimating preconsolidation stresses in these materials. Since the correlations are not appropriate for a depth range of 8 to 14 m, it would be appropriate to adopt an OCR profile based mostly on oedometer results.

Based on these evaluations, it would be appropriate to use a range of OCR profiles for design analyses. One such profile would assume a constant value of OCR equal to 7 for a depth range of 0 to 8 m and a constant value of OCR of about 4 for a depth range of 8 to 14 m.

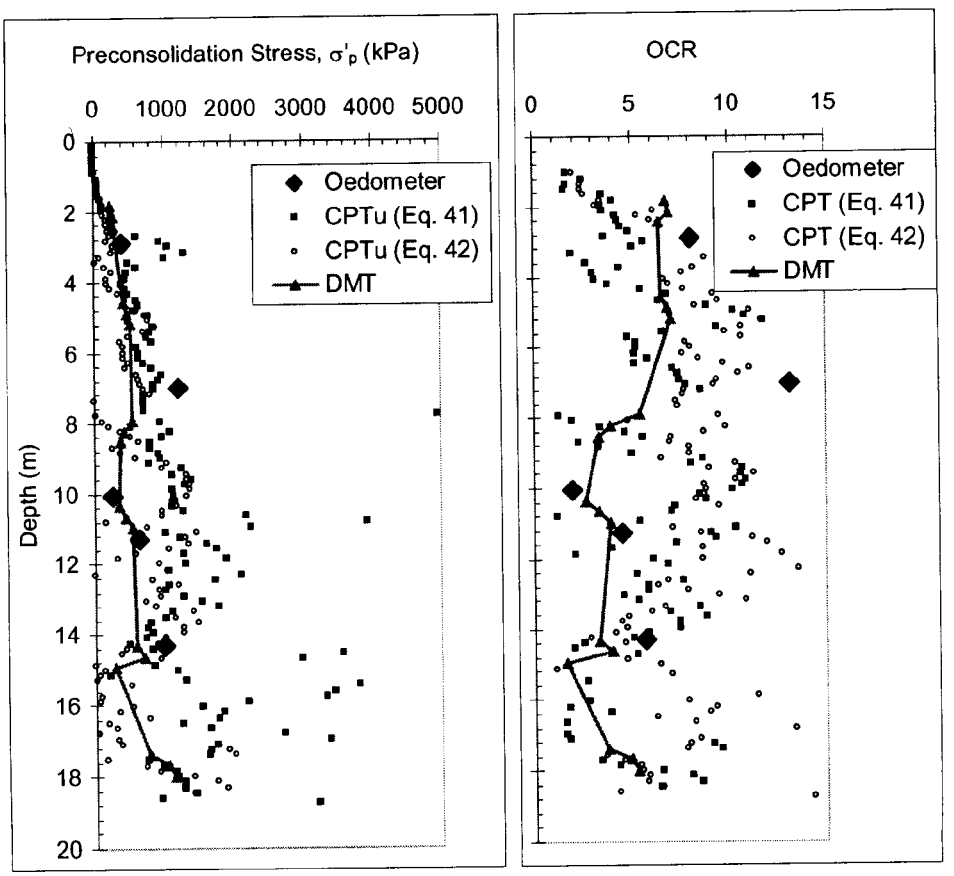

Figure A-61. σ_p' and OCR with depth from laboratory and in-situ tests.

IN-SITU HORIZONTAL STRESS STATE

In heavily overconsolidated soils, K_o can be an important design parameter since horizontal stresses can be significantly greater than vertical stresses. Figure A-62 shows values of K_o with depth for the site using various correlations. The SBPMT is a device that is capable of providing a direct measurement of the in-situ horizontal stress. For the SBPMT, K_o is calculated as the ratio of effective horizontal stress divided by vertical effective stress. The effective horizontal stress is given by $(p_o - u_o)$ where p_o is the pressuremeter lift-off pressure and u_o is the hydrostatic pore pressure in the ground.

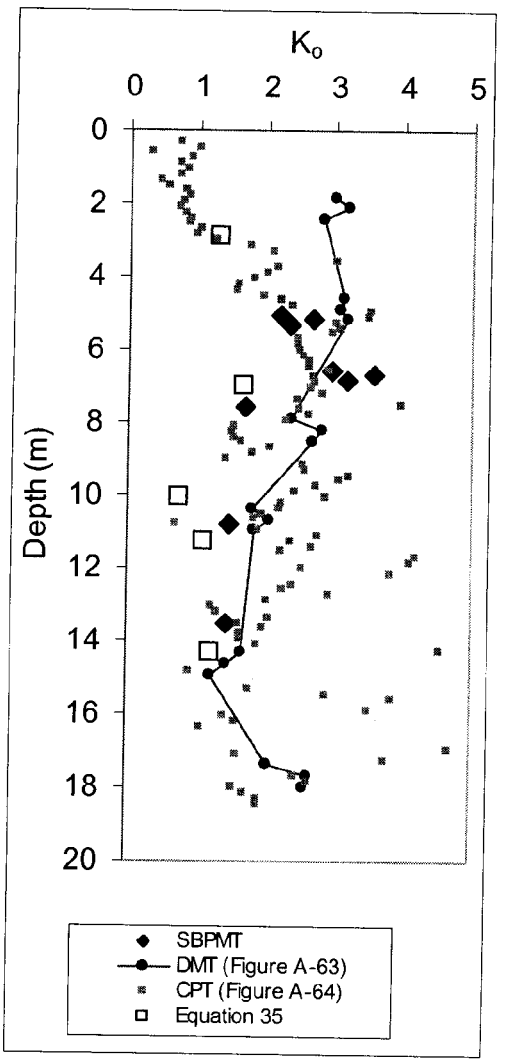

Figure A-62. Calculated K_o with depth from in-situ tests.

Parameters from other in-situ testing devices such as the SPT, CPT, CPTu, and DMT have been correlated to K_o. Figures A-63 and A-64 are used to evaluate K_o from CPTu and DMT data. K_o for the DMT is calculated based on the equation shown in Figure A-63 assuming β_k equal to 0.9 for fissured clays. Other correlations (not shown here) are available based on SPT N values and

penetration pore pressures from piezocones. For the methods shown in figures A-63 and A-64 (and others), the standard deviation is approximately 0.5. Values for K_o were also calculated according to equation 36 using OCR values from the oedometer test results with an assumed value for ϕ' of 25°.

For all methods, the overall trend of the data is similar; values of K_o closely follow the trend in OCR with higher values for K_o evident at the shallower depths (based on DMT and SBPMT) and progressively decreasing with depth. In selecting a profile for design, an upper and lower bound profile of K_o should be evaluated and then the design engineer should evaluate which K_o profile is critical. For example, a high K_o value may indicate that excellent resistance could be developed in a tiedown anchor while at the same time, a high value would indicate that a diaphragm wall would be subjected to potentially very large lateral loads during service.

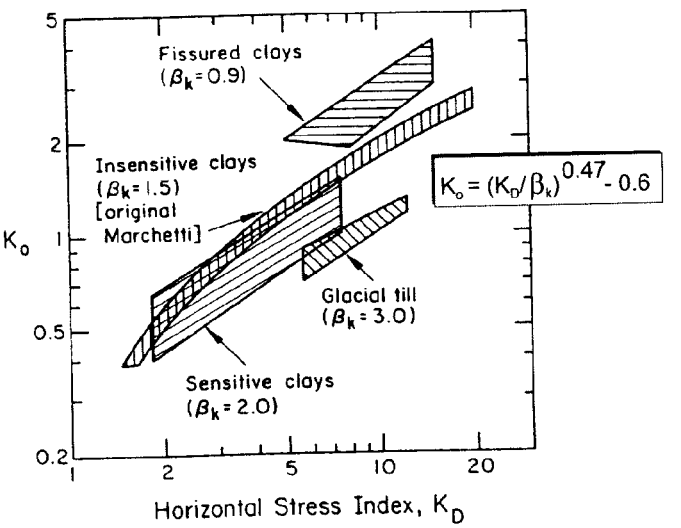

Figure A-63. K_o correlated with K_D from DMT data (Kulhawy and Mayne, 1990).

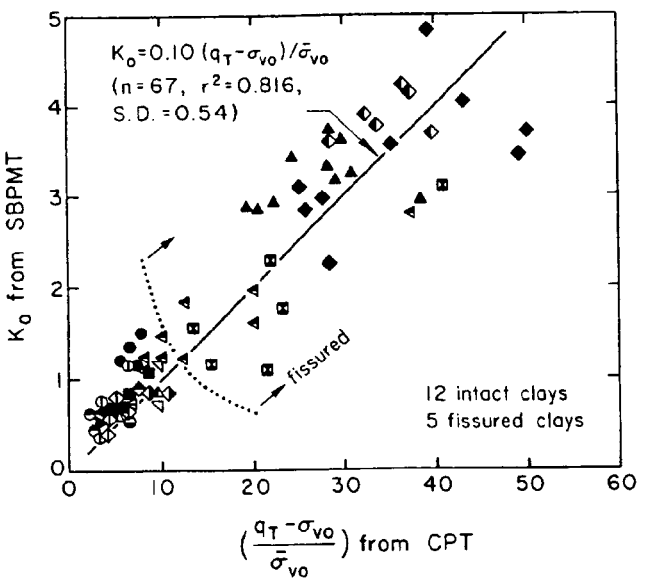

Figure A-64. K_o correlated with q_t from CPT data (Kulhawy and Mayne, 1990).

UNDRAINED SHEAR STRENGTH

Figure A-65 provides a summary of undrained shear strength, s_u, with depth for the Site. Laboratory UU and CIU triaxial tests are shown. The UU test results show significant scatter due in part to the local joint structure and the presence of sand and silt seams. Above 2 m, the UU test results show undrained strengths of approximately 150 kPa, on average. Below 2 m, the CIU test results are more consistent than the UU test results in that there is a general trend of increasing s_u with depth.

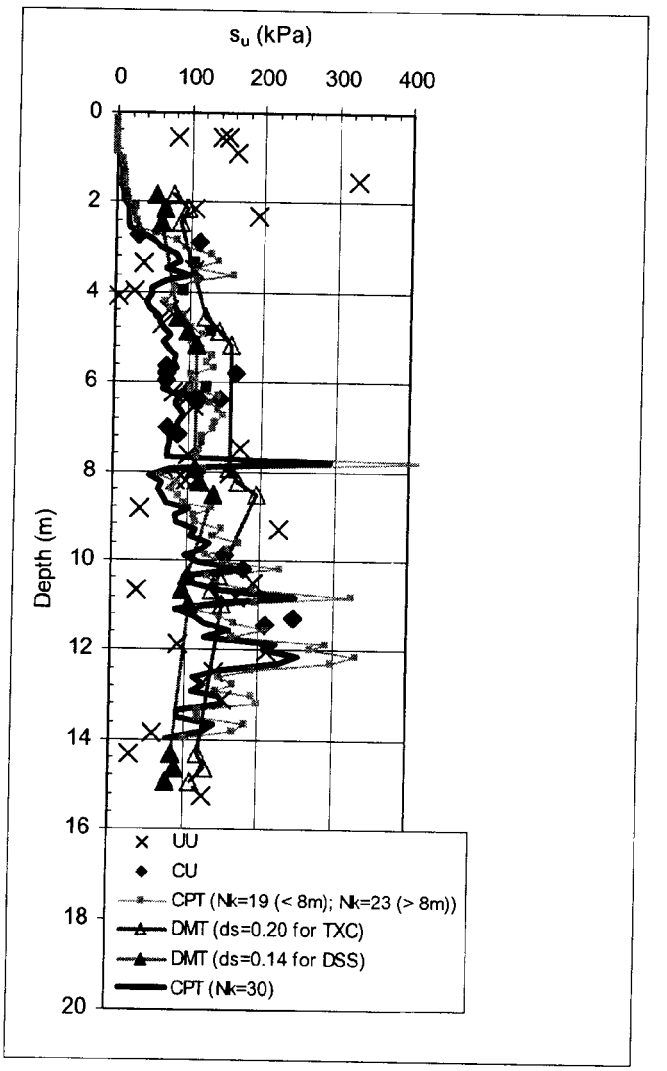

Figure A-65. Undrained shear strength, s_u, from laboratory and in-situ testing.

Several correlations using in-situ tests were also used to evaluate s_u. Undrained strength using CPTu results was calculated according to the following:

$$s_u = \frac{q_t - \sigma_{vo}}{N_k} \qquad \text{(Equation A-35)}$$

where N_k is equal to 19 in the Beaumont formation and 23 in the Montgomery formation. These values for N_k have been developed based on local calibration of CPT tip resistance results for soil

formations in the Houston area. In figure A-65, the data used for the CPT correlation are the average of soundings UHDU1 and UHDU3 (in which q_t can be evaluated since u_2 measured).

An additional correlation using the CPTu data is shown in figure A-65 for an assumed N_k factor equal to 30. As shown by Powell and Quarterman (1988), the effect of fissuring is to increase the correlated N_k factor, resulting in a lower correlated undrained shear strength for a given cone tip resistance. It is not possible to establish specific guidance relating the degree of fissuring to undrained shear strength, however, for highly fissured materials, the undrained shear strength appropriate for design analyses can be only 50 percent of the measured intact shear strength of the soil. This highlights the importance of understanding the degree of fissuring (e.g., size of soil "blocks" compared to cone tip size) when attempting to use undrained strength properties for design.

The correlation for the DMT uses the relationship $s_{uDMT} = d_s\sigma_{vo}' (0.5K_D)^{1.25}$ where d_s depends on the shear mode used. In figure A-65, values for d_s of 0.14 and 0.20 were used corresponding to triaxial compression and direct simple shear, respectively. The DMT data is the average of three soundings completed at the Site. The profiles of s_u from the DMT indicate that the correlation based on a triaxial compression mode of shear, on average, provides higher values of s_u as compared to other methods whereas the DMT correlation based on the direct simple shear mode appears to provide a good average fit to all the data. As with the interpretation of OCR, the correlations are much better for depths less than 8 m in the Beaumont formation.

Based on these data and the uncertainties associated with the evaluation of undrained shear strengths in fissured materials, it would be reasonable to select a constant value of s_u for design of 100 kPa for depths from 0 to 8 m. It is not clear whether an undrained strength characterization would be appropriate for depths greater than 8 m due to the increased sand content of this layer. However, based on figure A-65, depths up to 14 m could be conservatively assigned a constant undrained strength of 100 kPa or an undrained strength increasing from 100 kPa at 8 m to 150 kPa at 14 m.

SWELL POTENTIAL

Figure A-66 was used to evaluate swell potential for the soils at the Site. In using this figure, average index properties (i.e., in-situ dry density and liquid limit) were calculated for the soils of the Beaumont formation and for the Montgomery formation. The average data plotted on figure A-66 indicate that the Beaumont soils have high expansion potential compared to low expansion potential for Montgomery soils. As discussed in chapter 7, there are other methods available to evaluate swell potential, however, the information shown in figure A-66 would be sufficient to alert the engineer to the potential for significant swelling in the Beaumont formation (i.e., upper 8 or 9 m). Conservative local practice in these soils would likely preclude the use of shallow foundations unless specific measures were designed to minimize moisture changes in the upper reaches of the soil profile. To develop such designs would require more detailed information on swell potential such as that available from one-dimensional swell tests.

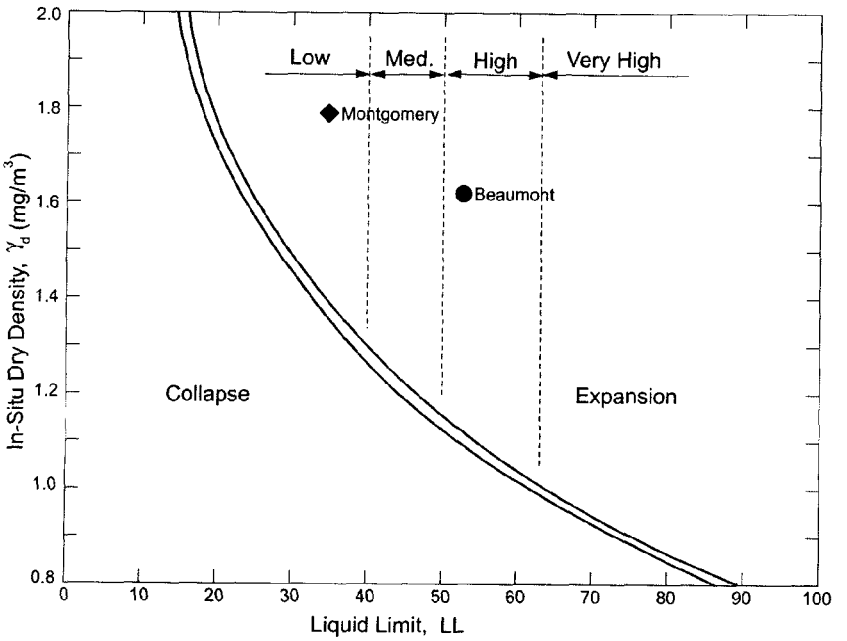

Figure A-66. Guide to expansion and collapse potential (adapted from Holtz and Kovacs, 1986).

APPENDIX B

CALCULATION OF THE COEFFICIENT OF CONSOLIDATION FROM LABORATORY DATA

B.1 OVERVIEW

The calculation of the coefficient of consolidation using laboratory data is typically performed using the following methods; (1) Casagrande's logarithm of time method; and (2) Taylor's square root of time method. These graphical methods provide an estimate of the time to reach a certain percentage of consolidation (e.g., 50 percent consolidation for the logarithm of time method and 90 percent consolidation for the square root of time method). Step by step procedures for the logarithm of time and square root of time methods are presented in the following sections.

B.2 LOGARITHM OF TIME METHOD

During a specific loading increment of an oedometer test, the deformation data will be recorded with time. To assess the vertical coefficient of consolidation, c_v, the data may be plotted versus time on a log scale. A graphical construction can be performed to assess the time to reach 50 percent consolidation, t_{50}. This procedure is described below and presented in figure B-1.

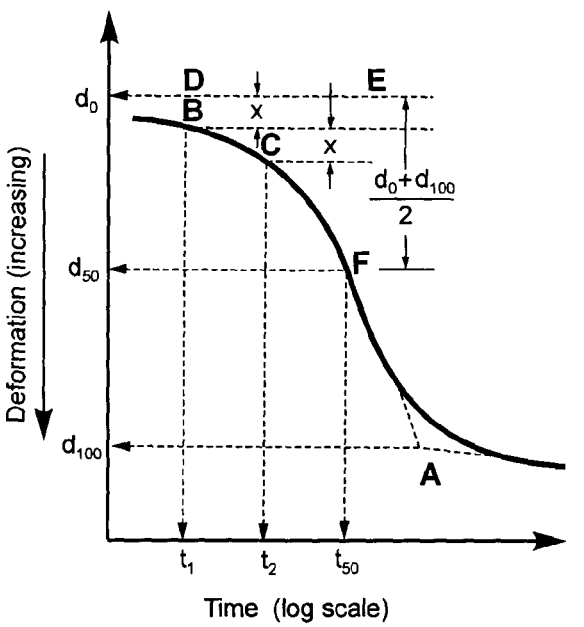

Figure B-1. Casagrande logarithm of time method for c_v calculation.

1. Extend the straight-line portions of primary and secondary consolidation so that they intersect. This point is marked A on figure B-1, and represents 100 percent primary consolidation.

2. Since the curve is on a log scale, the deformation value at t=0 will need to be estimated. The initial portion of the deformation – log time curve is approximated as a parabola. Select two

times, t_1 and t_2, such that $t_2 = 4t_1$. The difference in deformation values associated with these two time increments is identified as *x*.

3. Draw a horizontal line at the deformation value corresponding to *x* less than the deformation value at t_1 (line DE in Figure B-1). It may be desirable to perform this construction for a number of time pairs to increase the accuracy of the t=0 estimate. This deformation value (i.e., that corresponding to line DE) approximates zero percent consolidation.

4. Draw a horizontal line equal to the deformation value half way between the deformation at zero percent consolidation and the deformation value corresponding to 100 percent consolidation. This line intersects the time rate consolidation curve (point F on figure B-1) at a time equal to t_{50}.

5. The c_v value for this increment is calculated as:

$$c_v = \frac{0.197 \cdot H_{DR}^{\ 2}}{t_{50}} \qquad \text{(Equation B-1)}$$

where H_{DR} is the drainage height for the specimen. In a double drained specimen, H_{DR} is equal to the specimen height, and in a specimen with single drainage, H_{DR} is equal to half the specimen height.

B.3 SQUARE ROOT OF TIME METHOD

For this procedure, the deformation value for each time increment is plotted versus the square root of time. A graphical construction can be performed to assess the time to reach 90 percent consolidation, t_{90}. This procedure is described below and presented in figure B-2.

1. Extend the linear portion of the early part of the time rate consolidation curve, as indicated by line AB on figure B-2.

2. Draw a second line with the same origin on the y-axis (point A), and intersecting the x-axis at a value 15 percent greater than the line drawn for step 1. This implies that line OC=1.15 OB.

3. The square root of time value corresponding to the intersection of the line drawn for step 2 and the time rate consolidation curve (point D) is assumed equal to the square root of the time to reach 90 percent consolidation. The value for t_{90} is obtained by squaring this value.

4. The c_v value for this increment is calculated as:

$$c_v = \frac{0.848 \cdot H_{DR}^{\ 2}}{t_{90}} \qquad \text{(Equation B-2)}$$

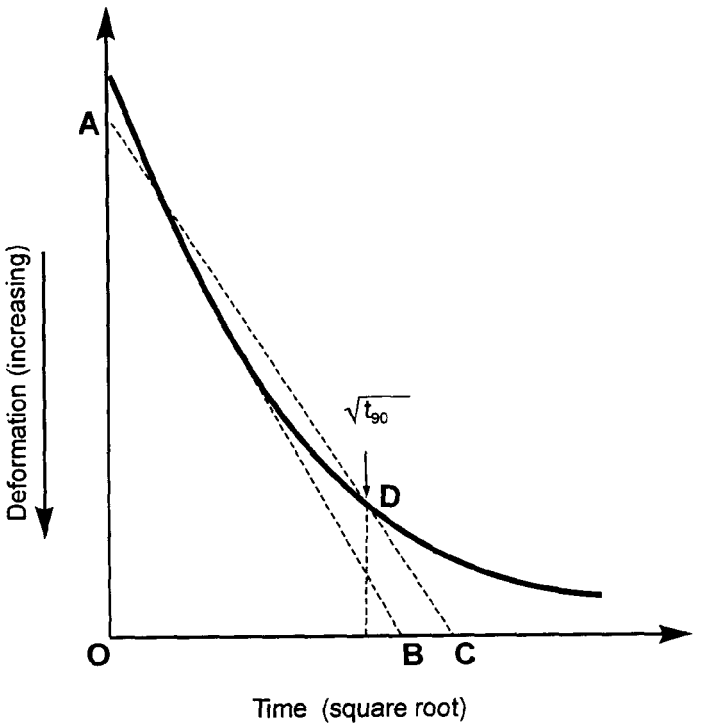

Figure B-2. Taylor's square root of time method for c_v calculation.

APPENDIX C

ALTERNATIVE APPROACH TO EVALUATE HORIZONTAL COEFFICIENT OF CONSOLIDATION VALUES FROM PIEZOCONE DISSIPATION TESTS

OVERVIEW

A method for evaluating the horizontal coefficient of consolidation, c_h, from piezocone dissipation test data (Burns & Mayne, 1998) is presented in this appendix. The solution presented below has been shown to work well for monotonic decay (Δu always decreasing) as well as a dilatory response (Δu increases for some or all of the dissipation).

CALCULATION OF RIGIDITY INDEX

To calculate c_h, the rigidity index, I_r, of the soil is estimated. This property is the ratio of the soil shear stiffness, G, to the undrained shear strength, s_u, and can be calculated from piezocone penetration test data and complimentary strength test data as:

$$I_R = \exp\left[\left(\frac{1.5}{M} + 2.925\right)\cdot\left(\frac{q_t - \sigma_{vo}}{q_t - u_2}\right) - 2.925\right] \qquad \text{(Equation C-1)}$$

where q_t is the cone tip resistance corrected for porewater pressures, σ_{vo} is the total vertical stress, u_2 is the penetration pore pressure measured behind the tip, and M is the slope of the critical state line equal to:

$$M = \frac{6\sin\phi'}{3 - \sin\phi'} \qquad \text{(Equation C-2)}$$

where ϕ' is the effective stress friction angle of the soil.

CALCULATION OF c_h

In lieu of merely matching one point on the dissipation curve (i.e., t_{50}), the entire curve is matched using the method presented herein to provide the best estimate of the value of c_h. The graph of pore pressure decay is plotted on a normalized scale as the ratio of excess pore pressure at time t, Δu_t, to the initial value of excess pore pressure during penetration, Δu_i.

The measured initial excess porewater pressure ($\Delta u_i = u_2 - u_o$) is expressed as:

$$\Delta u_i = (\Delta u_{oct})_i + (\Delta u_{shear})_i \qquad \text{(Equation C-3)}$$

The initial octahedral component of the excess porewater pressure $(\Delta u_{oct})_i$ is equal to:

$$(\Delta u_{oct})_i = (2M/3)(OCR/2)^{\wedge} \sigma'_{vo} \ln(I_R) \qquad \text{(Equation C-4)}$$

where OCR is the overconsolidation ratio, Λ is the critical state pore pressure parameter equal to about 0.8, and other parameters are as defined above.

The initial shear induced component of the excess porewater pressure $(\Delta u_{shear})_i$ is equal to:

$$(\Delta u_{shear})_i = \left[1-(OCR/2)^{\Lambda}\right]\sigma'_{vo} \qquad \text{(Equation C-5)}$$

The porewater pressures at any time are obtained in terms of the modified time factor, T*, from:

$$\Delta u_t = (\Delta u_{oct})_i\left[1+50T^*\right]^{-1} + (\Delta u_{shear})_i\left[1+5000T^*\right]^{-1} \qquad \text{(Equation C-6)}$$

$$T^* = (c_h t)/(a^2 I_R^{0.75}) \qquad \text{(Equation C-7)}$$

where a is the radius of the penetrometer.

To estimate c_h, an iterative solution will need to be performed.

1. Plot normalized dissipation data from the test on a semi-log scale of time vs. normalized porewater pressure, $\Delta u/\Delta u_i$ (see figure C-1 as an example).

2. Recalculate Δu_t using equation C-6, and iterate so that a good match of the data from step (1.) is computed. Equations C-1, C-2, C-4, C-5, and C-7 will need to be used for generation of the calculated dissipation curve. By varying the value of c_h in equation C-7, the value of T* will change and thus alter Δu_t. The value of c_h that yields the best match of field data is the best estimate of the field horizontal coefficient of consolidation.

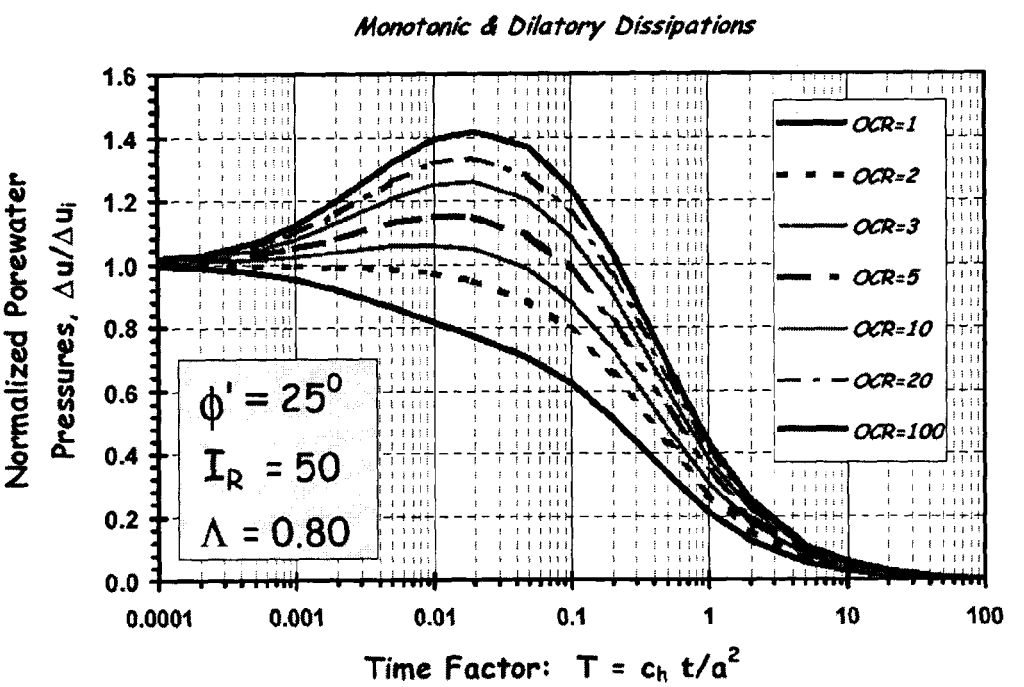

Figure C-1. Comparison of measured and predicted piezocone dissipation data.